REGIONAL SEAS

UNITED NATIONS ENVIRONMENT PROGRAMME

Proceedings of the Symposium/Workshop on oceanographic modelling of the Kuwait Action Plan (KAP) Region

UNEP Regional Seas Reports and Studies No. 70

Prepared in co-operation with

UNESCO

ROPME

UPM

PREFACE

The United Nations Conference on the Human Environment (Stockholm, 5-16 June 1972) adopted the Action Plan for the Human Environment, including the General Principles for Assessment and Control of Marine Pollution. In the light of the results of the Stockholm Conference, the United Nations General Assembly decided to establish the United Nations Environment Programme (UNEP) to "serve as a focal point for environmental action and co-ordination within the United Nations system" (General Assembly resolution (XXVII) of 15 December 1972). The organizations of the United Nations system were invited "to adopt the measures that may be required to undertake concerted and co-ordinated programmes with regard to international environmental problems", and the "intergovernmental and non-governmental organizations that have an interest in the field of the environment" were also invited "to lend their full support and collaboration to the United Nations with a view to achieving the largest possible degree of co-operation and co-ordination". Subsequently, the Governing Council of UNEP chose "Oceans" as one of the priority areas in which it would focus efforts to fulfil its catalytic and co-ordinating role.

The Regional Seas Programme was initiated by UNEP in 1974. Since then the Governing Council of UNEP has repeatedly endorsed a regional approach to the control of marine pollution and the management of marine and coastal resources and has requested the development of regional action plans.

The Regional Seas Programme at present includes eleven regions[1/] and has over 120 coastal States participating in it. It is conceived as an action-oriented programme having concern not only for the consequences but also for the causes of environmental problems through the management of marine and coastal areas. Each regional action plan is formulated according to the needs of the region as perceived by the Governments concerned. It is designed to link assessment of the quality of the marine environment and the causes of its deterioration with activities for the management and development of regional legal agreements and of action-oriented programme activities.[2/]

During its fourth session in 1976 the Governing Council of UNEP approved the Preparatory work for convening a Regional Conference on the Protection of the Marine and Coastal Environment of Bahrain, Iran, Iraq, Kuwait, Oman, Qatar, Saudi Arabia and the United Arab Emirates. Subsequently, on the basis of a fact-finding mission sponsered by UNEP and supported by several United Nations agencies, a draft action plan dealing with the scientific and socio-economic aspects for the protection and development of the marine environment of the region was prepared and reviewed by a

---

1/ Mediterranean Region, Kuwait Action Plan Region, West and Central African Region, Wider Caribbean Region, East Asian Seas Region, South-East Pacific Region, South Pacific Region, Red Sea and Gulf of Aden Region, Eastern African Region, South-West Atlantic Region and South Asian Region.

2/ UNEP: Achievements and planned development of UNEP's Regional Seas Programme and comparable programmes sponsered by other bodies. UNEP Regional Seas Seas Reports and Studies No. 1 UNEP, 1982.

series of technical meetings of Government-nominated experts. In April 1978 a Regional Conference of Plenipotentiaries was convened in Kuwait for the purpose of reviewing, revising and adopting the action plan and related legal instruments. The Conference, adopted on 23 April 1978,

(a) the Action Plan for the Protection and Development of the Marine Environment and the Coastal Areas of Bahrain, Iran, Iraq, Kuwait, Oman, Qatar, Saudi Arabia and United Arab Emirates,[3/]

(b) the Kuwait Regional Convention for Co-operation on the Protection of the Marine Environment from Pollution,[4/]

(c) the Protocol Concerning Regional Co-operation in Combating Pollution by Oil and other Harmful Substances in Cases of Emergency,[4/]

(d) resolutions on (i) interim secretariat, (ii) financial arrangements, (iii) steps to be taken for the establishment of the Marine Emergency Mutual aid Centre, and (iv) co-ordination between the regional marine meteorological and environmental programmes.[3/]

The Action Plan has subsequently become known as the Kuwait Action Plan.

The development of an oceanographic model for the region was one of these priority projects. A Symposium/Workshop on this subject was held at the University of Petroleum and Minerals (UPM) in Dhahran, Saudi Arabia, 15-18 October 1983. The Symposium was sponsered by the UPM, the Meteorological and Environmetal Protection Administration (MEPA) of Saudi Arabia; the Regional Organization for Protection of the Marine Environment (ROPME); the United Nations, Educational, Scientific and Cultural Organization (UNESCO); and the United Nations Environment Programme (UNEP).

The papers presented and discussed at this Symposium outlined the state of the art in the area of oceanographic modelling of the KAP Region and included suggestions for future work. On the basis of the discussions of these papers and the suggestions contained therein, the Symposium made a number of recommendations which appear at the end of the report.

This report includes the full text of all the scientific papers which were presented at the Symposium and were made available to UNEP for publication. In addition, it includes a paper which was submitted to the Symposium but was not presented or discussed due to the absence of the authors[5/].

3/ UNEP: Action Plan for the protection of the marine environment and the coastal areas of Bahrain, Iran, Iraq, Kuwait, Oman, Qatar, Saudi Arabia and United Arab Emirates. UNEP Regional Seas Reports and Studies No. 35. UNEP 1983.

4/ Kuwait Regional Convention for Co-operation on the Protection of the Marine Environment from Pollution and Protocol Concerning Co-operation in Combating Pollution by Oil and Other Harmful Substances in Cases of Emergency. UNEP 1983.

5/ C.P. Mathews and J.W. Lee: The development of oceanography in Kuwait.

TABLE OF CONTENTS

6/ This paper was submitted to the Symposium but was not presented or discussed.

7/ The two reports were presented as one paper at the Symposium but the authors have prepared them as two separate reports for this publication.

MEPA MARINE WEATHER SERVICES OPERATIONAL MODELS

by

Al-Deghaither, D. Brown*, R. Chao*, R. Langland*, H. Lewit*
C. Lozano*, V. Peterson*, and G. Rosenberger

Meteorology and Environmental Protection Administration (MEPA)
Jeddah, Saudi Arabia
* Affiliation: Global Weather Dynamics, Inc.
Monterey, CA, USA

ABSTRACT

MEPA Marine Weather Services include the routine computation of sea level pressure, surface winds, singular waves, mean currents, water heights and surface currents for both the Inner Gulf and the Red Sea. These computations support MEPA forecast services and the trajectory and evaporation-spreading oil spill models.

In addition, MEPA has hydrodynamic models for the major harbours and ports in Saudi Arabia and the capability of rapid model deployment for a new area.

This paper gives an overview of the above-mentioned models, including a critical appraisal of the data-base input, the heuristics and physics used in the models, and a discussion of the reliability of the model output. Suggestions are made for further improvements.

INTRODUCTION

MEPA Marine Forecasting Centers produce marine weather, sea state and wind forecasts, and warnings for the waters around Saudi Arabia. In order to support these activities, the National Meteorological and Environmental Center (NMEC) marine software generates sea level pressure and wind analyses, wave conditions, mean currents, surface heights and surface currents for both the Inner Gulf and the Red Sea every six hours. In addition to these operational products, NMEC marine software includes a data base to support observational data input and generated fields, a meteorological graphics package, a tide reduction package, and an oil spill programme.

The purpose of this paper is to give a critical review of NMEC marine software, especially in its application to the Inner Gulf regions. In the next sections, an overview of the entire marine software is provided, followed by a brief description of major software packages and an appraisal of the input and output data. Lastly, some suggestions for improvement are offered.

It should be noted that the heuristics involved in the construction of the marine software analyses are based on work produced by Global Weather Dynamics Inc. (GWDI) of Monterey, California. In fact, parallel marine software for this area has been run in Monterey. The Monterey products, which are transmitted via satellite, are used directly at the MEPA office in Dhahran.

MARINE SOFTWARE OVERVIEW

The major inputs and programmes in marine software are shown in Figure 1. Sea level pressure is analyzed on a global band grid using the observations and previous analyses available. The area covered in the global band and the indicative output are illustrated in Figure 2. A zoom of the analyzed pressure field in the Saudi Arabian area is used as a first-guess approximation in which to incorporate further observations with local corrections, such as land/sea breeze effects, normally disregarded in the global band grid. The regional analyzed pressure field as shown in Figure 3 is used together with wind observations and sea surface temperature analysis to create an analyzed surface wind field.

The analyzed wind field is an input to the wave, water circulation and surface current models. In addition, the circulation models (hydrodynamic) for the major basins use the analyzed pressure fields. The analyzed surface currents are used as an input to the oil spill model. Finally, the analyzed surface heights are an input to the tidal reduction package or the cotidal/corange programmes (see Figure 1). Some of the analyses of pressure, wind, and oil spill trajectories may be bogused.

The marine software data base, product presentation and communications are supported by a host of utilities and graphics output in a user-friendly environment.

DESCRIPTION OF MAJOR SOFTWARE PACKAGES

This section presents a brief description of the major packages outlined in the previous section. Details are given in the Marine Weather Service Project Manuals (Marine Wheather Services Project, 1983a,1983b and 1983c).

Sea level pressure analysis

The production of the required sea level pressure analysis fields is carried out using a nesting procedure. A 2.5 degree resolution Mercator global band grid extending from 40°S to 60°N is analyzed every six hours. All available surface land and ship observations are included. These data are received from the Global Telecommunications System (GTS) and from other sources, such as the satellite data circuit extending from NMEC to GWDI in the United States.

A first guess for a regional 1.25 degree Mercator sea level pressure analysis is interpolated from the global band output. The finer resolution of the regional grid that extends from 10°S to 60°N, 15°W to 85°E makes it possible to resolve mesoscale pressure patterns.

Data assimilation is accomplished using a least-squares minimization of the deviation of the local gradients and Laplacian from the original first guess. The model includes logic to accept or reject observations on any of three successive data assimilation scans.

Surface wind analysis

The first guess for the wind field is the geostrophic wind corrected for curvature and drag. The pressure field used to construct the quasi-geostrophic wind is the analyzed pressure field.

The initial guess is modified for the land/sea breeze effect of the Red Sea and Inner Gulf coastlines and for wind surges over water areas only.

Data assimilation is accomplished using a least-squares minimization of the deviations of local divergence, vorticity and gradient from the original first guess. The model includes logic to accept or reject observations on any of three successive data assimilation scans.

Singular wave analysis

The period and amplitude of the most significant wave (the average of the one third highest waves) are decomposed into sea (locally generated wave) and swell (advected wave). The wave generation scheme follows Bretschneider (1952) and Sverdrup & Munk (1947); the advection scheme is a variation of Haug (1968) due to Hubert (private communication). The advection scheme contains a correction for amplitude modification in shallow waters.

Hydrodynamic circulation models

The model for the vertically averaged current and surface height is a baroclinic model driven by wind stresses and tidal forces. It includes bottom friction (Nihoul, 1975). The discrete version is realized through an explicit finite difference scheme.

The circulation models for the Inner Gulf region are the Gulf model with a 20.3 km grid size (Figure 3), the western region of the Gulf with a 10.6 km grid size (Figure 4), and the models for Jubayl harbour and the docking and anchorage areas of Ras Tannurah and Ad Dammam, with grid sizes of 0.5, 0.4 and 1.0 km, respectively (Figures 5-7).

Surface currents

To obtain the surface current, the vertically averaged current generated by the circulation model and the local wind-generated surface current are added together. The local wind-generated current is obtained from a scheme of Madsen (1977).

Oil spill trajectories

Oil spill trajectories are constructed with the assumption that the oil spill is advected by the surface currents.

Oil spill evaporation and dispersion

The estimates for the evaporation and dispersion of various common types of oils are made following the parameterization of Aravamundan et al. (1982).

Tidal reduction

A least-squares fit to selected tidal constituents after appropriate filtering of data is used to predict tidal constants and generate tidal tables (from the algorithm designed by Foreman, 1977).

DATA QUALITY AND VALIDATION

Starting with the operational installation of the wind and pressure analyses early in June 1982, portions of the marine software have become fully operational. The outputs have shown stability and a reasonable range and disposition of values. Unfortunately, the available observational data are very limited and too scattered to permit the best validation procedure to be established.

It was realized at the outset of the project that the observational data would be sparse. A special effort therefore was made to design a software package amenable to an expansion of the data base having a sensible number of tuning parameters. Recently, more data have become available due to an oil spill in the Gulf. Some initial validation studies have been carried out.

The following two examples are indicative of data quality and computational output.

Surface winds

Surface land and ship observations are received at NMEC via the Global Telecommunications Circuit (GTS) and the data circuit from GWDI. Being a Regional Telecommunications Hub (RTH), NMEC Jeddah collects regional observations which are then made available for the analysis.

ARAMCO drilling platforms report wind and sea conditions twice daily via a regional communication circuit. Unfortunately, this circuit is not terminated at the NMEC message switching system and the observations are not in a suitable format for machine processing. These observations must thus be interactively entered by shift personnel into the observational data base, using a bogusing procedure. The total number of observations on

The total number of observations on the analysis grid from all the sources mentioned above rarely exceeds 70 for any of the six hourly analyses. The grid extends from just West of the Red Sea to East of the Inner Gulf, and from the Southeastern end of the Mediterranean Sea to the extreme Northwestern Arabian Sea. Of the available observations, only about 30 per cent are over or near the water areas of interest.

In the absence of observations, the ensuing wind analysis is based on the first-guess wind field as estimated from sea level pressure, sea breeze and surge algorithms. In certain regions, such as the Gulf of Suez and Bab al Mandab, local orographic influences dominate the wind flow and observations are critical in specifying correctly the wind conditions.

Since these wind analysis fields are the primary forcing function for all the subsequent processing (waves, HN, surface current, oil spill), the correct specification of wind fields is imperative.

Predicted tides near Ad Dammam

The output of the basin model includes hourly time history records at selected grid locations. Figure 8 shows the surface height produced by the model at latitude $26^{o}23'02"N$, and longitude $50^{o}22'08"E$, near Ad Dammam. The associated energy spectrum is shown in Figure 9. The characteristic semidiurnal tide of the area as well as the relative proportions of the major tidal constituents is well approximated by the record. Direct comparison with data recently provided by ARAMCO is in progress.

It should be pointed out that oceanographic data are much more sparse than meteorological data. There seems to be a need for a serious, cooperative effort to initiate a sensible oceanographical, observational network.

CONCLUSIONS

The ability to provide a reliable marine weather service both in normal and crisis situations hinges on a sufficiently dense observational network with high quality data and efficient, reliable data analysis.

Marine software is an aid in the forecasting activities at MEPA. MEPA is in the early stages of developing an observational network facility, and this software is considered to provide a firm basis for integrating and interpreting observations.

The next steps in the development of marine software should be more in-depth tuning and validation of analyses, using newly acquired observational data, and the integration of a regional atmospheric prognostic model to provide forecast wind fields.

It should be noted that all the marine models are currently capable of producing forecast output given the forecast input fields.

ACKNOWLEDGEMENTS

Assistance in preparing this manuscript was received from Mr. Samir Buhari, Director of NMEC, and the forecast staff at Jeddah and Dhahran.

BIBLIOGRAPHY

Aravumundan et al.(1982) Break-up of oil at rough seas, simplified model and step-by-step calculations. Coast Guard Report CG-D-28-82, Wahington, D.C.

Bretschneider, C.L. (1952) The generation and decay of wind waves in deep water. Transactions of the American Physical Union, Vol. 33, 381-389.

Foreman, M.G.G. (1977) Manual for tidal heights and prediction. Pacific Marine Science Report 77-10, Institute of Ocean Sciences, Patricia Bay, B.C. Canada.

Haug, O. (1968) A numerical model for the prediction of sea and swell. Meteorologiske annaler, Vol. 5, 139-161.

Madsen, O.S. (1977) A realistic model of the wind-induced Ekman boundary layer. J.Phys.Oceanogr., Vol. 7, 248-255.

Marine Weather Services Project (1983a) Software functional description Final Rept. Global Weather Dynamics, Inc. Monterey, CA, and Saudi Arabian Tech. Saudi Arabia.

Marine Weather Services Project (1983b) Software user's manual, Final Rept. Global Weather Dynamics, Inc., Monterey, CA, and Saudi Arabian Technology, Saudi Arabia.

Marine Weather Services Project (1983c) Software maintenance manual, Final Rept. Global Weather Dynamics, Inc., Monterey, CA, and Saudi Arabian Technology, Saudi Arabia.

Nihoul, C.J. (ed.) (1975) Modelling of marine systems, Chaps. 1 & 2. Elsevier Publ. Co., The Netherlands.

Sverdrup, H.U. and Munk W.H. (1947) Wind, sea and swell, theory of relations for forecasting. U.S. Navy Hydrographic Office, Publication No. 601, Washington, D.C.

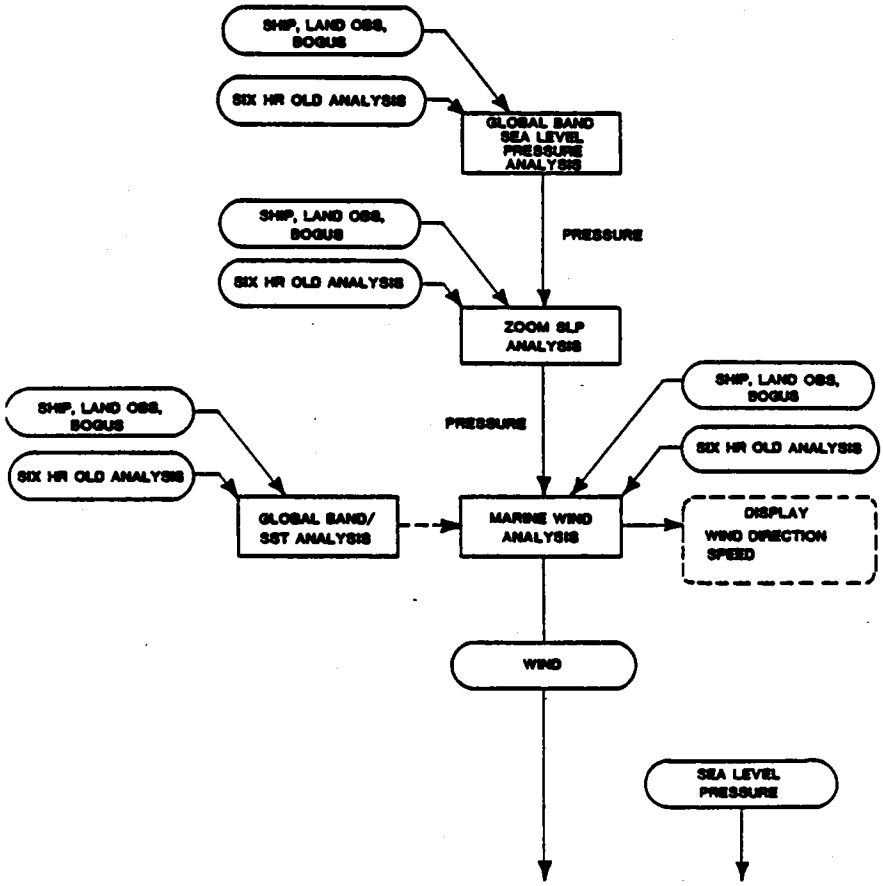

Figure 1: Marine weather software flow diagram: part I.

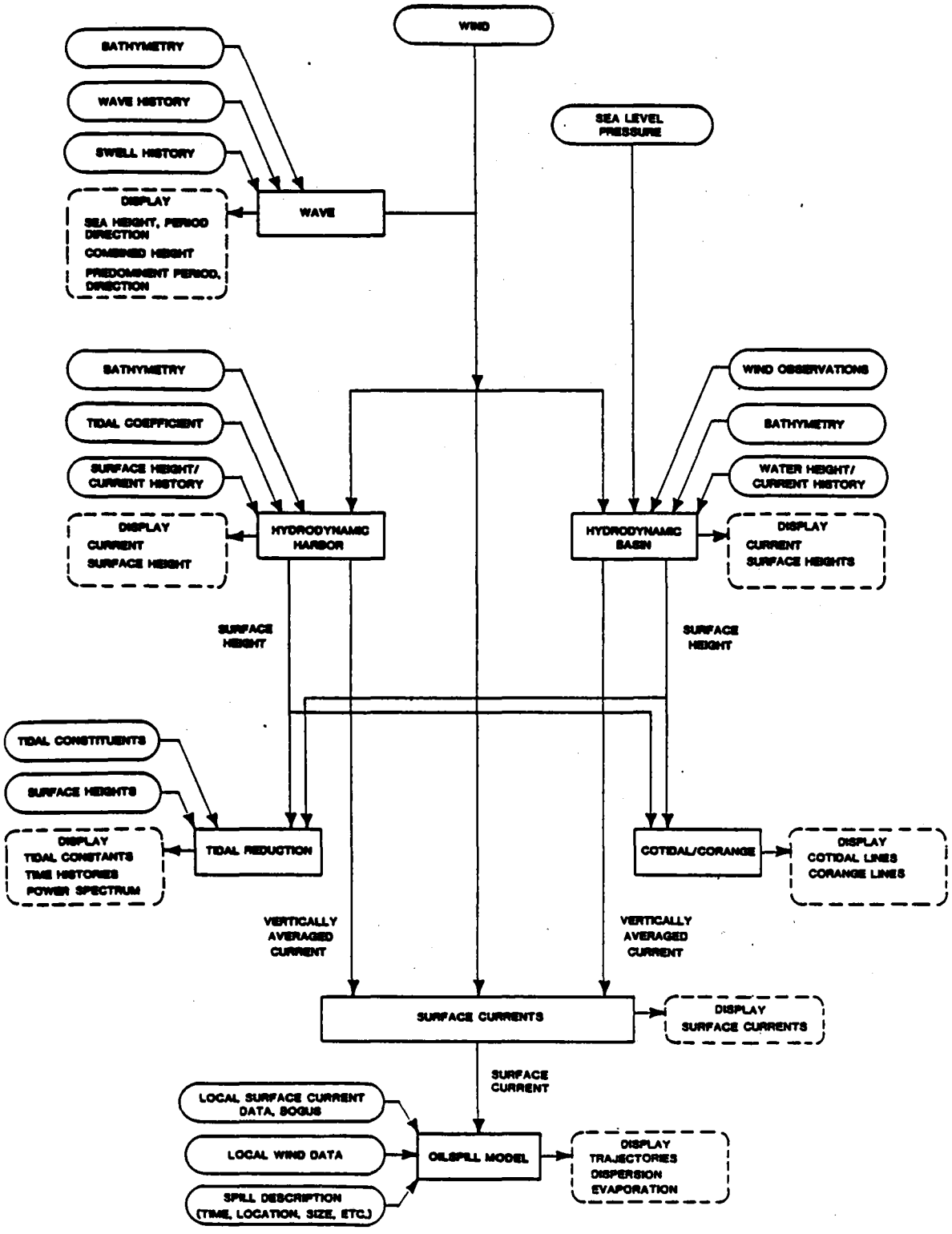

Figure 2: Marine weather software flow diagram: part II.

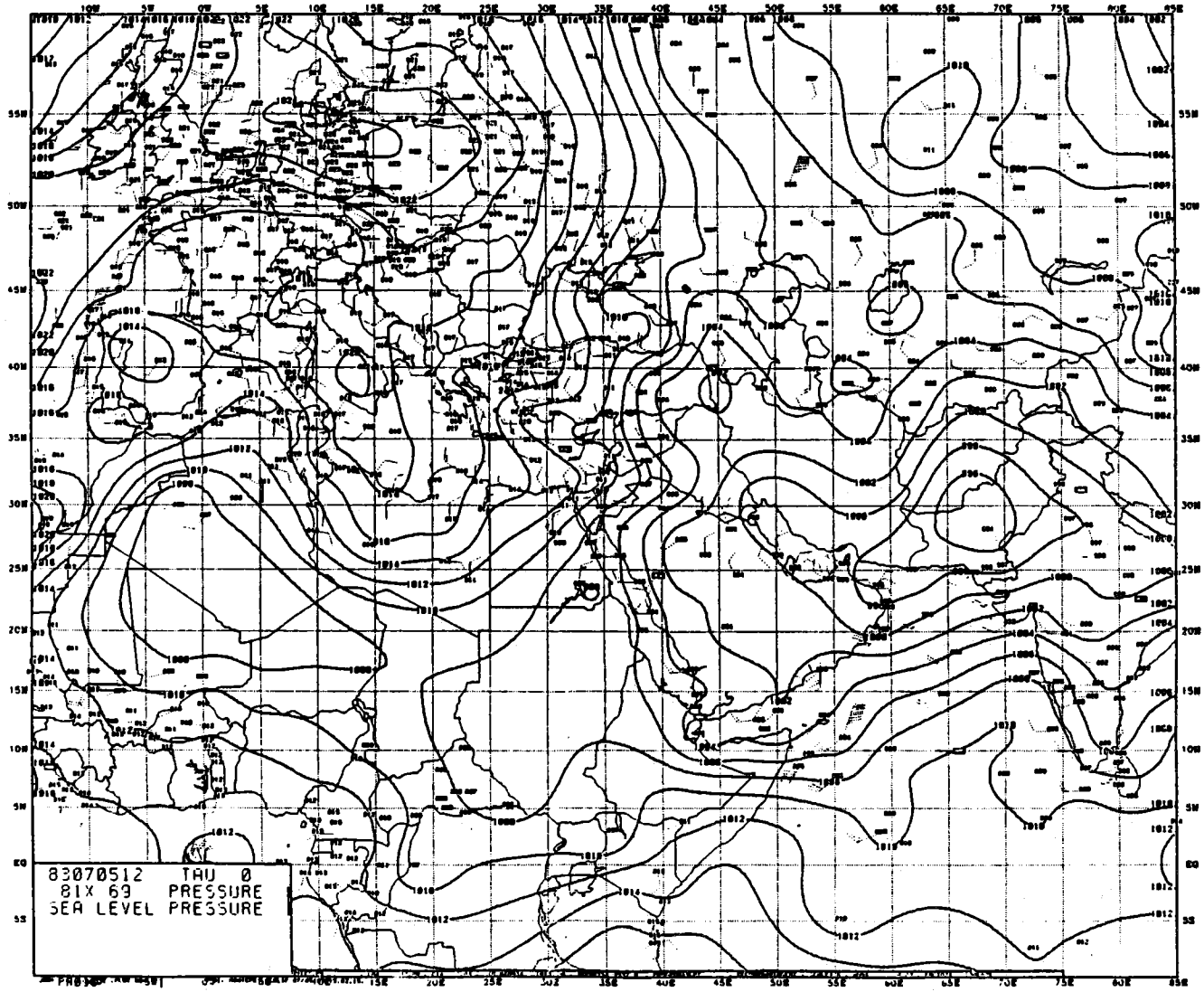

Figure 3: Surface pressure level analysis for 7 July 1983 at 12 GMT. The number of observations around the Gulf are about 7. This number of observations is unusually high.

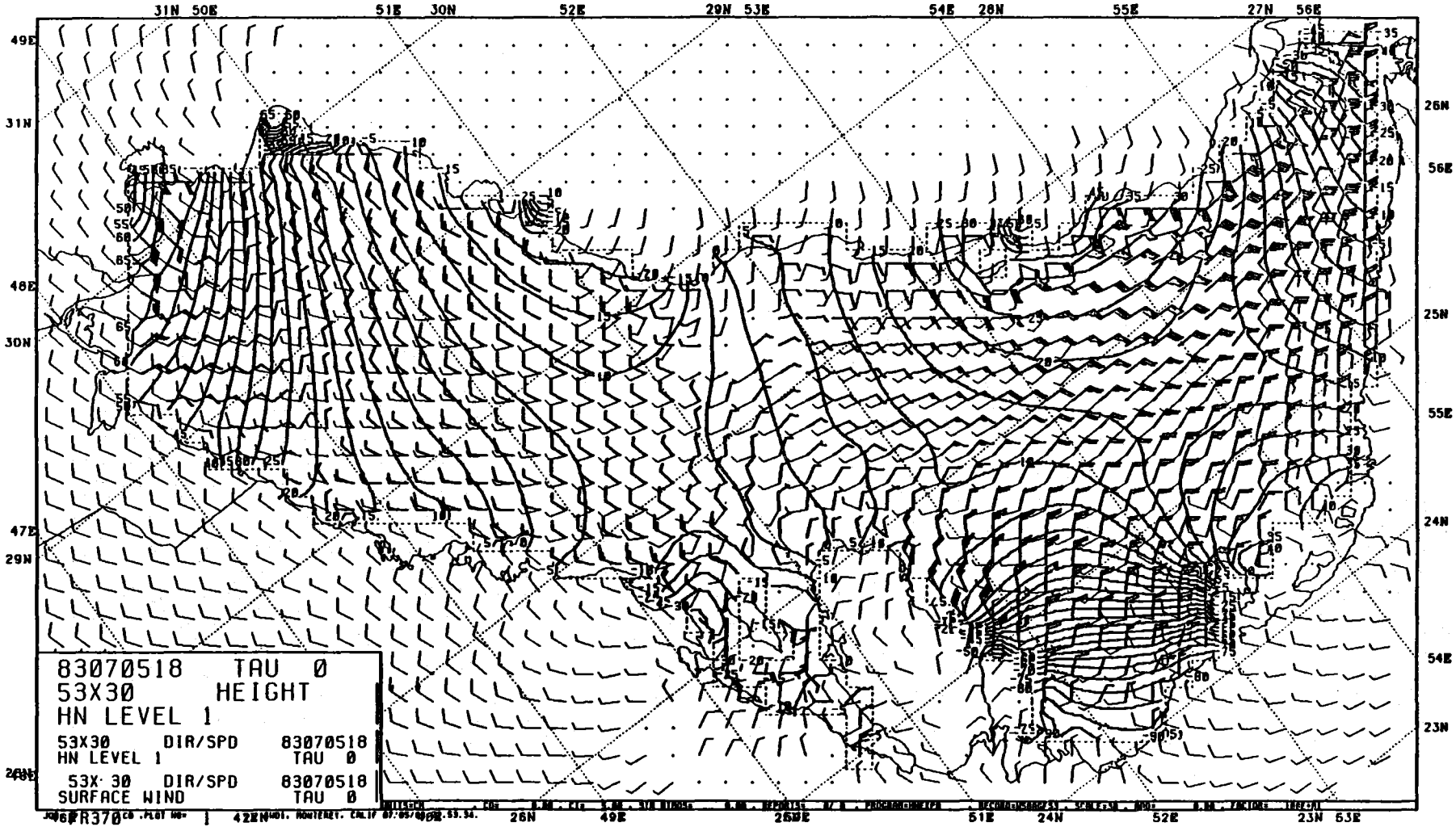

Figure 4: Inner Gulf hydrodynamic model output.

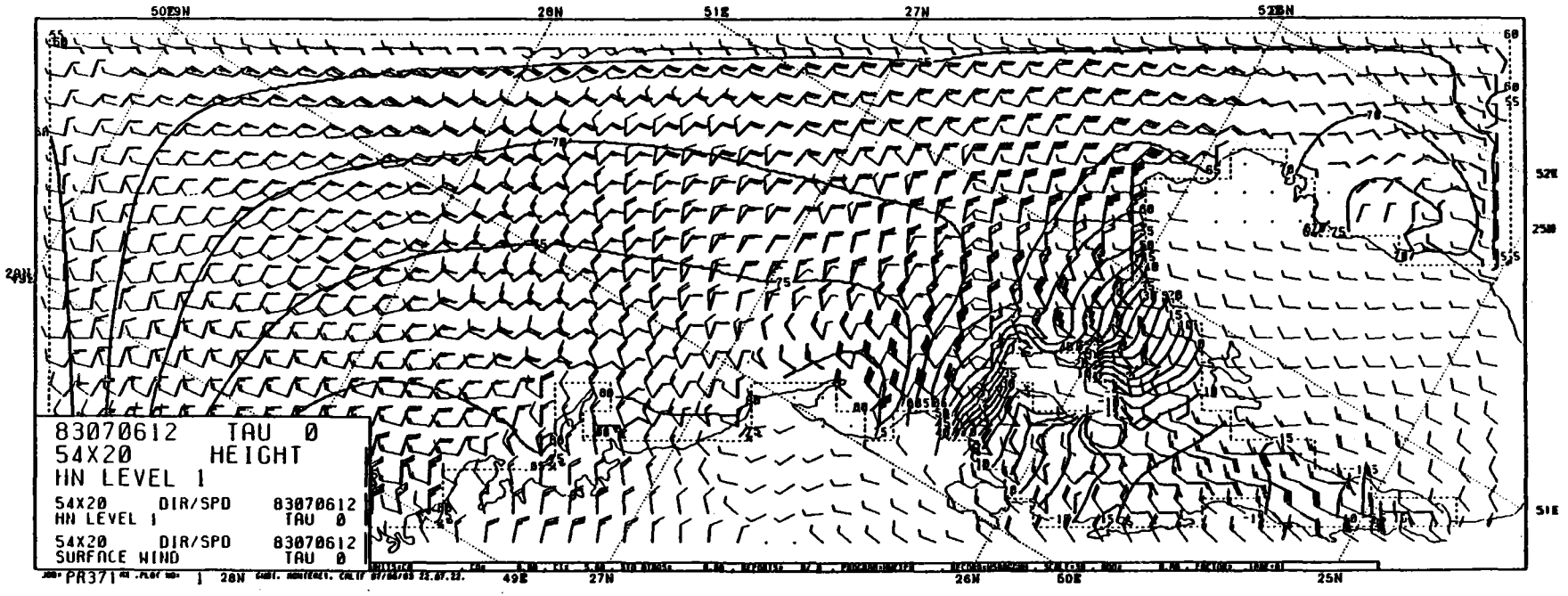

Figure 5: Western Inner Gulf region hydrodynamic model output.

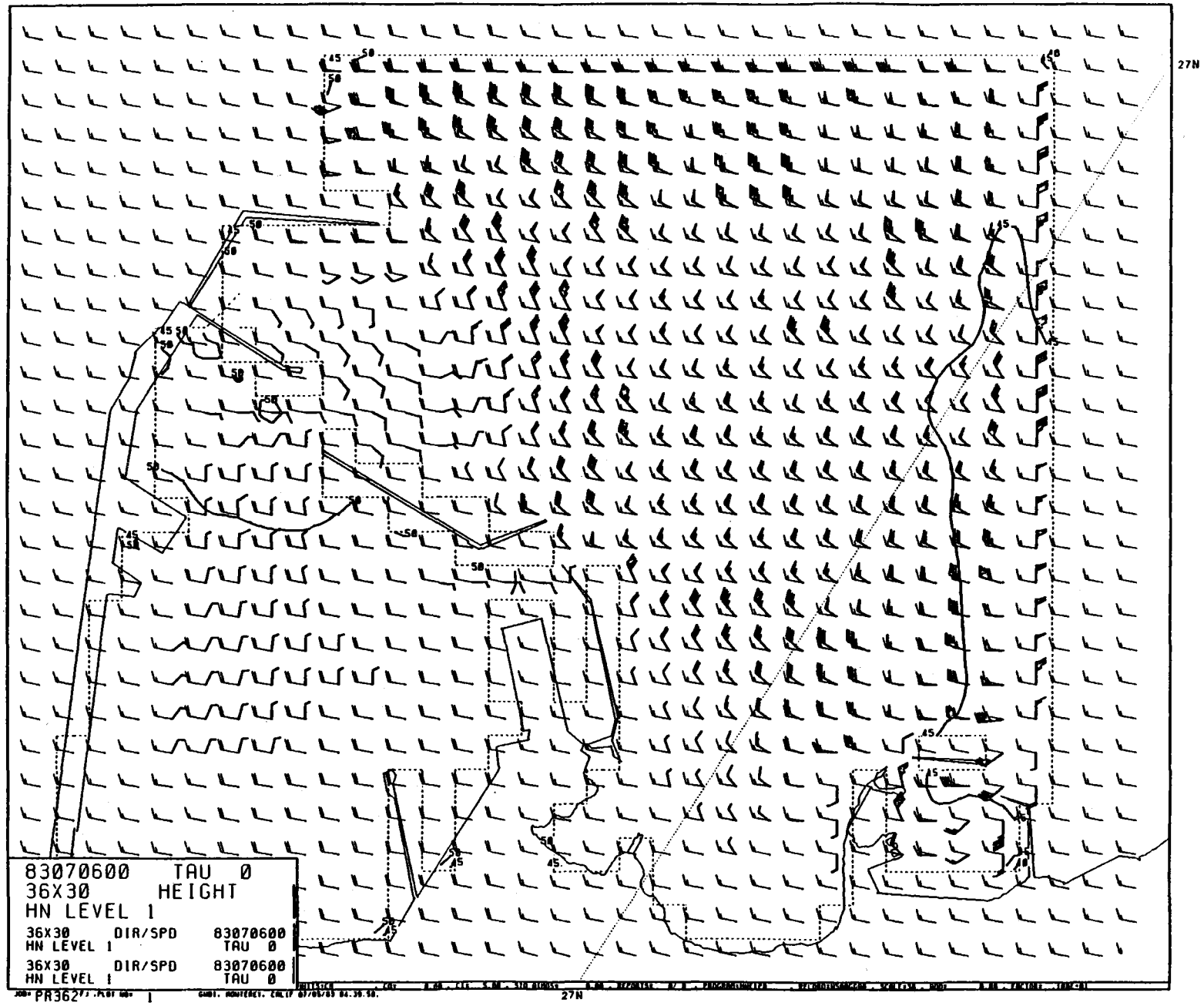

Figure 6: A typical circulation pattern by the model for Jubayi harbour.

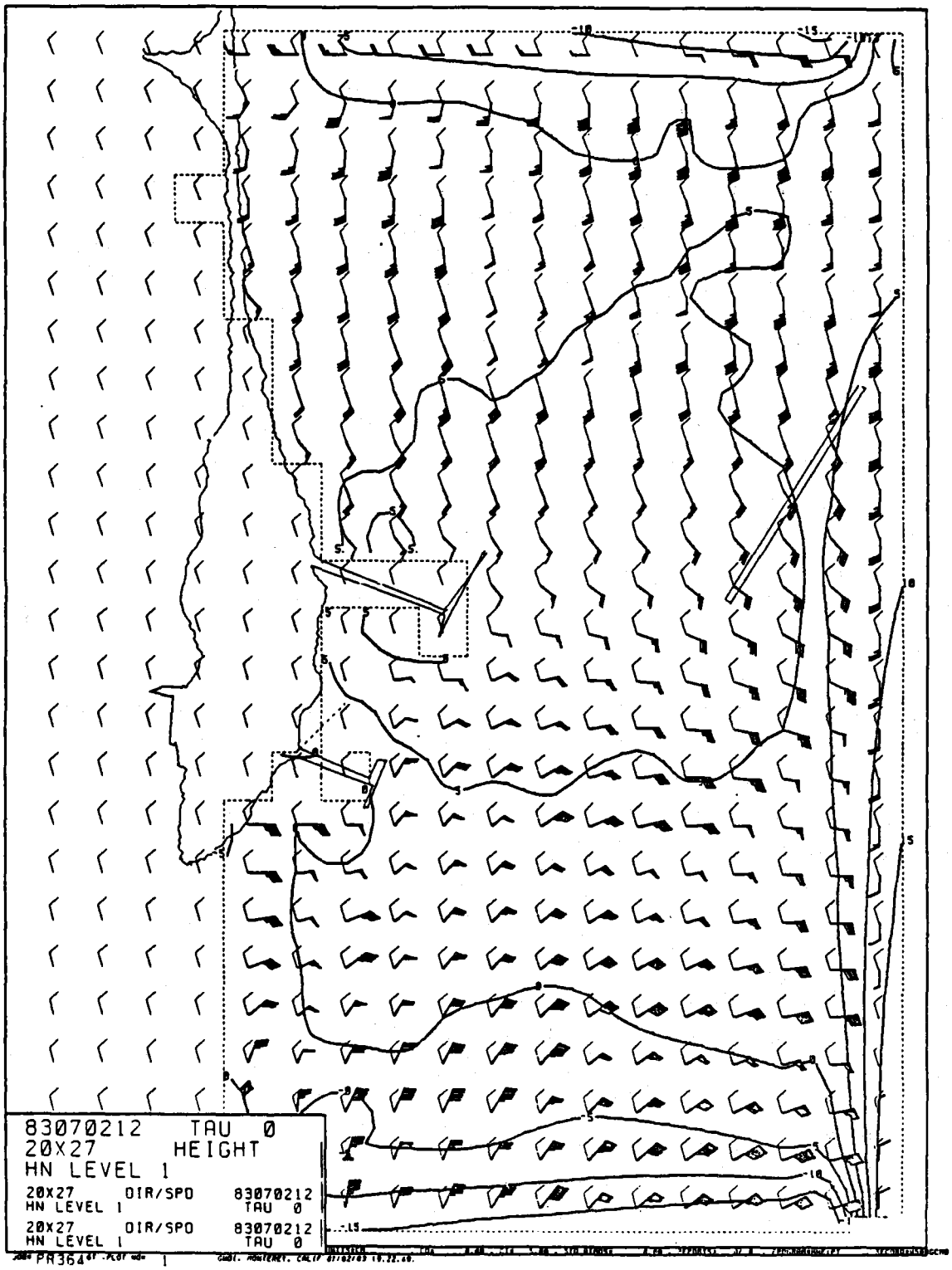

Figure 7: Nearshore circulation about Ras Tannurah.

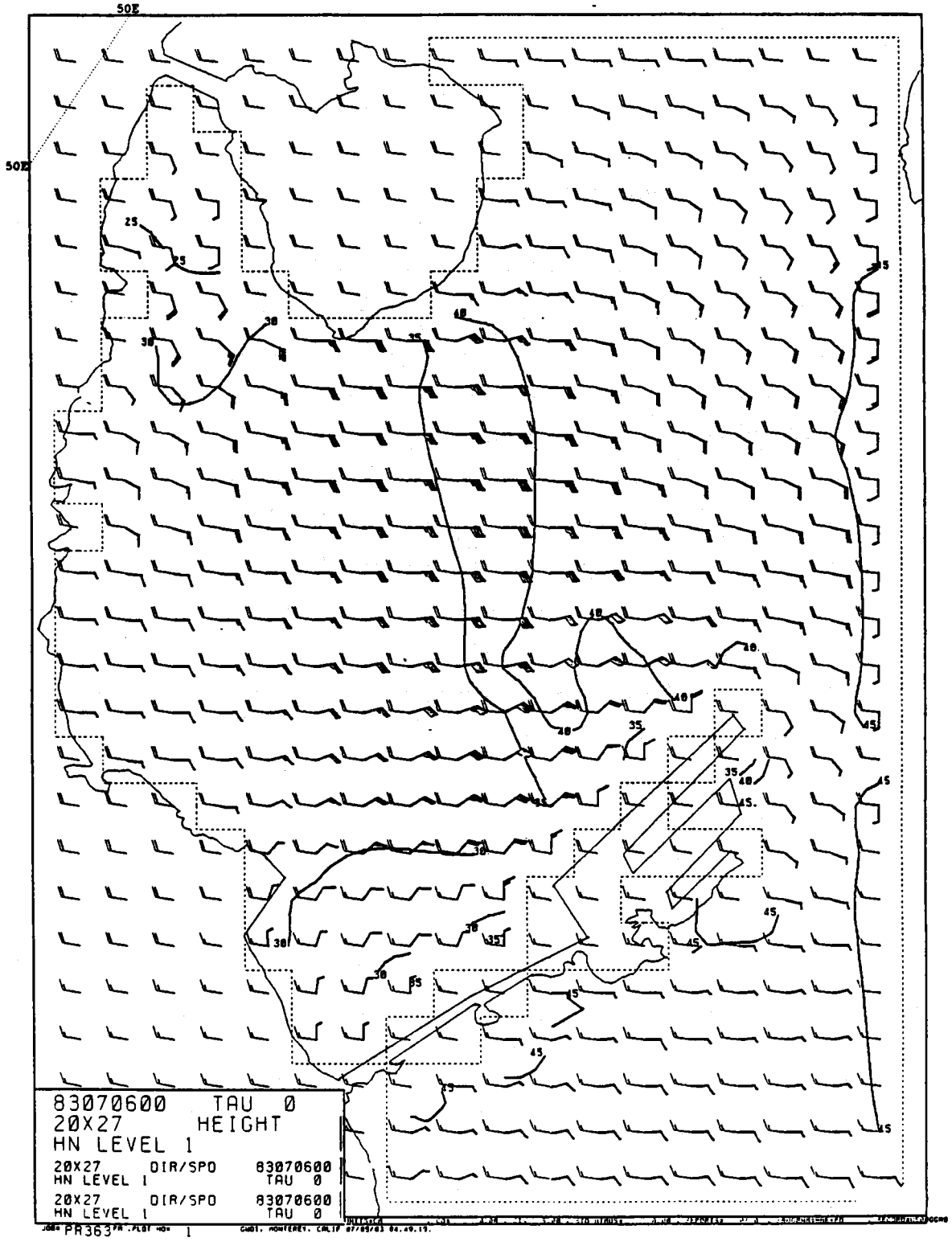

Figure 8: Ad Dammam model circulation.

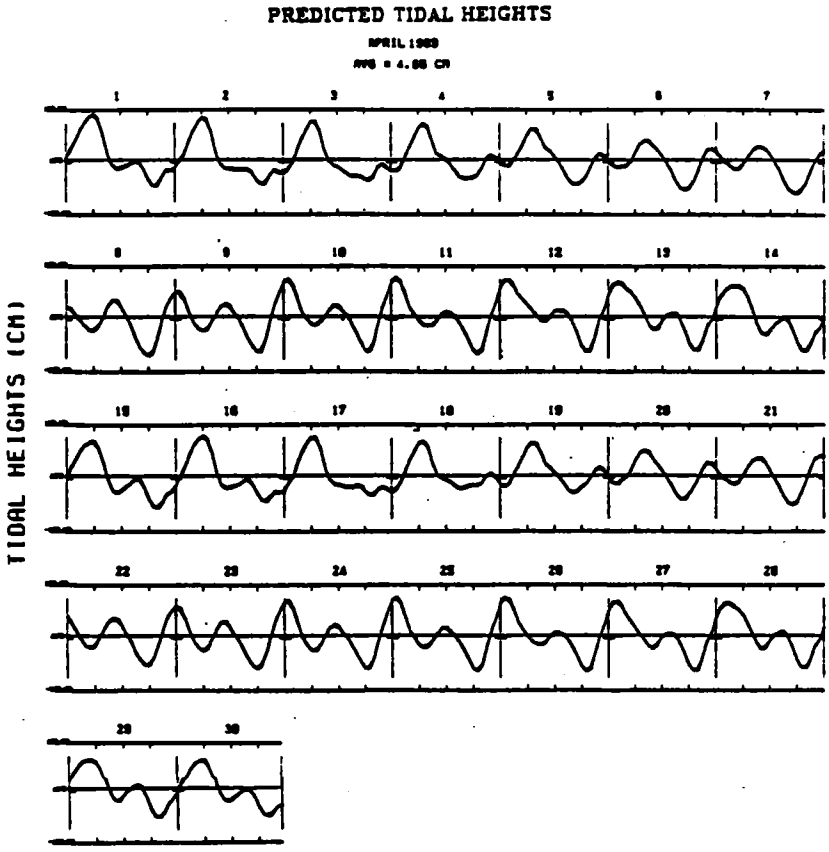

Figure 9: Time history of surface height near Ad Dammam during the month of April.

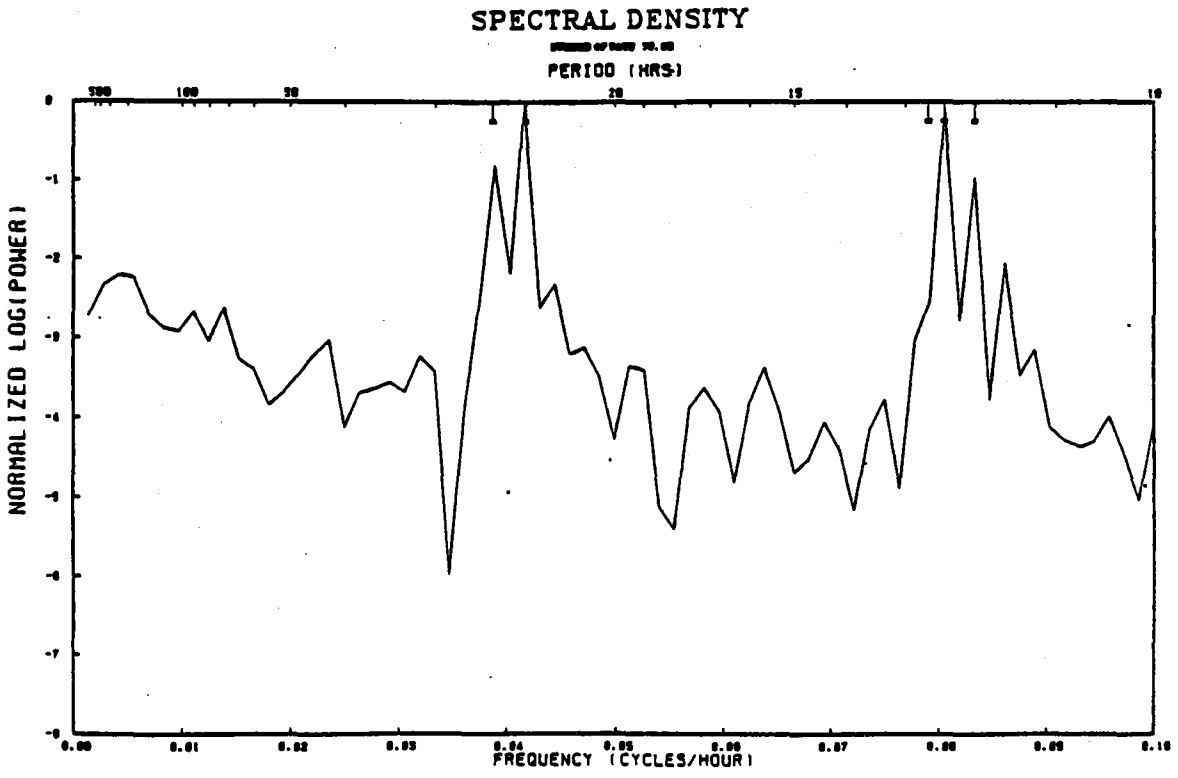

Figure 10: Power spectrum of the record shown in Figure 9. Note the contributions from the different major tidal constituents.

THE MODELLING OF TIDAL FLOWS IN ESTUARIES

by

Vernon H. Carr
ARAMCO/SIAL, Saudi Arabia

ABSTRACT

A numerical model of the tidal structure in various channels is constructed and a reduction of the waveforms into fourier components is employed to determine the magnitude of the inherent non-linearity in the vertically integrated equations for depth-averaged motion at positions along the channel.

An illustration is given of the tidal structure for pure lunar semi-diurnal forcing and a combined lunar-solar forcing. In addition, non-linear interactions between lunar and solar tides are investigated.

The effect of an imposed constriction of the channel on tidal structure and mean elevation profiles is presented and from the latter net flow is deduced.

INTRODUCTION

Over the past years, numerical modelling of tidal structures in specific river estuaries has been employed using the vertically integrated equations for depth-averaged motion. In this study, the same non-linear governing equations, which are non-linear, are used and the resulting tidal profiles are illustrated with respect to variations in the channel width parameter. The depth profile is constant and of exponential form throughout, and is representative of typical river estuaries.

Initially, the forcing at the open sea extremity was the lunar semi-diurnal tide (M2) and the resulting non-linear behaviour was shown to be of greater importance in shallower waters at the head of the channel.

Later, a solar tide S1 was included in the model, with the same period as M2, but with a different amplitude and phase. The simple technique of summing the system response to each forcing term (M2 and S1) and comparing this with the system response to the combined lunar and solar forcing clearly depicts the non-linearity throughout the cycle.

Mean elevation along the channel was shown to vary with respect to the width parameter, with a general slope towards the seaward limit. A significant change in the mean elevation profile of the system is effected by constricting the channel and, consequently, altering the mean velocity.

In all cases, the reduction of the waveforms into fourier components is incorporated in the model and a comparison of the strength of the higher harmonics is noted at appropriate points.

A quantitative analysis of the terms used in the governing equations is also given in a later section.

THEORY

Rectangular axes are chosen such that the origin, O, is at the open sea end of the estuary, positioned at the equilibrium level, the axis Ox is directed inland and the axis Oz is directed vertically upward. The displaced level of the free surface is given by z = (x,t) and the floor of the channel corresponds to z = -h(x). The breadth is given by b(x) as illustrated in the diagrams below:

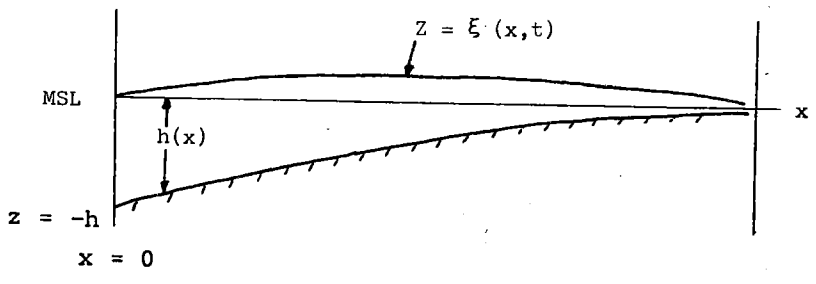

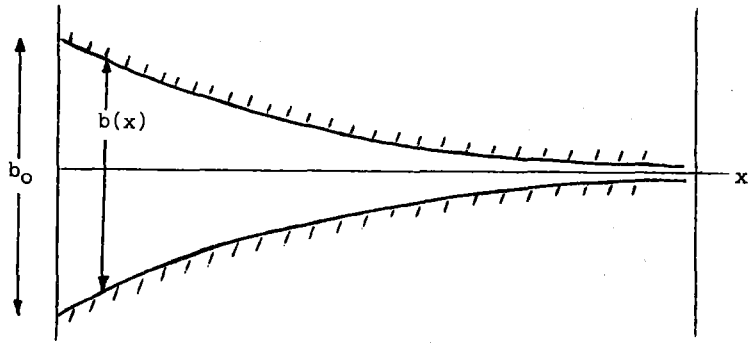

The horizontal and vertical components of velocity satisfy

$$\frac{\delta u}{\delta t} + \frac{u\delta u}{\delta x} + \frac{w\delta u}{\delta z} = -g\frac{\delta \xi}{\delta x} + \frac{1\delta \tau}{\rho \delta z} \quad . \; . \; . \; . \; A$$

where τ is the horizontal Reynolds stress, ρ the density of water and the pressure is hydrostatic. The equation of continuity may be written as

$$\frac{\delta \xi}{\delta t} + \frac{1}{b(x)}\frac{\delta}{\delta x}\left[b(x)\int_{-h}^{\xi} u dz\right] = 0 \; . \; . \; . \; B$$

Now, the depth averaged velocity $\bar{u}$ is defined as

$$\bar{u} = \frac{1}{\xi + h}\int_{-h}^{\xi} u dz$$

Integrating equations (A) and (B) vertically gives

$$\frac{\delta \bar{u}}{\delta t} + \frac{\bar{u}\delta \bar{u}}{\delta x} + \frac{1}{(\xi+h)}\frac{\delta}{\delta x}\left[(\xi+h)\;(u^2 - \bar{u}^2)\right] +$$

$$\frac{b'}{b}\;(\bar{u}^2 - \bar{u}^2) = -g\frac{\delta \xi}{\delta x} + \frac{1}{\rho(\xi+h)}\;(\tau_s - \tau_o)$$

where τ_s and τ_o are the surface and bottom stresses respectively. Ignoring any vertical structure in the flow, we assume that

$$\bar{u}^2 - \bar{u}^2 = 0$$

and that there is no surface wind stress ($\tau_s = 0$).

For pure tidal flow, the bottom stress is represented by

$$\tau_o = C_f \rho \bar{u}|\bar{u}|$$

where C_f is an empirically determined friction coefficient.

The equations then reduce to

$$\frac{\delta\bar{u}}{\delta t} + \frac{\bar{u}\delta\bar{u}}{\delta x} = -g\frac{\delta\xi}{\delta x} - C_f \frac{\bar{u}|\bar{u}|}{\xi+h} \quad \ldots\ldots 1$$

$$\frac{\delta\xi}{\delta t} + \frac{1}{b(x)}\frac{\delta}{\delta x}\left[b(x)\ (\xi+h)\ \bar{u}\right] = 0 \quad \ldots 2$$

At the seaward end of the channel, the surface elevation is determined by the open sea tide

$$\xi = \xi_o(t) \qquad \text{at } x = 0$$

At the landward extremity, the velocity is described in terms of the fresh water flow

$$u = -u_f \qquad \text{at } x = L$$

$\xi_o(t)$ has the form $\xi_o(t) = \Sigma_k A_k \sin\left(\frac{2\pi t}{T_k} + \phi_k\right)$

therefore the kth tidal component has amplitude A_k, period T_k and phase ϕ_k.

Finite difference scheme

The horizontal distance is defined by $x = x_i = i\Delta x$, where $i = 1,2,3....m$ and $\Delta x = \frac{L}{m}$

The time t is incremented $t = n\Delta t$ where $n = 1,2,3....$

Define a staggered grid as follows:

ξ	u	ξ	u		u	ξ	u
i = 1	i = 2	i = 3	i = 4		i = m-2	i = m-1	i = m

Elevations are computed at grid points $i = 3,5,7....m-1$. (At $i = 1$, the elevation is described by $\xi = \xi_o(t)$).

Currents are computed at grid points $i = 2,4,6....m-2$. (At $i = m$, the current is the fresh water flow $u = -u_f$)

Later, in the updating process ξ and u are both computed at all grid points $i = 1,2,3....m$. Note that u is now the depth- averaged velocity.

Finite difference equations

Notation: for any variable f(x,t) write $f(x_i,t_n) = f_i^n$ where f_i^n is the value of f at grid points i, time level n. Write equation (2) as

$$\frac{\xi_i^{n+1} - \xi_i^n}{\Delta t} = \frac{-1}{b_i}\left[\frac{\{u_{i+1}^n b_{i+1}(\xi_{i+1}+h_{i+1})\} - \{u_{i-1}^n b_{i-1}(\xi_{i-1}+h_{i-1})\}}{2\Delta x}\right]$$

$$\Leftrightarrow \xi_i^{n+1} = \xi_i^n - \frac{1}{b_i}\frac{\Delta t}{2\Delta x}\left[\{\cdots\cdot\}\right]$$

where $\{\cdots\}$ is $\overset{n}{\{ui+1bi+1(\xi i+1^{+}hi+1)\}} - \overset{n}{\{ui-1bi-1(\xi i-1^{+}hi-1)\}}$

(computed for i = 3,5,7....m-1).

Although this is only applied at i = 3,5,7....m-1, the terms in the square bracket require the elevation to be known at grid points 2,4,6....m. These are found from

$$\xi \overset{n}{}_{i} = \frac{1}{2} (\xi^{n}_{i+1} + \xi^{n}_{i-1}) \text{ for } i = 2,4,6....m-2$$

and $$\xi \overset{n}{}_{m} = \frac{1}{2} (3\xi^{n}_{m-1} - \xi^{n}_{m-3})$$

Thus, since ξ^{n+1}_{1} is specified, as equal to $\xi_{o}\{(n+1)\Delta t\}$ a complete updating of may be effected. Write equation (1) as

$$\frac{ui^{n+1} - ui^{n}}{\Delta t} + \frac{1}{2}\left[\frac{(u^2)^{n}_{i-1} - (u^2)^{h}_{i-1}}{2\Delta x}\right] = -g\left(\frac{\xi^{n+1}_{i+1} - \xi^{n-1}_{i-1}}{2\Delta x}\right) - \frac{C_f \left| ui^{n} \right| ui^{n+1}}{\xi^{n+1}_{i} + hi}$$

$$\Leftrightarrow \left\{1 + \frac{C_f \left| ui^{n} \right| \Delta t}{\xi^{n+1}_{i} + hi}\right\} ui^{n+1} = ui^{n} - \frac{\Delta t}{4\Delta x}\left[(u^2)^{n}_{i+1} - (u^2)^{n}_{i-1}\right] - g\frac{\Delta t}{2\Delta x}(\xi^{n+1}_{i+1} - \xi^{n+1}_{i-1})$$

(computed for i = 2,4,6....m-2)

Now, the updated values of the elevation have already been computed but to calculate the terms in the square bracket values of the velocity at grid points i = 3,5,7...m-1 are required. These are found from the equations

$$u^{n}_{i} = \frac{1}{2} (3 \overset{n}{}_{u2} - \overset{n}{}_{u4})$$

and

$$u^{n}_{i} = \frac{1}{2} (\overset{n}{}_{ui+1} + \overset{n}{}_{ui-1})$$

As u^{n}_{m} is constant and equal to the fresh water flow, $-u_f$, a complete updating of the velocity can now be effected. The entire process can be repeated as necessary.

The adopted procedure is to start the integration at t = 0 when the elevation and velocity are zero everywhere, except at the landward extremity (x = L); time (t) is then incremented repeatedly by a small amount Δ t. A suitable value of Δ t is chosen to ensure stability and the updating continued until any transient system reponse has decayed.

The numerical solution now has an oscillatory form which can be subsequently analyzed using Fourier analysis (see Appendix I).

NUMERICAL EXPERIMENTS

In the experiments, the length L of the estuary was 100 km. Values of the elevation and depth-averaged velocity were computed at 18 grid points with a grid

spacing of 5.55 km. The width parameter b(x) at x = 0 was chosen as 10 km (except for experiment 1). The variables h(x) and b(x) were taken to be of the form

$$h = h_o \exp - \alpha x \quad \text{and} \quad b = b_o \exp - \beta x$$

In experiments 2 to 8, the depth variation was from 10 m at x = 0(h_o) to 3 m at x = L, the corresponding being equal to 1.204×10^{-5} m^{-1}. The width coefficient was varied from 2.302×10^{-5} m^{-1} to 6.0×10^{-5} m^{-1} (corresponding to river widths of 1 km and 25 m, respectively). The fresh water flow $-u_f$ was taken as 20 cm/sec throughout the numerical experiments.

The elevation was initially zero everywhere and a lunar semi-diurnal tide (M2) of amplitude 2.6 m and period 12.4 hours forced at grid point one. Constant oscillatory response was obtained after several cycles of integration and the analysis of each system response was carried out during the tenth tidal cycle. There were one hundred time steps per cycle.

All width profiles are illustrated and a summary of results is given in table 1. Only the first and second harmonics are listed, since these are the dominant terms, and in all cases significant generation of the second harmonic and reduction of the first harmonic in progressively shallower waters is noted.

Further characteristics are noted from table 1 together with elevation profiles of experiments 2, 3 and 8.

(a) The hydraulic gradient is more pronounced for wider river estuaries, implying greater net outflow important in sediment or pollutant transportation.

(b) The tidal waveforms are initially amplified and the peak retarded for narrow estuaries.

(c) For wider estuaries the forcing waveform is rapidly damped and the higher phase angles of the first harmonic indicate that the tidal peak travels more slowly.

(d) $\frac{\delta \xi}{\delta t}$ during the flood tide is significantly greater than during the eff flow.

(e) Tidal range decreases in shallower waters (this is more pronounced in wider estuaries).

(f) Typical wave speeds vary from approximately 13 m/s in experiment 2 to approximately 8 m/s in experiment 3.

Significant changes in the system response were effected by constricting the channel. In experiments 7 and 8, constrictions introduced were 60% at grid point 7 and 10% at grid point 8 respectively, relative to seaward estuary width.

The following characteristics were observed:

(a) Mean elevation profiles were significantly different from those obtained using the exponential width parameters. A steady mean elevation resulted after the constrictions of higher magnitude for narrow estuaries (48 cm and 62 cm for experiments 7 and 8, respectively).

(b) The corresponding hydraulic gradient was small after the constrictions resulting in a reduction of the net flow, illustrated by the graphs of mean velocity and mean elevation for the two types of estuary. Hence, the numerical model predicts little sediment or suspension transport in the "Bulge" of the estuary.

The first six harmonics for the three types of channel, narrow, exponential, wide exponential and constricted, are given in table 2.

QUANTITATIVE ANALYSIS

Analysis of the terms in equation (1) shows that the updated velocity field is dependent on the balance of the two terms on the right hand side

$-g\frac{\delta \xi}{\delta x}$ varying from 6.3×10^{-4} ms^{-2} at $\frac{T_p}{4}$ to -2.3×10^{-4} ms^{-2} at $\frac{3T_p}{4}$.

The Reynolds stress term $\frac{-c_f \bar{u}|\bar{u}|}{\xi + h}$ varies from -5.3×10^{-4} ms^{-2} at $\frac{T_p}{4}$ to 2.0×10^{-4} ms^{-2} at $\frac{3T_p}{4}$ and $\bar{u}\frac{\delta \bar{u}}{\delta x}$, which is an order of magnitude smaller, and varies from -3.09×10^{-5} ms^{-2} at $\frac{T_p}{4}$ to -6.3×10^{-6} ms^{-2} at $\frac{3T_p}{4}$.

These are typical values during flood ($\frac{T_p}{4}$) and ebb ($\frac{3T_p}{4}$) tide in shallow water (grid point 16) for experiment 2. The numerical model, therefore, predicts larger time variation of the tidal current and related elevation during the flood tide, approximately 1.3×10^{-4} ms^{-2} and $\frac{\delta \bar{\xi}}{\delta t}$ 3.11×10^{-4} ms^{-1}. (See tidal profiles, grid point 16).

In deeper water the elevation profiles are dominated by the imposed tidal forcing and generated fluctuating velocity fields.

In addition, the updated velocity values are critically dependent on the empirically determined friction coefficient C_f which in this study is taken to be 4.6×10^{-3}, corresponding to a roughness length of z_o = 5 mm (Johns, 1978). An order magnitude less in C_f results in large values of $\frac{\delta \bar{u}}{\delta t}$ and the system becomes unstable too high. An order of magnitude results in the system being overdamped and the stress term in equation (1) dominating. This would imply $\frac{\delta \bar{u}}{\delta t}$ remaining effectively constant. Thus, the velocity structure becomes small, which in turn alters the elevation profile.

Illustration of the non-linear interaction between lunar and solar forcing

In the initial experiments, the forcing was of the form

$$\xi_1 = A \sin \frac{2\pi t}{T_p}$$

where A is the amplitude of the lunar semi-diurnal tide, taken as 2.6 m. The response of the system was then computed for forcing of the form

$$\xi_1 = A \sin \frac{2\pi t}{T_p} + A_s \sin \frac{2\pi t}{T_p} + \phi$$

where A_s is the amplitude of the solar tide taken as 46.6% of A, and ϕ is the phase angle of the solar tide relative to the lunar. The period of the solar tide was taken to be the same as that of the lunar one in order to eliminate effects resulting from using a 12 hour solar cycle (spring and neap tides).

Three values of ϕ were implemented $\frac{\pi}{2}$, $\frac{3\pi}{2}$ and $\frac{\pi}{4}$, in experiments 2A, 2B and 2C respectively. The width and depth parameters were the same as in experiment 2.

The non-linear behaviour is illustrated in the following graphs representing experiments 2A, 2B and 2C. In all cases, this behaviour was most pronounced in shallow waters.

ACKNOWLEDGEMENT

I wish to thank Dr. B. Johns of the Department of Meteorology, University of Reading, England for his guidance throughout this study.

REFERENCES

Johns, B. (1978) The modelling of tidal flow in a channel using turbulence energy closure scheme, Journal of Physical Oeanography, Vol. 8, pp. 1042-1049.

Defant (1961) Physical Oceanography, Vol 2. Macmillan & Pergamon Press, New York.

APPENDIX I

Fourier Analysis

The complex fourier series of an integrable function f(x) defined in the interval 0 to 2L is

$$f(x) \approx \sum_{n=-\infty}^{n=+\infty} A_n \exp\left(\frac{in\pi}{L}\right)$$

in which the complex fourier coefficients A are given by

$$A_n = \frac{1}{2L} \int_o^{2L} f(x)\exp\left(\frac{-in\pi x}{L}\right) dx \quad \text{for } n = 0,\pm1,\pm2..$$

In this case, the integrable function is the elevation (x,t) expressed as

$$\xi(x,t) = \bar{\xi}(x) + \sum_{s=1}^{\infty} \left[A_s \cos\frac{2\pi st}{T_p} + B_s \sin\frac{2\pi st}{Tp} \right] \ldots 3$$

The first term on the right hand side of equation (3) is the mean elevation and the second term denotes the additional harmonics. A_S and B_S are given by

$$A_s = \frac{2}{T_p} \int_o^{T_p} \xi\cos\frac{2\pi st}{T_p}\, dt \quad \text{and} \quad B_s = \frac{2}{T_p} \int_o^{T_p} \xi\sin\frac{2\pi st}{T_p}\, dt$$

therefore, in complex form,

$$A_s + iB_s = \frac{2}{T_p} \int_o^{T_p} \xi n \exp\frac{i2\pi st}{T_p}\, dt$$

where $t = n\triangle t$ and T signify the tidal period.

This integral is computed using the trapezoidal technique during the final tidal cycle. The amplitude of each harmonic is calculated from

$$A_s' = (A_s^2 + B_s^2)^{\frac{1}{2}}$$

with the phase angle ϕ_S' being given by $\phi_s' = \tan^{-1}\frac{B_s}{A_s}$

Hence, the elevation has been reduced to

$$\xi(x,t) = \bar{\xi}(x) + \sum_{s=1}^{\infty} A_s' \sin\left(\frac{2\Pi st}{T_p} + \phi_s'\right)$$

In this study, the first six harmonics were computed and tabulated at each grid point.

Table 1

Experiment No.		1	2	3	4
Depth (metres)		10 to 5	10 to 3	10 to 3	10 to 3
Width (km)		30 → 0.5	7.45→0.05	8.8 → 1.0	7.2→0.025
Amplitude /Phase	#4	2.56/-0.23	2.62/-0.19	2.30/-0.32	2.65/-0.16
of the first	#10	2.35/-0.82	2.25/-0.80	1.52/-1.15	2.39/-0.73
harmonic at	#16	2.30/-1.44	1.78/-1.71	1.23/-2.16	1.89/-1.60
grid points					
4,10,16.(m)/(rad)					
Amplitude /Phase	#4	0.13/-0.74	0.13/-0.68	0.17/-1.10	0.13/-0.63
of the second	#10	0.33/-2.11	0.46/-2.12	0.33/-2.60	0.52/-1.94
harmonic at	#16	0.77/ 2.73	0.70/ 2.20	0.36/ 1.50	0.75/ 2.42
grid points					
4,10,16.(m)/(rad)					

Experiment No.		5	6	7	8
Depth (metres)		10 to 3	10 to 3	10 to 3	10 to 3
Width (km)		8.5 → 0.15	8.0 → 0.18	-	-
Amplitude /Phase	#4	2.40/-0.29	2.52/-0.22	2.07/-0.33	2.57/-0.13
of the first	#10	1.72/-1.08	1.99/-0.96	1.13/-1.46	0.70/-1.30
harmonic at	#16	1.38/-2.06	1.59/-1.92	1.23/-2.07	0.77/-1.84
grid points					
4,10,16.(m)/rad)					
Amplitude /Phase	#4	0.16/-1.02	0.15/-0.90	0.20/-1.12	0.14/-0.34
of the second	#10	0.37/-2.51	0.43/-2.34	0.16/-2.96	0.09/-2.16
harmonic at	#16	0.43/ 1.63	0.54/ 1.86	0.35/ 1.67	0.17/ 2.35
grid points					
4,10,16.(m)/(rad)					

Experiment No.	1	2	3	4	5	6	7	8
Mean elevation #4	5	3	15	1	11	7	21	5
at grid points #10	17	16	48	10	40	29	48	62
4,10,16.(cm) #16	25	31	74	22	64	49	47	63

Table 2: Amplitude and phases of elevation for experiments 2, 3, and 8

Experiment 2					
	Grid point 4		Grid point 10		Grid point 16	
S	ξ (m)	ϕ_s (rad)	ξ (m)	ϕ_s (rad)	ξ (m)	ϕ_s (rad)
1	2.62	-0.185	2.25	-0.796	1.78	-1.714
2.	0.133	-0.683	0.46	-2.118	0.699	2.198
3.	0.043	2.342	0.111	1.932	0.261	-0.239
4	0.021	2.45	0.078	0.163	0.116	1.879
5	0.006	-2.02	0.02	1.233	0.078	0.420
6	0.003	-0.653	0.048	0.913	0.021	2.852
Experiment 3					
	Grid point 4		Grid point 10		Grid point 16	
S	ξ (m)	ϕ_s (rad)	ξ (m)	ϕ_s (rad)	ξ (m)	ϕ_s (rad)
1	2.30	-0.319	1.52	-1.151	1.23	-2.156
2	0.166	-1.101	0.328	-2.6	0.358	1.501
3	0.056	1.405	0.042	0.331	0.084	-1.706
4	0.026	1.236	0.072	-2.102	0.055	0.815
5	0.017	2.507	0.007	2.586	0.029	-2.152
6	0.012	2.329	0.020	-2.365	0.009	0.183
Experiment 8					
	Grid point 4		Grid point 10		Grid point 16	
S	ξ (m)	ϕ_s (rad)	ξ (m)	ϕ_s (rad)	ξ (m)	ϕ_s (rad)
1	2.57	-0.131	0.695	-1.3	0.769	-1.893
2	0.142	-0.337	0.085	-2.162	0.169	2.350
3	0.047	1.923	0.013	-1.444	0.144	2.824
4	0.011	2.501	0.028	-1.728	0.051	1.091
5	0.014	-2.095	0.01	-1.812	0.012	-0.772
6	0.015	-1.944	0.012	-2.830	0.013	-1.838

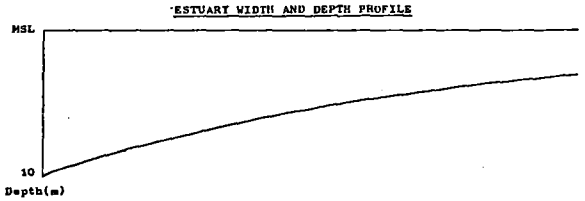
ESTUARY WIDTH AND DEPTH PROFILE
MSL
10
Depth(m)

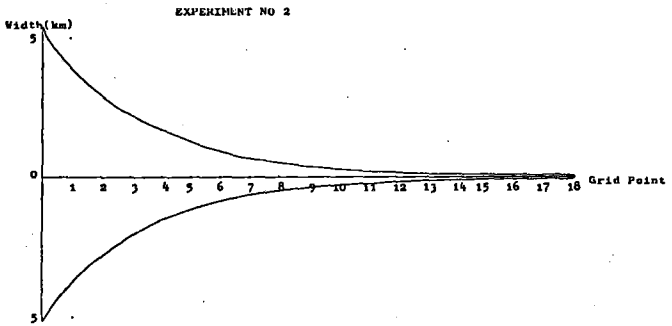
EXPERIMENT NO 2
Width(km)
5
0
5
1 2 3 4 5 6 7 8 9 10 11 12 13 14 15 16 17 18
Grid Point

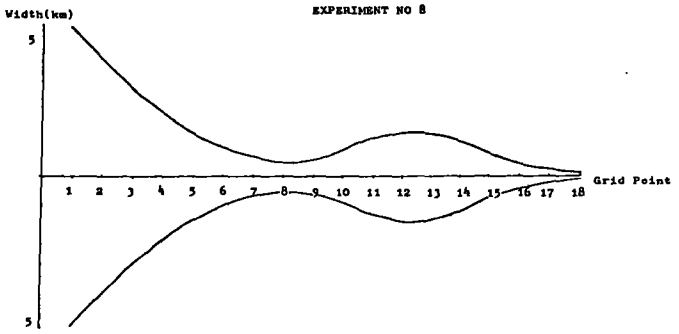
EXPERIMENT NO 8
Width(km)
5
5
1 2 3 4 5 6 7 8 9 10 11 12 13 14 15 16 17 18
Grid Point

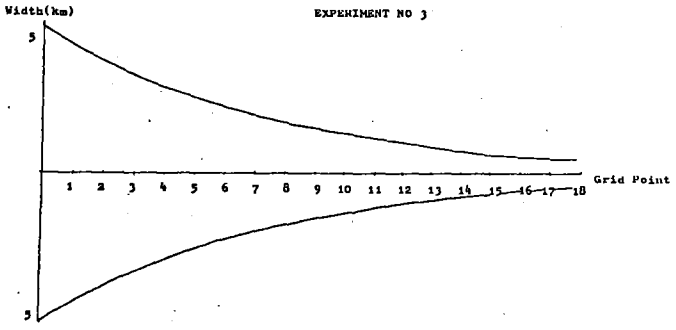
EXPERIMENT NO 3
Width(km)
5
5
1 2 3 4 5 6 7 8 9 10 11 12 13 14 15 16 17 18
Grid Point

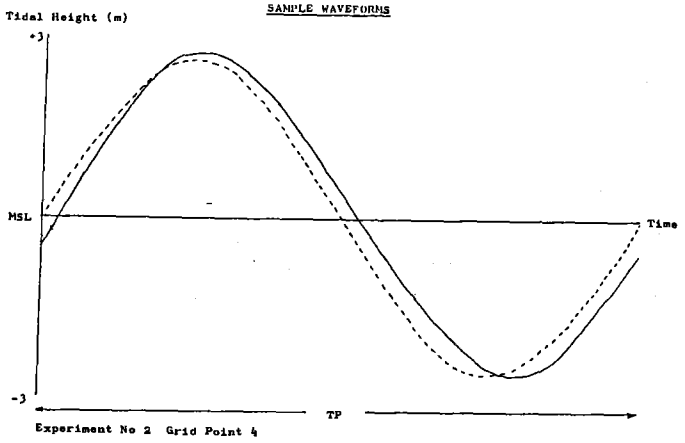
SAMPLE WAVEFORMS
Tidal Height (m)
+3
MSL
-3
Time
TP
Experiment No 2 Grid Point 4

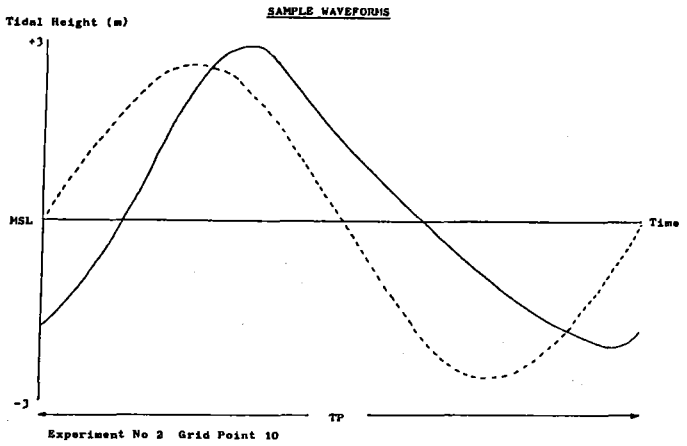

Experiment No 2 Grid Point 10

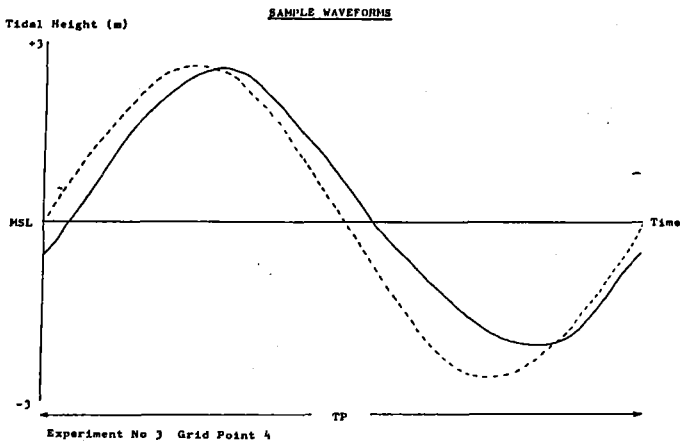

Experiment No 3 Grid Point 4

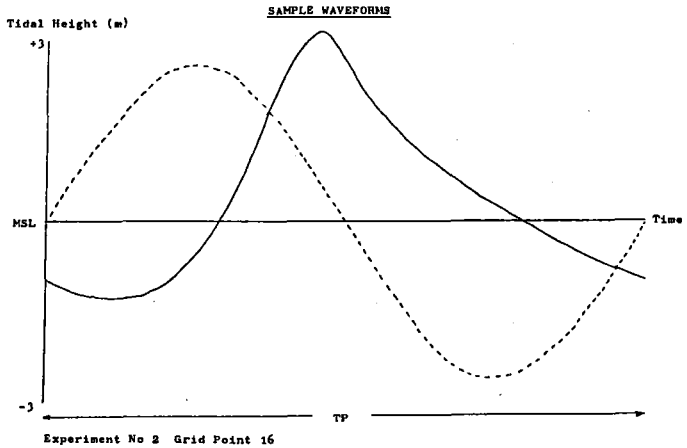

Experiment No 2 Grid Point 16

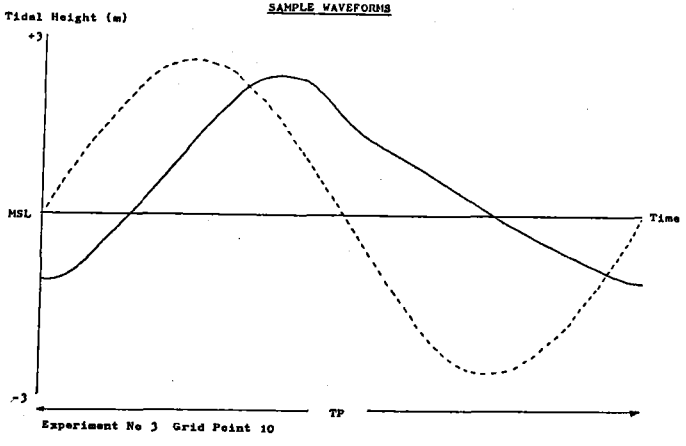

Experiment No 3 Grid Point 10

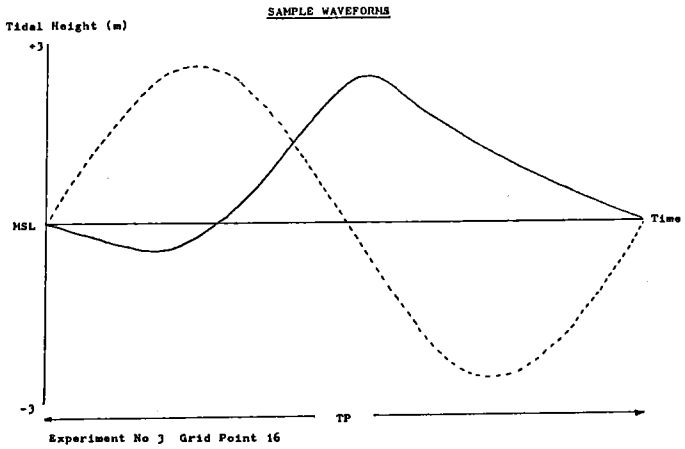

Experiment No 3 Grid Point 16

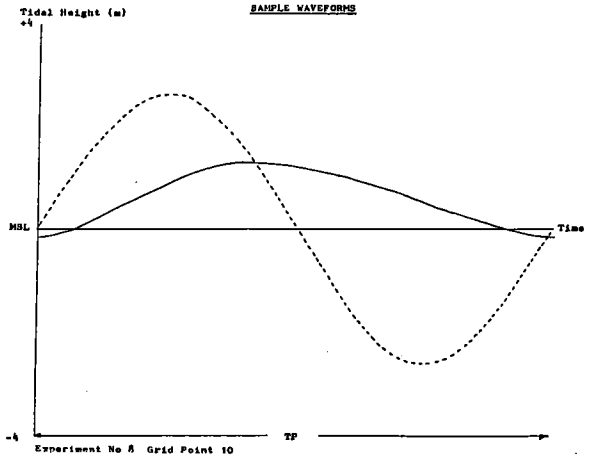

Experiment No 8 Grid Point 10

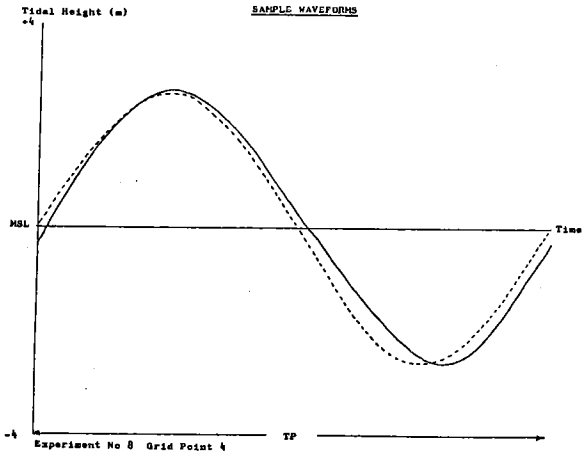

Experiment No 8 Grid Point 4

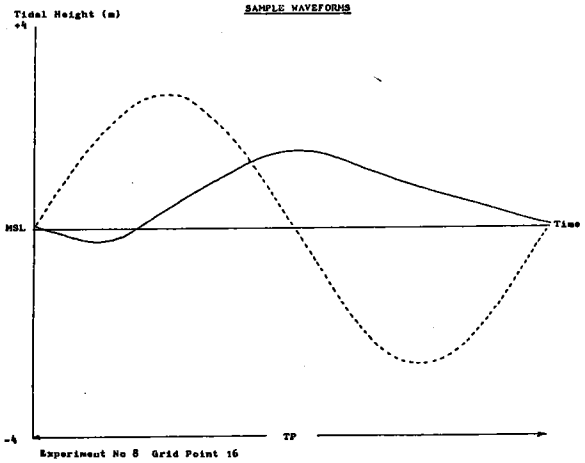

Experiment No 8 Grid Point 16

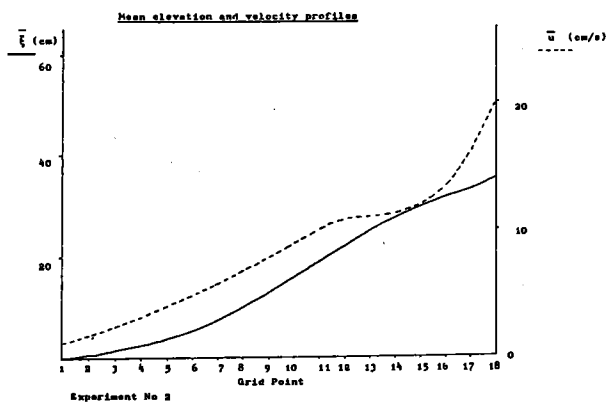
Mean elevation and velocity profiles
$\bar{\xi}$ (cm)
$\bar{u}$ (cm/s)
60
40
20
20
10
0
1 2 3 4 5 6 7 8 9 10 11 12 13 14 15 16 17 18
Grid Point
Experiment No 2

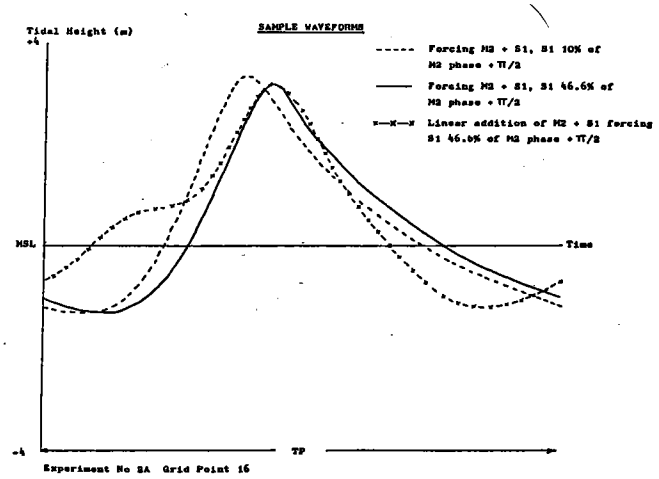
SAMPLE WAVEFORMS
Tidal Height (m)
+4
-4
MSL
Time
TP
Forcing M2 + S1, S1 10% of M2 phase + π/2
Forcing M2 + S1, S1 46.6% of M2 phase + π/2
Linear addition of M2 + S1 forcing S1 46.6% of M2 phase + π/2
Experiment No 2A Grid Point 16

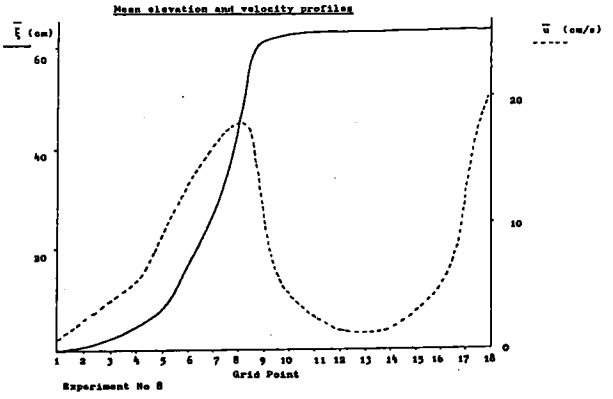
Mean elevation and velocity profiles
$\bar{\xi}$ (cm)
$\bar{u}$ (cm/s)
60
40
20
20
10
0
1 2 3 4 5 6 7 8 9 10 11 12 13 14 15 16 17 18
Grid Point
Experiment No 8

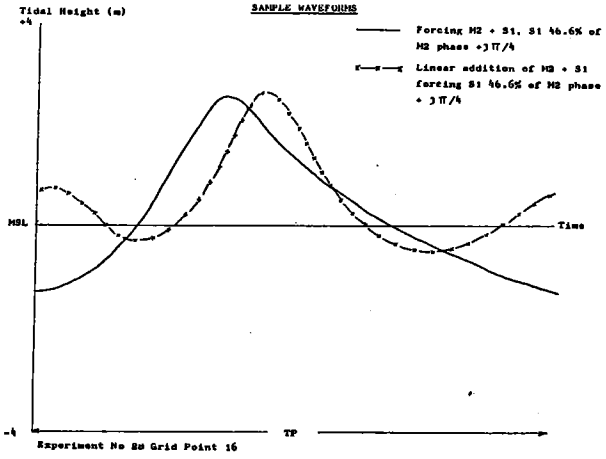
SAMPLE WAVEFORMS
Tidal Height (m)
+4
-4
MSL
Time
TP
Forcing M2 + S1, S1 46.6% of M2 phase +3π/4
Linear addition of M2 + S1 forcing S1 46.6% of M2 phase + 3π/4
Experiment No 8A Grid Point 16

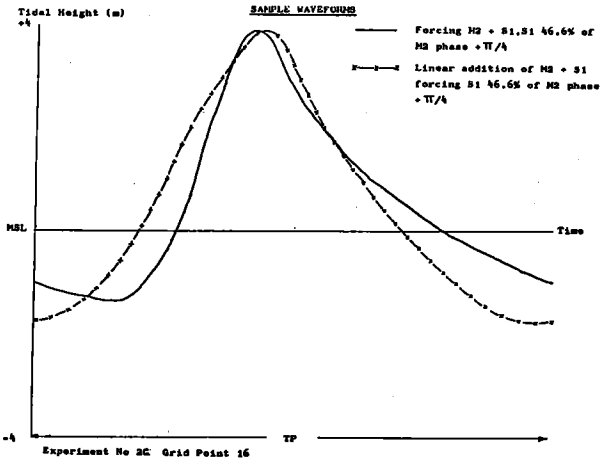
SAMPLE WAVEFORMS
Tidal Height (m)
+4
-4
MSL
Time
TP
Forcing M2 + S1,S1 46.6% of M2 phase + π/4
Linear addition of M2 + S1 forcing S1 46.6% of M2 phase + π/4
Experiment No 8C Grid Point 16

OIPASIPA - A POWERFUL TOOL FOR CONTINGENCY PLANNING

by

J. W. Dippner
Institut für Meeresforschung Bremerhaven

ABSTRACT

A new and powerful tool for quantitative oil spill contingency planning is presented in this paper. OIPASIPA (oil patch simulation package) is a deterministic numerical model for the simulation of the drift and fate of oil spills. It contains the important dynamical processes of slick formation, movement and weathering. The numerical framework is provided by a Lagrangian tracer technique. OIPASIPA includes drift by currents and wind is spreading and horizontal dispersion by turbulent diffusion and shear currents. Evaporation of different sorts of crude oil is calculated as a function of temperature and wind. Natural dispersion effects are simulated by an empirical relationship between wind speed and rate of natural dispersion. Comparisons with observation, e.g., the Bravo Ekofisk blow out, show excellent agreement.

The modular structure of OIPASIPA has a high flexibility and permits the convenient implementation of new developments as well as universal application to different kinds of oil spills. The model is designed to fit the requirements of users. It permits risk assessment and sensitivity analysis. OIPASIPA may also be run in an interactive mode. Hence, it is a powerful tool for quick decisions in clean-up strategy.

INTRODUCTION

Over the past decades, there has been marked growth in oil transport by sea, as well as increased offshore activities. Hence, there is a greater risk of marine pollution caused by tanker accidents, blow outs etc. Disastrous ecological and economic consequences can arise in the event of an accident. The problems and effects of oil pollution, the behaviour of crude oil in the sea and risk assessment have been important research fields. In addition, several numerical models have been developed to simulate the drift and extension of an oil spill. The oil drift model OIPASIPA presented in this paper was developed in cooperation between the Bremerhaven Institute of Marine Research and the Institute of Oceanography at the University of Hamburg, and sponsored by the Ministry of Research and Technology of the Federal Republic of Germany. The scientific aim was to forecast the drift, extension and stranding of crude oil after tanker accidents in the German Bight.

MAIN PROCESSES

The different processes occuring after an accident can, in general be divided into three groups:

1. Transport or advection processes.
   The oil is transported by wind, waves, tides and currents.

2. Extension processes.
   (a) Spreading, in which the motion is induced primarily by oil properties (density difference and surface tension);
   (b) Dispersion, in the presence of a velocity field, where there are extension processes due to turbulent mixing.

3. Weathering processes.
   These are time dependent processes which change the state and the composition of the oil. There are three different kinds of weathering:

   (a) Physical weathering: evaporation, mechanical dispersion, dissolution, direct air sea exchange, sinkage, sedimentation and tar lump formation;
   (b) Chemical weathering: photochemical oxidation, accomodation and emulsification;
   (c) Biological weathering: microbial degradation, uptake by organisms and biological dispersants.

It can clearly be seen from this list that oil spill modelling is a complex matter. On the other hand, there is no great sense in modelling all kinds of processes, since a lot of them are not yet really understood. In addition, the processes take place on different time scales. Hence, for a forecast model where quick decisions in clean-up strategy are required, processes with a time scale of a few days are important, while for risk assessment, a model which produces simple probable trajectories may be regarded as sufficient.

THE MODEL

Transport and extension

Transport and extension are based on the well known transport diffusion equation. The numerical framework is provided by a Lagrangian tracer technique (Maier-Reimer & SÜndermann 1981). The oil is divided in a finite numbers of particles and each particle has definite properties. A trajectory is computed for each individual particle. The ensemble of all particles describes the actual position of oil patch. The velocity of each particle is calculated as:

$$\vec{U}_o = \vec{U}_t + \vec{U}_s + \vec{U}_d \qquad (1)$$

Where $\vec{U}_t$ is the advection velocity, $\vec{U}_s$ the spreading velocity and $\vec{U}_d$ a diffusion velocity.

The advection velocity of the ambient water is an input value obtained from a hydrodynamic circulation model. This can be a two or three-dimensional model of a harbour, a river, a coast etc. The circulation model may be forced by tides, wind, waves or density driven currents. The influence of wind can act directly as acceleration in the nonlinear equation of motion or, for simple cases like accidents in harbours or rivers, can be considered as linear and superposed on the transport velocity.

According to Fay (1969), the spreading velocity is calculated under the assumption of Fickian diffusion.

Two processes are considered in the simulation of horizontal dispersion. Local mixing by shear currents is simulated by a statistical fluctuation of the actual advection velocity. Isotropic turbulence is calculated in a diffusion velocity model using a time dependent diffusion coefficient.

Weathering

Evaporation . Crude oil is a mixture of different sorts of hydrocarbons. Hydrocarbons may be divided into eight groups similar in molecular weight and boiling point. The evaporation is given by

$$\frac{dm_i}{dt} = - \alpha_i \, m_i \qquad i = 1, \ldots, 8 \qquad (2)$$

where m_i is the weight of the i-th group at the surface. All eight equations may be solved for each particle. The coefficients are:

$$\alpha_i = \frac{k p_i M_i A}{RT \rho_i V} \qquad (3)$$

where M_i and ρ_i are the molecular weight and density of the i-th component A, is the covered area, V the actual volume of the particle, R the universal gas constant, T the absolute temperature, and p_i the effective gas pressure according to Raoult's law. For the gas phase, the mass transfer coefficient k can be expressed as a linear function of wind speed (Liss 1973). Figure 1 shows the percentage change of mass of the eight groups for constant temperature and wind. The oil considered is crude Venezuelan. Figure 2 shows the change in the average density and volume for a constant wind speed of 5 m/s and three different temperatures.

Mechanical dispersion. Mechanical dispersion, also called natural dispersion, is a phenomenon which incorporates the oil from the sea surface into the water column. It can be forced by turbulence, wave set-up, wave breaking or Langmuir circulation. Mechanical dispersion is accelerated by chemical dispersants and is important for clean-up operations. Since this process is very complicated and not completely understood, a simple empirical dependence on the wind speed would seem to be sufficient.

Ambient input data

OIPASIPA may be run in an interactive mode in order to forecast short time variability due to meteorological events. Wind speed and direction are two input data. The advection velocity of the ambient water is also an input value. Additional input data are the geographical location coordinates of the accident, the discharge, the type of oil and the temperature. OIPASIPA can currently simulate seven different types.

The Bravo blow out

Besides the complexity of oil spill simulation, verification of the model is an additional problem. In general, very little or no data are available for the testing and verification of the numerical model. The detailed measurements carried out by the Norwegian Continental Shelf Institute during the Bravo Ekofisk blow out make this event an interesting one to model; the results of the simultation may then be compared with the actual measurements (Audunson et al. 1977). The advection velocity is calculated from a two-dimensional North Sea model (Dippner 1983). Figures 3 to 5 show the Norwegian measurements on the left hand side, and the results of OIPASIPA on the right hand side, in the same scale. These results show good agreement between observation and calculation regarding shape and drift pattern.

Application

The German Bight is an area with heavy traffic and a difficult region for navigation due to its complicated topography (Figure 6). There is thus a high risk of tanker accidents. Figures 7 to 10 show the development of a theoretical oil spill in the German Bight simulated using OIPASIPA. By the calculation of a large number spills at different places is under different environmental conditions, one can carry out a risk assessment for each region.

The German Bight is also an extensive is wadden area which is a varity in the world owing biotic & abiotic factors (Wesemüller & Augst 1979). Oil pollution would destroy the shell-banks and the juvenile fish cultures of plaice etc. The fishing industry would be damaged for some years as would tourism, the coast being a very important recreation area. If the environmental vulnerability is known (Figure 11), OIPASIPA may also be used for sensitivity analysis.

CONCLUSION

A deterministic numerical model is presented is containing the important dynamic processes of slick formtion, movement and weathering. OIPASIPA may be used for forecast and hindcast, as well as contingency planning. The modular structure has a high flexibility and permits universal application. The model is designed to fit the requirements of users; few input data are required and it is easy to handle. OIPASIPA may also be used for risk assessment and sensitivity analysis.

REFERENCES

Audunson T. et al. (1977) The Bravo blow out. IKU Report No. 90 Continental Shelf Institute Trondheim, Norway.

Dippner J. W. (1983) A hindcast of the Bravo Ekofisk blow out. Veröff. Inst. Meeresforsch. Bremerhaven No. 19.

Fay J. A. (1969) The spread of oil slicks on a calm sea. In: Oil at the sea, Hoult, D.P. (ed.) Plenum Press, New York.

Liss P.S. (1973) Processes of gas exchange across an air water interface, Deep Sea Res. 20, 221-238.

Maier-Reimer E. & Sündermann, J. (1981) On tracer methods in computational hydrodynamics. In: Engineering application of computation hydraulics, Abott M. B. and Cunge, J. A. (ed.) Pitman, London.

Wesemüller H. & Augst H. J. (1979) German waddensea, principles of a protection program, Niedersächsisches Landesverwaltungsamt, Hannover (in German).

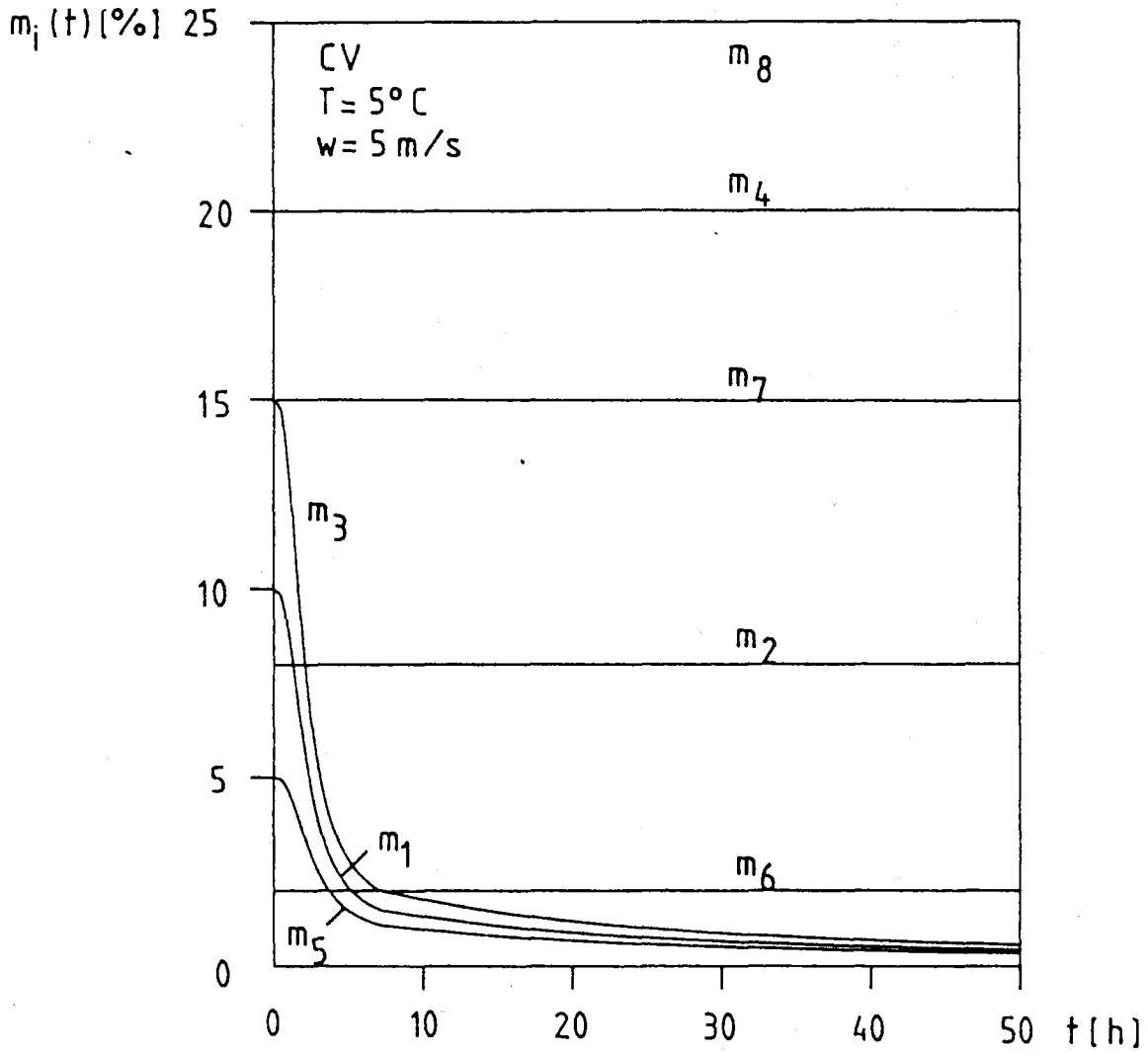

Figure 1: Percentage change of mass of the eight groups

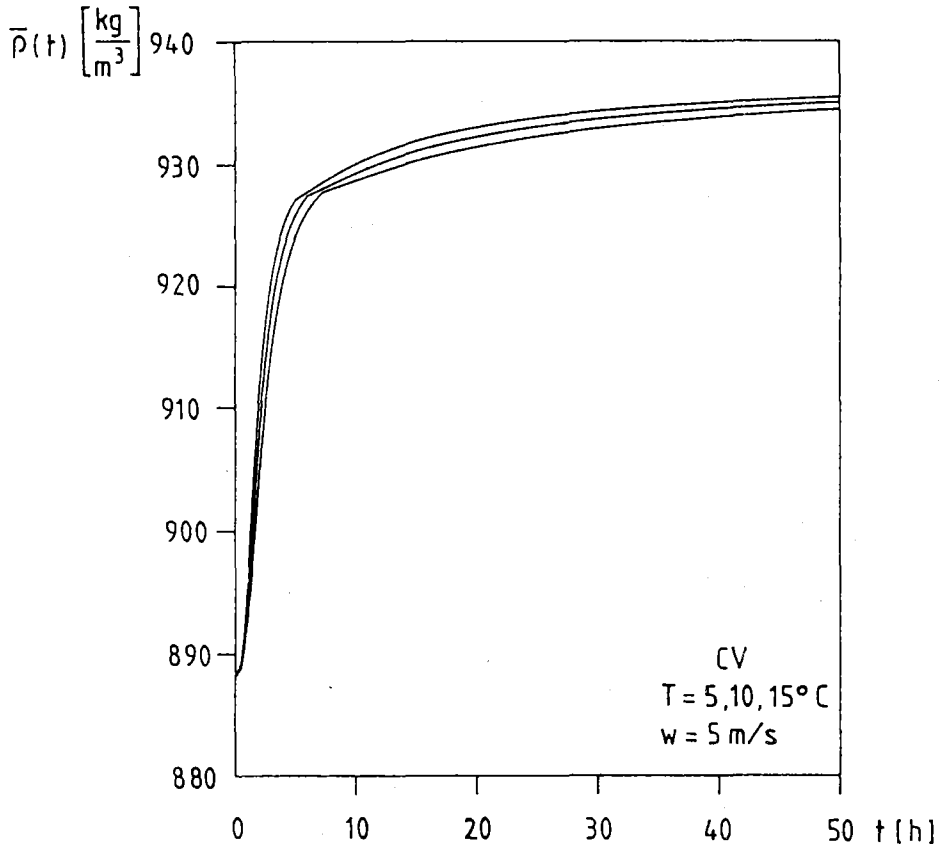

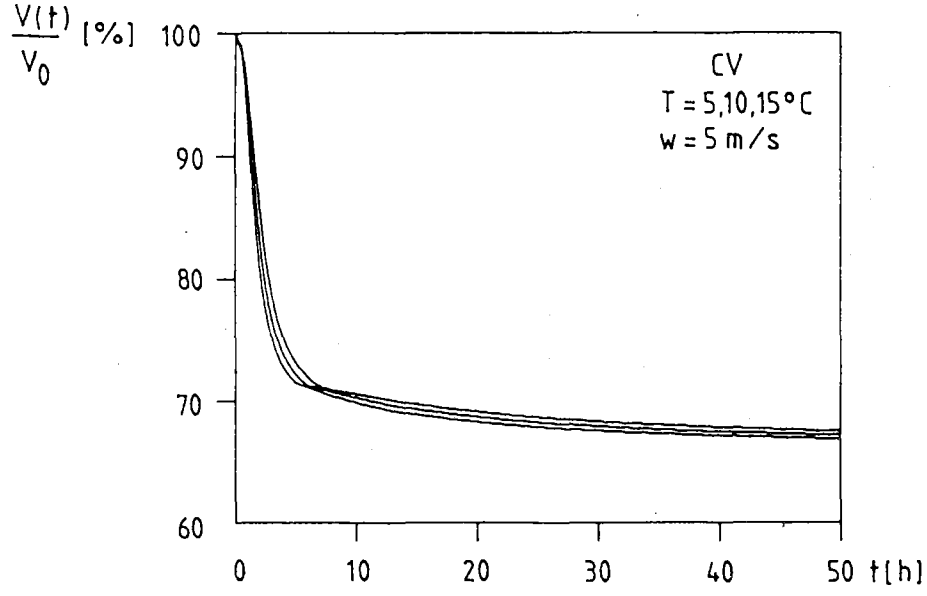

Figure 2: Change of density (a) and volume (b)

23. 4. 16°° h

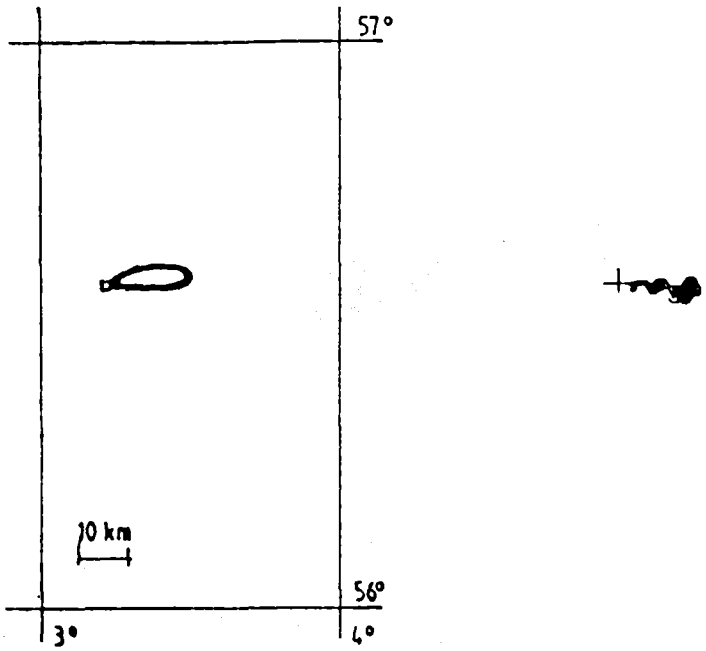

24. 4. 12°° h

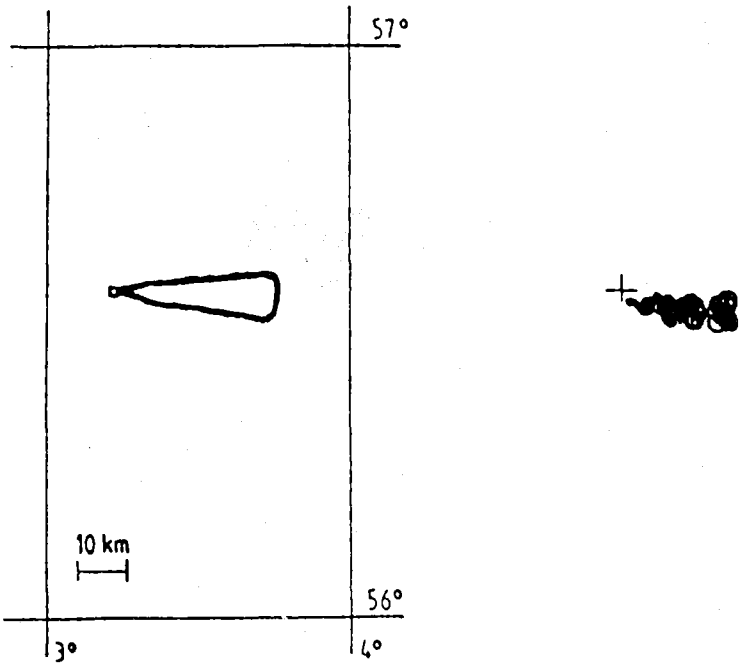

25.4. 14°° h

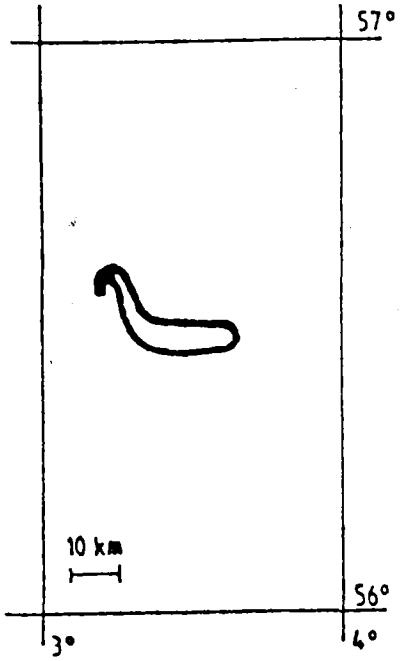

27.4. 8°° h

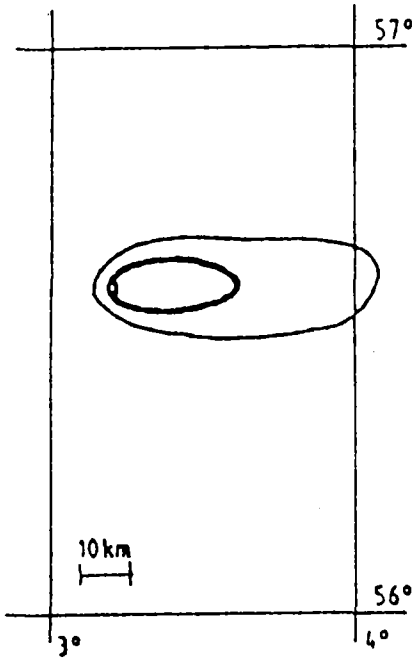

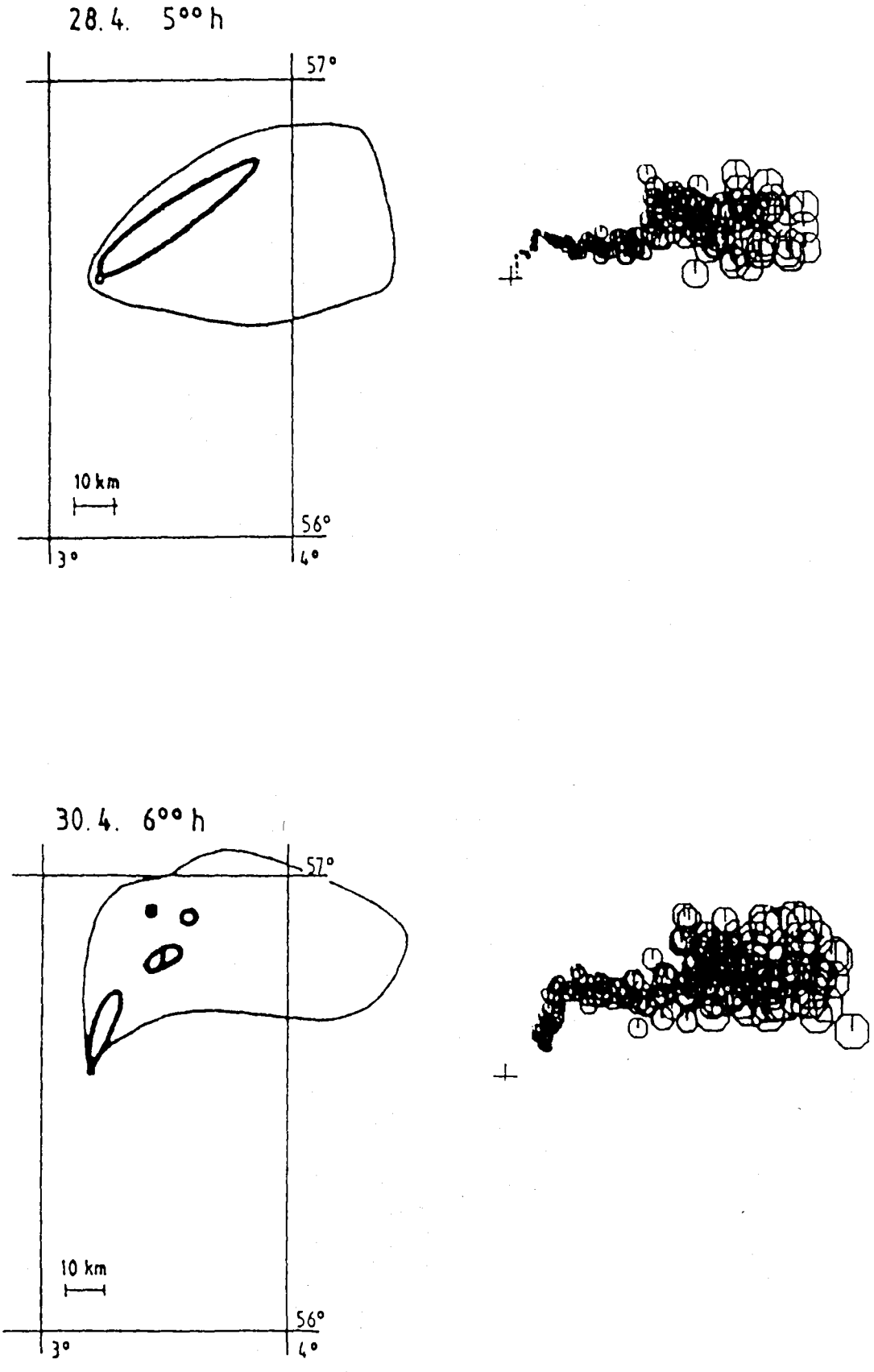

Figure 5: Observation (left) and simulation (right)

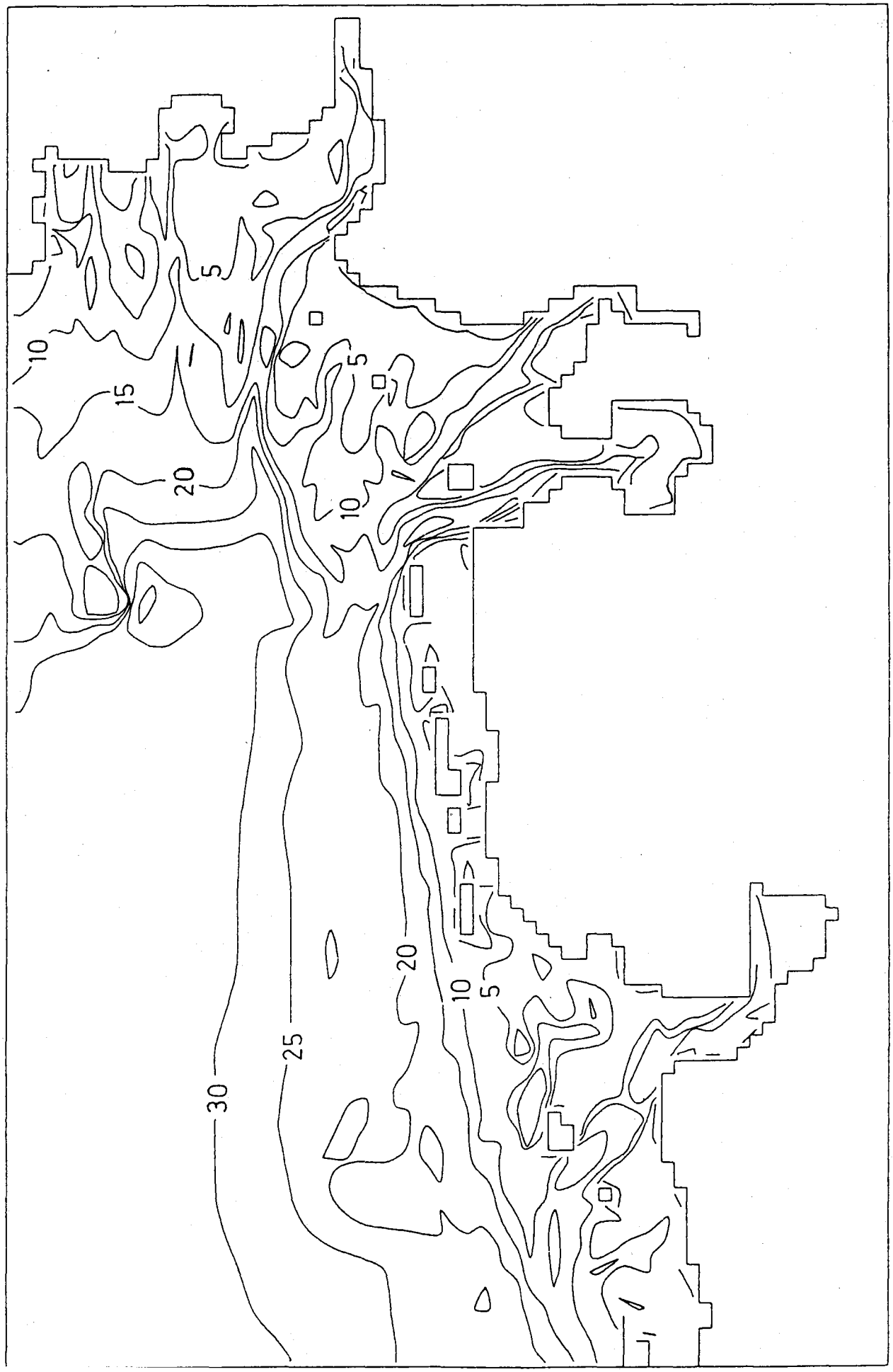

Figure 6: Depth distribution in the German Bight

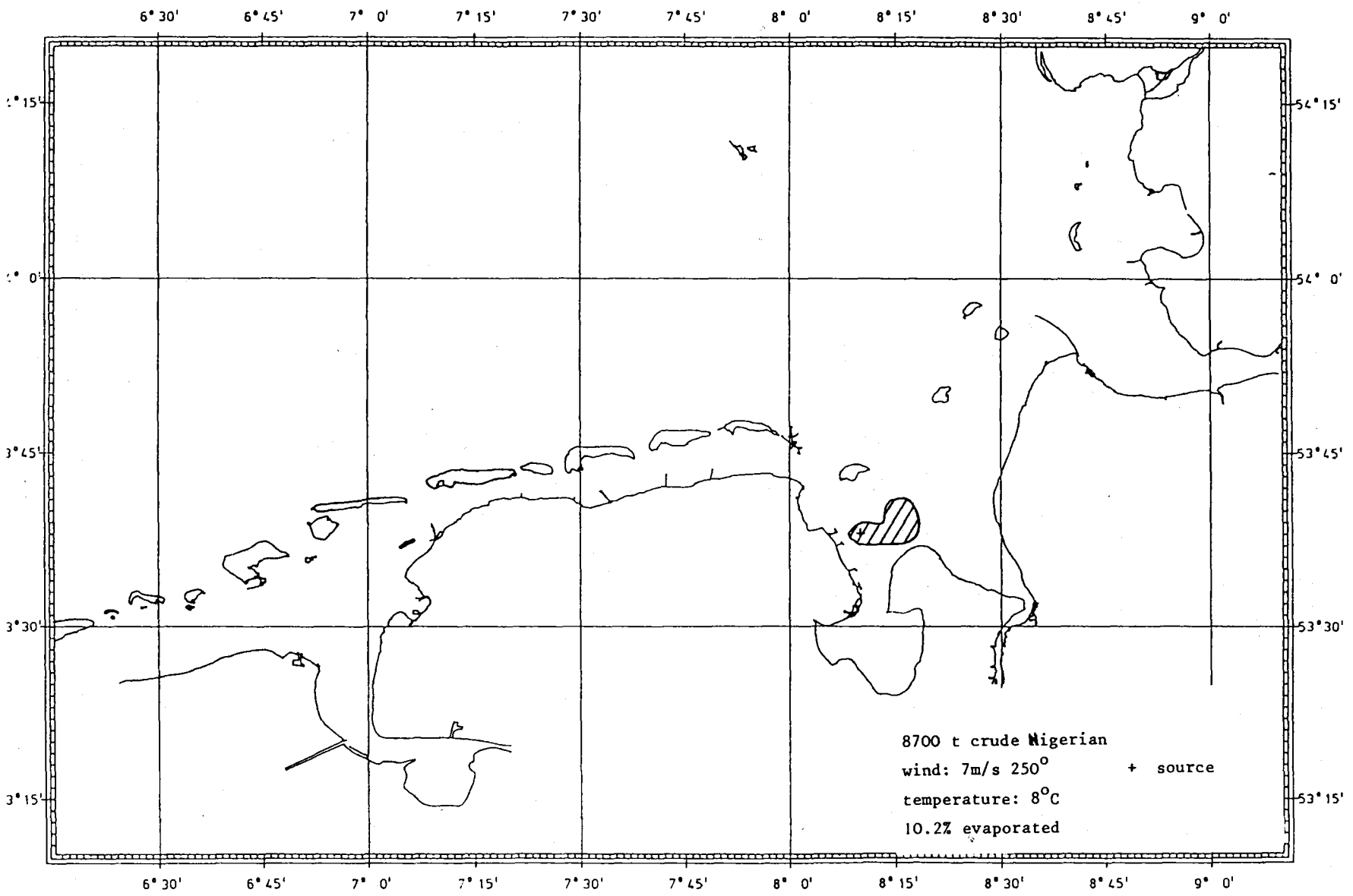

Figure 7: Simulated spill in the German Bight : 6 hours after spill

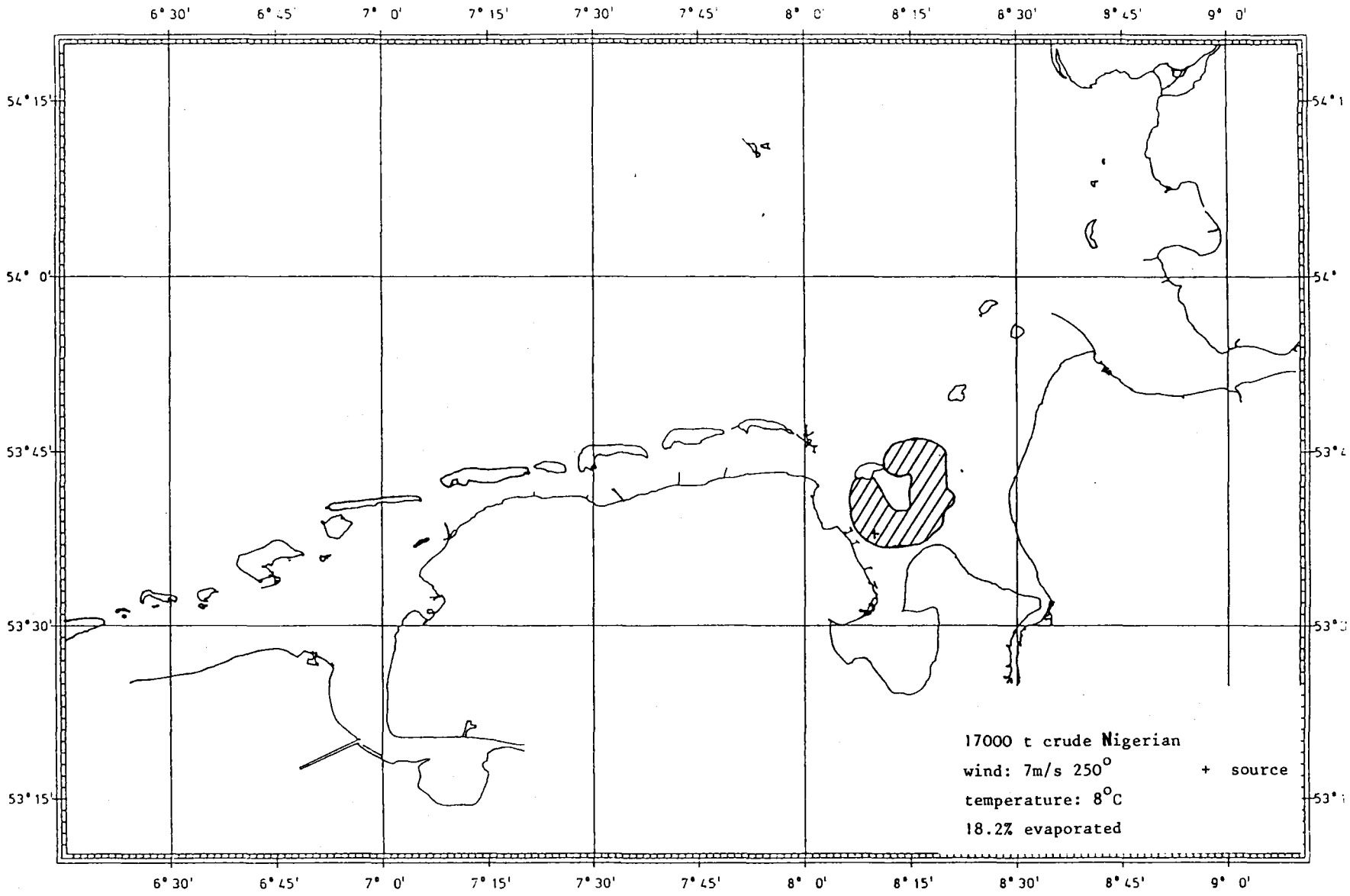

Figure 8: Simulated spill in the German Bight : 12 hours after spill

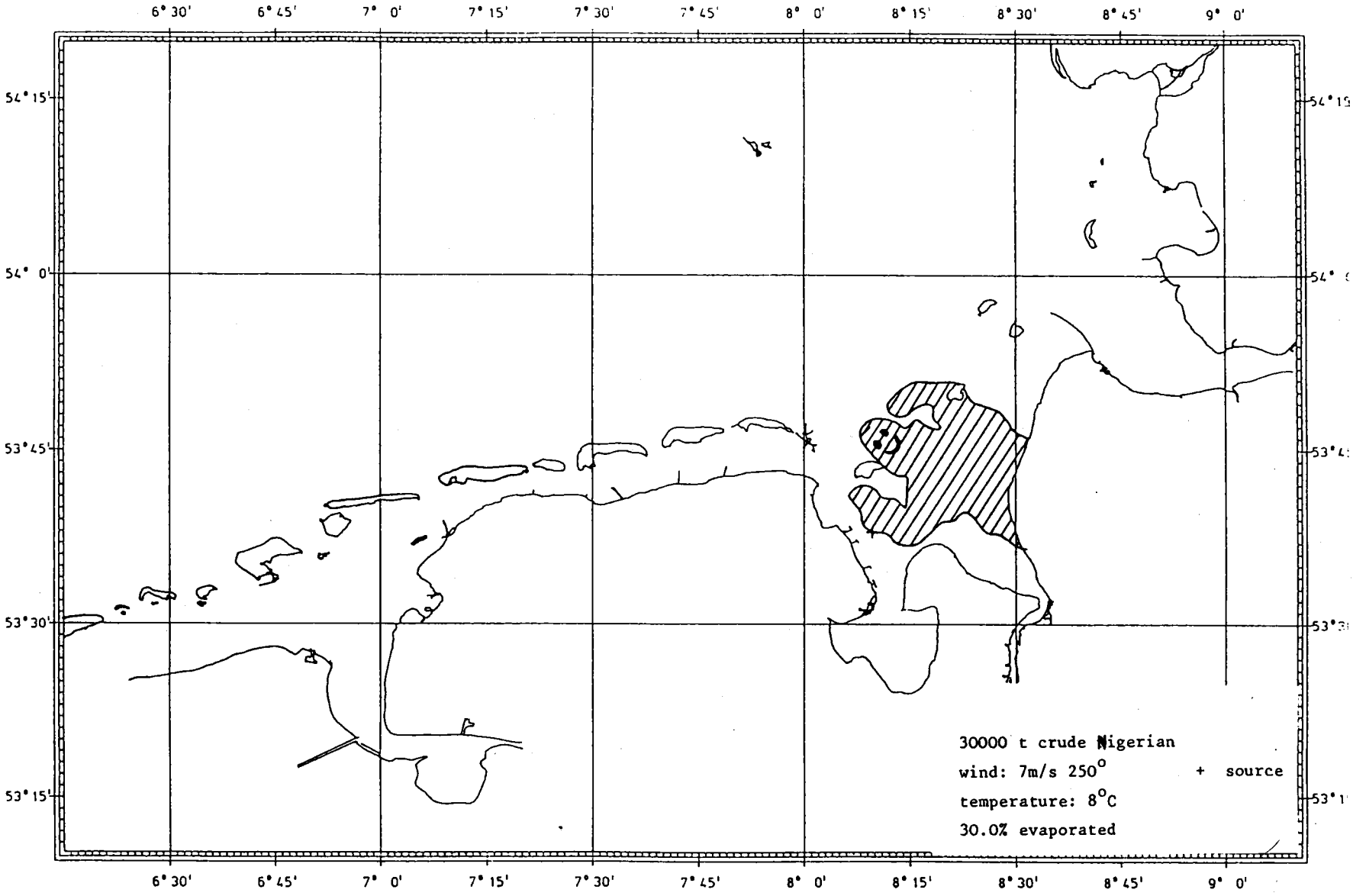

Figure 9: Simulated spill in the German Bight : 24 hours after spill

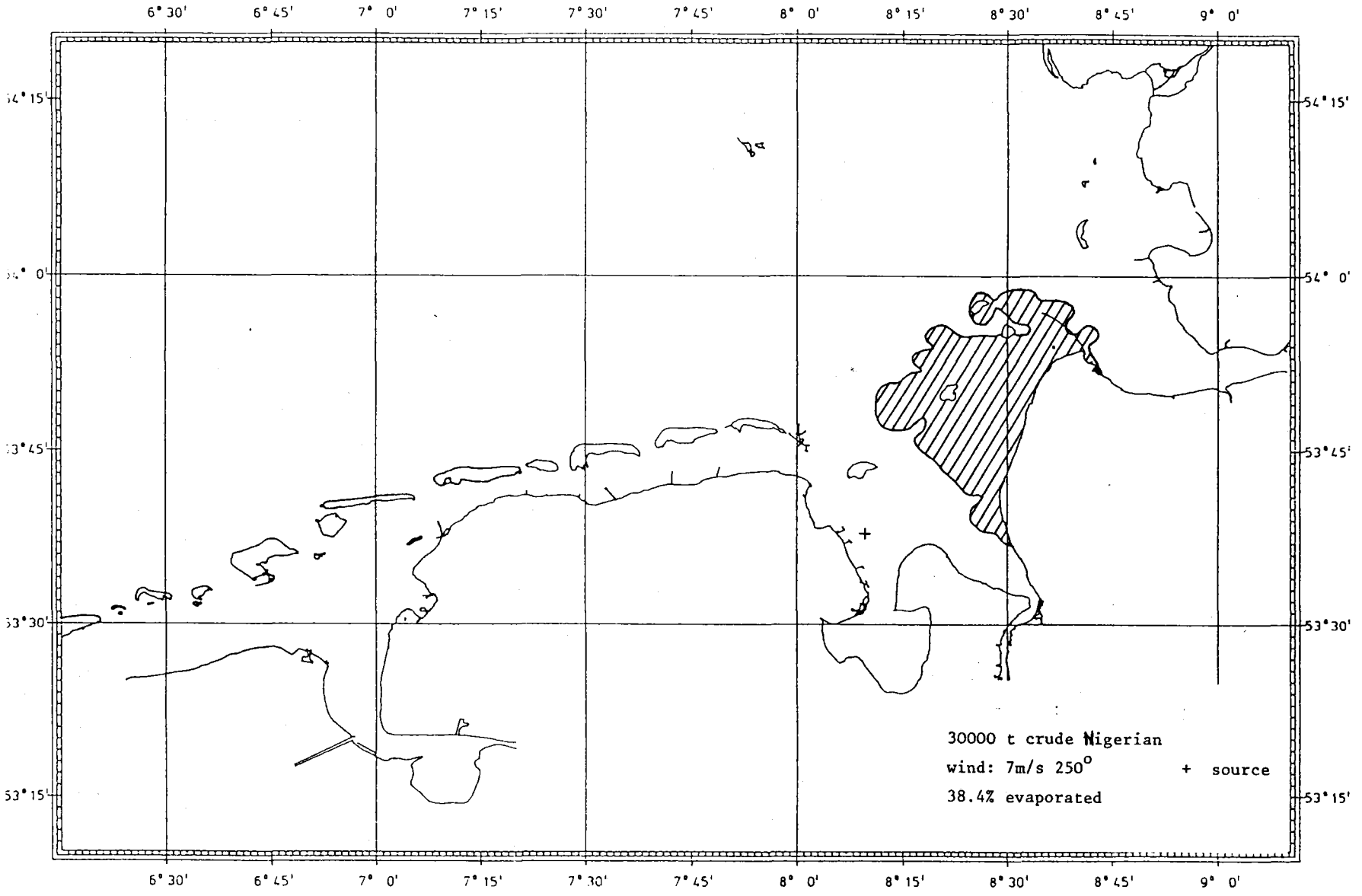

Figure 10: Simulated spill in the German Bight : 48 hours after spill

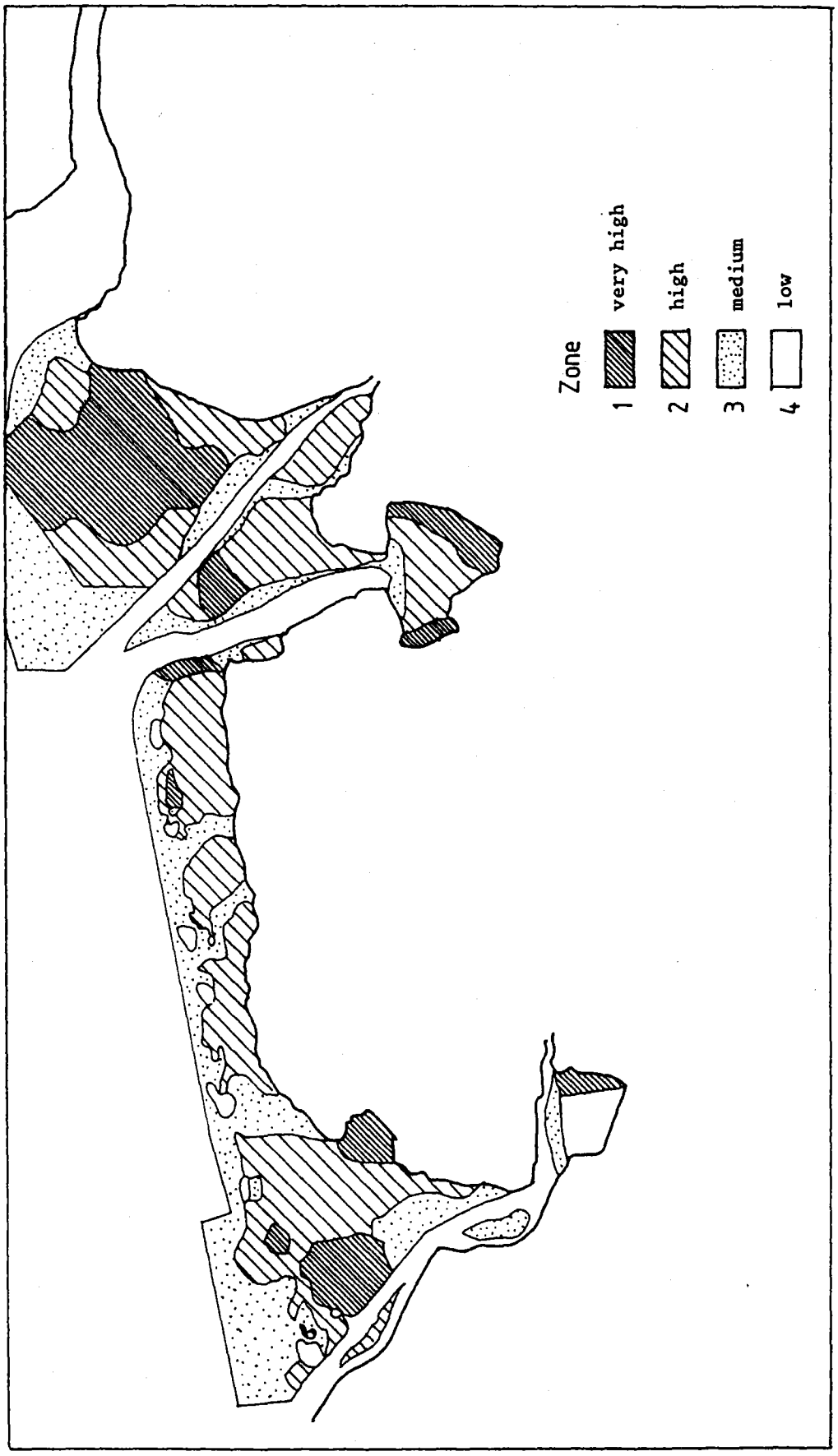

Figure 11: Environmental vulnerability

TIDAL CHARTS OF THE ARABIAN SEA NORTH OF 20°N

by

Khawaja Zafar Elahi
Department of Mathematics
King Saud University
Riyadh, Saudi Arabia

ABSTRACT

A depth-averaged two-dimensional numerical model (20°N to 25°N, 56°E to 70°E) of the Arabian sea, including the Bay of Oman, is developed to reproduce the major diurnal and semi-diurnal tidal constituents. The model has a resolution of $\frac{1}{2}°$ both latitude and longitude and an open boundary at latitude 20°N along which tidal input data, derived from the empirical cotidal charts of the Arabian Sea, is applied.

The classical non-linear hyperbolic initial and boundary value problem of long wave propagation in shallow waters is solved by the explicit finite difference technique. The results regarding tidal elevation are used to develop detailed cotidal and co-amplitude charts for principal tides. The charts make it possible to predict the tidal elevation at the coast and in the open sea area with greater accuracy. These predictions can be used as the driving force for the development of a numerical model to study the tidal dynamics in the Bay of Oman and the Inner Gulf.

NOMENCLATURE

U,V = components of vertically averaged velocity in the λ and ϕ directions, resp.

ξ = water elevation

A_h = horizontal eddy coefficient

g = acceleration due to gravity

h = mean water depth

$H = h + \xi$ actual depth

r = bottom friction coefficient

R = radius of the Earth

t = time

u,v = components of the wind velocity

λ,ϕ = geographical longitude and latitude

μ = surface friction coefficient

ω = angular velocity of the Earth's rotation

INTRODUCTION

Knowledge of tidal dynamics, currents and elevation constitutes a major part of the information required to solve coastal engineering problems. These factors may be used to study the flow dynamics of exceptional or rare events, and to investigate with greater accuracy the influence of constructional alternatives to tidal dynamics. Such information is also used as design criteria in engineering problems.

Tidal charts can be prepared either using the information available in the form of analyses of long and short sets of observations of waterlevel fluctuations on the coastal gauges or using numerical models. The information available about tides in the Arabian Sea will be summarized below.

McCammon and Wunsch (1977) constructed charts for the major semi-diurnal and diurnal tidal constituents of the Indian Ocean north of 15°S. The co-amplitude and cotidal lines in these charts are drawn on the basis of the analysed coastal tidal observational data. Fairbairn (1954) prepared a tidal chart for the K_2 - tide using Proudman's Theorem. Bogdonau and Karkove (1975) were the first to develop a mathematical model to analyse the tidal phenomena in the Indian Ocean. A small amount of information on the area is also available from the mathematical models of the world ocean prepared by Accad and Pekeris (1978), Zahal (1970, 1973) and Schwiderski (1980). In the existing tidal charts, consideration is mainly given to the position of the amphidromic system. A little information is provided about amplitude variation in the Arabian Sea but there is no information about the cotidal variation in the area.

The information produced with the help of the present numerical models (see Figure 1) presents a clear picture of phase and amplitude variation. The co-amplitude lines are drawn with a successive difference of 2 cm for M_2-tides, 1 cm for S_2- and K_1-tides, and 5 cm for O_1 tides. The successive difference in co-tidal lines is 1° for all four partial tides.

MATHEMATICAL MODEL OF THE NORTHERN ARABIAN SEA

The system of equations which describes the tidal dynamics of large fluid masses is derived from the hydrodynamic equations of motion and continuity. Because the flow field is turbulent in nature, the time-smooth velocity and pressure distribution must be considered. The external forces are the gravity force, the Coriolis force and the bottom friction together with Reynold's stresses. The water level variation as a function of time is prescribed on the open boundary in the place of a tide generating force. Since water movements are mainly horizontal and the horizontal dimensions are much greater than the depth, the system of equations has been simplified to a two-dimensional system in the model. The effect of the Earth's curvature is taken into account by considering the depth averaged equations of motion and continuity in spherical polar coordinates as follows:

$$\frac{\partial \xi}{\partial t} + \frac{1}{R \cos \phi} \left\{ \frac{\partial (HU)}{\partial \lambda} + \frac{\partial}{\partial \phi} (HV \cos \phi) \right\} = 0 \qquad (1)$$

$$\frac{\partial U}{\partial t} - 2 \omega \, \mathrm{Sin}\phi V + \frac{1}{H} \tau_b^x - A_h \nabla^2 U + \frac{g}{R \cos \phi} \frac{\partial \xi}{\partial \lambda} = 0 \qquad (2)$$

$$\frac{\partial V}{\partial t} + 2 \omega \, \mathrm{Sin}\phi U + \frac{1}{H} \tau_b^y - A_h \nabla^2 V + \frac{1}{R} \frac{\partial \xi}{\partial \phi} = 0 \qquad (3)$$

If u(z) and v(z) denote the horizontal velocity components at depth z below the undisturbed sea surface, then

$$U = \frac{1}{h + \xi} \int_{-h}^{\xi} u(z) dz \qquad (4)$$

$$V = \frac{1}{h + \xi} \int_{-h}^{\xi} u(z) dz \qquad (5)$$

The stresses due to roughness of the bottom (τ_b^x, τ_b^y) are parameterized empirically using the Newton-Taylor formulation:

$$\tau_b^x = r\, H^{-1}\, U(U^2 + V^2)^{\frac{1}{2}} \qquad (6)$$

$$\tau_b^y = r\, H^{-1}\, V(U^2 + V^2)^{\frac{1}{2}} \qquad (7)$$

in which r = .003 is the bottom friction coefficient.

The system of equations requires boundary and initial conditions for solution. No-slip is assumed along coastal boundaries. Thus, the normal and tangential components of velocity are zero at coastal points. Water elevation as a function of time is prescribed on the open boundry. As an initial condition, a "cold start" is given to the model, i.e., the values for water elevation and velocity are taken to be zero.

The computational parameters used in the model are as follows:

Computational points	15 x 30
Grid distance	$\Delta\lambda = \Delta\phi = 0.5°$
Time interval	$\Delta t = 2.5$ min.
Horizental eddy viscosity	$A_h = 10^6$ cm^2/sec
Friction coefficient	r = .003

The system of partial differential equations for the initial and boundary conditions is transfered into a set of algebraic equations by replacing the space derivatives by central differences and the time derivatives by forward differences. These equations can be solved numerically using the hydrodynamic numerical method developed by Hansen (1956).

The computational work was done on a CDC 7600 computer at Hannover Technical University. The numerical solutions were converged after 10 tidal cycles in the case of semidiurnal tides and 5 tidal cycles in the case of diurnal tides.

RESULTS: TIDAL CHARTS OF THE ARABIAN SEA NORTH OF 20°N

Semidiurnal tides

M_2-Tide (principal lunar). The values of phase given in the tide tables for the coastal gauges had a variation of 157° to 165°. The numerical model (Figure 2) produced similar results as the 160° cotidal line moved from the South East corner near Porbandar to the Bay of Oman. The value was 171° at Muscat. The 150° cotidal line in the tidal chart of McCommon and Wunsch (1977) is out of phase by 10° to 15°. The 60 cm and 70 cm co-amplitude lines are almost exactly the same as those reproduced in the numerical model.

S_2-Tide (principal solar). The tidal chart drawn by McCommon and Wunsch (1977) shows only an 180° cotidal line at 20°N of the Arabian Sea. The phases tend, however, to have a value between 180° and 210° and the amplitude a value greater than 20 cm. This is reproduced exactly in the tidal chart based on the numerical

model (Figure 3) which presents a detailed picture of the distribution of co-amplitude and cotidal lines. The variation of amplitude is between 24 cm and 30 cm and phase varies between 190° and 210°.

Diurnal tides

K_1-tide (luni-solar). Amplitudes in the numerical model for K_1-tide (Figure 4) vary from 33 cm to 44 cm; this is in accordance with observation. Co-tidal lines have a value of 344° to 350° and increase parabolically northwards. These results may be compared with the tidal charts drawn by McCommon and Wunsch (1977). In the modelled area, there is a co-amplitude line with a value of 30 cm and the value of the phases lies between 330° and 360°. As far as the phases are concerned, the modelled and observational charts are similar, numerical values agreeing well with the observed values on the coastal gauges.

O_1-tide (principal lunar). The tidal charts of McCommon and Wunsch (1977) have no co-amplitude or co-phase lines at 20°N in the Arabian Sea but the co-amplitude lines tend to increase northwards above 20 cm and the phase should lie between 330° and 360°. The numerical results (Figure 5) are in agreement with the above tendency, variation in amplitude being between 22 cm and 24 cm and the phase being between 340° and 350°.

The results of the numerical model may also be compared with observational values available from the following coastal tidal gauges: Poranbar, Karachi, Ormara, Pasni and Muscat (Table 1). Again, both computed and observed values match. The deviation between computed values and the observed harmonic constants at the Ormara gauge, for example, is due to an inaccuracy in observed value, since this value is derived only from the local tide table (Hydrographic Department, Pakistan Navy, 1978). The results at the Pasni gauge are excellent. The increase in phase by 12° and in amplitude by 6 cm for M_2-tide at the Muscat gauge is due to the fact that this gauge is under the influence of two open boundaries.

Table 2 presents the harmonic constants for four major tides in thirteen important areas on the coast of the Northern Arabian Sea mathematical model.

CONCLUSION

The tidal charts prepared using the hydrodynamic-numerical model had a high level of accuracy. They presented a detailed picture of the equal amplitude and phase distributions and hence provided the structure of the tidal wave of a given frequency. These results may be used to provide the necessary boundary values at the open boundary for numerical models of the near shore area and they can also be used to check the results of such models. These charts may also be used to check the accuracy of the results of short sets of observation at temporary tidal gauges.

REFERENCES

Accad, Y. & Pekeris C.V. (1978) Solutions of the tidal equations M_2 and S_2 tides in the world Oceans from a knowledge of the tidal potential alone. Phil. Trans. Roy. Soc. London, Ser. A, 290:235.

Bogdanov, K.T. & Karkov B.V (1975) Calculation of Indian Ocean tide. Oceanology, 15:156-160.

Fairbairn, L.A. (1954) The semi-diurnal tides along the equator in the Indian Ocean. Phil. Trans. Roy. Soc. London, Ser. A, 247:191-212.

Hansen, W. (1956) Theorie zur Errechung des Wasserstandes und der Stromungen in Randmeeren nebst Anwendungen, Tellus 8, No. 3, p. 287-300. Hydrographic Dept, Pakistan Navy (1978), Tide Tables for Pakistan Ports.

Hydrographic Department Pakistan Navy (PAK), Tide Tables for Pakistan Ports, 1978, Pak. Karachi.

McCommon, C. & Wunsch C. (1977) Tidal charts of the Indian Ocean, North of 15°S. J. of Geophy. Res. Vol. 82, No. 37.

Schwinderski, E.W. (1980) On charting Ocean Tides. Rev. of Geoph. and Sp. Phy. Vol 18, No. 1, p. 243.

Zahel, W. (1970) Die Reproduktion gezeitenbedingter Bewegungsvorgänge in Weltozean mittels des hydrodynamisch-numerisch verfahrens, XVII Mitt. d. Inst. f. Meereskunde d. Univ. Hamburg.

Zahel, W. (1973) The Diurnal K_1-tide in the world Ocean - A numerical investigation. Pageoph. Vol. 109, VIII.

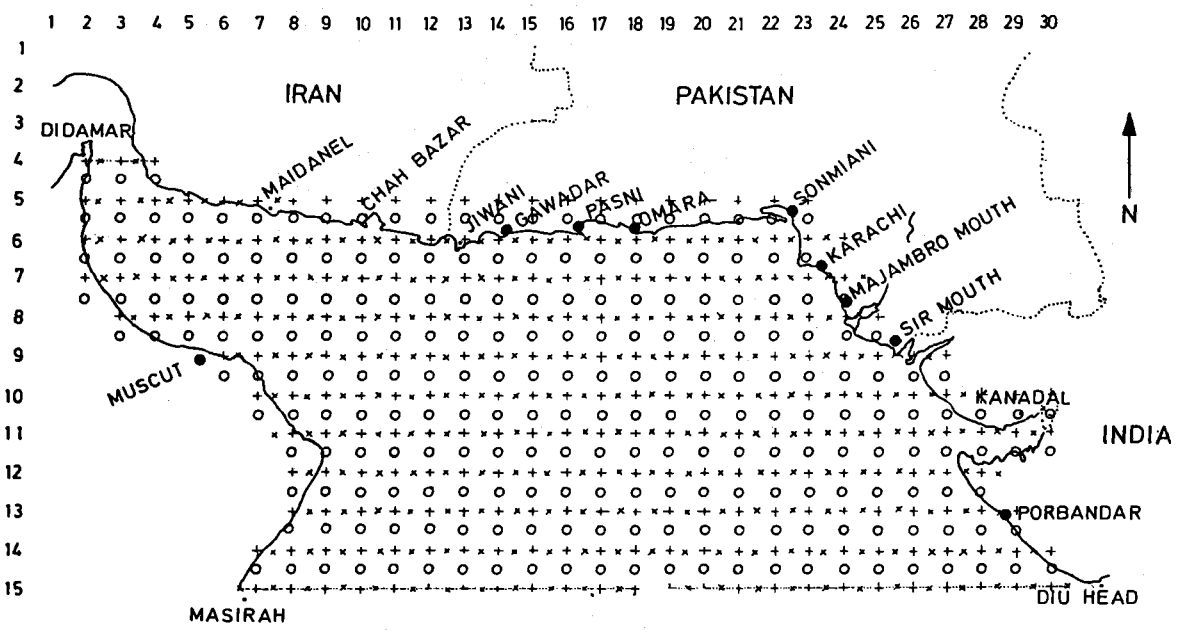

Figure 1: Finite-difference grid for the Northern Arabian Sea

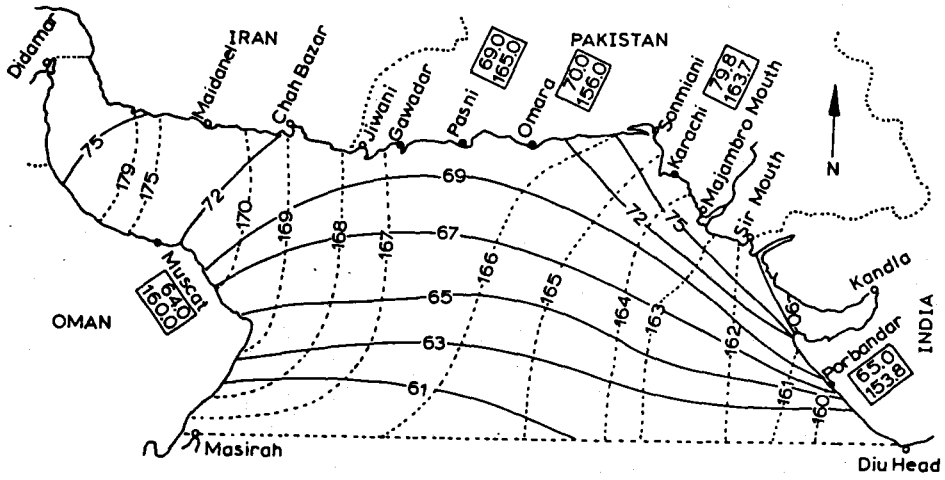

Figure 2: M_2-tide in the Northern Arabian Sea. Cotidal (_____) and co-range (-------) lines. The boxes show the observed values: amplitudes in cm upper values and phases in degrees lower values.

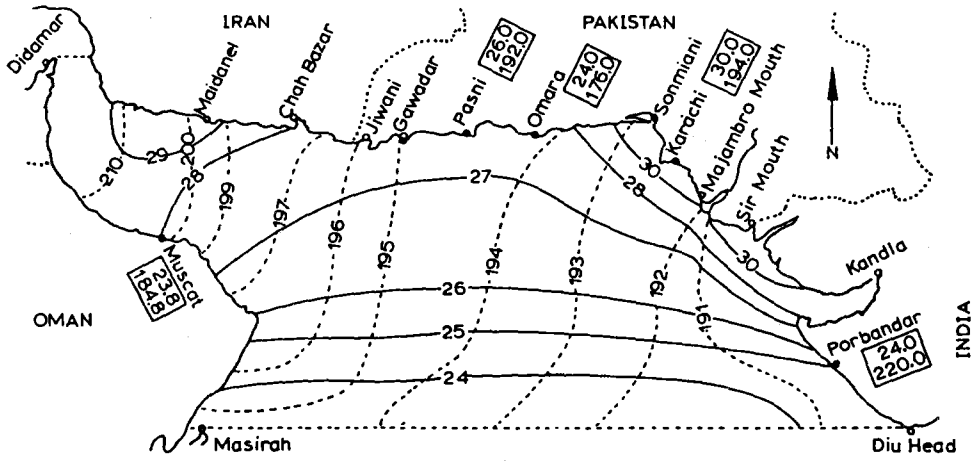

Figure 3: S_2-tides in the Northern Arabian Sea

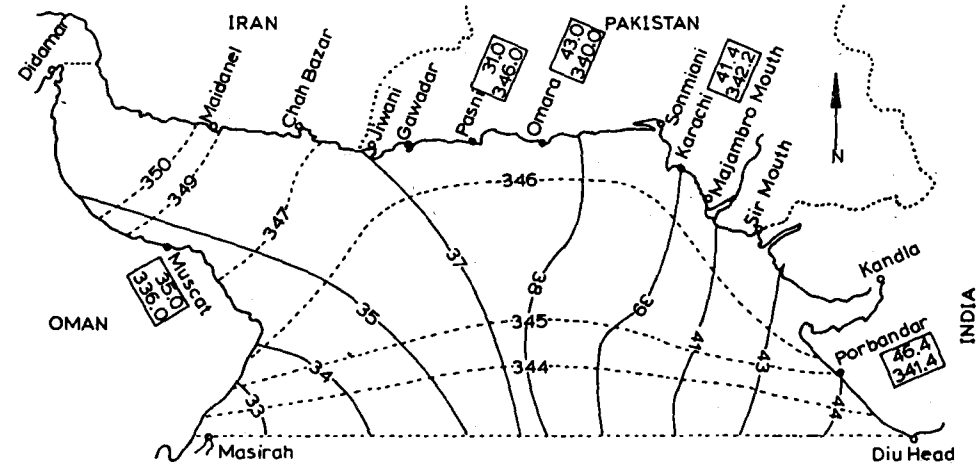

Figure 4: K_1-tides in the Northern Arabian Sea

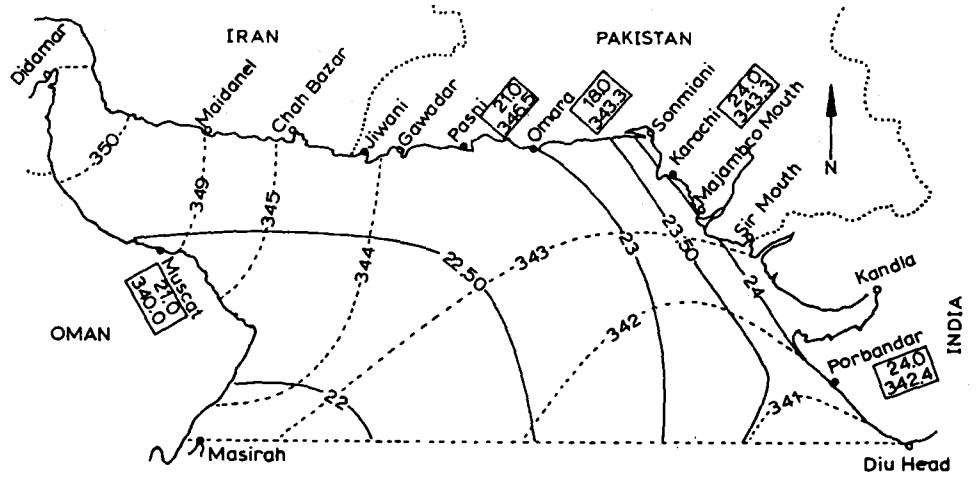

Figure 5: O_1-tides in the Northern Arabian Sea

Table 1: Computed (c), observed (o), amplitude (a), and phases (k) of the major tidal constituents.

TIDAL CONSTITUENT		M_2		S_2		K_1		O_1	
SITE	a(cm) κ(deg.)	c	o	c	o	c	o	c	o
Porbandar	a	67,92	65,o	27,57	24,o	45,17	46,o	24,11	24,o
	κ	161,43	157,o	191,51	220,o	345,89	336,o	342,10	342,o
Karachi	a	79,91	79,8	31,47	29,6	39,22	41,1	23,68	20,o
	κ	166,34	163,7	194,67	193,9	347,51	342,2	343,93	343,2
Omara	a	69,54	70,o	27,27	24,o	37,72	43,o	22,94	18,o
	κ	166,29	156,1	194,24	176,o	346,47	340,o	343,68	343,3
Pasni	a	68,98	69,o	27,07	26,o	37,38	31,o	22,91	24,o
	κ	166,37	165,o	194,48	192,o	346,42	346,o	343,79	346,3
Muscat	a	69,75	63,3	27,27	23,7	35,99	38,8	22,48	20,2
	κ	171,74	159,8	199,33	189,8	347,76	341,4	345,71	342,4

Table 2: Amplitude a (cm), phase k (deg), waterlevel at t=0 and at t = T/4, 1 and 2 (cm).

No.	PLACE	N	O		M_2	S_2	K_1	O_1
		o	o					
	PAKISTAN							
1	Sir Mouth	23.66	68.12	A	77.15	30.28	39.38	23.53
				K	165.37	193.83	347.99	343.59
				ξ1	-74.65	-29.49	38.96	22.57
				ξ2	19.49	-7.15	-8.29	-6.63
2	Majambro Mouth	24.10	67.32	A	77.50	30.48	39.82	23.57
				K	166.34	194.03	347.37	343.66
				ξ1	-75.31	-29.57	38.33	22.62
				ξ2	18.31	-7.39	-8.59	-6.65
3	Karachi	24.80	66.97	A	79.91	31.47	39.22	23.68
				K	167.32	194.67	347.51	343.51
				ξ1	-77.97	-30.44	38.29	22.75
				ξ2	17.54	-7.97	-8.48	-6.55
4	West Point	25.24	66.31	A	79.14	31.13	39.11	23.66
				K	168.66	196.18	347.75	344.51
				ξ1	-77.59	-29.89	38.22	22.80
				ξ2	15.56	-8.67	-8.30	-6.32
5	Omara	25.11	64.41	A	69.54	27.27	37.72	22.94
				K	166.29	194.24	346.47	343.68
				ξ1	-67.55	-26.43	36.67	22.06
				ξ2	16.48	-6.71	-8.82	-6.46
6	Pasni	25.20	63.50	A	68.08	27.07	37.38	22.91
				K	166.37	194.48	346.42	343.29
				ξ1	-67.07	-26.21	36.34	22.00
				ξ2	16.10	-6.77	-8.78	-6.39
7	Gwadar	25.11	62.33	A	69.12	27.16	37.11	22.86
				K	166.95	194.99	146.47	144.00
				ξ1	-67.33	-26.23	36.08	21.98
				ξ2	15.61	-7.03	-8.68	-6.30
8	Jiwani	25.06	61.83	A	69.41	27.28	37.02	22.87
				K	167.22	195.31	346.55	344.13
				ξ1	-67.69	-26.31	36.00	22.00
				ξ2	15.36	-7.20	-8.61	-6.25
	IRAN							
9	Chah Bazar	25.30	60.70	A	70.68	27.75	36.01	22.92
				K	168.79	197.06	347.08	344.81
				ξ1	-69.33	-26.53	35.88	22.09
				ξ2	13.74	-8.14	-8.23	-6.00
10	Maidanel	25.40	59.20	A	73.24	28.60	36.84	23.04
				K	171.06	199.61	348.25	345.87
				ξ1	-72.35	-26.94	36.06	22.34
				ξ2	11.39	-9.60	-7.50	-5.62
11	Maskat	23.62	58.60	A	68.75	27.27	35.99	22.40
				K	171.14	199.33	347.76	345.79
				ξ1	-68.92	-25.73	35.18	21.80
				ξ2	10.75	-9.03	-7.63	-5.52
12	Rasal Hadd	23.55	59.80	A	65.79	25.84	35.56	22.19
				K	169.06	197.08	346.50	344.81
				ξ1	-64.60	-24.70	34.58	22.95
				ξ2	12.49	-7.59	-8.30	-5.82
	INDIA							
13	Porbandar	21.63	69.62	A	67.92	27.57	45.17	24.11
				K	161.43	191.51	345.89	342.10
				ξ1	-64.38	-27.02	43.81	21.41
				ξ2	21.63	-5.50	-11.01	-7.41

STORM SURGES IN THE INNER GULF OF THE KUWAIT ACTION PLAN (KAP) REGION AND THE GULF OF OMAN

by

M.I. El-Sabhl and T.S. Murty

ABSTRACT

The Inner Gulf of the KAP Region is mainly affected by weather systems extra-tropical in nature. A meso-scale system that deserves special attention is the so-called winter squall. A two-dimensional numerical model is developped to study the storm surges in the Gulf. The results show that the more shallow part of the Gulf are subjected to major storm surges. Strong winds associated with the squall system, coupled with topography and tidal effects, can give rise to water level deviations of several meters. Recommendations for future work are given.

INTRODUCTION

The Inner Gulf of the Kuwait Action Plan Region (Figure 1) is mainly affected by extra-tropical weather systems (Murty and El-Sabh, 1984). The tracks more or less follow the axis of the Gulf. One of the interesting weather phenomena in the region is the so-called "Shamal", which is a meso-scale wind phenomenon. Shamal is used to refer to seasonal northwesterly winds occurring during the winter as well as the summer and has a significant influence in the Gulf region. Tropical weather systems do not traverse the Gulf. The Gulf being shallow, especially in the southwest part, could be subjected to large amplitude storm surges. On the other hand, the Gulf of Oman is deeper than the Inner Gulf. One would expect the storm surge threat in the Gulf of Oman to be somewhat less than in the Inner Gulf. The few available observations appear to suggest this fact. Table 1 summarizes the differences between storm surges generated by extra-tropical weather systems and tropical cyclones.

A knowledge of storm surges in the Inner Gulf and the Gulf of Oman is not only useful for navigation and coastal engineering works, but is essential for understanding the detailed movement of oil slicks, such as the oil slick due to the Nowruz spill in the early part of 1983. It can be shown that tidal motion may disperse the slick somewhat, but most of the movement is due to wind and storm surges associated with the Shamal.

METEOROLOGICAL CONDITIONS

Detailed descriptions of the weather systems in the Inner Gulf and Gulf of Oman region are discussed by Murty and El-Sabh (1984). As already mentioned, the sub-synoptic scale wind known as Shamal has a significant influence, particularly in the northern part of the Inner Gulf. The winter Shamal occurs mainly during November to March and is associated with mid-latitude disturbances travelling from west to east. It usually occurs following the passage of cold fronts and is characterized by strong northwesterly winds, mainly during December to February. The summer Shamal occurs during June and July and is associated with relative strengths of the Indian and Arabian thermal lows. The summer Shamal is not as important as the winter Shamal from a storm surge point of view. Based on duration, the winter Shamal can be divided into two types: a) those which last 24 to 36 hours, and b) those which last 3 to 5 days.

Although the winter Shamal typically occurs only once or twice every year, it brings some of the strongest winds to the Inner Gulf region. The shorter duration Shamal (24 to 36 hours) are more frequent. Shamal conditions rarely occur over the northern part of the Inner Gulf during the month of September (Perrone, 1981). Usually the Shamal occurs first in the northwestern part of the Inner Gulf and then spreads south and east behind the advancing cold front. It takes about 12 to 24 hours for the Shamal to spread from the northwest corner to the southern part of the Inner Gulf.

The onset of the Shamal is not easy to predict, mainly because of the difficulty in forecasting the associated upper air pattern. Once the Shamal had begun, it may subside within 12 to 36 hours after the passage of the cold front or it may persist for three to five days. At the onset of the Shamal, the wind direction is strongly influenced by the coastal orography. In the northern part of

the Inner Gulf the Shamal winds generally blow from a direction between N and WNW. In the middle part of the Gulf, Shamal winds tend to be from a direction between WNW and NW. On the southeast coast of the Gulf, the winds are westerly. In the Strait of Hormuz area, the Shamal winds are generally from the southwest.

In general, the speed of the Shamal winds ranges from 20 to 40 knots. Because of the large pressure gradient between the low over the Gulf of Oman and the high over Saudi Arabia, the Shamal winds are strongest in the southern and southeastern parts of the Inner Gulf. Average wind speeds in the southern and southeastern parts of the gulf range from 30 to 40 knots, with peak winds up to 50 knots. Winds over the northern part tend to be 5 to 15 knots less than the above values, on the average. Two areas of the Inner Gulf appear to experience stronger than average Shamal conditions (Perrone, 1981). These are areas near the Qatar Peninsula and Lavan Island (Figure 2).

NUMERICAL MODELLING OF STORM SURGES

The linearized versions of the shallow water equation are:

$$\mu_t = -(du)_x - (dv)_y \qquad (1)$$

$$u_t = -gu_x + fv - F^{(u)} + G^{(u)} \qquad (2)$$

$$v_t = -gu_y - fu - F^{(v)} + G^{(v)} \qquad (3)$$

where $\mu(x,y,t)$ = elevation of water surface above mean level

$u(x,y,t)$ = depth-averaged velocity in x-direction

$v(x,y,t)$ = depth-averaged velocity in y-direction

$d(x,y)$ = mean water depth

x,y = Cartesian coordinates in horizontal plane

f = Coriolis coefficient (assumed constant)

g = acceleration due to gravity

t = time

$F^{(u)}, F^{(v)}$ = friction terms

where the subscripts in equations (1) to (3) denote differentiation with that variable. One can either use a linear form for the bottom friction as in equation (4) or a quadratic form as in (5), where r is a linear friction coefficient and k is a dimensionless quadratic friction coefficient.

$$F^{(u)} = ru; \quad F^{(v)} = rv \qquad (4)$$

$$F^{(u)} = ku(u^2+v^2)^{\frac{1}{2}}/d; \quad F^{(v)} = kv(u^2+v^2)^{\frac{1}{2}}/d \qquad (5)$$

Figure 3 shows the square grid used in the computations, and the inset shows the finite-difference scheme. The Strait of Hormuz is taken as an open boundary. At the interior points of the grid, equations (1) to (3) have the following finite difference forms.

$$\frac{\mu'_{ij} - \mu_{ij}}{\Delta t} = - \frac{(d_{ij}+d_{i+1,j})u_{i+1,j} - (d_{i-1,j}+d_{ij})u_{ij}}{2\cdot\Delta x} - \frac{(d_{ij}+d_{i,j+1})v_{i,j+1} - (d_{i,j-1}+d_{ij})v_{ij}}{2\cdot\Delta y} \quad (6)$$

$$\frac{u'_{ij} - u_{ij}}{\Delta t} = - g\frac{\mu'_{ij}-\mu'_{i-1,j}}{\Delta x} + f\bar{v}_{ij} - F^{(u)}_{ij} + F^{(u)}_{ij} \quad (7)$$

$$\frac{v'_{ij} - v_{ij}}{\Delta t} = -g \frac{\mu'_{ij}-\mu'_{i,j-1}}{\Delta y} - fu'_{ij} - F^{(v)}_{ij} + F^{(v)}_{ij} \quad (8)$$

where

Δt = time step

$\Delta x, \Delta y$ = grid interval sizes in x,y directions respectively

d_{ij} = mean water depth at elevation point μ_{ij}

$$\bar{u}_{ij} = \frac{1}{4}\,(u_{i,j-1} + u_{i+1,j-1} + u_{ij} + u_{i+1,j}) \quad (9)$$

$$\bar{v}_{ij} = \frac{1}{4}\,(v_{i-1,j} + v_{ij} + v_{i-1,j+1} + v_{i,j+1}) \quad (10)$$

The following stability criterion is used in determining the optimum time-step.

$$\Delta t \leq \frac{\Delta x \cdot \Delta y}{[gd_{max}\,(\Delta x^2+\Delta y^2)]^{\frac{1}{2}}} \quad (11)$$

RESULTS

Storm surges in the Inner Gulf. Figure 4 shows schematically the spatial structure of the storm as it advances one grid space in the x-direction in one time-step. This storm thus has a life of about one day and is supposed to represent a short duration winter Shamal. Figure 5 shows the wind directions as simulated for a winter Shamal. Figure 6 shows the computed profiles of the M_2 tide and M_2 tide plus storm surge (due to a short duration winter Shamal). At selected grid points Figure 7 shows for the same locations computed profiles of tide (with three semi-diurnal and three diurnal constituents included), tide plus storm surge and storm surge alone.

Next we made additional simulations with the same wind directions, but for a longer duration (4 to 5 days) Shamal. The results for these simulations are shown in Figure 8. Figure 9 shows the results of the simulations with three times stronger wind stress while Figure 10 shows the results of the simulations when the wind constantly blows from the positive y direction. Plots of the horizontal distribution of the storm surge heights at two different times are shown in Figure 11. From these various types of plots, it can be seen that significant positive and negative storm surges can occur in the Inner Gulf. The tide is also important.

Storm surges in the Gulf of Oman

Next we will consider briefly the storm surge problem in the Gulf of Oman. Since the Gulf of Oman is deeper than the Inner Gulf, one would expect the storm surge threat in the Gulf of Oman to be somewhat less than that in the Inner Gulf, and the few available observations appear to suggest the same result. Most of the tropical cyclones of the Arabian Sea either travel westward or recurve and thus they rarely travel over the Gulf of Oman. This is not to say that significant surges do not occur in the Gulf of Oman; rather, that the frequency of their occurrence is small.

The Strait of Hormuz lies in the boundary region between the west to east travelling extra-tropical cyclones and the east to west travelling tropical cyclones. One could expect significant surges in the Strait of Hormuz, either from tropical cyclones or from extra-tropical cyclones.

Finally no storm surge forecasting in real time can be made without taking the tides into account. Since the Indian Ocean tide enters the Arabian Sea, travels into the Gulf of Oman, then into the Inner Gulf through the Strait of Hormuz, for a better understanding of the tides one should make measurements of the tides at the junction of the Arabian Sea with the Indian Ocean.

Summary and recommendations for future work

Some important results emerge from the present study. As already discussed, it is wind stress that is overwhelmingly responsible in generating storm surges in the Inner Gulf and the Gulf of Oman. The role of the atmospheric pressure gradients is relatively small, if not insignificant.

The Inner Gulf is traversed by extra-tropical weather systems, and the Gulf of Oman occasionally by tropical cyclones; the east to west travelling tropical storm tracks and the west to east travelling extra-tropical weather system tracks converge in the Strait of Hormuz area. Here one can expect complex and interesting storm surge effects.

Another significant point is the occurrence of negative surges in the shallow parts of the Inner Gulf. This may have implications for navigation, coastal engineering works and dispersal and movement of oil slicks and other pollutants, etc. In the deeper Gulf of Oman negative surges are unlikely to occur, but as shown in table 1, specialized observations are needed. In addition, whereas the duration of the storm surges in the Inner Gulf could be long (up to 2 days), in the Gulf of Oman they may last only a few hours. However, this tendency (which is due to the difference in the nature of tropical and extra-tropical weather systems) might be counteracted by on opposite tendency, namely, that bottom friction in the shallower Inner Gulf will tend to dissipate the surges faster than in the Gulf of Oman.

ACKNOWLEDGEMENTS

Mr. M. Rasmussen did all the computer programming for this study. We also thank Mrs. Jocelyne Gagnon for typing the manuscript, and Ms. Coralie Wallave for drafting the figures. This study was supported in part by grants from the Université du Québec à Rimouski and NSERC of Canada to M. El-Sabh.

REFERENCES

Murty, T.S. and M.I. El-Sabh (1984) Storm tracks, storm surges and sea state in the Arabian Gulf, Strait of Hormuz and Gulf of Oman. In: M.I. El-Sabh (ed.) Oceanographic Modelling of the Kuwait Action Plant (KAP) Region. UNESCO Repts. in Mar. Sci. No. 28:12-24.

Perrone, I.J. (1981) Winter Shamal in the Persian Gulf. Naval Environmental Prediction Research Facility. Monterey, Calif. Tech. Rept. I.R. 79-06.

Table 1: Differences between hurrican-generated and extratropical storm-generated surges

Parameter	Tropical system	Extratropical system
Size of storm.	Small.	Large.
Representation on weather charts.	Sometimes difficult to position on weather charts using ordinary weather reports. The vigorous portion of the storm may lie between two observing stations.	Easy.
Requirement of specialized observations such as satellite, weather reconnaissance, radar, aircraft.	Needed.	Usuallay not required. Standard weather reports usually adequate unless mesoscale systems are embedded.
Amplitude of surges.	Greater. The maximum surge created in the U.S. was at Gulfport (Miss.) following Hurricane Camille in August 1969 - 7.5 m.	Smaller. Largest surge of 2.5 m was at New York City in Nov. 1950.
Duration of surge.	Short. (Several hours to ½ day).	Long (Several days).
Inland inundation.	Large.	Little.
Length of coastline affected by the surge.	Less usually than 160 km.	Several hundred km.
Geometry of the storm.	Compact and nearly symmetrical.	111-defined and sprawling geometry.
Speed of movement of the storm.		Slow motion along a regular track.
Pressure gradients and wind stress associated with the storm.	Easy to model the driving forces. Could be represented analytically.	Difficult to model the driving fields.

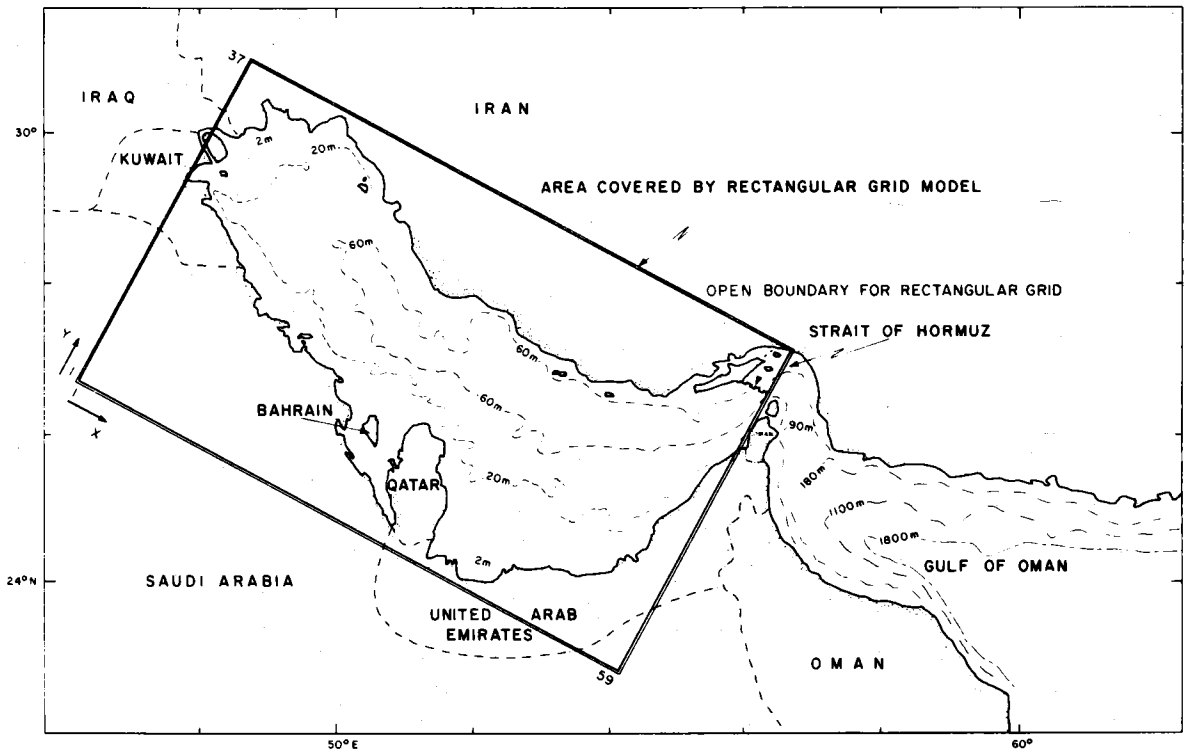

Figure 1: Bathymetry and geography of the Inner Gulf area.

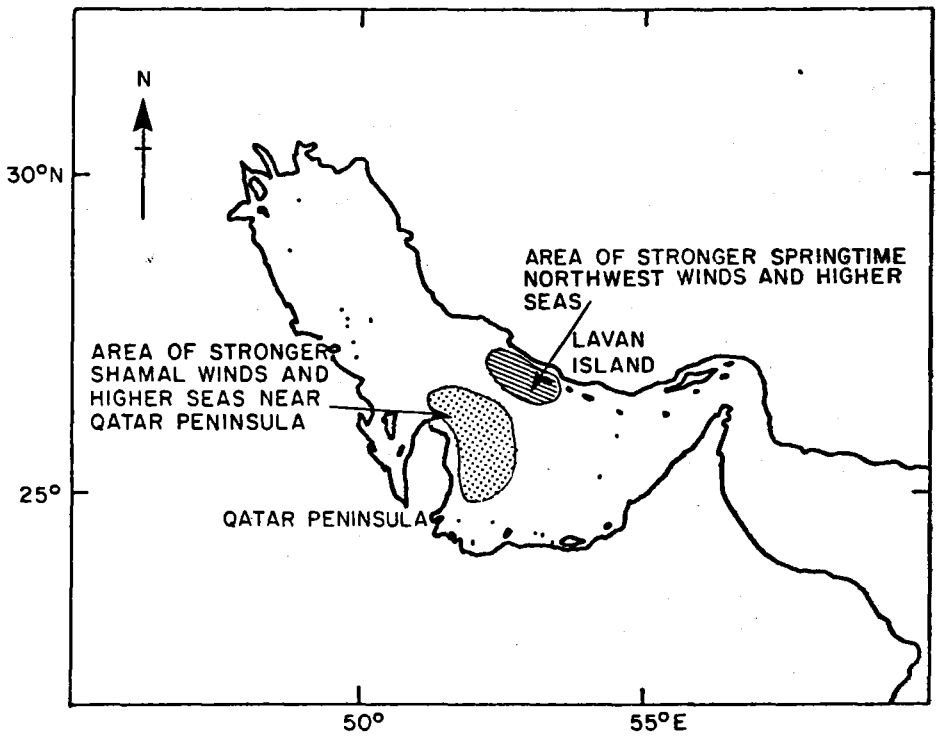

Figure 2: Areas of stronger than normal northwesterly winds and higher seas.

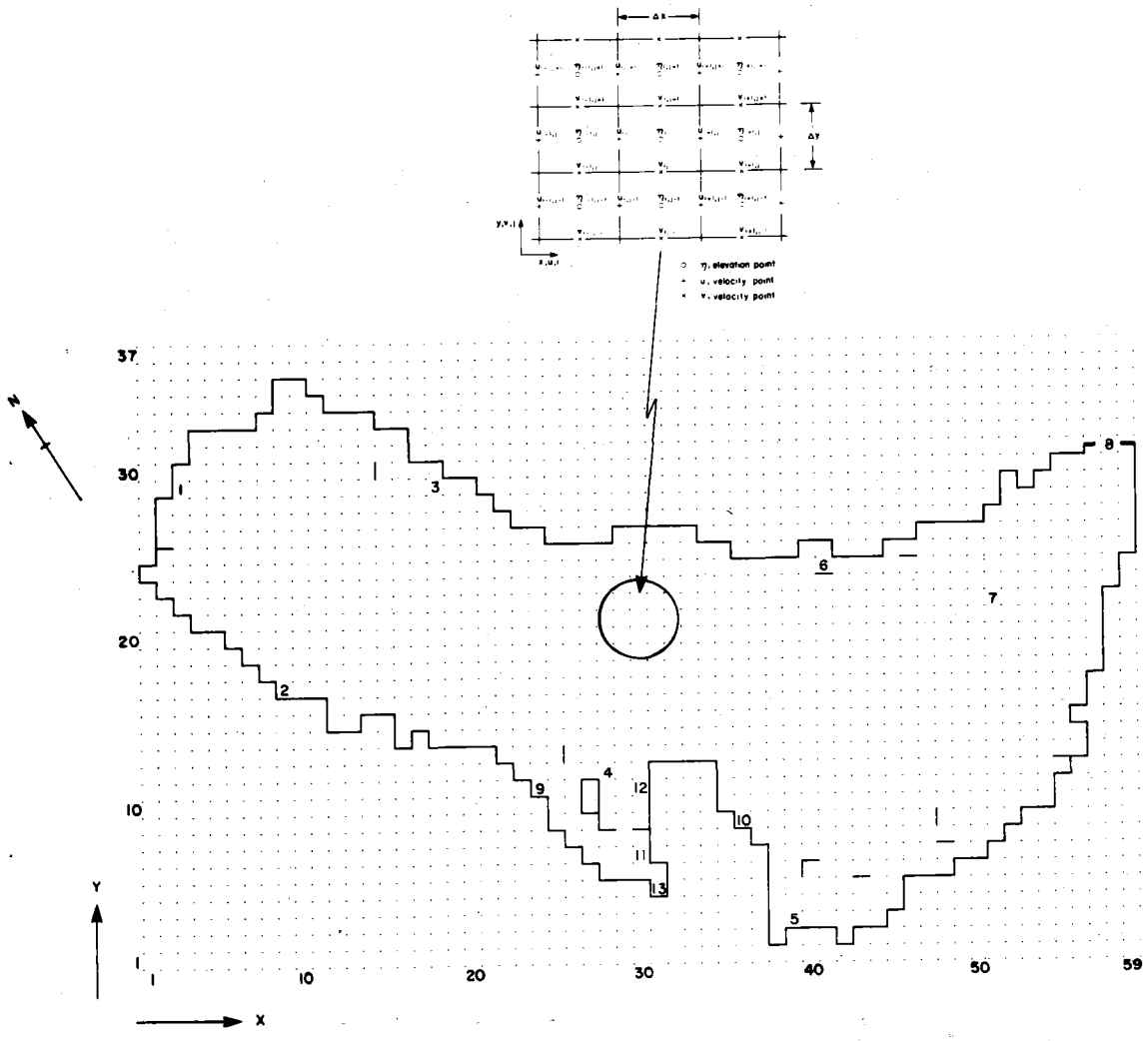

LEGEND

Station 1. Shat Al Arab Bar, Iran	**Station 8. Strait of Hormuz**
Station 2. Ras Al Mishaab, Saudi Arabia	**Station 9. Dammam, Saudi Arabia**
Station 3. Bushire, Iran	**Station 10. Doha, Qatar**
Station 4. Mina Salman, Bahrain	**Station 11. Janan, Qatar**
Station 5. Jazirat Ghagha, U.A.E.	**Station 12. Ras'Ashairiz, Qatar**
Station 6. Jazirat Shaikh Shuaib, Iran	**Station 13. Al Hamlah, Qatar**
Station 7. Jazirat, Sirri, Iran	

Figure 3: The square grid used in the computations. The inset shows the finite-difference scheme.

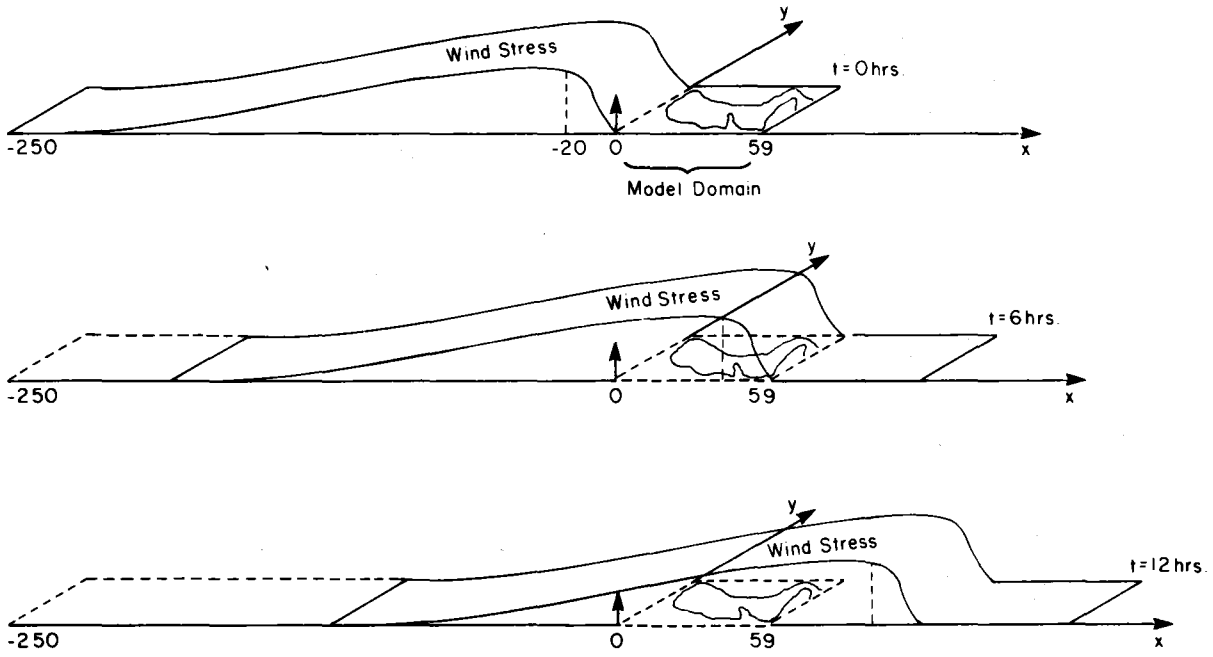

Figure 4: Schematic of the wind field used.

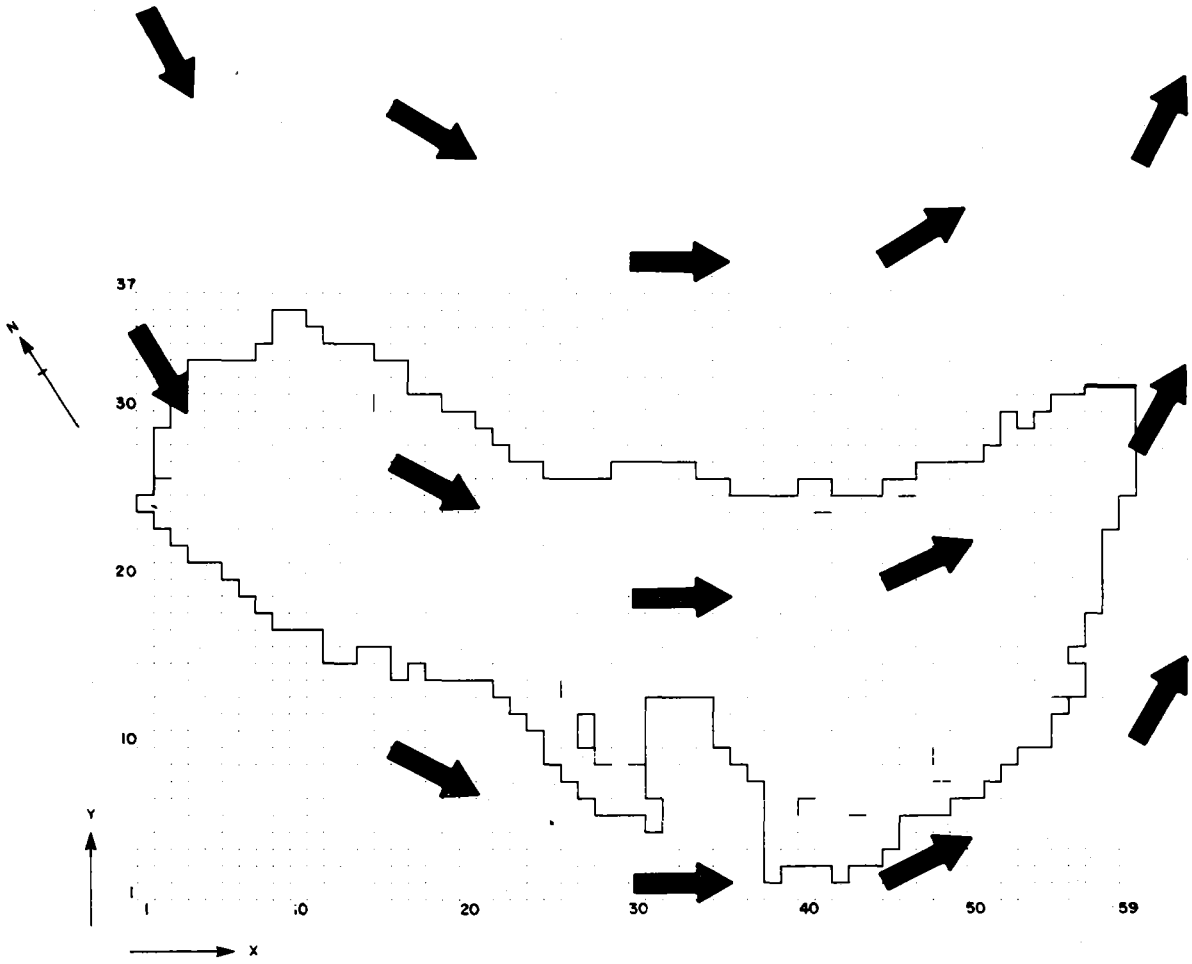

Figure 5: Wind directions used in the numerical simulation.

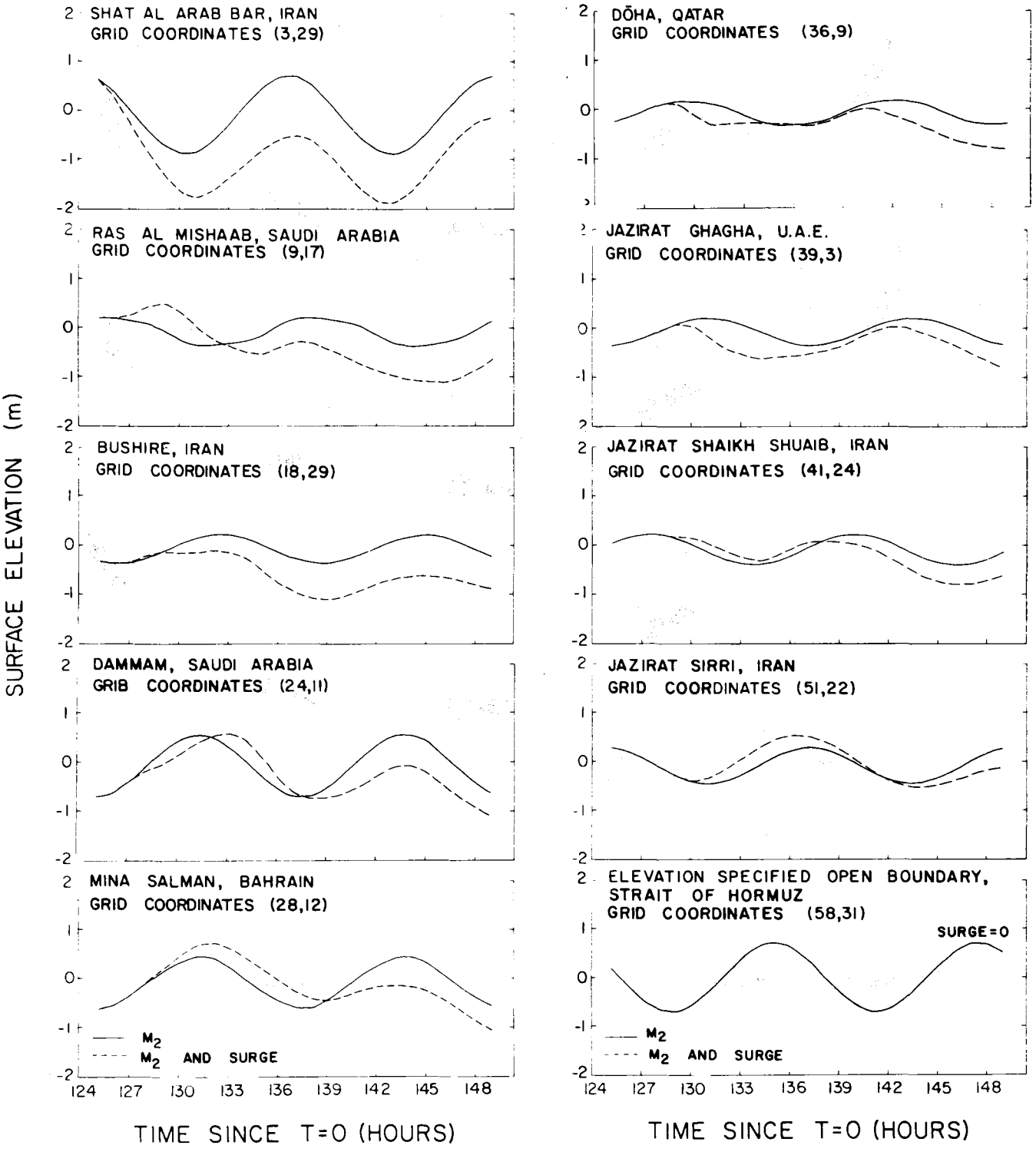

Figure 6: Computed profiles of the M_2 tide and the storm surge plus M_2 tide at selected locations.

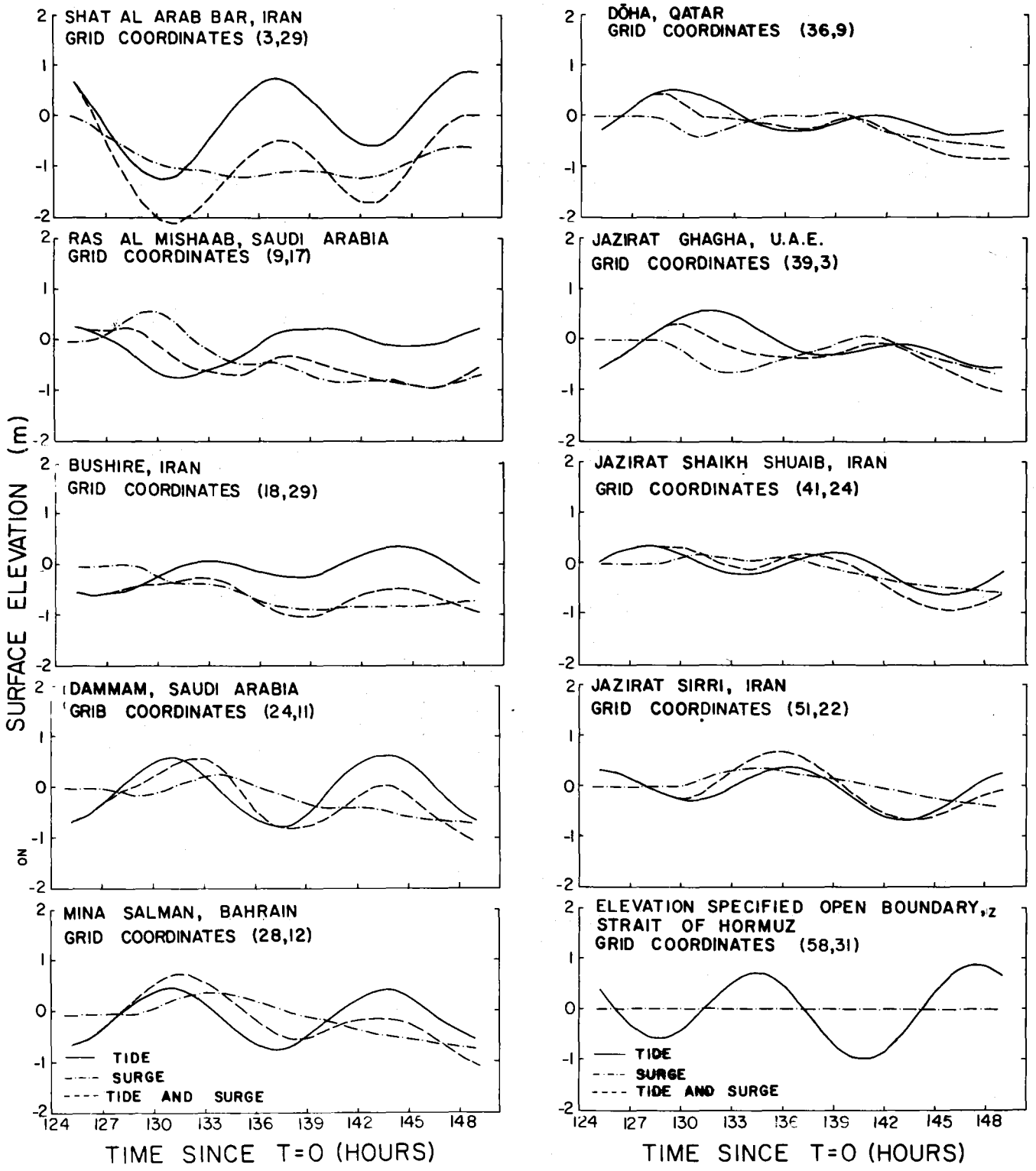

Figure 7: Computed profiles of the tide and six constituents (M_2, S_2, N_2, K_1, O_1, P_1) are included, surge plus tide and surge only at selected locations.

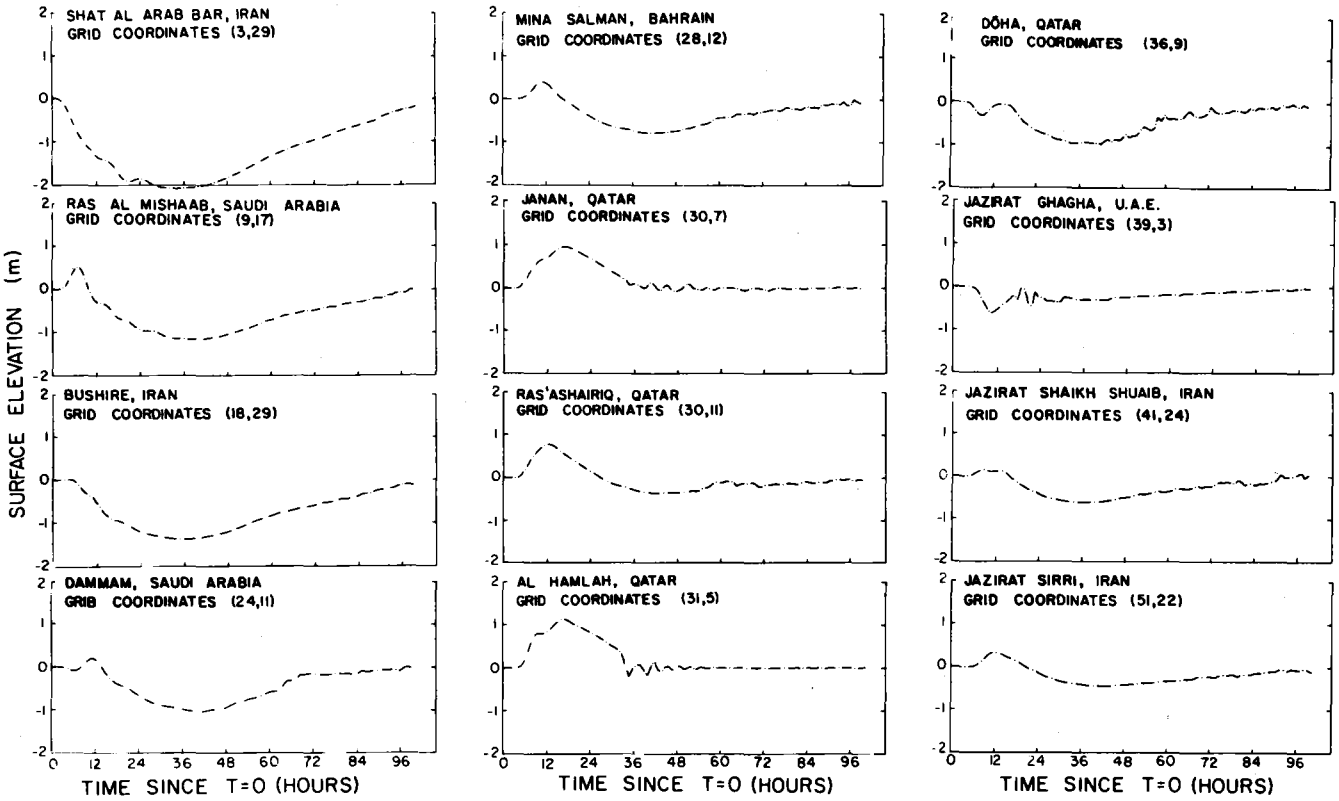

Figure 8: Results of simulations for longer duration winter Shamal.

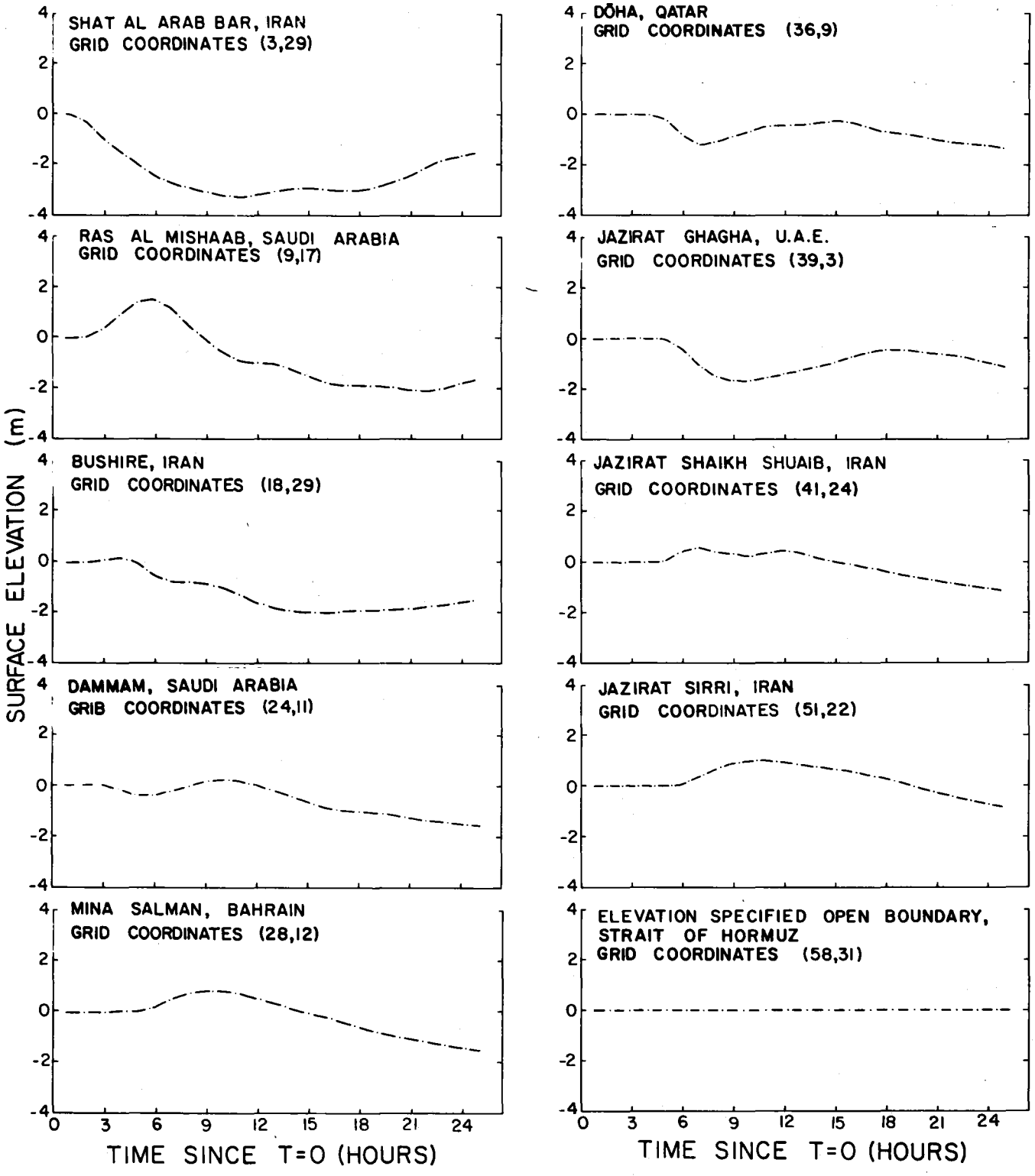

Figure 9: Results of simulations for long duration winter Shamal. Wind stress used is three Pascals.

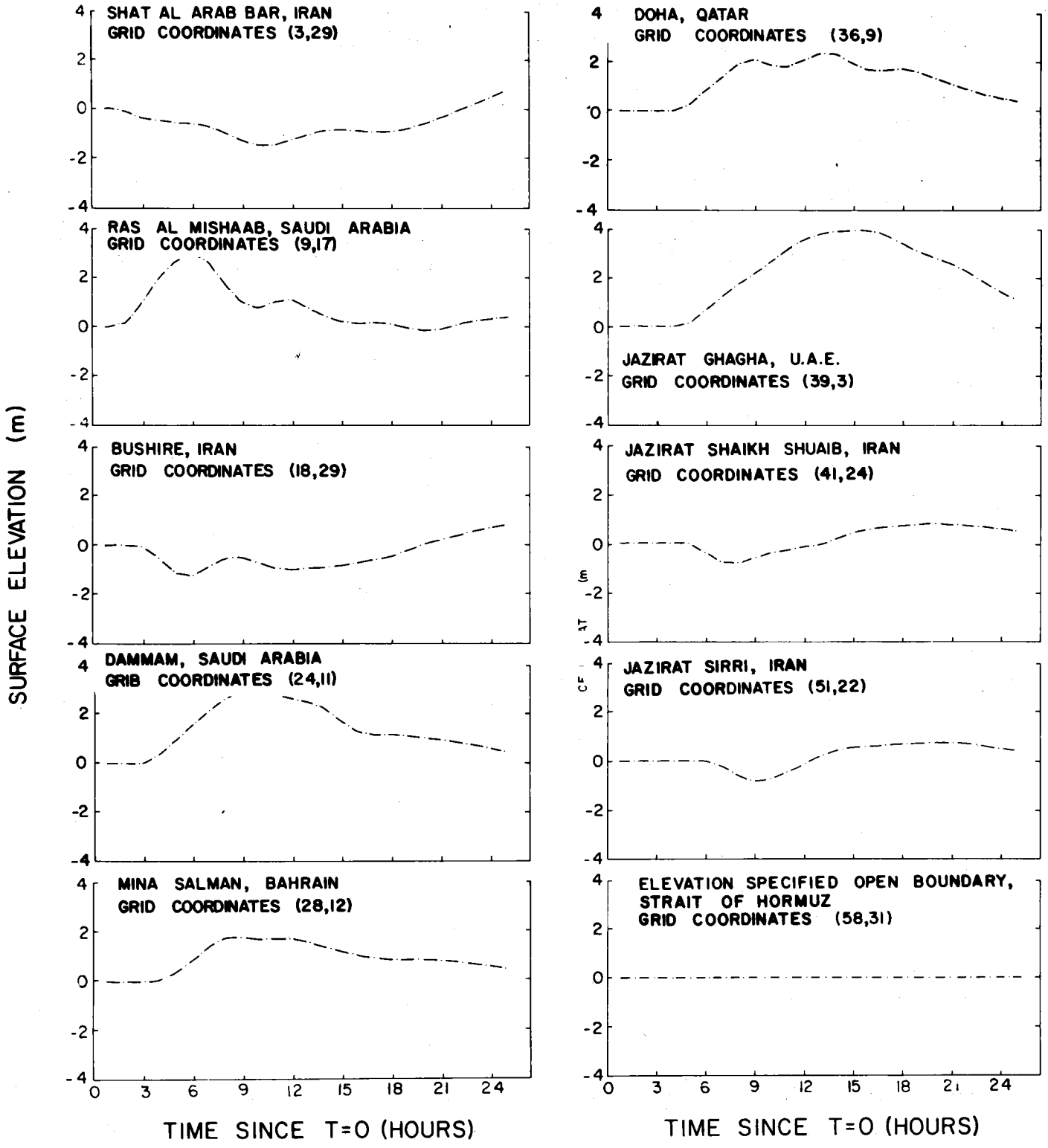

Figure 10: Results of simulations for long durations Shamal. The wind blows constantly from the positive y direction.

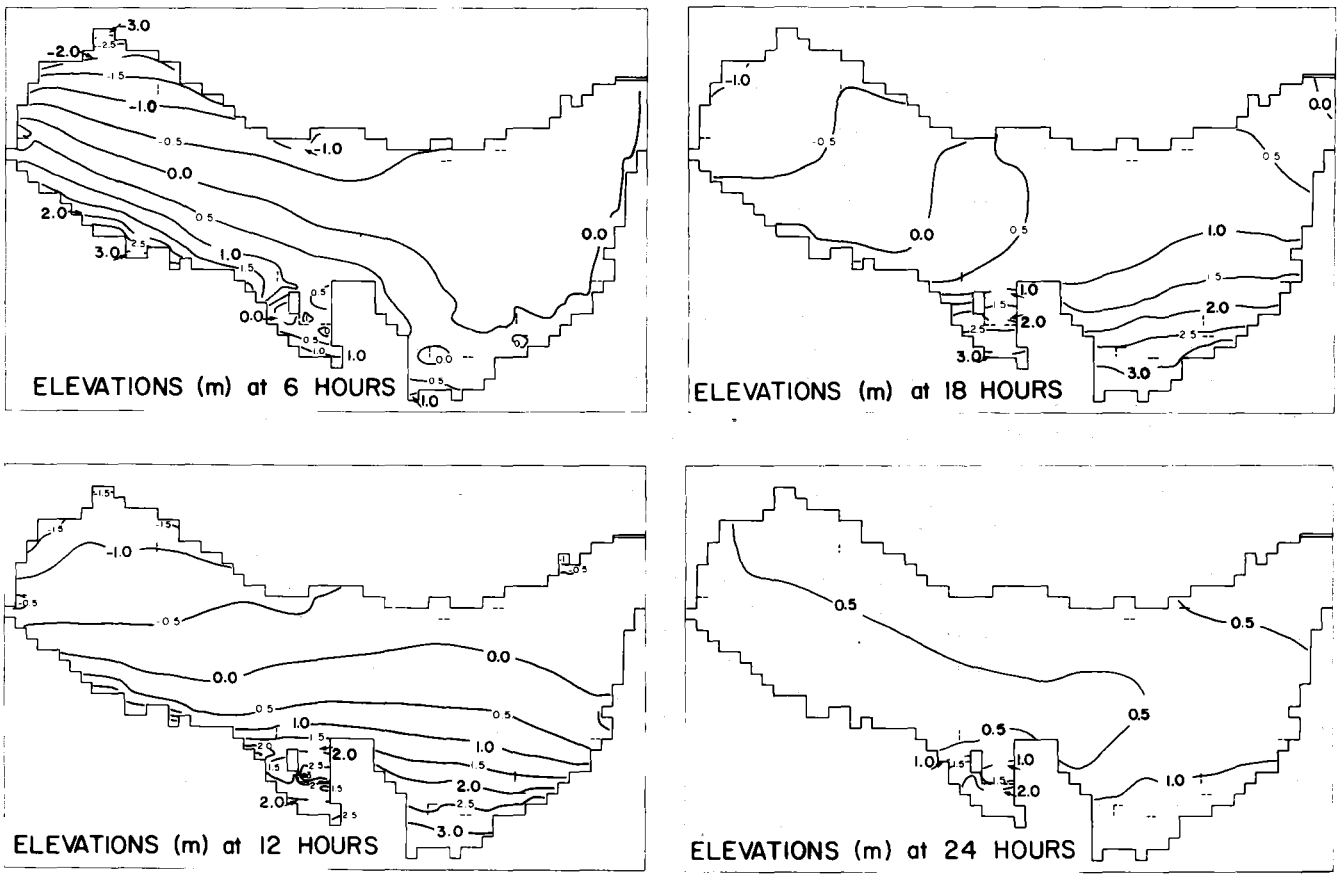

Figure 11: Distribution of storm surge heights.

Although different classifications are possible, those listed above have been found useful since specific algorithms can be applied to each of the categories and this breakdown generally corresponds to the terms in the classical mass balance or distribution of variables equation that is the fundamental underlying principle addressed by all spill trajectory models. In differential form, this equation can be written:

$$\frac{\partial c}{\partial t} + \vec{\nabla} (c\vec{v}) = \vec{\nabla} (k \vec{\nabla} c) + S \qquad (1)$$

where:

c = the pollutant concentration in an Eulerian sense (i.e., mass/volume or mass/area in the case of a floating pollutant)

$\vec{\nabla}$ = vector operator $\vec{i} \frac{\partial}{\partial x} + \vec{j} \frac{\partial}{\partial y}$

v = vector advective velocity

k = diffusion coefficient

The first term on the left-hand side of this equation gives the local time-rate change of the pollutant at a particular point, i.e., this is the rate of increase or decrease of pollutant that an observer would see if he were at a fixed location. The second term on the left-hand side of the equation is the advection, or movement, of the pollutant due to the movement of the media itself. More generally, this is any movement of the pollutant due to the deterministic fields and it can be represented as the divergence of the mass flux (cv). The first term on the right-hand side of equation (1) represents the diffusion, or sub-advection scale spreading, of the pollutant. Here it is written as simple Fickian diffusion (the details of how this formulation was reached and the assumptions that it entails will be discussed in the following sections). The final term in equation (1) represents the sources and sinks of the pollutant. These must include a description that specifies when, where and how each pollutant enters the environment (i.e., the characteristics of the spill) and how the pollutant is removed from the surface marine environment (i.e. evaporation, weathering, beaching, or cleanup).

With this as the basic conceptual framework the individual terms in this formulation are now discussed.

ADVECTIVE PROCESSES

A major and distinctive feature of the marine environment is its continual state of movement. The idea that pollutants introduced into water will move with the water is pretty well accepted and understood. Additionally, the common experience of walking along the beach and examining flotsam found there makes it clear that ocean currents can transport objects or pollutants very long distances. All of this points to the fact that one of the central, if not major, factors in pollutant trajectory analysis for the marine environment is to develop an understanding of ocean currents.

The understanding of ocean currents is an extremely ambitious undertaking and has held the attention of many physical oceanographers for a number of decades. Libraries are filled with the results of their work. Classical descriptive works,

SIMULATION OF MOVEMENT AND DISPERSION OF OIL SLICKS

by

J. A. Galt
National Oceanographic & Atmospheric Administration
Office of Oceanography and Marine Services
Seattle, Washington

ABSTRACT

A number of physical processes affect the movement and spreading of hydrocarbons in the marine environment. These processes typically include advection, spreading, turbulent diffusion, wave/oil slick interactions, weathering of the oil, and beaching. This paper discusses these physical phenomena and the various algorithms and procedures used to represent them. The sensitivity of the simulation results from these procedures is examined relative to realistic geophysical data and operational constraints.

For many applied problems, alternative model formulations or configurations, such as a priori assessment studies, contingency planning and tactical support for spill response, may be useful. These alternative formulations are examined and illustrated with examples.

INTRODUCTION

This work is intended to present a review of the physical processes and algorithms which affect the movement and spreading of oil slicks in the marine environment. It differs, however, from a typical review paper in several ways. First, there is no attempt to present a comprehensive bibliography, as these are available in a number of other sources (Stolzenhach et al., 1977; American Petroleum Institute 1977, 1979, 1981, 1983). Secondly, this work will confine its attention to floating pollutants and will not attempt to cover the problems of how hydrocarbons mix down into the water column. Once again, other authors have addressed this problem and the reader should refer to them (Kolpack, 1977, Reed et al., 1983).

Having introduced the caveats as to what this paper is not, the more positive aspects of what will actually be covered may be outlined. The procedures and opinions presented in this work are based on experience gained during eight years of activity in a national spill response programme. During these studies, well over one hundred spills or potential spills were investigated by the author. These spills ranged in size from a few gallons in protected inland waters to multi-million gallon spills associated with large tanker accidents or well blow outs. The duration of individual studies ranged from as short a time as one hour to as long as ten months.

It is perhaps worth reiterating that these studies were carried out in direct support of spill response and contingency planning activities. This introduces a different set of conceptual biases than might otherwise be the case. This approach is one of applied science, somewhere between the empiricism that is traditionally associated with engineering and the esoteric realm of pure science. To elaborate further on this approach; in investigating physical processes, details are pursued down to the point where they affect the simulation algorithms that can be used, and explored to the extent that available input or descriptive data have some likelihood of determining a particular trajectory estimate. Beyond this level of detail, the processes are only relative in obtaining error information. It is at least as important to know what is not included as to know what is included. That is, these "sub-resolution" interactions must be understood only to the extent that it is necessary to put appropriate caveats on the forecast estimates.

The next section of this paper outlines the basic formulation of the spill trajectory problem. The third to sixth sections address specific processes associated with advection, spreading and diffusion, weathering, and beaching. The seventh section covers general computer requirements for real time trajectory modelling support. The final section discusses alternative strategies for model use and possible future developments.

BASIC FORMULATION OF THE SPILL TRAJECTORY PROBLEM

The physical processes that affect the movement and spreading of floating oil can be categorized in a number of different ways. In this paper, all the processes are grouped under the general categories of advection, spreading or diffusion, and weathering (sources and sinks). An additional process which represents boundary conditions (rather than the fundamental transport processes associated with the differential equation or initial conditions) is associated with beaching, and it is discussed separately.

such as Defant (1961), are familiar examples of descriptive and dynamic oceanography. Pedlosky (1979) or von Schwind (1980) provide a more theoretical coverage.

Before the pollutant trajectory specialist tries to take on this truly Herculean task of understanding ocean currents, it is appropriate to pose the following questions. Exactly what needs to be known about the currents and where can the required information be obtained? To answer these questions, the advective processes and their mathematical representations must be considered in more detail, starting with the simplest conceptual component of advection.

Currents cause a displacement of water elements and, consequently, a displacement of any pollutants which are suspended in or floating on the water. This can easily be represented as a classical Lagrangian problem and, in fact, this is by far the most straightforward approach to take for spill trajectory modelling. Clearly, if it is not known which way the water goes, the trajectory analysis will be incorrect at the most primitive level. It is a near certainty that the very first question which a spill trajectory specialist will be asked is, "Which way is the spill going to go?"

Looking back at equation (1), it may be noted that advection is actually represented as a differential term and it is worthwhile looking in more detail at this formulation. In particular, if we expand out the divergence of the mass flux term then

$$\vec{\nabla} \cdot (c\vec{v}) = c \vec{\nabla} \cdot \vec{v} + \vec{v} \cdot \vec{\nabla} c \qquad (2)$$

The first term on the right-hand side of this equation indicates that the differential change associated with advection has a component associated with the divergence or convergence in the fluid flow. For a three-dimensional, geophysical, fluid-flow problem the divergence is always zero so this term does not contribute. On the other hand, for the description of the surface distribution of a floating pollutant the two-dimensional divergence is not necessarily zero. Because of this, problems can easily arise in the representation of the advective fields. Consider, for example, flow in an irregular channel. Increases in depth must be compensated for by a stretching of the water column, causing a horizontal surface convergence. Conversely, decreases in depth must shrink the water column, causing a horizontal surface divergence. Thus it can be seen that flows entering deeper water tend to concentrate a floating pollutant, while flows into shallower regions tend to reduce the concentration of floating pollutants. Familiar examples of this kind of effect can be seen where flotsam tends to accumulate along the edge of a lake where a stream flows in.

In addition to the horizontal convergences and divergences caused by irregular geometry, it is found that variable density allows layering in the marine environment and variable layered depths can also cause convergences and divergences in the horizontal advective fields. Tidal circulation within estuaries often causes convergent slick lines where incoming salty water will slide under and mix with the less saline river runoff water. Such interfaces or frontal zones typically accumulate floating pollutants and it is not uncommon for spill trajectories in estuarine areas to be dominated by the convergence patterns associated with these mixing fronts.

On a slightly smaller scale, irregularities in the wind-driven flow cause surface roll vortices, referred to as Langmuir circulation (Assaf,et al., 1971). This circulation results in a series of convergent and divergent patterns along the

sea surface. These patterns tend to accumulate floating material and cause linear features in the pollutant distribution associated with the convergence areas. These linear convergence lines are observed under moderate and strong wind conditions virtually everywhere at sea, and during spill events the floating oil will also be distributed as linear slick lines.

All of the effects mentioned above can easily be seen in real spills. The advective currents that are used in a spill trajectory model should ideally be able to represent all of them. To the extent that they do not, the trajectory analysis clearly cannot simulate or represent these distributions. Here, then, is an identification of some possible errors associated with the misrepresentation of realistic convergences or divergences in the marine environment. Unfortunately, the problem becomes more complicated in considering the available data sources to represent advective flow fields.

Many spill trajectory models simply input a velocity field that is available from literature reviews, ship drift data, hydrographic studies, or single point drift or current meter observations. When this is done, the available data must be interpolated onto a continuum so that pollutants throughout the field can be advective. It is often the case that the interpolation procedures that are developed make no allowances for the two-dimensional divergence. For example, consider a trajectory model that uses a uniform, spatially constant current vector. Such a model will clearly give a strong convergence along any shoreline where the dot product of the outward-directed normal and the current vector are positive, and a strong divergence along any shoreline where that product is negative. This clearly does not make good sense from a physical point of view, and the trajectory estimates derived from such a model are bound to show unrealistic concentrations in some areas and forbidden zones along some coastlines where it is impossible for oil ever to go. Another commonly used interpolation procedure is to take data from a number of sources and interpolate based on nearest neighbour considerations. Such schemes tend to distribute the divergences and convergences along line sources where the lines are bisectors between the given data points. Once again, using such fields leads to peculiar distributions in the estimated pollutant fields. Advective flow fields can be made to have a much smoother appearance by the application of Laplacian filters. While these do tend to reduce the divergence in the field they do not solve the actual problem associated with these kinds of misrepresentations.

Having noticed that the distribution of pollutant trajectories is strongly influenced by the real two-dimensional divergences and convergences in the marine environment and, consequently, can be badly misrepresented by unrealistic convergences and divergences, it is important to develop a strategy for processing advective field data for use in spill trajectory models. Ideally, advective fields to represent ocean currents should be generated by mass-conserving, hydrodynamic flow models (Galt, 1980; Galt and Payton, 1981). If observed or historical data are used in a spill model then it is imperative that the interpolation functions used to transfer the data to the conceptual continuum must conserve mass. However, the advective fields are represented in a spill model, the continuity-preserving or mass-preserving routines should include as fine a space scale as is practical. Scales which are not represented, for example Langmuir scales or estuarine fronts, must be identified or flagged as missing. When the overall trajectory analysis is being carried out, these missing components must be included in the estimates of uncertainty and in the descriptive documentation that should be presented at all spill trajectory estimate briefings.

A number of possible sources for advective information have been mentioned, i.e., ship drift, current meter data, numerical models, etc. None of these data sources gives truly representative values of surface currents. This clearly points

to the next major problem for trajectory analysis which still falls into the general area of advective processes, i.e., what is going on right at the ocean surface?

It is well known that, at the air-sea interface, a number of physical processes are active that cause currents which are present in only the top meter or so, and these are typically not represented in any of the standard current estimates. One of the primary components of this drift is caused by surface gravity waves. This so-called Stokes drift is a non-linear effect which is associated with the steepness of the waves. The wave steepness is dominated by the short gravity waves which, in turn, tend to be well-correlated with the local, real-time winds.

An additional surface current can be caused by the wind stress acting directly on the ocean surface. In steady linear theory this gives an Ekman drift. More complex theories may include Langmuir circulation (Assaf et al., 1971) or Prandtl layers. Regardless of which theories are used, the net result is a downwind current or nearly downwind surface current at approximately two per cent of the mean wind speed.

It is an observed fact that during an oil spill any organized slicks move through the water at a speed that is greater than the surface current in a downwind direction. This has been referred to as a leeway effect but the connotation is incorrect in that it implies that this drift is associated with direct wind stress forcing. The actual mechanism for this differential oil-water velocity is associated with the absorption of surface gravity waves by the slick. An oil slick looks smooth, or slick, because it dampens small capillary and surface gravity waves. The momentum that is present in the waves must then be transferred to the oil slick itself. This wave stress then pushes the oil in the direction of the dominant short gravity and capillary waves, which is downwind. Detailed studies of this mechanism have failed to pinpoint exactly how this process takes place, but the net result is clear and undisputed (Stewart, 1976). Since the oil slick is driven by the absorption of small gravity and capillary waves and these waves tend to be in equilibrium with the local real-time winds, there is once again an advective transport mechanism which is correlated with the wind.

It may be noted that all three of the surface active processes which have been described above are actually currents or momentum transfer and that they are all well-correlated with the wind. In addition, any floating hydrocarbons will be advected by these processes. When grouped together, these processes all make up what is referred to as the wind drift factor. Typical trajectory models take this to be a simple displacement at 3 per cent of the wind speed. Theoretical studies suggest that Ekman currents should have a slight rotation with regard to the wind direction, but considering the accuracy that is available for wind data in marine areas this is a moot point. No practical operational case is known to the author where the application of a small rotation angle would have made any relevant difference in the outcome of the trajectory analysis.

A advective processes covering all the organized and well-defined displacements associated with classical ocean flows, such as tides, geostrophic currents, estuarine flows and barotropic wind drift have been discussed. To these must be added the specific surface phenomena which are correlated with the wind but not directly related to stress-driven displacement of the oil. This combination will give a relatively complete description of advective processes, providing that care is taken not to misrepresent the divergence when using various interpolation schemes. Before leaving the subject of advective processes, a couple of additional pitfalls to be avoided should be pointed out.

In shallow marine areas such as bays and lagoons, the wind can set up and drive a significant barotropic mean flow (this is in addition to any Ekman or Stokes drift effects). The general advective circulation is then also correlated with the wind. This couples the general circulation and the wind drift factors and leads to a correlation in the transport components. With such a correlation, the variations in the winds take on an added significance, since the mean of the summed displacements is not the same as the sum of the mean displacements. This is a classical problem of the sums of random variables which are not independent of each other. Trajectory analysis routines should account for these correlations where possible and at least recognize them when they are not explicitly included in the trajectory estimates.

As a final point, many older trajectory models based on observed data have presented displacement algorithms that specify floating oil as moving at some fraction of the current (typically 70 per cent). From equation (1), it may be seen that this is equivalent to the statement that floating oil can swim upstream at 30 per cent of the current speed. Even the most blatant empiricist should question this statement, but somehow the notion has persisted and found its way into many operational manuals for oil spill trajectory forecasting. The origin of this myth is in fact not so hard to discover. Ten to fifteen years ago, current measurements were typically made with savonius rotor meters that simply sampled the direction of the flow and integrated turns on a rotor. These meters were subject to wave pumping that significantly over-estimated the currents whenever the measurements were made near the ocean surface (Halpern et al., 1974). Unfortunately, this instrument error somehow got translated into the oil spill literature as a pollutant transfer process. It should be recognized for what it is and discarded from any trajectory analysis algorithms.

Advective processes are central to trajectory analysis. They totally determine the centre of mass of a spill and include the dominant effects of winds and currents. It is paramount that these fields not only represent appropriate directional information but they must also have realistic divergence properties if good results are to be obtained. Temporal correlations and real geophysical geometry are also important factors that must be included in the trajectory analysis equations. To the extent that any of these advective characterizations are unresolved or poorly described, the resulting trajectory analysis will be degraded. Such uncertainties or degradations must be reflected in the non-deterministic portions of the trajectory analysis which will be covered next.

SPREADING AND DIFFUSION

Spreading and diffusion processes as envisioned in spill trajectory analysis encompass the effects of a number of different physical mechanisms and there is some ambiguity in how to classify them. There is, in fact, no clear distinction between advective processes and diffusive processes that can be invoked purely on physical grounds. (One man's advection is another man's diffusion). In spite of this potential confusion, there is a practical distinction which can be used to separate these processes. In particular, advection can be thought of as deterministic. Spreading and mixing are attributed to additional movement about which there is some uncertainty. This suggests that the more that is known about advective processes, the less they would be expected to be represented as spreading or diffusion. To get a better idea of how this works, an example will first be given of some of the processes or mechanisms that lead to motion that is non-deterministic or uncertain in a typical trajectory analysis.

On the smallest scale, thermal kinetic energy causes Brownian movement with individual molecules exhibiting random motion. Statistical mechanics has been successful in describing this type of behaviour and predicting the macroscopic properties of the resulting distribution. This leads to the classical notions of isotropic diffusion. Even with this simple conceptualization, several features are evident which will need to be carried through for nearly all of the spreading and diffusion algorithms that are commonly used for trajectory analysis. First, the diffusive movements are not known in detail and, secondly, as a result of these motions particles move apart such that areas of high concentration are reduced with a net transport of material down concentration gradients. These concepts provide the basic analogy for the description of all our diffusive algorithms.

Considering slightly larger scales of motion, we find that the interactions depend on the macroscopic properties of the pollutant as well as the properties of the marine environment. These studies have traditionally been applied for hydrocarbons by examining the effects of gravity, surface tension and viscosity for an oil-water-atmosphere interface (Fay, 1969). The conceptual model used here is that of a pool of hydrocarbon floating on seawater. The formulation then uses dimensional analysis to consider balances between the various forces, and a three phase spreading law is derived. This is envisioned as a deterministic process rather than a statistical process so that in some regards it does not fit into the diffusion and spreading analogy stereotype, although it certainly does lead to heavy concentrations spreading out. The real point that should be made, however, is that three phase spreading is never seen to occur in real geophysical settings; other dispersive and mixing processes always dominate. Experience with hundreds of real spills indicates that three phase rules do not operate to yield useful improvements in simpler spreading and diffusion algorithms.

An examination of real geophysical flows in either the atmosphere or the ocean reveals that steady flows are rarely present. Winds always exhibit gustiness and ocean currents have eddies or vortices embedded in the larger scale flows that may, in turn, be seen as eddies in yet larger scale current patterns. This geophysical turbulence is fundamentally related to the non-linear advective terms (Hinze, 1959) that occur in the Navier-Stokes equation. Although these processes are of immense importance and have been the subject of extensive atmospheric, oceanographic and engineering research, formal mathematical solutions have proved elusive in spite of more recent applications of massive computer power.

Pioneering work by Reynolds established the early recognition that turbulent processes act in a dispersive manner, and a powerful mixing length analogy tied this much more complex turbulent diffusion back to the simpler molecular diffusion with the introduction of an eddy or turbulent diffusion coefficient.

Although the use of eddy coefficients is extremely helpful in representing mixing and spreading processes in natural geophysical domains, complexities still exist. The actual numerical values for eddy coefficients clearly depend on the scale that is being considered. For example, the small eddies behind a pier caused by tidal currents mix in qualitatively the same way as mesoscale eddies spawned off instabilities in the Gulf Stream, but the appropriate diffusion coefficients will vary by many orders of magnitude. In practice, these diffusion coefficients can only be evaluated empirically, and this requires a good deal of experience as well as a clear understanding of what processes the trajectory analysis is actually trying to represent.

To be a little more specific, if flows are modelled along a smooth but highly developed coastline and the mean flow is represented but the eddies behind piers, jetties and breakwaters are not resolved, then the empirical eddy diffusion

coefficient must represent the mixing associated with the turbulence induced by these "roughness elements". Alternatively, in modelling a large estuary, thermohaline flow patterns may be included while ignoring tidal currents as part of the advection. In this case, the turbulent diffusion coefficients must represent mixing associated with the energy input of tidal oscillations and its associated dispersion. The latter case typically requires much larger numerical values for the diffusion coefficients than the former. As a final example, consider modelling a shallow expansive coastal area by using seasonal or monthly current patterns. At this level, the wind-driven currents associated with individual weather systems (although deterministic to some degree) are uncertain, random or turbulent to the degree of resolution that is proposed. Once again, the turbulent eddy coefficients must be chosen to represent this uncertainty.

It may be noted that spreading and diffusive processes have covered such conceptually different things as spreading and turbulent diffusion on the one hand, and uncertainty on the other. This is a common source of confusion and many trajectory models use diffusive algorithms to represent both. These alternative views lead to quite different interpretations of the trajectory analysis results. As long as this is kept clearly in mind, no particular problem arises from the dichotomy. If, for example, a single plume of oil emanating from a ruptured hull is modelled, the mean flow carries the oil away, and mixing or turbulence widens the plume. A suitable specification of the diffusion coefficient will result in a plume with the correct aspect ratio. (Too big a diffusion coefficient and the plume widens excessively, too small a diffusion coefficient and the simulated trajectory is too filamentous). When properly done, the trajectory results can be interpreted as actual oil concentrations. Now, if the same problem were addressed with uncertainties concerning variations in the current or wind direction, then the diffusive algorithms could be used to represent uncertainty or measurement errors. The model would predict a similar plume but, in this case, the results would be interpreted quite differently. The plume distribution would now represent a probabilistic distribution of the oil and scatter would show possible locations for the pollutant, not actual concentrations. Such output is characteristic of trajectory analysis that is carried out for assessment purposes or which uses climatologically-based current and wind data. In any case, this dual use of diffusive algorithms must be carefully distinguished and the proper interpretation presented as a standard part of the briefing documentation that should accompany all trajectory analysis results.

The above discussion has focused on a number of processes which tend to be diffusive in nature. This selection presents a diverse and theoretically difficult, if not impossible, task to be addressed by trajectory models. Random events, observational errors, and forecasting uncertainties all appear. Given the actual difficulties associated with modelling spill events, it is unrealistic and unjustifiable to develop elaborate diffusion or spreading algorithms when the observational data, initial conditions and our understanding of geophysical processes will never be able to distinguish such subtle differences. Faced with this, a simple approach accompanied by careful interpretation and appropriate caveats seems to be the best. For example, with a Lagrangian formulation, a random walk diffusion algorithm has proved useful and easy to interpret. In these models, the diffusion operator in equation (1) is replaced by a Monte Carlo formulation.

Before leaving the subject of spreading and diffusive processes, it should be pointed out that state-of-the-art trajectory models do not have computers to deliver the whole analysis. It should always be kept in mind that advective processes indicate where the pollutant is going to go, but spreading and diffusive processes point to what it is going to look like when it gets there. In any real spill, the small scale processes determine the form in which the oil is going to appear.

Langmuir cells line the oil up in wind rows and thin linear features. Convergent zones in estuaries trap and hold oil. Radiation stress from waves can actually compress pools of oil such that individual large pancakes or patches can exist hundreds of kilometers from the spill site. Weathered tar balls can obtain a density close enough to seawater so that wave induced turbulence mixes them below the surface and down throughout the upper mixed layer. Under these conditions they may be nearly invisible to observational aircraft or even ships. All of these observational details may be important to response personnel. Any computer trajectory model which uses simple isotropic diffusion will always result in spill trajectory estimates that look like Gaussian plumes. On the other hand, no real spill will look like a Gaussian plume. Once again, any presentation of computer-generated trajectory analysis should include briefing documentation (oral or written) and it is here that the trajectory modeller must explain what the model includes and what it does not include. Careful explanations to the response personnel of what they are actually likely to observe in the field are necessary. Consideration has be given to advective processes describing where a floating pollutant will go and diffusive processes determining what it will look when it gets there. Consideration is now given to weathering which will address how much of the pollutant will actually arrive.

WEATHERING

The present paper is concerned with weathering processes that remove floating oil or hydrocarbons. This is obviously a somewhat restricted view since many potential pollutant transformations cause problems in other parts of the marine environment. Since this work deals with the trajectory modelling of floating hydrocarbons as pollutants, this framework will be maintained throughout the present discussion.

Oil and hydrocarbon products are combinations of thousands of molecular species. In addition, sea water is a chemically, biologically and, occasionally, geologically complex mixture. It is not surprising, then, that many different types of reactions are possible. Evaporation, agglomeration to sediments, dissolution, micell formation, oxidation and ingestion are some of the possibilities (Wolfe, 1977; Rosen, 1978). Each of these interactions has been studied in laboratory settings and, to a lesser extent, in the actual marine environment. As these potential interactions occur simultaneously, it is not surprising that no operative trajectory model tries to parameterize all these processes in detail.

Recent experience with the Nowruz oil spill suggests that sandfall may also provide a significant weathering mechanism, at least in the northern section of the Gulf. Data from sand traps in Kuwait indicate dust and sandfall as high as 100 tons/km2/month. This corresponds to 0.01 g/cm2/month. Weathered Nowruz tarballs appear to have densities close to that of the surface sea water. Under these conditions, sand deposits on the floating oil could easily increase its density to the point where it would sink. Unfortunately, little is known about the distribution of sandfall over the water of the Gulf so it is difficult quantitatively to evaluate the significance of this process.

Aggregate weathering algorithms have been proposed by a number of authors to represent many of these weathering processes (Kolpack, 1977; Mackay, 1980; Mackay and Leinonen, 1977). More recently, specific work has addressed how best to classify and parameterize hydrocarbons to describe their physical weathering properties (Mackay et al., 1983). It is perhaps not surprising that, until now,

most of the information developed about hydrocarbons has been presented by the petroleum industry and relates to information necessary either to refine, ship or pump the products (i.e., pour point, specific gravity, and distillation curves). In spite of major simplifications, most of the proposed aggregate algorithms still require more input data than is typically available during a short-term spill response. From a pragmatic point of view, an even simpler approach is needed. A crude approximation which can recognize major trends will be more useful than a detailed representation that does not have a very high probability of obtaining appropriate input data or the observational verification necessary to use the algorithm.

The development of a weathering algorithm can begin with the recognition that any hydrocarbon is made up of a great variety of molecules which have different molecular weights. It is also known that some of the major weathering processes depend roughly on molecular weight. This then suggests that hydrocarbons should be classified by their molecular weight fractional distribution (this also is closely related to the fractional distillation curves which is information that is typically available for most crude oil supplies).

How many different weight fractions are considered for any particular hydrocarbon pollutant is somewhat a matter of taste, but if each hydrocarbon is considered as being made up of a light, an intermediate and a heavy fraction (i.e., three weight classes), useful results can be obtained.

A simplified algorithm can be generated by assuming exponential loss (i.e., a half-life loss law) for each of the three fractional components. The lighter fraction will disappear quickly, the intermediate fraction more slowly, and the heavier fraction more slowly still. Although the exponential loss law behaves like a classical evaporation model, the evaporation rates are empirically derived and really represent a combination of evaporation, dissolution and other forms of accommodation. This is admittedly a simplistic approach and it is realized that research is being conducted which may lead to more effective weathering algorithms but for the present this approach provides a useful expedient. It has been used in a number of trajectory modelling studies (Galt and Payton, 1983; Gilbert, 1983; Torgrimson, 1983a,b).

An obvious question related to weathering algorithms is how to handle non-natural weathering processes such as the use of dispersants (by the limited definition of weathering used in this paper, effective dispersant use should be included in the trajectory analysis as a weathering process). Laboratory investigations of dispersant effectiveness have been presented (Mackay and Szeto, 1981) but the author is unaware of any large scale quantitative documentation for actual spills. Dispersants were used during the Amoco Cadiz spill and the IXTOC 1 spill, and there is no question that some fraction of the oil was removed as a surface pollutant, but in both of these cases the actual amount of spill material was so overwhelming that the results did not appear to be quantitatively significant. Nonetheless, for smaller spills and as more effective application techniques become available, the effects of dispersant use should certainly be included in spill trajectory analysis and weathering algorithms.

From a computational point of view, it should be noted that the three-part exponential weathering law described above can be implemented in a Lagrangian framework using a Monte Carlo formulation. This can be calculated in such a way that pollutant particles need not carry age or type data associated with them and this has the potential of saving considerable computer storage. On the other hand, if individual Lagrangian pollutant elements are allowed to be characterized by such additional descriptors as age and pollutant type, many other empirically-derived

weathering algorithms can prove useful. For example, experience in observing and tracking many spills at sea has shown that, as oil concentrations get smaller and individual patches weather, observability decreases. In this case, overflights, even with trained observers, may return negative results. Modellers want to keep track of such conditions since landfalls of even widely scattered tarball concentrations can make significant coastal impacts even though the same oil concentrations may go undetected at sea. To represent these conditions in trajectory analysis, the following algorithms have been used: when oil concentrations become small and the average age of the pollutant Lagrangian particles goes beyond three or four half-lives of the intermediate weight class for the type of pollutant spilled then the spill trajectory output maps indicate a low probability of detection. This introduces the concept of trace quantities of pollutants into the trajectory analysis results and, although it is based on empiricism, the results tend to be useful and have held up as qualitiatively verifiable over the course of a number of spills.

Having introduced the idea of observability and trace quantities of pollutants, this section will close with a consideration of a few processes that are not strictly weathering but which definitely affect the reliability of trajectory analysis. These processes affect the appearance and the temporary location of the floating hydrocarbons.

As scattered tarballs weather, their density increases and under rough wave conditions they will tend to mix down throughout the upper mixed layer of the ocean. This has the effect of making them extremely difficult to observe from the air or even from small boats, and has led in numerous spills to reports that the oil is sinking. Although it is not impossible for oil to sink in this fashion, it rarely happens and quantitative studies by divers (Hooper, 1981) have shown that in a number of cases the tarballs, or small oil patches, are mixed down by wave energy but remain buoyant and that as seas calm down and low energy conditions prevail, the oil refloats and reappears at the surface. This process has occurred at nearly every major spill and has led to considerable confusion and disagreement among observers who fly out and try to report the location of the oil. The ensuing credibility arguments and squabbles do little to clarify where or how the oil is actually being transported.

Under extremely heavy wave conditions, mousse and thick oil patches can also be broken up and driven down into the upper layer of the ocean. Under these conditions, even very heavy concentrations of oil can be seen to disappear mysteriously. Once again, calm conditions restore the dominance of the buoyancy forces and the oil will again float to the surface. In addition, the liquid condition of mousse allows it to be accumulated in pools by the radiation pressure of the small gravity waves and large pools of oil can then be seen to coalesce and reappear.

Most floating oil appears as black or brown, with occasional tinges of red in it. All of these colors and their observability in the visual range are dramatically affected by lighting conditions. Stormy or near-dusk conditions can seriously affect whether oil is observable or not, and overflights at mid-day and in the late afternoon can be expected to come back with significantly different reports on the amount of oil seen, even if reported by the same observer.

All of the above-mentioned observability factors have the potential to degrade the observational data base required to verify and improve the weathering algorithms. As can be seen, the state-of-the-art in computing weathering procedures for trajectory analysis is quite primitive. In spite of this, the empirical results based on observations with a modest reliance on the underlying processes are still useful and produce helpful insights on how spills will persist as surface problems.

BEACHING

The beach, or more precisely the edge of the marine environment, is the boundary to the partial differential equation solution domain. The distribution equation (1) cannot be solved without some information on how the variable coefficients behave in this region, and how the dependent variables (oil particles or concentration values) are affected by this boundary.

As oil approaches the shoreline, a number of different processes become operative. First, the regional oceanographic currents are deflected by the shoreline itself. This is a simple kinematic constraint associated with the local geometry and continuity considerations. Approaching the shoreline, turbulent diffusive processes may also be reduced due to decreased mixing lengths. Even nearer the shore, diffusion processes may increase again because of a focusing of energy in the surf zone. Atmospheric forcing is also modified by the presence of a coastline and variations in the winds are commonly seen. Coastlines with high relief show orographic effects and regions where high thermal contrasts exist between land and adjacent marine areas often show adiabatic or drainage winds, as well as sea breeze phenomena. To the extent that any of these processes are known, they should of course be included in the advective and diffusive algorithms of the trajectory model.

Even closer to the shore, there are a number of boundary scale phenomena that affect the pollutant distribution for floating hydrocarbons. For example, steep shorelines reflect wave energy, and the resulting standing wave patterns have been observed to hold oil offshore (Hess, 1978). Wave refraction can also turn and channel pollutant movements as they near the shoreline. An important secondary offshoot of wave refraction is the generation of alongshore currents. These alongshore currents develop strongly within the surf zone and tend to propel a pollutant parallel to the beach with the net effect that, as oil comes ashore, it tends to be smeared and moved along a broader section of beach face than it would have if it had come directly ashore in the absence of these kinds of processes. Alongshore currents also feed what is referred to as "rip current systems" (Shepard, 1963). These rip currents are offshore-directed counter-currents which take the oil from the nearshore surf zone and re-inject it out through the breakers into the offshore region, sometimes reaching as far as one kilometer from the beach. This phenomenon also has the net effect of distributing pollutants along a beach face and has been documented as operative in a number of spills.

All of the above-mentioned processes affect the oil or pollutant as it nears the shoreline. Once it actually comes in contact with the shoreline, what happens depends on a somewhat different complex set of conditions. The behaviour of the oil will depend on the sediment size of the beach, the steepness of the beach face, the porosity and interstitial water pressure in the beach, and the amount of wave energy along the beach face. Climatic factors such as the amount of sunlight and air temperatures may also be significant. As with weathering, what is needed to incorporate all these processes into trajectory models is a simplified algorithm which recognizes the basic processes and is consistent with the rather large body of observational experience that is now available from studies that have taken place over the course of many spills. To develop a basic beaching algorithm, the first consideration is how beaches might be classified with regard to oil pollution. Fortunately, such a classification has been made by Gundlach and Hayes (1978). These researchers have developed a one to ten scale for classifying beaches which combines the effects of wave energy, morphology and beach porosity. In this sytem, low-scale values correspond to short residence times for stranded pollutants and high-scale

values correspond to long residence times. To incorporate this scale into a beaching algorithm, the scale numbers are used to define the half-life probability that oil will remain on the beach if it could refloat. For example, rocky headlands (a scale value 1 beach) will rewash half of their hydrocarbon pollutants approximately every two days. On the other hand, salt marshes (a scale value 10 beach) will rewash half of their pollutant load only every six years. The numbers here are obviously open to discussion, but a simple algorithm of this nature does represent the essential first-order characterization of various beaches.

The incorporation of a refloating half-life into a beaching routine requires a specification of how oil actually adheres or sticks to the beach face in the first place. Theoretical considerations indicate that oil cannot contact the beach face due to currents alone; currents do not inundate the shoreline, with the arguable exception of percolation into mangrove swamps or marshes. There must be an onshore component of the wind or waves to bring oil in to contact with the beach face.

Observations point to the fact that oil will not stick to the beach face on a rising tide. A falling water level and onshore winds are the conditions under which oil will be stranded and stuck on the beach face. From this point on, the beached oil is subject to a probabilistic refloating (based on beach type) whenever that the water level is sufficiently high to wet it. Once refloated or reinjected into the water, the oil is free to rebeach, sink or be carried offshore to move to another region.

This proposed beaching algorithm retains its simplicity while emulating the main observed behaviour that has been documented for a number of spills. These are, of course, the essential features of any successful simulation.

COMPUTER REQUIREMENT FOR TRAJECTORY MODELLING SUPPORT

A number of the physical processes that affect the movement and spreading of hydrocarbon pollutants on the sea surface have been discussed above. Once these are successfully converted into algorithms and, in turn, transformed into computer code it is possible to run trajectory models and have the computer act as a synthesizer and data manager for all of the various components. The output from this is the computer trajectory simulation which forms the basic guidance that the spill trajectory specialist uses to prepare the actual trajectory briefings which are, of course, the final product of the entire endeavour. Quite clearly, whether all this can be successfully completed or not will depend on the computational facilities that the trajectory modeller has available and his or her ability to get these functional in an appropriate time scale. This section of the paper briefly considers some of the minimum requirements of a computational system and outline some general trends in computer modelling capability. It should also be pointed out that computer hardware development is perhaps one of the most rapidly changing technological fields and the one certainty is that the availability of new machinery will be changing.

The fundamental requirements of all spill trajectory modelling systems are to be quick to implement and user-friendly. No matter how much pre-planning and contingency planning has been done, nearly all spills occur as unexpected accidents. This means that input data must be set up rapidly and that the trajectory modelling team needs to have uncomplicated and straightforward communication links with the machines. Programme codes should be interactive and interrogative, i.e., the programmes should key the user and inform him or her what the next input sequence of

information should be. The programme should also provide the user with echo checks of the data that is input. Wherever possible, input data should be automated. To input basically graphical information such as the shape of a region and its bathymetry by hand is not only archaic, it is also very prone to error. Digitizing marine charts with a light pen is an order of magnitude faster and much more accurate. Television scanner-digitizers are also on the market and it is quite likely that most major trajectory models will receive their basic geometry and topographic information in this format within a very short time.

Considering the rapid development of microcomputer technology and the dramatic cost reductions of these units, it is obvious that spill trajectory models developed in the future should take advantage of this type of unit. Useful spill trajectory algorithms should be developed for stand-alone microcomputers that offer a high degree of portability. These will offer a field support capability that is unknown at present. In the near future, there will be spill trajectory models stored in cassette form that can be plugged into any number of standard micro-CPU units. Every terminal operator, platform superintendent or port captain should have a spill trajectory model available for his local area on which he can play through alternative scenarios with the ease with which he can now play computer games: the required hardware is much the same.

As spill trajectory algorithms are developed for specific sites and specific operational areas, they should also be linked into localized data sources. For example, when a platform operator is faced with a spill scenario, he should be able to plug in his trajectory model and it, in turn, should call on the local sources of environmental information, such as anemometer readings off the platform's flight deck and current velocity measurements off a meter attached to one of the legs of the platform. This kind of real-time data input could easily be automated and would significantly improve the reliability of the local trajectory estimates that are produced.

It should always be kept in mind that the output from a computer trajectory simulation will be the basis of briefing documents that the trajectory analysis specialist will be presenting to planners or spill response personnel. The products should thus all be in graphic format. The computer should generate maps with some kind of quantitative as well as qualitative overlays that are easy to interpret by anyone familiar with the area in which the spill takes place. Complex numerical or tabular data is of extremely limited use in spill response where, typically, dozens of different specialists of varying backgrounds must all communicate information to each other in a timely manner.

Computer systems for spill trajectory work need to be designed in such a way that the output from the analysis can be transmitted over standard communication lines. No matter where a spill occurs or where the trajectory analysis takes place, there are bound to be many other locations where the information is needed. Home offices, field response personnel, headquarters units and press briefing rooms will all want pictures of the output and basic briefing information. Spill trajectory modelling systems should keep this in mind and be designed so that they have standard communication posts that can send information over existing microwave or telephone line systems.

A final requirement that should be kept in mind when designing spill trajectory models is really imposed by the nature of the oil industry itself and the government bureaucracies that tend to deal with the oil industry. This is the requirement that standardized terminology and graphic outputs should be developed. Standardization is important because of the high degree of mobility of individual participants in oil development and oil spill response. In any single spill, experts from dozens of

different technical fields all may need to consider the consequences of various spill trajectory estimates. A year later, these same people will most certainly be working in different areas, in different oil fields and, perhaps, in different sections of the international market. For them to have to learn a new format for trajectory output each time they move to a new area will not only seriously degrade their ability to respond quickly in spill situations, but will also significantly detract from the spill trajectory modeller's capability to provide useful information.

STRATEGIES FOR TRAJECTORY MODEL USE

To carry out spill trajectory analysis successfully it is necessary first to identify the relevant physical processes responsible for the movement and spreading of floating hydrocarbons. Next, these must be translate into algorithms which can simulate or describe the processes and at the same time use the input data available. Having done this, it is necessary to support these components with appropriate computer hardware and communications interfaces so that the input data can be quickly acquired and the output analysis clearly displayed and disseminated. All of this does nothing more than assemble the necessary pieces. The final step of developing strategies for the use of these tools is essential and critical for the success of the entire endeavour. This subject is discussed below.

A common and straightforward technique for the use of trajectory analysis is simply to provide tactical support when there is a spill. That is, when the modeller is informed of an accident in which oil was lost, a mad scramble is initiated to collect enough environmental data to feed all of the pre-assembled computational algorithms, a spill forecast is carried out, the results are output, and a briefing is prepared to inform response personnel of the probable track of the spilled pollutant. It is hoped that all of this can take place before the spill is over. The time-critical aspects of the problem are familiar to anyone who has worked in spill response and there are a number of helpful approaches to solving the problem. Automated data inputs and telecommunication equipment have already been mentioned . Equally important are 24-hour a day, seven day a week access to key personnel, up-to-date libraries (this year's tide tables, etc.), and current lists of organizational phone numbers. Even with all of this, there will still be problems.

Experience has led to the conclusion that it is seldom useful to go straight for a state-of-the-art spill trajectory product after the initial notification call. First, this will take too long and, secondly, initial reports are always sketchy and usually incorrect (much effort can be wasted going in the wrong direction). During a spill response, trajectory analysis should be continuous and the results applied like coats of paint. There will be something to work with right away and the results should get better as time goes on.

After the initial spill notification, the first trajectory estimates should be available within ten to thirty minutes. This product will probably not use any computer analysis routines but will be based on a quick look at the tide tables, a call to the meteorological service, and perhaps a call to a colleague in an oceanographic department at a university or research laboratory who has studied the area near the spill. The briefing results for these trajectory estimates should be delivered over the telephone and will serve little more than to alert response personnel to major problems and give some indication the direction in which the pollutant is likely to go.

Within two hours after the initial spill notification, a second level analysis should be available. By then, detailed maps should have been studied (also digitized and entered into computer routines), key threatened resources should be identified and the potential time of impact estimated. For this, simple algorithms will suffice and although the computer is essential for data management, its contribution to the trajectory calculations may or may not be significant. At this stage, briefings are still probably being presented over the telephone, but teletype and telefax equipment may also prove useful.

By the fourth hour after initial spill notification, computer-generated current patterns should be available and graphic representations of tidal and wind forecasts should be ready for transmission. The briefing should include specific coastline sections that may be threatened and enough current data to help in recommendations for boom placement and other containment or mitigation procedures.

Within six to eight hours following initial notification, standard trajectory maps and composite summaries should be available for telecommunication to all interested parties, with accompanying briefings via telephone conversation or electronic mail.

By the second day of the spill, hindcasts should be made to check trajectory forecast accuracy. Recommendations should be available for the routing of observational and monitoring overflights. Such details as estuarine effects, results of beach surveys, interviews with local fishermen and marine operators, and the results of regional studies should all be factored into the analysis and briefings that are available. Tactical spill trajectory support requires close ties between modellers and operational response groups, and involves a continual process of upgrading input, analysis, forecasting and hindcasting. Experience, communication links, computers and endurance are all needed for successful results.

Although most spills are unexpected, this is not universally true. Many spills continue for a long time and there may even be some degree of choice as to when they occur. This suggests a second way in which trajectory analysis procedures can be used for spill response. Consider the following cases:

Case 1. A grounded ship may require relatively high risk operations to refloat the hull or lighten the cargo. When shall this be done?

Case 2. A crippled ship may need to be beached to carry out salvaging operations but there is considerable choice as to which beach should be used. Where should it go?

Case 3. Mutineers take over a tanker and threaten to jettison the cargo if demands are not met. How should negotiators take a hard line and when should they back down?

Case 4. A grounded and burning tanker continues to leak for eight weeks with a small but significant threat to a very sensitive area which could be protected. At what point and under what forecast conditions should expensive protection equipment be called out and put in place?

All of these are real cases in which trajectory analysis was used as part of the overall planning and response strategy. In each case, the analysis centred around using the computer to run a series (sometimes a large number) of scenarios. This is not a typical forecast, but rather an exploration of the situation. Using these results, the consequences of alternate plans of action can be compared. As before, the analysis must include detailed briefings and an explanation of all

graphics output. In this case, the trajectory analysis team must usually also be part of the response planning group.

Large oil spills can assume oceanic proportions, and to plan for them or prepare a response as they unfold across the marine environment can prove an extremely taxing endeavour. In such spills, it also usually becomes obvious that for most open ocean areas little can, or should be, done in the way of response. The questions then become ones of when should action be initiated, how long will response personnel have to respond, which areas are threatened by particular hydrocarbon concentrations as they approach the coastline, how much equipment will be needed and at what level of alert should it be kept ready, and so forth. All of these questions relate to subjects which will be covered in any good regional contingency plan. A third type of trajectory analysis, receptor mode analysis, is particularly useful to answer this type of question (Gilbert, 1983; Galt and Payton, 1983).

Receptor mode trajectory analysis starts by choosing a particular high value target site (i.e., marina, public beach, or high value fisheries resources) and the algorithms then proceed to calculate where the oil might have come from such that it could threaten this high value area. Computationally, these algorithms run the trajectory problem backwards. At each time step, a probabilistic distribution of where the oil could have come from is calculated and this process is extended backwards in time. The output of receptor mode analysis is presented in the form of two distribution maps. The first map is a joint probability distribution map that shows the likelihood of a pollutant moving from any location to the high value target area. These contour lines then define the threat probability that any particular target can be impacted.

The second form of output will be time-of-travel maps. These time-of-travel maps indicate how long a response group would have to effect countermeasures or mitigation procedures. The use of receptor mode analysis results can dramatically decrease the number of false starts, unnecessary standby costs, excessive costs associated with continual overflights and distribution mapping and, in general, focus scarce resources on the problem areas which are most likely to be affected.

CONCLUSION

It is hoped that this paper has pointed out that spill trajectory analysis is a combination of a number of different elements. It must begin with a clear understanding of the physical processes which transport oil. In every case, these processes must be understood in terms of the local or regional marine environment. Some areas, for example, will be dominated by tides, others may have permanent oceanic currents that approach coastlines, while yet others may be totally dominated by estuarine and thermohaline forcing. After the physical processes in the local marine environment are understood, it is then necessary to develop the appropriate analysis and computational algorithms to represent these processes. This, of course, will not be useful until the appropriate hardware and communication links are put together. Finally, successful strategies for the use of all these tools are required. It perhaps goes without saying that every situation will be slightly different and each of the spill trajectory analysis teams that are formed will turn out to be slightly different. Trajectory analysis is but one small piece of a larger response organization and thus each team will have to fit into a different national, industrial or regional spill response organization.

REFERENCES

American Petroleum Institute (1977) Proceedings of the 1977 Oil Spill Conference, Washington D.C.

American Petroleum Institute (1979) Proceedings of the 1979 Oil Spill Conference, Washington D.C.

American Petroleum Institute (1981) Proceedings of the 1981 Oil Spill Conference, Washington D.C.

American Petroleum Institute (1983) Proceedings of the 1983 Oil Spill Conference, Washington D.C.

Assaf, G., Gerard R. and Gordon A.L. (1971) Some mechanisms of oceanic mixing revealed in area photographs. Journal of Geophysical Research, Vol.26, No. 27, pp. 6550-6572.

Defant (1961) Physical oceanography. Macmillan Co. and Pergamon Press, New York, Volumes I and II.

Fay, J.A. (1969) The spread of oil slicks on a calm sea. Fluid Mechanics Lab. Publication No. 69-6. Department of Mechanical Engineering, MIT, Mass.

Galt, J.A. (1980) A finite element solution procedure for the interpolation of current data in complex regions. Journal of Physical Oceanography, Vol. 10 , No. 12, pp. 1984-1997.

Galt, J.A. and Payton D.L. (1981) Finite element routines for analysis and simulation of nearshore circulation. Presented at the International Symposium on the Mechanics of Oil Slicks, September 1981, Paris.

Galt, J.A. and Payton D.L. (1983) The use of receptor mode trajectory analysis techniques for contingency planning. Proceedings of the 1983 Oil Spill Conference, American Petroleum Institute, Washington D.C., pp. 307-311.

Gilbert, T.E. (ed.) (1983) Technical guidelines for offshore oil and gas development, Pennwell Publishing Co., Tulsa, Oklahoma, p. 330.

Gundlach, E.R. and Hayes M.D. (1978) Classification of coastal environments in terms of potential vulnerability to oil spill impacts. Mar. Tech. Soc. Jour. Vol 12, No. 4, pp. 18-27.

Halpern, D., Pillsbury R., and Smith L., (1974) An intercomparison of three current meters operated in shallow water. Deep Sea Research, No. 21, pp. 489-497.

Hess, W.N. (ed.) (1978) The Amoco Cadiz Oil Spill. NOAA/EPA Special Report, p. 283.

Hinze, J.O. (1959) Turbulence. McGraw-Hill, New York, p. 586.

Hooper, C.H. (ed.) (1981) The IXTOC 1 oil spill: the federal response. NOAA Office of Marine Pollution Assessment. NOAA Special Report, December 1981.

Kolpack, L. (1977) Priorities in fate of oil spill research. Proceedings of the 1977 Oil Spill Conference, American Petroleum Institute, Washington D.C. pp. 483-485.

Mackay, D. (1980) Solubility, partition coefficients, volatility and evaporation rates, In: Handbook of environmental chemistry, Hutzinger, O. (ed.), Springer-Verlag, Vol. 2, Part A, pp. 31-45.

Mackay, D. and Leinonne P.J. (1977) Mathematical model of the behaviour of oil spills on water with natural and chemical dispersion. Report EPS-3-EC-77- 19, Environment, Canada, Ottawa, Ontario., p. 89.

Mackay, D., Stiver W. and Tebeau A. (1983) Testing of crude oils and petroleum products for environmental purposes. Proc. of the 1983 Oil Spill Conference, API, Washington D.C., pp. 331-337.

Mackay, D. and Szeto F. (1981) The laboratory determination of dispersant effectiveness: method development and results. Proc. of the 1981 Oil Spill Conference, API, Washington D.C., pp. 11-17.

Pedlosky, J. (1979) Geophysical fluid dynamics. Springer-Verlag, New York, p. 624.

Reed, M., Spaulding, M.L. and Saila S.B. (1983) Assessing the impacts of oil spills on Georges Bank Fisheries. Proc. of the 1983 Oil Spill Conference, API, Washington D.C., p. 579.

Rosen, M.J. (1978) Surfactants and interfacial phenomena. John Wiley and Sons, New York, p. 303.

Shepard, F.P. (1963) Submarine geology. Harper and Row, New York, p. 557.

Stewart, R.J. (1976) The interaction of waves and oil spills. Report No. MITSG 75-22 Massachusetts Institute of Technology Sea Grant Program, Cambridge, Mass. p. 192.

Stolzenhach, K., Madsen, O.S., Adams, E.E., Pollack, A.M. and Cooper, C. (1977) A review and evaluation of basic techniques for predicting the behaviour of surface oil slicks. Ralph M. Parsons Laboratory, Department of Civil Engineering, MIT, Report No. 222.

Torgrimson, G.M. (1983a) A comprehensive model for oil spill simulation. Proc. of the 1983 Oil Spill Conference, API, Washington, D.C. pp. 423-428.

Torgrimson, G.M. (1983b) The on-scene-spill model. NOAA Hazardous Materials Response Branch Technical Report (in press).

von Schwind, J.J. (1980) Geophysical fluid dynamics for oceanographers. Prentice - Hall, Englewood Cliffs, New Jersey. p. 307.

Wolfe, D.A. (ed.) (1977) Fate and effects of hydrocarbons in marine organisms and ecosystems, New York. p. 478.

APPLICATIONS OF TRAJECTORY ANALYSIS FOR THE NOWRUZ OIL SPILL

by

J.A. Galt, D.L. Payton, G.M. Torgrimson, and G. Watabayashi
National Oceanic and Atmospheric Administration (NOAA)
Seattle, Washington 98115 USA

ABSTRACT

Early in the calendar year in 1983 an accident in the Nowruz oil field in the northern part of the Kuwait Action Plan Region began a spill that continues up to the time of this writing. This paper describes modelling and trajectory analysis procedures that were carried out to investigate the oil lost from these wells. These studies included a large-scale analysis of the entire Inner Gulf region and a more detailed small-scale analysis of the northwest section of the Gulf centered on Kuwait. Four high-value areas in Kuwait were identified and a second type of trajectory study referred to as "receptor mode analysis" was investigated for these sites.

INTRODUCTION

The movement and spreading of oil on the surface of the sea is controlled by a number of complex processes including advection by currents, indirect wind forcing, turbulence, and weathering; these processes will not be discussed in detail in this paper. The reader is referred to Galt (1984) for a discussion of these topics.

The next section of this paper will discuss the initial Inner Gulf modelling work and trajectory analysis. The third section discusses the higher resolution, more detailed development of trajectory analysis components for the northwest portion of the Gulf. The fourth section describes the use of receptor mode trajectory analysis for specific high-value sites along the Kuwait coast. The final section presents some conclusions based on this analysis, and makes some recommendations for the utilization of these trajectory studies in response and contingency planning activities.

LARGE-SCALE ANALYSIS

As an initial axiom, the data required for trajectory analysis will have to cover the area of concern with an appropriate scale to resolve the details of interest. Figure 1 shows the large-scale Inner Gulf map used for this trajectory analysis study. The eastern basin and the northwest basin are distinguishable.

Given the large-scale map it is next necessary to estimate the advective current fields. A number of sources for this data are available for the Inner Gulf. One such source of current estimates has been compiled by the U.S. Defense Mapping Agency. Oceanographic cruises in the Inner Gulf (Ross and Stoffers, 1978) have mapped temperature and salinity distributions for various seasons. Quite detailed tidal flow models are also available to provide tidal height and current patterns. In addition, there are numerous site specific studies all along the Gulf where developmental activities have required local investigations.

Most of the available current data is empirically derived and there has been no particular effort during the subsequent analysis to examine the divergence of the composite velocity field. If these velocity patterns are then used for trajectory analysis, the potential divergence errors are a serious draw-back (Galt, 1984). Faced with this problem, computational modelling procedures that ensure mass conserving advective patterns to describe the fundamental components of the advective field are used. The resulting patterns will then need to be scaled by the observed data to ensure that we have predicted currents which are scaled correctly and give plausible results.

Since we are interested in the larger scale trajectory analysis problem, we will ignore advective processes caused by the tides. These will be oscillatory in nature and an examination of predicted tidal flow fields suggests that the pollutant excursion associated with these currents will be smaller than our map resolution.

A major component of the steady-state circulation in the Inner Gulf is due to the prevailing winds. With much of the Gulf shallow, an integrated transport formulation is likely to prove useful. The particular form of the equations we use are:

$$\frac{\partial \vec{v}}{\partial t} + 2\vec{\omega} \times \vec{v} = -g\nabla\xi - \frac{c|\vec{v}|\vec{v}}{h} + \vec{\tau}$$

$$\frac{\partial \xi}{\partial t} + \nabla(\vec{v}h) = 0$$

where:

$\vec{v}$ = is the horizontel vector velocity

$\vec{w}$ = rotation vector of the earth (Coriolis parameter)

ξ = free surface elevation

c = drag coefficient for bottom friction

h = undisturbed water depth

$\vec{\tau}$ = wind stress vector

These equations were solved using a finite element time-stepping procedure. Quasi-steady solutions were obtained by applying a steady, uniform wind and running the model for 48 hours from an initial condition of rest. The major spin-up of the model is related to the natural seiche period of the basin which is of the order of 24 hours. Thus, in 48 hours the time-dependent oscillations are quite small.

A number of alternate scenarios were investigated with this model. The first test case hypothesized was for a 5 m/sec wind from the northwest. The results of this case can be seen in Figure 2.

Examination of patterns derived from the wind forcing to the south and east imply currents for any wind direction and can also be approximately represented by the sum of these two basic component patterns.

A second current component identified for the Inner Gulf is caused by surface waters that come in through the Strait of Hormuz to replace the evaporative losses that take place over the entire Inner Gulf. The distribution of this current (Figure 3) can be estimated by an examination of salinity distribution data (Dubach, 1964; Grice and Gibson, 1978) and the use of another finite element circulation analysis routine (Galt and Payton, 1981). At the northern end of the Inner Gulf a small amount of fresh water runoff comes in from the major river systems. The flow pattern associated with this can also be estimated using the same analysis techniques.

Each of these components to the current can now be scaled and linearly added together to best represent the observational data available for the Inner Gulf. Figure 4 presents the results of this combination. The major features of the predicted Gulf-wide current system can now be examined.

One major feature of the circulation is a current moving to the southeast along the western shore. This is seen to develop first in southern Kuwait and then to move south along the Saudi Arabian coast, gaining strength as it moves. By the time it reaches the Gulf of Bahrain, some of it moves south along the western shore of

Bahrain, but the majority of the flow is bathymetrically steered to the south and east over towards the northern tip of Qatar where some small fraction of it rounds the Qatar coast and moves into the eastern basin of the Gulf. Some re-circulation north of Qatar can also be seen. The maximum speed associated with this current is on the order of a half-knot along the southern coast of Saudi Arabia and north of Bahrain and Qatar.

A second major feature of the derived current pattern is coastal flow along the eastern shore or the southwestern coast of Iran. This current is seen to be both weaker and more narrow than the one along the Saudi Arabian coast. Suspended sediment patterns seen in satellite pictures of the Inner Gulf clearly indicate the position and width of this current. Throughout the center of the northwestern basin there is seen a weak return flow that covers the deeper segments of the Gulf. This continues towards the northwest where it approaches the shoreline and bifurcates about mid-way down the Kuwait coast. This is the basic advective field used in the large-scale trajectory analysis. Given this, we now consider available wind data.

Wind statistics are available from a number of stations around the Gulf (IMCOS, 1976). Actual wind observations are reported from a number of stations around the Gulf every six hours. From this and pressure field data the Marine Environmental Protection Agency (MEPA) in Saudi Arabia has carried out a regional analysis which estimates surface wind patterns for the entire area.

With this collection of wind data, current patterns, and the spill characteristics, a number of trajectory experiments were carried out.

Two experiments used the mean averaged currents with statistical winds from Kharg Island and Bahrain. A third and fourth test used the mean averaged currents and the actual or analyzed winds available from MEPA first for the Kharg Island region, and then for an area in the central Gulf north of Bahrain.

Since the wind-driven current analysis suggested that the Inner Gulf takes more than six hours to come into even an approximate state of equilibrium with an applied wind stress, an additional series of trajectory experiments was carried out. In this set, various combinations of mean averaged currents and variable currents were keyed to the observed winds.

The results from each of these trajectory experiments were compared to the available observational sitings of oil that had been compiled by the Regional Office for Protection of the Marine Environment (ROPME). Figure 5 indicates the predicted distribution on May 5 and is an example of the typical model results. The oil can be seen to move southeast down the centre of the Gulf. By approximately the hundreth day of the spill, the heaviest part of the distribution is extending southeast to the vicinity of Qatar.

The distribution estimates include the primary effects of the major weathering processes. Sand-fall data from Kuwait indicates that this may also be an effective weathering or sinking mechanism in the Inner Gulf; however, this factor has not been included in these trajectories.

From experience gained in previous spills and reports of the observations made during the Nowruz spill, it is possible to describe what the surface pollution will look like in the areas covered by this trajectory analysis. Major concentration areas indicated by concentrations of dots can be expected to contain relatively large numbers of dense tarballs and small oil patches. In the nothern sections some consolidated patches and larger pools of oil may be present. At the extremes of the distribution, one would expect to see widely scattered tarballs which will become

ubiquitous as time goes on. These tarballs appear to be quite dense and contain highly weathered oil. In this form any mechanical mixing associated with wave activity can stir them below the surface where they are particularly difficult to observe from either aircraft or ships.

REGIONAL ANALYSIS-KUWAIT

The large analysis presented in the previous section gives a relatively low-resolution overview of the expected spilled oil distribution. Major threat areas are identified and the general characteristics of the floating pollutant have been described. We now focus our attention upon a higher resolution analysis. The region chosen for study is Kuwait. We begin the investigation by looking at higer resolution maps. Their relationship to the Inner Gulf map is shown in Figure 6. From a trajectory analysis point of view, these higher resolution regions are thought of as a sequence of nested maps embedded in the next level higher resolution. The larger of the two maps covers the entire Kuwait coastline while the smaller, higher resolution map covers only the region of Kuwait Bay.

Figure 7a indicates the bathymetric contours that are resolved by the computer simulation in the larger of the two maps. Major bathymetric features are seen to be the large shoal area surrounding Failaka Island and the relatively deep submarine valley that leads along the coastline and up into the Kuwait Harbour.

For this section of the Gulf, a dominant steady-state current caused by the wind stress is expected. We start out as before by an investigation of the vector wind components. With a wind from the north we can clearly identify southerly flow over the shoal region along Failaka Island, and along the shallow section adjacent to the Kuwait coast. A wind from the west presents a quite different circulation picture with easterly flow over the shoal area around Failaka Island, and a relatively strong compensating flow up the submarine canyon and along the northern section of the Kuwait coastline.

A characteristic wind direction for the Kuwait region is from the northwest and Figure 8 indicates the expected current patterns associated with this kind of forcing. This pattern indicates a number of interesting features. There is a clock-wise gyre south of Failaka Island and slightly offshore. At the coastline in the vicinity of the Shuaiba industrial complex, the currents are seen to bifurcate with weak northerly flow north of that area and weak southerly flow south of the area. As we move south along the Kuwait coast, the current is seen to increase in magnitude and develop into a much more organized coastal current structure parallel to the shore. Although throughout the year in Kuwait a northwesterly or north-northwesterly wind is the most common, there are periods in the year when a bimodal wind direction distribution is present. In these cases, the secondary maximum in the wind direction indicates flow from the southeast. Examination of the expected current distribution for this type of wind forcing indicates that this pattern is very nearly the negative of the northwest wind pattern. This also reconfirms that we can represent the current patterns for any particular direction of wind focing by a linear combination of the component currents that are derived from the west wind and north wind cases.

We now move to a consideration of our third level zoom map which focuses specifically on the Kuwait Harbour region. Figure 7b indicates the map used for this analysis and the bathymetric contours that are resolved in the computer analysis.

Once again, we expect one of the major components of the current to be the wind-driven flow. Figure 9 indicates the expected current pattern that would result from the northwest wind and thus represents the most common case expected in this region. Evident in this flow pattern is the north-westerly flow up the submarine canyon with easterly flow south of Failaka Island. Within the bay itself, the northern portion of the bay still exhibits a relatively well-defined counterclockwise circulation, while the eastern or inner bay segment shows a much more complex circulation with generally weaker flows. Comparison with the expected current pattern that would result from southeasterly winds can once again be seen to be the negative of the previous case.

Within Kuwait Harbour the tidal currents become significant. Near the mouth of the harbour, just off Ra's al Ard, the tidal currents can reach two knots in magnitude. For trajectory analysis at this higher resolution level, we can no longer ignore the tidal excursions compared to the other transport processes. To estimate the tidal current pattens a kinematic transport analysis is used (Galt and Payton 1981). The results of this analysis are show in Figure 10.

Given the advective current patterns described above, we must now consider wind forcing and wind forcing data for the higher resolution Kuwait studies. Regular wind reports are available from the Kuwait International Airport and Mina al Ahmadi. Long statistical records are available from the airport, Mina al Ahmadi, and south at Ra's al Khafji. A close examination of the statistical wind distribution indicates that the coastal stations show evidence of sea breeze phenomena which are typically not present in the data from the Kuwait International Airport. For offshore trajectory analysis the coastal stations probably provide a more realistic statistical distribution of winds.

Now that we have developed the current pattern distributions and possible wind data sources it will be useful to look into a comparison of the modelled processes and available observational data. This will provide a strategy for the actual set-up and use of the model computations.

Looking first at the tidal current in Kuwait Bay, we may calculate the tidal prism associated with the predicted tidal elevation changes. This gives the volume of water that must be carried into the bay by the flood currents. The volume flow in is directly proportional to the time rate of change of the surface elevation. This yields a "keying stategy", i.e., a way to predict real-time currents using available geophysical data (predictions from the Tide Table).

Lacking current data from the southern Kuwait coast, our keying strategy will be to use wind data as the independant forcing variable. To do this, we divide the wind into north and west components and use these, along with a steady mean component, to represent the flow which is not balanced by the instantaneous wind. A linear dependence is hypothesized which is the appropriate formulation for shallow regions where the bottom stress is the major dissipation process.

Our proposed keying strategy for the wind-driven currents is admittedly empirical but it does preserve a number of circulation features that can be seen in the area. For example, the predicted currents respond to variations in the wind but do not go to zero during short calm periods; currents in the vicinity of Shuaiba will be weak and variable with a slightly negative correlation to the wind varriations; and a general southeasterly current is seen to increase in strength as one moves south along the coast towards Saudi Arabia. All of these are observed features and the predicted magnitudes of the current patterns are consistent with a much wider body of observational data that is available for the Kuwait coast.

To carry out the trajectory analysis, we must also specify the diffusion and spreading processes. Small-scale dye studies from power plant effluent studies provide some information for diffusion along the Kuwait coast. However, because of the slightly larger scale of resolution used in the model, larger diffusion coefficients will be necessary. Typical coastal values are on the order of 1-5 x 10^5 cm2/second.

We now have all the components necessary to assemble a trajectory analysis model for the Kuwait region:

1) Three nested maps are considered (Figure 6);

2) North- and west wind current response patterns which can be linearly summed to predict all wind forcing cases are associated with each map
   a) Figure 2 is associated with the Inner Gulf map
   b) Figure 8 is associated with the Kuwait coast map
   c) Figure 9 is associated with the Kuwait Harbour map;

3) The tidal current patterns (Figure 10) are associated with the Kuwait Harbour map;

4) The diffusion coefficient is set between 1 and 5 X 10^5 cm2/sec with the understanding that it should be adjusted during the course of the trajectory analysis study based on observations of the spill as it develops (An iterative hindcast/forecast process is obviously suggested);

5) 25 per cent of the long-term mean wind components are keyed to each of the wind-driven component patterns;

6) 75 per cent of the varaible six-hour averaged winds components are keyed to each of the wind-driven component patterns;

7) The six-hour averaged wind vectors are used to key the indirect surface transport processes; and

8) The time-dependence of the tidal height curve for Kuwait Harbour is associated with the tidal current pattern.

This now completes the description of the Kuwait regional trajectory analysis model. With a spill model configured as indicated above, and loaded into an iterative, interactive simulation programme, we are in a position to perform trajectory analysis studies with a minimum amount of actual data input at run time. Tidal height predictions, forecasted winds, and monthly historical mean winds, along with the initial distribution and type data on the pollutant are sufficient input parameters to carry out real time trajectory analysis for support of spill response activities. If forecasted winds are replaced by observed winds it is possible to perform hindcast analysis with this same model configuration. When carrying out trajectory analysis for time or length scales longer than those dominated by tidal excursions for use in assessment or contingency planning modes, the only required input data will be the statistical wind distribution divided into speed and direction classes. These cases include the extremely important class of receptor mode trajectory analysis which we will now consider.

RECEPTOR MODE ANALYSIS

Trajectory analysis is most commonly carried out to support real time or tactical spill response. In this case, a spill is hypothesized, environmental data is entered, and the questions of "Where will the pollutant go?", "When will it get there?", and "What will it look like?", are all addressed. For the problems associated with spill response planning or contingency planning, an alternate formulation, referred to as receptor mode analysis, is particularly useful (Galt, 1984; Galt and Payton, 1983; Gilbert, 1983). In this mode of analysis, a high value receptor site is identified, and we then address the question of where a pollutant could come from such that it could reach the high value receptor site or target. To do this, a statistical ensemble of hypothesized spills are traced back-wards in time and space. The output from this type of analysis is presented as two maps or distribution fields that can be graphically combined.

The first map is a probability distribution which indicates the chance that a pollutant would have of moving from any location in the marine environment to the high value receptor site. The second map shows the minimum time-of travel contours. This data defines a threat zone for the high value target or receptor and indicates how long response personnel would have to set up and implement mitigation procedures.

To carry out this analysis for Kuwait, four high value receptor sites were identified. For these studies, statistical winds from Mina Al Ahmadi were used to key the indirect wind transport processes and the wind-driven current components. As an example, Figure 11 shows a contour plot of the statistical wind distribution for the month of November.

Because a statistical ensemble of spill trajectories is being considered, tidal currents were not explicitly included in the receptor mode analysis since the tidal phase would be random and the net effect would only be an increased scatter or uncertainty in the displacements. To compensate for this effect, a diffusion coefficient of 2.5×10^5 is used for all of the receptor sites. This diffusion coefficient value is well within the normal range for the offshore region but slightly higher than the norm for the inner bay.

For each site 250 spills were considered in the statistics and their displacements were traced for five days during the month of November. Figure 11 indicates the receptor mode analysis results for one of these sites for the month of November. The threat probability distribution is contoured with four solid, heavy lines. The inner contour surrounds the region where the receptor site has a greater than 40 per cent probability of being impacted if the pollutant is found within this contour. The second contour surrounds the area with a greater than 10 per cent probability of impacting the receptor site. The third contour surrounds the greater than 1 per cent probability of threat area; and the fourth contour indicates the maximum extent of any possible threat zone to the receptor site.

Figure 12 shows the minimum time-of-travel contours with a contour interval of 24 hours. These contours are indicated by dotted lines.

These receptor mode maps now provide a basis for developing an efficient and cost-effective response plan for oil pollution protection for the four sites studied. Surveillance programmes need only to cover the threat zones indicated. Beyond that range, oil sitings are not likely to be relevant to the five-day problem. Once significant oil is identified within the threat perimeter, its

relative seriousness can be ascertained. Pre-designated response personnel can be alerted and equipment moved to "ready to deploy" positions. At this point, modelling activity should shift to a tactical support mode and regular forecast/hindcast procedures started. The model, observation, and response components designated in contingency plans should all continue close cooperation and information exchange throughout the duration of the threat alert. After the threat passes, all units can return to the surveillance level programme.

CONCLUSIONS

In order to investigate the significance of these impacts, estimate their time and space distributions, and to effectively plan defensive strategies, a number of environmental questions must be answered. Trajectory analysis has the ability to provide some of the required answers. In this particular case, the initial level of trajectory analysis focused on the entire Inner Gulf. Major components of the advective flow were associated with, 1) wind-driven currents, 2) thermohaline or estuarine flow including evaporative and runoff effects, and 3) tidal currents. Based on time and space scales of the analysis, displacements due to tidal currents were seen to be insignificant so these processes were not considered further in the large scale analysis. Each of the relevant current factors was estimated using mass-conserving algorithms and the results were scaled to match available observational data. Wind data considered in the large-scale analysis came from statistical climatological data or real-time hindcast and local meteorological analysis. Combinations of keying strategies for wind and current data were investigated in a series of trajectory experiments. The model output was compared to observed oil siting data. Trajectory analysis results indicate that the primary threat area for coastal impacts covers the southeast coast of Saudi Arabia, Bahrain, Bahrain Bay, and the northern coast of Qatar. Time of travel to these impact areas will be between one to three months and thus pollutants will arrive in a highly weathered state and appear as stiff, dense, tarballs. The long transit times and basically closed nature of the Gulf means that outside of the major plume scattered tarball concentrations will also be likely.

In addition to the Gulf-wide trajectory studies, a regional investigation covered Kuwait waters and used two nested high-resolution maps (Figures 7a, 7b). For this study, wind-driven and tidal flow components were estimated. Alternate keying strategies considering the variations and the mean components of the wind were compared. The statistical wind distribution and similar current statistics for location offshore of Shuaiba were compared. The current statistics showed a large amount of scatter and a weak negative correlation with the wind statistics. Dynamic considerations suggest that this is associated with a coastal bifurcation in the current pattern that shifts up and down the northern half of Kuwait's open coast. On the average, its position appears slightly south of Shuaiba.

Climatological wind data available for Kuwait was used as forcing for a receptor mode analysis for four high-value sites in Kuwait. For each of these locations, threat zone and time-of-travel maps are developed for each month of the year. These maps indicate where offshore sitings of floating oil represent a significant threat to any of these high-value target areas.

With the analysis and experiments presented in this work, it is possible to make some general statements about the large-scale distribution of oil from the Nowruz field as a threat to Kuwait, and some recommendations for how to use these components in developing a modelling response strategy:

1) Given the general Gulf-wide circulation, location of the Nowruz spill, and the statistical winds for the Northern Gulf, the probability of large coherent patches of oil impacting Kuwait are slight. Coastal impacts are more likely going to be associated with peripheral scatter from the edges of the major plume and from impacts due to indirect and widely scattered divergent paths. Relatively long transit times will be associated with either of these pollutant routes.

2) The form of the pollutant reaching Kuwait will most likely be dense, heavily weathered tarballs. As these will have densities close to that of seawater, any turbulent mixing will distribute them down into the mixed layer and away from the surface. This situation often leads to observational reports of "sinking" or "disappearance" of the oil, neither of which may be true. Actual sinking is likely, as the tarballs get into the surf zone, where sediment can agglomerate into the oil, and may result from sandfall at sea, but little is known about this process. Once these weathered tarballs are beached, high temperatures can cause them to melt, whereupon they can then flow together and form heavy tar mats.

3) Receptor mode analysis can form the basis for determining threat zones for the four selected high value targets along the Kuwait coast. These threat zones define where regular offshore surveillance would be required. Until significant concentrations are sited within these threat zones, no particular defensive response activities are warranted.

4) If significant oil concentrations are present within a designated threat area tactical modelling support should be initiated with forecast/hindcast activities and response or protection plans should be activated with the issuance of an alert to response personnel. As the probability of impact increases, continual modelling trajectory analysis should work closely with and support actual cleanup and protection procedures.

The overall approach outlined above is believed to offer a conservative and effective oil spill defense strategy for Kuwait waters. At the same time, it will minimize the demands on key scientific and response personnel by evaluating threats and discarding as false alarms sitings with a low probability of impact to the major areas of concern.

REFERENCES

Dubach, H.W. (1964) A summary of temperature-salinity characteristics of the Persian Gulf. National Oceanographic Data Center, General Series Publication G-4.

Galt, J.A. (1964) Simulation of the movement and dispersion of oil slicks. Oceanogaphic modelling of the Kuwait Action Plan Region. UNESCO Reports in Marine Sciences No.28.

Galt, J.A. and Payton D.L. (1981) Finite element routines for analysis and simulation of nearshore circulation. In: Proceedings of the International Symposium on the Mechanics of Oil Slicks, Paris, France.

Galt, J.A. and Payton D.L. (1983) The use of receptor mode trajectory analysis techniques for contingency planning. In: Proceedings of the 1983 American Pertroleum Institute Oil Spill Conference, San Antonio, Texas.

Gilbert, John T.E. (ed.) (1983) Technical guidelines for offshore oil and gas development. Pennwell Publishing Co., Tulsa, Oklahoma, 330 pp.

Grice, George D. and Victoria Gibson R. (1978) General biological oceanographic data from the Persian Gulf and Gulf of Oman. Report B., Woods Hole Oceanographic Institution Technical Report No. WHOI-78-38, 35 pp. Unpublished manuscript.

IMCOS Marine Ltd., (1974) Handbook of the weather in the Gulf between Iran and the Arabian Peninsula - Surface Wind Data, Bibliography.

IMCOS Marine Ltd., (1976) Handbook of the weather in the Gulf between Iran and the Arabian Peninsula - Surface Wind - Discussion, General Climate - Discussion and Meteorology of the Gulf.

Ross, David A. and Peter Stoffers (1978) General data on bottom sediments including concentration of various elements and hydrocarbons in the Persian Gulf and Gulf of Oman, Report C. Woods Hole Oceanographic Institution Technical Report No. WHOI-78-39, 107 pp. Unpublished manuscript.

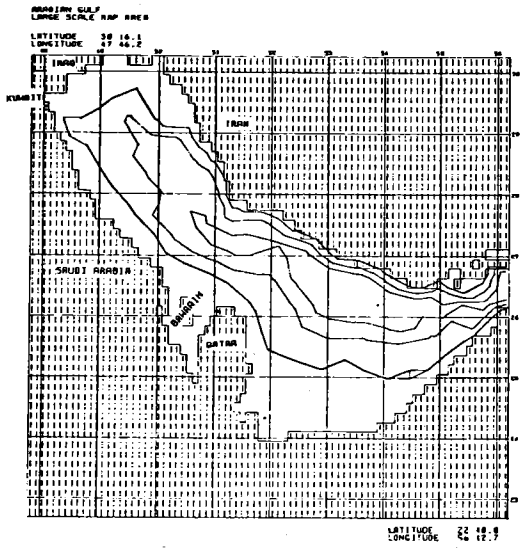

Figure 1: Large-scale map of the Inner Gulf depth contours at 20, 40 and 60 m are shown

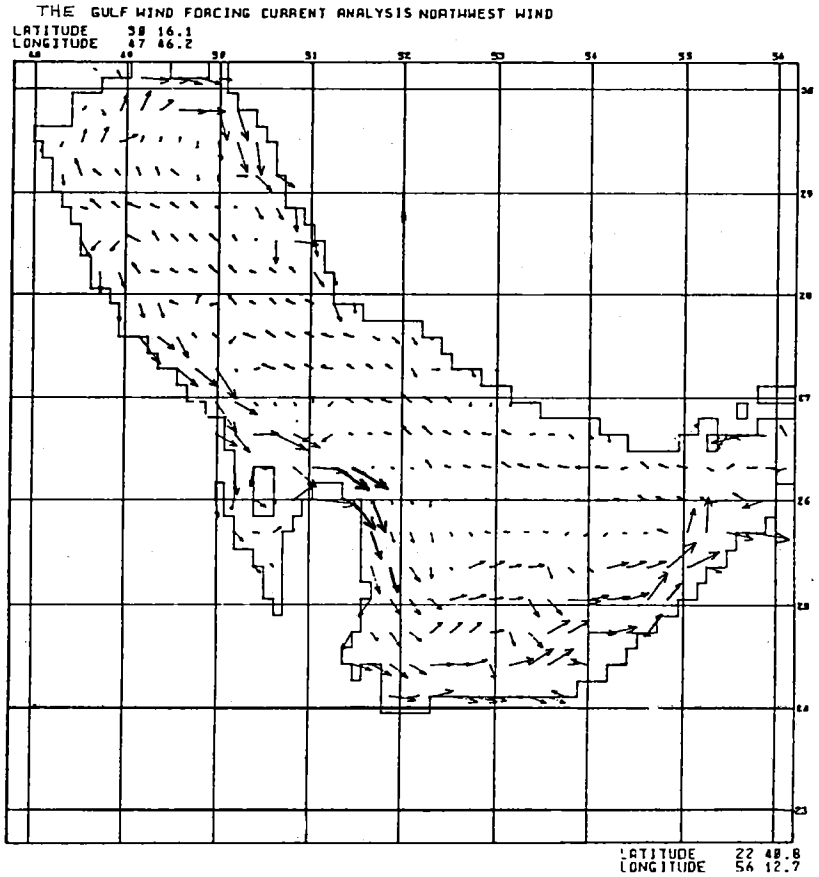

Figure 2: Surface current component due to wind stress using a 5m/s wind from the northwest

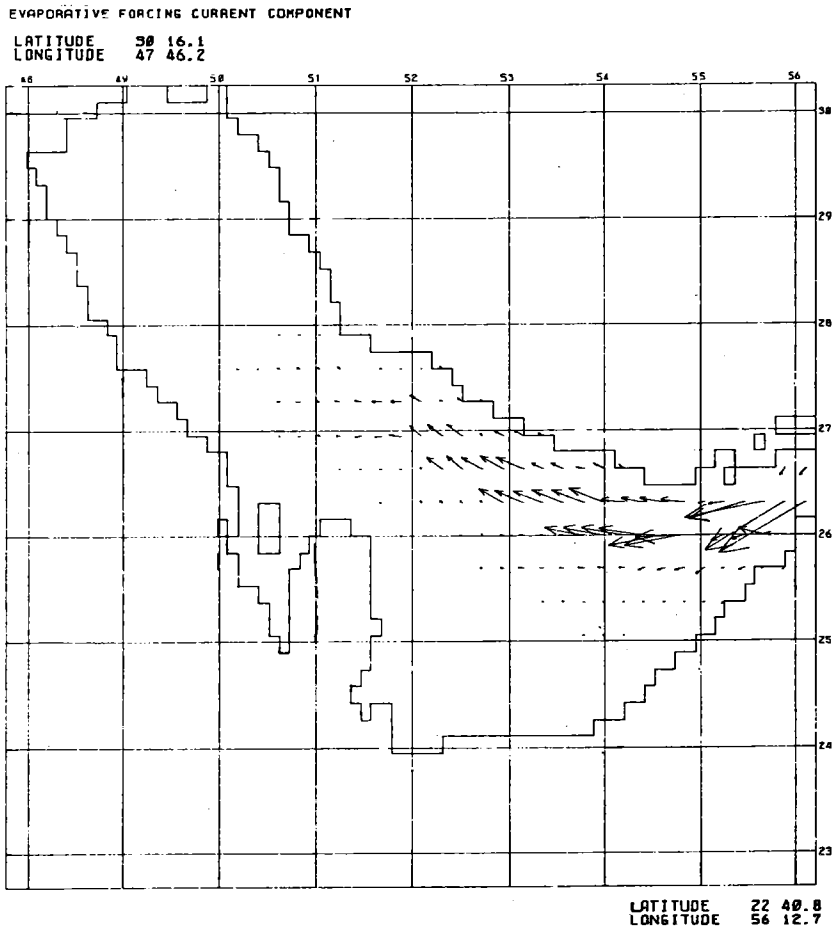

Figure 3: Surface current representation due to evaporative forcing and inflow through the Strait of Hormuz

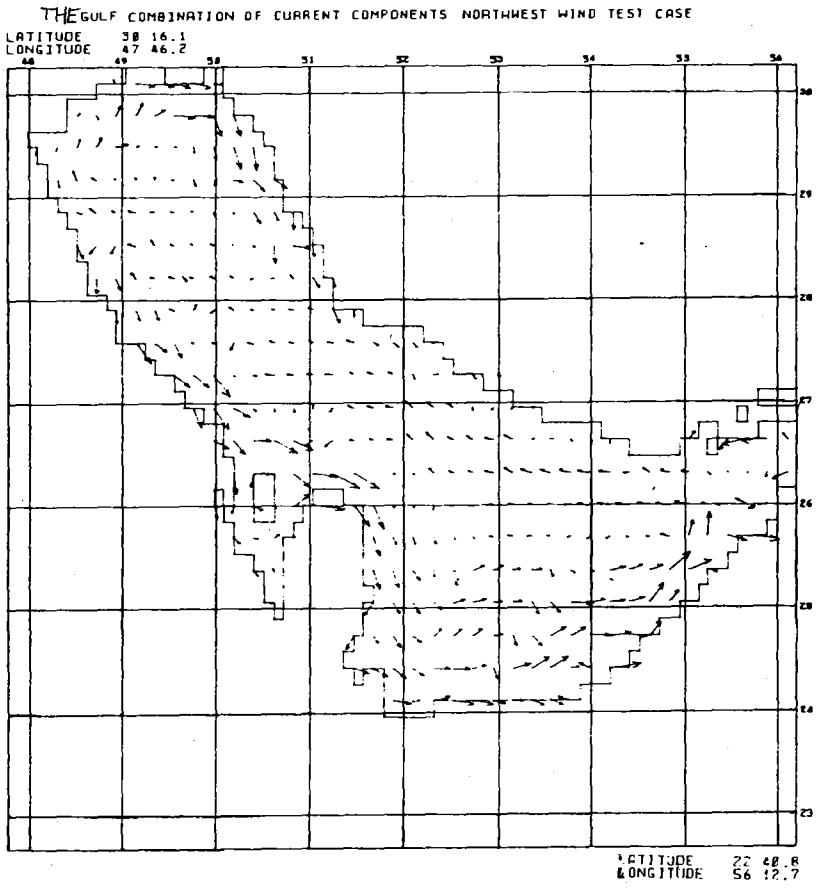

Figure 4: Linear Sum of current components scaled to be consistent with observational data

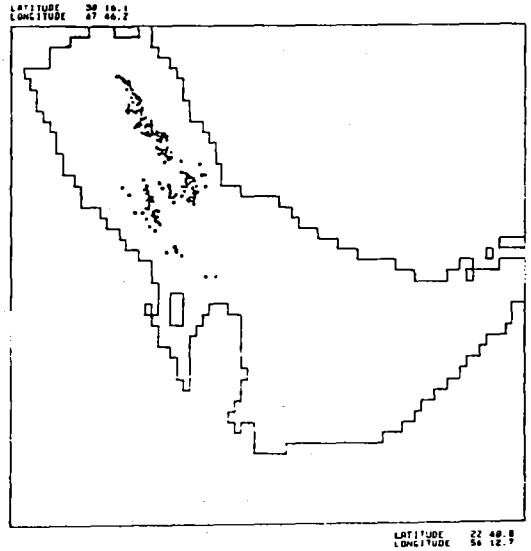

Figure 5: Example of trajectory analysis results for May 5, 1983

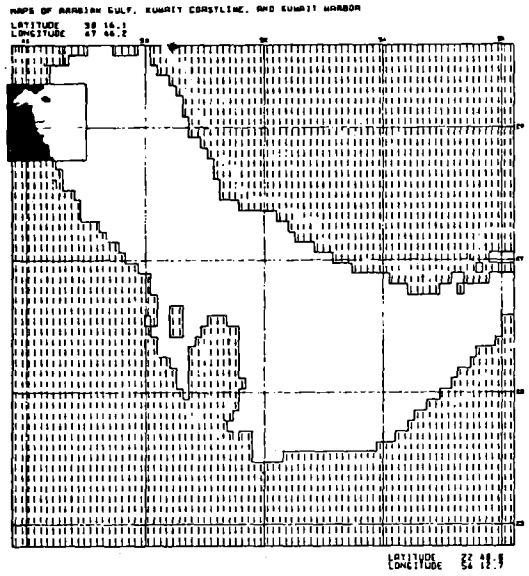

Figure 6: Representation of three maps used for the Kuwait Regional Study

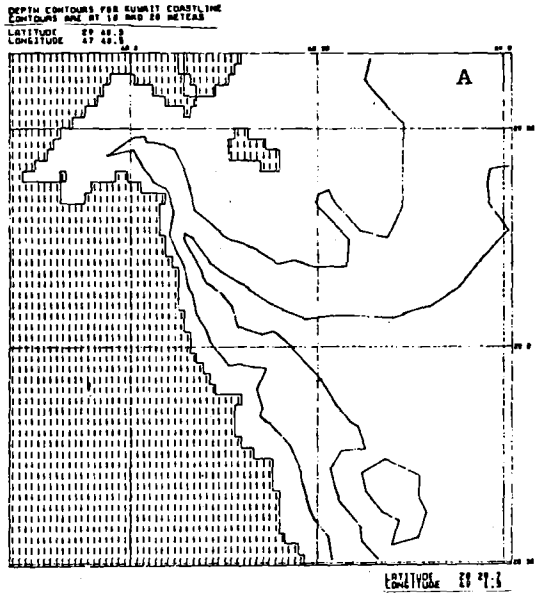

Figure 7a: Map of Kuwait coastal area. Contours at 10 and 20 m are shown

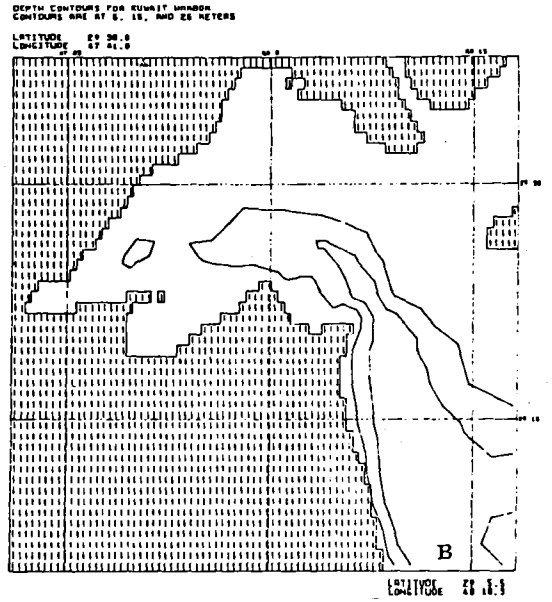

Figure 7b: Map of Kuwait Harbour area. Contours at 5, 15 and 25 m are shown

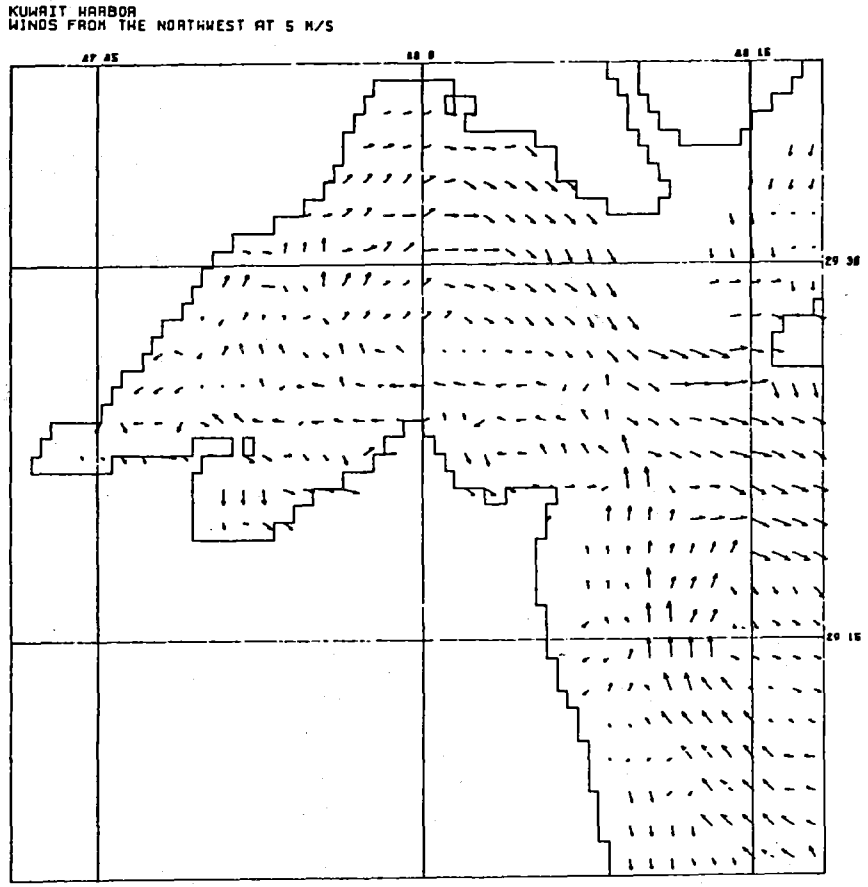

Figure 8: Surface current component due to wind stress using a 5m/s wind from the northwest

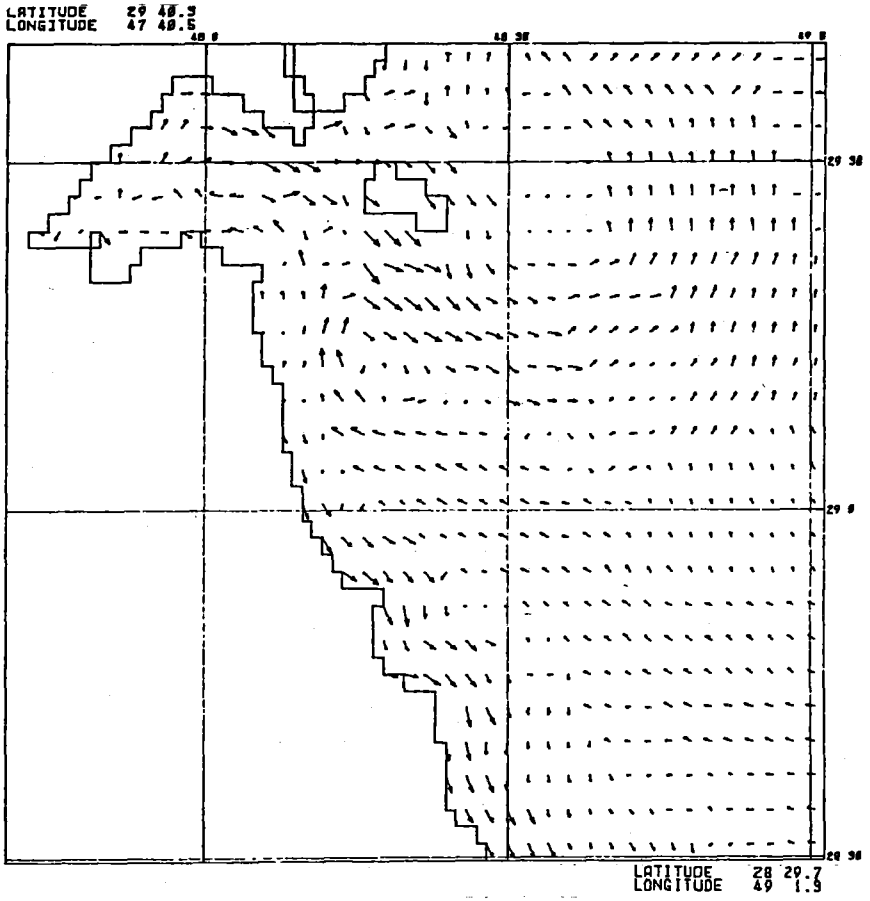

Figure 9: Surface current component due to wind stress using a 5m/s wind from the northwest

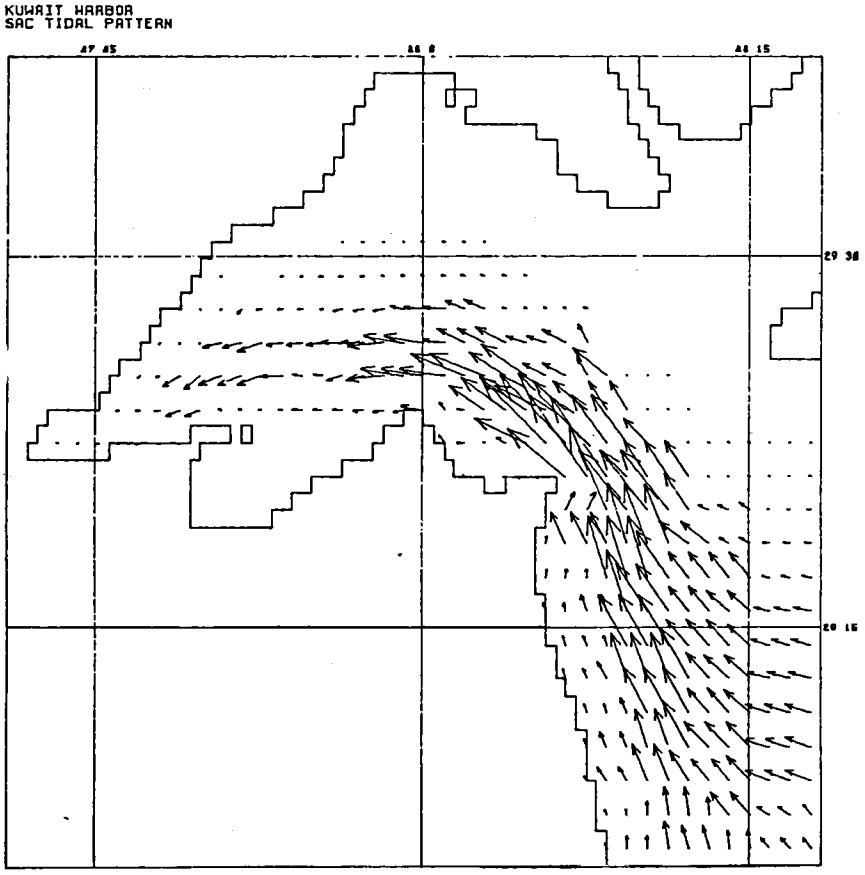

Figure 10: Representation of flood tidal current patterns for Kuwait Bay

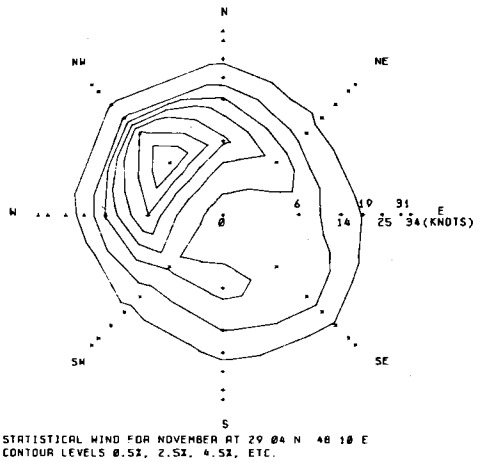

Figure 11: Contour map of the statistical wind distribution for November from data collected at Mina Al Ahmadi

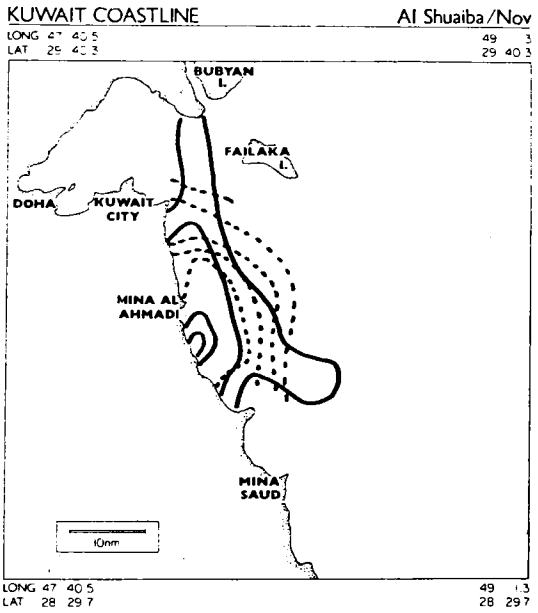

Figure 12: Example of reception mode analysis for November at Al Shuaiba Site. Probability contours are solid and correspond to areas of 40%, 10%, 1% and greater than 0% probability. Dotted contours indicate time of travel in days

A COUPLED NUMERICAL MODEL FOR PREDICTING THE EXTENT OF STORM SURGE FLOODING

by

T. C. Gopalakrishnan
Kuwait Institute for Scientific Research
Safat, Kuwait

ABSTRACT

Several numerical models have been developed in the past to compute storm surge intrusion, with given storm parameters and coastal conditions. Most of these models do not consider the extent of flooding due to wave attack over the storm surge. The present study evaluates coastal inundation due to both storm surge and storm wave attack over the enhanced water levels. Storm surge some distance offshore is computed using a two-dimensional finite element model. Using the values of storm surge thus predicted, a one-dimensional moving boundary model is used to compute the extent of intrusion on land due to the surge and wave at individual locations of interest. The application of the model to the North Carolina coast in the U.S. is briefly explained.

INTRODUCTION

Evaluation of storm surge and the consequent flooding of coastal areas is an essential aspect of disaster prevention and safety zoning in coastal regions. It involves choosing a design storm and computing the resulting elevation of water level near the coastline. The extent of flooding depends not only on the storm surge but also on the storm wave riding the enhanced water level that has already intruded the onshore areas.

In the present study, this problem is modelled in two phases: first, using a two-dimensional resolution in the offshore region and, secondly, connecting the storm surge thus predicted to the onshore motion of the water. The onshore motion itself is composed of two phenomena, the intrusion of water inland due to the enhanced sea level, and the motion of waves over it. The second phase, namely the onshore motion, is based on a one-dimensional resolution because a two-dimensional moving boundary model is computationally very expansive.

THEORY

The numerical model for the resolutions mentioned above are based on the vertically integrated momentum and continuity equations. The vertical accelerations (which become significant during the onshore motion) are, however, included in the one-dimensional model. For details of the governing equations (in relation to the offshore and nearshore models), the reader is referred to Taylor and Davis (1975) and Gopalakrishnan (1978).

Boundary Conditions

For the offshore model, the two-dimensional grid is terminated at the shore line, as shown in Figure 1. This boundary is assumed as fixed and hence velocities normal to it are zero. The side lines of the offshore grid are open boundaries which are chosen well away from the region of interest on the shore. Along these lines the water elevation is considered to be a result of astronomical and barometric tidal fluctuations only. This will, no doubt, introduce an error into the analysis but past investigators indicate that it is of second order only. The seaward open boundary is chosen to be beyond the continental shelf and hence, again, the water level there is specified as for the lateral boundaries. This is based on the fact that the storm surge beyond the shelf is not significant because of the great depth.

Specifying the boundary conditions for the one-dimensional model presents interesting features in view of the fact that the downstream end of it has a moving extremity. The upstream end, i.e. the seaward end, has the storm surge or the incoming wave serving as the boundary condition. On the downstream side, Lagrangian acceleration is used to follow the leading particle with regard to its velocity and distance covered. Details of this are given in Gopalakrishnan (1978).

THE NUMERICAL PROCEDURE

Figure 1 shows how the region under consideration is discretized using triangular finite elements. The co-ordinates of the nodes are supplied as part of the input. Based on the governing equations and boundary conditions mentioned in the previous section, a system of algebraic equations can be developed, with the water transport and levels (denoted by Eta n) as the unknowns. The solution of this system then gives the values of transport and levels, thus leading to the storm surge evaluation at the shoreline. The algebraic system indicated above is set up using the Galerkin finite element procedure.

The nearshore one-dimensional model

The shoreline has been assumed as fixed in the two-dimensional resolution mentioned above. This, however, is not true as the water body moves inland, due to enhanced water levels. Hence, in the one-dimensional moving boundary approach, the storm surge at some distance from the shore (say 4 km) obtained from the above resolution is considered as the forcing function for driving water inland. The error introduced by the assumption of a fixed boundary in the two-dimensional resolution will decrease with distance seaward of the shoreline. The speciality of the one-dimensional model is that it can handle a changing problem domain. The finite element near the edge of the water body is designed to be flexible in the sense that it expands and contracts according to the position of the tip of the water body, denoted by B in Figure 2. Details of this procedure can be found in Gopalakrishnan and Tung (1980).

The one-dimensional model is applied in two phases: it is first used for the region shown in Figure 2, the forcing function being the storm surge at the point A, as predicted by the two-dimensional model. The storm wave is then used as the forcing function at A over the water body which is thus affected and moved inland. The latter is the one actually responsible for the extensive flooding on the coast.

As mentioned above, an analysis is given for the prediction of the storm wave of a given hurricane. It is based on established methods as given in Ippen (1966).

Hurricane parameters

In the present analysis, Hurricane Hazel (1954) was used as the forcing function for the storm surge. The track of this hurricane is shown in Figure 3. The wind and pressure fields were computed based on the approach described by Graham and Nun (1959). From this computation, the wind velocities and pressures at the various nodes of the two-dimensional grid were supplied.

COMPUTATIONS AND RESULTS

The numerical model described above was applied to the North Carolina Coast in relation to Hurricane Hazel.

The computation domain was divided into 469 triangular elements having 270 nodes in all. A linear shape function was used for interpolating the variables. The typical length of an element varied between 14 km in deep water areas to 6.5 km

near the shore. The friction coefficient and eddy viscosity coefficient were estimated as ranging from zero to 0.002 and 1,500 m2/sec to 4,000 m2/sec, respectively. The time increment Δt was adopted as 200 sec starting from $t = 0$ when the hurricane was located at 30°N latitude and 78.8°W longitude. A total period of 18 hours was covered. The corresponding computation time on an IBM 370 computer was 6 minutes, 8 seconds. Figure 4 is an example of the storm surge near the North Carolina Coast.

In the one-dimensional model, line elements were adopted in conjunction with a cubic shape function. The longest element was 100 m in length for the storm surge evaluation and 20 m for the wave propogation. A typical onrush of wave over the shore areas is presented in its evolutionary pattern in Figures 5, 6 and 7.

The Computation time for a single run is approximately 1 minute for time steps of 0.1 seconds and a field time of 12 minutes. These figures are less while following the storm surge on shore.

The results presented here are more to highlight the methodology rather than to describe the actual analysis of the flooding of the North Carolina coast.

ACKNOWLEDGEMENTS

This work was sponsored by the Office of Sea Grant, NOAA, US Department of Commerce, under Grant No. R/CZS-18 and the North Carolina Department of Administration. J.S. Wei, graduate student of the Marine, Earth and Atmosphere Sciences Department, North Carolina State University, did most of the computations and the plotting of results.

REFERENCES

Gopalakrishnan, T.C. (1978) Galerkin finite element analysis of wave shoaling and run-up. Doctoral thesis, Center for Marine and Coastal Studies, North Carolina State University, Raleigh, NC, USA.

Gopalakrishnan, T.C. and Tung, C.C. (1980) Run-up of non-breaking waves: a finite element approach. Coastal Engineering, 4, 3-22.

Graham, H.E. and Nun, D.E. (1959) Meteorological considerations pertinent to standard project hurricane, Atlantic and Gulf Coasts of the United States. Report No. 33, National Hurricane Research Project, US Department of Commerce.

Ippen, A.T. (1966) Estuary and coastline hydrodynamics. McGraw Hill, New York.

Taylor, C. and Davis, J. (1975) Tidal and long wave propagation: a finite element approach. Computers and Fluids, 3, 125-148.

Wei, J.S., Chen, M.S. and Machemehl, J.L. (1980) Finite element model for hurricane surge and coastal flooding: urban storm water management in coastal area, ASCE, 205-214.

Zienkiewicz, O.C. (1971) The finite element method in engineering science. McGraw-Hill, New York.

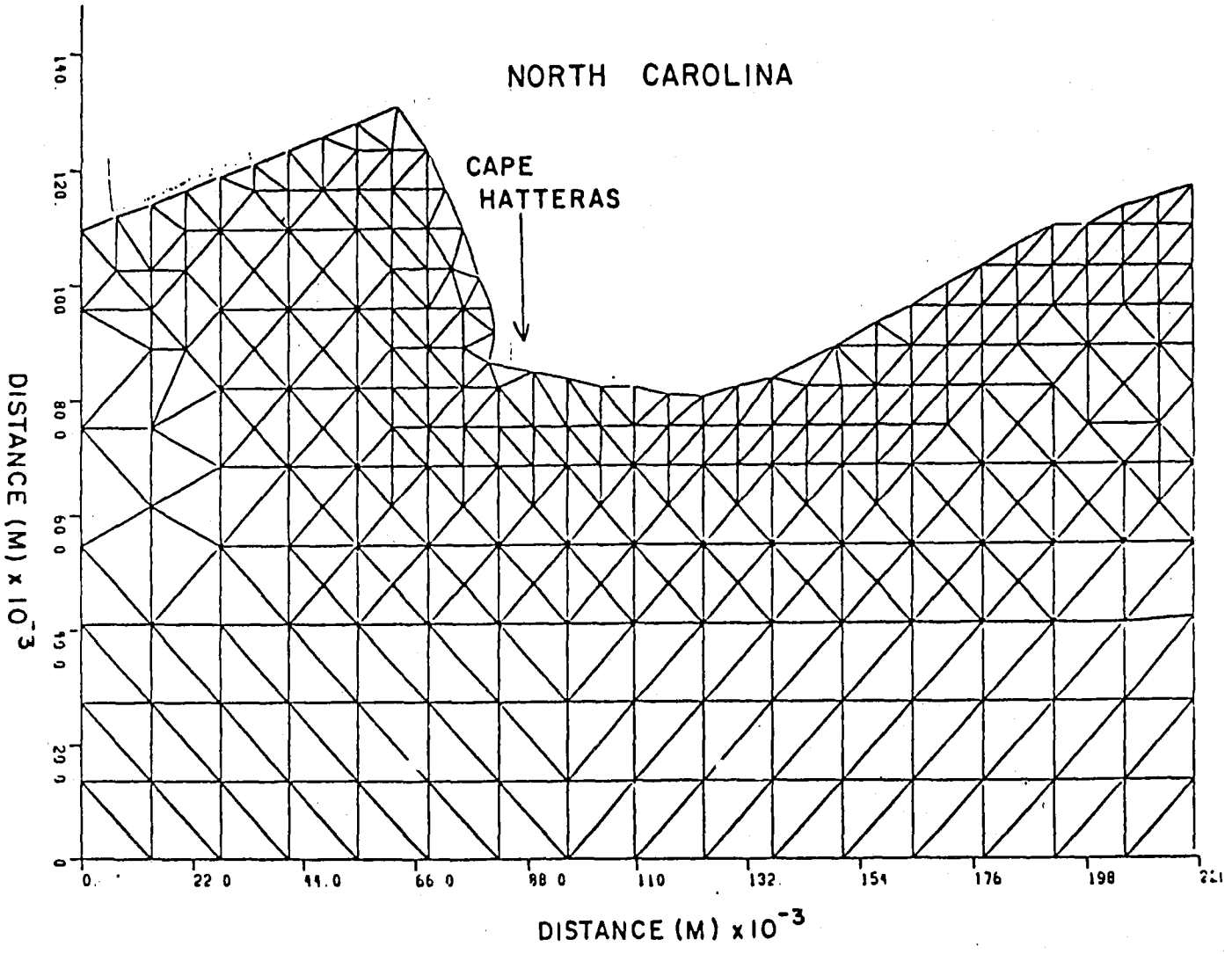

Figure 1: Discretization of the region east of Cape Hatteras.

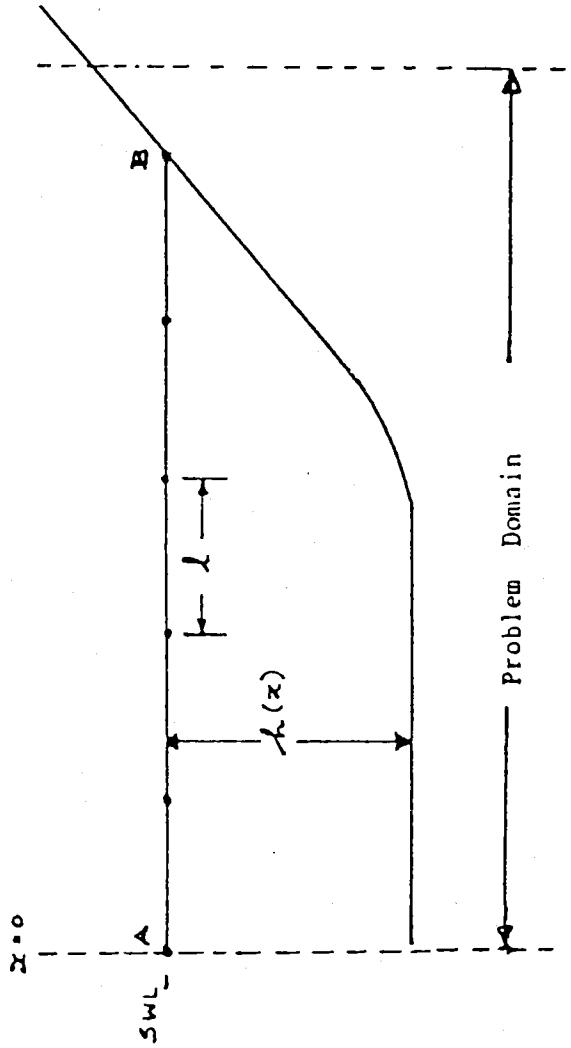

Figure 2: Spatial discretization.

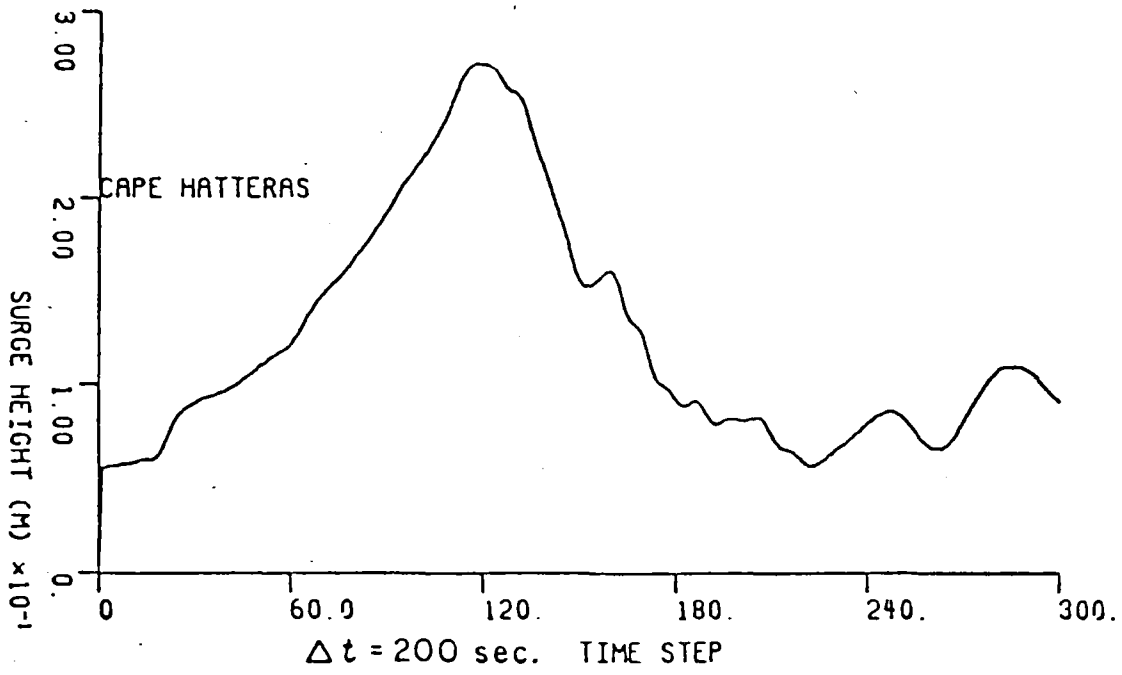

Figure 4: Storm tide -HZØ- Cape Hatteras.

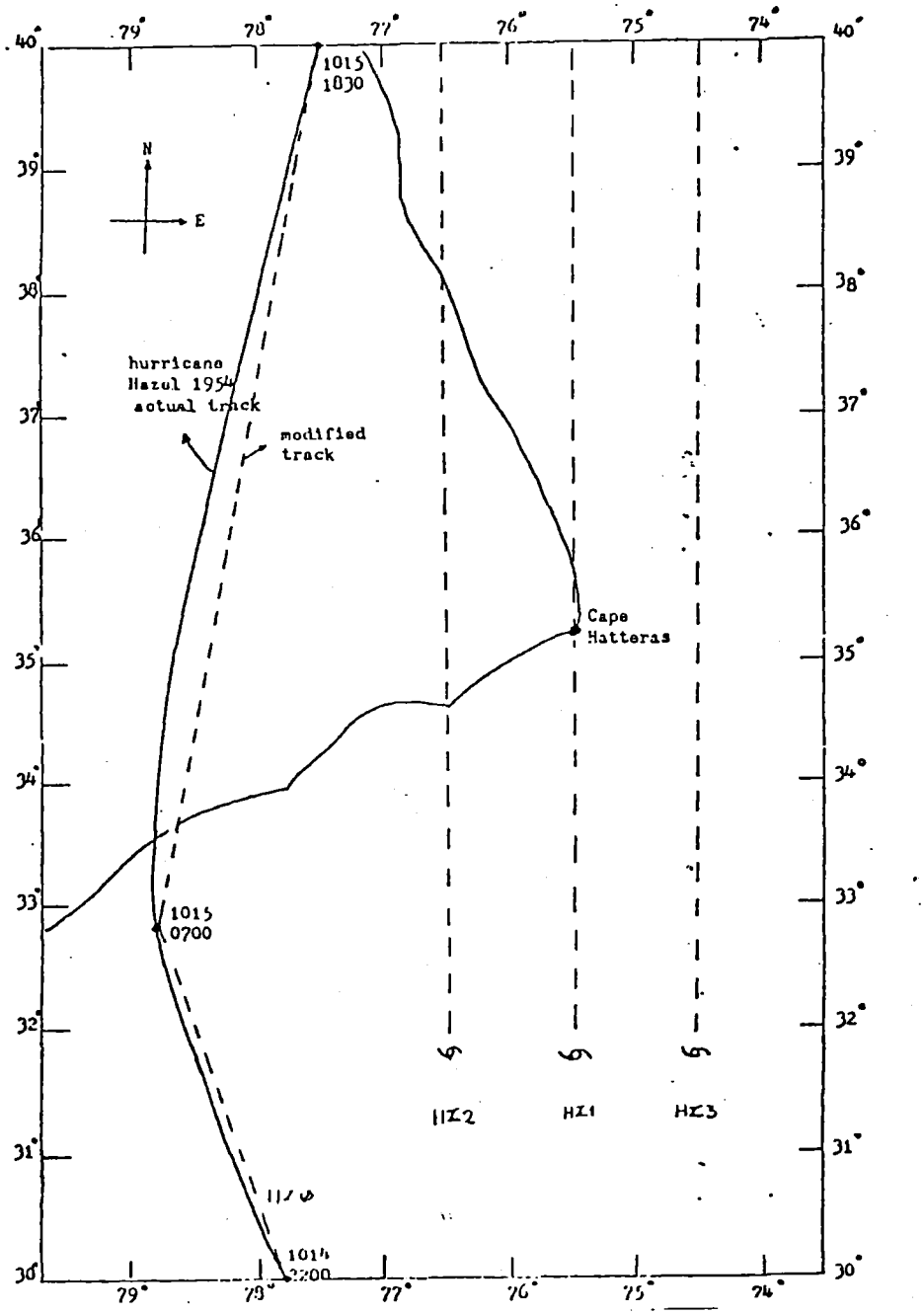

Figure 3: Actual and hypothetical paths of Hurricane Hazel.

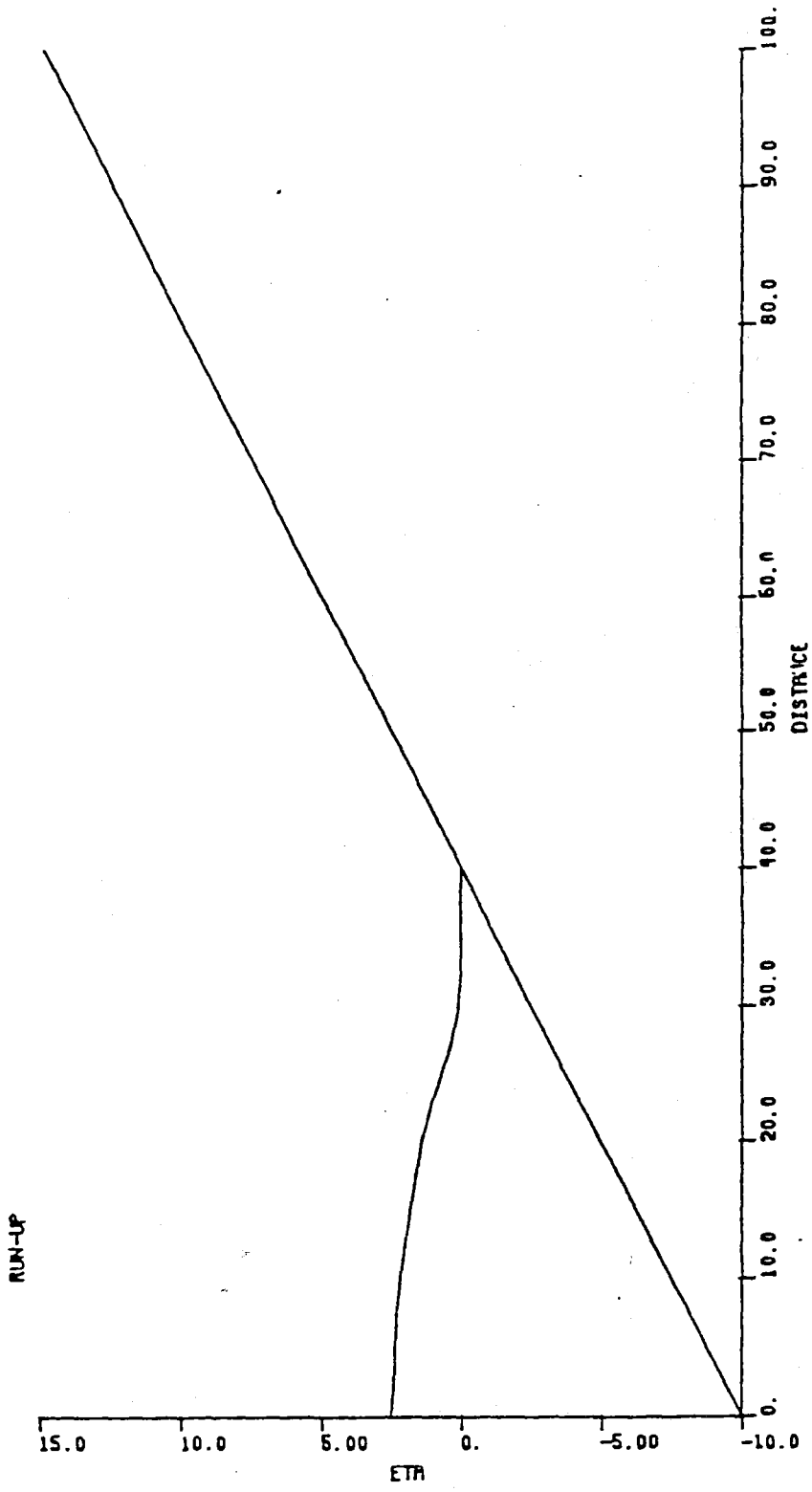

Figure 5: Wave entering the coastal waters.

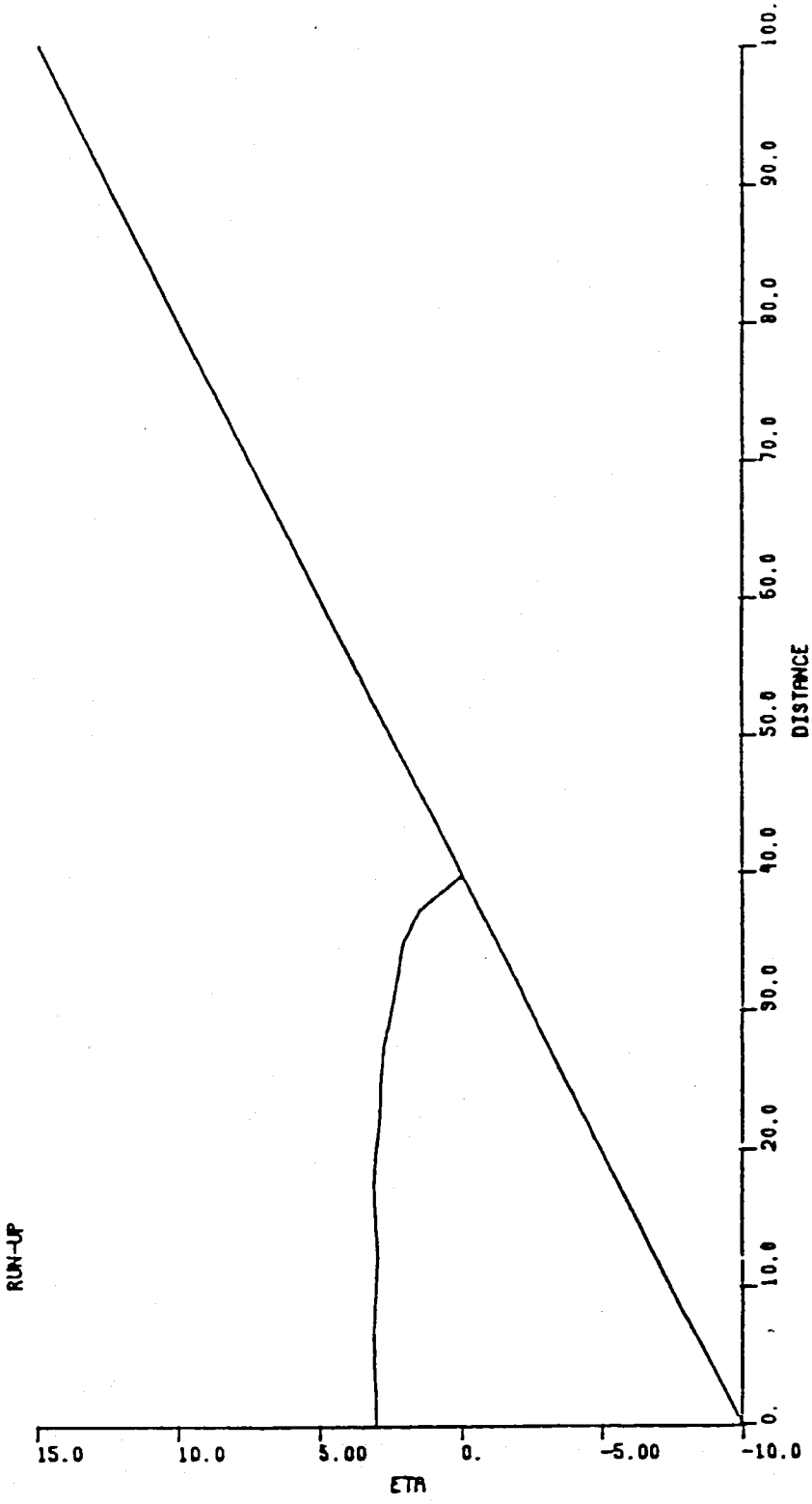

Figure 6: Wave beginning to climb the dry beach.

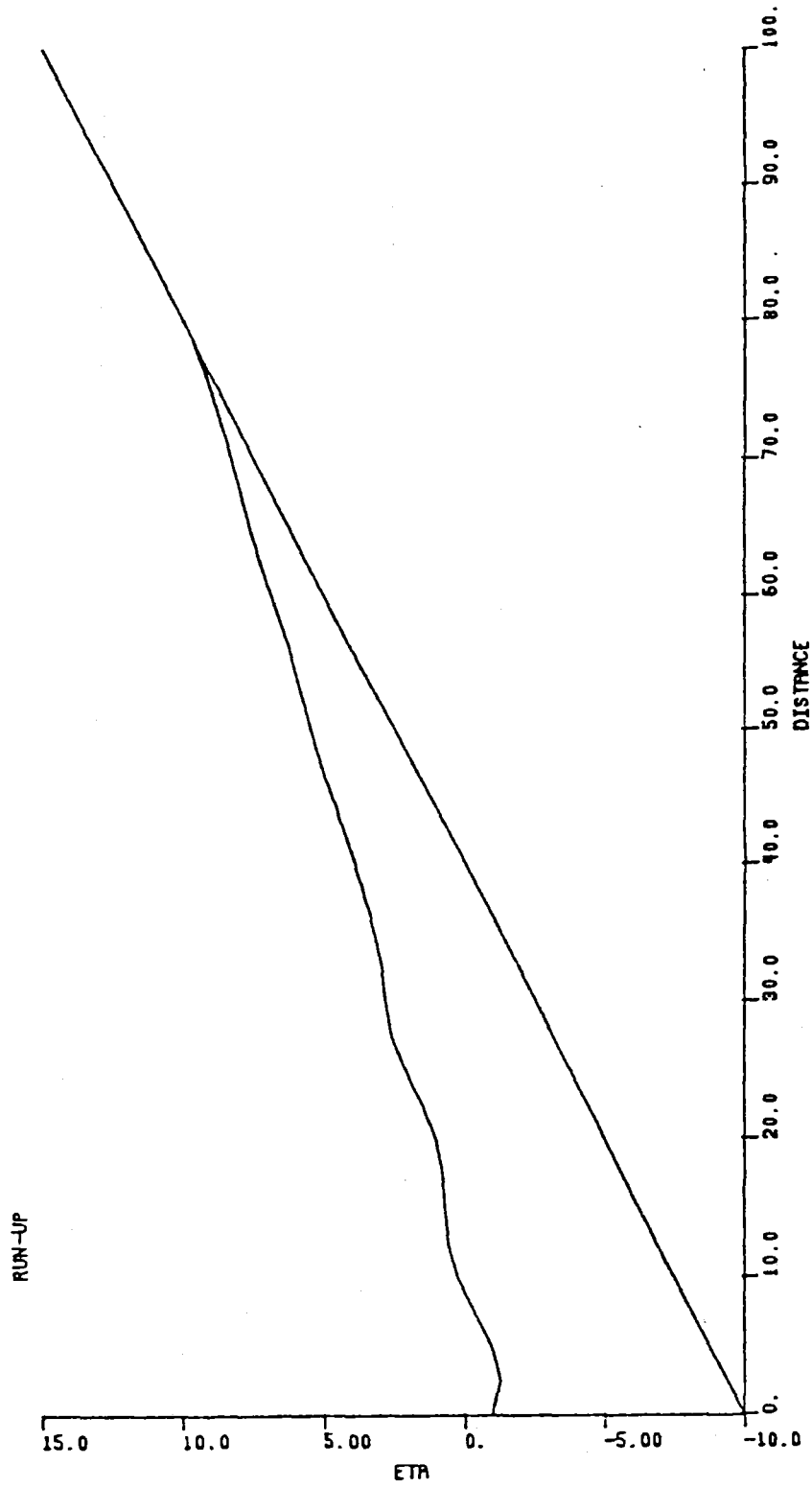

Figure 7: Wave uprush towards the end of the flooding.

HYDRODYNAMIC MODELLING: AN OVERVIEW

by

A'Alim A. Hannoura
College of Engineering, University of Qatar

ABSTRACT

The progress that has been made in the field of automated computations and numerical methods over the last three decades has made it possible to simulate a very wide range of hydrodynamic processes. Perhaps the most common problem involved in these processes is the determination of a free surface. Once the free surface is obtained, internal flow phenomena, such as velocity field and pressure distribution, could be found from the solution of the internal flow governing equation.

This paper presents a survey of hydrodynamic modelling techniques, governing equations and different hybrid approaches to the solution of hydrodynamics problems and those relating to the transport of foreign elements. Specific examples of wave-structure interaction are discussed to illustrate numerical procedures as well as their limitations.

INTRODUCTION

Since the beginning of life, water, in its different forms, has been recognized as the most precious element on earth. The word element is, of course, used here in its classical context, not in a chemical sense. In some ancient civilizations water was considered to be sacred. Today, water and its hydrological cycle are still valued as a reminder of the wisdom of God. The actions of mankind over the years have, however, failed to preserve and protect this precious source of life. Problems associated with water such as droughts, floods, undesirable physical and chemical properties of water, waterborne diseases, soil salinity, erosion and sedimentation may have taken on different weights and magnitude but they have been with us through the ages.

The evolution of knowledge has been very much related to the challenge of life and the quest for improving living standards. Our present day understanding of water systems has gone through distinctive phases of growth. First there was the period of observation and speculation, followed by a time of experimentation and measurement; this led to modernization and the periods of empiricism, rationalization and theorization. It would not have been possible to reach today's level of knowledge and expertise in the area of hydrodynamic modelling without the contributions of all of these phases, particularly the periods of modernization and theorization.

It was not until recently that mankind realized the importance of sound planning and management of water resources systems and their close association with the quality of our life. In the planning and management of water systems, it is important to understand the behaviour of the system when it is subjected to differend hydrological and meteorological conditions or operated under various policies. Physical models or electrical analog techniques are not fully capable of studying these varying conditions or policies. Conceptual models in the form of partial differential equations with appropriate boundary and initial conditions can be developed to represent the problem under consideration. Due to the complicated geometry of natural water systems and the nonlinearity of some of the flow or the domain parameters and properties, exact analytical solutions are not possible. The ever-progressing technology in the field of high speed digital computers has made it possible to use numerical methods to solve these conceptual models.

NUMERICAL METHODS

The number of available conceptual models in the areas of hydrodynamic (e.g., rivers, lakes, estuaries, tides, wave-structure/sea bed interaction) and transport (e.g., sediments and water quality related substances) processes is increasing daily. This growth is strongly related to advance in computation techniques, quantitative understanding of physical processes, and machine capabilities.

These models have utilized different numerical techniques to solve the conceptual equations of the problem under consideration. Two methods, finite difference and finite elements, have been used extensively. In the finite difference method of numerical solution, the derivatives in the conceptual model, i.e., the governing equations of flow, are replaced by difference approximations. In the finite element method, which has been gaining in popularity over the last few decades, the governing partial differential equation is integrated over the problem domain, and the divergence theorem is used to simplify the resulting equation. This

weak form of the equation is equivalent to the governing equation and has the same solution. The numerical solution of the weak form is then obtained for the potential function which is usually expressed in terms of a continuous polynomial.

The advantages and disadvantages of both methods have been the subject of several publications. While both methods have yielded similar accuracies in the solution of the governing hydrodynamic equations of a given system, the finite element method seems to approximate the solution of the transport equation better than the finite difference method.

GOVERNING EQUATIONS

In general, the hydrodynamics of a given flow system is composed of four equations in four unknowns. The hydrodynamic partial differential equations are the three motion equations and the continuity equation. These equations are solved for the three velocity components and the pressure with respect to a space-reference system (coordinates). The most general form of the motion equations for an incompressible fluid, i.e., constant density, is that given by the Navier-Stokes equations:

$$\frac{\partial u}{\partial t} + u\frac{\partial u}{\partial x} + v\frac{\partial u}{\partial y} + w\frac{\partial u}{\partial z} - 2\omega\sin\phi\, v = -\frac{1}{\rho}\frac{\partial p}{\partial x} + \nu\left(\frac{\partial^2 u}{\partial x^2} + \frac{\partial^2 u}{\partial y^2} + \frac{\partial^2 u}{\partial z^2}\right) \qquad (1)$$

$$\frac{\partial v}{\partial t} + u\frac{\partial v}{\partial x} + v\frac{\partial v}{\partial y} + w\frac{\partial v}{\partial z} + 2\omega\sin\phi\, u = -\frac{1}{\rho}\frac{\partial p}{\partial y} + \nu\left(\frac{\partial^2 v}{\partial x^2} + \frac{\partial^2 v}{\partial y^2} + \frac{\partial^2 v}{\partial z^2}\right) \qquad (2)$$

$$\frac{\partial w}{\partial t} + u\frac{\partial w}{\partial x} + v\frac{\partial w}{\partial y} + w\frac{\partial w}{\partial z} = -\frac{1}{\rho}\frac{\partial p}{\partial z} - g + \nu\left(\frac{\partial^2 w}{\partial x^2} + \frac{\partial^2 w}{\partial y^2} + \frac{\partial^2 w}{\partial z^2}\right) \qquad (3)$$

in which u, v and w are the velocity components in the x, y and z directions, where z is assumed to be vertical; $2\omega\sin\phi$ = Coriolis parameter, where ω = Earth's angular velocity and ϕ = latitude; ρ = density; p = pressure; and ν = kinetic viscosity.

In addition to these equations, the continuity equation is required to solve for the four unknowns, u, v, w and p:

$$\frac{\partial u}{\partial x} + \frac{\partial v}{\partial y} + \frac{\partial w}{\partial z} = 0 \qquad (4)$$

Physical interpretation of the governing equations

Equations 1 to 3 represent the energy balance of the system; terms such as

$\frac{\partial}{\partial t} + u\frac{\partial}{\partial x} + v\frac{\partial}{\partial y} + w\frac{\partial}{\partial z} \equiv$ the creeping flow; total acceleration;

$2\omega r\sin\phi \equiv$ mass force due to Coriolis acceleration;

$g \equiv$ surface force due to gravity;

$\frac{1}{\rho}\frac{\partial p}{\partial} =$ surface force due to pressure; and

$\nu(\frac{\partial^2}{\partial x^2} + \frac{\partial^2}{\partial y^2} + \frac{\partial}{\partial z^2}) \equiv$ surface force due to viscosity of the fluid

Equation 4 gives the mass balance. These equations have to be modified when they are applied to the simulation of hydrodynamic systems such as stratified flow, to take into account the density variations.

Governing equations and turbulence

When the time-dependent variables are integrated over time, following classical fluid mechanics and turbulence procedures, and the result of this process is applied to the Navier-Stokes equations, a new set of equations, known as the Reynolds equations, is obtained. Average values of velocities and pressure now replace the instantaneous ones and additional stresses appear due to the turbulent nature of the flow. Equations 1 to 3 are rewritten as:

$$\frac{\partial \bar{u}}{\partial t} + \bar{u}\frac{\partial \bar{u}}{\partial x} + \bar{v}\frac{\partial \bar{u}}{\partial y} + \bar{w}\frac{\partial \bar{u}}{\partial z} - 2\omega r\sin\phi\,\bar{v} =$$

$$-\frac{1}{\rho}\frac{\partial \bar{p}}{\partial x} + \nu\nabla^2\bar{u} - (\frac{\partial}{\partial x}\overline{u'u'} + \frac{\partial}{\partial y}\overline{u'v'} + \frac{\partial}{\partial z}\overline{u'w'}) \qquad (5)$$

$$\frac{\partial \bar{v}}{\partial t} + \bar{u}\frac{\partial \bar{v}}{\partial x} + \bar{v}\frac{\partial \bar{v}}{\partial y} + \bar{w}\frac{\partial \bar{v}}{\partial z} + 2\omega r\sin\phi\,\bar{u} =$$

$$-\frac{1}{\rho}\frac{\partial \bar{p}}{\partial y} + \nu\nabla^2\bar{v} - (\frac{\partial}{\partial x}\overline{v'u'} + \frac{\partial}{\partial y}\overline{v'v'} + \frac{\partial}{\partial z}\overline{v'w'}) \qquad (6)$$

$$\frac{\partial \bar{w}}{\partial t} + \bar{u}\frac{\partial \bar{w}}{\partial x} + \bar{v}\frac{\partial \bar{w}}{\partial y} + \bar{w}\frac{\partial \bar{w}}{\partial z} = -\frac{1}{\rho}\frac{\partial p}{\partial z} - g$$

$$+ \gamma \nabla^2 \bar{w} - \left(\frac{\partial}{\partial x}\overline{w'u'} + \frac{\partial}{\partial y}\overline{w'v'} + \frac{\partial}{\partial z}\overline{w'w'} \right) \quad (7)$$

and the continuity equation (Equation 4) becomes

$$\frac{\partial \bar{u}}{\partial x} + \frac{\partial \bar{v}}{\partial y} + \frac{\partial \bar{w}}{\partial z} = 0 \quad (8)$$

The Reynolds equations and the Navier-Stokes equations are actually the same if we recall that any instantaneous quantity q in equation 3 has been replaced by an average term, $\bar{q}$, plus a time dependent term, q', as follows:

$$q = \bar{q} + q' \quad (9)$$

The same procedure is also applied to the continuity equation. Of course, some new terms will be cancelled due to the nature of the random term q' and the fact that its integration over a certain time scale is equivalent to zero. On the other hand, a number of terms containing the temporal average of the products of random fluctuations, i.e. $q_i'; q_j'$; will appear, as stated above. It is apparent from comparison of the structure of this new group of terms in equations 5, 6 and 7 with the viscosity-stress terms in equations 1, 2 and 3 that they are of a similar nature.

In the Navier-Stokes equations, the stresses due to viscosity, t, are often expressed as

$$\frac{\tau_{ij}}{\rho} = \frac{\partial u_i}{\partial x_j} + \frac{\partial u_j}{\partial x_i} \quad (10) \quad (10)$$

in which u and x represent velocity and one-dimensional space, respectively, while i and j denote direction or component. An analogous expression in the Reynolds equation for stresses due to turbulence may be written as

$$\frac{\bar{\tau}_{ij}}{\rho} = -\overline{u_i u_j} = \varepsilon_{ij}\left(\frac{\partial \bar{u}_i}{\partial x_j} + \frac{\partial \bar{u}_j}{\partial x_i}\right) \quad (11) \quad (11)$$

in which ε_{ij} = turbulent viscosity. This is not a property of the fluid, however, but a tensor which depends on the hydrodynamic characteristics of the flow domain.

Additional governing equations

The equations presented above are sufficient to describe the hydrodynamics of homogeneous, incompressible and isothermal conditions. Where these conditions do not hold due to thermal or salinity processes, additional equations should be included. Such equations might include some or all of the following: a state equation to relate density to temperature and salinity, a heat budget equation, and

an auxiliary set of equations to give expressions for viscosity, bottom friction and surface wind stresses.

SIMPLIFICATIONS OF THE GENERAL GOVERNING EQUATIONS

Various difficulties arise in the application of the hydrodynamic equation, presented in the previous section, to real world problems in physical oceanography. Among these difficulties are the geometric boundaries involving the sea bed and coastline, and the nonlinearity of some of the parameters involved in the determination of different stresses. The following approximations are often made in order to simplify the general hydrodynamic equations into a more manageable form:

(1) In some problems, the value of terms considered to be small with respect to others may be neglected.

(2) Special linearization procedures are often used to approximate nonlinear terms. This is usually done in the form of an iteration process.

(3) The representation of stresses due to turbulence and the fact that the turbulent viscosity term in equation 11 is a function of space have both presented major difficulties in the simulation of hydrodynamic systems. If computation time and storage problems are solved, however, recent developments in turbulence computations, such as k-ε models, could be used. This approach would require the addition of two extra equations for the distribution of k, turbulent kinetic energy, and ε, the rate of dissipation of kinetic energy. The value of the turbulent viscosity would then be estimated using k and ε.

(4) The number of independent variables may be reduced whenever it is great enough to determine the average value of a certain variable, whether spatial or temporal. This is done by integration with respect to the independent variable to be averaged. Such approximations which reduce three-dimensional models to two dimensional ones or unsteady applications to steady ones are made to study spatial rather than temporal variations.

(5) When uncoupling space-time processes such as time-dependent free surface problems, two-dimensional models could be used to obtain the free surface. Once the free surface is known, the spatial variations could be examined for the momentary domain, neglecting time variations. This is similar to, but more refined than, the assumption of rigid lid models.

Special cases

In physical systems where the special characteristics of the flow lend themselves to one or more of the simplifications outlined above, the system may be reduced to a two- or even a one-dimensional application of the general problem, without great loss of accuracy. The following examples are some of these cases.

Two-dimensional models. Motion in rivers, lakes and estuaries is generally characterized by a very small velocity in the vertical direction compared with the horizontal velocity components of the flow. This is also true when these systems are subjected to tides or flood waves. It is not, however, a valid assumption for wind-generated waves. In the former case, the equation may be integrated over the vertical direction to obtain mean values of the horizontal velocity components.

Neglecting vertical acceleration compared to gravity reduces equation 7 to a hydrostatic equation. On the other hand, in the latter case, such approximations would not simulate the hydrodynamic feature of wind-generated waves. In order to simulate such features, the vertical variation in the horizontal velocity components must be considered; some such models have been called, incorrectly, three-dimensional models.

The use of depth-averaged or depth-varying models, discussed above, depends on the desired accuracy and the purpose of the simulation process. Depth-averaged models are useful in predicting general circulation patterns, mass transport and tides. The simulation of wind-induced currents predicting the trajectory of surface pollutants, and design information for offshore structures would, however, require the use of so-called three-dimensional models.

One dimensional models. This is a further extension of the approximations outlined above. In this case, motion is mainly unidirectional and variations in the other two directions are neglected. Some co-efficients have to be introduced to account for these approximations; for example, momentum or energy coefficients to account for the nonuniformity of the velocity distribution, and a depth-dependent friction coefficient to account for the resistance variation along the bed and sides of the flow boundaries. Typical application of one-dimensional models are found in well-mixed narrow estuaries.

TRANSPORT AND DIFFUSION EQUATIONS

In studies concerned with water quality and mass transport, the analysis often starts with the solution of the hydrodynamic equation and then proceeds to the solution of the mass transport equation.

Taking a substance such as a pollutant, with a certain concentration, then the transport equation would be as follows:

$$\frac{\partial c}{\partial t} + \frac{\partial cu}{\partial x} + \frac{\partial cv}{\partial y} + \frac{\partial cw}{\partial z} = K\left(\frac{\partial^2 c}{\partial x^2} + \frac{\partial^2 c}{\partial y^2} + \frac{\partial^2 c}{\partial z^2}\right) + S \qquad (12)$$

in which K = diffusion coefficient, and S = source or sink term. The left hand side of equation 12 represents the total change of the substance concentration, i.e., the rate of change in time and space at a particular location, given by the advection terms resulting from the motion of the fluid. The first term on the right hand side represents the diffusion of the substance considered and the last term, S, is a possible input or output term of the substance considered. Resuspension of bed material or settlement of the same suspended substance, are examples of this term.

Equation 12 gives the transport of a substance under laminar flow conditions where the left hand side of the equation gives the transport process and the right hand side gives the molecular diffusion. In turbulent flow, an additional term would appear due to random terms in the velocity components and concentration, i.e.,

$$\frac{\partial \bar{c}}{\partial t} + \frac{\partial \overline{cu}}{\partial x} + \frac{\partial \overline{cv}}{\partial y} + \frac{\partial \overline{cw}}{\partial z} = K V^2 \bar{c}$$

$$+ \left(\frac{\partial \overline{c'u'}}{\partial x} + \frac{\partial \overline{c'v'}}{\partial y} + \frac{\partial \overline{c'w'}}{\partial z}\right) + \bar{S} \qquad (13)$$

This quantity represents a new transportation factor. In this case, turbulent flow is much more important than viscosity and molecular diffusion. Equation 13 could be rewritten, after a series of manipulations similar to those above, so as to eliminate the new term accounting for molecular and turbulent diffusion.

The approximations discussed in the previous section are often applied to the transport equation in order to simplify it to two- or one dimensional applications. Other approximations may be introduced depending on the physical processes of the problem, e.g. the contribution of the turbulence components and the vertical gradient of the velocity to the transport process in stratified flows.

THE USE OF HYBRID TECHNIQUES IN NUMERICAL MODELS FORMULATION

In some hydrodynamic processes where more than one numerical technique many be used to formulate the numerical model, it may be possible to achieve greater accuracy and a saving of computer time and storage. An example of this hybrid approach is the use of the finite difference method to solve for the hydrodynamic part of an overall study of water quality, followed by the use of the finite element method for the transport process. In wave-structure interaction, where the process can be approximated by a two-dimensional representation of the wave and a rubble-mound breakwater, the problem can be solved in two stages. First, the unsteady, two-dimensional problem is approximated to a one-dimensional form, then a finite difference algorithm is used to integrate the time-dependent governing equations. The method of characteristics may be employed to provide a criterion for the time step in order to ensure stability and convergence. Secondly, the unsteady, two-dimensional problem is approximated to a momentary, two-dimensional form and the finite element method is used to integrate the space-dependent governing equation. Thus inertia effects will be dealt with using the finite different method in the characteristic phase, and the finite element method will be used to handle the irregularity of the structure boundaries as well as the inhomogeneity of the solution domation.

BIBLIOGRAPHY

Bennett, J.R. et al. (1983) A two-dimensional lake circulation modelling system: Programs compute particle trajectories and the motion of dissolved substances. NOAA Tech. Memo. ERL GLERL-46, GLERL, Ann Arbor, MI.

Cecchi, M.M. (1980) Finite element in transport phenomena. 3rd FEM Conf. In: Water Resources, Univ. of Miss., Oxford, Miss.

Chen, C.W. and D.J. Smith (1980) Preliminary insights into a three-dimensional ecological-hydrodynamic model. Chapter 10. In: Lake Ecosystem Modelling, Ann Arbor Science publisher, Ann Arbor, MI.

Cooper, C.K. and B.R. Pearce (1977) A three-dimensional numerical model to calculate currents in coastal waters utilizing a depth varying vertical eddy viscosity, Rep. No. 226, Dept. of Civ. Eng., MIT.

Csanady, G.T. (1967) Large-scale motion in the Great Lakes. J. of Oceano. Res., Vol 72, No. 16.

Fay, J.A. (1971) Physical processes in the spread of oil on water surface. Proc. Joint Conf. on Prevention and Control of Oil Spills, American Petroleum Institute, Washington, D.C.

Fallah, M.H. and R.M. Stark (1976) Literature review: Movement of spilled oil at sea. Mar. Tech. Soc. J., 10:3-17.

Fisher, H.B. (1976) Mixing and dispersion in estuaries. Ann. Rev. Fluid Mech.

Gallagher, R.H. et al. (ed.) (1975) Finite element in fluids. Vol. I. J. Wiley, New York.

Galt, J.A. (1983) Simulation of the movement and dispersion of oil slicks. Symposium/workshop on oceanographic modelling of the KAP Region, Dhahran.

Hannoura, A.A. (1980) A hybrid finite element model applied to unsteady flow problems. 3rd FEM Conf. in Water Resources, Uni. of Miss., Oxford, Miss.

Hunter, J.R. (1983) A review of the residual circulation and mixing processes in the KAP Region, with reference to applicable modelling techniques. Symposium/workshop modelling of the KAP Region, Univ. of Petroleum and Minerals, Dhahran.

Leendertse, J.J. et al. (1973-1975) A three-dimensional model for estuaries and coastal seas. Vols 1-5, the Rand Corporation, Santa Monica, CA.

Liggett, J.A. and K.L. Kwang (1971) Properties of circulation in stratified lakes. J. of Hyd. Div., ASCE, Vol. 97, No. HYI.

Ramming, H.G. and Z. Kowalik (1980) Numerical modelling of marine hydrodynamics. Elsevier Oceano. Series, No. 26, Elsevier Sci-Pub. Comp., New York.

Shen, Y.P. and W. Lick (1979) The transport and suspension of sediment in a shallow lake. J. of Geoph. Res., Vol. 84, No. C4.

Stolzenbach, K.D. et al. (1977) A review and evaluation of basic techniques for predicting the behaviour of surface oil slicks. Report No. 222, Dept. of Civ. Eng, MIT.

Thacker, W.C. (1978) Comparison of finite-element and finite-difference schemes. Part I and II, J. of Phys. Oceano., Vol. 8.

NUMERICAL MODELLING CAPABILITIES AND LIMITATIONS

by

E. M. Hassan
Chairman, Department of Marine Sciences
Qatar University

ABSTRACT

Assumptions underlying modelling are discussed. Different kinds of models are described and conditions and limitations are mentioned. Examples are given of special conditions in the Gulf, and a proposal is made for the establishment of a high-level modelling centre in the ROPME region.

NUMERICAL MODELLING CAPABILITIES AND LIMITATIONS

Models are used for various objectives, the most important of which are:

(1) To isolate and test hypotheses;

(2) To predict the behaviour of systems at future times or under specified conditions;

(3) To help control systems by investigating the effects of modifying certain conditions.

The basic assumptions underlying modelling are: that nature follows certain laws (even if, under certain circumstances or in certain instances, they are stochastic); that natural systems are heirarchically separable; and that natural systems can be approximated as linear by parts. The first condition allows modelling in principle, if the laws are known or approximated. They do not have to be understood. An example is the tidal prediction in ports. Although it is well known that the gravitational forces of the moon and the sun cause the tides, these can be predicted from a long record of water elevations without reference to the tidal producing forces. The second condition allows a system to be modelled without modelling the underlying systems, e.g., in modelling oceanic circulation, no account is taken of the fact that water is composed of molecules of Hydrogen and Oxygen. The third condition allows a part of the universe, say the ocean, or a subsection of it, say the surface layer, to be isolated and modelled without modelling the whole universe. Without the second and third assumptions, the simplest model of anything would be the thing itself and the shortest time taken to make a model would be the real time required to create the physical entity.

Modelling is a characteristic brain activity, usually carried out subconsciously, to make generalisations, projections or predictions and thus allow for the maximum and most efficient use of the brain rather than cramming it with unrelated items of information. The brain, thus, organizes information in patterns and uses rules to connect these patterns; this is the essence of modelling. Numerical modelling is usually done outside the human brain, in the "brain" of a computer, itself a brain-child and an external extension of the human brain. The computer, of course, needs rules and data to enable it to proceed.

A model needs the following elements: initial data (even a set of zeros), rules to define its development and the routes it would take at logical branches, and boundary conditions in space and time (or other appropriate variables). In order for the system to be soluble, certain mathematical conditions have to be satisfied to ensure the existence and uniqueness of the solution. This cannot always be worked out from the mathematical formulation; even if it can, the process may be extremely complicated. Most modellers, however, proceed happily where mathematicians fear to tread. The mathematical equations representing the model have to be complete from the mathematical point of view (necessary and sufficient), and correct from the natural (or physical) point of view. Inaccuracies in the initial or boundary conditions can be tolerated to some extent by models. If the rules that control the development of the model are wrong, however, the deviation between the model and the prototype will increase with the number of iterations or of time steps. Other restrictions and errors are imposed on the model by the numerical process itself. These will be mentioned later.

Models can be classified in many ways. Four of the most important types will be briefly mentioned below:

(1) Discrete and continuous models

In a discrete model, the variables are defined at a set of points in the space-time matrix. Interpolation between points may or may not be possible, or it may be possible if further assumptions are made regarding the model. In a continuous model, the variable is known at all points in space and at all instants of time. This occurs in analytically solved models and in analog models. Mixed models can be found where some variables are continuous in certain directions and discrete in others, or continuous in time but discrete in space, etc. Generally, numerical models are discrete. The discreteness imposes additional mathematical restrictions, as will be discussed below.

(2) Kinematic and dynamic models

A kinematic model models motion without relating it to its causes, i.e. without consideration of cause and effect. An example of this type of model is the prediction of tides; for over a hundred years, the prediction has been based on observation of water levels, rather than on a calculation of lunar and solar gravitational forces. This kind of model depends to a great extent on the regularity of the phenomenon. Dynamic models use causes (usually forces) as a starting point. They thus require a deeper level of understanding of the different relationships and boundary conditions of the system, but not necessarily as long a record as kinematic models. Examples of dynamic models are weather prediction models and oceanic circulation models.

(3) Deterministic and stochastic models

A deterministic model does not have random variables in its system and always reaches the same ending from the same beginning, through the same pathways. This is exemplified by a complete system of equations with fixed coefficients. Stochastic models contain random variables; thus successive runs of the model, starting with the same data and using the same conditions, produce different results. An example of this type of model is a circulation model using windstress with a random element. Random variables in the model sometimes reflect the existence of variables below the level of detection or resolution of the model.

(4) Stationary (or steady state) models and time dependent models

A stationary model is independent of time and its results remain constant with respect to time. The steady state can, however, appear variable if presented in another framework. An example of this is that the magnitude of a harmonic component appears as a constant in frequency space, whereas the velocity appears as a variable in time space. Time dependent models, however, appear non-stationary in any framework due to the effect of non-stationary functions. The results continue to grow, settle in an equilibrium range or die out according to whether the generative forces exceed, equal or become less than the dissipative forces.

Because numerical models always contain discrete elements, they are subject to two further limitations. The first concerns the resolution of the model. It is obvious that the model cannot "see" to a resolution finer than the spacing of its network. Thus, the level of detail required in the result is an important factor in deciding the mesh size of the model. In particular, any periodic variable that has a period exactly equal to the mesh size will not be detected and will propagate through the system. The second is the problem of "aliasing". This results from variables that have periods slightly different from the mesh size. These would be "seen" by the model as variables with longer periods and cannot be separated from them.

Another kind of problem results from instabilities in the model when certain conditions about the sizes of different meshes are not observed, e.g., relationships between the time step and space step in the problem of diffusion, or when a certain kind of differences are used instead of another, such as using central differences in space under certain circumstances rather than one-sided differences. These conditions can be established in simple cases, e.g., simple diffusion, but difficulties increase rapidly as the system becomes more elaborate, and conditions can rarely be determined by theoretical considerations.

The above comments briefly outline the choices and difficulties faced by the numerical modeller in modelling aspects of the Gulf. Many kinds of models have to be used, however, to model the Gulf environment. The papers presented in this symposium show that a start has already been made in developing these models. An enormous number of systematic and coordinated observational and experimental programmes will have to be carried out, however, to provide data for the models and to test them, particularly in features that are unique to the Gulf. For example, the shallowness of the Gulf necessitates very careful considerations of the topography of the bottom and of bottom friction as a major dissipative force. Another feature is the amount of oil reaching the Gulf water daily in normal operations. This would cover an area of about 2000 km2 daily to a thickness of 10 microns, affecting both energy and material exchange between the Gulf water and the atmosphere, and the characteristics of the water surface. What is the lifetime of this layer (before it dissolves or evaporates) and how much of the Gulf is covered by oil at any one time? Again, with a residence time of water in the Gulf between one and five years, what is the residence time of oil that reaches this water? Is it blown by the wind or does it move with the currents? Again, what is the effect locally and in the whole Gulf of the fresh water systematically removed from the Gulf and the heat systematically added?

One complete area of modelling that is woefully deficient in the Gulf is eco-system modelling. In certain respects, this is the culmination and purpose of other modelling, the results of which would be inputs to models of the eco-system. This area needs further attention and examination.

Modelling requires a powerful concentration of manpower of different disciplines, as well as powerful computing tools backed by good mathematical and statistical help and banks of observational material to construct and test models. Experience has shown that, while the observational programme is of necessity diffuse, the modelling programme should be concentrated in one location (e.g., NOAA fluid dynamic laboratory in Princeton) and it is suggested that ROPME and its States consider the establishment of such a modelling centre of excellence.

To conclude, numerical modelling is a very powerful tool for understanding, predicting and helping to control natural phenomena and for planning courses of action. It is limited by the limits of observations, the correctness of the laws used, the limits of detection and a host of mathematical difficulties. Continuing interaction should be maintained between the modeller and the observational programme. By its nature and as shown experience, modelling is best carried out in a strong centre of excellence. It is suggested that such a centre be considered for the ROPME area.

A REVIEW OF THE RESIDUAL CIRCULATION AND MIXING PROCESSES IN THE KAP REGION WITH REFERNENCE TO APPLICABLE MODELLING TECHNIQUES

by

J.R. Hunter

Marine Science Laboratories;
Menai Bridge, Anglesey, North Wales
United Kingdom

ABSTRACT

The available literature concerning the main aspects of the residual circulation and mixing processes in the KAP Region is reviewed.

Unfortunately, there are virtually no published reports of direct measurements of residual currents in the Region, and estimates up until now have been based on observations of ships' drifts and of the distribution of salinity, and on the modelling of the dynamics of the water movement. All three methods are prone to various errors but it is shown that a reasonably consistent picture of the overall circulation pattern (an anti-clockwise density-driven flow, somewhat modified by the surface wind stress) can be obtained from them. It is noted that, whereas numerical hydrodynamic models have been very successful in accurately predicting tidal currents in the coastal sea areas of the world, their usefulness in predicting residual currents is rather limited; they are still primarily research tools, to be used with caution in conjunction with other techniques.

Estimates of the turn-over time (the time for all the water in Gulf to come within the influence of the open sea boundary at the Strait of Hormuz) and the flushing time (the time for all the water in the Gulf to be exchanged with water from the open sea) are made from our knowledge of the residual flow, from computations based on the water and salt balance of the basin and from an understanding of the physical processes operating in the Region.

Applicable modelling techniques are reviewed, ranging from simple (but often very useful) single-box models to complex three-dimensional models of the momentum, water, heat and salt balance of the sea.

INTRODUCTION

The physical oceanography of the KAP Region has been reviewed by Grasshoff (1976), Hughes and Hunter (1979) and Hunter (1982a, 1982b). More general reviews of the marine environment of the Region have been given by Hartmann et al. (1971), Purser (1973), UNESCO (1976) and Kashfi (1979). A recent bibliography of the marine science of the Region has been given by Farmer and Docksey (1983).

It is evident that there are virtually no published direct measurements of residual currents (i.e., the currents left behind after the removal of tidal oscillations) or of mixing processes. The former could be obtained by a long (e.g., one month) time series of observations using current meters or Lagrangian drifters, while the latter could be obtained using a dissolved tracer such as dye. Hence we have to resort to indirect methods, such as the analysis of the drifts of ships at sea, or of "conventional" oceanographic variables (such as temperature and salinity), in order to investigate these phenomena.

The problem is further complicated by the fact that neither residual currents nor mixing processes are constant in time; both display fluctuations due predominantly to meteorological forcing and, less importantly, to tidal variations such as the Spring-Neap cycle. The time scales involved range roughly from the diurnal variations (e.g., sea-breeze effects), through the scales of short-term meteorological variability (e.g., of the order of days), through seasonal changes and ultimately to long-term climatic trends. It is generally assumed that an environmental data set averaged over a long enough period provides a measure that has some significance for future predictions. As a general rule, averages taken over a period of the order of a month are often indicative of conditions for that season of the year (although of course, for example, no two winters are identical), and averages taken over a period of the order of a year are indicative of some long-term mean (but again we should bear in mind that the weather varies significantly from year to year). Furthermore, the data within a set must be sampled frequently enough to include all the significant variations; for instance, it would be incorrect to produce an estimate of an annual mean current, based only on observations taken during the daytime, as nightime residuals may be significantly different.

There is also the problem of spatial averaging, as oceanographic parameters do not necessarily follow smooth variations in space. Quite often, coarse sampling grids completely miss some important phenomenon, and it is only through careful planning and flexible execution of an experiment that an oceanographer can be reasonably sure that his data set reflects the real world.

The twin objectives of long data sets (adequately sampled in time) and closely-spaced observation points must be balanced against logistic constraints, and so real data sets generally fall far short of the scientific ideal. As an example, probably the most comprehensive set of "conventional" oceanographic observations (temperature, salinity and chemical measurements), pertaining to winter conditions in the Region, has been reported by Brewer et al. (1978). This was based on a single cruise of the research vessel "Atlantis II", covering a period of only 10 days. During this time, 48 oceanographic stations were visited, and observations were reported at approximately every 10 m of depth (although temperature and salinity would have actually been sampled far more frequently in the vertical). The station pattern consisted of a "leg" up the deep-water axis of the Region, and 5 main transverse sections. The transverse sections were separated by roughly 200 km, and stations within each section by typically 30 km. Such coverage represents an intelligent compromise, but necessarily involves large "holes" of area, roughly

20,000 km2 within which no observations were made at all. At present, an understanding of the physical oceanography of the Region has to be based on data sets of this type.

An understanding of the physical processes at work in the sea may be furthered through the use of modelling techniques. These may range from simple equations defining, say, a one-box flushing model, to complex three-dimensional models of the momentum, water, heat and salt balance of the sea. The latter may at present be implemented only on the largest of modern computers. Modelling makes it possible to combine current (limited) knowledge of mechanisms with observational data and to give fresh insight into the relevant processes or to predict observable parameters not previously measured. A particularly successful example has been in the use of vertically-averaged numerical hydrodynamic models to predict tidal elevations and currents in shelf seas. The physical processes which determine such tidal motions have been quite well understood for a long time, and there are also numerous records of tidal elevations from ports around the coasts. There is, however, rather a deficiency in observations of offshore tidal elevations and currents in many shelf sea areas of the world, and numerical tidal models have served as useful and verifiable tools for the prediction of these variables from existing data. Models are hence used in this way as "intelligent" (i.e., they include information based on an understanding of the mechanisms at work in the sea) interpolators of observations that are sparse, in the sense that they come mainly from the coasts rather than from offshore areas. There have been two quite successful models of the tidal motions in the Region (von Trepka, 1968; Evans-Roberts, 1979).

Vertically-averaged hydrodynamic models of the type used to predict tidal motions have been used extensively in attempts to predict residual currents in shelf seas. While they have been quite successful in predicting "surge" events (i.e., strong time-varying motions of time scales of the order of a few days, associated with moving meteorological systems, e.g., Davies and Flather, 1977), they have really been quite unsuccessful in predicting longer term variations of the residual currents. This failure arises from three main factors, all associated with the process of vertically averaging (which is used for computational efficiency, since it reduces a three-dimensional problem to a two-dimensional one):

(a) An inherent assumption in such models is that the currents do not vary dramatically over the depth. It is known (Hsu et al., 1982) that a significant proportion of the momentum transferred to the water by the wind goes (initially at least) into the generation of surface gravity waves. Associated with these waves, there is a residual flow (the Stokes drift) of roughly 3 per cent of the wind speed (Kenyon, 1969), which resides in a surface layer about one quarter of a wavelength thick (typically 10 m in shelf seas). The effect of the rotation of the Earth may also lead to the formation of a surface Ekman layer in which the other part of the residual flow would be concentrated. These flows are clearly not treated correctly in vertically-averaged models.

(b) The bottom stress is generally assumed to be parallel to the vertically-averaged velocity and related to it by a simple linear or quadratic power law. This is a reasonable approximation if the velocity does not vary much over the depth but can be quite incorrect when effects due to the rotation of the Earth lead to the formation of a bottom Ekman layer, in which case the bottom stress may lie at a considerable angle to the depth-averaged current.

(c) Residual currents are often generated by horizontal pressure gradients arising from density variations in the sea (caused either by temperature or salinity changes). Vertically integrated models can only treat such situations very

crudely, and can give no indication of the resultant vertical shear in the water column.

These problems can be partially removed by resorting to three-dimensional models, with their inherent disadvantage of much increased computational cost. Further complications arise from the necessity to introduce extra parameterisations to cope with variation in the vertical direction (such as the introduction of vertical eddy viscosity). These paramaterisations are generally poorly understood, especially in regions where the water density is vertically stratified, and often have to be "tuned" to obtain the optimum model results.

Computer models of mixing processes (dispersion models) in the sea suffer from other disadvantages:

(a) As with dynamic models, many of the paramaterisations (such as, in this case, eddy diffusivities) are poorly understood, especially in regions where the water density is vertically stratified.

(b) Many numerical models rely on finite-difference schemes as approximations to define partial differential equations. In most simple schemes, the simulation of advective processes is generally poor, leading to numerically-induced diffusion of the dissolved contaminant. This problem may be alleviated completely by resorting to particle-tracking techniques, but here it is the diffusive terms that pose a problem. A solution is through the use of a random-walk (or Monte-Carlo) method to simulate diffusion but this can lead, in some cases, to a great increase in computational cost. The numerical diffusion caused by many advective finite-difference schemes does not pose nearly so much of a problem with hydrodynamic models, as in these cases the advective terms (for momentum) are generally rather small, whereas they are normally dominant in dispersion models.

There have been few attempts to model either residual currents or mixing processes in the Region.

OBSERVATIONS OF THE RESIDUAL CIRCULATION OF THE REGION

It has been known for a long time that evaporation exceeds precipitation in the Gulf, and so it would be expected that the more saline dense water would sink and pass out of the Strait of Hormuz, giving rise to a compensating surface flow of less dense water into the Gulf. The effect of the Earth's rotation would be to deflect these flows to the right, giving a surface flow west and north-west along the Iranian coast, and a deep flow to the south-east and east along the coasts of Saudi Arabia and the United Arab Emirates; the deep flow would be further contrained to these latter coastlines as the shallow sea areas of high evaporation lie in these regions. This circulation pattern would undoubtedly be modified by forcing by wind and atmospheric pressure, but it has been generally supported by observations of drifts of ships at sea.

Evidence for this anti-clockwise residual circulation in the Gulf, driven predominantly by evaporation (giving rise to horizontal density and pressure gradients) has been described by Schott (1918), Barlow (1932a, 1932b, 1932c), the British Admiralty (1941), Emery (1956), Sugden (1963), Hartmann et al. (1971), Szekielda et al. (1972), Purser and Seibold (1973), Grasshoff (1976), Szekielda (1976) and Brewer et al. (1978).

Szekielda et al. (1972) and Szekielda (1976) reported that data from ships' drifts indicated two separate anti-clockwise circulations, one in the northern part of the Gulf and one in the southern part. However, an analysis of all the ship drift data collected by the British Meteorological Office up to 1981 (Hunter, 1982a) does not support this view. These latter data consisted of 1806 observations distributed over 28 "one degree" (latitude and longitude) squares, divided up both by month and by season. Simple statistical tests were applied to indicate if the vector average for a given "one degree" square represented a significant residual flow; if not, then that data set was rejected. This would not necessarily mean that the residual at that square was small, but rather that the variability was too large for a constant residual to be detectable. Figure 1, reproduced from Hunter (1982a), shows the resultant data for the whole year after statistical selection; vector tails are centred on each "one degree" square, and a black circle indicates the centre of a square where the observed residual was not statistically significant. These vectors show considerably less spatial variability than the raw data i.e., including every observed drift, and generally indicate a surface flow westward into the Gulf along the Iranian coast of magnitude about 0.1 m/s. There is also the suggestion of an anti-clockwise circulation. The analysis was also carried out for the four seasons. The results did not differ markedly from those for the whole year, except that less "one degree" squares were accepted since there were, on average, less observations per square, the westward flow into the Gulf appeared strongest in summer (about 0.2 m/s) and weakest in spring and autumn (about 0.1 m/s) and there was little evidence of an anti-clockwise circulation (i.e. no eastward return flow was present).

Current estimates based on ship drift observations may be subject to a number of errors (HMSO, 1977), one of the main ones being due to the ship's windage, tending to bias estimates in the direction of the prevailing wind if sufficient allowance is not made for this factor. The prevailing wind in the Gulf, however, is from the north-west and west (IMCOS, 1974), in opposition to the dominant inferred flow. It would hence appear that the ship drift observations are an indicator of the "long-term" circulation pattern, namely a surface inflow towards the west along the Iranian coast, between 0.1 m/s and 0.2m/s in strength (strongest in summer). There are, unfortunately, few data on the currents in the south and south-west regions of the Gulf, due to the absence of ships' observations in these areas.

The northwestern part of the Gulf is undoubtedly influenced by the fresh water inflow of the Tigris, the Euphrates and the Karun (entering the Gulf via the Shatt Al-Arab). This inflow appears to be deflected to the right by Coriolis force to form a river plume of width approximately 20 km, flowing along the Iraqi coast into Kuwait waters (Mathews et al., 1979). This phenomenon is also indicated by observations on a somewhat larger scale by Dubach (1964) and Brewer et al. (1978).

The inflow of water from the Gulf of Oman, near the Iranian Coast, and conditions in the Strait of Hormuz have been observed by Sonu (1979). In the Strait of Hormuz, the inflow was estimated to occupy the top 30 m of the water column, a mixing layer the middle 20 m and the outflow the bottom 30 m. Current observations were made from on board ship, near Kish Island, off the Iranian coast, but no effort was made to remove the tidal oscillations (which probably exceed the residual flow in this area), or even to report at what time in the tidal cycle the observations were made.

The deep saline outflow of water from the Strait of Hormuz into the Gulf of Oman has been observed by Sewell (1934a, 1934b), Emery (1956), Duing and Koske (1967), Duing and Schwill (1967) and Leveau and Szekielda (1968). Unfortunately, the time of year during which the observations were made is not clear from some of these reports. It appears, however, that a tongue of saline water flows out of the

Strait of Hormuz at a depth of about 100 m, sinks to about 200 m in the Gulf of Oman and finally sinks to about 500 m in the south Arabian Sea. Duing and Koske (1967) reported a seasonal variation in the northern parts of the Arabian Sea (and hence, probably in the Gulf of Oman). Sewell (1934a) described a second tongue of saline water passing out of the Gulf of Oman from the surface to about 50 m depth (it is believed that these observations were made in the winter).

The residual circulation in the Gulf of Oman (and indeed in the southern part of the Gulf) is undoubtedly influenced by the seasonal effect of the south-west and north-east monsoons. It has long been realised that these give rise to a seasonal reversal of currents in the North Indian Ocean (Warren, 1966), the currents being generally to the west during the north-east monsoon (winter) and to the east during the south-west monsoon (summer). The surface currents observed from ship drifts in the Gulf of Oman do not appear to show a consistent seasonal pattern. Barlow (1932a) reported earlier observations up until that time which indicated a surface outflow in the Gulf of Oman during the winter, and a surface inflow in the summer. Barlow (1932b, 1932c) then described later observations that indicated an outflow in the Gulf of Oman in the summer as well. Barlow also described the interesting phenomenon that, between February and April, the "south-west monsoon" type of circulation is established in the Arabian Sea while the north-east monsoon is still blowing. The current Admiralty Pilot (British Admiralty, 1967) indicates, in winter, an inflow along the northern coast of the Gulf of Oman and an outflow to the south of this, with a reversal of this situation in summer.

Published accounts of direct observations of currents in the Region are few. The observations of Sonu (1979) have been referred to above. British Admiralty charts report a few observations in the form of tidal stream "diamonds", but these are based on records of generally short duration, and the residual flow has usually been removed from the data before presentation. Peery (1965) probably gave the most complete set of direct current observations in the Region, but these were based on records durations of 3 days or less, and were made from on board an anchored ship. These results were hence probably contaminated by ship movement, and would not anyway be representative of any long-term residual flow. They do, however, serve as a useful data set to be used with numerical model results as indicators of tidal currents in the Region. Dubach and Wehe (1959) reported observations in Kuwait harbour, but these are only indicative of tidal flows.

There have undoubtedly been many observations taken by moored recording current meters in the Region, as part of commercial survey programmes. These data sets are difficult to obtain partly because they are presented only in the form of internal reports, and partly for reasons of confidentiality. Many of these would have been recorded in coastal regions and would hence not be of great value in indicating the overall features of the residual circulation in the Region.

SIMPLE MODELS OF THE RESIDUAL CIRCULATION

It would appear that the dominant forcing mechanism for residual currents in the Gulf is through pressure gradients arising from evaporation-induced density variations. Horizontal variations in water density give rise to horizontal pressure forces which vary with depth. These lead to vertically varying horizontal water velocities, which balance the density forces by the following mechanisms:

(a) by internal friction (i.e., turbulent stresses), and
(b) by a Coriolis force at right angles to the water flow.

Superimposed on these depth-varying currents may also be a baratropic flow balanced by a surface slope and Coriolis force, and a bottom Ekman layer (which probably exists in the Gulf, as the "Ekman depth" is in many places less than the water depth (Hunter, 1982a)).

A technique used by the deep-sea oceanographer is to assume that between the surface and bottom Ekman layer (the former caused by the wind stress), i.e., the bulk of the ocean, the dominant process determining the vertical variations in horizontal velocity is a balance between density forcing and Coriolis accelerations (mechanism (a) above). This leads to the well-known geostrophic computation, which allows the oceanographer to determine velocity variations from estimates of sea water density made over two adjacent vertical profiles. Hunter (1982a) considered four vertical density profiles on a transverse oceanographic section in the southern part of the Gulf, reported by Brewer et al. (1978), and performed geostrophic computations for two pairs of these profiles. He showed that the density structure was consistent with a velocity difference from surface to bottom of between 0.1 and 0.2 m/s. As the density data were recorded in the winter, this result is in approximate agreement with the estimate of surface inflow obtained from ship drift data (Hunter, 1982a). Hence it would appear that, in winter at least, the inflow and outflow passing along the axis of the Gulf is geostrophically balanced (i.e., balanced by Coriolis force) across the channel. It is probable that similar agreement would be found for geostrophic computations carried out on data collected in the summer (the only comprehensive set of summer oceanographic data is due to Emery (1956), who unfortunately gave little density information).

However, if it is postulated that the Coriolis force at right-angles to the current is balanced by pressure forces due to density variations and surface slopes, the condition of a force balance parallel to the flow must also be satisfied. Internal friction in the fluid due to vertical shears in the horizontal velocity must also be balanced by density and surface slope driven pressure forces. Unfortunately, the present understanding of the internal viscous stresses due to turbulence in a stratified fluid is poor, and it is difficult to make reliable predictions of the estuarine-type circulation due to this balance of forces. Hughes and Hunter (1979) hence concluded that the density-induced forces would not be sufficient to sustain the observed circulation pattern, while subsequent computations of Hunter (1982a) indicated that they would. A simple model of the Gulf as a two-layer stratified system shows how this is possible. Consider the longitudinal section of a channel containing a layer of light fluid overlaying a layer of dense fluid, as shown in Figure 2. For simplicity, the two layers are of the same thickness, and the flows in the two layers are equal and opposite. The sea surface and interface are sloped so as to support the shear stresses at the interface and bottom. These shear streses may be derived from quadratic friction laws, and corresponding dimensionless drag coefficients. It can be simply shown that:

$$u^2 = g d \frac{\partial \eta}{\partial x} \left(\frac{\rho_2 - \rho_1}{\bar{\rho}} \right) \Big/ \left(8 C_I + C_D \right) \qquad (1)$$

where: u is the velocity in each layer,

g is the acceleration due to gravity,

d is the layer thickness,

$\frac{\partial \eta}{\partial x}$ is the interface slope

ρ_2 is the density of the lower layer,

ρ_1 is the density of the upper layer,

$\bar{\rho}$ is a (constant) reference density,

C_I is the interfacial drag coefficient, and

C_D is the bottom drag coefficient.

The interfacial stress has been taken as:

$$\bar{\rho} C_D u^2 \qquad (2)$$

and the bottom stress as:

$$4 \bar{\rho} C_I u^2 \qquad (3)$$

Inserting typical values:

g = 9.8 SI units

d = 25 m

$\frac{\partial \eta}{\partial x}$ = .0002 in winter (Brewer et al. 1978)
or .00004 in summer (Emery, 1956)

$\frac{\rho_2 - \rho_1}{\bar{\rho}}$ = .00075 in winter (Brewer et al, 1978)
or .0025 in summer (Emery, 1956)

C_I = .0004 (Bo Pedersen, 1980)
C_D = .0025 (Proudman, 1953)

gives:

u = .08 (winter)
and .07 (summer)

These are of the same order as the surface currents obtained from ship drift data, so it appears that the observed longitudinal density gradients are sufficient to drive these currents against internal friction. On the basis of a geostrophic force balance across the Gulf and a frictional balance along the Gulf, Hunter (1982a) indicated the circulation schematically by the diagram shown in Figure 3. Evaporation in the shallow areas of the southwestern and southern Gulf leads to a

sinking of dense water that is deflected to the right by Coriolis force to flow out at the bottom of the Strait of Hormuz. This flow is compensated by a surface inflow along the Iranian coast. This circulation will be modified by the effect of surface wind stress, especially in shallow areas where the effect of density forcing will be small; this is evident from the form of equation (1).

Gulfs in which evaporation exceeds precipitation and runoff are generally called inverted estuaries, as an analogy with conventional estuaries where fresh water inflow is diluted by salty water entering from the sea. The latter have been usefully classified by the method of Hansen and Rattray (1965, 1966), which consists of a simplified model of the central region (longitudinally) of an estuary, involving equations defining the balance of momentum, water and salt. The analysis indicates that an estuary may be classified by only two parameters, two pairs of which were given by Hansen and Rattray:

(a) The ratio between the surface velocity and the sectional mean velocity (the latter is due to the fresh water flow); and the ratio between the surface to bottom salinity difference and the sectional mean salinity.

(b) The densimetric Froude number, defined by the ratio between the sectional mean velocity and a densimetric velocity (which is a function of the estuary depth and the densities of fresh water and sea water); and the ratio between the sectional mean velocity and the root mean square tidal velocity (there is an implicit assumption here that mixing in the estuary is driven primarily by tidal currents).

The basic classification consists of plotting the parameter pair (a) as horizontal and vertical axes respectively. The model of Hansen and Rattray predicts the ratio between the upstream salt flux due to horizontal diffusive processes, and the total upstream salt flux (the remainder of the upstream salt flux is due to the density-induced circulation), as a function of these two parameters. This prediction uses no empirical data, and depends only on the constraints of the conservation equations used, and on certain similarity assumptions. It allows an estimate to be made of the relative importance of density-induced circulation from a knowledge of the parameter pair (a) only (which must be measured for each particular estuary).

On the assumption that estuaries could also be classified by parameter pair (b), Hansen and Rattray obtained empirical relationships between (b) and (a), using data from eight real estuaries. If both parameter pairs (a) and (b) are known, a check may be made on the consistency of Hansen and Rattray's model and, hence, an indication is given of the physical processes involved.

It seems reasonable to be able to classify an inverted estuary in the same way, if the loss of fresh water by evaporation is understood as equivalent to a negative fresh water inflow. The evaporation rate for the Gulf, for different times of the year, has been given by Privett (1959). For the present classification, the fresh water flow was taken as half the total estimated evaporation rate for the Gulf; this is roughly the fresh water flow half-way up the Gulf.

The Gulf geometry as given by Emery (1956) and the following values are assumed:

Surface velocity

= 0.1 m/s in winter (Hunter, 1982a)
or 0.2 m/s in summer (Hunter, 1982a)

Fresh water flow due to evaporation

= 0. 001 m/s in winter (Privett, 1959)
or 0.0005 m/s in summer (Privett, 1959)

Salinity difference over water column

= 2 ppt in winter (Brewer et al, 1978)
or 2 ppt in summer (Emery, 1956)

Sectional mean salinity

= 39 ppt in winter (Brewer et al, 1978)
or 40 ppt in summer (Emery, 1956)

Depth of water for evaluation of densimetric velocity

= 50 m

Density of sea water

= 1025 SI units

Density of fresh water

= 1000 SI units

Root mean square tidal velocity

= 0.14 m/s (von Trepka, 1968)

The winter and summer conditions fall on the classification diagram as shown in Figure 4. Winter and summer positions are shown for each of the parameter pairs. It is seen that classification by the two methods agrees well along the horizontal axis, but disagrees by about an order of magnitude on the vertical axis. This disagreement can be rectified by the simple adjustment of increasing the root mean square tidal velocity by a factor of 4 to 0.6 m/s. These adjusted points are also shown in Figure 4. The necessity of making this adjustment suggests that mixing processes in the Gulf are not solely due to tidal processes. This is not unexpected, as the density-driven current is of the same order as the tidal current (and can hence contribute to the supply of mixing energy), also, wind-induced mixing must play an important role. The positions of the points based on parameters (a) and adjusted parameters (b) indicate that the ratio between the upstream salt flux due to horizontal diffusive processes, and the total upstream salt flux, is about probably less than 0.01 in both winter and summer (using data from Hansen and Rattray 1966). Compared with conventional estuaries, the Gulf falls on the borderline between partially-mixed estuaries where longitudinalsalt transfer is by both advection and diffusion (Type 2) and those where the longitudinal salt transfer is primarily by advection (Type 3). Winter conditions are not very different from those of the Mersey Narrows, England, although of course the spatial scales differ by about two orders of magnitude.

From this simple classification of the Gulf as an inverted estuary, two important point emerge:

(a) The longitudinal transfer of salt is dominated by the density-induced circulation. This effect will probably also dominate the transport of dissolved contaminants in the Gulf.

(b) Mixing processes in the Gulf are not solely driven by tidal currents. Both density-driven flows and surface wind stress will play an important part.

A NUMERICAL MODEL OF THE RESIDUAL CIRCULATION

It is clear that the circulation of the Region is complex and three-dimensional. The only numerical three-dimensional model of the overall residual currents in the Region, known to the author, is by Hunter (1982b). The model was used to simulate the steady-state response of the Gulf to a specified density distribution (derived from the winter observations of Brewer et al. 1978) and a uniform wind stress. Specific features of the model were:

(a) The computation was on a flat Earth, using the beta-plane approximation and variable topography.

(b) The equations were time-dependant and linearised, with the damping effect of the tides included through appropriate bottom friction.

(c) Sigma coordinates were used in the vertical (i.e., the vertical axis was scaled by the local depth).

(d) A quadratic law was used to relate wind stress to wind velocity.

(e) A fixed sea level was prescribed at the open boundary.

(f) The density data were not subject to modification by the model.

(g) The vertical eddy viscosity and linear bottom friction coefficient were best guesses from the available data, and were not tuned to obtain optimum model results.

(h) The model mesh consisted of 331 cells in the horizontal, each divided into 5 levels.

(i) The model was run to steady state (for the internal velocity field), which took about 23 days.

(j) Two model runs were implemented: one for the case of no wind, and one for the case of a typical wind.

Figure 5 shows the predicted surface and bottom currents under conditions of a 5 m/s wind from the north-west, a typical wind for the Gulf. "Noise" present in the predicted velocities was attributed to the use of relatively sparse density data collected over a period of only one month. The predictions indicate a surface inflow of strength around 0.1 m/s along the Iranian coast, some evidence of river inflow at the northwestern end of the Gulf, and an outflow of water along the bottom

from the coastal areas off Saudi Arabia, Qatar and the United Arab Emirates. The wind stress generates clear Ekman rotation and a surface inflow into the region north of the United Arab Emirates.

MIXING PROCESSES IN THE REGION

Mixing processes in the Gulf were reviewed by Hughes and Hunter (1979). They showed, from simple analysis of the limited oceanographic data available that:

(a) The time to obtain 90 per cent mixing of a contaminant over a water column in the Gulf would be around 16 days (longer in summer, due to the presence of vertical thermal density stratification, inhibiting mixing).

(b) Exchange of water in the horizontal direction is dominated by the residual circulation. In some sea areas of the world vertical mixing can interact with vertical shears in the tidal currents, but this is not an important mechanism in the Gulf. Horizontal turbulence is also not an important contributor to the transport processes.

Two time scales may be defined for a basin such as the Gulf, in relation to the overall mixing processes.

The turn-over time

This is the time for all the water in the basin to come within the influence of the open sea boundary. Consider a basin of volume, V, and a surface current of total transport, Q, flowing parallel to the basin axis. By continuity, this transport must be balanced by a return flow somewhere else in the basin cross-section. If there is no exchange of water with the open sea, and if the flow, Q, is the dominant process turning over the basin, then we may define the turn-over time by:

$$V / Q \qquad (4)$$

From flow estimates from ship drift data, a typical current in the surface inflow is about 0.1 m/s (allowing for a somewhat reduced current near the head of the Gulf). If this current acts across half the average cross-sectional area of the Gulf, A, then the transport, Q, is defined by:

$$Q = 0.1\ A/2 \qquad (5)$$

and the turn-over time is:

$$2\ V / (0.1\ A) = 20 \times (\text{length of Gulf in meters}) \qquad (6)$$

From Emery (1956), the length of the Gulf is 990 km, giving a turn-over time of 230 days. This estimate is, however, modified by vertical mixing processes, which effectively short-circuit the flushing circulation described above, and increases the estimated turn-over time to about 2.4 years (Hughes and Hunter, 1979).

The flushing time

This is the time for all the water in the basin to be exchanged with water from the open sea. It must clearly be longer than the turn-over time. The flushing time may be estimated by considering the conservation of water and salt, and the evaporation rate over the sea surface. Assuming that the exchange in the Strait of Hormuz was due to shear flow, Koske (1972) derived a flushing time of 3 years and deduced an outflow velocity of about 0.1 m/s for the bottom water in the Strait. Using a somewhat similar approach but a less restrictive model of the exchange in the Strait, Hughes and Hunter (1979) derived a time for 90 per cent flushing of 5.5 years.

As the spatial scales of the Gulf and the Gulf of Oman are so very different (their typical depths differ by an order of magnitude), the two areas must be considered as distinct oceanographic regimes, joined by the Strait of Hormuz. The Gulf is a shallow inverted estuary where tidal currents and wind effects exert an importnat influence (the latter especially in shallow areas) on circulation and mixing processes. Exchange of dissolved contaminants within the Gulf can be understood as a process of horizontal redistribution by residual currents and vertical redistribution by turbulence (both processes being modified by the presence of vertical density stratification, which is strong in the summer). The time scales involved are of the order of tens of days for vertical mixing, and years for horizontal turn over. Exchange between the Gulf and the Gulf of Oman does not appear to offer an overiding constraint on the total flushing of the Gulf, as estimates of the flushing time are not much larger than the estimate of the turn-over time; indeed, the estimates made here are clearly subject to quite large errors and it is probable that the present evidence does not suggest any significant difference between the flushing time and the turn over time. It is unlikely that the Gulf of Oman imposes any significant restriction on the flushing of the Gulf as it is basically an extension of the Arabian Sea (which itself forms part of the North Indian Ocean); the major part of the Gulf of Oman is deeper than 1000 m and as wide as the Gulf.

The above estimates of turn-over and flushing of the Region relate only to the gross features of a contaminant distribution, once it has been transported significantly away from the shore. There will, of course, also be local problems of removal of effluent (say, from small embayments or from coastal discharges at places where the local currents are weak). This short review of mixing processes only relates to the exchange processes acting on large scale distributions of dissolved substances (i.e., of the order of the size of the sea basins involved).

Contaminants that are predominantly associated with the sea surface (e.g., floating oil) must also be considered separately. Advective processes at the air-sea interface are generally stronger than elsewhere. As a rule-of-thumb, floating substances travel at about 3 per cent of the wind speed (typically 0.15 m/s in the Gulf) relative to the underlying water (i.e., of the order of 10 m below the surface). Further, a floating effluent is not subject to vertical mixing processes, so a turn-over time in the absence of wind, of around 200 days (see equation (6)) would be appropriate.

RECOMMENDATIONS FOR MODELLING OF THE RESIDUAL CIRCULATION AND MIXING PROCESSES IN THE REGION

There can be no single model that will serve as a predictor of any required oceanographic parameter at all length and time scales over the whole Region. What is required is a suite of models varying from the very simple (e.g., single-box models) to the very complex (e.g., three-dimensional numerical models), covering different requirements (e.g., some modelling the hydrodynamics only, others modelling flushing processes) and different spatial and temporal scales (e.g., some modelling local coastal processes, others modelling the gross features of exchange in the Region). For certain applications, it is not possible to divide up the effort into a number of discrete models, due to the interactions between oceanographic variables. For instance, the residual circulation of the Gulf can only be modelled successfully by considering the balances of momentum, water and salt, and none of these three components can be omitted from the computations. It should be taken as a general rule, however, that it is more computationally efficient to model separately those variables that do not mutually interact. Included in the latter are variables that interact in one direction only (e.g., momentum and a passive contaminant, as the former affects the latter by advection and diffusion processes, but the latter does not affect the former), but not variables that interact in both directions (e.g., momentum and salinity, as salinity also affects momentum through variations in density and, hence, in the generation of stable vertical stratifications and of horizontal pressure forces).

The basic requirements for a model of the residual circulation of the Region are:

(a) The model should be three-dimensional if it is adequately to predict observed features of the circulation. It is, however, possible that models of fewer dimensions may be sufficient in certain local areas (e.g., two-dimensional (in plan) models may be capable of describing the circulation in shallow areas, although applications of these types of models in other areas of the world have not been particularly successful).

(b) The model should include the effects of density and wind forcing, both of which are important in determining the circulation pattern. The former may be defined from observational data (e.g., the model of Hunter, 1982b), but for predictive purposes (rather than simply for use as a tool to understand the physical processes at work) it is preferable that the density distribution be a modelled variable.

(c) The model should include the effect of bottom friction, as the Gulf is effectively a shallow sea area, where bottom currents are a significant part of the total circulation.

(d) The model should include the effect of surface evaporation, runoff and precipitation.

A simplification often used in models of the deep ocean is to ignore vertical motions of the sea surface and to impose a constraint known as the rigid lid approximation. This removes all motions associated with external gravity waves (e.g. conventional tidal oscillations and meteorologically- induced surges) and hence such models serve as predictors of the internal motions (e.g., steady density-driven shear flows and internal waves) only. This would probably be an adequate approximation for the estimation of the long-term circulation pattern, but

would not of course describe surge events which are known to be significant and to last several days (IMCOS, 1975: Hughes and Hunter, 1979). Another approximation is to divide the vertical water column into a few (often two) discrete layers (often of constant density) (e.g., Hurlburt and Thompson, 1976). Such models are generally used to describe internal motions of a wave-like nature, and do not cope well with steady circulations where it is required that water be exchanged between the layers (e.g., in upwelling or downwelling situations). Even simpler models of internal wave-like motions consist of a single layer (often used to model a thin light surface layer) and are called "reduced gravity" models, e.g., O'Brien, Adamec and Moore, 1978). Because of their simplicity, they may be of use in modelling transient motions in the surface layers of the Region.

The requirements described above correspond closely to three-dimensional estuary-type models (with the inclusion of surface evaporation, which is quite simple). It may be thought that they also correspond to models of the deep ocean, but these generally use the rigid lid approximation and ignore bottom friction (e.g. Semtner 1974). There are four main ways with which to cope with the vertical variations of numerical models of the sea:

(a) By splitting the model into a number of discrete layers, within each of which the physical parameters (e.g., current, salinity and density) are generally assumed constant. The interfaces between layers are generally fixed relative to the water and hence move by vertical advective processes. A two-layer example is given above.

(b) By a simple finite-difference scheme, dividing the water column into a number of (not necessarily equally spaced) horizontal layers. A disadvantage of this approach is that the vertical resolution is good in deep areas, but relatively poor in shallow areas (in the sense that in the latter there are fewer mesh points over the depth). They are often called grid box models. Common examples are the models of Leendertse's group in the Rand Corporation (e.g., Leendertse et al., 1973).

(c) A variant of (b) is to scale the vertical coordinate system by the local depth, yielding conservation equations defined in terms of a sigma coordinate.This has the advantage over (b) in that, in shallow areas, the vertical resolution is better, but this may lead to some problems of frictional instability in these regions. An example is the Gulf model of Hunter (1982b).

(d) Over the past 10 years, a technique of splitting the vertical variations into a relatively small number of discrete functional forms (modes) has been developed (Heaps, 1972). Each mode leads to a set of conservation equations. This method apparently promises to offer improved computational efficiency over other schemes; it also preserves resolution in shallow areas. At present, the main application has been in the solution of the hydrodynamic equations under conditions of constant density. Owen (1980) and Davies (1982), however, laid down the theoretical background for including advection and diffusion of salt (and hence of density), and Heaps (1982) described a combination of the modal approach and the layer approach, point (a) above, whereby the velocity within each constant density layer was described by a summation of modes.

Models of mixing processes in the Region may be based on the diffusion and advection schemes used in the above hydrodynamic models. As has been noted earlier, however, many of these schemes lead to numerically-induced diffusion. An alternative is the use of particle-tracking techniques, utilising a random-walk method to simulate diffusion (e.g., Bork and Maier-Reimer, 1977). These latter

models are at their most computationally efficient when the contaminant exists as a relatively small patch in a larger sea area. They have hence been used successfully in oil slick modelling (e.g., Ahlstrom, 1975; Hunter, 1980). When the contaminant covers the whole sea area (such as is the case with salinity), this technique is, however, rather inefficient.

An example of a simple single-box model has been given above in the calculations of the flushing time of the Gulf. Another quite successful simple model is the cross-sectionally averaged one-dimensional model used to predict water quality variables such as biological oxygen demand and dissolved oxygen in an estuary (e.g., Stommel, 1953; Tracor, 1971). These models are often time-averaged over a tidal cycle, and hence derive their advection velocity from the fresh water flow (in the case of Gulf, this would be equivalent to the evaporation rate). The longitudinal diffusion coefficient (which describes many processes such as turbulence, and the interaction of this with the lateral and vertical shears in both the tidal and the mean flow) is generally obtained from observation of the salinity distribution in the estuary. This is probably the reason for the success of these highly paramaterised models, since they are very closely tied in with experimental data from the region under consideration.

Other simple yet successful models are those describing the near-field plumes of buoyant effluent, such as those due to outfalls of sewage or the cooling water from thermal power stations. There exist a number of analytic and similarity solutions of both the two- and three-dimensional problem, based on a mixture of theoretical reasoning and empirical results. The complexity of calculations required for these solutions range from the very simple to the relatively uncomplicated numerical integration of a series of differential equations. These types of model have been reviewed by Agg (1978), MacQueen (1978) and Fischer et al. (1979).

RECOMMENDATIONS FOR ASSOCIATED COLLECTION OF OBSERVATIONAL DATA

It is clear that there is a great lack of published observations of conventional oceanographic data, of current velocity data and of any mixing experiments (e.g., using tracers such as dye to indicate factors such as the vertical mixing time for the water column) in the Region. There must exist a considerable quantity of such data that has been collected as part of the industrial development and oil exploitation in the area. It is considered imperative that a concerted effort be made to obtain this information by consultation with both the survey companies (who collected the data) and the clients (who commissioned the data collection). To the author's knowledge, there at present exist year-long records of current meter observations from the deep-water areas of the Gulf. An analysis of these would prove invaluable in furthering our understanding of the circulation process. It will only be when a thorough inventory of such data has been made that it will be reasonable to plan any future large-scale oceanographic experiments in the Region. Collection agencies for oceanographic data exist in many countries (e.g., the Marine Information and Advisory Service in the United Kingdom) and these serve as useful sources of conventional oceanographic observations, mainly collected by governmental organizations, however. It is only during recent years that current velocity measurements have been collected by these agencies and then again most of these come from governmental organizations. The situation as regards meteorological data is somewhat better, as co-operation exists both between governments (i.e., the World Meteorological Organization) and between commercial companies (i.e., the Oil Companies Weather Co-ordination Scheme), so that meteorological observations in the Region are reasonably freely available.

The types of observation that are particularly required are:

(a) Long period (greater than one month) observations of current velocity over the whole Region.

(b) Large-scale conventional oceanographic observations over the whole Region.

(c) Smaller-scale conventional oceanographic observations in certain significant areas such as:

  (i) The shallow areas of high evaporation in the southwestern and southern areas of the Gulf.

  (ii) The area around the fresh water inflow of the Shatt Al-Arab.

  (iii) The Strait of Hormuz, as an aid to understanding exchange processes between the Gulf and the Gulf of Oman.

(d) Mixing experiments involving the use of tracers such as dye. A particularly important factor to measure is the vertical mixing time, as this, together with observations of current velocities, will yield estimates of the horizontal exchange rate.

(e) The rate of inflow of fresh water via the Shatt Al-Arab, which clearly has an important effect on the oceanographic conditions at the northern end of the Gulf. There is much evidence that this has declined considerably during this century due to irrigation schemes (Ubell 1971). Discharge data for the Tigris, Euphrates and the Karun are published fairly frequently by UNESCO (e.g, UNESCO, 1974), but these reports generally have to be corrected for downstream withdrawal of water for irrigation. Thus, there is a need for more accurate estimates of the quantity of fresh water actually entering the Gulf.

REFERENCES

Agg, A.R. (1978) Investigations of sewage discharges to some British coastal waters, Chapter 6, Initial dilution, Technical Report TR92, Water Research Centre, Stevenage, Herts., U.K.

Ahlstrom, S.W. (1975) A mathematical model for predicting the transport of oil slicks in marine waters, Battelle Pacific Northwest Laboratories, Richland, Washington, U.S.A.

Barlow, E.W. (1932a) Currents in the Persian Gulf, northern portion of the Arabian Sea, Bay of Bengal, etc. I. Summary of previous knowledge, The Marine Observer, Vol. IX, No.99, pp. 58-60.

Barlow, E.W. (1932b) Currents in the Persian Gulf, Northern portion of the Arabian Sea, Bay of Bengal, etc. II. The S.W. monsoon period, The Marine Observer, Vol. IX, No. 105, pp. 169-171.

Barlow, E.W. (1932c) Currents in the Persian Gulf, Northern portion of the Arabian Sea, Bay of Bengal, etc. III. The N.E. monsoon period and general summary, The Marine Observer, Vol. IX, No. 108, pp. 223-227.

Bo Pedersen, F. (1980) A monograph on turbulent entrainment and friction in two-layer stratified flow, Series Paper 25, Institute of Hydrodynamics and Hydraulic Engineering, Technical University of Denmark.

Bork, I. and Maier-Reimer, E. (1978) On the spreading of power plant cooling water in a tidal river applied to the River Elbe, Advances in Water Research, Vol. 1, No. 3, pp. 161-168.

British Admiralty (1941) Water movements and related information, Persian Gulf, (Sheet II), Oceanographical Chart No. 13, C. 6120.

British Admiralty (1967) Persian Gulf Pilot, the Hydrographer of the Navy, London.

Brewer, P.G., Flear, A.P., Kadar, S., Shafer, D.K. and Smith, C.L. (1978) Report A, Chemical oceanographic data from the Persian Gulf and Gulf of Oman, Report WHOI-78-37, Woods Hole Oceanographic Institution, Massachusetts, U.S.A.

Davies, A.M. (1982) On computing the three dimensional flow in a stratified sea using the Galerkin method, Applied Mathematical Modelling,.Vol. 6, pp. 347-362.

Davies, A.M. and Flather, R.A. (1977) Computation of the storm surge of 1 - 6 April 1973 using numerical models of the North West European continental shelf and North Sea, Deutsche Hydrographische Zeitschrift, Vol. 30, No. 5, pp. 139-162.

Dubach, H.W. (1964) A summary of temperature-salinity characteristics of the Persian Gulf, Publication NODC-G-4, National Oceanographic Data Center, Washington, D.C.

Dubach, H.W. and Wehe, T.J. (1959) Descriptive oceanography of Kuwait Harbour, Technical Report TR-55, U.S. Navy Hydrographic Office, Washington D.C.

Duing, W. and Koske, P.K. (1967) Hydrographic observations in the Arabian Sea during the N.E. monsoon period 1964/65, "Meteor" Forschungsergebnisse, Series A, No. 3, pp. 1-43.

Duing, W. and Schwill, W.D. (1967) Spreading and mixing of the highly saline water of the Red Sea and the Persian Gulf, "Meteor" Forschungsergebnisse, Series A, No. 3, pp. 44-66.

Emery, K.O. (1956) Sediments and water of Persian Gulf, Bull. Am. Assoc. Petrol. Geol. Vol. 40, No. 10, pp. 2354-2383.

Evans-Roberts, D.J. (1979) Tides in the Persian Gulf, Consulting Engineer, June 79.

Farmer, A.S.D. and Docksey, J.E. (1983) A bibliography of the marine and maritime environment of the Arabian Gulf and Gulf of Oman, Kuwait Bull. Mar. Sci. No. 4, Mariculture and Fisheries Dept., Kuwait Institute for Scientific Research, Kuwait.

Fischer, H.B., List, E.J., Koh., R.C.Y., Imberger J. and Brooks, N.H. (1979) Mixing in Inland and Coastal Waters, Academic Press.

Grasshoff, K. (1976) Review of hydrographical and productivity conditions in the Gulf region. In: Marine Sciences in the Gulf Area, UNESCO Technical Papers in Marine Science 26, pp. 39-62.

Hansen, D.V. and Rattray, M. (1965) Gravitational circulation in straits and estuaries, J. Mar. Res., Vol. 23, No. 2, pp. 104-122.

Hansen, D.V. and Rattray, M. (1966) New dimensions in estuary classification, Limnology and Oceanography, Vol. 11, No. 3, pp. 319-326.

Hartmann, M., Lange, H., Seibold E. and Walger, E. (1971) Surface sediments in the Persian Gulf and Gulf of Oman, In: Geologic-hydrologic setting and first sedimentological results, "Meteor" Forschungsergebnisse, Series C, No. 4 pp. 1-76.

Heaps, N.S. (1972) On the numerical solution of the three-dimensional hydrodynamical equations for tides and storm surge, Extrait des Mémoires de la Société Royale des Sciences de Liège, Series 6, No. 11, pp. 143-180.

Heaps, N.S. (1982) Development of a three-layered spectral model for the motion of a stratified sea. Paper presented at the NATO Advanced Research Institute, Os, Norway, 6-11 June 1982 (to be published in Coastal Oceanography, Plenum Publishing Corp., New York).

HMSO (1977) The Marine Observers Handbook, Her Majesty's Stationery Office, Meteorological Office, Report M 522.

Hsu, C.T., Wu, H.-Y., Hsu, E.-Y. and Street, R.L. (1982) Momentum and energy transfer in wind generation of waves, Jour. Phys. Oceano., Vol. 12. pp. 929-951.

Hughes, P. and Hunter, J.R. (1979) Physical oceanography and numerical modelling of the Kuwait Action Plan Region, UNESCO, Division of Marine Sciences, report MARINF/278.

Hunter, J.R. (1980) An interactive computer model of oil slick motion. Paper presented at Oceanology International 80, Brighton, U.K.

Hunter, J.R. (1982a) The physical oceanography of the Arabian Gulf: a review and theoretical interpretation of previous observations. Paper presented at the First Gulf Conference on Environment and Pollution, Kuwait, 7-9 February, 1982.

Hunter, J.R. (1982b) Aspects of the dynamics of the residual circulation of the Arabian Gulf. Paper presented at the NATO Advanced Research Institute, Os, Norway, 6-11 June, 1982 (to be published in Coastal Oceanography, Plenum Publishing Corp., New York).

Hurlburt, H.E. and Thompson, J.D. (1976) A numerical model of the Somali Current, Jour. Phys. Oceano., Vol. 6, pp. 646-664.

IMCOS (1974) Handbook of the weather in the Gulf, between Iran and the Arabian Peninsular, Surface Wind Data, IM. 102, IMCOS Marine Ltd., London.

IMCOS (1975) Gulf tidal anomalies, 17-19 January 1973, Technical Note No. 1,IM.112, IMCOS Marine Ltd., London.

Kashfi, M.S. (1979) Marine Science in the Gulf, Impact of Science on Society, Vol. 29, No. 2, pp. 135-144.

Kenyon, K.E. (1969) Stokes drift for random gravity waves, Jour. Geophys. Res. Vol. 74, No. 28, pp. 6991-6994.

Koske, P.H. (1972) Hydrographic conditions in the Persian Gulf on the basis of observations aboard R.V. "Meteor" in spring 1965, "Meteor" Forschungsergebnisse, Series A, No. 11, pp. 58-73.

Leendertse, J.J., Alexander R.C. and Liu, S.K. (1973) A three-dimensional model for estuaries and coastal seas: Volume 1, principles of computation, Report R-1417-OWRR, Rand Corporation, Santa Monica, California.

Leveau, M. and Szekielda, K.H. (1968) Situation hydrologique et distribution du zooplankton dans le N.W. de la Mer d'Arabie, Sarsia, Vol. 34, pp. 285-298.

MacQueen, J.F. (1978) Turbulence and cooling water discharges from power stations. In: Mathematical modelling of turbulent diffusion in the environment, (ed.) Harris, C.J. Academic Press.

Mathews, C.P., Samuel M. and Al-Attar, M.H. (1979) The oceanography of Kuwait waters: some effects on fish population and on the environment, Annual Research Report 1979, Kuwait Institute for Scientific Research, Kuwait.

O'Brien, J.J. and Adamec, D. (1978) A simple model of upwelling in the Gulf of Guinea, Geophysical Research Letters, Vol. 5, No. 8, pp. 641-644.

Owen, A. (1980) A three-dimensional model of the Bristol Channel, Jour. Phys. Oceano., Vol. 10, pp. 1290-1302.

Peery, K. (1965) Results of the Persian Gulf - Arabian Sea Oceanographic Surveys 1960-61, Technical Report TR-176, U.S. Naval Oceanographic Office, Washington D.C.

Privett, D.W. (1959) Monthly charts of evaporation from the North Indian Ocean (including the Red Sea and the Persian Gulf), Quarterly Journal of the Royal Meteorological Society, Vol. 85, pp. 424-428.

Proudman, J. (1953) Dynamical oceanography, Methuen, London.

Purser, B.H. (ed) (1973) The Persian Gulf, Holocene Carbonate Sedimentation and Diagenesis in a Shallow Epicontinental Sea, Springer-Verlag, Berlin.

Purser, B.H. and Seibold, E. (1973) The principal environmental factors influencing Holocene sedimentation and diagenesis in the Persian Gulf. In: The Persian Gulf, Holocene Carbonate Sedimentation and Diagenesis in a Shallow Epicontinental Sea, (ed.) Purser, B.H. pp. 1-9, Springer-Verlag, Berlin.

Schott, G. (1918) Ozeanographie and Klimatologie des Persischen Golfes und des Golfes von Oman, Annalen der Hydrographie und Maritimen Meteorologie, Vol. 46, pp. 1-46.

Semtner, A.J. (1974) An oceanic general circulation model with bottom topography, Technical Report No. 9, Department of Meteorology, University of California, Los Angeles.

Sewell, R.B.S. (1934a) The John Murray Expedition to the Arabian Sea, Nature, Vol. 133, pp. 86-89.

Sewell, R.B.S. (1934b) The John Murray Expedition to the Arabian Sea, Nature, Vol. 133, pp. 669-672.

Sonu, C.J. (1979) Oceanographic study in the Strait of Hormuz and over the Iranian shelf in the Persian Gulf, U.S. Office of Naval Research, final report, contract no. N00014-76-c-0720, TC 3675.

Stommel, H. (1953) Computation of pollution in a vertically mixed estuary, Sewage and Industrial Wastes, Vol. 25, No. 9, pp. 1065-1071.

Sugden, W. (1963) The hydrology of the Persian Gulf and its significance in respect to evaporite deposition. Am. Jour. Sci., Vol. 261, pp. 741-755.

Szekielda, K.H. (1976) Spacecraft oceanography, Oceanogr. Mar. Biol. Ann. Rev. Vol. 14, pp. 99-166.

Szekielda, K.H., Salomonson V. and Allison, L.J. (1972) Rapid variations of sea surface temperature in the Persian Gulf as recorded by Nimbus 2 HRIR, Limnology and Oceanography, Vol. 17, No. 2, pp. 307-309.

Tracor (1971) Estuarine modelling: an assessment, Tracor Inc., Austin, Texas, USA.

Von Trepka, L. (1968) Investigations of the tides in the Persian Gulf by means of a hydrodynamic-numerical model, Proc. of the Symp. on Mathematical-Hydrodynamical Investigations of Physical Processes in the Sea, No. 10., Inst. für Meers. Univ. Hamburg, pp. 59-63.

Ubell, K. (1971) Iraq's water resources, Nature and Resources, Vol. VII, No. 2, pp. 3-9.

UNESCO (1974) Discharges of selected rivers of the world, the UNESCO Press, Paris.

UNESCO (1976) Marine sciences in the Gulf area, UNESCO Technical Papers in Marine Science 26.

Warren, B.A. (1966) Medieval Arab references to the seasonal reversing currents of the North Indian Ocean, Deep-sea Research, Vol. 13, pp. 167-171.

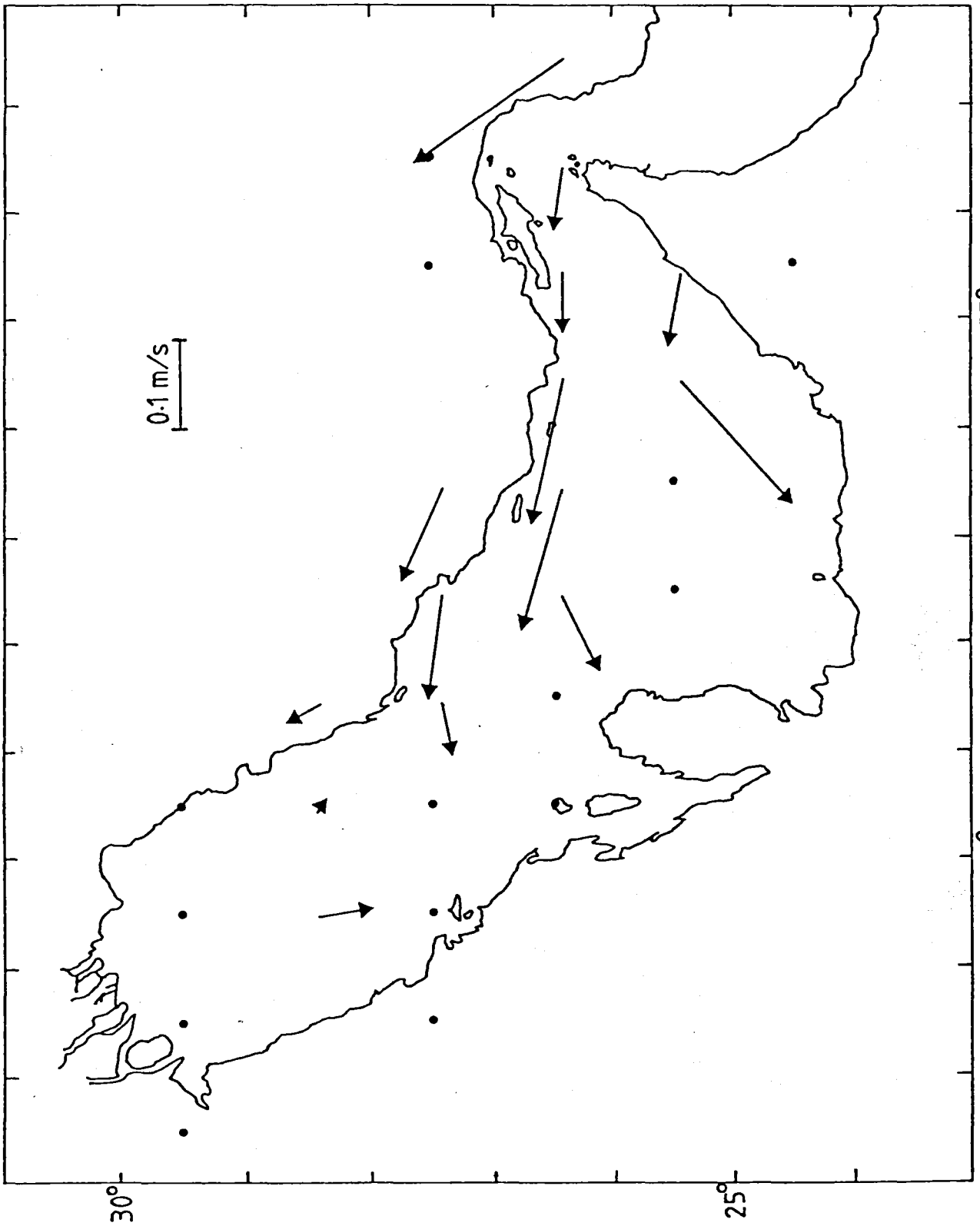

Figure 1: Selected ship drift data for whole year (after Hunter, 1982a)

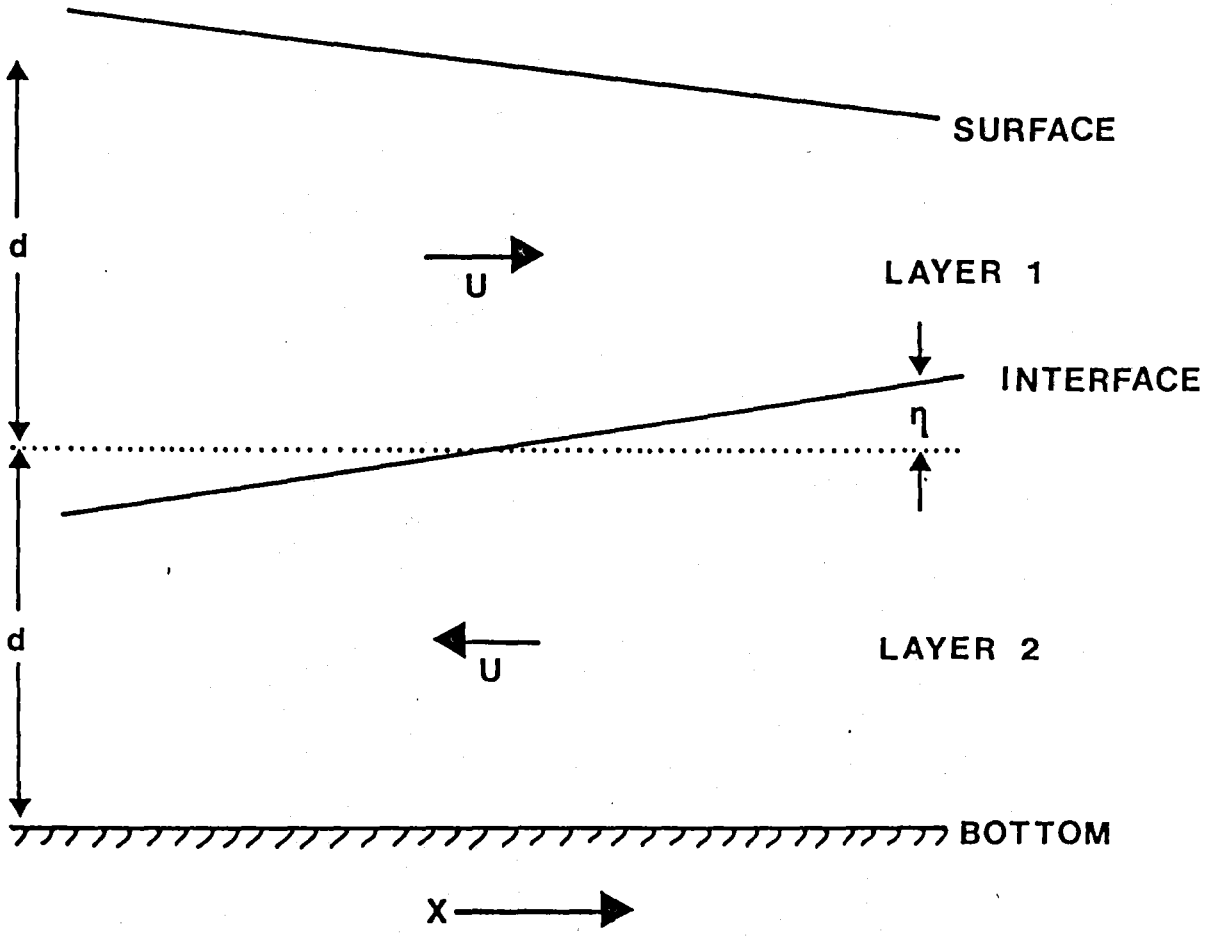

Figure 2: Simple two-layer longitudinal model of the Gulf

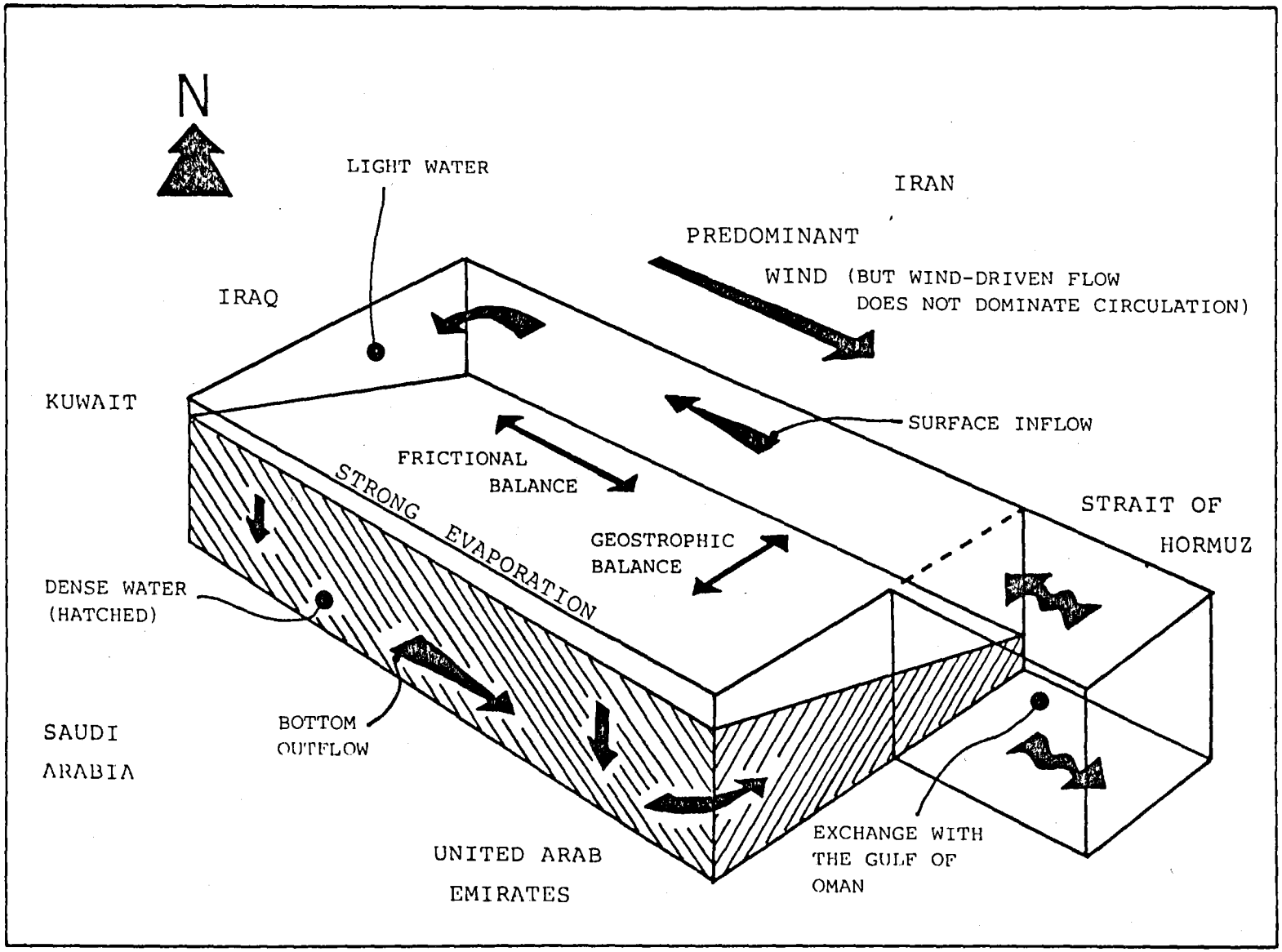

Figure 3: The probable circulation pattern in the Gulf (after Hunter, 1982a)

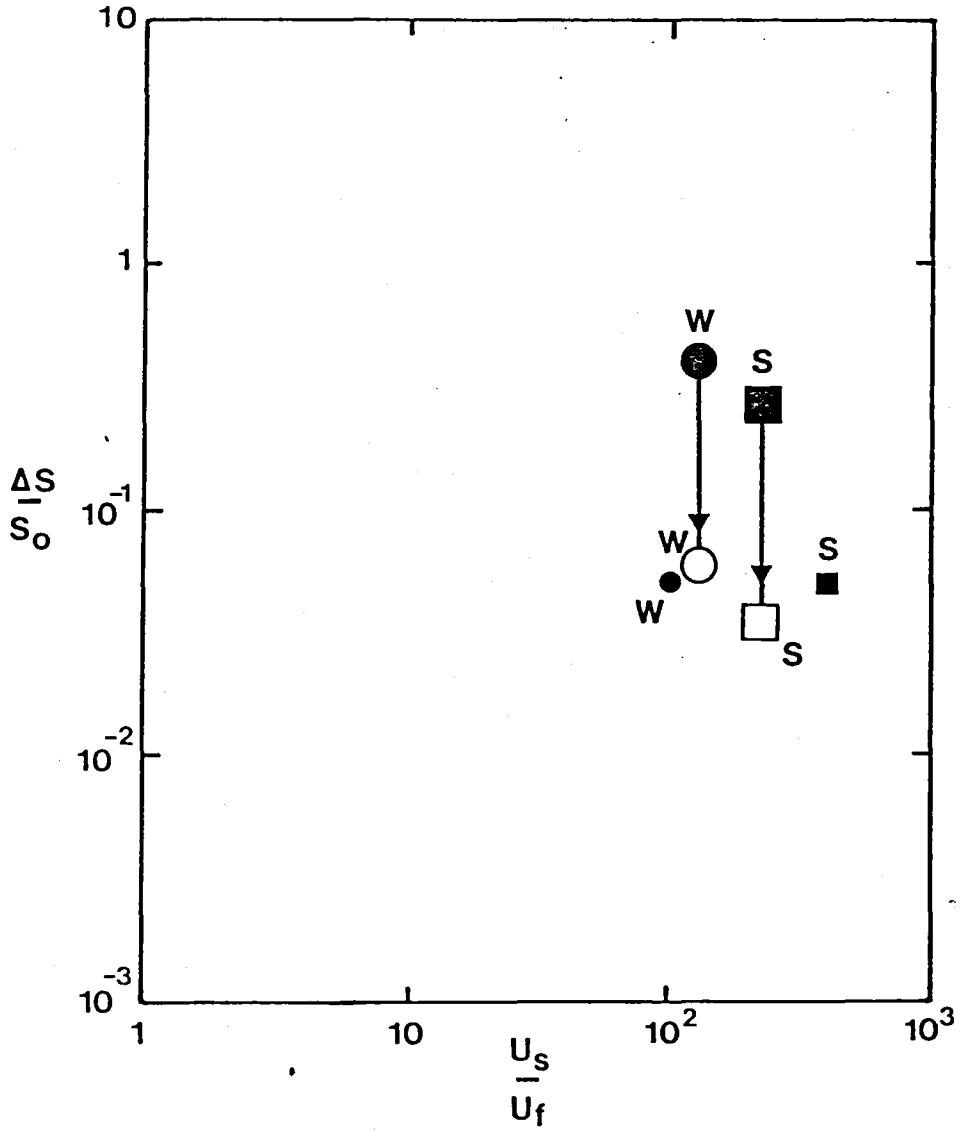

Figure 4: Classification of the Gulf as an inverted estuary.

Key:
- ΔS : surface to bottom salinity difference
- S_o : sectional mean salinity
- U_s : surface velocity
- U_f : sectional mean velocity
- "W" : winter data
- "S" : summer data

small full circle and square : from parameter pair (1)
large full circle and square : from parameter pari (2)
large open circle and square : from adjusted parameter pair (2)

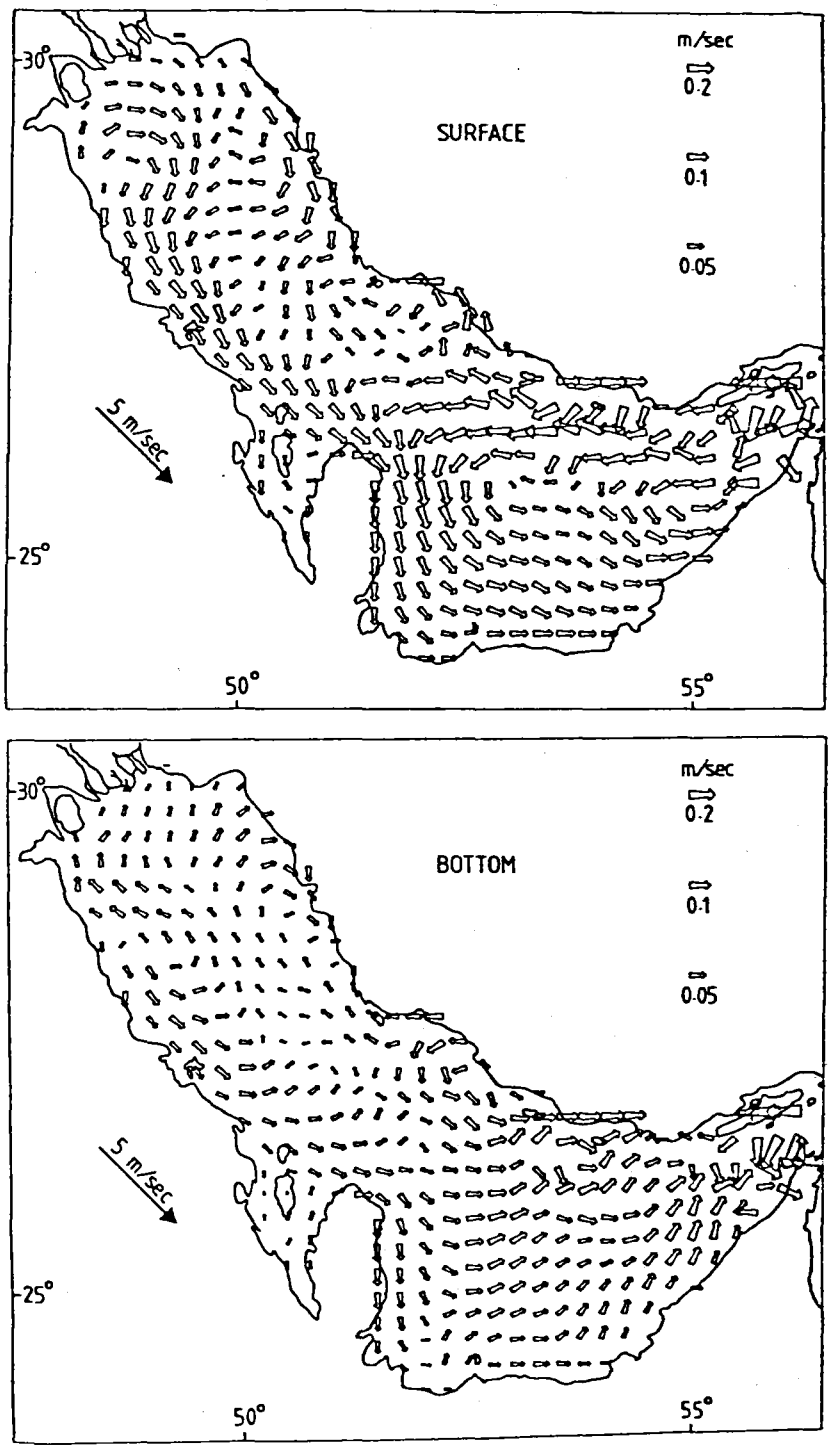

Figure 5: Predicted model velocities for surface and bottom cells with prescribed wind stress (vector lengths proportional to cube root of velocity) (after Hunter, 1982b)

A BRIEF SURVEY OF OCEANOGRAPHIC MODELLING AND OIL SPILL STUDIES IN THE REGION

by

William J. Lehr
Research Institute, University of Petroleum & Minerals
Dhahran, Saudi Arabia

ABSTRACT

The Kuwait Action Plan Region is characterized by shallow waters of high temperature. The Gulf, making up the northern part of the region, has little fresh water inflow. This, combined with liberal evaporation, causes highly saline conditions particularly in parts of the Western Gulf. Water balance is maintained by flow through the straits of Hormuz resulting in a flushing time of a few years. Winds in the area generally blow from the Northwest with some variation in this pattern in winter and spring.

Tidal height patterns in the region are fairly well established and several two-dimensional tidal models that agree reasonably well with actual results have been produced. Residual current models, however, are less perfected due in part to lack of adequate data and uncertainties over the driving mechanisms of the current.

Because of the abundant petroleum industry activities in the region, oil pollution is widespread. Oil spill modelling has shown some usefulness in the Gulf, particularly the estimates of spill trajectories of the Hasbah and Nowruz oil spills. Standard models of the fate of spilled oil, however, may have to be modified to fit the unique Gulf conditions. Also, different types of models are needed for different modelling purposes in the Region.

INTRODUCTION

The Nowruz oil spill highlights the importance of studying the hydrodynamics of the KAP Region and thereby ascertaining the movement of spilled oil and other pollutants. The purpose of this paper is to provide a brief 'state of the art' review of the known information about the topics covered in the symposium/workshop. A review of the general environmental conditions of the KAP Region is followed by a discussion of the tides and tidal models for the area, a look at residual current work and, finally, an examination of relevant oil spill studies.

General environment

With an average length of 1000 km, a width of between 55 and 340 km and total area of about 240,000 km2, the Gulf is relatively small compared to other offshore oil producing areas such as the North Sea, twice its size, or the Gulf of Mexico, five times as large. It is also relatively young, geologically speaking, having been formed only 3 or 4 million years ago. During its brief history it has been reduced several times to an estuary of the Tigris-Euphrates river system when world-wide sea level lowering occurred. The most recent such episode ended less than 20,000 years ago with the Gulf refilling during the sea level rise known as the "Flandrian Transgression", reaching its present level about 5000 years ago (Kassler, 1973).

The entire basin lies on the continental shelf whose slope into deeper waters occurs only in the Gulf of Oman. The result is that the Gulf is very shallow, rarely deeper than 100 meters, with an average depth of between 31 to 37 meters. It is asymmetrical in profile with a gentle slope from the western to eastern side. A wide area of mud bottom is found in the northern and eastern parts of the Gulf, with sand bottom predominant in the southern and western part. Rock is present at the bottom of the straits of Hormuz and in reef and island margin areas.

The eastern coastline is marked by mountains and cliffs whereas the western shore is often sandy. Industrial and commercial activities in populated areas have affected the shoreline and altered nearshore current patterns.

Studies by Emery (1956) found a nearly uniform summer surface temperature in the Gulf of around 90°F, with a general decrease of temperature to about 75°F in the Arabian Sea. Compilation of Winter surface measurements by Schott (1908) and Blegvad (1944) show a variation of between 60°F in the northern Gulf to about 75°F at the straits of Hormuz. Due probably to extensive vertical mixing, Emery found only a small vertical temperature gradient with bottom and top water temperatures varying by about 20°F.

Privett (1959) has estimated the evaporation rate for the Gulf to vary between 0.2 and 0.6 gm/cm2 day. This means that the volume of water evaporated each year is equivalent to the volume of 4 million Nowruz spills. Privett claims that evaporation is at a maximum in December and a minimum in May, although measurements conducted by some oil companies in the northern part of the Region suggest the opposite situation, at least for the upper Gulf.

Fresh water inflow has been estimated (Grasshoff, 1976) at between 5 to 100 km3 per year. This represents only about 1.3 per cent to 28 per cent of the water loss to evaporation. Since precipitation is light in the Region, consideration of the differential flow through the straits of Hormuz is crucial to the water balance in

the Gulf. Koske (1972), assuming a shear flow through Hormuz, computed a flushing time for the basin of about 2.5 years. Hughes and Hunter (1979), using a less restrictive model, derived a time for 90% flushing of 5.5 years. They also estimated the turnover time, the time it takes for all the water in the Gulf to come within the influence of the open sea boundary, of 230 days. If the interaction of vertical mixing is included with the residual current in the Gulf in their estimate, however, the turnover time increases to 2.4 years.

Highly saline conditions are found in the Gulf. Surface salinities in the summer range from 37o/oo in the Gulf of Oman to 42o/oo just off Bahrain. In fact fact, salinities as high as 70o/oo have been reported in the Gulf of Salwah at its extreme southern extremity (Basson et al., 1977). The salinity in winter is somewhat higher than in summer, apparently due to the variation of fresh water influx through the Shatt-Al-Arab, and meteorological effects, particularly evaporation (Schott, 1918). Offshore winds in the Gulf area blow mainly from the Northwest and are particularly strong in early summer when, due to a counter-clockwise wind circulation around a low pressure area over the Asian continent, the so-called shamals (Arabic for North) blow down the Gulf with gusts of as much as 100 km/hr (Williams, 1979). The most serious interference with this wind pattern occurs in Winter or early Spring, when passing depressions affect the Gulf in their movement from West to East. These can cause wind flow to change from Northwest to Southeast. Such exceptional wind patterns can last for a number of days before they revert to normal patterns (Wennink and Nelson-Smith, 1977).

Tides and tidal models

The tides in the Gulf are complex, consisting of a variety of tidal types (Figure 1). The tidal ranges are large throughout the Gulf, being over a metre everywhere and exceeding 3 metres at Shatt-Al-Arab. These large amplitudes cause strong tidal currents which commonly exceed 0.5 m/sec at maximum ebb or flood (Defense Mapping Agency, 1975). The tides generally flow Westward and Northwestward and ebb in the opposite directions. This gives the appearance of the tide progressing up the Iranian coast and down the Saudi side, with the range increasing from the middle of the Gulf in Kelvin wave style. The dimensions of the Gulf are such that the oscillations in the tide are not too far from resonance (Hughes and Hunter, 1979). The four main harmonic constituents of the tidal regime in the Gulf are M_2, S_2, O_1, and K_1. For a particular combination of the main constituents to repeat itself requires about 19 years, although suitable approximations can construct an artificial tide cycle of about 24.8 hours which enables the main features of the Gulf tides to be studied (Evans-Roberts, 1979). The M_2 and S_2 constituents have two amphidromic points, one in the Northwestern part of the Gulf and the other in the Southwestern part (Figure 2). The K_1 and O_1 have a single amphidromic point.

Several two-dimensional models of tides in the Gulf already exist (Trepka, 1968; Dames and Moore, 1975; Evans-Roberts, 1979; Danish Hydraulic Institute, 1980; Lardner et al., 1982; Le Provost, 1983; Murty and El-Sabh, 1983). An analysis of the one developed at the Research Institute of the University of Petroleum and Minerals (Lardner et al., 1982) demonstrates the general nature of such models. The basic equations to be solved are the Navier-Stokes equation and the equation of continuity, which are subjected to the so-called shallow-water approximation, i.e., the equations are depth averaged for the horizontal X and Y components and the hydrostatic equation approximates the vertical Navier-Stokes equation. The model neglects eddy viscosity and meteorological conditions, and considers water density to be vertically uniform. Then the governing equations can be reduced to

Then the governing equations can be reduced to

$$\frac{\partial \zeta}{\partial t} + \frac{\partial}{\partial x}(H\bar{u}) + \frac{\partial}{\partial y}(H\bar{v}) = 0$$

$$\frac{\partial \bar{u}}{\partial t} + \bar{u}\frac{\partial \bar{u}}{\partial x} + \bar{v}\frac{\partial \bar{u}}{\partial y} = f\bar{v} - g\frac{\partial \zeta}{\partial x} + \tau_b{}^x$$

$$\frac{\partial \bar{v}}{\partial t} + \bar{u}\frac{\partial \bar{u}}{\partial x} + \bar{v}\frac{\partial \bar{v}}{\partial y} = -f\bar{u} - g\frac{\partial \zeta}{\partial y} + \tau_b{}^x$$

where

u, v are depth averaged horizontel fluid velocity components

f is the coriolis term

H is the total water depth

ζ is the height of free water surface above the reference plane Z = 0

$\tau_x{}^b$ and $\tau_y{}^b$ are the bottom stress expressed in the form

$$\tau_x{}^b = -\frac{g\rho}{c^{-1}}(\bar{u}^{-1} + \bar{v}^2)^{\frac{1}{2}}\bar{u}$$

$$\tau_y{}^b = \frac{g\rho}{c^{-1}}(\bar{u}^{-1} + \bar{v}^2)^{\frac{1}{2}}\bar{v}$$

with C (the Chezy coefficient) empirically determined as a function of H. The boundary conditions chosen were zero normal velocity flow on any land boundary and specification of the water height at any open ocean boundary. A finite difference scheme using a coarse mesh (20 km mesh size) was chosen for the whole Gulf with the option of interfacing with finer mesh for local regions of interest. The computations were started with initially flat conditions everywhere except the open boundary across Hormuz where each component was specified based on its co-tidal chart. The model was run for 75 hours of real time to allow for steady conditions to be reached. Figures 3 and 4 demonstrate the predicted tide amplitudes for the M_2 and K_1 components. As expected, the M_2 shows the existence of two amphidromic points and K_1 shows only one. One consistent discrepancy between the model and empirical results was in the M_2 and S_2 amplitudes, the model predictions of the former being somewhat smaller than observed and the model predictions of the latter being somewhat too large. One suggested explanation for this discrepancy was the neglecting of the linear damping mechanisms.

The tidal current model by the Danish Hydraulic Institute (Danish Hydraulic Institute, 1980) is fairly similar to the University of Petroleum and Minerals model although it is only a part of a more general package. It uses an 8 km coarse grid mesh for modelling the whole Gulf. It also has the capability of using the output of the coarse grid as input to a finer mesh grid for any localized area in the Gulf. The other models are discussed in another paper in this workshop (Le Provost, 1983).

Tidal currents in the southern part of the KAP Region have also been modelled (Elahi, 1983).

All of the models either have been used for or are capable of, predicting tidal currents as well as heights but there is almost a complete absence of systematic

current surveys to measure tidal current in detail in the Gulf (Hughes and Hunter, 1979) to provide empirical verification. IMCOS Marine (Hibbert, 1980) claims to have developed a verified model to predict currents from tide height predictions applicable to any part of the Gulf.

Residual currents

Very little information exists describing the residual current field in the region. Schott (1918), Koske (1972) and Brewer et al. (1978) describe an anticlockwise drift around the Gulf. Claims have been made that ship drift data support such a circulation pattern. Recent work by Hunter (1982), however, criticizes circulation patterns based on such ship drift data and claims that, considering only locations where there was sufficient and acceptable drift information, there was little evidence to suggest an anticlockwise pattern. Cognizant of Hunter's criticism of using drift information alone, the Research Institute has combined these data with some basic hydrodynamic considerations to develop a semi-empirical approach to residual currents. A multiple gyre pattern results (Lehr and Fraga, 1983).

Past studies have presented mixed answers for the major contributing factor to residual flow in the Gulf. Hughes and Hunter (1979) concluded that the major contributor to the residual flow was wind driven currents based on Ekman dynamics. More recently, Hunter (1982, 1983) has argued that a better hypothesis would be to assume a density driven flow that is geostrophically balanced across the Gulf, though it may be modified by surface and bottom Ekman layers.

Current patterns in certain local areas of the Gulf have been studied and modelled by organizations in the Region. Three areas, in particular, are the coastline industrial areas of Saudi Arabia, (Tetra Tech, 1977; Williams, 1983) the West coast of Qatar (Beltagy, 1980) and the Kuwait offshore areas, (Mathews and Lee, 1983). Galt et al. (1983) showed that fresh water runoff had a significant impact on the residual currents in the Northern Gulf region.

Murty (1983) has examined the effects on the current patterns in the Gulf and Northern Arabian Sea during storm conditions.

Oill spill studies

As the world centre of the oil industry, the Gulf region is constantly subject to environmental damage posed by oil spills, as the Nowruz spill amply demonstrates.

Excluding disastrous spills such as Nowruz, different researchers have come up with different estimates of the amount of oil which will be spilled in the Gulf over the coming decade. Taking a 5 per cent annual increase in oil production over the next ten years, Hayes and Gundlach (1977) estimate that 3 million tons will be spilled. Golub and Brus (1980), using a more realistic production increase estimate of 1.7 per cent annually, predicts, that 1.5 million tons of oil will be spilled. In both predictions, the major source is seen to be related to tanker transport, with offshore production and discharges by coastal refineries and other industries being the next major contributors.

Examining vessel reported slicks in the Gulf in 1978, Ootsdam (1980) concludes that the spill rate is less than half the world rate because risk due to human error is less at the start of outward bound journeys and most oil from ballast water on inward bound voyages would have been released before the vessels reached the Gulf.

Nevertheless, he calculates spilled oil in the Arabian Gulf in 1978 to be over 150 000 tons, a figure which may be too high since he uses too large a thickness estimate for oil spill sheen. A study by the Research Institute (Belen et al., 1983) concludes that the average annual oil spillage from marine transport is 45 000 to 60,000 tons. Another study (Lehr and Cekirge, 1981) concludes that the shoreline impact of this spilled oil is seasonally sensitive. Surveys of oil on the shore have been conducted for particular regions in the Gulf (Al-Hamri & Anderlini, 1979).

Several computer models have been used to simulate oil spills in the Gulf. The SLIKFORCAST model developed by the Continental Shelf Institute and Det Norske Veritas and widely used in the North Sea was applied to the 1980 oil spill in the Hasbah offshore oil field (Krogh, 1980) with satisfactory results. Global Weather Dynamics Incorporated, under contract to the Saudi Arabian Meteorology and Environmental Protection Administration (MEPA) has conducted simulation studies on the Nowruz Oil Spill. Unfortunately, details of the predictions of the model were unavailable. The National Oceanic and Atmospheric Administration (NOAA) applied its model, OSSM, to the same spill (Galt, et al., 1983) and concluded that the Southern coast of Saudi Arabia, Bahrain and Qatar would suffer the heaviest impact of Nowruz pollution mainly in the form of tar balls. A third model applied to the Nowruz spill, developed by Murty and El-Sabh (1983), indicated that the Southern Iranian coastline was the area of greatest pollution risk.

The Research Institute has developed an oil spill simulation package, GULFSLIK (Figure 5), specifically for the Gulf region. The first model developed for the package, GULFSLIK I (Lehr and Cekirge, 1979) was a simple trajectory model based on seasonal average winds and currents and is perhaps a good illustration that usefulness is not synonymous with complexity. Not only did it provide at least as good a prediction of the Hasbah oil spill path (Figure 6) as the more complicated SLIKFORCAST model, but also has been used to provide information about the possible source of a large (40,000 barrel) spill which struck Bahrain in the summer of 1980 (Lehr and Belen, 1983). In early March of 1983 GULFSLIK I was applied to the Nowruz oil spill (Lehr, 1983) and indicated that the shorelines most at risk were the Saudi coastline near Abu Ali Island, Bahrain, Northern Qatar and the Southern Iranian coastline near Hendorabi Island. Comparison of these predictions, as well as the predictions of the other models mentioned, with the actual results of the Nowruz spill has been difficult, due in part to the nature of the spill and the lack of slick observation information from the Eastern part of the Gulf.

Trajectory models designed for the whole Gulf are of limited use for near shore spills. The OSSM model of NOAA has the capabilities of being applied to a smaller area of interest within a larger region and was thus used on the nearest shore areas of Kuwait (Galt et al., 1983). Certain coastal industrial sites have developed simplified models as part of their oil spill contingency plans. Under contract to the Arabian American Oil Company, the Research Institute developed GULFSLIK II, a spread and transport model for certain near shore areas of the Saudi Arabian coastline. It provides a good example of the type of information such models can provide.

GULFSLIK II receives as input data the initial volume of spilled oil, oil density, statistical tables of historical current and wind patterns and shoreline coordinates. To simulate a spill incident, the model divides the slick into nine Lagrangian elements located 40° apart on the edge of the spill. For each Lagrangian Lagrangian element, a transport vector is constructed from a percentage of the wind vector at 10 meters, the residual current and a spread vector. Spreading in the model was originally based on the well known Blokker formula (Blokker, 1964), with the spread vector for each spill edge element assumed to be radially outward from the centre of mass of the slick.

Initial values for the transport vectors are chosen using Monte Carlo simulation as are subsequent vectors, with a time interval of three hours. Details of the simulation and the approximation used to construct the conditional probabilities for the transport vectors are provided in Lehr et al., (1981).

For a particular spill site, the model is run 100 times with the spill edge element locations recorded for each run on a grid appropriately chosen for the geography of the spill site. The grid block occupation numbers for some specified time after initial spill occurrence are then plotted on a map to provide an overall picture of the expected behaviour of the spill. The block occupation numbers relate to the probability that the edge of the slick would be found in the corresponding grid block. Figure 7 shows a typical output for a simulated 1000 barrel 30 API spill at the Sea Island offshore loading platform at Ras Tanura.

Movement of oil is only one factor in oil spill simulation. Equally important is the mass loss and alteration of the oil due to weathering. While oil spill weathering models exist for the Gulf (Belen et al., 1981), a recent series of four test spills carried out by the Research Institute and the Arabian American Oil Company suggest that many common assumptions of such models may have to be modified for Gulf conditions. In particular, widely used spreading formulas, such as the Blokker formula or the Fay formula (Fay, 1971), compared quite poorly with the actual measured results (Lehr et al., 1983). Figure 8 shows the contrast between the area predicted by the Blokker formula and the actual area for a 51 barrel spill of Arabian light oil.

Work on the GULFSLIK package and its applications has highlighted the requirements for a useful and usable oil spill modelling programme for the KAP Region.

Basically, the need for oil spill models falls into two categories; first, contingency planning for oil pollution and, secondly, combat strategy in the case of an actual spill. The first category is suitable for models that do not operate in real-time and include sophisticated hydrodynamic packages requiring the use of a main-frame computer. Such models may need highly skilled and experienced operators to operate the package and interpret the results into a form useful for contingency planning. In the second category however, the users may not be computer experts. Such programmes should be interactive, providing simple prompts for necessary input data, and should display output in an easily understood manner. A minicomputer is probably more suitable for such a programme.

In either category, however, it is essential that the model be calibrated to, and preferably initially designed for, the conditions of the KAP Region.

REFERENCES

Al-Hamri, L. and Anderlini, V. (1979) A survey of tar pollution on beaches of Kuwait. KISR Annual Research Report, ISSN 0250-4065, Kuwait, p.82.

Basson, P., Burchard, J., Hardy, J. and Price, A. (1977) Biotopes of the Western Gulf. Arabian American Oil Co., Dhahran, p.27.

Belen, M., Lehr, W. and Cekirge H. (1981) Spreading dispersion and evaporation of oil slicks in the Arabian Gulf. Proceedings 1981 Oil Slick Conference 2 to 5 March 1981. API, Atlanta, pp 161-166.

Belen, M, Faraga, R. and Cekirge H. (1983) Statistical determination of oil spills in transport operations in the Arabian Gulf. Presented at First Saudi Engineering Conference, 14 to 19 May 1983, Jeddah.

Beltagy, I. (1980) IMCO/UNEP Workshop on combatting Marine pollution from oil exploration and transport in the Kuwait Action Plan region 6 to 10 December 1980, Bahrain.

Blegvad, H. (1944) Fishes of the Iranian Gulf: Danish Scientific Expendition in Iran (1935-1938), part 3 Copenhagen, pp 1 - 247.

Blokker, P. (1964) Spreading and evaporation of petroleum products on water. Proceedings Fourth Int. Harbon Conf. Antwerp. pp 911-919.

Brewer, P., Fleer, A., Kadar, S., Shafer, D. and Smith, C. (1978) Chemical oceanographic data from the Persian Gulf and Gulf of Oman, Woods Hole Oceanographic Institution Technical Report, WHOI - 78 - 37, pp 105.

Dames & Moore (1975) Final report, cooling-water system investigation, Iran 1 and 2 Nuclear Power Plan, Halileh, Iran.

Danish Hydraulic Institute (1980) Applications of System 21 in the Gulf, Horsholm, Denmark.

Defense Mapping Agency, USA (1975) Sailing Directions for the Persian Gulf, Hydrographic Center, Washington D.C.

Elahi, K. (1983) Tidal Charts of the Arabian Sea North of 20°N, pressented at the Symposium/workshop on oceanographic modelling of the Kuwait Action Plan Region, Dhahran, 15 to 18 October 1983.

Emery, K. (1956) Sediments and water of Persian Gulf. Bull of the Am. Assoc. of Pet. Geologist, 40, pp. 2354 - 2383.

Evans-Roberts, D. (1979) Tides in the Persian Gulf. Consulting Engineer, June 1979.

Fay, J. (1971) Physical processes in the spread of oil on a water surface. Proceedings Joint Conference on Prevention and Control of Oil Spills, 15 to 17 June 1971, API, Washington, D.C. pp 463-467.

Galt, J., Payton, D., Torgrimson, G. and Watabayashi, G. (1983) Trajectory analysis for the Nowruz oil spill with specific applications to Kuwait, NOAA, Seattle.

Grasshoff, K. (1976) Review of hydrographical and productivity conditions in the Gulf region, Marine Sciences in the Gulf Area, UNESCO Technical Papers in Marine Science, 26.

Golub, R. and Brus E. (1980) Analysis of oil pollution in the Kuwait Action Plan Region, IMCO/UNEP Workshop on combatting marine pollution from oil exploration, exploitation and transport in the Kuwait Action Plan Region, 6 to 10 December 1980 Bahrain.

Hayes, M. and Gundlach, E. (1977) Oil pollution in the Arabian Gulf: A preliminary survey. Research Planning Institute Report No. 1-GOP.

Hibbert, D. (1980) The Gulf Weather Forecast Scheme: 21 years on, Proceedings Petroleum and Marine Environment:Petromar 80, Monaco, pp 635-663.

Hughes P. and Hunter, J. (1979) A proposal for a physical oceanography programme and numerical modelling of the KAP Region. Project for KAP 2/2, UNESCO, Paris.

Hunter, J. (1982) The physical oceanography of the Arabian Gulf: A review and theoretical interpretation of previous observations, presented at First Gulf Conference on Environment and Pollution February 7-9 1980, Kuwait.

Hunter, J. (1983) A review of the residual circulation and mixing processes in the KAP Region, with reference to applicable modelling techniques, presented at the Symposium/workshop on oceanographic modelling of the Kuwait Action Plan Region, Dhahran, 15 to 18 October 1983.

Kassler, P. (1973) The structural and geomorphic evolution of the Persian Gulf. In: Purser, B. (ed.) The Persian Gulf, Springer-Verlag, New York, Heidelberg, Berlin, pp 11 - 32.

Koske, P. (1972) Hydrographische Verhaltnisse in Persischen Golf Grand von Beobachtungen von F.S. Meteor in Fruhjahr 1965, Meteor Forsch Ergnbn. · Gebruder Borntraeger, Berlin, pp 58 - 73.

Krogh, F. (1980) Computer simulation of oil spills IMCO/UNEP Workshop on combatting marine pollution from oil exploration, exploitation and transport in the Kuwait Action Plan Region, Bahrain 6 to 10 December 1980.

Lardner, R., Belen, M. and Cekirge, H. (1982) Finite difference model for tidal flows in the Arabian Gulf, Comp. and Maths. with Appls., 8, pp. 425 - 444.

Lehr, W. (1983) Information on Nowruz oil field spill, Research Institute, internal report, Dhahran.

Lehr, W. and Belen, M. (1983) The fate of two large oil spills in the Arabian Gulf, Proceedings 1983 Oil Spill Conference, 28 February to 3 March 1983, API, El Paso, pp 377 - 380.

Lehr, W., Belen, M. and Cekirge, H. (1981) Simulated oil spills at two offshore fields in the Arabian Gulf, Marine Pollution Bull. 12, pp 371 - 374.

Lehr, W. and Cekirge, H. (1979) GULFSLIK I: A computer simulation of oil spill trajectories in the Arabian Gulf, Research Institute, internal report, Dhahran.

Lehr, W. and Cekirge, H. (1981) Oil slick movements in the Arabian Gulf, Proceedings Petroleum and Marine Environment Petromar 80, Monaco, pp 737 - 742.

Lehr, W., Cekirge, H., Fraga, R. and Belen, M. (1983) Empirical studies of the spreading of oil spills, Oil and petrochemical pollution 2, pp 7-11.

Lehr, W. and Fraga, R. (1983) A semi-empirical method of estimating residual surface currents in the KAP region, presented at Symposium/workshop on oceanographic modelling of the Kuwait Action Plan Region, Dhahran, 15 to 18 October 1983.

Le Provost, C. (1983) Model for tides in the KAP Region, presented at the Symposium/workshop on oceanographic modelling of the Kuwait Action Plan Region, Dhahran, 15 to 18 October 1983.

Mathews, C. & Lee, J (1983) The development of oceanography in Kuwait. (Unpublished).

Murty, T. (1983) Storm tracks and storm surges in the Arabian Gulf, Strait of Hormuz and Gulf of Oman, presented at the Symposium/workshop on oceanographic modelling of the Kuwait Action Plan Region, Dhahran, 15 to 18 October 1983.

Murty, T. and El-Sabh, M. (1983) Movement of oil slicks in the Arabian Gulf during stormy periods, presented at the Symposium/workshop on oceanographic modelling of the Kuwait Action Plan Region, Dhahran, 15 to 18 October 1983.

Ootsdam, B. (1980) Oil pollution in the Persian Gulf and approaches, 1978, Marine Pollution Bull, 11, pp. 138 - 144.

Privett, D. (1959) Monthly charts of evaporation from the N. Indian (including the Red Sea and Persian Gulf), Quart. J. Roy, Meteorol Soc. 85, pp. 424 - 428.

Schott, G. (1908) Der Salzgehalt des Persischen Golfes und der Angrenzenden Gewasser, Annalen der Hydrographie und Maritimen Meteorologie, 36, pp. 296-299.

Schott, G. (1918) Oceanographie und Klimatologie des Persischen Golfes und des Golfes von Oman, Annalen der Hydrographie und Maritimen Mateorologie, pp. 1 - 46.

Tetra Tech (1977) Marine and atmospheric surveys, Report for Royal Commission for Jubail and Yanbu.

Trepka, L. (1968) Investigations of the tides in the Persian Gulf by means of a hydrodynamic - numerical model. Proceedings of Symposium on Mathematical--Hydrodynamical Investigations of the Physical Processes in the Sea, Institute für Meereskunde der Universität Hamburg, pp. 59 - 63.

Wennink, C. and Nelson-Smith A. (1977) Coastal oil pollution evaluation study for the Kingdom of Saudi Arabia, Vol.2 IMCO, London, p. 28.

Williams, R. (1979) Meteorologic and oceanographic data handbook, Arabian American Oil Co., Dhahran.

Williams, R. (1983) Oceanographic modelling applications for industry in the Arabian Gulf, presented at the Symposium/workshop on oceanographic modelling of the Kuwait Action Plan Region, Dhahran, 15 to 18 October 1983.

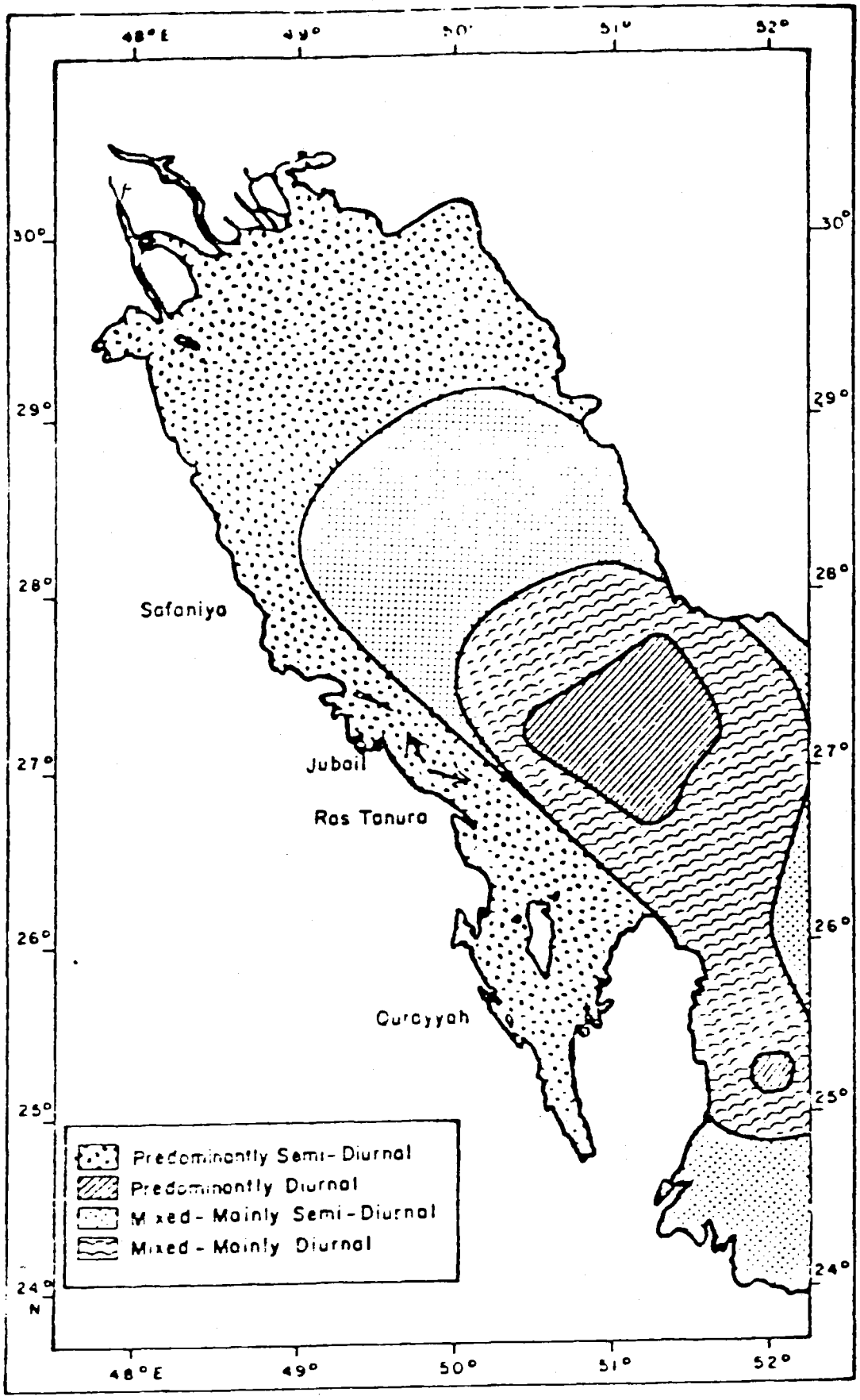

Figure 1: Tidal current regime for Northern Gulf (Williams, 1979).

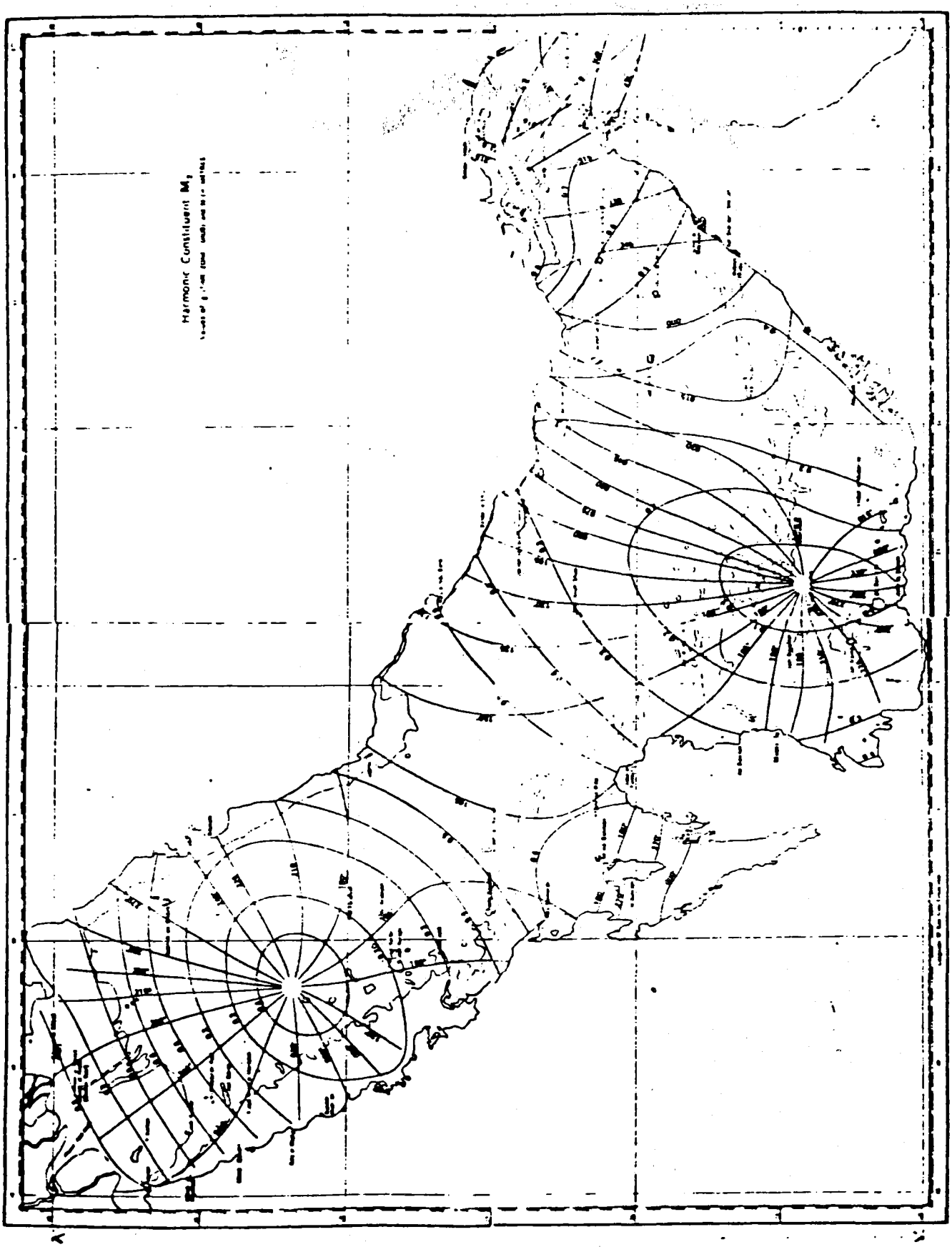

Figure 2: M2 tide heights and phases.

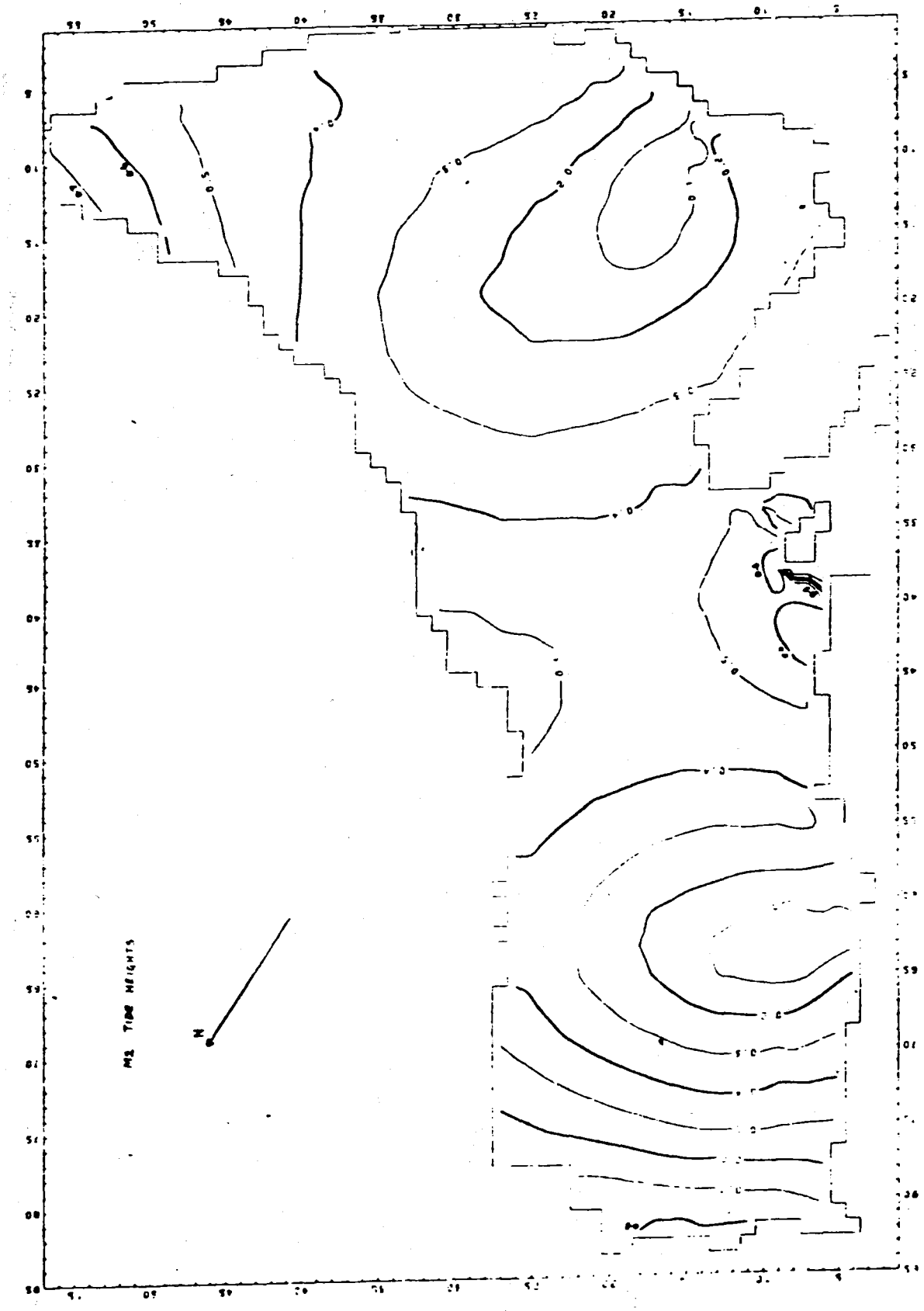

Figure 3: M2 tide heights from the University of Petroleum and Minerals model.

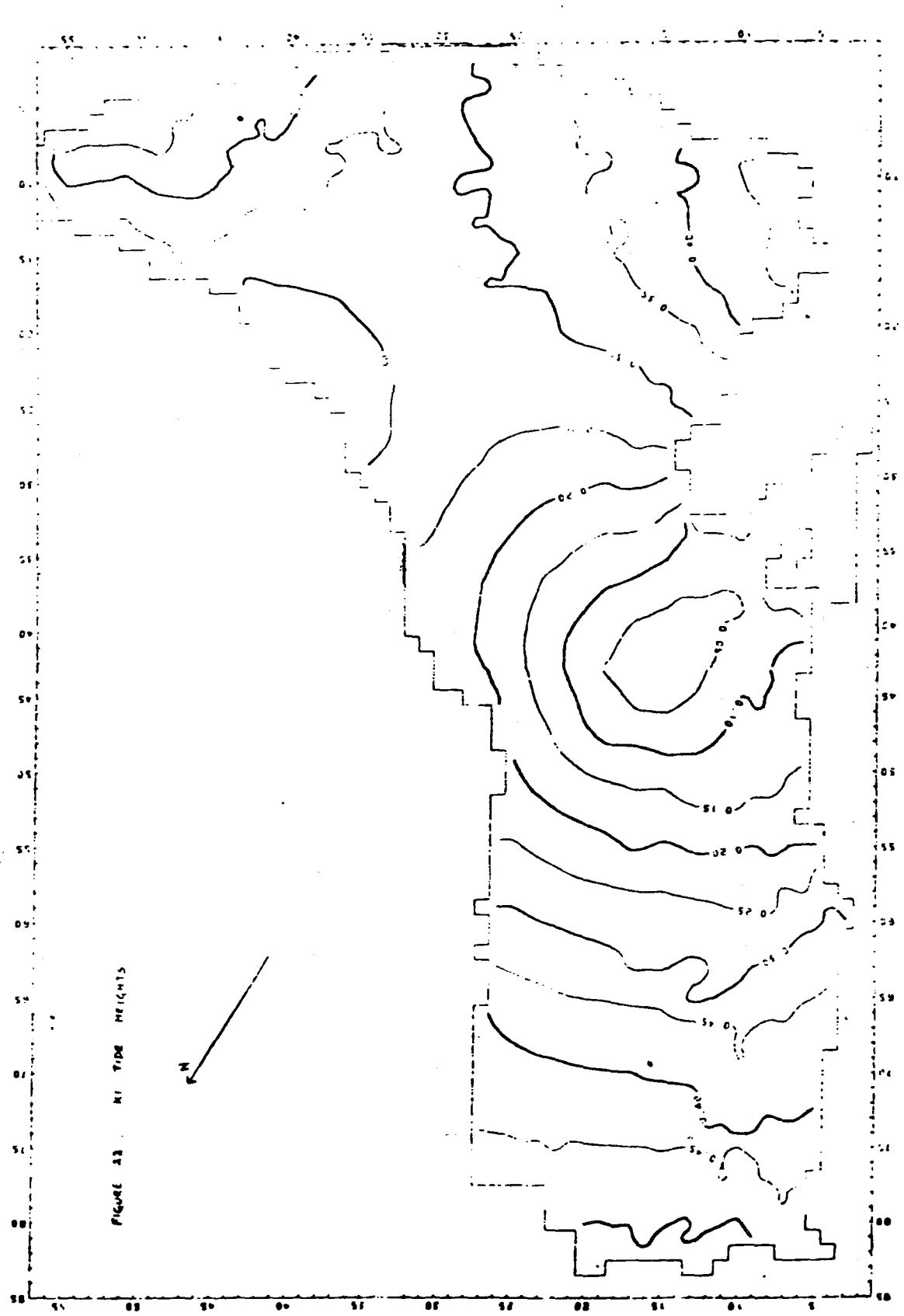

Figure 4: K1 tide heights from the University of Petroleum and Minerals model.

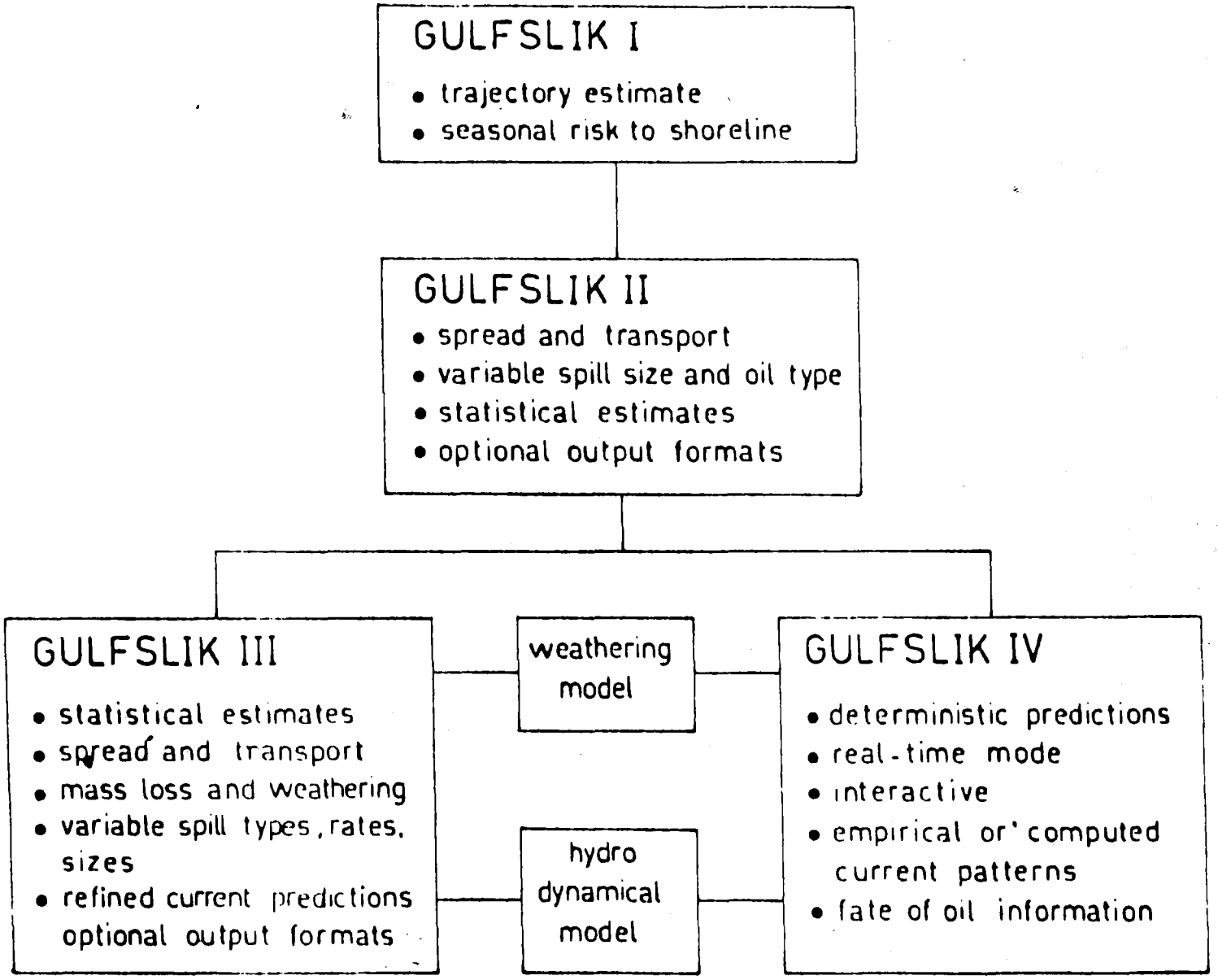

Figure 5: Diagram of GULFSLIK oil spill modelling package.

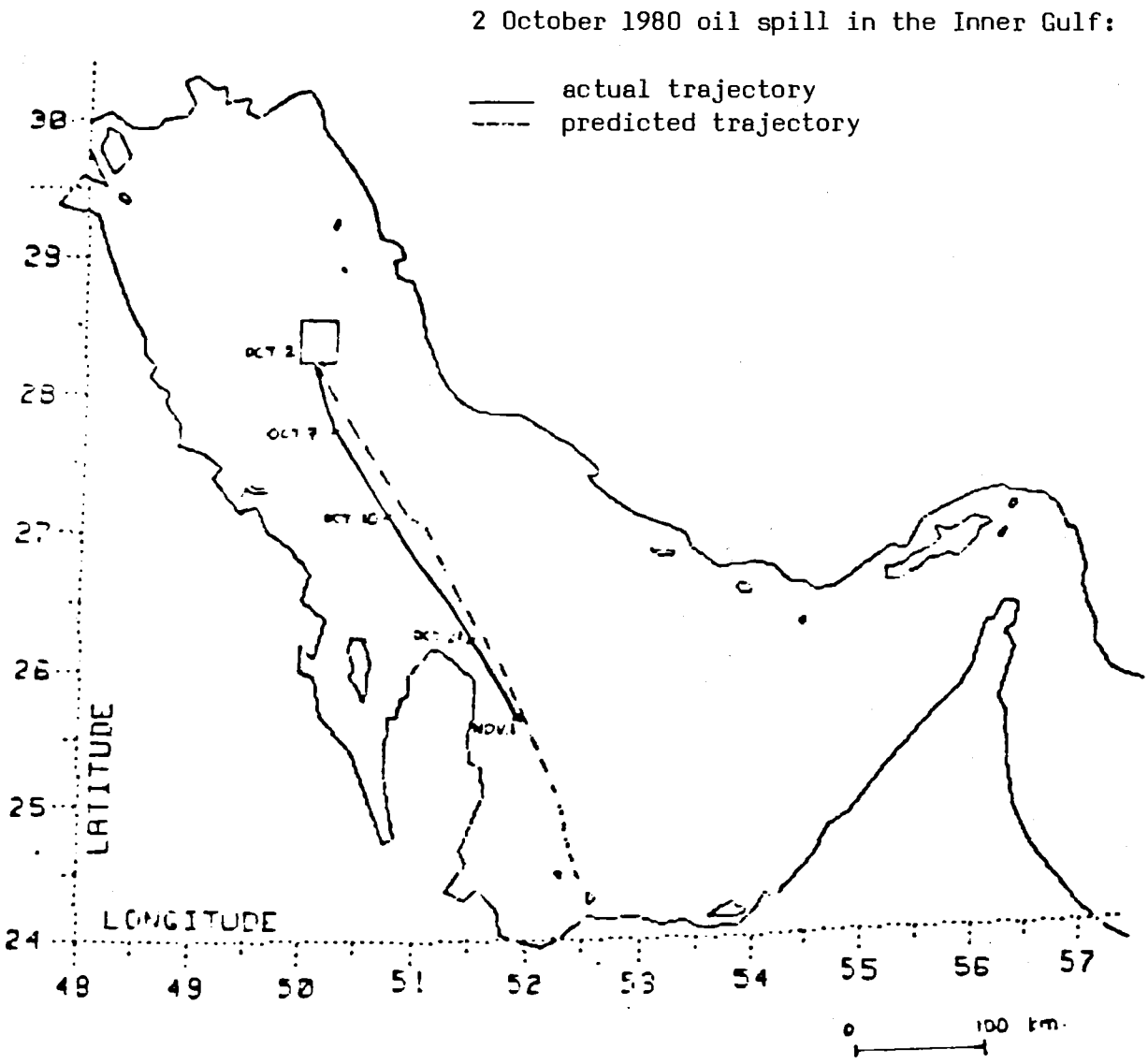

Figure 6: Prediction of Hasbah oil spill trajectory by GULFSLIK I.

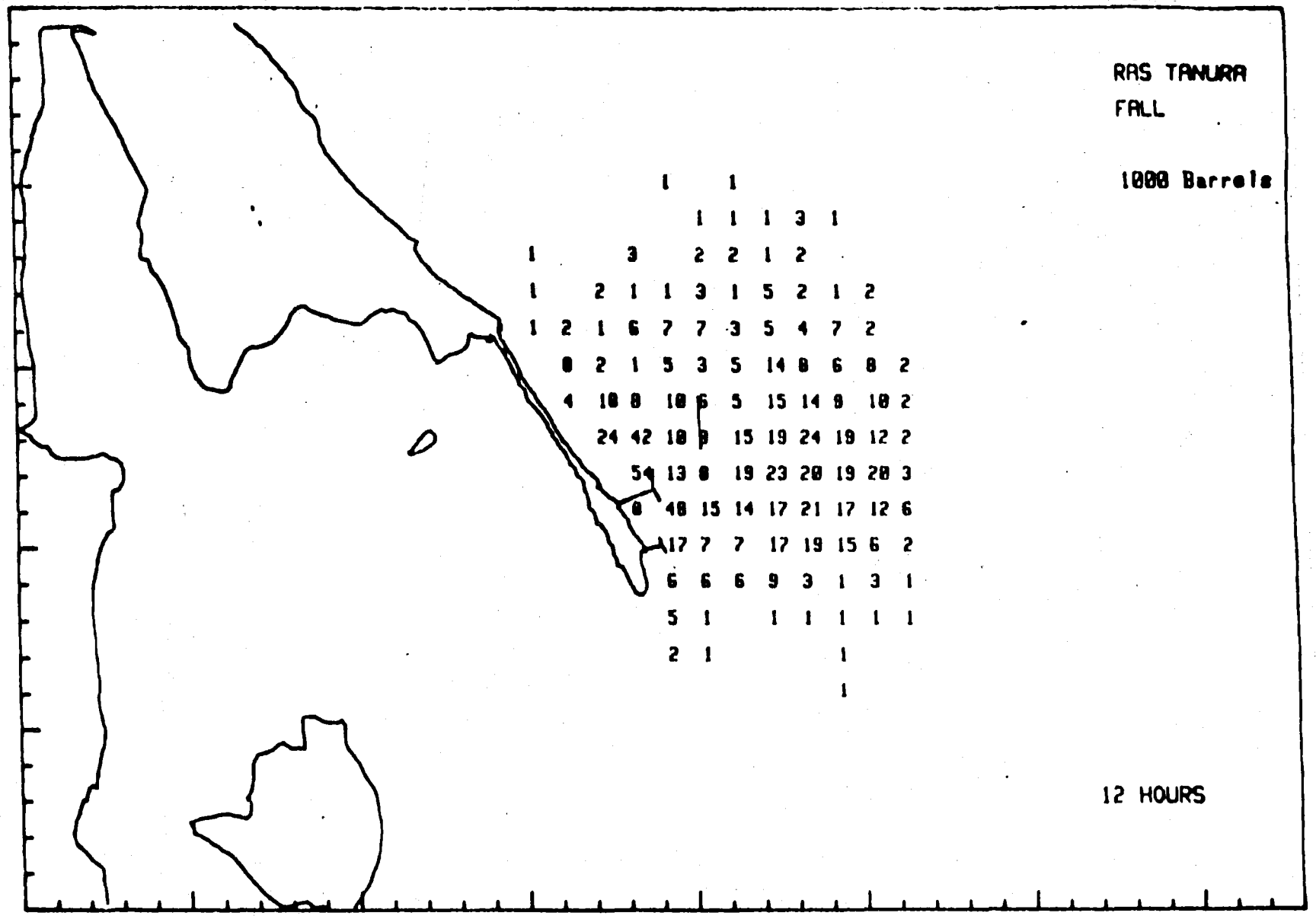

Figure 7: Sample output for GULFSLIK II model, twelve hours after simulated at Ras Tanura Sea Island.

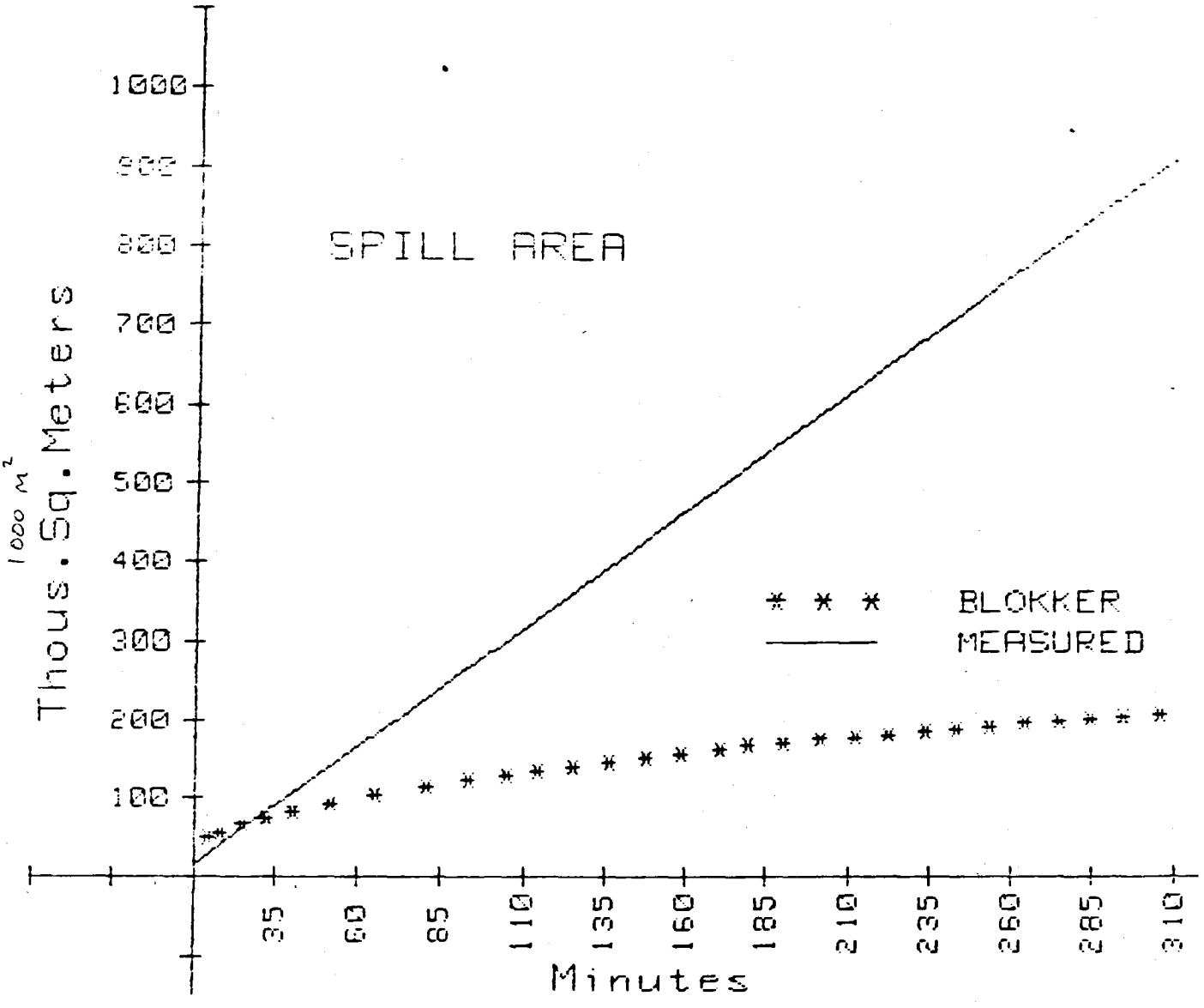

Figure 8: Area predicted by the Blokker formula compard with the actual area for a 5l barrel spill.

A SEMI-EMPIRICAL METHOD OF ESTIMATING RESIDUAL SURFACE CURRENTS IN THE KAP REGION

by

William J. Lehr

and

Robert J. Fraga

Water Resources and Environment Division
Research Institute
University of Petroleum and Minerals
Dhahran, Saudi Arabia

INTRODUCTION

The modelling of oil spills and other surface pollutants in the Inner Gulf, of the Kuwait Action Plan region mirror image of whose topography is shown in Figure 1, requires an accurate description of their transport. This transport is basically accomplished in three ways: time-dependent wind-driven leeway, for which empirical formulas exist for drift rate and angle as a function of wind velocity (Lehr & Cekirge, 1979);tidal currents, for which well-established models exist in the Gulf (lardner et al., 1982); and steady state residual surface currents. Unfortunately, very little information exists describing the residual current field in the region. The studies of Schott (1918), Koske (1972) and Brewer et al., (1978) describe an anti-clockwise drift around the Gulf. Studies by the United States Naval Hydrographic Office (Tetra Tech, 1979) and the National Oceanographic Data Center (1980) based on ship drift data indicate a similar but slightly more complicated result. A recent paper by Hunter (1982), however, criticizes circulation patterns based on such ship drift data and claims that when only locations in the Gulf where sufficient and acceptable drift information were used, there was little evidence to suggest an anti-clockwise circulation.

SEMI-EMPIRICAL INTERPOLATION OF STEADY STATE RESIDUAL SURFACE CURRENTS

Knowing of Hunter's criticism of ship drift data alone, the authors combined this information with some basic hydrodynamic considerations to develop a semi-empirical approach to residual surface currents. From some general approximations involving time averaging of the two-dimensional Navier-Stokes equation, it is possible to write a streamline equation for the steady state residual current (Nihoul, 1975). To accomplish this, the nonlinear advection terms in the Navier-Stokes equation for the residual current are dropped. This is justified by a Rossby number, the ratio of inertial to Coriolis forces, of around 10-2 assuming a characteristic length of at least 100 km in the Gulf. Also, the dispersion term involving the second derivative of the current velocity is considered to be small compared with contributions from bottom friction. It is then possible to write the streamline equation in the form

$$A \nabla^2 \Psi + B \, \partial\Psi/\partial x + C \, \partial\Psi/\partial y = D \qquad (1)$$

Here

Ψ = stream function

and , if v is the residual velocity, then

$$v_x = -\partial\Psi/\partial y$$

$$v_y = \partial\Psi/\partial x$$

The coefficients in the equation are defined by Nihoul (1975) as follows:

A = frictional coefficient proportional to the average magnitude of the time dependent wind and tidal currents;

B,C = Coriolis terms which are functions of depth and latitude;

D = stress term incorporating such factors as wind and tidal stress.

The values of A, B and C can be reasonably estimated for the conditions of the Gulf. According to Nihoul, a good approximation for A is

$$A = K \langle||v||\rangle$$

where K is a drag coefficient and $\langle||v||\rangle$ is a long-term time average of the fluctuating part of the current. According to a study by Hughes & Hunter (1979), appropriate Gulf values for these two terms are 0.003 and 0.2 m/sec, respectively.

B, C take the form

$$B = - f\,\partial H/\partial y - (2A/H)(\partial H/\partial x)$$

$$C = f\,\partial H/\partial x - (2A/H)(\partial H/\partial y)$$

where

f = Coriolis parameter for Gulf
= .000066 sec-1

H is the depth (tidal elevations neglected and small non-zero values used at boundaries to avoid numerical difficulties).

It is, however, difficult to construct an accurate estimate for D. The authors therefore, used equation (1) at points where, according to Hunter, reasonable estimates for residual current and hence the gradient of could be determined, along with selected boundary points where the velocity is set to zero. This gave a total of 34 selected locations (see Figure 2) on the edge or inside the Gulf where the value of D could be determined empirically. Using the computer software system SURFACE II (Sampson, 1978), these values of D were then interpolated throughout the Gulf using a constrained distance-squared weighting function. Figure 3 shows the results of this interpolation.

B and C are determined at the 34 selected locations in the Gulf from geometric considerations of the known topography at those points and these values interpolated throughout the Gulf, as for D.

The 34 points were supplemented by 99 others located in an evenly- distributed fashion in the Gulf and along its boundary. The resulting 133 points became the nodes for a finite-element network consisting of 175 simple triangular elements. The streamline function Ψ was assumed to be approximated by

$$\Psi = \sum_{j=1}^{133} \Psi_j \Phi_j$$

where

Ψ_j = value of Ψ at the j-th node

Φ_j = linear basis function whose value at the j-th node is 1.

Various assumptions can be made as to the way the terms B,C and D vary over the domain. Following Pinder & Gray (1977), they are assumed to vary in the same way as the basis functions.

Thus

$$B = \sum_{j=1}^{133} B_j \phi_j$$

where

Bj - value of B assigned a priori at the j-th node.

C and D are similarly dealt with.

The resulting set of equations is solved using the Galerkin method with a boundary condition of no flow across the Gulf boundary, even for the Strait of Hormuz. This last assumption is made to avoid numerical difficulties and is subject to modification in future work.

RESULTS

A contour map for the Ψ values computed by the Galerkin method is given in Figure 4. A similar map is presented in Figure 5 in Ψ which was re-calculated on the assumption that the Gulf bottom is flat.

Figure 6, taken from Galt (1983), shows a linear sum of current components due to wind stress using a 5 m/sec wind from the Northwest, evaporative forcing and inflow through Hormuz, fresh water runoff and entrainment.

Despite the difference in levels of sophistication between the two models, there is a measure of agreement between them, notably in the counterclockwise gyre present Northeast of Qatar.

BIBLIOGRAPHY

Brewer, P.G. et al. (1978) Chemical oceanographic data from the Persian Gulf and Gulf of Oman, Woods Hole Oceanographic Institution Technical Report, WHOI-78-37.

Galt, J.A. et al. (1983), Trajectory analysis for the Nowruz oil spill with specific applications to Kuwait, Modelling and Simulation Studies, Hazardous Materials Response Branch NOAA, Seattle, WA, pp. 6-15.

Hughes, P. & Hunter J.R. (1979) Physical oceanography and numerical modelling of the Kuwait Action Plan (KAP) Region.

Hunter, J.R. (1982) The physical oceanography of the Arabian Gulf: a review and theoretical interpretation of previous observations, presented at First Gulf Conference on Environment and Pollution, 7-9 February 1980, Kuwait.

Koske, P. (1972) Hydrographische Verhaltnisse im Persischen Golf Grund von Beobachtungen von F.S. "Meteor" in Fruehjahr 1965, "Meteor" Forsch. Ergbn., Gebrueder Borntraeger, A.11, Berlin, pp. 58-73.

Lardner, R. et al. (1982) Finite difference model for tidal flows in the Arabian Gulf, Comp. and Maths. with Appls., Vol. 8, pp. 425-444.

Lehr, W. & Cekirge, H. (1979) Gulfslik I: a computer simulation of oil spill trajectories in the Arabian Gulf, Research Institute Internal Report, Dhahran.

National Oceanographic Data Center (1980) Surface Current Data System (Ship Drift Data for Arabian Gulf).

Nihoul, J. (1975) Modelling of marine systems, Elsevier Scientific Publishing Co., Amsterdam, pp.59-62.

Pinder, G. & Gray, W. (1977) Finite element simulation in surface and subsurface hydrology, Academic Press, New York.

Sampson, R.J. (1978) Surface II graphics system: number one series on spatial analysis, Kansas Geological Survey, Lawrence, Kansas.

Schott, G. (1918) Oceanographie und Klimatologie des Perischen Golfes und Golfes von Oman, Annalen der Hydrographie und maritimen Meteorologie, pp. 1-46.

Tetra Tech (1979) Final report water transport studies. Royal Commission for Jubail and Yanbu Contract No. 001-C04.

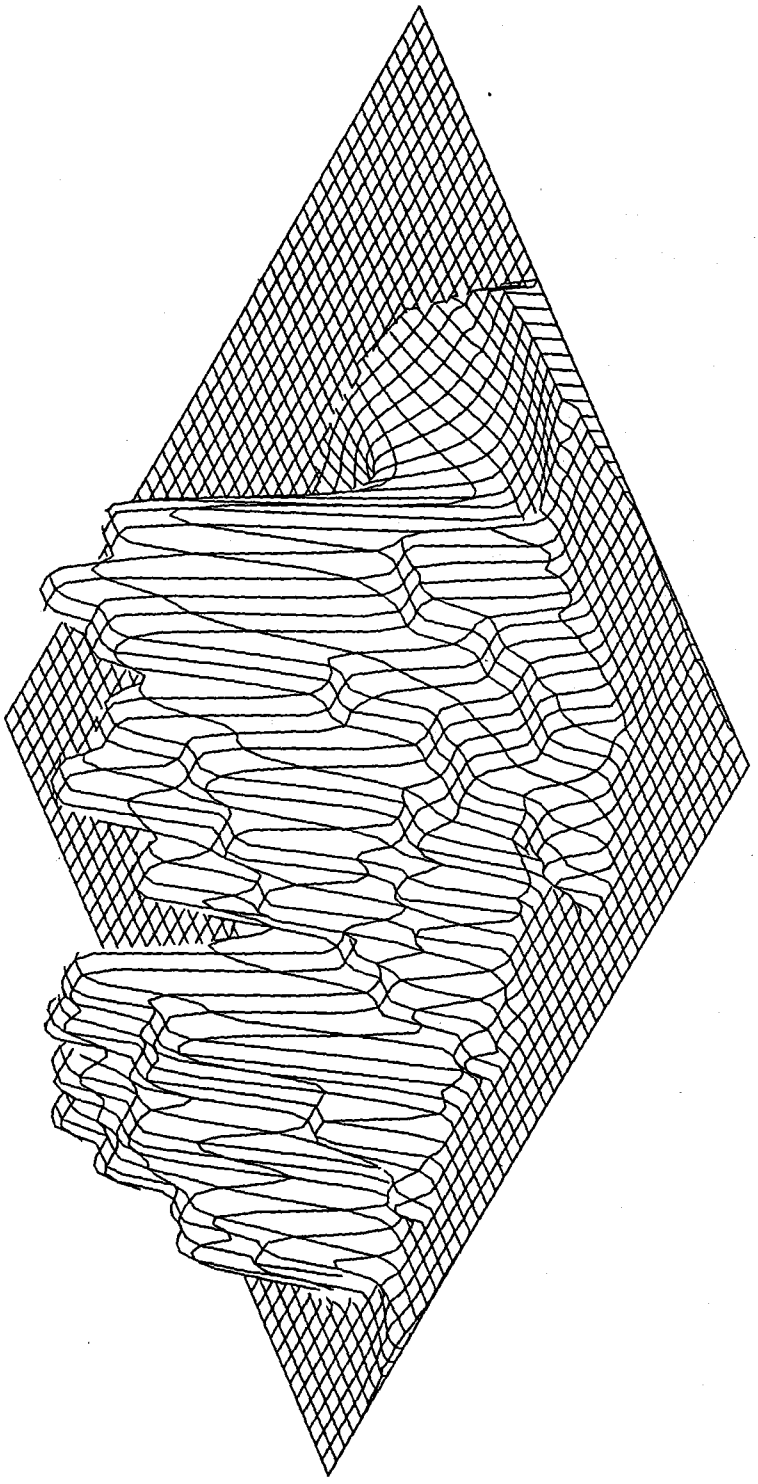

Figure 1: Mirror image of Gulf topography constructed by using SURFACE II

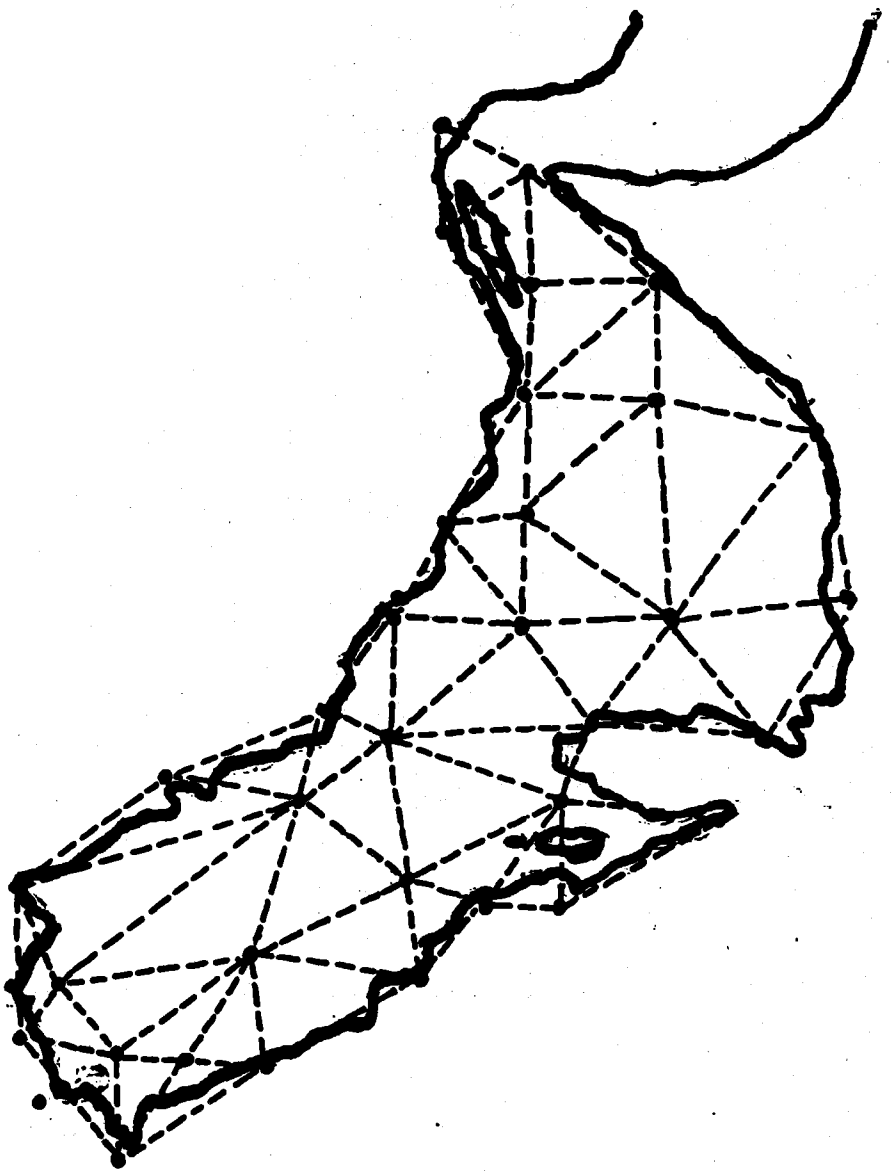

Figure 2: Location of sites where empirical estimates of residual current were determined

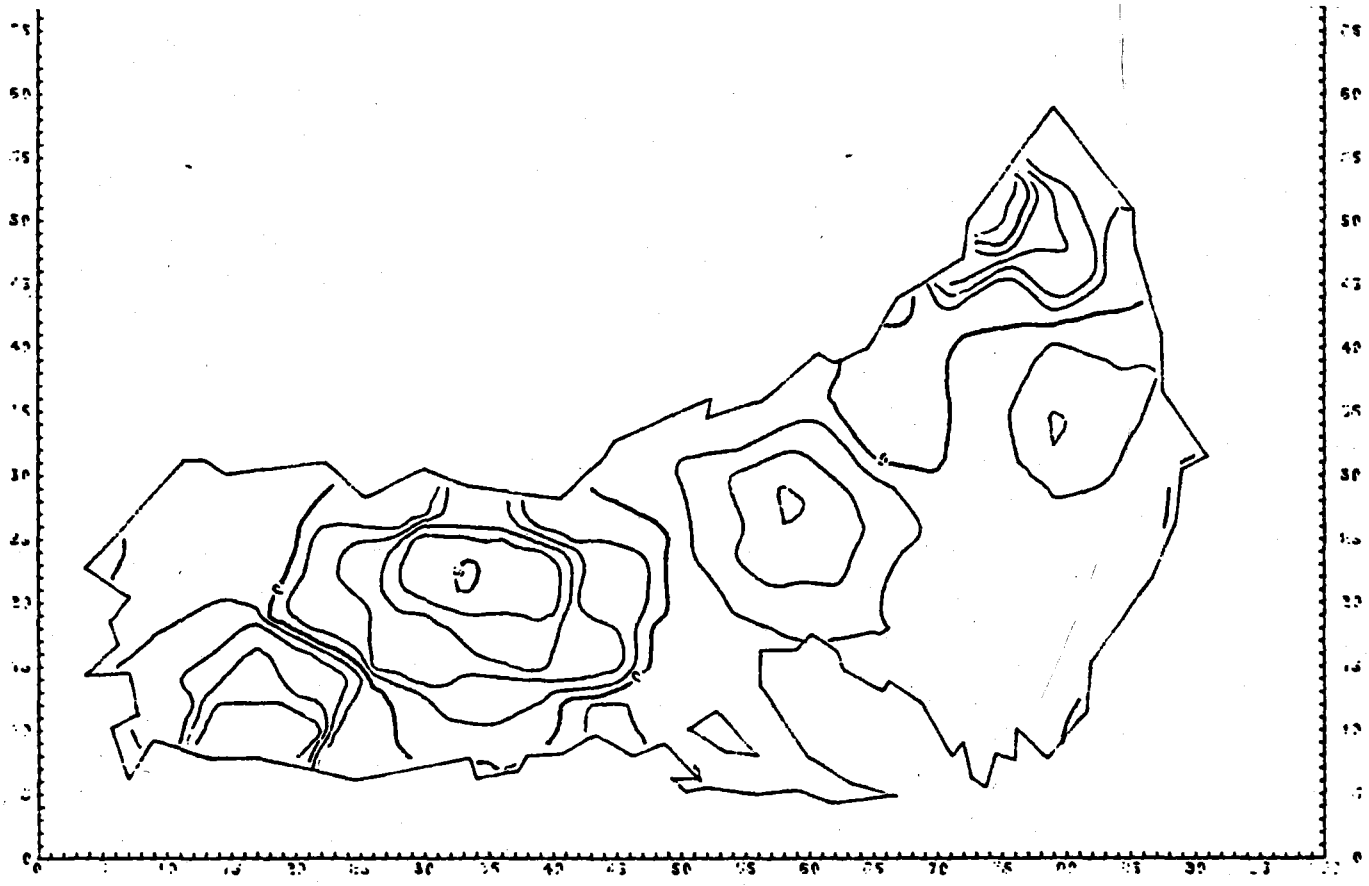

Figure 3: Contour map of D values interpolated throughout the Gulf

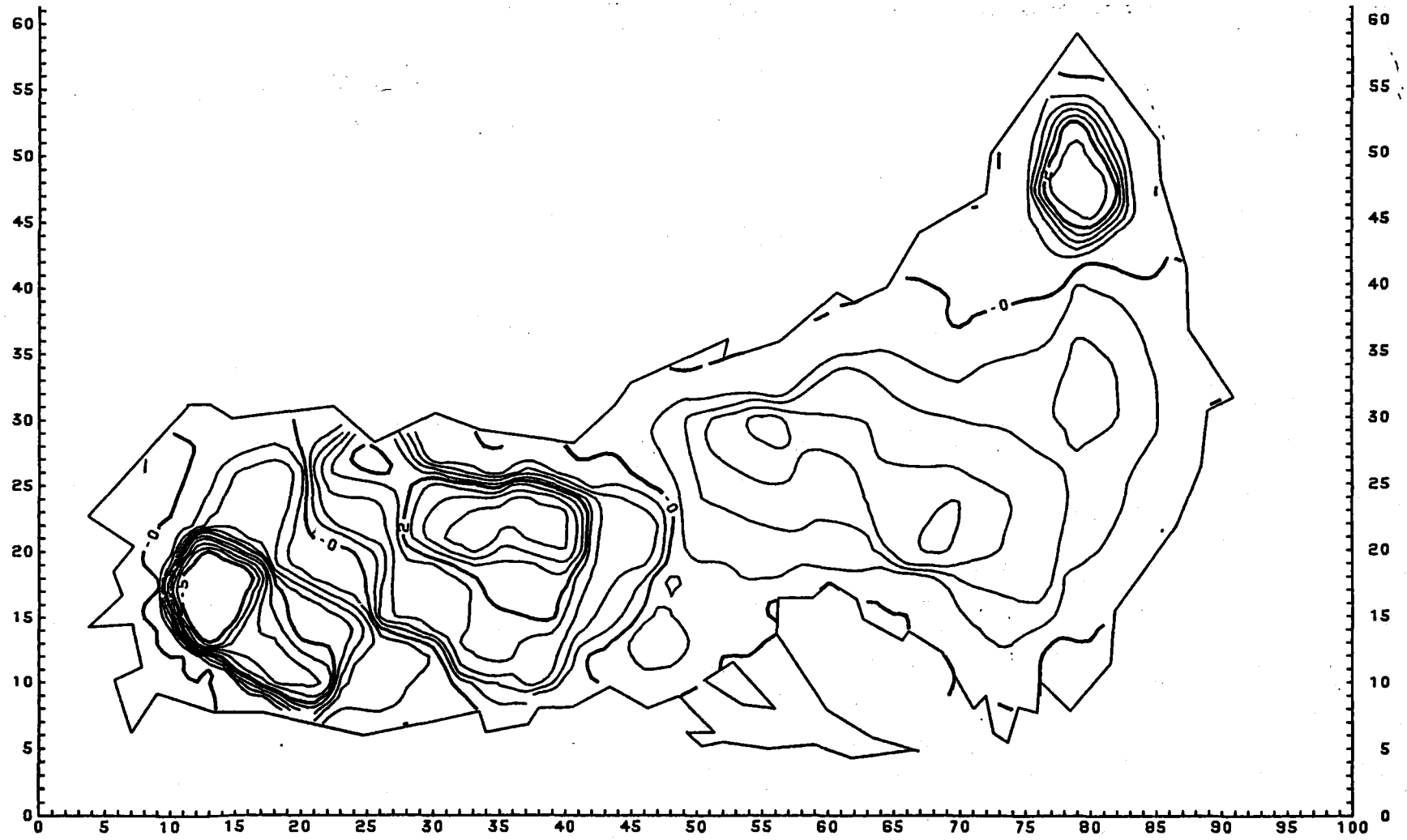

Figure 4: Level curves for Ψ computed troughout the Gulf, using variable topography

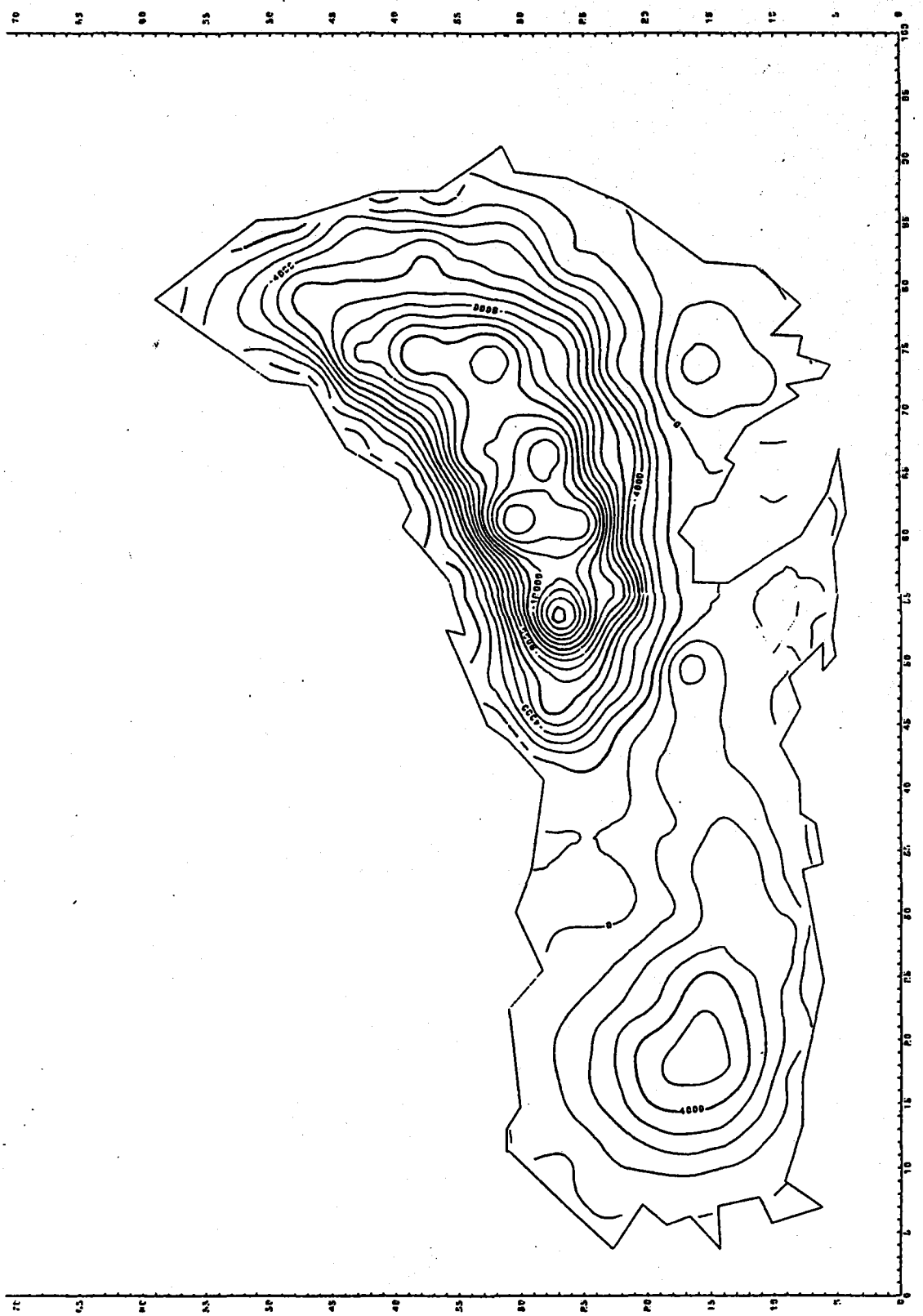

Figure 5: Ψ contours calculated on the assumption that the Gulf bottom is flat.

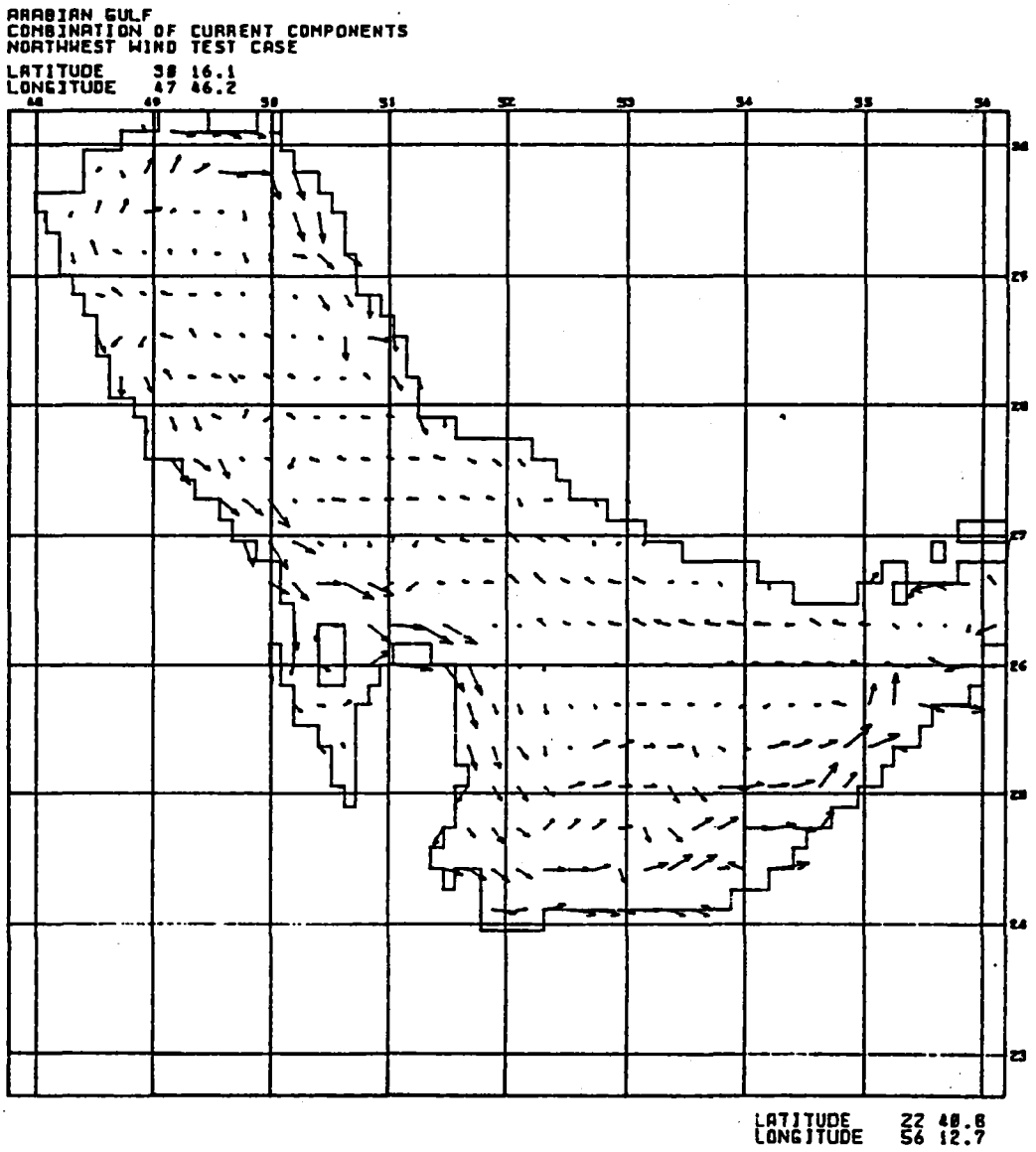

Figure 6: Linear sum of current components scaled to be consistent with observational data (Galt, 1983)

MODELS FOR TIDES IN THE KUWAIT ACTION PLAN (KAP) REGION

by

C. Le Provost
Institute de Mécanique de Grenoble, C.N.R.S., France

ABSTRACT

Existing knowledge about tides in the KAP Region is outlined in the first section of this paper which presents an analysis of the harmonic constituents of tides in the Inner Gulf of the Kuwait Action Plan Region and the Gulf of Oman. The description is not restricted to major constitutents; it extends to non-linear constitutents which are non-negligible in some places. The second part of the paper presents classical numerical modelling techniques applicable to tidal problems, illustrated by reference to three models of the Inner Gulf that are fully documented in the literature. The performance of these models is discussed and their limitations are pointed out. In the last section, recommendations are made for future work to improve present knowledge about tides in the KAP Region: complementary in situ observations of offshore tidal elevations and, in particular, tidal currents, and new numerical modelling experiments based on methodologies successfully applied to similar problems in other coastal areas throughout the world.

INTRODUCTION

Tides in the KAP Region, which includes the Inner Gulf and the Gulf of Oman, may be said to be quite well known depending, of course, on the physical variable concerned and on the precision expected. In the present paper, it will be seen that tidal elevations have been quite well observed and analysed, at least along the coast of the Inner Gulf, giving a satisfactory picture of the components of tidal elevations all over the region. This empirical knowledge has been confirmed and completed, to some extent, by several numerical models which will be examined below. Even for tidal elevations, however, it will be seen that some problems are still to be solved if precise predictions are expected. It should also be pointed out that tides in the Gulf of Oman have been less well observed and identified, partly because of the oceanic characteristics of that area. But the main lack of data is on the velocity field. Very little is known from observation about water velocities. Although numerical models have been used to produce a global view of the main tidal components, this information has to be checked against a minimum set of in situ observations. The first part of this paper will give a brief description of the tides in the region, based on the observed sea surface elevation along the coasts. Anticipating the results of the numerical models, a classification of the different tidal types (diurnal or semi-diurnal) for elevations and currents will also be presented because of the exceptional variety of tidal regimes present in the Region. The second part of the paper will present some numerical models described in the literature on the KAP region. Their main characteristics and differences will be pointed out and a comparative analysis of their results will be given. The last section will give a summary of the different unsolved problems, and make some recommendations for future work based on methodologies successfully applied to similar problems in other coastal areas throughout the world.

THE PHYSICAL CHARACTERISTICS OF TIDAL MOTIONS OVER THE KAP REGION

Tidal motions are typically pseudo-periodic, varying markedly with time. The motions are dominated by some main semi-diurnal and diurnal components, and constantly evolve through fortnightly, monthly, semi-annual, annual and even longer modulations, the strict periodicity of tides being 18.6 years. Such a complex situation can, however, be described quite simply by the harmonic theory of tides.

The harmonic theory of tides

Doodson (1921) was the first to give a full expansion of the tide-generating force in terms of harmonic series based on Brown's expansions of the Moon's parallax, longitude and latitude. These were recomputed by Cartwright & Tayler (1971) and Cartwright & Edden (1973) with modern astronomical constants and greater accuracy. It appears from these expansions that the energy in the tidal spectrum is

localised in four narrow bands, called "species": (0) long-period, (1) diurnal, (2) semi-diurnal and (3) terdiurnal. Some hundred terms are necessary in this harmonic expansion to define the potential to an accuracy of about 1 per cent, but only a few of them are of practical importance. Figure 1 is an illustration of the shape of that spectrum, indicating the location of the main constituents and giving the symbols originally allocated by Darwin (1883). The characteristics of the constituents are also presented in table 1.

Following the dynamic theory of tides, it may be assumed that each constituent of this tide-generating potential, corresponds to a wave in the ocean; consequently, the sea surface elevation due to tides in the ocean can be written as:

$$H(x,y,t) = H_o(x,y) + \sum_{i=1}^{N_p} fi\ Ai(x,y) \cos [\omega_i t + (V_o+u)_i - g_i(x,y)] \qquad (1)$$

with: $H_o(x,y)$: mean sea level at point (x,y)

$A_i(x,y)$: amplitude of the constituent i at point (x,y)

$g_i(x,y)$: phase lag, related to the phase of the corresponding constituent in the tide-generating potential, the reference being taken on the Greenwich meridian

v_{oi} : phase of the constituent at t = 0

f_i and u_i: nodal correction factor and nodal phase correction slowly varying with a basic period of 18.61 years

N_p : number of significant constituents.

Equation (1) can still be used for shallow water areas, but new frequencies must be introduced into the spectrum because of the non-linear effects governing the dynamics of propagation of the different astronomical tidal waves coming from the ocean. The frequencies of these non-linear components are easy to deduce from the frequencies of their generating waves. They correspond to harmonics or interactions and are distributed in new species (quarter-diurnal, sixth-diurnal, etc) or superimposed on already existing astronomical species (long-period, diurnal, semi-diurnal, terdiurnal).

Thus the harmonic theory of tides assumes that the variation of the sea surface elevation can be developed from a form similar to (1), with a number of constituents NR greater than NP. The parameters A_i (x,y) and g_i (x,y) are typical parameters of the tidal spectrum at point (x,y), constant in time, and completely define the time-varying quantity H (x,y,t). Classically, these parameters are deduced from the harmonic analysis of time series of <u>in situ</u> observations (note that such an analysis requires long time series because of the proximity of some frequencies). The definition of Ai and gi then, allows the prediction of H (x,y,t) for any time t.

Harmonic tidal data for the KAP Region

Tidal elevations have been well observed along the coasts of the Inner Gulf. Figure 2 shows the locations for which a set of harmonic constituents exists (B.H.I. source). More than fifty data sources are sufficient to provide an accurate picture of the tides in the area. The density of observation points is particularly high along the western coast of Saudi Arabia, Qatar and United Arab Emirates. Very few data, however, exist for the Gulf of Oman.

It can be seen from Figure 2 that the Inner Gulf is a shallow area with a deeper channel on the Iranian side, while the Gulf of Oman is very deep, with quite a narrow continental shelf and more than 2,000 m deep in its eastern part. Consequently, it would be expected that the tides in the Gulf of Oman would, in fact, be part of the Indian Ocean cotidal system, while in the Inner Gulf the tides would be locally induced by the limits, i.e., the Strait of Hormuz.

Main tidal constituents. It is well known that the Inner Gulf is a coastal area where the semi diurnal and diurnal tides can give rise to resonance oscillations. Given its geometry (about 850 km long, 250 km wide, with a mean depth of 50 m), Defant (1961) estimated that the free oscillation period of the basin is between 21.7 h and 22.6 h. In practice, large semi-diurnal and diurnal tides are observed. Figure 3 and table 2 give the maximum values of the main constituents observed along the coasts. The higher values are located in the Strait of Hormuz (Bandar Abbas and Khor Kani) and at the end of the Gulf (Fao and Khor Musa Bab). Large semi-diurnal amplitudes are also observed in the vicinity of Bahrain. Empirical cotidal charts have been produced for the main constituents from the set of observed data by the Hydrographic Department of the British Admiralty. Figure 4 presents the three dominant constituents, M_2, S_2 and K_1. It can be seen that the semi-diurnal constituents are, in fact, areas of maxima and result in a system of two amphidromic points, while the diurnal K_1 gives one amphidromic point in the middle of the Gulf.

Such systems are the well known Kelvin-Taylor amphidromes, described mathematically by Taylor (1921) for co-oscillating waves in rectangular frictionless channels closed at one end, and situated in a rotating frame. In the Inner Gulf, the energy enters through the strait of Hormuz and propagates for each constituent as a Kelvin wave sloping up towards the Iranian coast. These waves are reflected at the end of the Gulf, and come back along the other side of the channel. The resultant of these two opposite Kelvin waves forms a set of amphidromes with a first amphidromic point of zero amplitude at a quarter of a wave length from the end of the channel, for each constituent. If the incident and reflected waves had the same amplitude, the amphidromic points would be equidistant from the two lateral coasts of the channel; but here, because of frictional damping, the outgoing wave is weaker, and the amphidromic points are consequently shifted from the axis of the channel towards the Arabian coast.

The M_2 and S_2 cotidal charts presented in Figure 4 look very similar, and an obvious question arises about the possibility of deducing the cotidal maps of any constituent from information on one constituent in each species, as well as

fixing the ratio between them and their phase lag. The ratio and phase lags for all the significant constituents are given in table 2. A relatively constant ration was observed for the semi-diurnal constituents related to M h2 H at various observation points:

S_2/M_2 : 0.31 to 0.37 $gS_2 - gM_2$ = 36° (at the entrance) to 62° (at the end)

N_2/S_2 : 0/20 to 0.25 $gN_2 - gM_2$ = -18° (at the entrance) to -34° (at the end)

K_2/M_2 : 0.10 to 0.13 $gK_2 - gM_2$ = 34° (at the entrance) to 50° (at the end)

L_2/M_2 : 0.05 to 0.08 $gL_2 - gM_2$ = 9° (at the entrance) to 25° (at the end)

$^u2/M_2$: 0.02 to 0.07 $gM_2 - gM_2$ = 89° (at the entrance) to 110° (at the end)

These ratios are close to those of the components of the tide-generating force, except for S_2 , because of the radiational contribution to the tides. Similar values have been observed for the English Channel (Le Provost, 1974). The same observations hold for the diurnal constituents, related to K_1:

O_1/K_1 : 0.58 to 0.64 $gO_1 - gK_1$ = - 3° (at the entrance) to -47° (at the end)

P_1/K_1 : 0.24 to 0.32 $gP_1 - gK_1$ = 0° (at the entrance) to -10° (at the end)

Q_1/K_1 : 0.07 to 0.10 $gQ_1 - gK_1$ = -51° (at the entrance) to 61° (at the end)

The corresponding ratios for the tidal potential are quite similar for P_1, but larger for O_1 and Q_1 because of the radiational contribution to K_1 and P_1, which does not affect O_1 and Q_1 .

Secondary constituents. It may be observed from Figure 3 and table 2 that some significant non linear terdiurnal and quarter diurnal constituents exist in the observed spectra.

It is difficult to draw conclusions about the terdiurnal non-linear constituents, as significant amplitudes are only observed at the end of the Gulf, at Fao and Khor Musa Bab. They appear to result from non-linear interactions between semi-diurnal and diurnal constituents: M_2 and $K_1 \rightarrow MK_3$, M_2 and $O_1 \rightarrow MO_3$, S_2 and $O_1 \rightarrow SO_3$ (but why not SK3?). If these interactions actually occur, attention must be paid to the similar non-linear contribution to diurnal constituents: M_2 and $K_1 \rightarrow O_1$, M_2 and $O_1 \rightarrow K_1$, S_2 and $K_1 \rightarrow P_1$. This perhaps explains the smallness of the O_1/K_1 and P_1K_1 ratios at Fao.

Quarter diurnal constituents probably exist in the Gulf, as the areas of maxima appear to be located in the areas of minima of semi-diurnal amplitudes (except the area of the end of the Gulf), as expected from the theory of non-linear constituent generation (Le Provost, 1974). Significant amplitudes may be observed at Ras AL-Mishaab and Al Doha. Moreover, the amplitude ratio MS4/M4 seems to be relatively constant and very close to the theoretical value $2A(M_2)xA(S_2)/A(M_2)^2$ expected from the theory, and the phase lag is equal to that of the generating constituents $g(S_2)-g(M_2)$.

These secondary constituents are reqired in making precise predictions because, in the harmonic method, all the significant constituents have to be taken into account. Moreover, higher order constituents can contribute to interpreting complexity of tidal currents when differences are observed between ebb and flows.

Classification of tidal types

As noted above, tides in the KAP Region present typical semi-diurnal and diurnal amphidromes, leading to a particular tidal cycle due to the configuration of the area. Evans-Roberts (1979) has recently produced maps for classification of tides and currents, based on numerical simulations. The numerical procedure used by Evans-Roberts is described below. Figure 5, however, presents these classifications. The maps divide the Inner Gulf into areas of semi-diurnal ($M_2 + S_2/K_1 + O_1 < 0.5$), predominantly semi-diurnal (0.5 - 1.0), predominantly diurnal (1.0 - 1.5) and diurnal (>1.5) tides and currents. The diurnal character of the tide appears of course around the amphidromic points of the semi-diurnal cotidal maps. This classification is particularly interesting for currents, as very little is known about them at present from observation and they are an important parameter. Evans-Roberts numerical results imply that diurnal constituents for currents arise in the central part of the Inner Gulf over an area where tides are semi-diurnal, and vice versa for semi-diurnal constituents. This is apparently due to the amphidromic shape of these tides, maximum amplitude of currents being located in the areas of minimum amplitude of sea surface elevations.

NUMERICAL MODELLING OF THE KAP REGION

Over the last 20 years, increased computer facilities have led to intensive development in the numerical modelling of tides and its successful application to the investigation of tidal motions in many coastal areas. An enormous number of such numerical models are reported in the literature. It is difficult to draw up a complete list of models even for a particular, restricted area. This paper is devoted to the KAP Region and reference will be made to three of the models developed for the Inner Gulf, Von Trepka (V.T.) (1968), EVans-Roberts (E.R.) (1979), and Lardner, Belen & Cekirge (LBC) (1982), and to one of the more recent ocean tide models for the Gulf of Oman, reported by Schwiderski (1979).

The Inner Gulf

Equations and approximations in the formulation. The basic equations to any of these approaches are the Navier-Stokes equations and the equation of continuity, written either in cartesian or polar coordinates, depending on the size of the area being investigated and the degree of approximation acceptable. In practice, most of the tidal models used are limited to an average version of these equations over the vertical, resulting from the so-called shallow water approximation, reducing the problem to a two dimensional system involving u and v, the eastward and northward mean depth velocity components, and , the sea surface elevation:

$$\frac{\partial u}{\partial t} + \frac{u}{R\cos\phi}\frac{\partial u}{\partial \lambda} + \frac{v}{r}\frac{\partial u}{\partial \phi} - \frac{uv}{R}\tan\phi - 2\Omega \sin\phi\, v + Cu\,(u^2+v^2)^{\frac{1}{2}} + \frac{g}{R\cos\phi}\frac{\partial \zeta}{\partial \lambda} = \frac{g}{R\cos\phi}\frac{\partial P}{\partial \lambda} \qquad (2a)$$

$$\frac{\partial v}{\partial t} + \frac{u}{R\cos\phi}\frac{\partial v}{\partial \lambda} + \frac{v}{R}\frac{\partial v}{\partial \phi} + \frac{u^2}{R}\tan\phi + 2\,\Omega \sin\phi\, u + Cv\,(u^2+v^2)^{\frac{1}{2}} + \frac{g}{R}\frac{\partial \zeta}{\partial \phi} = \frac{g}{R}\frac{\partial P}{\partial \phi} \qquad (2b)$$

$$\frac{\partial \zeta}{\partial t} + \frac{1}{R\cos\phi}\left(\frac{\partial}{\partial \lambda}(h+\zeta)u + \frac{\partial}{\partial \phi}(h+\zeta)\, v\cos\phi\right) = 0 \qquad (2c)$$

in which the following symbols denote:

λ, φ = east longitude and latitude, respectively;
t = time;
ζ = elevation of the sea surface above the equilibrium level;
h = the equilibrium water depth;
R = the radius of the Earth;
Ω = the angular speed of the Earth's rotation;
g = the acceleration due to gravity;
u,v = eastward and northward mean depth components of current, respectively;
P = tide-generating potential; and
C = bottom friction coefficient.

In order to solve these equations, appropriate boundary conditions have to be specified. On any land boundary, the normal velocity component must be zero. Along the open boundaries, the most appropriate boundary condition is to prescribe the flux of water, but such a condition is usually difficult to estimate, and it is easier to specify the sea surface elevation, deduced from observations at the coast. Thus, the boundary conditions are generally of the form:

$$\ell u + m v = 0 \quad \text{on } \Gamma_1 \text{ (land boundary)} \qquad (3a)$$

$$\zeta = \zeta_o \quad \text{on } \Gamma_2$$

where (ℓ, m) is the unit normal to the shore line, and ζ_o is the prescribed values of the water height along the open boundary.

Some simplifications are applied to the system (2) for practical applications. For shallow water tides, the generating potential is generally neglected. For restricted areas, the equations (2) are written in cartesian coordinates, thus neglecting the Earth's curvature: this is the case for the V.T. and LBC models, but not for the E.R. model in which a spherical polar system is retained. It should be noted that, given the latitudinal extension of the Gulf from 24°N to 30°N, it is better not to make this approximation. In order to save computational work, equations (2a) and (2b) are sometimes linearized. Such simplification is largely justified when the modelled area is not too shallow and there are no large velocity gradients. It was used by V.T., following Hansen's formulation (1956, 1962, 1966), but the analysis presented above indicates the existence of harmonic and interaction constituents in the spectrum which cannot be reproduced in the models if these non-linear terms are excluded.

The bottom friction parametres used are very important factors for the efficiency of these models. Several laws are classically applied, but they must all postulate at least a quadratic velocity dependence. Thus, V.T. used a friction friction coefficient inversely proportional to the depth of the water column, $C = r/(h+\zeta)$. LBC introduced a more complex formulation in their model, following Leendertse (1967), $C = \frac{\rho g}{k^2}$ with $k = C_1 \ln (C_2 h + C_3)$, where C_1, C_2 and C_3 are constant values dependent on the nature of the bottom.

Finite difference approximations. The system (2) of differential equations is transformed into a set of finite difference equations for numerical integration. The precision of the numerical solutions depends, of course, of the properties of the finite difference scheme adopted.

V.T. used the well known Hansen scheme. The LBC model is based on a splitted method developped by Leendertse, which consists of dividing each time step into two half-steps. During the first half-step, equations (2a) and (2c) are solved to compute a new value of ζ and u, and the new v value is then computed from equation (2b), using the new values of ζ and u. During the second half-step, the process is reversed.

With finite difference techniques, it is necessary to use constant grid spacing. As the size of the mesh greatly influences the precision of the results, it is often difficult to reconcile the fineness of the mesh size with the volume of computation required. V.T. used a regular mesh-sized of 14 km, while E.R. used a mesh of 10 minutes latitude and longitude (approximately 9 by 10 nautical miles). LBC developed a multi-block technique consisting of a relatively coarse mesh (approx. 20 km) covering the whole Gulf, with a secondary block of finer mesh (about 10 km) over the shallow coastal areas along the south-east, south-west and north-west shores.

Simulation conditions and analysis of results. One of the main differences between the simulations produced by V.T., LBC and E.R. is the way in which they approximate tidal forcing at the Strait of Hormuz. A simple approach was employed by LBC. They studied the different constituents separately by forcing them at the open boundary and carried out simulations for 75 hours of real time, starting from rest, since the dynamics had reached equilibrium after a spin-up phase of about two days. They retained the last day of simulation to estimate the amplitudes and phases of the simulated constituent over the whole area thus producing cotidal maps for M_2, S_2 and K_1. Figure 6 gives the charts of equal amplitudes for M_2 and K_1. These maps should be compared to those presented above, in Figure 4, based on extrapolations of observed values. Their solutions look quite good. The semi-diurnal tide exhibits two amphidromic points situated in the right place, and high tidal amplitudes at the entrance of the Gulf, in the region between Saudi Arabia, Qatar and the Iranian coast on the other side, and at the bottom of the Gulf; the diurnal tide presents a single amphidromic point correctly located, north of Bahrain, and large amplitudes at the bottom of the Gulf and off the eastern Qatar and Southern Emirates coast. From a detailed analysis of the M_2 solution, however, it appears that these amplitudes are too small in the Central part of the Gulf, between Bahrain and the Iranian coast, by about 10 per cent; the same remark applies to K_1 between Qatar and the Emirates coasts. It might appear at first that the

bottom friction coefficient is not appropriate, and is too strong; but this argument is probably not the right one, because these cotidal charts are in good agreement with the observations elsewhere. In fact, it will be seen below that the non-linear damping interactions between M_2 and K_1 cannot be neglected. The authors also noticed that their S_2 constituent, convenely, was too big. It is evident here that a secondary wave like S_2 cannot be simulated alone; its damping is dominated by the velocity field of the dominant waves propagating with it, at least M_2, but probably also K_1.

V.T. first investigated M_2 and K_1 separately. His M_2 solution is presented in Figure 7. Overall, the amplitude seems to be better. In the central part of the basin, the solution is higher than that of LBC, and the author noted that, even in the Bahrain area with its complicated coastline and very shallow waters, his solution was very good.

Careful examination of this solution, however, shows that this M_2 wave is too strong all along the eastern coast of Qatar and the southern coasts of the Emirates, the discrepancies attaining more than 20 per cent in that area. This brings us back to the same conclusion as above about the impossibility of correctly representing even the dominant waves separately. V.T. himself reached the same conclusion when trying to reproduce O_1 and S_2. As in LBC simulations, the amplitudes of these waves were too big.

V.T. carried out an interesting experiment to take into account the non-linear interactions between the different constituents. He prescribed a real prediction of sea surface elevations at the entrance of his model, which included seven constituents, for 40 days beginning on 5 August. To save computer time, a mesh size of 42 km was used. The results of the simulation were checked with the predictions of high and low water levels given in the tide tables. The differences in height in Kuwait harbour were typically less than 10 cm, with a maximal difference of 36 cm; the mean deviation in time was about 20 minutes, and it was observed that these deviations were not cumulative. The author concluded that, with a finer grid net, and more than seven constituents, these difference would be reduced, and that harmonic analysis would then show the influence of tide-tide interactions. This idea will be taken up again in the last section of this paper.

E.R. developed a low cost method to reproduce the M_2-K_1 interaction by simulating the M_2 constituent together with an artificial diurnal tide (AM1) having the amplitude and phase of K_1 but period exactly twice M_2. This produces a tide cycle which is repeated at intervals of 24.8 hours. The economy is evident: the the main features of the tides can thus be studied without the need to generate and analyze vast quantities of results. This method, however, does not allow the other constituents of the tides, such as S_2 and O_1, or the non linear inter action noted above to be studied. The cotidal map of M_2 produced by E.R. is presented in Figure 8. As the author noted, the amplitudes generated for M_2 tended to be lower than those observed in situ, or those in the Admirality cotidal charts. This is a little surprising. The question arises as to whether it is due to the fairly coarse grid used. This point requires further clarification.

All these models also produce velocity fields corresponding to mean depth currents but this information cannot be checked because of the lack of observational data on tidal currents in the Gulf. Similar models have, however, been successfully applied throughout the world, and these results can thus be treated with some confidence. As an example of the currents in the Inner Gulf, Figure 9 presents a chart giving the magnitude and the direction of the maximum M_2 velocity, obtained by V.T. It can be seen that this field is quite complicated and strongly influenced by the topography of the coast and of the sea bed. These mean velocities are typically of the order of 20 cm/sec and do not exceed 0.4 m/sec. As already noted above, however, attention must be paid to the diurnal contribution which can produce diurnal currents in areas where semi-diurnal currents are weak or, alternatively, increase and weaken these semi-diurnal velocity fields in particular areas.

Local models around Bahrain

Because of the complexity of the topography around the Island of Bahrain and its vulnerability to environmental problems, local models have been developed for that region, which deserve mention because of their practical importance.

The Danish Hydraulic Institute has developed four hydrodynamic models with successively finer grids, focusing on the particular studied area (Al Khobar in Saudi Arabia): a model of the Gulf, with 8 km grid, a secondary model (Dawhat Salwa) with a grid of 3 km; a regional model, between Bahrain and the Saudi Arabian coast, with a grid mesh of 740 m; and a local model going down to 247 m. Unfortunately, this system of models is not documented in the literature and it is thus impossible to analyse its corresponding results.

Another example of a local model, produced by LBC (1982) as an extension of their multi-block model discussed above, will be used as an illustration. This model covers the area between the Arabian coast South of Ras Tanura and the West coast of Qatar, (see Figure 10). The grid mesh here is of 5 km. The simulated amplitudes for M_2 and S_2 are presented in Figure 10. If these solutions are compared with observed data, it may be seen that the results correctly represent the complex structure of the tides in that area.

The Gulf of Oman

As noted above, tides in the Gulf of Oman are of a different type because the area opens directly on to the Indian Ocean, and it is very deep, more than 2000 m in its eastern part. From a modelling point of view, these tides consequently require another class of models, those dealing with oceanic tides. An example of this class of models is provided by Schwiderski (1979). Such models generally include the tidal force, the loading tide and bodily tide. The amplitudes and phases of the main constituents of the tides are computed over the globe as a whole. The space resolution of these models is, consequently, very coarse. In Schwiderski's model, the resolution is of $1^\circ \times 1^\circ$, thus only a few values have been computed for the present area of interest. An examination of the results for the Gulf of Oman leads to the conclusion that the tides must be quite homogeneous throughout the area:

M_2'	:	amplitude	: 63 cm to 72 cm
		phase	: 160° TU (quasi constant)
S_2	:	amplitude	: 22cm to 24 cm
		phase	: 194° to 199° TU
K_1	:	amplitude	: 32 cm to 37 cm
		phase	: 339° to 348° TU

These values fit in very well with in situ observations because the Schwiderski model is designed to adjust the computed solution to the data obderved along the coasts.

CONCLUSION AND RECOMMENDATIONS FOR FUTURE WORKS

As this review shows, tides in the Inner Gulf and the Gulf of Oman are quite well known and understood. Tidal elevations have been well observed along the coasts and several models have recently been developed which give a quite satisfying overview of the KAP area. There are, however, some gaps in observational data, and some improvements are necessary in modelling.

Need for observation

Long-period observations taken offshore, for example from oil rigs, would enable more accurate cotidal charts to be drawn. It is recommended that preference be given to particular locations, such as the middle of the Gulf between Bahrain-Qatar and the Iranian Coast, to evaluate exactly the amplitude of the semi-diurnal constituents in this area of maximum values.

Evidently, tidal currents need to be observed. As the model results show, the effects and the characteristics of this major parameter have a very complicated distribution over the region. With the help of these model results, it would be possible to choose a set of observation stations correctly distributed such as to increase current knowledge and check numerical solutions. It is important to bear in mind that, given the complexity of the tidal spectrum, long-period of observations are needed, at least of the order of a month.

Need for improvement in modelling

It is obvious from the analysis of the different models presented above that a more satisfactory simulation is required combining all the positive properties of the previous models. An interesting framework for a new model would be as follows, if limited to at least a two dimensional classical model:

- formulated in spherical coordinate;
- completely non-linear, with careful attention being paid to the non-linear terms in the finite difference scheme adopted;
- applied with the highest possible space resolution;
- driven a long time in such a way that the non-linear interactions between the main tidal constituents are correctly reproduced;
- using improved bottom friction laws.

Such a simulation has recently been carried out for the English Channel by Le Provost and Fornerino (1985). Using a grid resolution of 10 km, a second order finite difference scheme and a month-long simulation with 22 constituents, a complete analysis of the tides in the area has been obtained, providing a detailed description of all the significant tidal constituents and fitting the observations of elevations and mean depth currents very well. A model for the predition of tidal elevations and tidal currents was developed on the basis of these results. Comparison with in situ observations obtained from tidal guage data or satellite altimetric measurements of sea surface variations confirms that the order of precision of the tidal elevation prediction model is within 15 cm for several metres of variability (up to 13 meters in the St. Malo Gulf); see Le Provost, 1981. Comparison with long-period observations of tidal currents shows that the tidal current prediction model reproduces mean depth velocities with a mean square error of some 10 cm/sec for currents of the order of 1 or 2 m/sec maximum amplitude (Fornerino & Le Provost, 1985).

These two-dimensional models are, however, limited by their formulation in providing a better representation of the tidal flows, especially the vertical distribution of the velocity field. Three-dimensional models are now available (see Davies, 1977). These models consume more computer time and simulations probably should be limited to certain tidal cycles. It is consequently recommended that some combined projects be established to include long-time simulation with two-dimensional models, and shorter simulation with three-dimensional models, to provide better knowledge of the vertical distribution of the tidal currents.

These global models would of course, serve to provide boundary conditions for local models, which could be three-dimensional and of very fine resolution.

REFERENCES

HMSO, Admiralty Charts. Persian Gulf, principal harmonic constituents.

Brown, E.W. (1919) Tables of motion of the moon. 3 vols. New Haven, Conn. Yale Univ. Press.

Cartwright D.E. & Edden, A.C. (1973) Geophys. J.R. Astrono. Soc. 33, pp. 253-264.

Cartwright D.E. & Tayler, R.J. (1971) New computations of the tide generating potential. Geoph. J.R. Astro. Soc. 23, pp. 45-74.

Darwin, G.H. (1883) Report on harmonic analysis of tidal observations. British Ass. for Adv. Sc. Rep. pp. 48-118.

Davies, A.M. (1977) The numerical solution of the three-dimensional hydrodynamic equations using a B-spline representation of vertical current profile in bottom turbulence. J.C. NIHOUL (ed.) Elsevier Oceanography series, 19, pp. 1-25.

Defant, A. (1961) Physical oceanography, vol. 2, Pergamon Press.

Doodson, A.T. (1921) The harmonic development of the tide generating potential. Proc. Roy. Soc. A 100, pp. 305-328.

Evans-Roberts, D.J. (1979) Tides in the Persian Gulf. In: Consulting Engineer.

Fornerino, M. & Le Provost, C. (1985) Un modèle de pridiction des courants de marie en Manche. Revue Hydrographique Internationale - July issue.

Hansen, W. (1956) Theorie zur Errechnung der Wasserstander und der Strùmugen in Randmeeren nebst Anwendungen, Tellus, 3.

Hansen, W. (1962) Hydrodynamical methods applied to oceanographic problems. In: Proc. of the Symp. on Math. Hydrody. Methods of Physical Oceanography, Mitt. d. Inst. f. Meereskunde, 1, Hamburg.

Hansen, W. (1966) Die Reproduktion der Bewegungsvorgänge in Meere mit Hilfe hydrodynamisch numerischer Verfehren. Mitt. d. Inst. f. Meereskunde, V, Hamburg.

Lardner R.W., Belen M.S. & Cekirge, H.M. (1982) Finite difference model for tidal flows in the Arabian Gulf. Comp. and Math. with Appls. vol. 8, no. 6, pp. 425-444.

Leendertse, J.J. (1967) Aspects of a computational model for long period water-wave propagation. Rand Corporation Report, RM-5294-PR.

Le Provost, C. (1974) Contribution à l'étude des marées dans les mers littorales: Application à la Manche. Thesis, 228 pages, I.M.G. Grenoble.

Le Provost, C. (1981) A model of prediction of tidal elevations over the English Channel. Oceanologica Acta, 4, 3, pp. 279-288.

Le Provost, C. & Fornerino, M. (1985) Tidal spectroscopy of the English Channel with a numerical model. Jour. of Phys. Oceanogr., July issue.

Taylor, G.I. (1921) Tidal oscillations in gulfs and rectangular basins. Proc. of the London Math. Soc. 2 XX, pp. 148-181.

Schwiderski (1979) Global ocean tides. Atlas of tidal charts and maps. Naval surface weapons Center. NSWCTR 79-414, Silver Spring, MD 20910.

Von Trepka, L. (1968) Investigations of the tides in the Persian Gulf by means of a hydrodynamic-numerical model. Proc. of the Symp. on Math. Hydrody. Invest. of Phys. Processes in the Sea. Inst. für Meer. der Univ. Hamburg, 10, pp. 59-63.

Table 1: Characteristics of the main tidal constituent potential.

	Name of partial tides	Symbol	Period in solar hours
Long-period components	Lunar fortnightly	Mf	327.86
	Lunar monthly	Mm	661.30
Diurnal components	Principal lunar diurnal	O_1	25.82
	Luni-solar diurnal	K_1	23.93
	Large lunar elliptic	Q_1	26.87
	Principal solar diurnal	P_1	24.07
Semi-diurnal components	Principal lunar	M_2	12.42
	Principal solar	S_2	12.00
	Large lunar elliptic	N_2	12.66
	Luni-solar semi-diurnal	K_2	11.97
	Smaller lunar elliptic	L_2	12.19
	Variational	μ_2	12.87
	Large lunar evectional	ν_2	12.63
	Lunar elliptic second order	$2N_2$	12.91
	Smaller lunar evectional	λ_2	12.22
	Large solar elliptic	T_2	12.01

Table 2: Maximum of amplitudes for the main constituents.
- Ratio/biggest amplitude in the species and phase lag by reference to that biggest constituent.

	SEMI-DIURNAL											
	M_2		S_2		N_2		K_2		L_2		μ_2	
FAO	82.7	337°	25.3	39°	16.7	303°	10.7	27°	6.9	351°	5.6	87°
	Ratio/M2 phase lag		0.31	62°	0.20	- 34°	0.13	50°	0.08	140°	0.07	110°
KHOR MUSA BAB	86.9	313	31.3	13°	18.8	289°	9.2	9°	4.5	322°	4.3	52°
			0.36	60°	0.22	- 24°	0.11	56°	0.05	90°	0.05	99°
MINA SALMAN	66.1	152°	21.8	213°	14.7	121°	6.9	195°	4.6	177°	1.3	241°
			0.33	61°	0.22	- 29°	0.10	43°	0.07	25°	0.02	89°
KHOR KANI	68.9	309°	25.3	347°	17.4	286°	6.7	347°				
			0.37	38°	0.25	- 23°	0.10	38°				
BANDAR ABBAS	100.0	298°	36.0	334°	21.9	280°	10.4	332°				
			0.36	36°	0.22	- 18°	0.10	34°				
Tidal Potential			0.47		0.19		0.12		0.04		0.03	

	DIURNAL								QUARTER DIURNAL			
	K_1		O_1		P_1		Q_1		M_4		MS_4	
FAO	43.8	315°	25.4	268°	10.6	312°	3.1	264°	6.0	258°	4.3	326°
			0.58	-47°	0.24	- 3°	0.07	- 51°			0.7	+ 68°
KHOR MUSA BAB	49.5	301°	31.7	253°	15.8	291°	4.7	240°	3.8	172°	3.0	241°
			0.64	- 48°	0.32	- 10°	0.10	- 61°			0.8	+ 69°
KHOR KANI	26.2	70°	15.8	67°	8.5	70°			2.7	182°	2.1	261°
			0.60	- 3°	0.32	0°					0.8	+ 79°
BANDAR ABBAS	33.8	64°	20.7	52°	11	62°			3.7	156°	3.0	246°
			0.61	- 12°	0.33	- 2°					0.8	+ 90°
Tidal Potential			0.71		0.33		0.14					
RAS AL-MISHAAB									4.0	16°	2.0	86°
											0.5	+ 70°
AL DOHA									4.5	166°	3.5	226°
											0.8	+ 60°

	THIRD DIURNAL					
	MK_3		MO_3		SO_3	
FAO	8.1	224°	6.3	187°	4.6	233°
KHOR MUSA BAB	2.8	159°	2.1	140°	2.5	259°

$\frac{A_{M_2} A_{S_2}}{A_{M_2}{}^2}$	$\simeq .07$

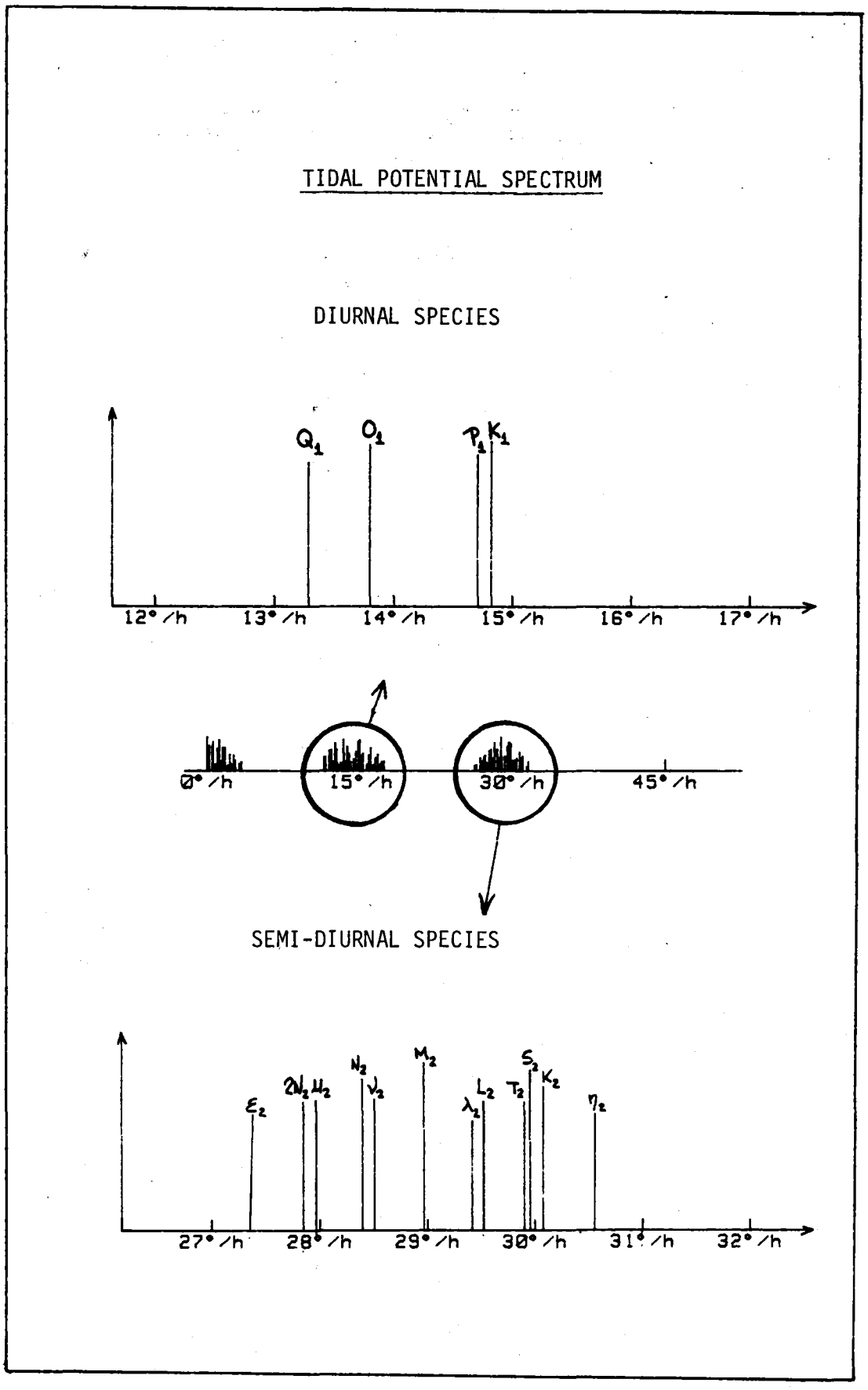

Figure 1: Tidal potential spectrum

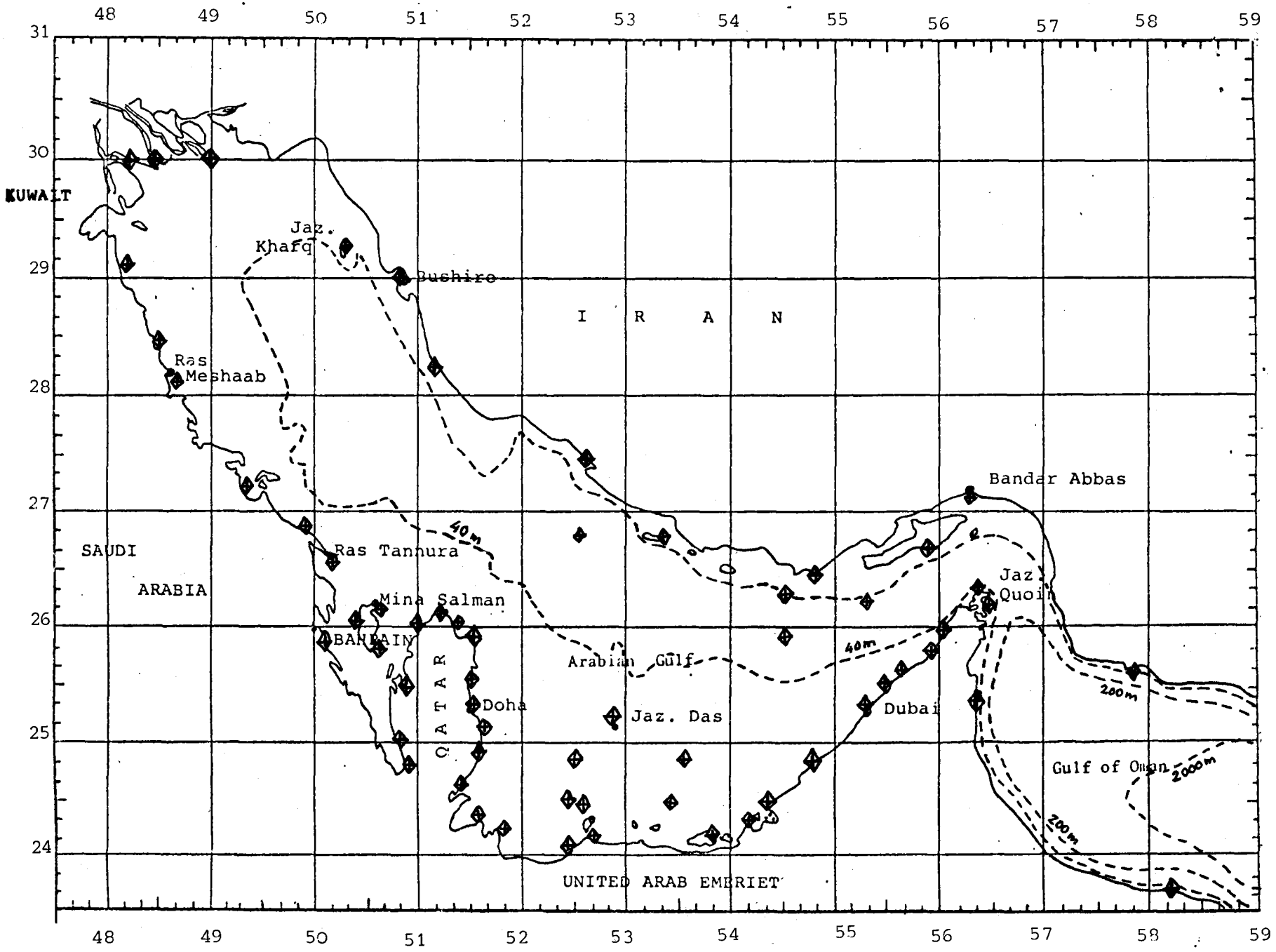

Figure 2: Location of observed tidal data.

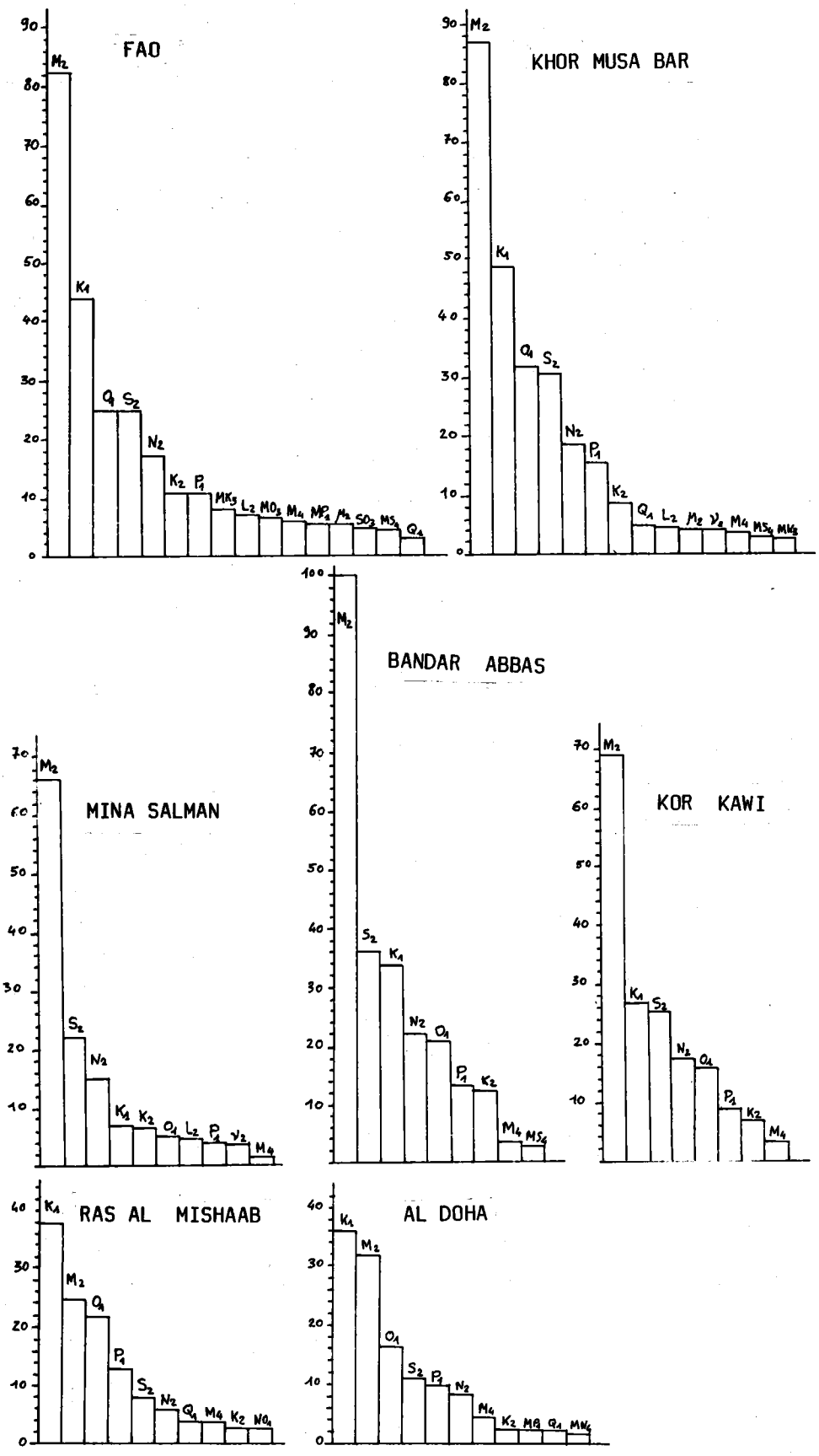

Figure 3: Observation points of maximum amplitude for the main tidal constituents

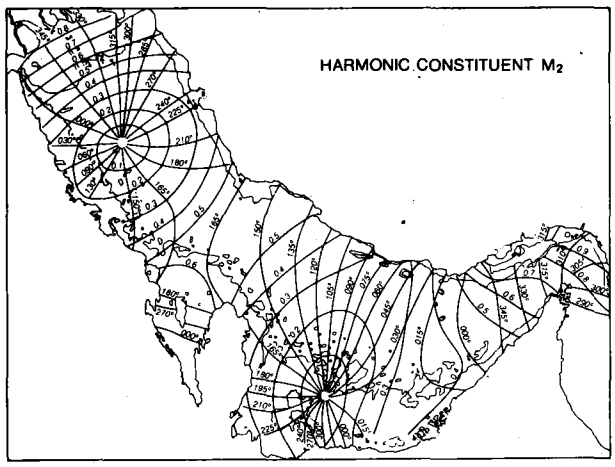

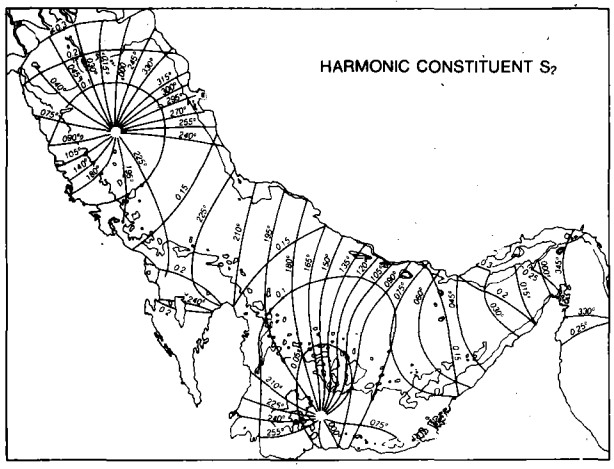

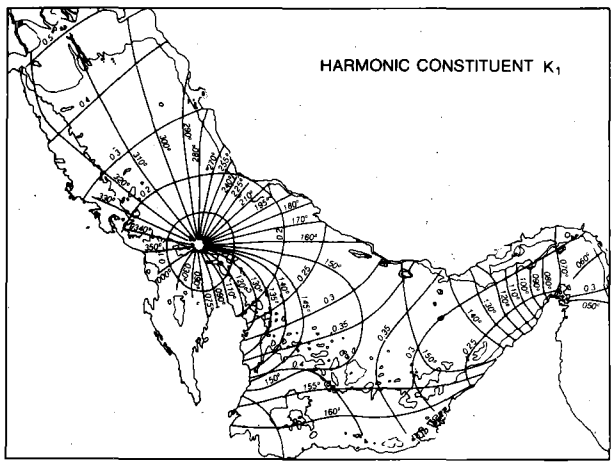

Figure 4: M_2, S_2 and K harmonic y). constituents (from British Admirality). g = time zone. 4, H in meters.

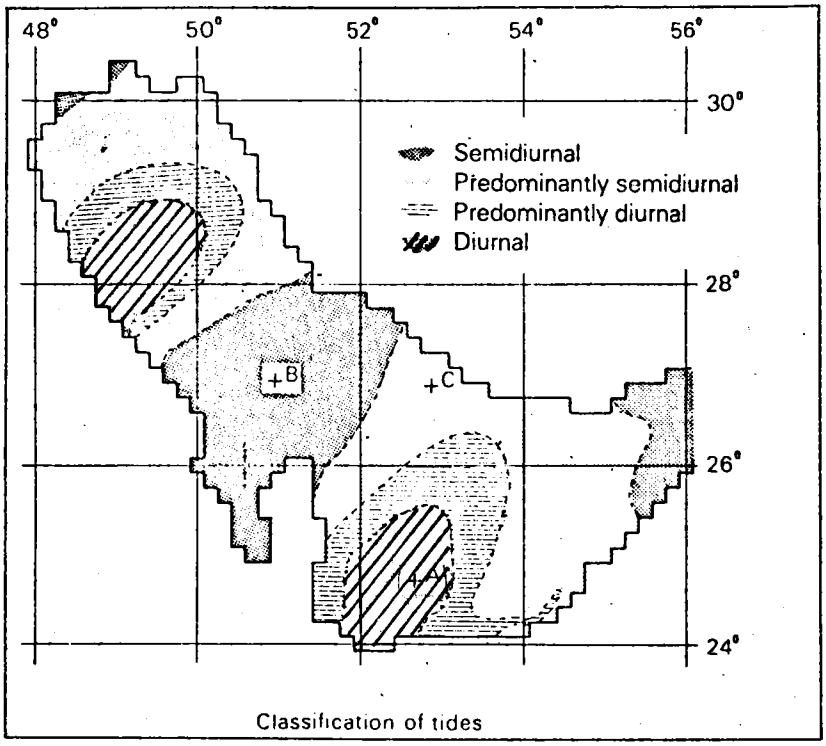

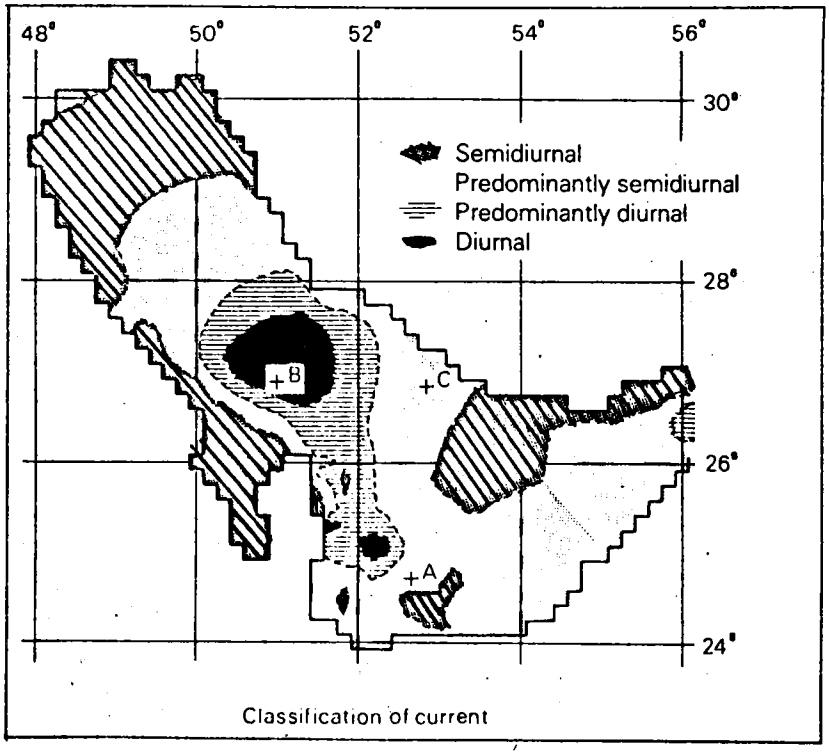

Figure 5: Classification of tidal types following Evans-Roberts (1979).

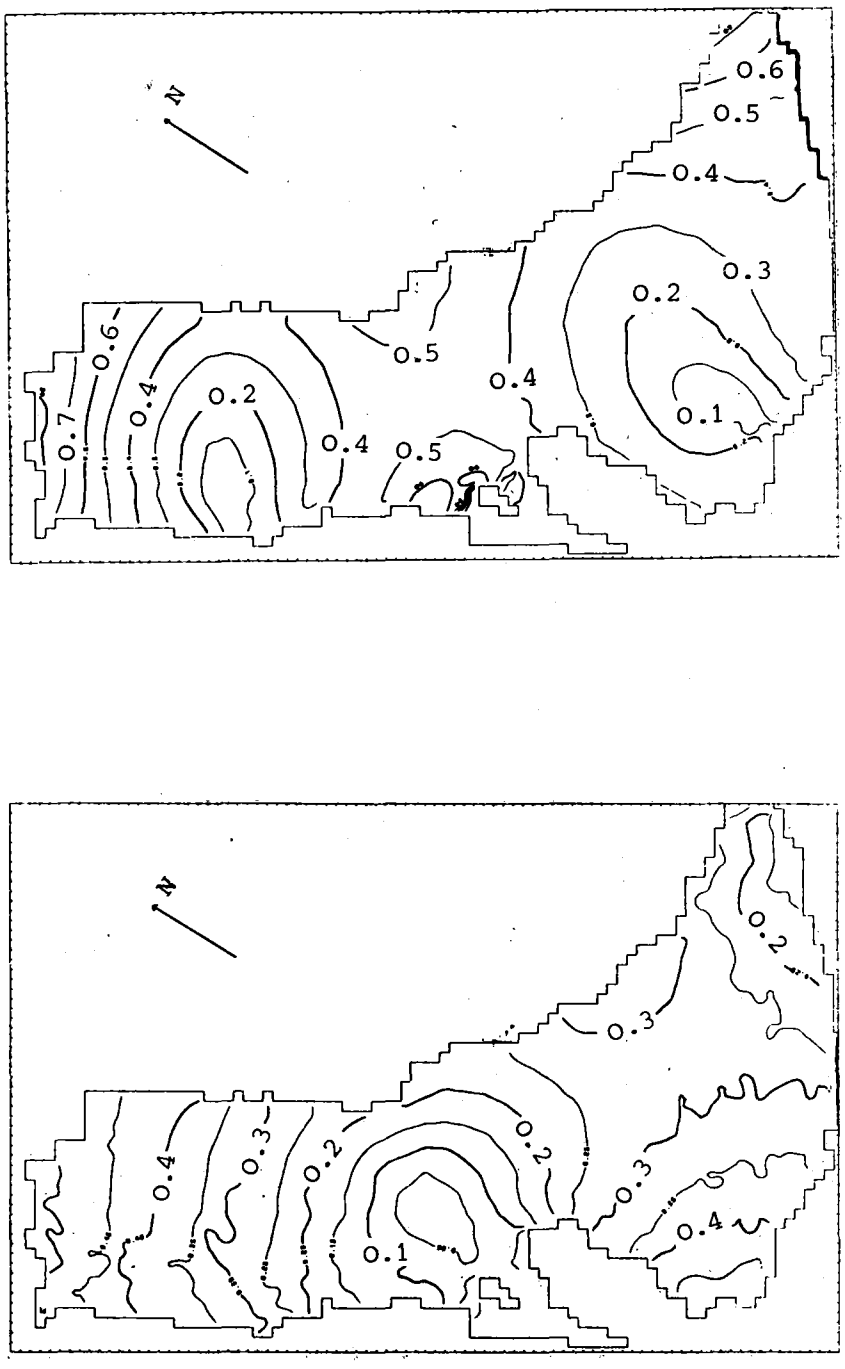

Figure 6: Amplitudes for M_2 and K_1 in meters simulated by Lardner et al (1982).

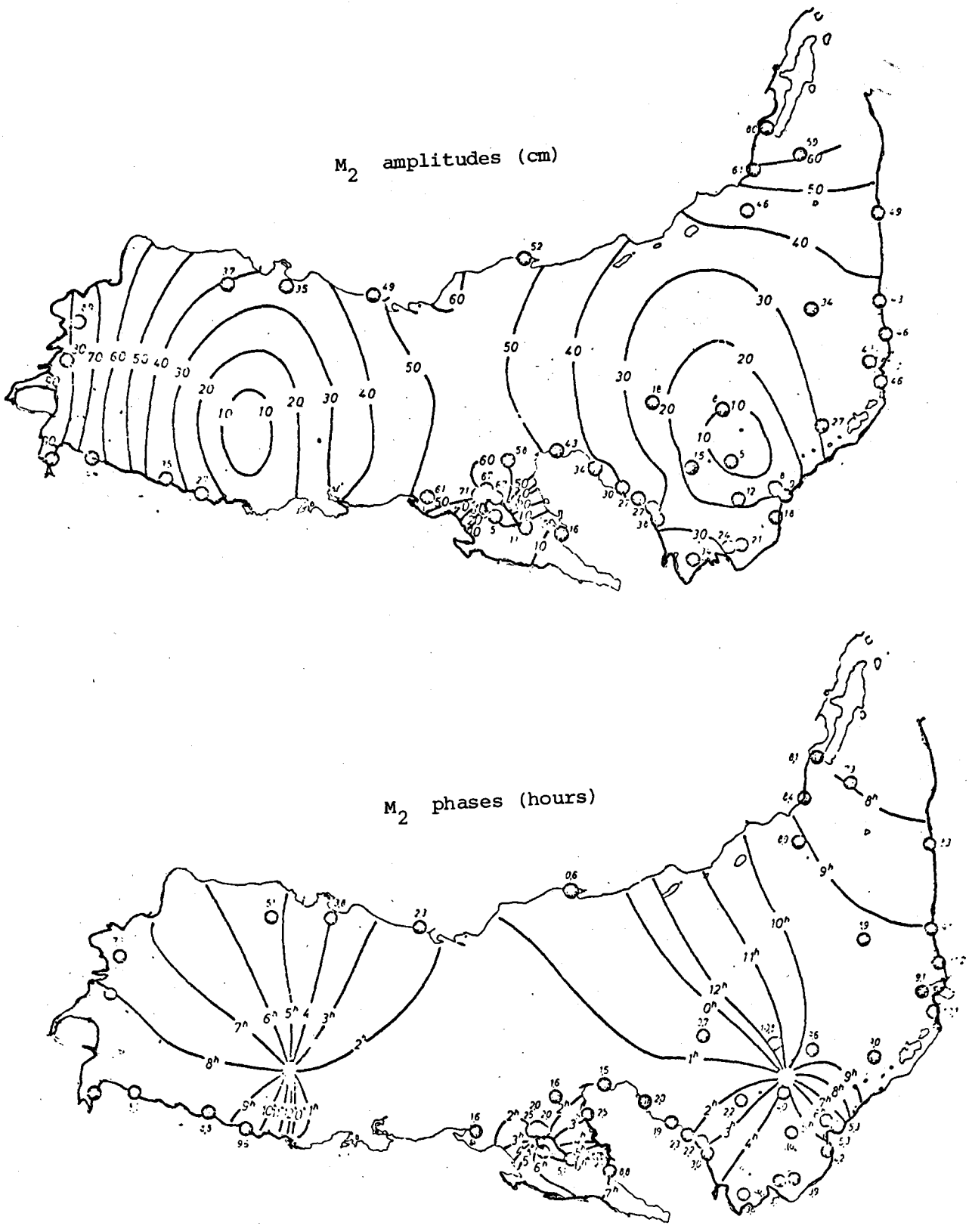

Figure 7: Amplitudes and phases for M_2 simulated by Von Trepka (1968).

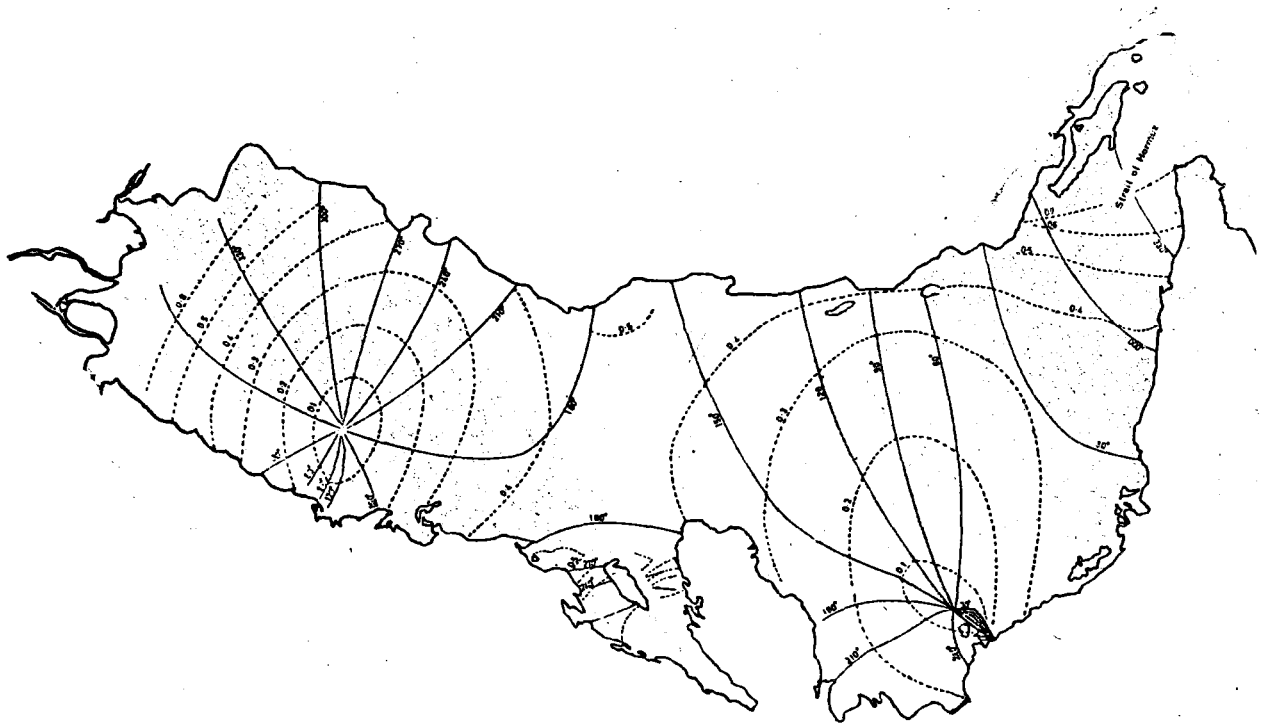

Figure 8: The M_2-tide simulated by Evan-Roberts (1979).

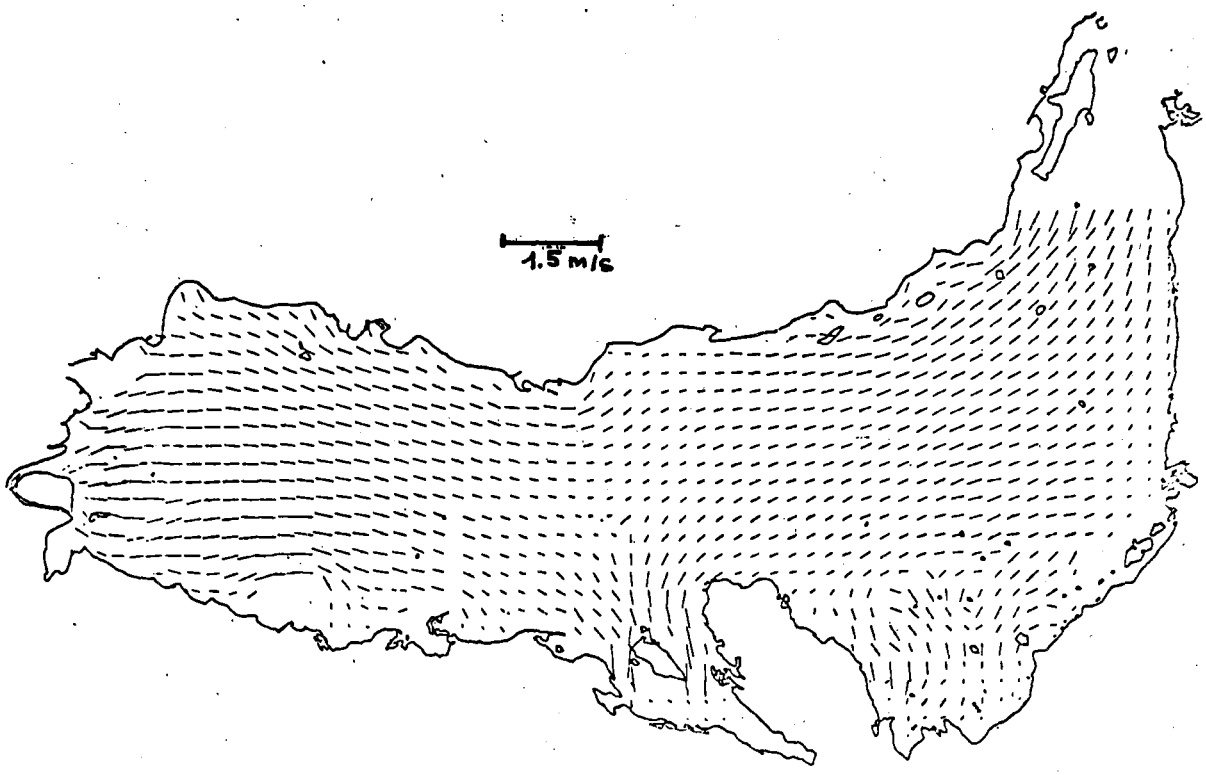

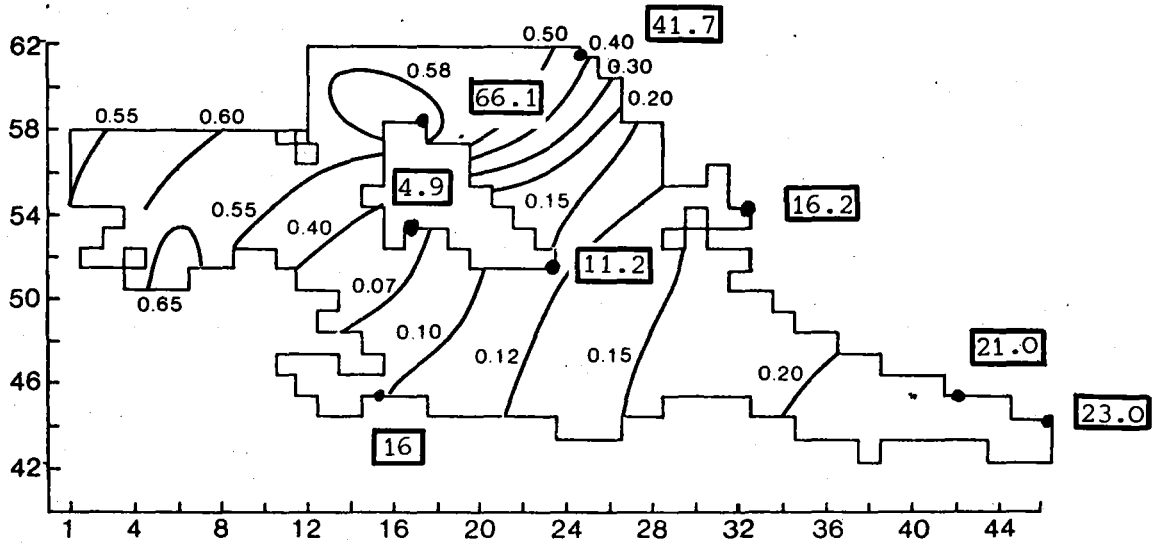

M_2 tidal amplitude (m) - 41.7 observed data (cm)

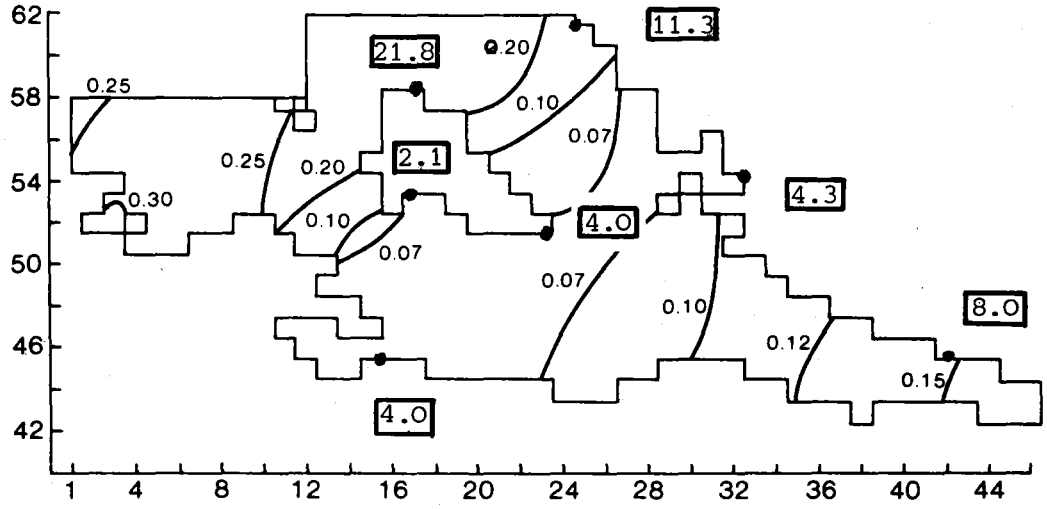

S_2 tidal amplitude (m) - 4.0 observed data (cm)

Figure 10: Example of local model. The Inner Gulf between new coast of Qatar and the south of Ras Tanura with the Island of Bahrain (from Lardner et al. (1982).

THE DEVELOPMENT OF OCEANOGRAPHY IN KUWAIT*

by

C. P. Mathews and J. W. Lee

Mariculture and Fisheries Department
Food Resources Division
Kuwait Institute for Scientific Research
Salmiya, Kuwait

---

* This paper was submitted to the Symposium but was not presented due to the absence of the authors.

INTRODUCTION

The history of the states with coasts on the Inner Gulf of the Kuwait Action Plan (KAP) Region has been deeply influenced by the geography of the area. The two most significant factors have been the desert (including the presence and absence of sources of freshwater) and the sea. The sea has been for a long time a major influence and source of wealth, both directly as a source of food and through pearl fishing, and indirectly through providing a major trade route between the Arabian countries and India and the Far East. A review of the history and economies of the area is outside the scope of this paper, but Al-Shamlan (1975, 1978) has provided an authoritative review of the history and technology of pearl industry from its inception to the present time in the Gulf as a whole, and for Kuwait in particular; and he described the historical and social aspects of this trade in some detail.

A good deal of marine research has been conducted during the last century in the Gulf, but its strategic importance, together with the interest stimulated in oceanography (in its broadcast sense, including marine biology and ecology) by the importance of the harvests of fish, shrimp and pearls, has caused greater interest in certain disciplines than in others. For instance, land-based (and, to a much lesser extent, ship-based) meteorology has been conducted on a semi-regular basis for some time; routine reports have been collected over a series of years, often with interruption, in several areas and periodic publications of data and other results have been carried out for some time. Relevant publications include these by Bannerji (1931, 1975a,b), BOAC (1960), Dallas (1881, 1889, 1891), Gaskell and Hibbert (1969), Gordon (1966), IMCOS Marine (1974a,b, 1975, 1976, 1977), a list of 29 publications from the Meteorological Office, London (Farmer and Docksey, 1983), Pedgely (1969) and Privett (1959), while Srinivasan (1978) provided some idea of the usefulness of weather satellites in the Gulf. Although data at certain times and in many areas are lacking, sufficient information is available for use by oceanographers.

Hydrographic surveys and observations have been carried out from time to time; the most interesting studies include those carried out by Barlow (1932a,b,c), Crossley and Parkinson (1967), Curries et al. (1973), Dubach (1974), Defant (1961, 1969), Emery (1956), Grasshoff (1975, 1976), Hydrographic Office (1942, 1943), IMCOS Marine (1974a,b, 1975, 1976), La Violette and Frontenac (1967), Naqvi et al. (1978), Panomareva (1975), Sonu (1979) and von Trepka (1970). Recently Brewer et al (1978) reported the results of a major oceanographic cruise covering the Iranian (eastern) portion of the Gulf and including all of the basic physical, chemical and biological parameters normally studied by oceanographers. Most of the studies conducted, however, covered fairly short periods and generally included the physical parameters of temperature and salinity. The most useful of these studies may be those of Grasshoff (1976), Dubach (1959) and La Violette and Frontenac (1967). Very few of the studies conducted include any work on currents; most of the work reported on currents is based on surface current observations carried out by vessels of opportunity.

One area in which studies have been carried out with some degree of frequency is the small area in the Northwestern Gulf into which the waters of the Shatt-al-Arab enter. Al-Saadi, Arndt and Hussein (1975), Arndt and Al-Saadi (1975), Mohammed (1965a,b), Saad (1978) and Saad and Hussein (1978) have all conducted oceanographic and hydrological surveys in this area. The results are all useful, although the studies were generally severely limited in time and space, while in some instances only simple equipment was available for conducting research.

Relatively few studies have been carried out on zooplankton. These include work by Frontier (1963a,b), Gopalkrishnan and Brinton (1969), Lenz (1973), Leveau and Szekieldi (1968), Martini and Muller (1972) and Weigman (1970, 1971). Again, thorough work has been conducted, but only covering relatively short periods. Even less work has been conducted in the ichthyoplankton; Cohen (1973), Nellen (1973a,b) and Ponomareva (1975) have done some work in this area.

Quantitative modelling of the physical oceanography of the Gulf has been carried out by Chakrabarti and Cooley (1978), and von Trepka (1968).

Work on the fisheries of the Gulf has also been conducted. Blegvad (1938) and Blegvad and Loppenthin (1944) concentrated on the taxonomy and distribution of the fish in the Gulf while Selim, in a series of papers (1966, 1968a-h), covered in some detail the traditional fishing techniques used in Kuwait, as well as the fishing grounds and the fleet operations. He also provided some of the first fisheries data for the Kuwait fishing fleet, especially for the artisanal boats. More recently, Farmer and Abdul Ghaffar (1983) have described fishing gear at present used in Kuwait. FAO, in a series of publications, has provided stock assessment advice on the state of the shrimp fisheries of the Gulf, FAO (1982) provides a bibliography. Farmer and Docksey (1983) also cover this area. More recent publications by FAO include work on demersal fish stocks (Grantham, 1980; FAO, 1981a,b).

The work reported above is all valuable and provides a very useful foundation for future work. With the notable exception of the papers by Al-Shamlan on the pearl oyster fishery of the Gulf (Al-Shamlan, 1975, 1978) and the series of papers by Salim (1966, 1968a-h), however, oceanographic work has been carried out mainly by foreigners and foreign organizations visiting the Gulf for particular purposes. For instance, significant as they were, the expeditions conducted by Blegvad and Loppenthin (1944) and Brewer et al. (1978) represent only a temporary scientific incursion into the Gulf. Useful as they were, the fisheries surveys conducted under FAO auspicies are now complete and no follow through exists. With the general exception of the meteorological work, which has been continued in Kuwait and in some other countries, most of the work has not resulted in the creation of a continuing, Gulf based capability. In Kuwait, however, a strong interest has been felt in marine studies for some time, and it is the object of this paper to describe in some detail the development of a modern oceanographic capability in Kuwait, using the "oceanographic" in the widest sense to include marine biology and ecology.

THE DEVELOPMENT OF OCEANOGRAPHY IN KUWAIT

The Kuwait Institute of Scientific Research (KISR) was established in 1967 by the State of Kuwait and the Arabian Oil Company (actually a Japanese owned company), the latter acting at the request of the Government of Kuwait. One of the first three divisions created was the Marine Biology and Fisheries Division (MBFD) later renamed the Mariculture and Fisheries Department (MFD). In 1967, MFD had a total staff of 4, and pilot projects were started initially on shrimp and fish culture. At this early stage it was not possible to undertake any major oceanographic work because of the restrictions on manpower and the lack of a research vessel.

From its inception, MFD was interested in the oceanography of the Gulf in general and of Kuwait in particular because of the effects that oceanographic and other environmental conditions can have on Kuwait's fisheries, and also on aquaculture activities. The lack of research vessels and KISR's early association with Japanese technicians and scientists led to a joint cruise conducted in 1968,

using the R/V Umitaka Maru, belonging to the Tokyo University of Fisheries; the Ueno Zoological Garden, Tokyo, and Kuwait University also shared the cruise (Khuronuma, 1974a). Areas of research covered during the cruise included fishing gear research (Kuronuma, 1974b), benthos dredging and benthic community structure (Kuronuma, 1974c), studies of the nekton (Kuronuma and Hiroshi, 1974), thermal and salinity structure of the Gulf (Kihara, 1974), bottom sediments (Oshite, 1974a) and of suspended matter (Oshite, 1974b), studies on the seagulls during the cruise (Nakamura, 1974) and zooplankton studies (Yamazu, 1974). Figure 1 shows the cruise track and the stations covered. The objective of the cruise was to obtain a qualitative and quantitative idea of the main differences in the areas studied in the different parts of the Gulf, as a background for focusing future pure and applied oceanographic and biological work in Kuwait, especially at KISR. The cruise of the Umitaka-Maru was probably the first Gulf-wide cruise including Arabian personnel, and had a lasting effect on the development of Marine Science in Kuwait.

A book on the fishes of Kuwait was published by Kuronuma and Abe (1972), who updated the work of Blegvad (1938) and Blegvad and Loppenthin (1944) with special reference to the fishes taken in Kuwait, particularly the commercial fishes. The research was conducted in Kuwait and in Japan. From 1972 onwards, the basic routine identification of fishes in Kuwait became possible. Although many taxonomic problems still exist (especially with respect to elesmobranch fishes), the necessary foundation for fisheries research was established. This fact made possible the development of subsequent work on Kuwait's fisheries.

Work was conducted at KISR from 1972 onwards on various applied projects, including experiments on the growth feeding and mortality of Penaeus semisulcatus with a view to restocking the Kuwaiti population and to increasing landings and later on, from 1980 onwards, with a view to culture to market size for direct sales. Studies on other decapoda were also conducted and, from 1975 onwards, on several species of fish. An appraisal of the culture activities conducted at MFD until 1980 was published by Mathews, Farmer and Clunan (1983). They document the very large amount of biological work, including early fisheries work, which provided a strong and continuous impetus for oceanographic work and for obtaining a general and detailed understanding of Kuwait's marine environment, so as to provide knowledge of the parameters which affect fish and shrimp being held in captivity, especially a knowledge of those parameters which are crucial in closing the life cycles of organisms being cultured, as well as in obtaining an understanding of the main parameters which affect the marine populations, particularly those of commercial importance. Farmer and Docksey (1983) provide a complete bibliography of the Gulf, covering all references and material in these and related subjects.

From 1974 onwards, it became clear that the Kuwait shrimp fishery was in a difficult situation. While MFD assisted FAO in collecting data for some early stock assessment studies, it was felt necessary to create a Kuwaiti capability in this area and projects for managing both the shrimp and fin fisheries of Kuwait started in 1977 and 1978 respectively.

The publication in 1974 of the results of the R/V Umitaka Maru's cruise in 1968, combined with the early work of Enomoto (1971), Al-Attar and Ikenoue (1974) and Ul-Hassan (1976) on the oceanography of the shrimp nursery grounds created a clear demand for further oceanographic work. Al-Attar & Ikenoue (1974), for instance, suggested that changes in bottom temperature on spawning grounds were crucial in triggering the spawning of sexually ripe Penaeus semisulccatus, while Ul-Hassan (1976) reported vertical temperature gradients of up to 6°C over the Qita Al-Arfyan fishing ground, one of the most important areas for Penaeus semisulcatus.

In 1975, MFD acquired a major capability: R/V Asmak IV (later renamed Oloum I). A description of this vessel is provided by Anon (1980); it has been used ever since its acquisition. It was originally used mainly as a source of broodstock for the shrimp and fish culture projects, and from 1978 onwards it became a major tool for oceanographic and fisheries research. By 1980, it was carrying out 130-150 sea days of research per year.

In 1978, the Fisheries Management Project was started with, as one major task, the objective of studying the oceanography of Kuwaiti waters; these studies were, however, aimed at supporting all fisheries, including aquaculture research. The strategy established was to conduct monthly or bimonthly cruises and to determine the structure of Kuwait waters, so that fisheries data on the species composition, distribution and catch rates of the main species of fish and shrimp could be correlated with such oceanographic variables as temperature, salinity and dissolved oxygen. Initially, samples were taken only at the surface and bottom. Cruises were started on a regular basis in 1978 and Mathews, Samuel and Lee (1983) presented a data report covering the years 1978-1980, while Mathews, Samuel and Abdul-Elah (1979, 1983) presented preliminary results on the same subject. There is a suggestion of the influence of freshwater inflow from the Shatt-Al-Arab and of low oxygen concentrations in Kuwait Bay near the southern coastline; however, more data points need to be collected in both cases, and during these studies, samples were collected only at the surface or on the bottom. Figure 2 shows the Kuwait National Sampling Grid which was established so as to facilitate co-ordinated fisheries and oceanographic research during these years.

In 1981 the quality of the oceanographic data was upgraded by the introduction of sophisticated electronic measuring equipment, and quality was controlled through the establishment of a small oceanographic calibration capability, so that all physical measurements were taken in accordance with internationally acceptable standards. Salinometers, thermometers, oxygen meters and electronic probes have been calibrated at MFD for all oceanographic research since 1980. At this time two manuals were also prepared at MFD for use in Kuwait (ROPME, 1983) for the instruction of junior scientists in basic oceanographic techniques in Kuwait and the Gulf, respectively.

In 1980, oceanographic cruises were upgraded to include profiles at each station and the following variables were measured routinely: temperature, salinity, dissolved oxygen, water colour, Secchi disk reading and various meteorological parameters. In 1983, turbidity was added to the list of parameters measured routinely. In 1980, the Kuwait national grid was also extended to include stations in areas of crucial interest, such as Kuwait Bay (a major spawning and nursery area for this species) and Qita-Al-Arfyan, a major fishing ground for this species. Results of the monthly cruises have been published by Lee (1983a). Figure 3 shows that air temperature increased from about 22°C in March to about 34°C in July and by October had declined to about 32°C; surface and bottom temperatures followed closely similar patterns. Gaps in the record arise from the unavailability of sea time during certain periods. In spite of this, the general temperature changes may be determined. For instance, increasing sunshine hours and temperature provide clear vertical stratification in April and May; stratification in June was much less marked, and was absent in September and even in October when cooling had already become marked. Lee (1983a) provides a fuller interpretation of these and other related phenomena.

During 1980, a programme for releasing surface drogues and bottom drifters was undertaken (Lee and Samuel, 1982, Lee, 1983b). A total of 2,800 drifters and drogues were released from February to April 1981. Figures 4 and 5 summarize some of the results obtained; surface currents show a generally anti-clockwise net movement with recoveries as far south as Ras-Al-Tanura (Saudi Arabia), while bottom

currents show at least some anti-clockwise movements. The low returns from the bottom drifters, however, suggest this needs confirmation. Similar work in Kuwait Bay shows that net surface currents are clockwise while bottom currents probably occur in a clockwise direction. The current movements in the vicinity of Ras Salmiyah are clearly complex and further work is required. All of these studies refer to releases effected from February to April 1980, while recoveries occur at a maximum of 230 days from release. Similar studies are planned for other times of the year, when current structures and circulation patterns may be very different.

During 1981, a very detailed survey of the physical and chemical oceanography of Kuwait Bay was carried out (Anderlini, Jacob and Lee, 1982). This work provided a detailed monthly coverage of the Bay and one of the most detailed carried out anywhere in the Gulf.

During 1980 and 1981, MFD also carried out work on zooplankton and ichthyoplankton. Al-Matar and Houde (1984) studied the ichthyoplankton distribution of Kuwait waters during 10 cruises and at 19 stations, from September 1979 to August 1980. Results included the distribution of larvae and eggs of 31 families of ichthyoplankton, estimates of the biomass and yield of pelagic species of fish from Kuwait waters, and a study of the correlation between planktonic fish, temperature and salinity. Full results have yet to be published, but preliminary estimates of the yield of small pelagic species show that over 70,000 tons of these may be available annually from Kuwait waters. This study tends to confirm the potential importance of small pelagic fish which was suggested by previous work in the Gulf (FAO, 1981b).

A series of cruises was also carried out by Solobiof et al. (1980) covering Gulf waters. Although the data were gathered sporadically over several years, they covered a total of over 80 stations and provided a broad picture of the general oceanography of the Gulf. These surveys were carried out by the Ministry of Public Works R/V Sabah. Simultaneously with the ichthyoplankton work, Michel et al. (1982) and Michel et al. (1983) studied the zooplankton of the area. Their work showed that Kuwaiti waters were rich in zooplankton, and Michel and Shoushani (1983) noted that the results suggested the possibility of using Chaetognatha as indicators of different water masses in Kuwait waters, while the data of Michel et al. (1982) suggest that this may be feasible for the Gulf as a whole.

From 12 February to 3 March, 1981 a cruise was held which provided a complete coverage of the western and southern portions of the Gulf. For the first time, a total of 36 stations in these areas were covered, in addition to the Kuwaiti stations. During this cruise, detailed observations of salinity, temperature and dissolved oxygen were taken in addition to zooplankton and ichthyoplankton samples. Measurements of several nutrients, especially of phosphate, were also taken. Mathews and Samuel (1982) presented some preliminary results, while Samuel and Mathews (1983) have provided a full report of this work.

During 1982 and 1983, there has been an expansion of KISR's oceanographic services with several contracts from governmental agencies and the private sector in Kuwait containing major elements of oceanography (including marine biology and ecology). This has allowed KISR expertise in physical, chemical and biological oceanography to be made available to the scientific community in Kuwait as a whole, as well as continuing to provide the essential supporting data for fisheries and aquaculture work, which was the programme's original objective.

In addition, work has now been started on related projects, such as studies of Kuwait's coral reefs and pearl oysters. The need for these studies was perceived because of new and significant environmental concerns. Some of Kuwait's reefs appear to be in serious and deteriorating condition (Downing 1981a,b).

The aquisition of so much field data suggested the need for advanced modelling. Hunter (1980) developed a tidal model for Kuwait waters and extended this to include vertical and horizontal stratification (1981). Lee et al. (1985) has started a series of monthly 24-hour cycle observations at three stations in Kuwait waters. Kadib (1979), Kadib and Al-Madani (1980) and Kadib, Safaie and Esen (1980a,b) described work near the Shuaiba industrial complex in Kuwait using stationary data-collecting towers; their work was aimed at predicting the incidence of thermal and other pollution associated with the power stations in this area. Although this work was primarily coastal in nature, a significant monitoring capability was established.

DEVELOPMENT OF A MARINE POLLUTION CAPABILITY IN KUWAIT

In 1976, KISR started work on marine pollution and several projects have been successfully completed. Although such work lies outside the area covered by this paper, it is interesting to note that capabilities for tackling work in the areas of sewage, heavy metal and, more recently, hydrocarbon pollution exist in Kuwait. These capabilities have been developing hand in hand with growth of the oceanography programme in Kuwait.

FUTURE WORK

The development of Kuwait's oceanography capabilities from the first day when MFD had a total of 4 people, through the initial phases of seagoing work when a foreign vessel (R/V Umitaka Maru) was used, to the aquisition of MFD's first major seagoing capability and the subsequent expansion into a fully developed and sophisticated oceanography programme has been described. In 1982, the Kuwait Institute for Scientific Research commissioned the construction of R/V Bahath, a 41m stern trawler fitted out as a fisheries oceanography research vessel. This ship, due for delivery in January 1984, is designed for cruises in the Gulf and the sea of Oman, as well as in Kuwait waters. It is designed to cover all of Kuwait's oceanographic and fisheries work as well as to be capable of covering a considerable amount of pollution oriented work during the next one to two decades. It is hoped that R/V Bahath will allow the development of joint work with other Gulf countries. Synoptic work on the Gulf is particularly necessary, as it has never been carried out in any detail before. Further work on net currents is necessary and is planned for 1984. An essential component of future work will also consist of contracts from governmental agencies and the private sector in Kuwait and, if possible, from other countries.

The development of oceanography in Kuwait has therefore been remarkably rapid from its small beginings in around 1970, to the small but very significant capability of international quality in 1983. The change from an essentially foreign inspired and equipped presence to the vigorous capability now in existence represents a significant achievement. This background for development of oceanography in Kuwait has been special because it has always followed the needs of aquaculture and fisheries management work, and only very recently has it branched out into a full strength oceanographic capability. This background has ensured, however, the relevance of oceanography to Kuwait. It has been, and is still, an essentially applied discipline, and work is carried out entirely because of the applied needs felt at KISR and in Kuwait as a whole.

REFERENCE

Al-Attar, M.H. and Ikenoue, H. (1984) Spawning season of shrimp Penaeus semisulcatus in the sea along the coast of Kuwait. Kuwait: Kuwait Institute for Scientific Research, 16 pp.

Al-Matar and Houde (1984) Preliminary study of pelagic fish stocks in Kuwait waters with special reference to the small pelagic fish and their commercial potential. In: Proceedings of the Third Shrimp and Fin Fisheries Management Workshop, (ed. C.P. Mathews), Kuwait Institute for Scientific Research, p 217-261.

Al-Saadi, H.A. (1975) Accumulation of potassium and sodium in aquatic plants of Shatt Al-Arab and adjacent areas. The Arab Gulf, 3:198-190.

Al-Saadi, H.A. and Arndt. E.A. (1973) Some investigations about the hydrographical situation in the lower reaches of Shatt Al-Arab and the Arabian Gulf. Wissenschaftliche Zeitschrift der Universität Rostock, Mathematisch-Naturwissenschaftliche, Reihe, 22(10):1169-1174.

Al-Saadi, H.A., E.A. Arndt and N.A. Hussain (1975) A preliminary report on the basic hydrographical data in the Shatt Al-Arab and the Arabian Gulf. Wissenschaftliche Zeitschrift der Universität Rostock, Mathematisch-Naturwissenschaftliche, Reihe, 24(6):797-802.

Al-Shamlan, S.M. (1975) (Pearl Diving History in Kuwait and Arabian Gulf, Part 1. Pearl Diving History in Kuwait) Kuwait: Kuwait Government Press, 480 pp. (in arabic)

Al-Shamlan, S.M. (1978) (Pearl Diving History in Kuwait and Arabian Gulf, Part 2. Pearl Diving History in Kuwait) Kuwait: Kuwait Government Press, 568 pp. (in Arabic)

Anderlini, V., P.C. Jacob and J.W. Lee (1982) Atlas of physical and chemical oceanographic characteristics of Kuwait Bay. Kuwait Institute for Scientific Research, 474 pp.

Arndt, E.A. and H.A. Al-Saadi (1975) Some hydrographical characteristics of the Shatt Al-Arab and adjacent areas. Wissenschaftliche Zeitschrift der Universität Rostock, Mathematisch-Naturwissenschaftliche, Reihe, 24(6):789-796.

Anonymous (1980) Research Activities, Mariculture and Fisheries Department, Kuwait Institute for Scientific Research, 16 pp.

Banerji, B.N. (1931) Meteorology of the Persian Gulf and Mekran. Calcutta: India, Meteorological Department, 65 pp.

Banerji, B.N. (1975) A report on the building up of a statistical system for the of marine fisheries statistics in the United Arab Emirates. Food and Agriculture Organization of the United Nations, report, IOP/TECH/75/4, 21 pp.

Banerji, S.K. (1975) Fishery statistics needed for development planning. FAO Fisheries Circular, (630):9 pp.

Barlow, E.W. (1932) Currents in the Persian Gulf, northern portion of Arabian Sea, Bay of Bengal, etc. Part 1. Summary of previous knowledge. Marine Observer, 9(99):58-60.

Barlow, E.W. (1932) Currents in the Persian Gulf, northern portion of Arabian Sea, Bay of Bengal, etc. Part 2. The S.W. monsoon period. Marine Observer, 9(105): 169-171.

Barlow, E.W. (1932) Currents in the Persian Gulf, northern portion of Arabian Sea, Bay of Bengal, etc. Part 3. The N.E. monsoon period and general summary. Marine Observer, 9(108):223-227.

Blegvad, H. (1938) Rapport sur les recherches de pêche effectuées au Golfe Persique pendant l'hiver 1936-1937. Iran: Ministry of Finance.

Blegvad, H. and B. Loppenthin (1944) Fishes of the Iranian Gulf. Danish Scientific Investigations in Iran, 3:247 pp.

BOAC Meteorological Section (1960) Temperature data - aerodromes in Persian Gulf. London:British Overseas Airways Corporation, Meteorological Section.

Brewer, P.G., Fleer A.P., Kadar, S., Shafer, D.K., and Smith (1978) Chemical oceanographic data from the Persian Gulf and Gulf of Oman. Woods Hole Oceanographic Institution, Massachusetts, technical report WHO 1-78-37, A, 107 pp.

Chakrabarti, S.K. and Cooley, R.P. (1978) Further correlation of Scott spectra with ocean wave data. American Society of Civil Engineers, Waterway, Port, Coastal and Ocean Division, Journal, 104(WW4):443-446.

Cohen, D.M. (1973) Kinds and abundance of fish larvae in the Arabian Gulf and Persian Gulf. Ecological Studies, (3):415-430.

Crossley, A.F. and I.N. Parkinson (1967) Distribution of jet streams at 200 mb in the Middle East. Journal of the Institute of Navigation, 20:397-404.

Curries, R.I., Fisher, A.E. and Hargreaves, P.M. (1973) Arabian Sea upwelling. In: The Biology of the Indian Ocean, (ed. B. Zeitzshel), p. 37-52, Springer Verlag, NY

Dallas, W.L. (1887) Memoir on the Winds and Monsoons of the Arabain Sea and North Indian Ocean. Calcutta, 45 pp.

Dallas, W.L. (1891) An inquiry into the nature and course of storms in the Arabian Sea and a catalogue and brief history of all recorded cyclones in that sea form 1648 to 1889. Indian Meteorological Department, Cyclone Memoirs, 4:301-424.

Dallas, W.L. (1899) Investigation into the mean temperature, humidity and vapour tension conditions of the Arabian Sea and Persian Gulf. Indian Meteoroligical Memoirs, 6:9-88.

Defant, A. (1961) Tides in the Mediterranean and adjacent seas, observations and discussions. In: Phys. Oceano. Vol 2. p. 407-417, Pergamon Press, London, U.K.

Defant, A. (1969) Aerologische Daten gewonnen dürch Radiosondenanefstiege und Radar-windmessungen während der Indischen Ozean Expedition 1964/1965 des Forschungs-schiffes 'Meteor'. 'Meteor' Forschungsergebnisse Series B (4):1-120.

Downing, N. (1981) Evaluation of potential for expanding the sport fishing industry through the establishment of artificial reefs. Kuwait Institute for Scientific Research, 19 pp. (restricted).

Downing, N. (1981) The fourth International Coral Reef Symposium. Kuwait Institute for Scientific Research, 21 pp. (restricted).

Dubach, H.W. (1964) A summary of temperature-salinity characteristics of the Persian Gulf. National Oceanographic Data Centre, report. NODC-G-4, 223 pp.

Dubach, H.W. and Wehe, T.J. (1959) Descriptive Oceanography of Kuwait Harbor. U.S. Naval Hydrographic Office, Technical Report, (55):43 pp.

El-Zahr, C. and Teng, S.K. (1982) A Preliminary Study of the effects of aeration rates on the survival and growth of hamoor larvae. Kuwait Institute for Scientific Research, Annual Report, (1980):78-80.

Emery, K.O. (1956) Sediments and water of Persian Gulf. Bulletin of the American Association of Petroleum Geologists, 40(1):2354-2383.

Enomoto, Y. (1971) Oceanographic survey and biological study of shrimp in the waters adjacent to the eastern coasts of the State of Kuwait. Bulletin of the Tokai Regional Fisheries Research Laboratory, (66):1-74.

FAO (1980) Environmental conditions in the Gulf and the Gulf of Oman and their influence on the propogation of sound. Food and Agriculture Organization of the United Nations report, FI:DP/RAB/71/278/12, 62 pp.

FAO (1981a) A report on the demersal resources of the Gulf and Gulf of Oman. Food and Agriculture Organization of the United Nations report, FI:DP/RAB/71/278/10, 122 pp.

FAO (1981b) Environmental conditions in the Gulf and Gulf of Oman and their influence on the propogation of sound. Food and Agriculture organization of the United Nations report, FI:DP/RAB/71/278/12, 62 pp.

FAO (1981c) Pelagic resources of the Gulf and Gulf of Oman. Food and Agriculture Organization of the United Nations report, FI:DP/RAB/71/278/11. 144 pp.

FAO (1982) Assessment of the shrimp stocks of the west coat of the Gulf between Iran and the Arabian peninsula. Food and Agriculture Organization of the United Nations report, FI/DP/RAB/80/015, 163 pp.

Farmer, A.S.D. and Abdul-Ghaffar, A.R. (1983) Traditional fishing. In: Kuwait's Natural History, An introduction (ed. David Clayton). Kuwait Oil Company, Kuwait, 274-293 pp.

Farmer, A.S.D. and Docksey, J.E. (1983) A bibliography of the marine and maritime environment of the Arabian Gulf and Gulf of Oman. Kuwait Bulletin of Marine Science, (4):121 pp.

Gaskell, T.F. and Hibbert, D. (1969) Monitoring the mideast weather. Ocean Industry 4(8):59-61.

Gopalakrishnan, K. and Brinton, E. (1969) Preliminary observations on the distribution of Euphausiacea from the International Indian Ocean Expedition. In: Proceedings of the symposium on Indian Ocean, New Delhi, 2-4 March 1968. Bulletin of the National Institute of Sciences of India, (38) 2:594-611.

Gordon, A.H. (1966) The mean wind structure over Bahrain and Aden in 1962. Journal of the Atmosphere Sciences, 23:712-719.

Grantham, G.J. (1980) The prospects for by-catch utilization in the Gulf area. Food and Agriculture Organization of United Nations report, FI:DP/RAB/71/278/14, 43 pp.

Grasshoff, K. (1975) Brief outline of hydrographical and hydrochemical situation in Arabian Gulf. In: Report on the consultation Meeting on Marine Science Research for the Gulf states. Paris: United Nations Educational, Scientific and Cultural Organization.

Grasshoff, K. (1976) Review of hydrographical and productivity conditions in the Gulf region. In: Marine Sciences in the Gulf Area, p. 39-62. UNESCO Technical Papers in Marine Science, (26):66 pp.

Hunter, J.R. (1980) An appraisal of the physical oceanography of Kuwaiti waters. Existing knowledge and future research needs. Kuwait: Kuwait Institute for Scientific Research, 40 pp.

Hunter, J.R. (1981) A stratification/mixing model of Kuwait waters. Kuwait: Kuwait Institute for Scientific Research, Technical Report, 17 pp.

Hydrographic Office (1942) Persian Gulf pilot, comprising the Persian Gulf and its approaches from Ras Al-Hadd in the south-west to Cape Monze in the east. London: Hydrographer of the Navy.

Hydrographic Office (1943) Strategical aerological survey. Coast of the Persian Gulf and Gulf of Oman (Kuwait, Bahrain, Muscat). Washington: U.S. Navy Dept., Bureau of Aeronautics, (22).

IMCOS Marine (1974a) Handbook of the weather in the Gulf between Iran and the Iranian Peninsula. Bibliography. London: International Meteorological and Oceanographic Services, 103 pp.

IMCOS Marine (1974b) Handbook of the weather in the Gulf between Iran and the Iranian Peninsula. Surface wind data. London: International Metoerological and Oceanographic Services, 103 pp.

IMCOS Marine (1975) Gulf tide anomalies: 17-19 January 1973. IMCOS Technical Note, (1):6 pp.

IMCOS Marine (1976) A handbook of the weather in the Gulf between Iran and the Iranian Penisula. General climate data. London: International Meteorological and Oceanographic Services, 101 pp.

IMCOS Marine (1977) Water level oscillations Das Harbour. IMCOS Technical Note, (2):8 pp.

Kadib, L.A. (1979) Oceanographic monitoring program in the Shuaiba offshore area. Kuwait: Kuwait Institute for Scientific Research, 125 pp.

Kadib, L. and Al-Madani, N. (1980) Forecast of design waves for the coastline of Kuwait. Kuwait Institute for Scientific Research, Annual Report (1979):98-105.

Kadib, L.A., Safaie, B. and Esen, I. (1980) A proposal for the construction of a hydraulic laboratory. Kuwait: Kuwait Institute for Scientific Research, 250 pp.

Kadib, L.A., Safaie, B. and Esen, I. (1980) Shuaiba offshore area. Kuwait: Kuwait Institute for Scientific Research.

Kihara, K. (1974) Bathythermography and the stratification of temperature and salinity in the Arabian Gulf, December 1968. Transactions of the Tokyo University of Fisheries, (1):18-24.

Kuronuma, K. (ed.) (1974a) Arabian Gulf fishery-oceanography survey by the Umitaka-Maru, training-research vessel, Tokyo Univ. of Fisheries in collaboration with Kuwait Institute for Scientific Research, 1968. Transactions of the Tokyo Univ. of Fisheries, (1):118 pp. (Individual sections cited separately)

Kuronuma, K. (1974b) Introduction: organization of the survey: itinerary of the survey: results of the survey. Transactions of the Tokyo University of fisheries, (1):1-12.

Kuronuma, K. (1974c) Dredging bottom deposits and benthos. Transactions of the Tokyo University of Fisheries, (1):52-54.

Kuronuma, K. and Abe, Y. (1972) Fishes of Kuwait. Kuwait: Kuwait Institute for Scientific Research, 123 pp.

Kuronuma, K, and Hiroshi, I. (1974) Nekton collection by larva net. Transactions of the Tokyo University of Fisheries, 1:67-71.

La Violette, P.E. and Frontenac, T.C. (1967) Temperature, salinity and density of the world's seas: Arabian Sea, Persian Gulf and Red Sea. U.S. Naval Oceanographic Office, informal report IR 67-49,105 pp.

Lee, J.W. (1983) Oceanographic characteristics of Kuwait waters in 1981. Kuwait Institute for Scientific Research, Annual Research Report (1982):100-104.

Lee, J.W. (1983) Water movements in coastal waters of Kuwait, 1981-1982. Kuwait Institute for Scientific Research, Annual Research Report, (1982):104-107.

Lee, J.W. and Samuel, M. (1982) Water movements in Kuwait coastal waters. Kuwait Institute for Scientific Research, Annual Research Report, (1981):113-116.

Lee, J.W., Arar, M.I., Shalash, I. and Saif, I. (1985) Variations in oceanographic parameters at two diurnal stations in Kuwait waters (March 1983-March 1984). KISR, 174A, Kuwait Institute for Scientific Research.

Lenz, J. (1973) Zooplankton biomass and its relation to particulate matter in the upper 200m of the Arabian Sea during the NE monsoon. In: The Biology of the Indian Ocean (ed. B. Zeitzschel and S.A. Gerlach), p. 239-241. Chapman and Hall, London. Springer-Verlag, Berlin.

Leveau, M. and Szekielda, K.-H. (1968) Situation hydrologique et distribution de zooplankton dans le N.W. de la Mer d'Arabie. Sarsia, 34:285-298.

Martini, E. and Muller, C. (1972) Nannoplankton aus dem nordlichen Arabischen Meer. 'Meteor' Forschungsergebnisse, Series C, (10):63-74.

Mathews, C.P., Farmer, A.S.D. and Clunan, D. (1980) Research Activities at the Mariculture and Fisheries Department of Kuwait Institute for Scientific Ressearch. Kuwait Institute for Scientific Research, 47 pp.

Mathews, C.P., Samuel H., and Abdul-Ellah, K. (1979) Fisheries Management studies in Kuwait. Kuwait Institute for Scientific Research, Annual Research Report, (1979):48-57.

Mathews, C.P., Samuel, M. and Abdul-Ellah, K. (1983) Oceanography and fisheries of the northern Arabian Gulf with special reference to Kuwiat waters. In: Proceedings of the Symposium on the Coastal and Marine Environment of the Red Sea, Gulf of Aden and Tropical Western Indian Ocean. Vol. II. 9-14 January 1980 in Khartoum. Jeddah, Saudi Arabia: The Red Sea and Gulf of Aden, Environmental Programme (ALESCO), p. 309-325.

Michel, H.B., Behbehani, M., Herring, D., Arar, M., Shoushani, M. and Brakoniecki, T. (1983) Zooplankton diversity, distribution and abundance. In: Kuwait waters: final report. Kuwiat Institute for Scientific Research, 154 pp.

Michel, H.B., Behbehani, M., Herring. D., Brakoniecki, T., Arar, M. and Shoushani, M. (1982) Diversity, distribution and biomass of zooplankton in the western Arabian Gulf. Kuwait Institute for Scientific Research, Annual Research Report, (1980):92-94.

Mohammad, M.-B.M. (1965) A faunal study of the Cladocera of Iraq. Bulletin of the Biological Research Centre, Baghdad, 1:1-11.

Mohammad, M.-B.M. (1965) Further observations on some environmental conditions of Shatt Al-Arab. Bulletin of the Biological Research Centre, Baghdad, 1:71-79.

Nakamura, K. (1974) Observations on the seabirds in the Arabian Gulf. Transactions of the Tokyo University of Fisheries, (1):13-17.

Naqvi, S.W.A., DeSouza, S.N. and Reddy, C.V.G. (1978) Relationship between nutrients and dissolved oxygen with special reference to water masses in western Bay of Bengal. Indian Journal of Marine Science, 7(1):15-17.

Nellen, W. (1973) Fischlarven des Indischen Ozeans. Ergebnisse der Fischbrutlunter-untersuchungen während der ersten Expedition des Forschungsschiffes 'Metero' in den Indischen Ozean und den Persischen Golf, Okotober 1946 bis April 1965. 'Meteor' Forschungsergebnisse, Series D, (14):1-66.

Nellen, W. (1973) Kinds and abundance of fish larvae in the Arabian Sea and the Persian Gulf. In: The Biology of the Indian Ocean (ed, B. Zeitzschel and S.A. Gerlach), p. 415-530. London: Chapman and Hall; Berlin: Springer-Verlag.

Oshite, K. (1974) Diatoms in the core samples of bottom deposits collected in the Arabian Gulf, December 1968. Transactions of the Tokyo University of Fisheries, (1):62-66.

Oshite, K. (1974) Suspension collected in the Arabian Gulf. Transactions of the Tokyo Univeristy of Fisheries, (1):72-81.

Pedgley, D.E. (1969) Cyclones along the Arabian coast. Weather, 24:456-468.

Ponomareva, L.A. (1975) (Euphausiids of the Indian Ocean and the Red Sea). Nauka, Moskow, 84 pp. (In Russian)

Privett, D.W. (1959) Monthly charts of evaporation from the north Indian Ocean (including Red Sea and the Persian Gulf). Quarterly Journal of the Royal Meteorological Society, 85:424-428.

ROPME (1983) Mannual of Oceanographic Observations and Pollutant Analysis Methods. The Regional Organization for the protection of the Marine Environment, Kuwait.

Saad, M.A.H. (1978) Seasonal variations of some physico-chemical conditions of Shatt Al-Arab estuary, Iraq. Estuarine and Coastal Marine Science, 6:503-513.

Saad, M.A.H. and Hussain, N.A. (1978) Preliminary studies on sodium, magnesium, calcium and potassium in the north-west Arab Gulf. The Arab Gulf, (9):19-27.

Samuel, M., Mathews, C.P. and Lee, J.W. (1983) Oceanographic data from 1978 to 1980. Kuwait Institute for Scientific Research, 73 pp. (restricted).

Selim, H. (1966) (The five year plan 1966-71. Plan for improving fisheries in Kuwait). Kuwait: Ministry of Public Works. (In Arabic)

Selim, H. (1968a) (Survey of the catching areas of the Kuwait fisheries, in tables). Kuwait: Ministry of Public Works. (In Arabic)

Selim, H. (1968b) Scientific, common and local names of Kuwaiti fishing grounds, Kuwait: Ministry of Public Works. (Mimeograph).

Selim, H. (1968c) (Living resources in the Arabian Gulf). Kuwait: Ministry of Public Works. (In Arabic)

Selim, H. (1968d) (Methods of planning of the fisheries resources development in Kuwait). Paper presented at the Conference of Oceanography and Water Wealth, Congress of the Arab League, 19-30 October, 1968, Cairo, Egypt. (In Arabic)

Selim, H. (1968e) Detailed study on fishing methods and gear used in Kuwait. Paper presented at the Conference of Oceanography and Water Wealth, Congress of the Arab League, 19-30 October, 1968, Cairo, Egypt. (In Arabic)

Selim, H. (1968f) (Analysis of the fishing operations of the local fleet in Kuwait). Paper presented at the Conference of Oceanography and Water Wealth, Congress of the Arab League, 19-30 October, Cairo, Egypt. (In Arabic)

Selim, H. (1968g) (Hydrobiology of the Arabian Gulf). Paper presented at the Conference for Oceanography and Water Wealth, Congress of the Arab League, 19-30 October, 1968. Cairo Egypt. (In Arabic)

Selim, H. (1968h) (A report on the resources of the sea in Kuwait.) Paper presented at the Conference for Oceanography and Water Wealth, Congress of the Arab League, 19-30 October, 1968. Cairo, Egypt. (In Arabic)

Solobiof, L.S., Goubanov, E.P., Azizov, E.Z., Mourad, H.A.H., Rashoud, A.K. and Ashkanani, A.H. (1980) (Principles of the protection of fisheries resources and the organization of fisheries catch in Kuwait, ed. Y. Boukaneevich and N. Abu-Shleib). Kuwait: Ministry of Public Works, 47 pp. (In Arabic)

Sonu, C.S. (1979) Oceanographic study in the Strait of Hormuz and over the Iranian shelf in the Persian Gulf. U.S. Office of Naval Research, Final report, contract No. N00014-76-c-0720, TC 3675, 53 pp.

Srinivasan, V. (1969) Satellite information in the study of Indian Ocean meteorology In: Proceedings of the Symposium on Indian Ocean, New Delhi, 2-4 March 1967. Bull. of the National Institute of Sciences of India, (38)2:990-997.

Trepka, L. von. (1968) Investigations of the tides in the Persian Gulf by means of hydrodynamics-numerical model. Mitteilungen des Institute für Meereskunde der Universität Hamburg, (10):59-63.

Trepka, L. von. (1970) Physical and chemical data observed by the research vessel 'Meteor' in the Persian Gulf 1975. 'Meteor' Forschungsergebnisse, Series A, (8):43-90.

Ul-Hassan, H. (1976) Biology of commercial shrimps of Kuwait, Arabian Gulf. Kuwait: Kuwait Institute for Scientific Research, 21 pp.

Weigmann, R. (1970) Zur Okologie und Ernahrungsbiologie der Euphausiaceen (Crustacea) im Arabischen Meer. 'Meteor' Forschungsergebnisse, Series, D, (5):11-52.

Weigman, R. (1971) Eine isolierte Population von Pseudeuphausia latifrons (Crustacea Euphausiacea) im Persischen Golf. Marine Biology, 8(4):351-355.

Yamazi, I. (1974) Analyses of the data on temperature, salinity and chemical properties of the surface water, and the zooplankton communities in the Arabian Gulf. Transactions of the Tokyo University of Fisheries, (1):26-51.

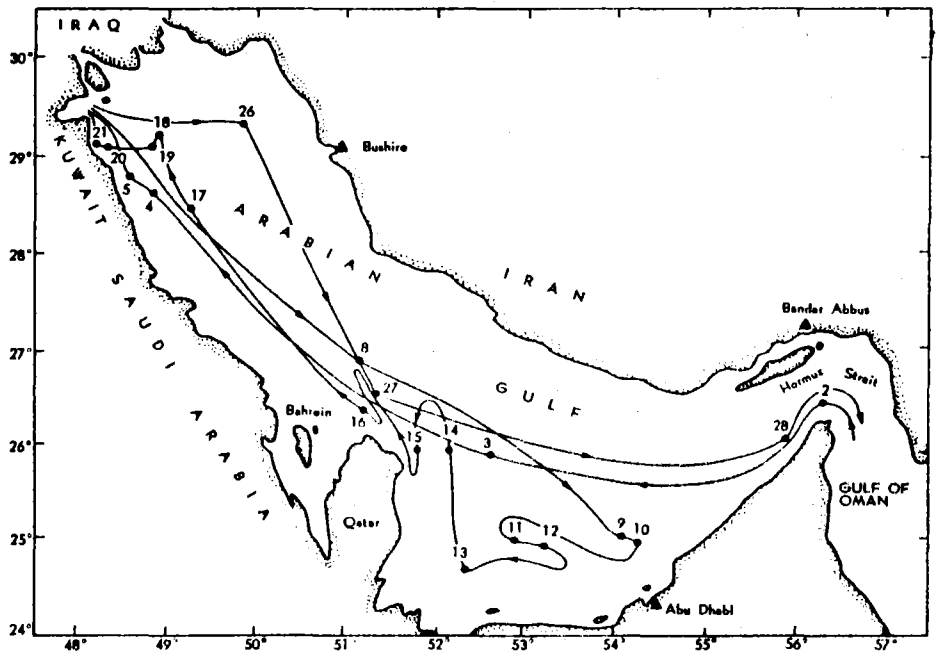

Figure 1: Map of Inner Gulf showing the cruising track of the Umitaka-Maru on fishery oceanography survey in December, 1968.

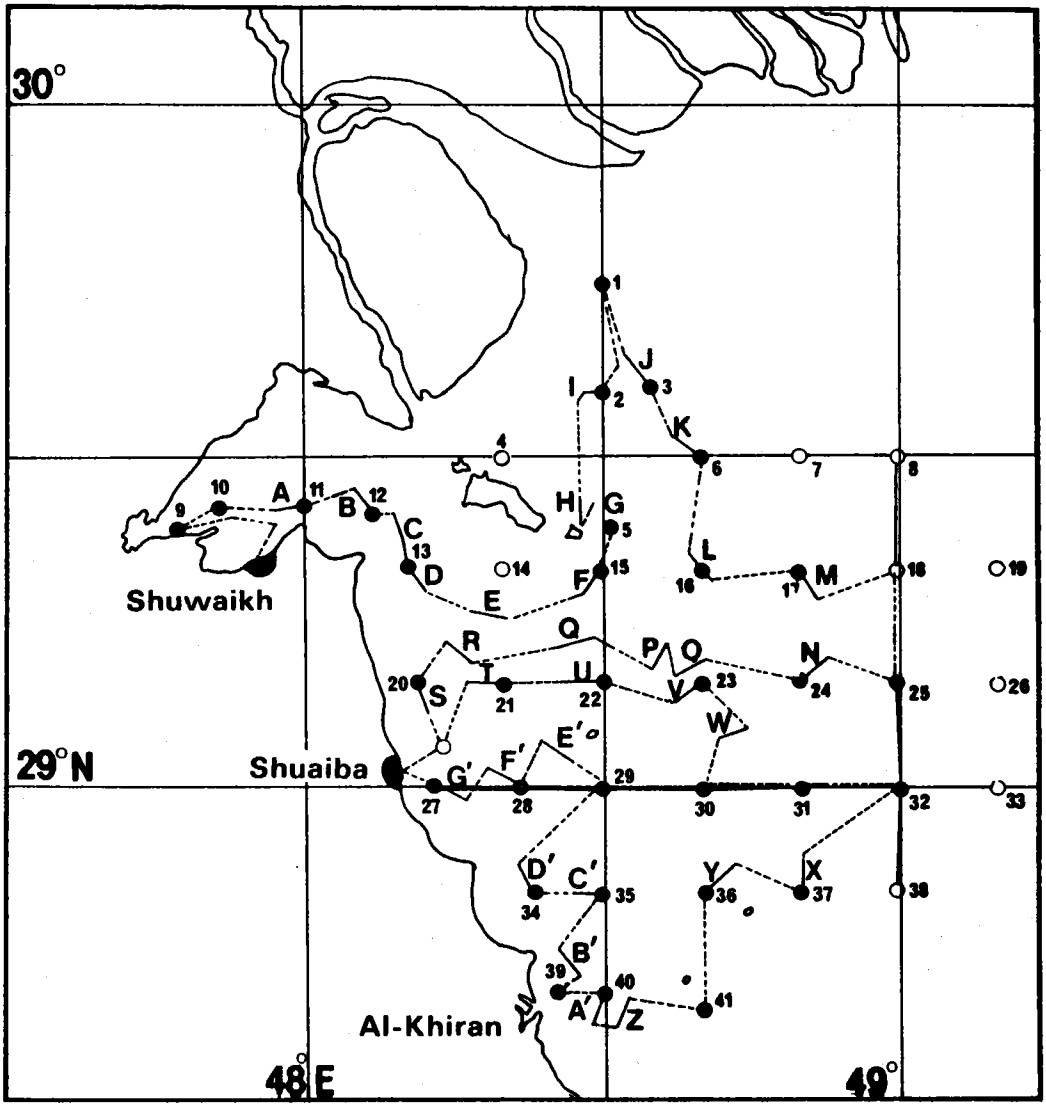

Figure 2: Kuwait National Sampling Grid (fisheries and oceanography) Letters - trawl stations: numbers - hydrographic stations.

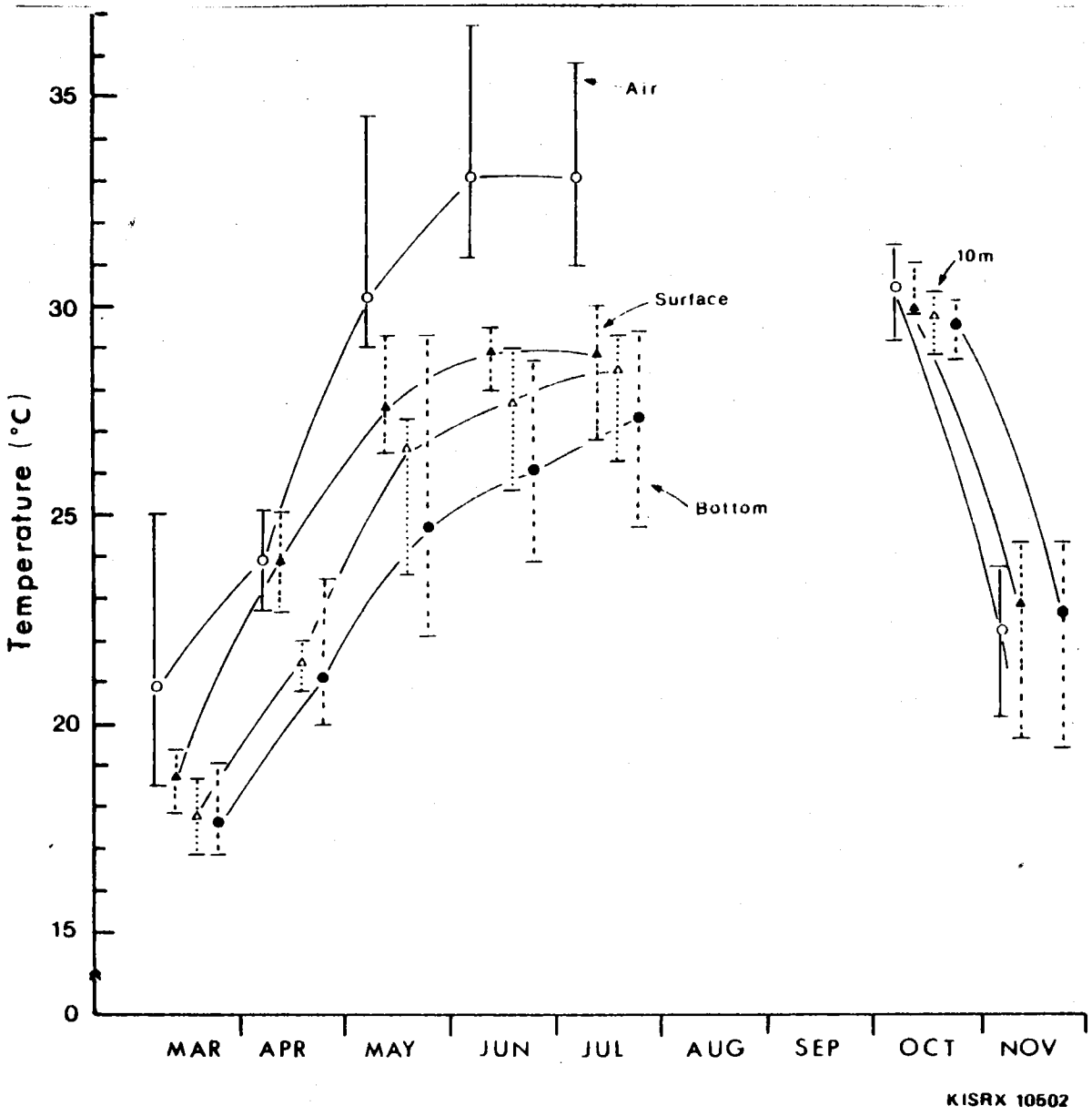

Figure 3: Mean and range of air seawater temperature.

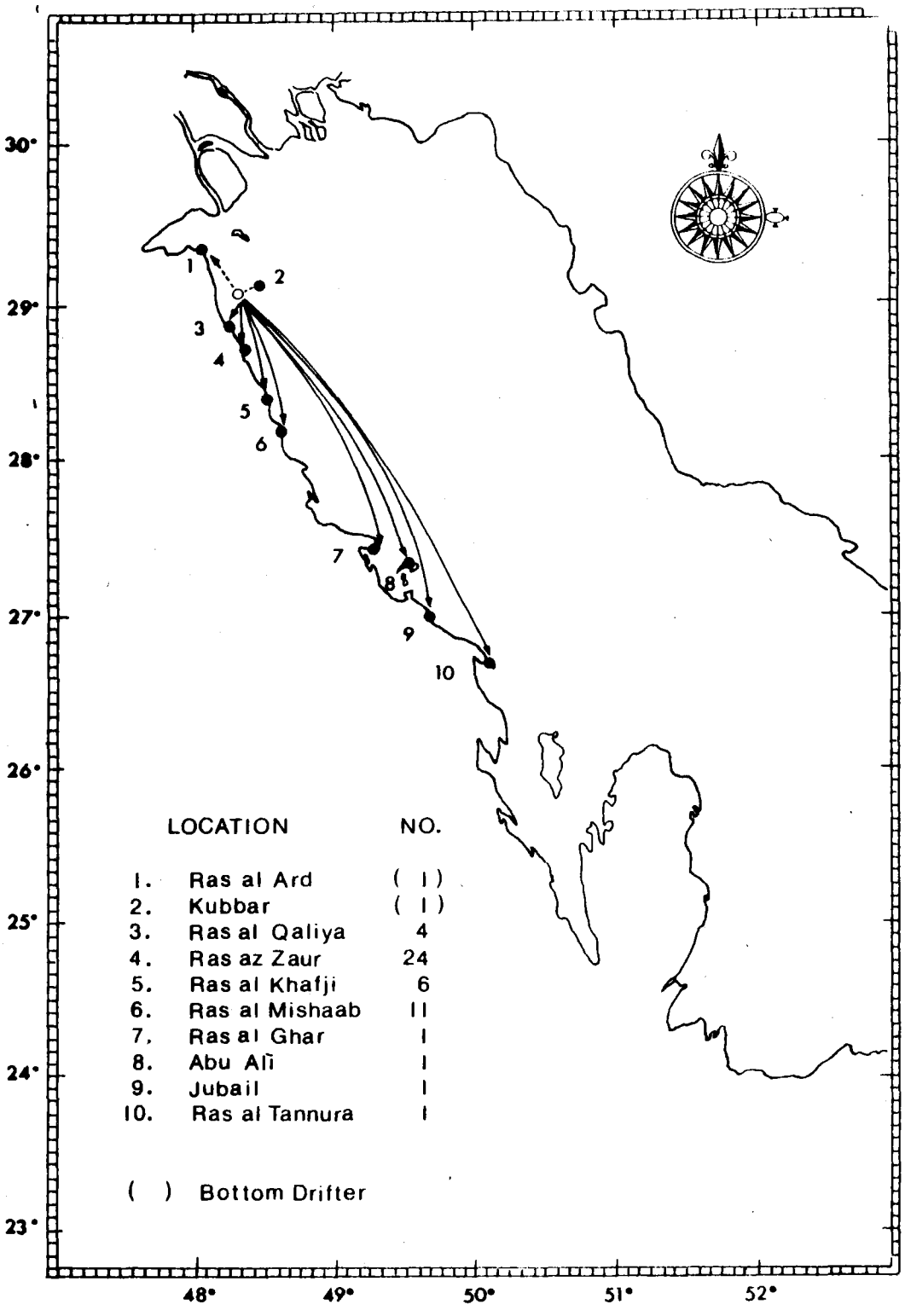

Figure 4: Estimated tracks of surface and bottom ( ) drifters.

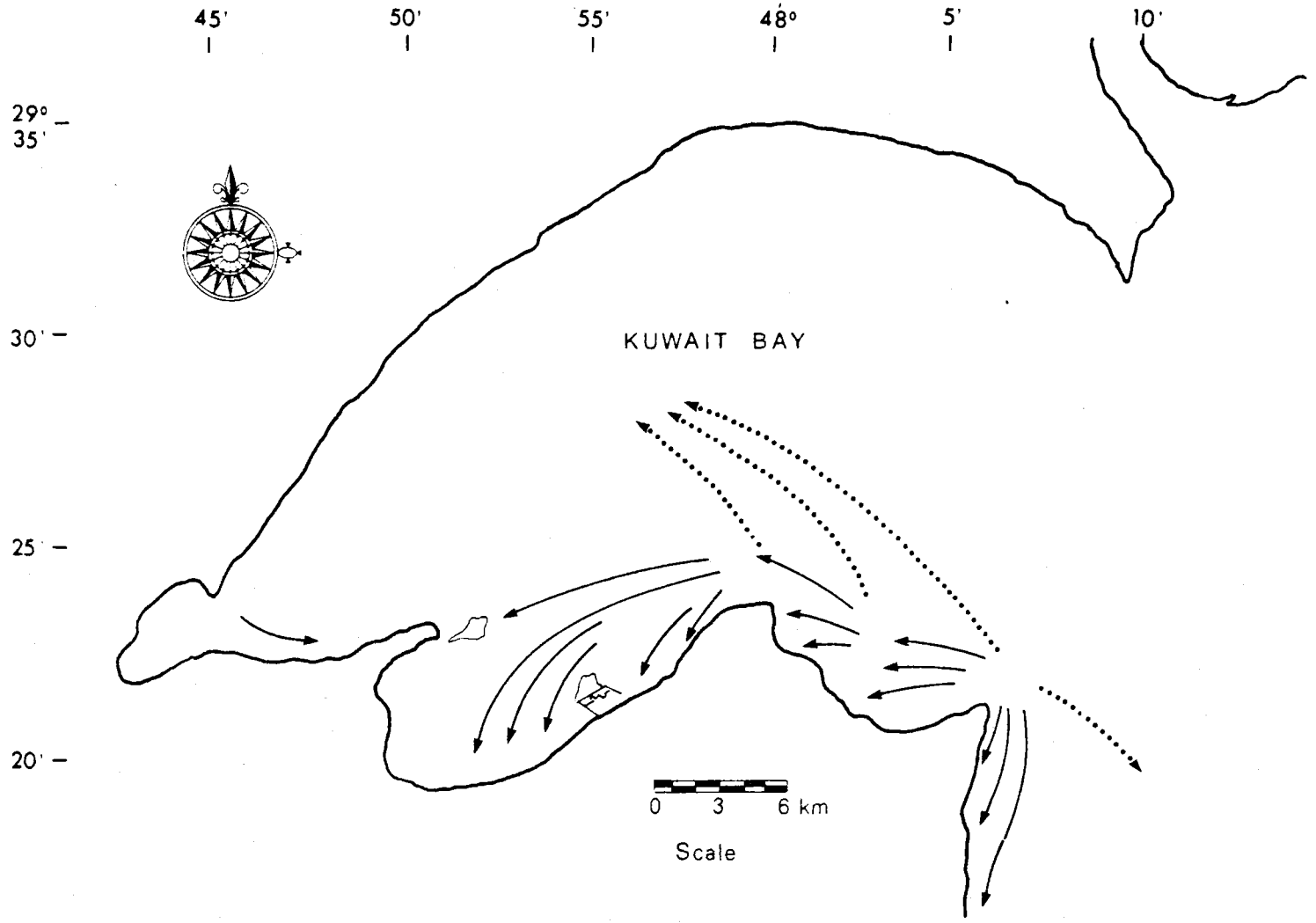

Figure 5: Estimated tracks of surface and bottom residual currents in Kuwait Bay.

STORM TRACKS AND SEA STATE IN THE KUWAIT ACTION PLAN (KAP) REGION: A REVIEW

by

T. S. Murty and M.I. El-Sabh
Institute of Ocean Sciences
Department of Fisheries and Oceans
Sidney, BC Canada

ABSTRACT

A review of the storm tracks and sea state in the KAP Region includes the Inner Gulf, the Strait of Hormuz and the Gulf Oman. The Inner Gulf is mainly influenced by extra-tropical weather systems, whereas the Gulf of Oman is mostly under the influence of tropical weather systems. The west-to-east directed extra-tropical cyclone tracks and the generally east-to-west directed tropical cyclone tracks converge near the Strait of Hormuz. Special attention has been given to the meso-scale phenomenon referred to as Shamal. The sea state is also discussed.

INTRODUCTION

The KAP Region consists of the following water bodies: the Inner Gulf, the Strait of Hormuz and the Gulf of Oman. There are eight nations bordering these water bodies (Figure 1): Bharain, Iran, Iraq, Kuwait, Oman, Qatar, Saudi Arabia and United Arab Emirates. The deeper Gulf of Oman joins the Arabian Sea towards east and south and is connected to the shallower Inner Gulf through the Strait of Hormuz. Since the climate of the region is influenced strongly by orography, a brief description of the geography of the area is useful.

The region under discussion consists of low-lying central areas enclosed by mountains (Perrone, 1981); the Inner Gulf and the Tigris-Euphrates Valley are at low elevations. Figure 2 shows the Taurus family of mountains in southern Turkey, the Pontic mountains in northeast Turkey, the Caucasus mountains of Iran, and the Hajar and Hejaz mountains of the Arabian Peninsula. Table 1 summarizes the heights of these mountain peaks.

The Inner Gulf is mainly affected by extra-tropical weather systems, whereas the Gulf of Oman is at the northern edge of tropical weather systems. The Strait of Hormuz region thus forms the boundary between the generally west-to-east travelling extra-tropical weather systems and the east-to-west travelling tropical weather systems. This paper is organized as follows: section two is concerned with extra-tropical weather systems mainly affecting the Inner Gulf; section three deals with the tropical weather systems that influence the Gulf of Oman and section four discusses the sea state. The paper concludes with a summary and suggestions for future work.

EXTRA-TROPICAL WEATHER SYSTEMS AFFECTING THE INNER GULF

Figure 3 shows the extra-tropical cyclone tracks across Asia (Haurwitz and Austin, 1944). It can be seen that the tracks more or less follow the axes of the Inner Gulf and the Gulf of Oman. One of the interesting weather phenomenan in the Inner Gulf region is the Shamal, a sub-synoptic scale wind phenomenon that occurs in this region with sufficient frequency and influence on the local weather to be significant operationally (Peronne, 1981). Shamal is an Arabic word meaning north. It is used in the meteorological context to refer to seasonal northwesterly winds that occur during winter as well as summer in the Inner Gulf region. In the following discussion, our source of information is the excellent technical report by Perrone (1981).

The winter Shamal occurs mainly during November to March and is associated with mid-latitude disturbances travelling from west to east. It usually occurs following the passage of cold fronts and is characterized by strong northwesterly winds (mainly during December to February). Perrone (1981) mentions that the winds at most locations in the Inner Gulf exceed 20 knots only for less than 5 per cent of the winter duration. Although infrequent, the winter Shamal is not insignificant from an operational point of view, because it sets in with great abruptness and force (the March 1983 oil spill event in the Inner Gulf occurred during a winter Shamal).

The summer Shamal occurs with practically no interruption from early June throughout July and is associated with the relative strengths of the Indian and Arabian thermal lows. From the point of view of the strength of the wind and

associated weather conditions, the summer Shamal is not as important as the winter Shamal. In the following discussion, consideration is restricted to the winter Shamal. Two types of Shamal can be distinguished, based on duration: those which last between 24 and 36 hours and those which last between three and five days.

The intense winter Shamals are preceded by a movement of cold air from the north into the Inner Gulf region. All but the most intense of such incursions are stopped by the mountains of Turkey, the Georgian S.S.R. and Iran. Cold air can, however, arrive in the Inner Gulf area by at least two indirect routes. One of these is via the Aegean Sea. The other enables cold air to move over the shorter mountain chain in western Turkey, then across the eastern part of the Mediterranean Sea, finally travelling either over or around the low mountains in Syria and Lebanon (with heights ranging from 914 to 1,829 m) and into the Tigris-Euphrates Valley.

The orography also affects the airflow within the Inner Gulf region. The sharply rising mountains to the north and east and the more gently rising mountains to the west and southwest channel the airflow at low level from northwest to southeast. Perrone (1981) gives the following six stages in the life cycle of a typical Shamal of three to five days duration.

(i) An upper trough is reflected in a surface low advected over Syria from the eastern Mediterranean Sea.

(ii) The upper trough and the associated surface low travel eastward. From the low extends a cold front, first towards south and then towards west. From the Red Sea, another low moves eastward across Saudi Arabia. Then, a southeasterly wind, referred to as Kaus, blows over the Inner Gulf.

(iii) The trough aloft moves eastward and a new low forms on the front, this low extending from the southern part of the Tigris-Euphrates Valley to the central part of the Inner Gulf. The original low either fills over the Nothern part of Iraq or retains some surface identity during its advection along with the upper trough towards the Caspian Sea. Then subsidence occurs in the lower troposphere, and this creates a surface high pressure zone in the northern part of Saudi Arabia. To the west of the new surface low, a strong but shallow air stream moves in; this is the winter Shamal. During the shamal, gale force winds occur as well as thunderstorms and high seas, and the visibility over the Inner Gulf is sharply reduced owing to advection of sand and dust in the air.

(iv) The new surface low formed in stage (iii) develops fully. It is advected into the eastern part of Iran by the trough aloft, but the surface low lies somewhat ahead of the trough. The cold front associated with this low travels southward over the Inner Gulf over to the Arabian Sea.To the west of the upper trough, over the Nothern part of Saudi Arabia, subsidence continues into the lower part of the troposphere. The surface pressure over Saudi Arabia increases, and the pressure gradient between the low pressure area over the Gulf of Oman and the Saudi Arabian high sustains the gale force winds of the Shamal. The high seas, thunderstorms and poor visibility continue.

(v) The upper trough either becomes stationary over the Strait of Hormuz or moves slowly over the southern part of the Inner Gulf, whereas the surface low moves to the northeast. A new orographically-induced low forms over the Gulf of Oman. Subsidence continues over Saudi Arabia in the lower troposphere,and this is followed by the formation of a second high pressure area, this time

over the Iranian Plateau. The orientation of the Zagros mountains is such that a lee trough that forms stretches from the low over the Gulf of Oman northwestward along the eastern shore of the Inner Gulf. The Shamal and the associated weather elements still continue. To the west of the trough, subsidence occurs over a wide area and, due to to this, thunderstorm and rainfall are inhibited over the Inner Gulf.

(vi) Ultimately, the upper trough moves away towards the east. Subsidence in the lower troposphere is now stronger over the Iranian Plateau than over Saudi Arabia. The high pressure over Saudia Arabia weakens and the lee trough moves westward over the Inner Gulf. Now the Shamal weakens and on the western side of the Inner Gulf winds subside, whereas on the eastern side of the Gulf the Shamal winds are replaced by either local sea breezes or weak southeasterlies or a combination of both.

Although the winter Shamal is a relatively rare event, typically occurring only once or twice each winter, it brings some of the strongest winds and highest seas of the season to the Inner Gulf region. Consideration will now be given to the more frequent shorter duration Shamals (24 to 36 hours). The synoptic situation described above generally applies to these Shamals also, with one important exception. The upper air trough does not stall over the Strait of Hormuz, but travels fast to the east. Hence stage (v) above does not occur for short duration Shamals. It should be noted that the stages described here are somewhat idealized and important variations can occur in individual cases.

Shamal conditions rarely occur over the northern part of the Inner Gulf in September. As it is associated with the movement of cold fronts or mid-latitude lows either over or to the north of the Inner Gulf, a Shamal may start at any time of the day. Before the onset of the Shamal, winds in the area ahead of the approaching cold front blow from south to southeast. These southerly winds (called Kaus in Arabic or Shakki in Persian) slowly increase in intensity as the front approaches, and may reach gale force before the passage of the front (Perrone, 1981). Due to the channelling effect of the low level air flow by the Zagros mountains in western Iran, the strongest of these southerly winds occurs on the eastern side of the Inner Gulf (Figure 4).

Usually, the Shamal occurs first in the northwest part of the Inner Gulf and then spreads south and east behind the advancing cold front. It takes about 12 to 24 hours for the Shamal to spread from the northwest corner of the Inner Gulf to the southern part. The onset of a typical mid-sinter Shamal is associated with the advection of a cold intense upper air trough at 500 mb to a location over Syria and Iraq (east of the Taurus mountains of Turkey). Figure 5 shows a surface low that usually forms to the Eeast of the upper trough in the area of strongest positive vorticity advection. The relatively warm waters of the Inner Gulf act as a significant heat source and the cyclogenesis is also due to the mechanical uplifting of the low level westerly or southwesterly flow by the Zagros mountains. The strong southwesterly airflow over the Zagros mountains further enhances this upward motion. The release of latent heat of condensation from the uplifted Arabian Gulf air further helps the cyclogenesis.

The following information is taken more or less directly from Perrone (1981). Just before the Shamal begins, a shallow narrow tongue of relatively cold air over the upper Tigris-Euphrates Valley advances southeastward down the lower part of this valley to run under and lift the warmer moist local Gulf air. The potential energy in the thermal contrast of the adjacent cold and warm surface air masses is converted to kinetic energy as the cold air lifts the warmer air. The energy

conversion relationship forms the basis of a forecast technique for predicting the initial velocity of the Shamal as it enters the Inner Gulf at the northwest corner. Just before the onset of the Shamal, the vertical air column over the northern part of the Inner Gulf and the Tigris-Euphrates Valley is usually conditionally unstable.

The onset of the Shamal is difficult to predict, mainly because of the difficulty in forecasting the associated upper air pattern. Once the Shamal has begun, it may subside within 12 to 36 hours after the passage of the cold front or it may persist for three to five days. The relationship between the surface and upper air patterns determines which duration and sequence is most likely to occur. Once the Shamal sets in, the wind direction is strongly influenced by the coastal orography. In the northern part of the Inner Gulf, the Shamal winds generally blow from any direction between north and west-northwest. In the middle parts of the Gulf, Shamal winds tend to be from a direction lying between west-northwest to northwest. On the southeast coast of the Gulf, the winds are westerly. In the Strait of Hormuz area, the Shamal winds are generally from the southwest. Usually the speed of the Shamal winds ranges from 20 to 40 knots.

For the longer duration Shamals, the upper air trough stalls over the strait of Hormuz. The Shamal winds persist for three to five days at gale force and blow from northwest over the whole Inner Gulf. Because of the large pressure gradient between the low over the Gulf of Oman and the high over Saudi Arabia, the Shamal winds are strongest in the southern and southeastern parts of the Inner Gulf. Average wind speeds in this area range from 30 to 40 knots, with peak winds in excess of 50 knots, not uncommon in this type of Shamal. Winds over the northern part of the Inner Gulf tend, on the average, to be 5 to 15 knots less than the above values.

According to Perrone (1981), two areas of the Inner Gulf appear to experience stronger than average Shamal conditions. These are shown in Figure 6. One area is near Qatar Peninsula, the other is near Lavan Island. The Shamal which is due to interaction between the synoptic scale and the meso-scale extra-tropical weather systems, is subject to modification by local conditions.

TROPICAL WEATHER SYSTEMS THAT AFFECT THE GULF OF OMAN

Figure 7 shows the ocean basins which give rise to tropical cyclones. The preferred annual tracks of tropical cyclones are shown in Figure 8. Figure 9 shows the tracks of tropical cyclones across Asia. The average speed in knots of storm movement is shown in Figure 10. The common tracks of Arabian Sea tropical cyclones are shown in Figure 11. Table 2 lists the number of cyclones (Beaufort greater than or equal to 12) and cyclonic storms (Beaufort greater than or equal to 8) over the whole Arabian Sea during the period 1890 to 1950 and the number of occurrences along the Arabian coast during the period 1891 to 1967. For details of the Beaufort Scale see Table 3. Table 4 lists some cyclones near the coast of the Arabian Peninsula during 1943 to 1967.

The specifications of the tropical cyclone disturbances in general use are: (a) depression, when winds reach up to 33 knots (Beaufort 7); (b) moderate storm, when winds are from 34 to 47 knots (Beaufort 8 to 9); and (c) severe cyclonic storm, when winds are from 48 to 63 knots (Rao, 1981). Table 5 lists the monthly and annual number of depressions and storms which formed in the Arabian Sea during 1930 to 1969.

Rao (1981) states that in the 70-year period from 1891 to 1960, the number of depressions and storms formed in the Arabian Sea in the months of May, June, October and November were 17, 24, 21 and 15, respectively. The area of formation stretches from south of 7.5°N to 23°N latitude and from 55°E to 77.5°E. For the months of May, October and November, however, the main area of formation lies between 10°N and 12.5°N. For the month of June, the area of formation is between 17.5°N and 20°N. About 80 per cent of the depressions formed in the area between 10°N and 12.5°N in both May and June. About 70 per cent of the depressions and storms formed in the area between 67.5°E and 72.5°E. In October and November, about 50 per cent formed between 10°N and 12.5°N. The longitudinal positions, however, varied widely between 62.5° and 75°E.

The Arabian Sea is in the area of the monsoon, a seasonal wind regime in which surface winds blow persistently from one general direction in summer, and just as persistently from a markedly different direction in sinter (Brody, 1977). The most satisfactory criteria for determining whether a region is monsoonal or not have been developed by Ramage (1971), who defined an area as monsoonal if the January and July surface circulations are such that the following four criteria are satisfied: (a) the prevailing wind direction shifts by at least 120° between January and July; (b) the average frequency of prevailing wind directions in both January and July exceeds 40 per cent; (c) the mean resultant winds in at least one of these two months exceed 3 m/sec; (d) fewer than one cyclone-anticyclone alteration occurs every two years in either January or July in a 5° latitude-longitude rectangle.

These criteria suggest that, for an area to be considered monsoonal, there must be highly persistent winds from different directions in winter and summer. Also the fourth criterion excludes the regions in which the seasonal wind shift is only due to a shift in the average tracks of the travelling weather systems. Figure 14 shows the monsoonal areas over the globe (Rammage, 1971) and it can be seen that, whereas the Gulf of Oman is included in this area, the Inner Gulf does not fall into the monsoon zone.

Although tropical cyclones do not usually occur in the Arabian Sea area, they do have a significant effect on the local weather (Brody, 1981). In spite of the low frequency of their occurrence along the Arabian Coast, where they influence the weather on an average of only once in three years, their associated torrential rains make up a significant portion of the total rainfall. During the 25-year period 1943 to 1967, a quarter of the total rainfall at Salalah was associated with tropical cyclones. In addition, their winds and associated sea conditions make the tropical cyclone a dangerous meteorological event in the Arabian Sea region.

Brody (1977) used a tropical cyclone classification that is somewhat different from that used by the India Meteorological Department for the north Indian Ocean. The differences are summarized in Table 6.

The Arabian Sea is the least active of the various tropical cyclone development regions on the globe. Only about 1 per cent of the world's tropical cyclones of at least tropical storm intensity develop in the Arabian Sea, in contrast to 5 per cent in the Bay of Bengal, which is somewhat smaller in area than the Arabian Sea. During a seventeen year period (1951 to 1967), no tropical storms were observed in the Arabian Sea for seven years, whereas a maximum of only three were observed in two of the 17 years. More recent satellite data appears, however, to suggest that the occurrence of tropical storms in the Arabian Sea might be more frequent than previously believed especially in the southwestern areas where virtually no data were available earlier.

In the Arabian Sea region, the tropical cyclones develop mainly during the spring and autumn transition seasons. The same bimodal distribution is applicable for tropical cyclones that reach hurricane intensity. The rarity of tropical storms in the Arabian Sea region can be seen from the fact that only 92 tropical cyclones reached storm intensity during the 80-year period 1891 to 1970. Slightly more than half of these reached hurricane intensity.

Occasionally tropical storms generated in the Bay of Bengal cross the peninsular part of India and develop in the Arabian Sea. Figure 15 shows the tracks of two tropical storms that developed in the Arabian Sea in the spring of 1974. Figures 16 to 30 show tropical cyclone tracks for the Arabian Sea including the region of the Gulf of Oman. It can be seen that tropical storms south of about 15°N usually move towards the northwest quite far from the west coast of India. north of 15°N this track splits, with some of the storms moving westward while the others move northward.

Brody (1981) states that, because of the extensive mountain barrier to the north of the Arabian Sea, the region's winter monsoon is much weaker than the northeast monsoon of the south China Sea, for example. Wind directions during the winter monsoon are generally from the northeast. In the northern part of the Gulf of Oman, however, the winds are generally light and variable. During the winter monsoon, cloudiness is generally slight and there is good visibility over the Arabian Sea. A common meteorological phenomenon in the northern part of the Arabian Sea is the occurrence of dust associated with cold fronts moving off the Arabian Peninsula. Among mesoscale effects to be expected are land-sea breezes along the coastlines of the Arabian Sea.

Tropical cyclones are extremely rare during the winter monsoon, and the few recorded ones occurred during December (Brody, 1981). The major meteorological events of the spring and autumn transitional seasons are the tropical storms. According to Brody (1981), as long as the near-equatorial trough remains over the sea, and the farther it moves from the equator (as during spring), the more often tropical cyclones will develop in the sea.

The Arabian Sea summer monsoon is usually firmly established by June. Surface winds reach a maximum during July. During June, the near-equatorial trough occasionally re-intensifies over the Arabian Sea and this gives rise to tropical cyclones. Tropical cyclones reaching storm intensity in June generally develop off the west coast of India and move northwestward, causing high winds at Karachi, Pakistan.

Brody (1981) states that, as the amount of insulation received over the northern hemisphere decreases as summer progresses into autumn, the heat trough over Pakistan and vicinity weakens and the near-equatorial trough again reappears over the Arabian Sea, with a second maximum of tropical cyclones occurring in the autumn. The October surface winds are again light and variable over most of the Arabian Sea, as they were in April. Intensification of the near-equatorial trough (whether or not there is tropical cyclogenesis) leads to augmented northeast winds over most of the Arabian Sea, north of the trough. Since passage of cold fronts is extremely rare in October, there is no increase in northeasterly winds associated with cold fronts over the northern part of the Arabian Sea. By November, fairly moderate northeasterlies with speeds of less than 22 knots are established over most of the Arabian Sea. Again, as in April, in the northern part of the Gulf of Oman, the winds are light and variable. Increases in the intensity of the monsoon flow during November are associated with tropical cyclogenesis as well as the intensification of the near-equatorial trough and the passage of cold fronts into the northern Arabian Sea.

SUMMARY AND RECOMMENDATIONS FOR FUTURE WORK

The extra-tropical cyclones that affect the Inner Gulf have been discussed above, with particular emphasis on the Shamal wind. The Gulf of Oman is affected by tropical cyclones from the Arabian Sea. The wind waves and storm tracks from these weather systems have been considered. The following studies should be made to obtain detailed knowledge of the sea-state and storm tracks in the Inner Gulf and the Gulf of Oman.

(i) Better observations should be made of the tracks of the extra-tropical cyclones that affect the Inner Gulf.

(ii) Detailed studies should be made of the winter and summer Shamals.

(iii) An attempt should be made to better understand the differences between Shamals of shorter and longer durations.

(iv) Better observations should be made of the tracks of tropical cyclones that affect the Gulf of Oman.

(v) An understanding is needed of the weather systems in the Strait of Hormuz area which forms the boundary between west-to-east travelling extra-tropical cyclones and east-to-west travelling tropical cyclones.

(vi) Better and detailed measurements are required of the wind waves in the Gulf of Oman, the Strait of Hormuz and the Inner Gulf.

(vii) Theoretical relationships between wind speed and wave height in shallow water should be developed.

REFERENCES

Brody, L.R. (1981) Meteorological phenomena of the Arabian Sea. Naval Environmental Prediction Research Facility, Monterey, California, NAVENPREDRSCHFAC, Applications Report, AR-77-01 (March 1977), Second Printing, November 1980, no pagination.

Crutcher, H.L. and Quayle, G. (1974) Mariners world-wide climatic guide to tropical storms at sea, published by the Commander, Naval Weather Service Command, NAVAIR, 50-1C-61, Superintendent of Documents, U.S. Govt. Print. Off. Wash. D.C. 114 pp.

Gray, W.M. (1978) Hurricanes: their formation, structure and likely role in the tropical circulation. In: "Meteorology over the tropical oceans", D.B. Shaw (ed.) Roy. Met. Soc., Bracknell, U.K., ISS-218.

Haurwitz, B. and Austin J.M. (1944) Climatology, McGraw-Hill Inc., N.Y. 410 pp.

Pedgley, D.E. (1969) Cyclones along the Arabian coast, Weather, Vol. 24, 456-468.

Perrone, I.J. (1981) Winter Shamal in the Persian Gulf, Naval Environmental Prediction Research Facility, Monterey, California, Technical Report I.R.-79-06, August 1979, Second Printing, January 1981, no pagination.

Ramage, C.S. (1971) Monsoon meteorology, Academic Press, N.Y. 296 pp.

Rao, K.N. (1981) Tropical cyclones of the Indian seas, Chapter 4. In: Climates of southern and western Asia, K. Takahashi and H. Arakawa (eds.) Elsevier Company, Amsterdam, p. 257-280.

Schalkwijk, W.F. (1947) A contribution to the study of storm surges in the Dutch coast. Report no. 125. Koninklink Nederlandsch Meteorologisc Institut, Debilt Series B, no. 7, 110 pp.

Table 1: Heights of the mountain peaks in the KAP and surrounding regions

Mountain peaks	Height (m)
Highest peaks of the Taurus chain in Turkey	2,743
General elevation in eastern Taurus and Pontic mountains	2,743 to 3,658
Ridge heights of the Caucasus chain	2,743 to 3,658
Some peaks of the Caucasus chain	Greater than 3,658
Zagros mountains of Iran	1,829 to 2,743
Some isolated peaks in the central part of Iran	Greater than 2,743
Hajar and Hejaz mountains of the Arabian Peninsula	914 to 1,829
Isolated peaks in the southwest Arabian Peninsula	1,829 to 2,743

Table 2: Number of occurrences of cyclones (Beaufort $\geq$ 12) and cyclonic storms (BF $\geq$ 8) over the whole Arabian Sea during the period 1890 to 1967 (from Pedgley, 1969)

	Jan	Feb	Mar	Apr	May	Jun	Jul	Aug	Sep	Oct	Nov	Dec	Year
Cyclones and cyclonic storms over the whole Arabian Sea	1	0	0	4	10	11	2	1	4	15	12	3	63
cyclones and cyclonic storms along the coast of Arabia	0	0	0	0	8	5	1	0	0	7	6	1	28
Cyclones along the coast of Arabia	0	0	0	0	6	2	0	0	0	2	2	1	13

Table 3: International and Bleck equivalents of the Beaufort Scale (from Schalkwijk, 1947)

Degrees Beaufort	International equivalent of wind ($m.\ sec^{-1}$)	Bleck equivalent of wind speed $m.\ sec^{-1}$
1	1.1	1.8
2	2.5	4.4
3	4.3	7.0
4	6.3	9.6
5	8.6	12.2
6	11.1	14.8
7	13.8	17.4
8	16.7	20.0
9	19.9	22.6
10	23.3	25.2
11	27.1	27.8
12	>29.0	>29.0

Table 4: Cyclones near the coast of the Arabian peninsula during 1943 to 1967 (from Pedgley, 1969)

Date of approach or crossing the coast	Nature of the Cyclone
June 6, 1946	Decaying before approaching Masirah from ESE.
October 1, 1948	Decaying before approaching coast between Masirah and Ras al Hadd from east.
October 25, 1948	Cyclonic storm crossed Salalah, approaching from SE.
May 24, 1959	Severe cyclone crossed Salalah, approaching from ESE.
October 18, 1959	Severe cyclone crossed near Ras Madraka, approaching from east.
May 18, 1960	Severe cyclone crossed coast at Ras Fartak.
November 23, 1960	Cyclonic storm approached entrance to Gulf of Aden from east.
May 30, 1962	Decaying before crossing coast at Ras Madraka.
May 26, 1963	Severe cyclone, passed just south of Salalah, approaching from east south east and then turning towards WSW.

Table 5: Monthly and annual number of depressions and storms in the Arabian Sea, 1930 - 1969 (from Rao, 1981)

Year	Jan.	Feb.	Mar.	Apr.	May	June	July	Aug.	Sep.	Oct.	Nov.	Dec.	Annual
1930						2				1			3
1931													0
1932					2					1			3
1933					1		1						2
1934						1			1				2
1935	1					1							2
1936						1					1		2
1937						1				1			2
1938					1						1		2
1939										1	1		2
1940										1	1		2
1941					1					1			2
1942				1									1
1943											1		1
1944						1		1					2
1945											1		1
1946						1							1
1947				1					1				2
1948						2				2	1		5
1949					1								1
1950							1		1				2
1951				1		1					1		3
1952												1	1
1953													0
1954				1		1	1						3
1955													0
1956						1				1			2
1957					1				1	1			3
1958													0
1959					1	1	1			1			4
1960					1		1				2		4
1961					1	1	2						2
1962					1		1						2
1963					1					1	2		4
1964						1		1			1		3
1965												1	1
1966									1	1			2
1967													0
1968													0
1969						1							1

Table 6: Classification of tropical cyclones

Wind speed	Brody's Terminology	Indian Meteorological Department terminology
Less than 34 knots	Tropical depression	Tropical depression
34 to 47 knots	Tropical storm	Moderate cyclonic storm
48 to 63 knots		Severe cyclonic storm
Greater than 63 knots	Hurricane (Typhoon)	Severe cyclonic storm with a core of hurricane winds

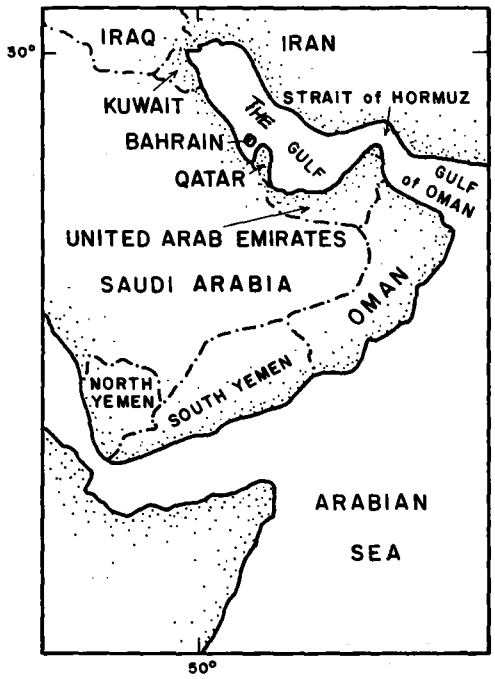

Figure 1: The eight nations of the KAP Region

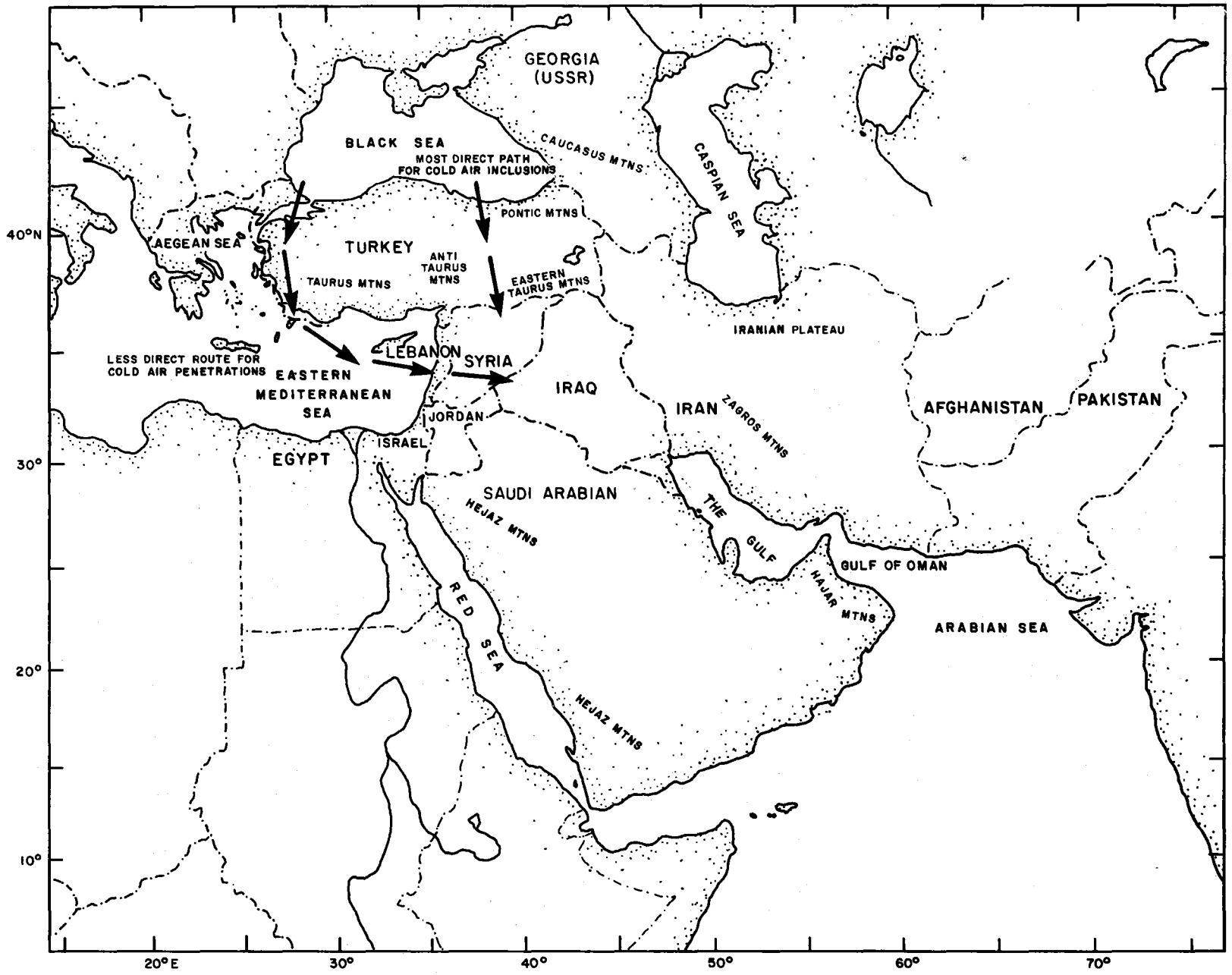

Figure 2: Geographical map of the Inner Gulf area.

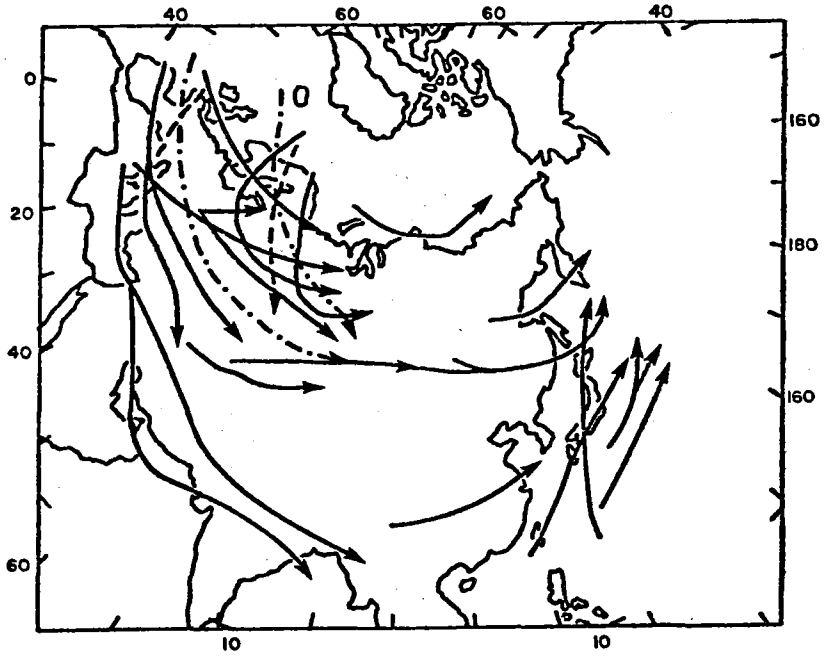

Figure 3: Extra-tropical cyclone tracks across Asia (from Haurwitz and Austin, 1944)

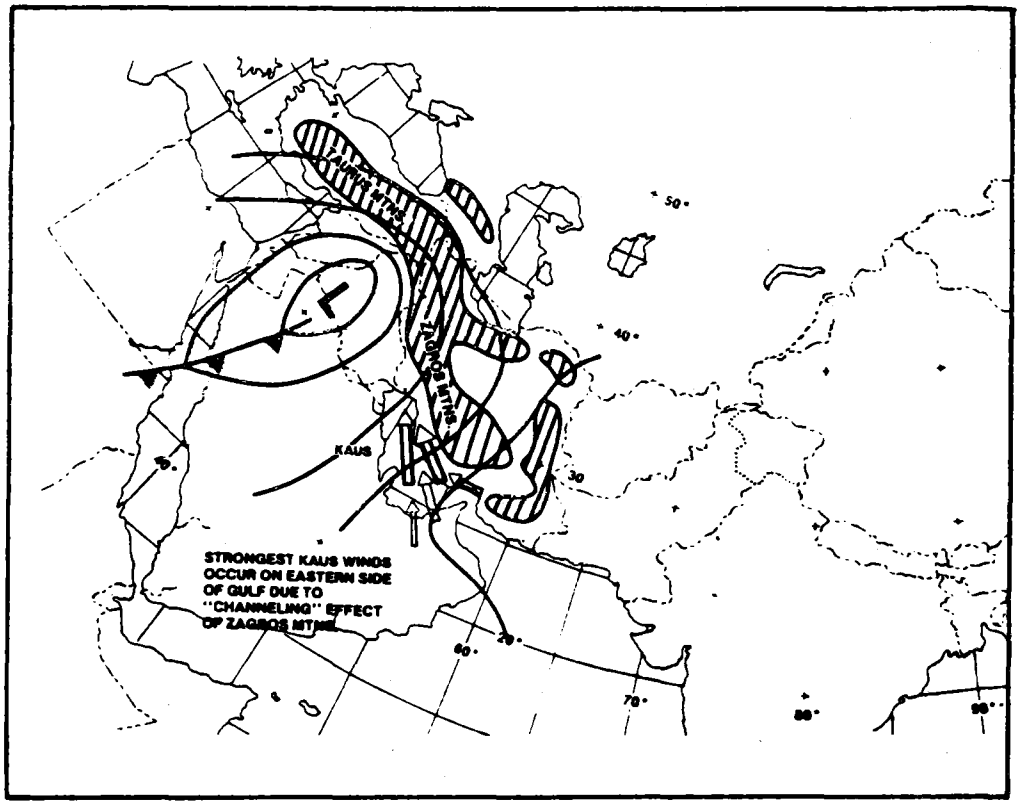

Figure 4: Channeling effect of the Zagros Mountains on Kaus winds (from Perrone, 1981)

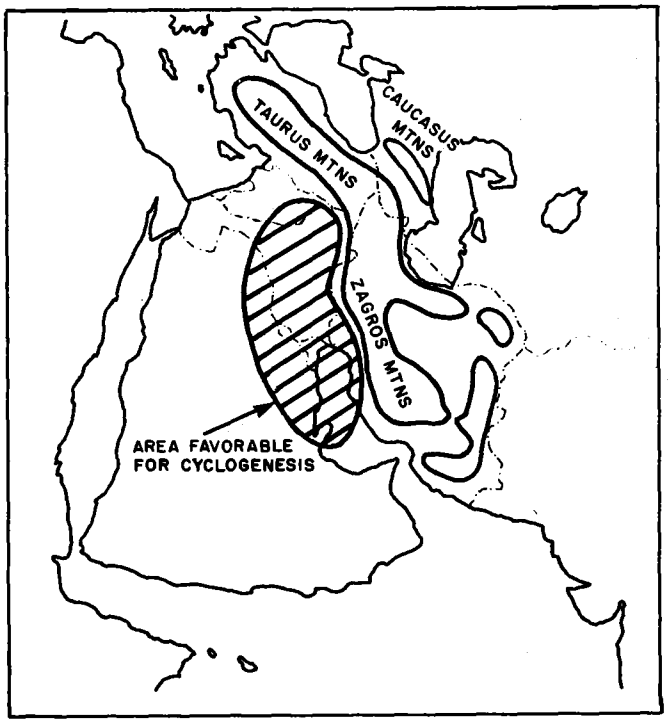

Figure 5: Area favorable for Shamal-associated cyclogenesis (from Perrone, 1981)

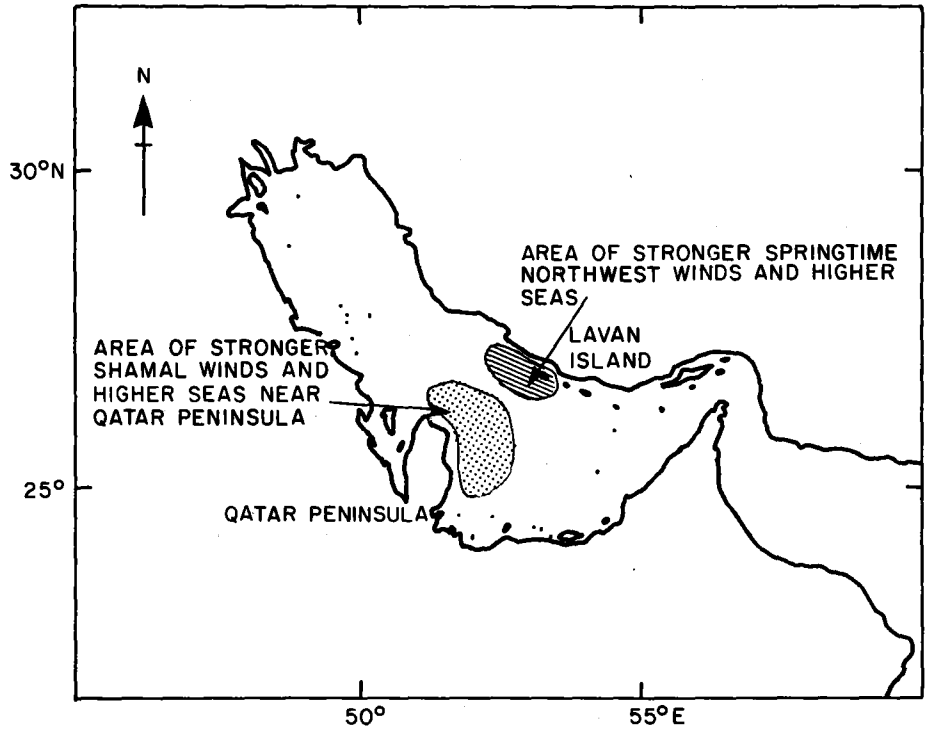

Figure 6: Areas of stronger than normal northwesterly

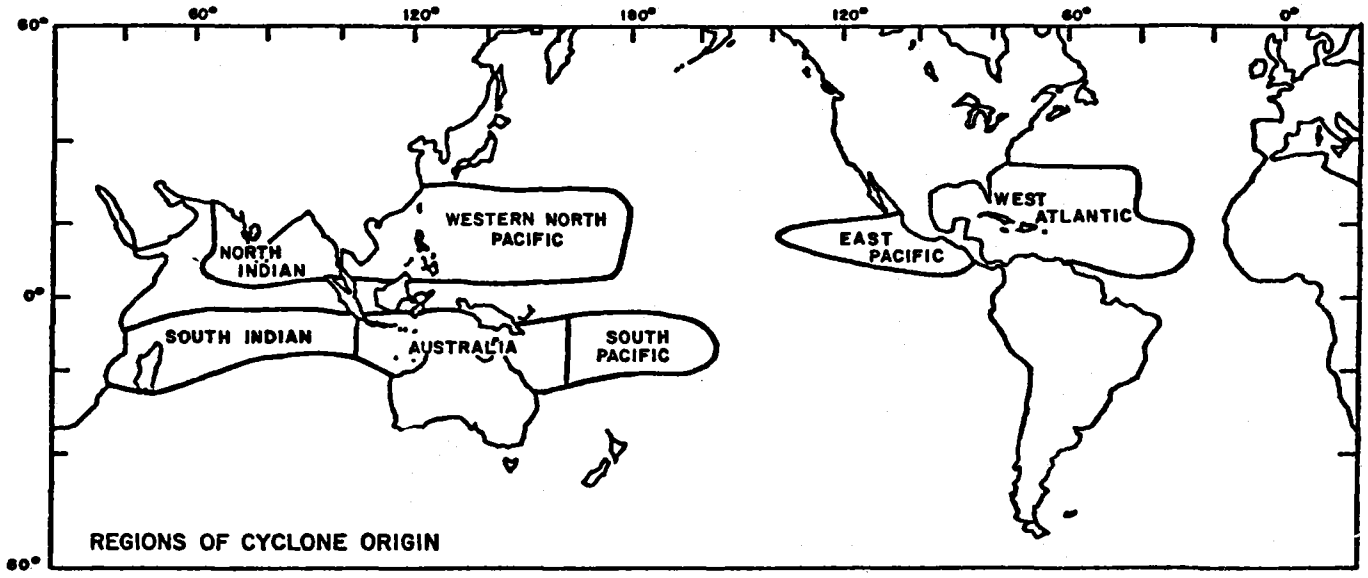

Figure 7: Ocean basins where tropical cyclones are generated (from Gray, 1978)

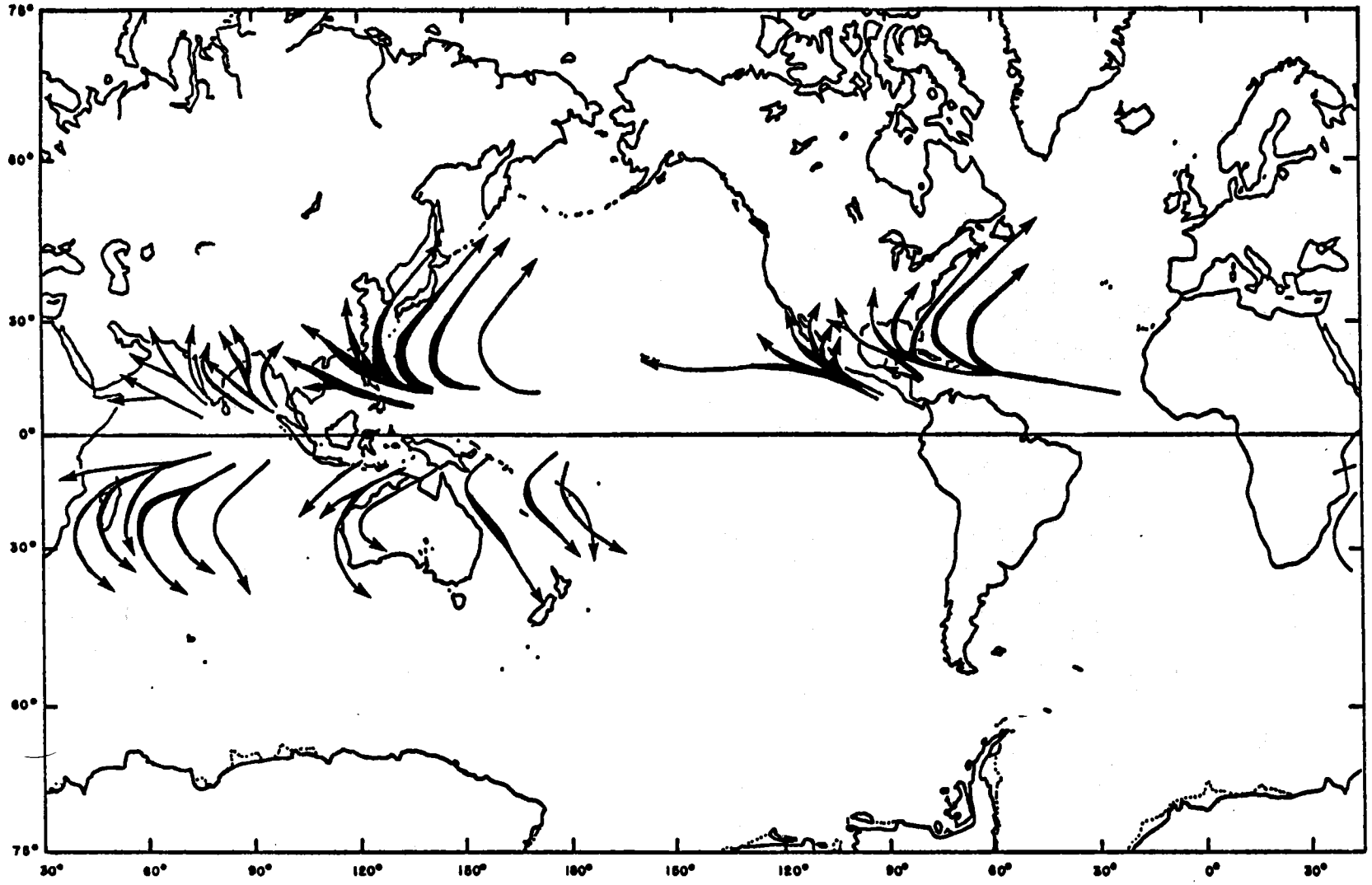

Figure 8: Preferred annual tropical cyclone tracks. Arrow widths are proportional to storm frequencies along indicated paths (from Gray, 1978)

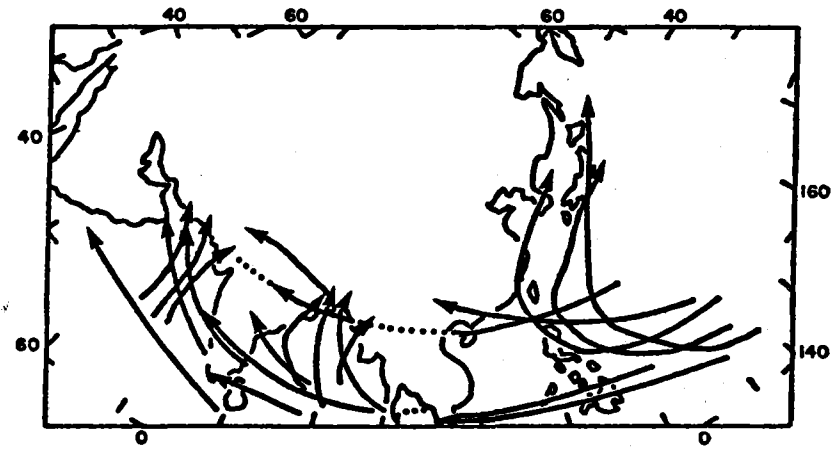

Figure 9: Tropical cyclone tracks across Asia (from Haurwitz and Austin, 1944)

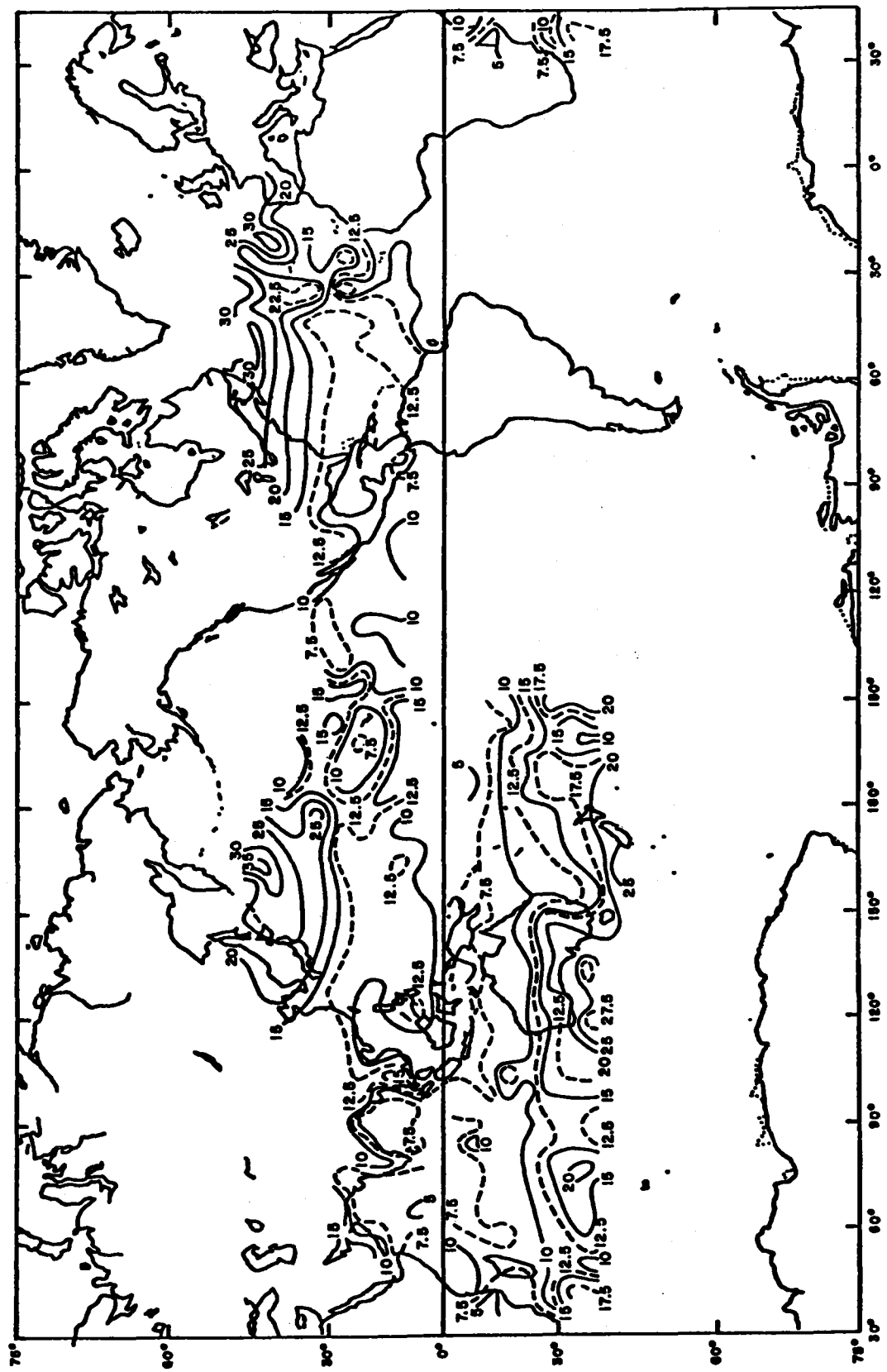

Figure 10: Average (for annual data) speeds, in knots, of storm movement (from Crutcher and Quayle, 1974)

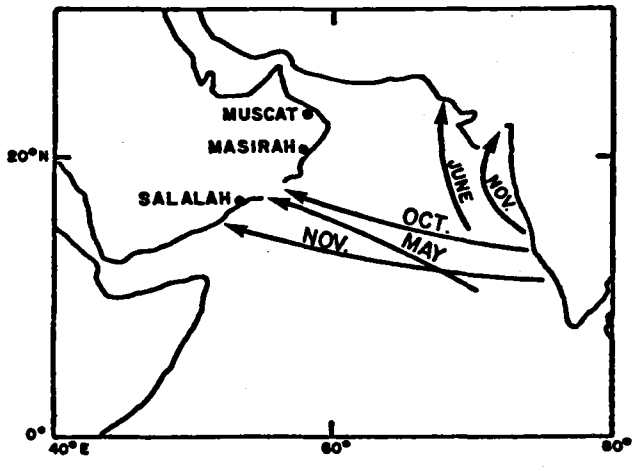

Figure 11: Common tracks of Arabian Sea cyclones (from Pedgley, 1969)

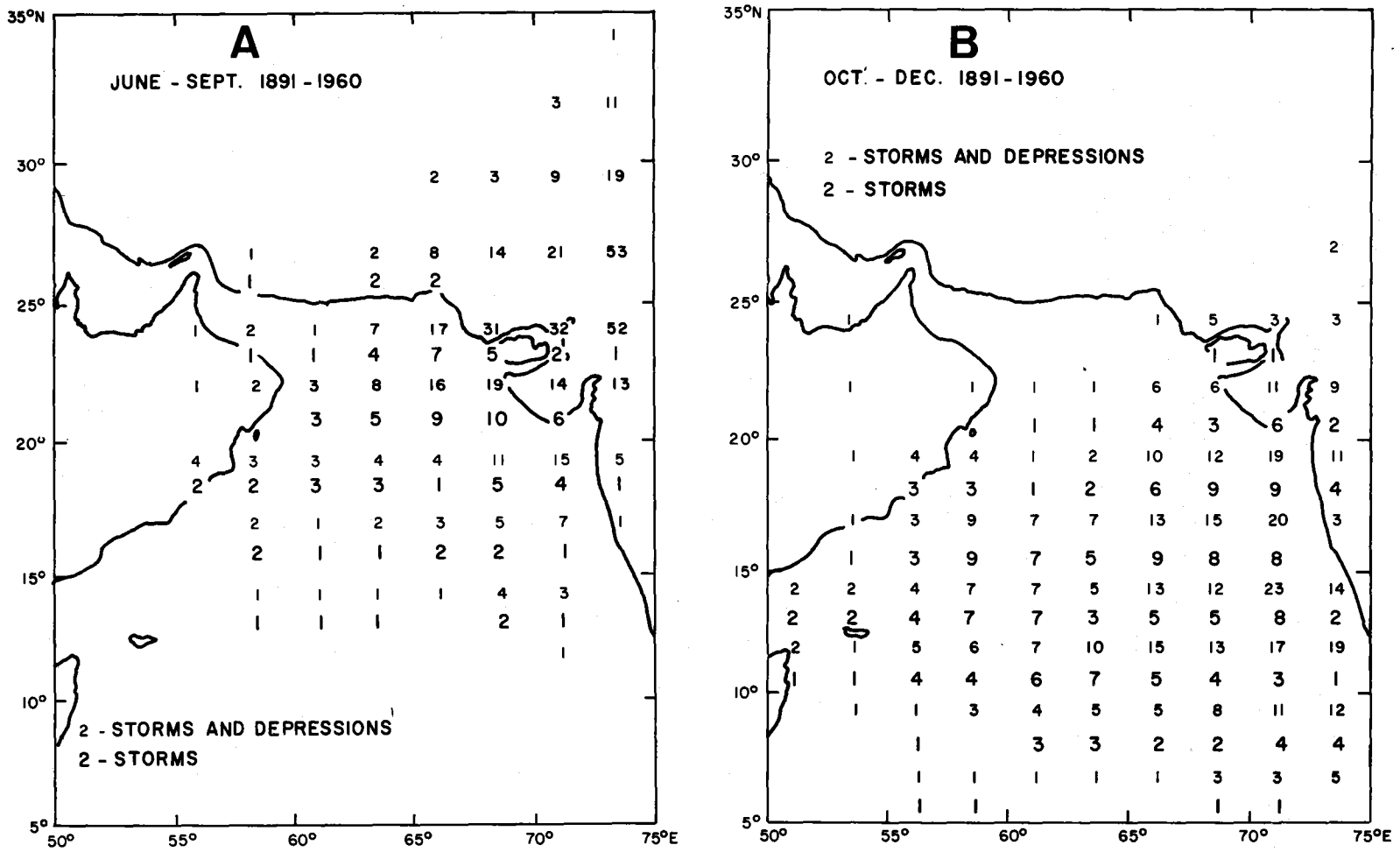

Figure 12: Frequency of formation and dissipation of storm and depressions (1891 - 1960): a) June to September, and b) October to December (from Rao, 1981)

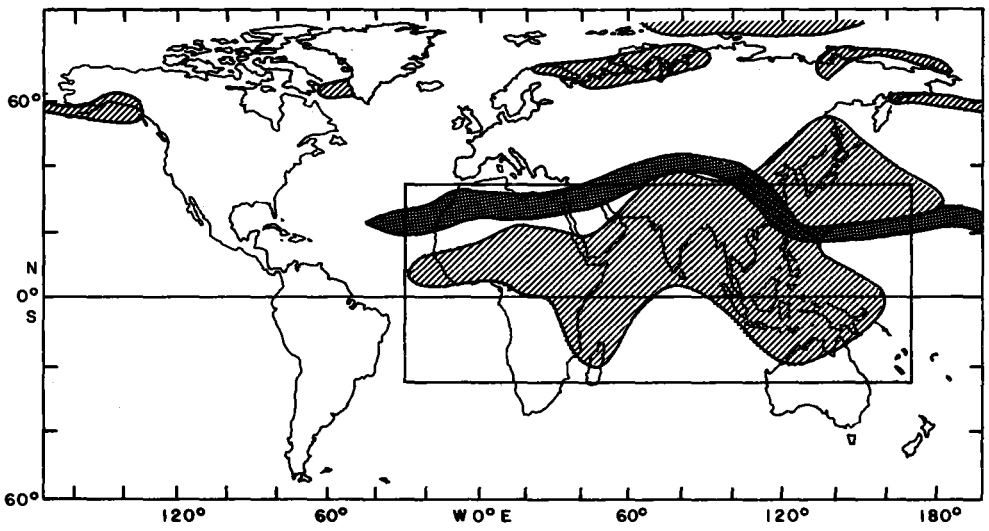

Figure 13: Delineation of the Monsoon regions of the globe. Hatched areas are defined by the first three criteria for a monsoonal regime, whereas the heavy line marks the northern limit of the fourth criterion. The rectangle encloses the Monsoon region (from Ramage, 1971)

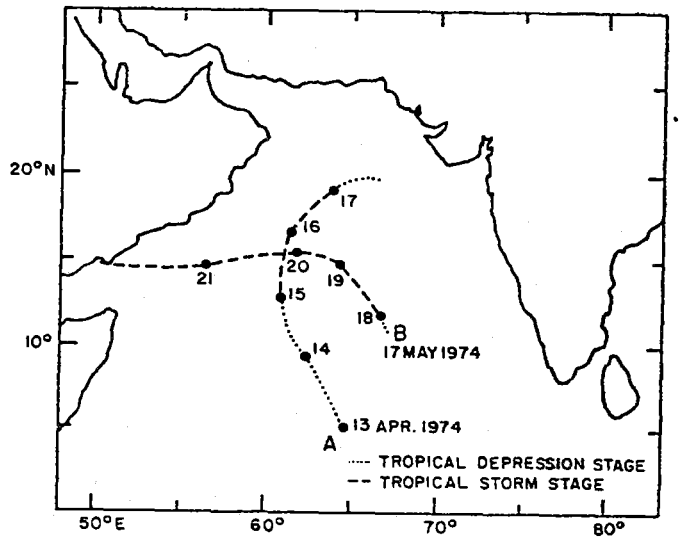

Figure 14: Tropical storms that originated in the Arabian Sea during the spring transition of 1974. Storm A: 13-17 April; Storm B: 17-21 May (from Mariner's weather log, 1974)

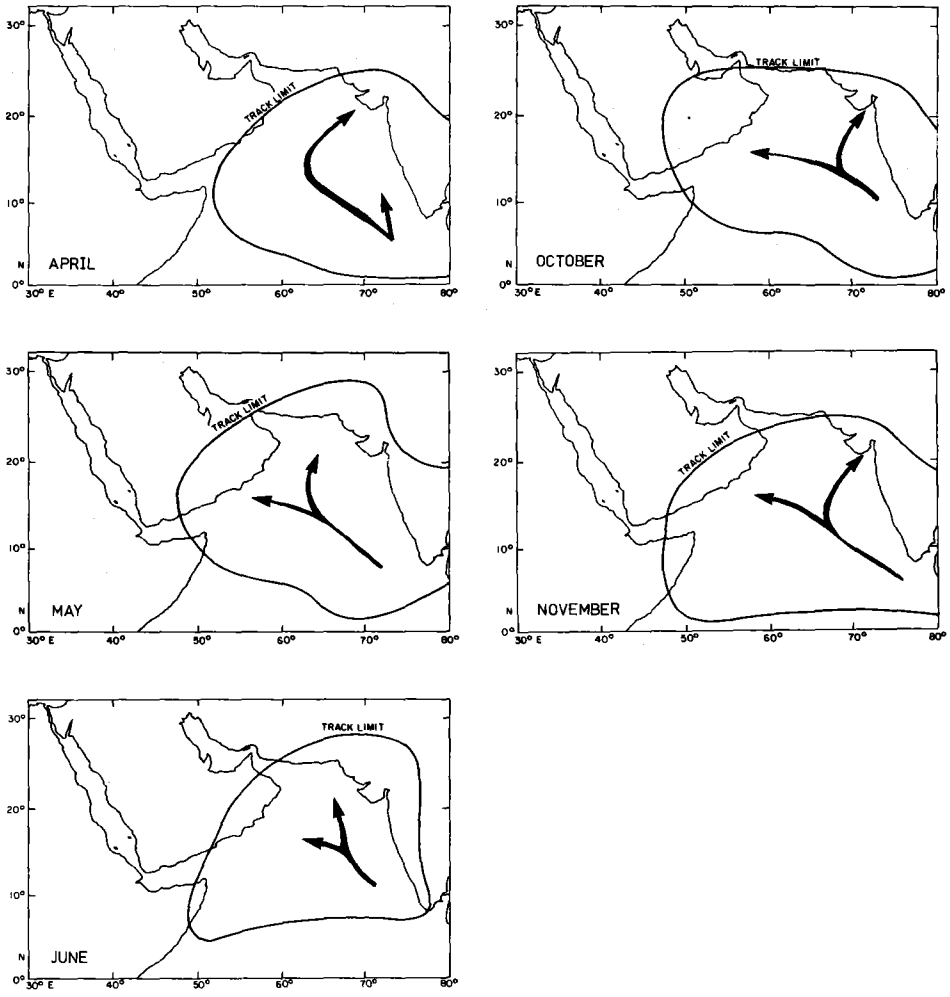

Figure 15: Mean tropical storm tracks for the Arabian Sea (from U.S. Naval Weather Service Command, 1974)

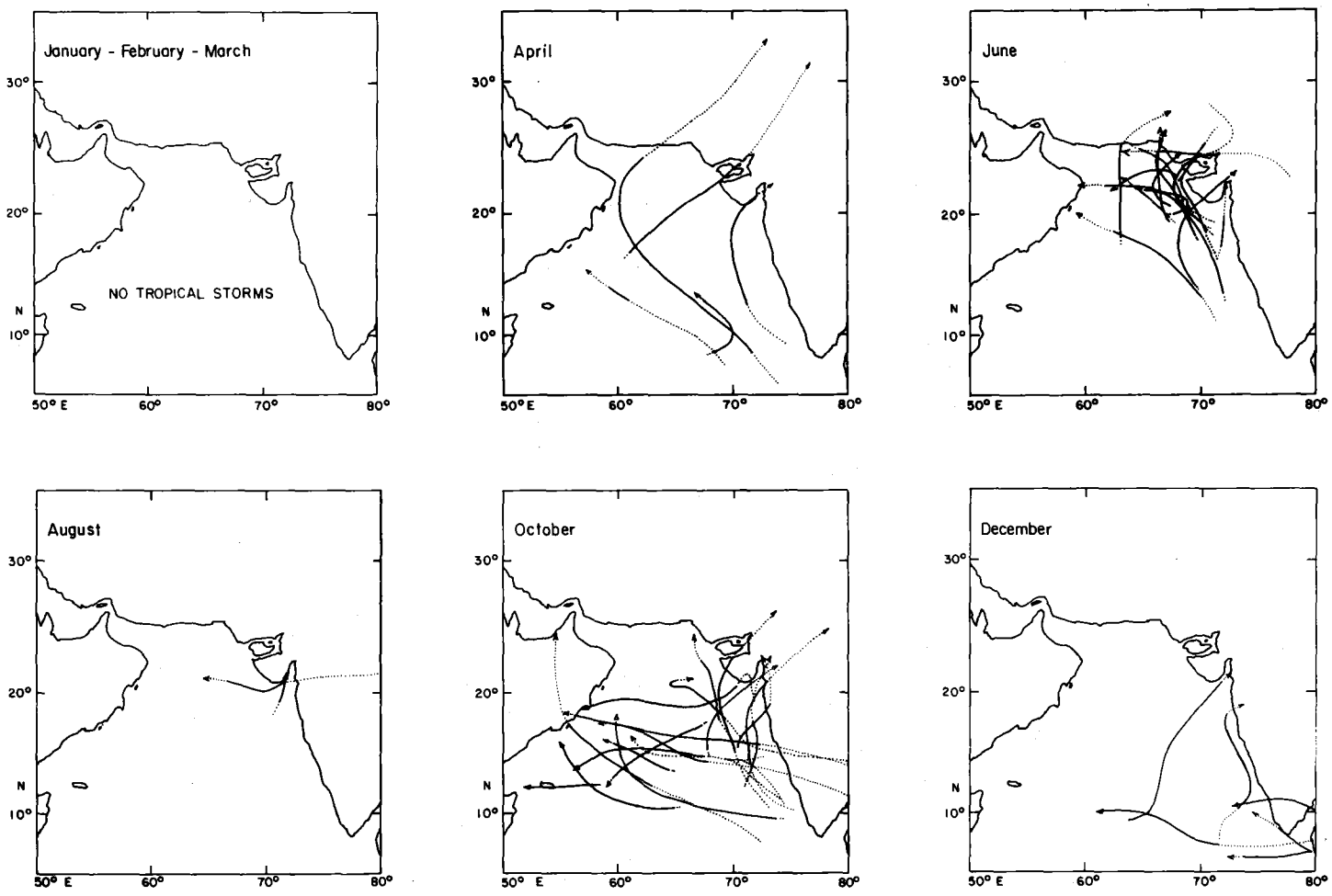

Figure 16: Tracks of tropical cyclones which reached tropical storm intensity in the Arabian Sea (dotted line indicates depression stage). The period of record is 1891-1970

MODELLING OF MOVEMENT OF OIL SLICKS IN THE INNER GULF OF THE KUWAIT ACTION PLAN REGION DURING STORMY PERIODS: APPLICATION OF THE NOWRUZ SPILL

by

T.S Murthy
Institute of Ocean Sciences, Sidney, B.C., Canada
and M.I. El-Sabh
Université du Quebec a Rimouski, Québec, Canada

ABSTRACT

A time dependent, two dimensional numerical model has been developed to simulate the movement of oil slicks in the Gulf. Initially, the oil is assumed to spread under the action of gravity, inertia and surface tension forces, but most of the movement is due to the currents in the water column due to wind-driven circulation and tides. The output from tidal and storm surge numerical models for the Gulf are used as input for the oil slick model which computes the trajectory, as well as the area by the oil slick, as a function of time. A two-dimensional square grid of 15 km size was used with 59 x 37 grid points and a time step of six minutes was used in the numerical integration. To approximately simulate the movement of the oil slick in the Gulf that occured during March-April 1983 at the time of a meteorological situation known as "Shamal", realistic values for the amount of crude oil being discharged into the water (about one thousand metric tons per day) as well as appropriate valued for the winds and tides were used. The numerically simulated results show reasonable agreement with the observations. It is concluded that wind is the primary agent in the movement of oil slicks.

INTRODUCTION

The Gulf is a semi-enclosed sea measuring 1000 km in length and varies in width from a maximum of 340 km to a minimum of 60 km in the Strait of Hormuz (Figure 1). It has an area of 226,000 km2 whereas its average depth is about 35 m. The important topographic feature is the deep water near the Iranian Coast and shallow areas in the southern parts of the coasts of Saudi Arabia, Qatar and United Arab Emirates. Grasshoff (1976), Hughes and Hunter (1979) and Hunter (1982) reviewed the physical oceanography of the Gulf. The oceanographic conditions in the Gulf vary drastically from summer to winter. High evaporation, low rainfall and limited exchange with the Indian Ocean lead to salinity valued in excess of $40^{o}/_{oo}$ and may rise to $50^{o}/_{oo}$ in the shallow coastal areas. The Gulf undergoes wide and rapid temperature changes in response to daily and seasonal cycles of heating and cooling. As with salinites, the highest water temperatures are found in the shallow bays and lagoons where the annual temperatures can range from 15*C in winter to 40*C in summer. Even well offshore temperature can range from 18*C in winter to 36*C in summer. Water circulation in the Gulf is governed by three factors: water movements resulting from evaporation; tidal currents and wind driven currents.

The extensive oil drilling and transportation activities in the Gulf increased the possibility of oil spills and consequent threat of oil pollution to the regional ecology. For example, in August and October 1980, two large oil spills occurred in the Gulf involving respectively about 3000 and 7000 metric tons (Lehr and Belen, 1982). More recently, in March 1983, another major oil spill occurred.

There is a large amount of literature on oil spills and simulation of their movements in various water bodies on the globe. We will not attempt to review all the literature but mention only those works dealing with oil spills in the Gulf. Most of the oil slick models for the Gulf were developed by the Water and Environment Division, Research Institute, of the University of Petroleum and Minerals, Dharan, Saudi Arabia. A series of numerical models referred to as GULFSLIK-I,II,III,IV were developed. These models are quite sophisticated and include the movement of the oil not only due to the primary forces (wind and tide) but also include spreading due to inertia, gravity, viscosity, surface tension, evaporation, etc. Also effects of weathering and turbulence are included. The simulations compared well with two actual spill events (Lehr, et al., 1981; Cekirge and Lehr, 1981; Lehr and Cekirge, 1980; Lehr et al., 1982). In these models, the Gulf was devided into 72 blocks with each block being 0.5 degree latitude in length and 0.5 degree longitude in width.

The present study describes a two-dimensional time-dependent numerical model to simulate the spreading and movement of oil slicks similar to the recent one which occurred in March 1983 at the Nowruz oil field. The model includes topography, movement due to wind-generated currents and tides, and the spreading due to gravity, inertia and viscosity.

Galt et al. (1984) and Lehr et al. (1983) simulated the movement of the Nowruz oil slick. Our work differs from these two models mainly in the manner in which the meteorological forcing terms are incorporated. We paid particular attention to the fact that most of the initial spreading occurred during a meteorological situation known as a winter "shamal". Since as is shown here that wind-generated currents are the primary mechanism for the movement of oil slicks, the meteorological forcing terms, deserve special attention in the oil slick models.

THE NUMERICAL MODEL

A two dimensional square grid model was developed for the Gulf which uses the Strait of Hormuz as an open boundary. Figure 2 shows the grid used for this model with 59 grid points along the length and 37 points along the width, the grid size being 15 km.

With reference to a cartesian coordiante system with horizontal x,y axes and the vertical z axis pointing upwards and with the origin of coordinates at the equilibrium level of the water surface, the linearized forms of the continuity equation and the momentum equations in the depth-averaged form are:

$$\frac{\partial \eta}{\partial t} = -\frac{\partial}{\partial x}(du) - \frac{\partial}{\partial y}(dv) \qquad (1)$$

$$\frac{\partial u}{\partial t} = -g\frac{\partial \eta}{\partial x} + fv - F^{(u)} + G^{(u)} \qquad (2)$$

$$\frac{\partial v}{\partial t} = -g\frac{\partial \eta}{\partial y} - fu - F^{(v)} + G^{(v)} \qquad (3)$$

where $\eta(x,y.t)$ = water surface elevation with reference to its equilibrium position; $u(x,y,t)$, $v(x,y,t)$ are the depth-average velocities in the x and y directions; $d(x,y)$ is the water depth; f is the Coriolis paramenter; g is gravity and t is time.

For the bottom friction terms $F^{(u)}$ and $F^{(v)}$, the following quadratic forms are used:

$$F^{(u)} = ku\,(u^2+v^2)^{\frac{1}{2}}/d; \quad F^{(v)} = kv\,(u^2+v^2)^{\frac{1}{2}}/d \qquad (4)$$

with the friction coefficient k being given a value of 0.0025. The terms $G^{(u)}$ and $G^{(v)}$ represent the forcing from surface wind stress.

Figure 3 shows the scheme for the finite-difference forms of the above equations. It should be noted that the grid points shown in Figure 2 form of the corner points of Figure 3. With reference to Figure 3, the finite difference forms of equations 1 to 3 are as follows:

$$\eta_{ij}^{t+\Delta t} = \eta_{ij}^{t} - \frac{\Delta t}{2\cdot\Delta x}\left\{[u_{i+1,j}^{t}\,(d_{ij}+d_{i+1,j})] - [u_{ij}^{t}\,(d_{i-1,j}+d_{ij})]\right\}$$
$$- \frac{\Delta t}{2\cdot\Delta y}\left\{[v_{i,j+1}^{t}\,(d_{ij}+d_{i,j+1})] - [v_{ij}^{t}\,(d_{i,j-1}+d_{ij})]\right\} \qquad (5)$$

$$u_{ij}^{t+\Delta t} = u_{ij}^{t} - \frac{g}{\Delta x}(\eta_{ij}^{t+\Delta t} - \eta_{i-1,j}^{t+\Delta t}) + f\tilde{v}_{ij}^{t} - F_{ij}^{(u)^t} + G_{ij}^{(u)^t} \qquad (6)$$

$$v_{ij}^{t+\Delta t} = v_{ij}^{t} - \frac{g}{\Delta y}(\eta_{ij}^{t+\Delta t} - \eta_{i,j-1}^{t+\Delta t}) - f\tilde{u}_{ij}^{t+\Delta t} - F_{ij}^{(v)^t} + G_{ij}^{(v)^t} \qquad (7)$$

where Δt = time step

$\Delta x, \Delta y$ = grid interval sizes in x,y directions respectively

d_{ij} = mean water depth at elevation point η_{ij}

$$\tilde{u}^t_{ij} = \frac{1}{4}\left[u^t_{i,j-1} + u^t_{i+1,j-1} + u^t_{ij} + u^t_{i+1,j}\right] \quad (8)$$

$$\tilde{v}^t_{ij} = \frac{1}{4}\left[v^t_{i-1,j} + v^t_{ij} + v^t_{i-1,j+1} + v^t_{i,j+1}\right] \quad (9)$$

The time step used in the numerical integration was the period of the M_2-tide divided by 125 which is 357.7 seconds (approximately 6 minutes). This is less than the 8 minutes maximum value for the time step as required by the C-F-L stability criterion (Courant-Friedrichs-Lewy stability criterion).

At the land boundaries, the flow normal to the coast is specified as zero. At the open boundary in the Strait of Hormuz, the tide is specified from observations. The Gulf is small enough so that the independent tide (i.e. due to tidal potential) in the Gulf is negligible and only the co-oscillating tide with the Arabian Sea through the Gulf of Oman was considered. The observed tides at Hangam Island and Khor Kawi were specified (table 1) and linear interpolation was used for the grid point in between.

The tidal currents, used as input for the oil slick model were obtained from the output of a two-dimensional time-dependent munerical tidal model from the Gulf. This tidal model uses ;the same grid system as shownin Figure 2 and includes the six most important tidal constituents, namely M_2, S_2, N_2, K_1, O_1, and P_1. Figures 4 and 5 respectively'show the tidal current patterns for M_2 only and the six constituents together. Previous computer models of the tides in the Gulf (von trepka, 1968; Evans-Robert, 1979; Lardner et al., 1982; Pelissier et al., in preparation) have been quite succesful in predicting the observed surface elevations. As there is little observational data on tidal currents in the Gulf, verification of the velocity predictions of these models is difficult.

The March 1983 oil spill occurred during a synoptic situation referred to as a winter shamal and this has been use to specify the wind stress. Figure 6 shows the general pattern of winds over the Gulf area. The wind forcing terms in equations 6 and 7 are defined as follows:

$$G^{(u)t}_{ij} = \frac{2\, u^t_i \cos A_i}{\rho_w\,(d_{i-1,j}+d_{ij})} \quad (10)$$

$$G^{(v)t}_{ij} = \frac{2\, u^t_i \sin A_i}{\rho_w (d_{i,j-1}+d_{ij})} \quad (11)$$

where ρ_w is the water density (kgm m^{-3}), u^t_I is the wind at the point i at time t (pascals)1/ and A_i is the angle of the wind vector at point i from the x-axis in a counter-clockwise direction. The shamal moves from west to east as shown in Figure 4 and the time-dependence of the wind field is specified as follows:

1/ Pascal corresponds to 60 km/h

$$u_i^t = \begin{cases} 0 \quad \text{for all } i > k \\ u_{max} \{\sin^2 [\frac{\pi}{2} \frac{(k-i)}{n_1}\} , \quad (k-i) = 1 \text{ to } n_1 \\ \qquad\qquad \text{for } i \le k \\ u_{max} \{\sin^2 [\frac{\pi}{2} (1 - \frac{n_2 - (k-i)}{n_2}]\} , \quad (k-i) = n_1 \text{ to } n_2 \\ \qquad\qquad \text{for } i \le k \end{cases}$$

where $i = 1,n$; k = time step · $t = k \cdot \Delta t$

The wind direction A_i is specified as follows:

$$A_i = A_1 + \frac{(i-1)}{m} (A_m - A_1) \qquad (13)$$

where A_1 = angle defined at i=1

A_m = angle defined at i=m

MOVEMENT AND SPREADING FO THE OIL SLICK

We simulated here an oil spill of 1000 metric tons per day (7000 barrels per day) which corresponds to the March 1983 spill. In each time step the movement due to hydrodynamic forces (tide and wind) and the spreading due to gravity, inertia, viscosity and surface tension are computed and the results are presented as trajectories of the oil slick movement as well as an envelope of the spreading slick. In the model, it was assumed that when the oil slick hits land it does not spread any further. It is also assumed that the slick moves with the same speed as the water current (vertically integrated) due the wind. Furthermore, the oil moves with the same speed and direction as the tidal current.

As for the spreading of the slick due to inertia under the effect of gravity, it is assumed that (Ages, 1983) this spreading operates only during the 1st hour after the spill and the following formula is used:

$$\ell_1 = \tfrac{1}{2} (\Delta g \cdot v t^2)^{\frac{1}{4}} \qquad (14)$$

where ℓ_1 is the radius of spreading and

$$\Delta = (\rho_w - \rho_{oil})/\rho_w = 0.10 \qquad (15)$$

where ρ_w is water density, ρ_{oil} is the oil density g is gravity, v is the volume of oil spill in cubic meters (1 ton of oil ~ 7 barrels ~ 1.12 m^3) and t is time since the oil spill started.

The spreading due to viscosity is applied only during the first 6 hours after the spill and the radius ℓ_2 of spreading is given by

$$\ell_2 = \tfrac{1}{2} (\Delta g \cdot v^2 \cdot t^{3/2} / \upsilon^{\frac{1}{2}})^{1/6} \qquad (16)$$

where Δ , g, v, t, are the same as in (14) and υ is the kinematic viscosity of oil ($1.4 \times 10\text{-}6$ m^2/s).

The spreading due to surface tension is assumed to act at all times and the radius of preading ℓ_3 is given by

$$\ell_3 = \tfrac{1}{2} (\sigma^2 t^3/\rho^2 \upsilon)^{\frac{1}{4}} \qquad (17)$$

where σ is the surface tension of oil on water (0.02 newtons/m) and the density ρ of sea water is taken as 1025 kgm/m^3.

DISCUSSION OF THE RESULTS

In the numerical experiments. a patch of oil is released at the beginning of each M_2 tidal cycle, with a total relaease of 1000 metric tons per day. Figure 7a shows the positions of the first patch of oil at the beginning of the next seven M_2 tidal cycles. Note that in this simulation, the wind field and the M_2 tide only are included. Figure 7b shows the corresponding envelope of the oil slick for this case. The positions of not only the first patch but the next seven oil patches (assuming that an equal amount of oil is released at the beginning of each M_2 tidal cycle) for the same wind and tidal conditions is shown in Figure 7c. The patterns of Figures 7a would be identical, but for the influence of the wind. The numerical experiment is repeated with the same wind coditions, but instead of just including the M_2 tide, we included five other tidal consituents namely S_2, N_2, K_1, O_1 and P_1. The results of this simulation are shown in Figure 8 in a manner similar to that in Figure 7. A comparison between Figures 7b and 8b shows that the influence of the additional tidal constituents is to make th slick envelope somewhat narrower.

In order to determine the influence of wind, a third numerical experiment consisted of simulations with only the six tidal constituents and no wind. Figure 9 shows the position of the oil slick after every M_2 tidal cycle for a total of eight cycles. It can be seen that the movement of the oil slick is not significant compared to its movement when a wind field was included as shown in Figure 8. Thus one can conclude that the wind field is the primary agent in causing the oil patch to move and any future oil slick movement simulations for the Gulf provide for an accurate wind field to be specified.

Figure 10 shows a satellite photograph of the oil slick in the Gulf taken in April 1983 (about three months after the start of the spill. As can be seen the slick has broken into three parts, with the major part being closer to the source of spill. Although direct comparisons cannot be made with our simulation because our numerical simulation covers only about four days, it can be seen from a comparison of Figures 8 and 10 that the movement pattern of the slick is reasonably well simulated.

SUMMARY

The present study describes the simulation of the movement and spreading of oil slicks in the Gulf during a stormy period similar to the event of the March 1983 spill. The model is two-dimensional, time-dependent and incorporates topography, tides, and wind-induced circulation. The model is reasonably satisfactory for the Gulf, but the 15 km grid used here is not small enough either to include the Strait of Hormuz or to obtain detailed simulations in the shallow parts of the Gulf.

It is proposed here that a better way of modelling the Gulf and the Gulf of Oman, including the Strait of Hormuz, is through the development of an irregular triangular grid model for the whole area. Figure 11 shows a regular triangular grid for the Strait of Hormuz and it can be seen that indeed such a grid will provide enough resolution. Irregular triangular grid allows for bigger triangles in the deep water where one does not need fine resolution. The computations could be done in the finite-difference framework with which the oceanographic modellers are familiar with and not in the finite-element scheme. Our previous experience with multiple grids (telescopic grids) shows that, from a numerical point, use of irregular triangular grid gives better results.

ACKNOWLEDGEMENTS

We thank Mike Rasmussen for computer assistance and Jocelyne Gagnon for typing the manuscript.

REFERENCES

Ages, A. (1983) Personnel communication. Intitute of Ocean Sciences, Sidney, BC. Canada.

Cekirge, H.M. and W.J. Lehr (1981) Fate and threat of Oil Slicks in the Arabian Gulf. Amer. Soc. Mech. Engng. (in press).

Evans Robert, D.J. (1979) Tides in the Persian Gulf. The consulting Engng.

Grasshoff, K. (1976) Review of hydrographic and productivity conditions in the Gulf region. In: Marine Sciences in the Gulf Area. UNESCO Tech. Papers in Marine Science, 26:39-62.

Hughes, P. and J.R. Hunter (1979) Physical oceanographic and numerical modelling of the Kuwait Action Plan Region. UNESCO Division of Marine Sciences, Rept. MARINE/27 106 p.

Hunter J.R. (1982) The physical oceanography of the Arabian Gulf: A review and theoretical interpretation of previous observations. Proc. First Arabian Gulf Conference on Environment and Pollution, Kuwait, (in press).

Lardner, R.W., M.S. Belen and H.M. Cekirge (1982) Finite-difference model for tidal flows in the Arabian Gulf. Joint Oceanographic Assembly, Halifax, N.S. Canada.

Lehr W.J. and M.S. Belen (1982) The fate of two large oil spills in the Inner Gulf. Unpublished Manuscript.

Lehr, W.J. and H.M. Cekirge (1980) Oil slick movements in the Arabian Gulf. Proc. Petromar-80 - Petroleum and Marine Environment Conf., Monaco, pp. 677-683.

Lehr, W.J., M.S. Belen and H.M. Cerkige (1981) Simulated oil spills at two offshore fields in the Arabian Gulf. Mar. Poll. Bull., 12:737-741.

Lehr, W.J., M.S. Belen, H.M. Cekirge and N. Gunay (1982) GULFSLIK - An oil spill modelling program for the Arabian Gulf. Proc. First Arabian Gulf Conf. on Environment and Pollution, Kuwait, (in press).

Pelissier, M., M.I. El-Sabh and C. Le Provost (in preparation) Tides in the Arabian Gulf: Spectral analysis and modelling.

Von Trepka, L. (1968) Investigation of the tides in the Persian Gulf by means of a hydrodymanic-numerical model. Proc. Symposium on Mathematical-Hydrodynamical Investigations of the Physical Processes in the Sea. Institut für Meereskunde der Universität Hamburg, 10:59-63.

Table 1: Amplitudes (cm) and Phases (in degrees with reference to Time zone-4) for the six most important tidal constituents in the Strait of Hormuz.

Station	M_2		S_2		N_2		K_1		O_1		P_1	
	Amp.	Phase	Amp.	Phase	Amp.	Phase	Amp.	Phase	Amp.	Phase	Amp.	Phase
Hangam Island	73.8	320	25.0	007	17.4	292	29.0	088	20.4	070	09.4	088
Khor Kawi	68.9	309	25.3	347	17.4	286	26.2	070	15.8	067	08.5	070

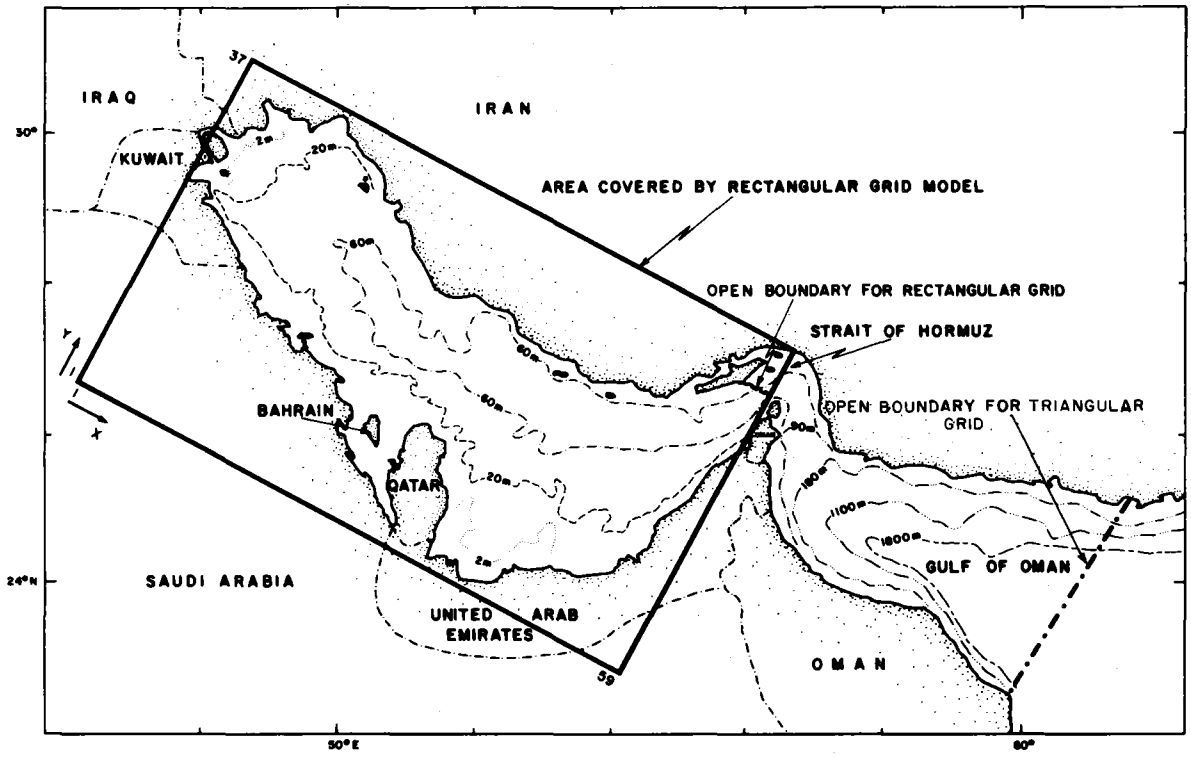

Figure 1: Geography and bathymetry of the Inner Gulf.

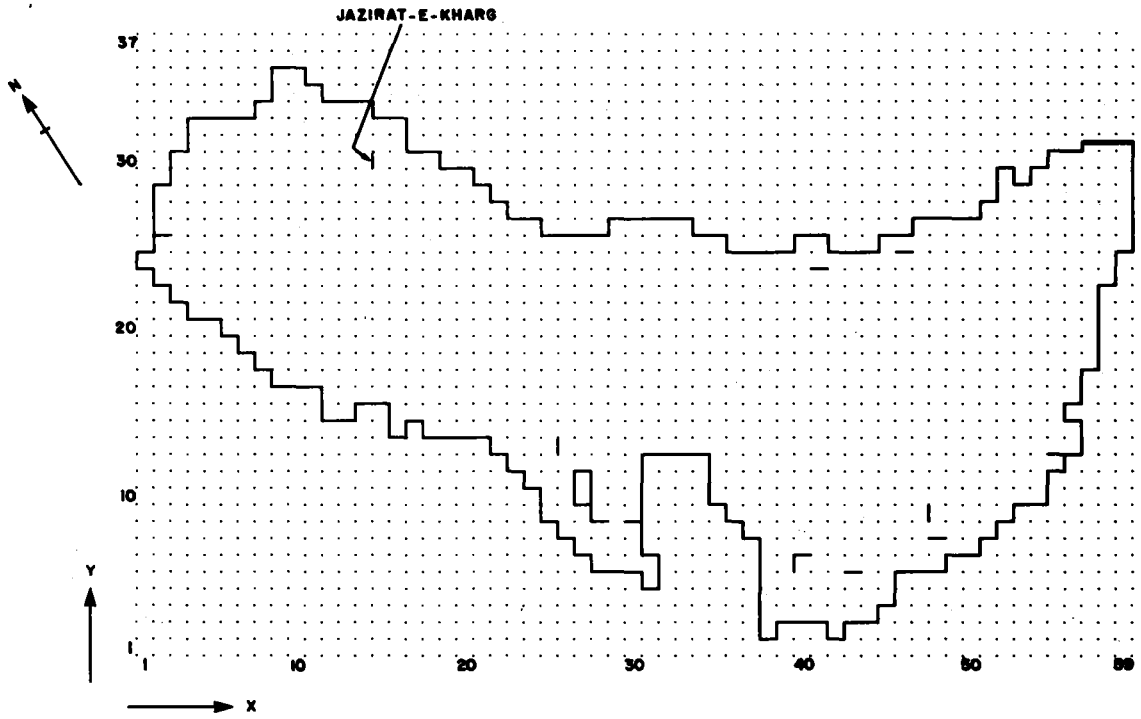

Figure 2: Grid for the numerical model.

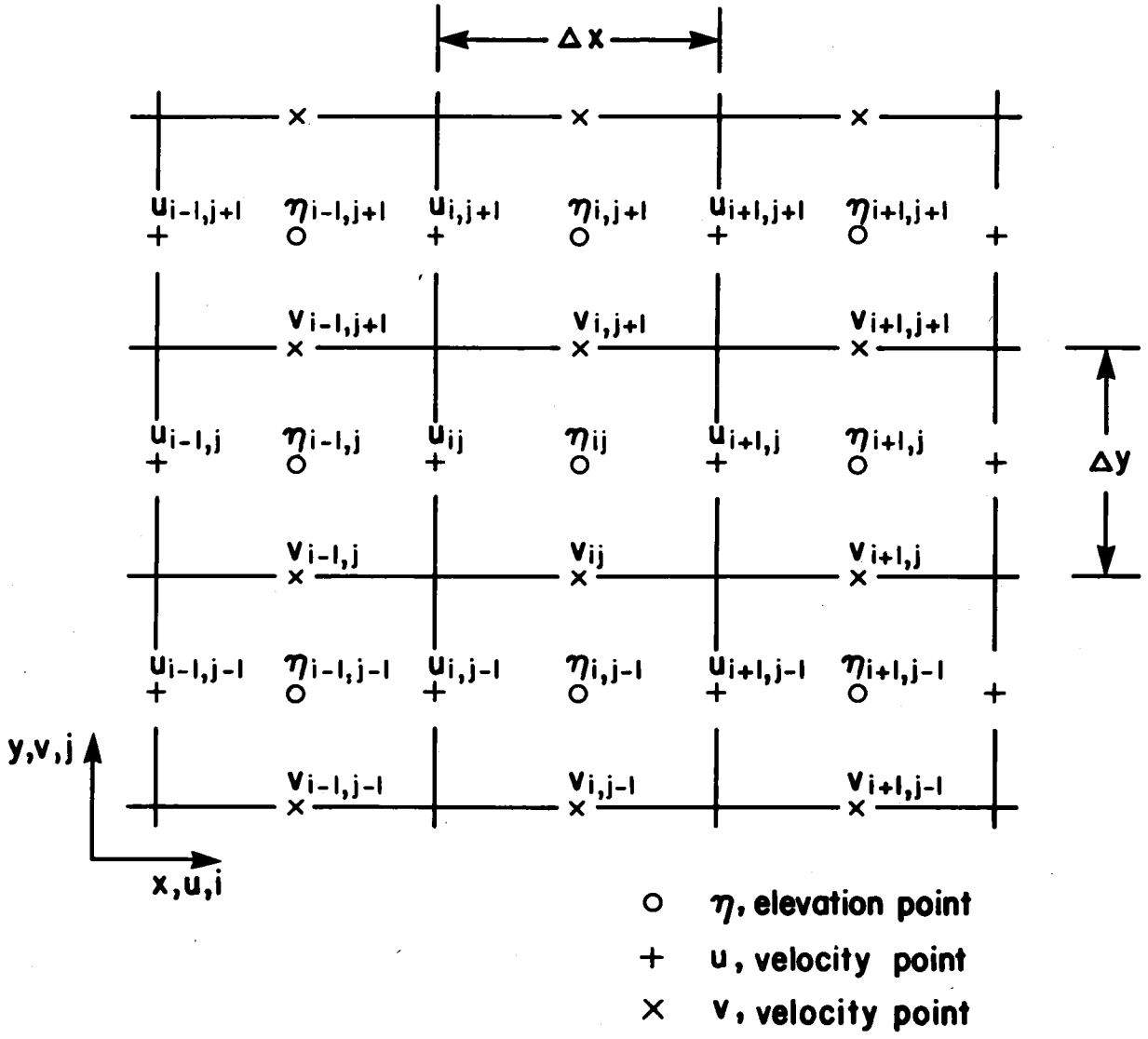

Figure 3: Notation used in the finite-difference scheme.

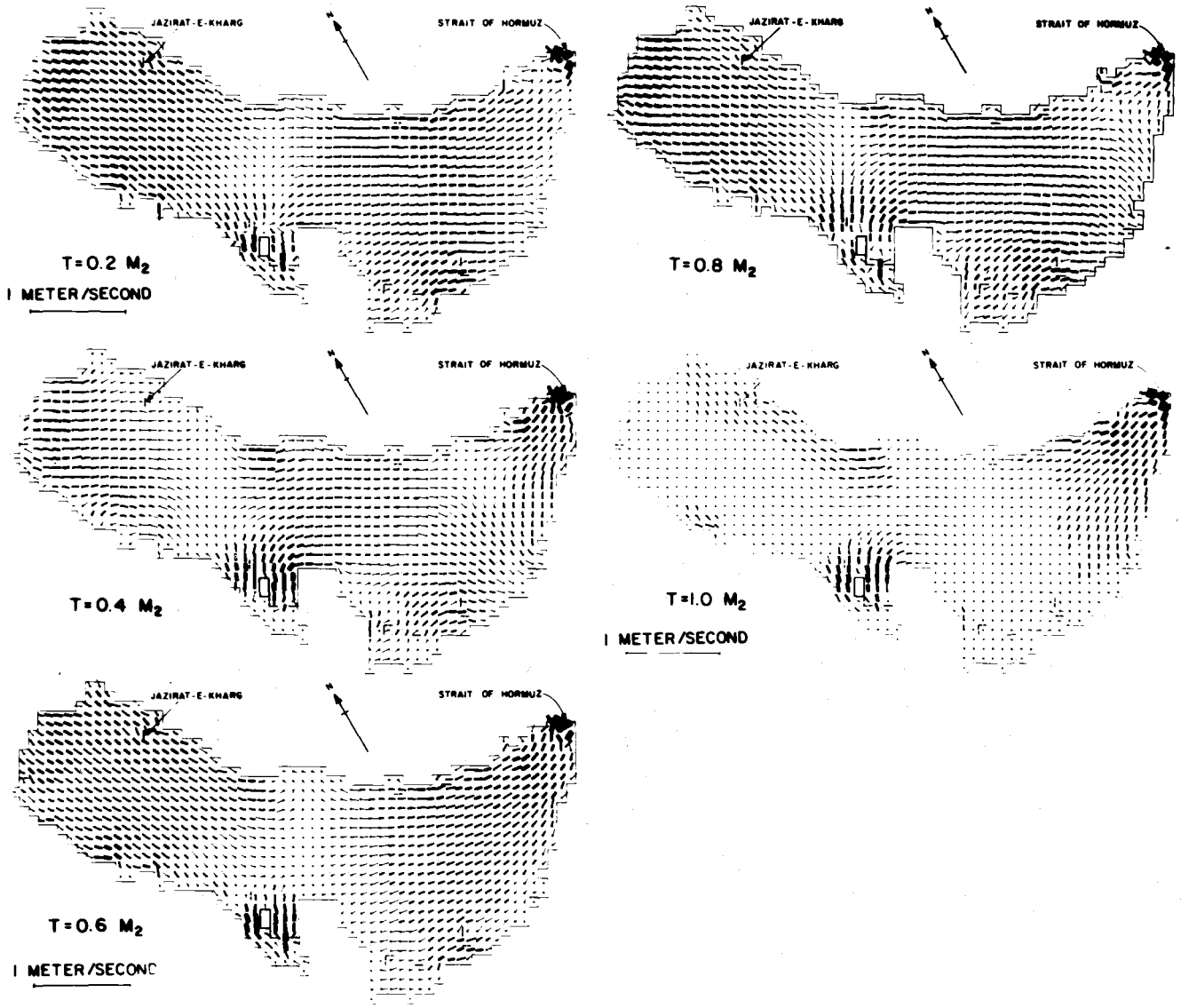

Figure 4: Currents in the Inner Gulf due to the M_2 tide.

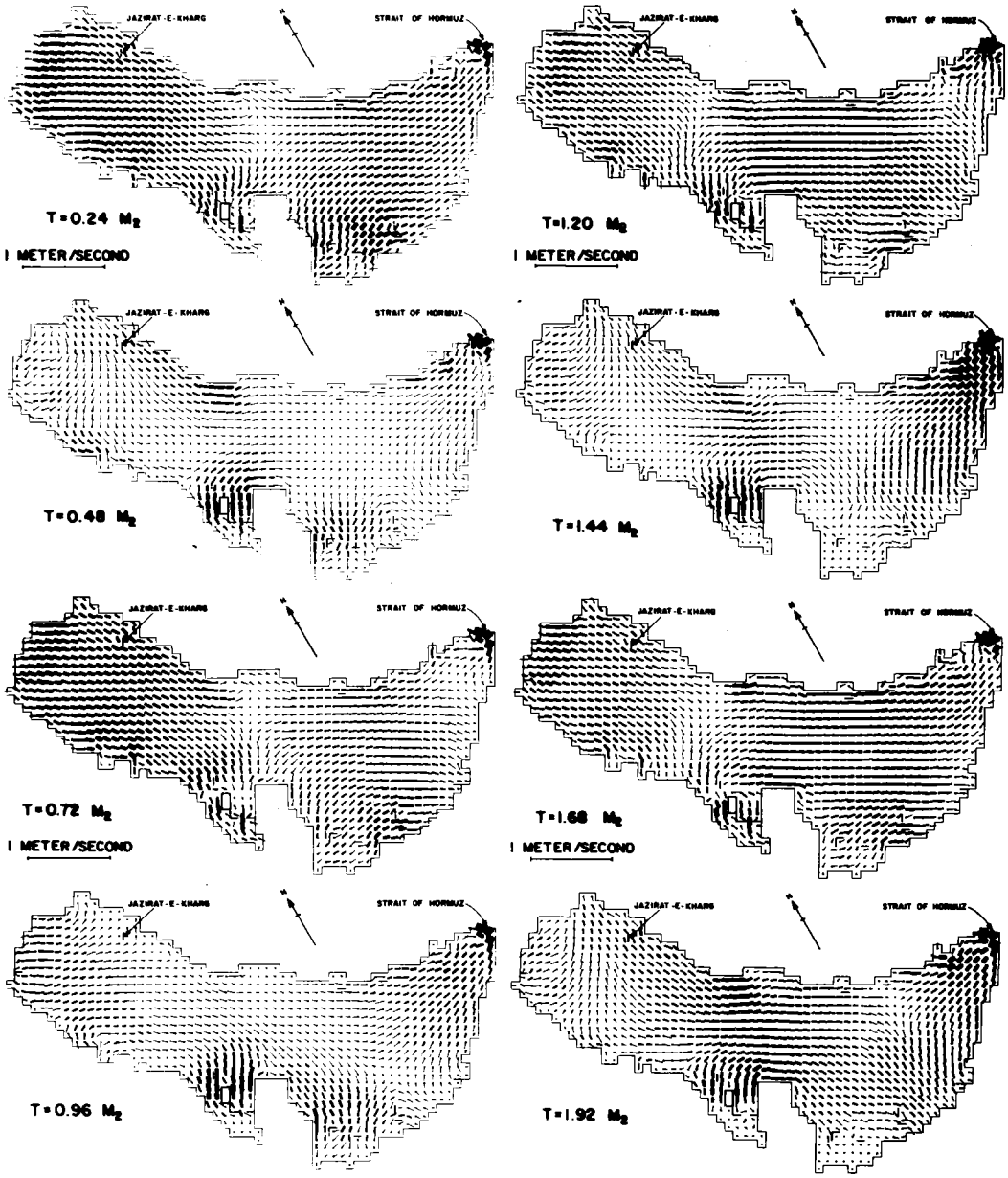

Figure 5: Currents in the Inner Gulf due to the six tidal constituents M_2, S_2, N_2, K_1, O_1, P_1.

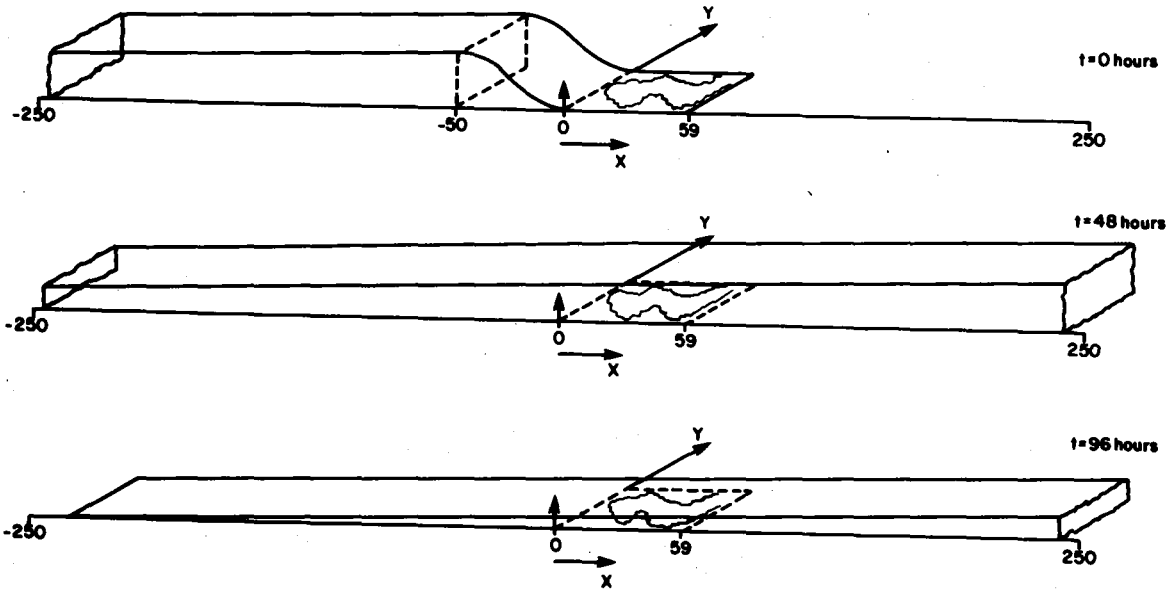

Figure 6: Wind field configuration.

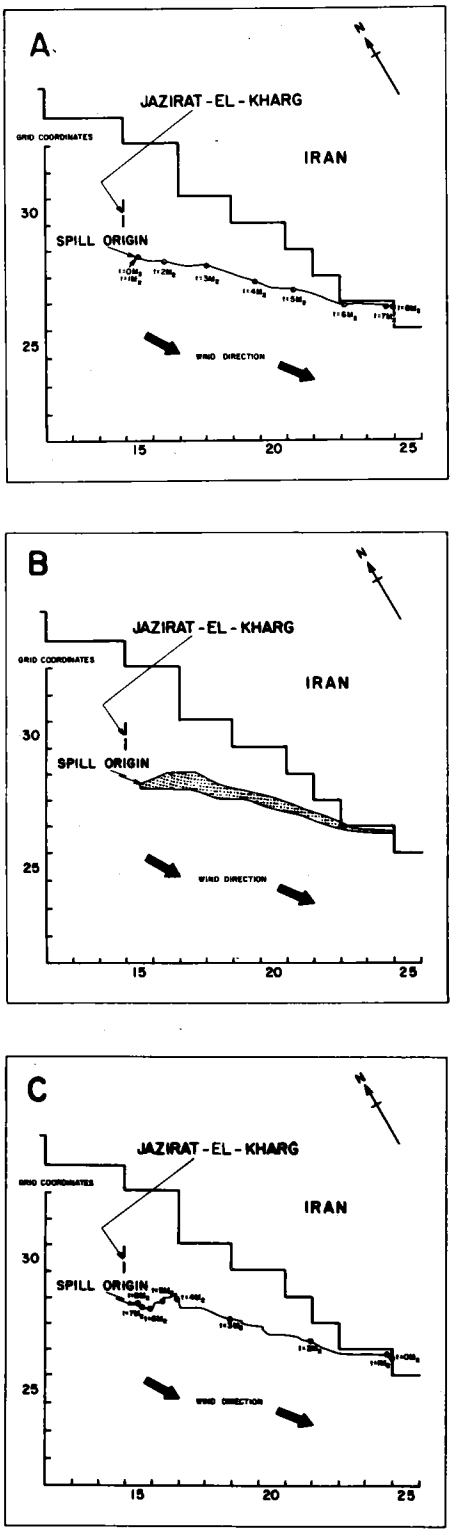

Figure 7: M_2 tide and wind field:
a. Position of the first oil patch after each M_2 tidal
b. Envelope of the oil slick
c. Position of eight successive oil patches.

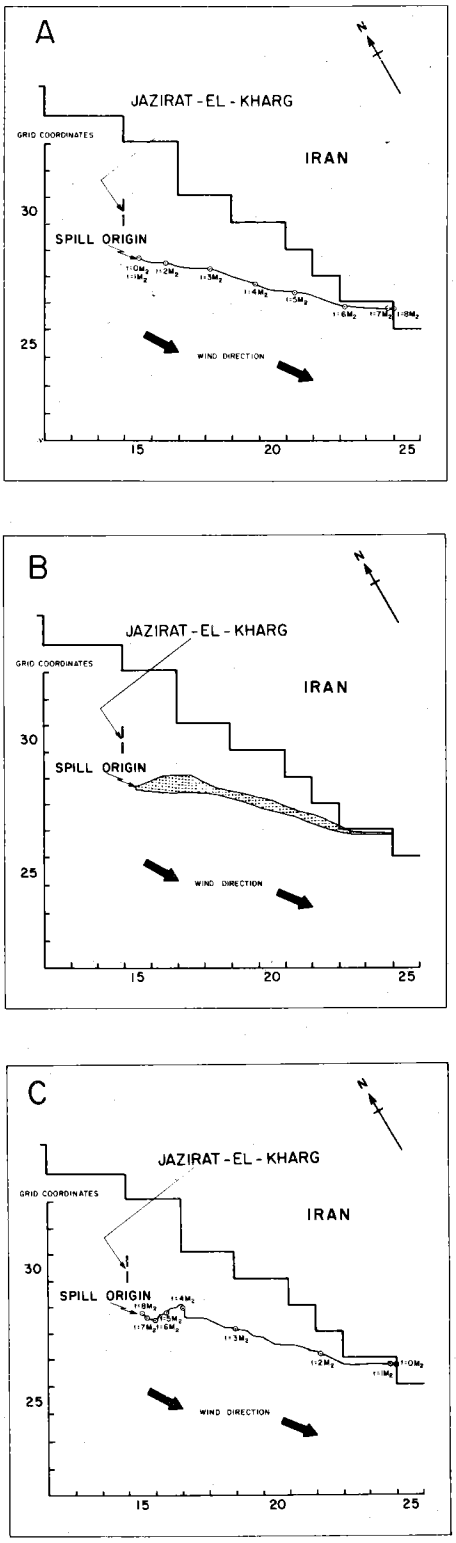

Figure 8: Six tidal constituents and wind field: a,b, c same as in Figure 7.

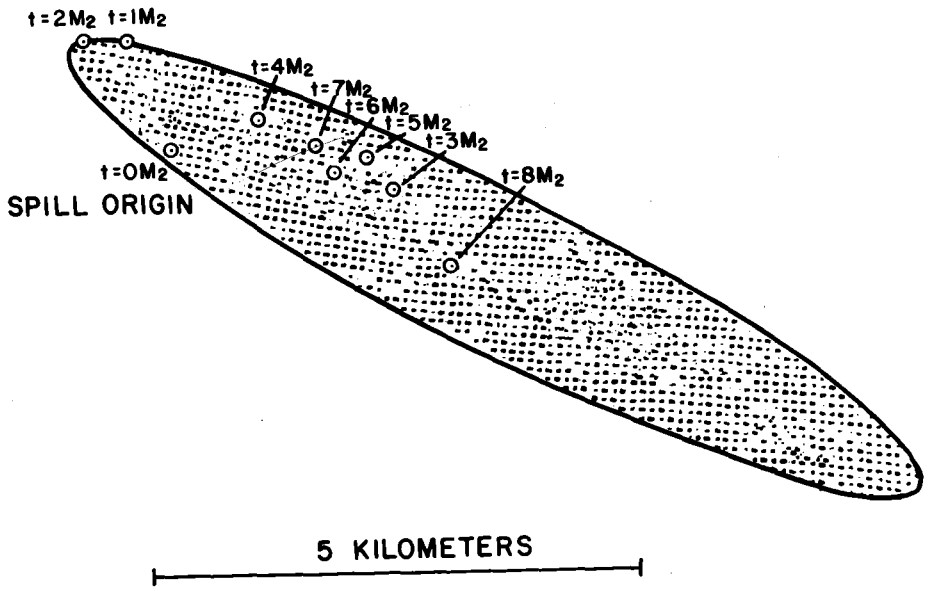

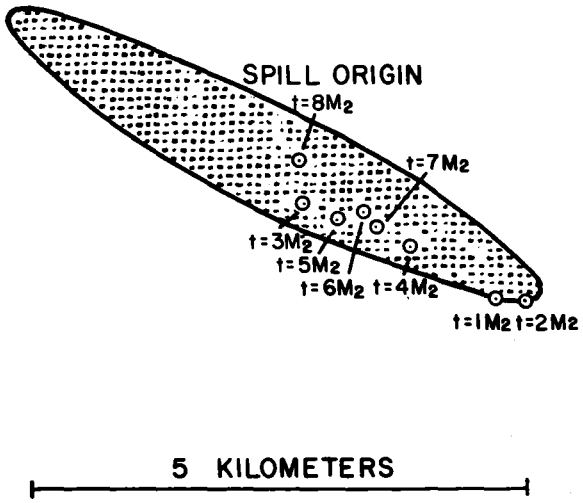

Figure 9: No wnd field, six tidal constituents.

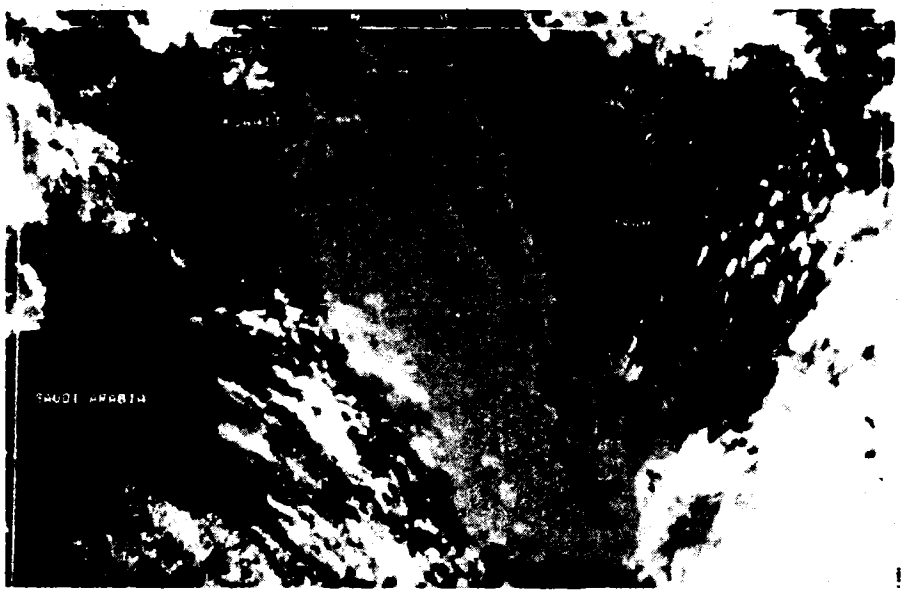

Figure 10: Satellite photograph of the oil slick in the Inner Gulf taken in April 1983.

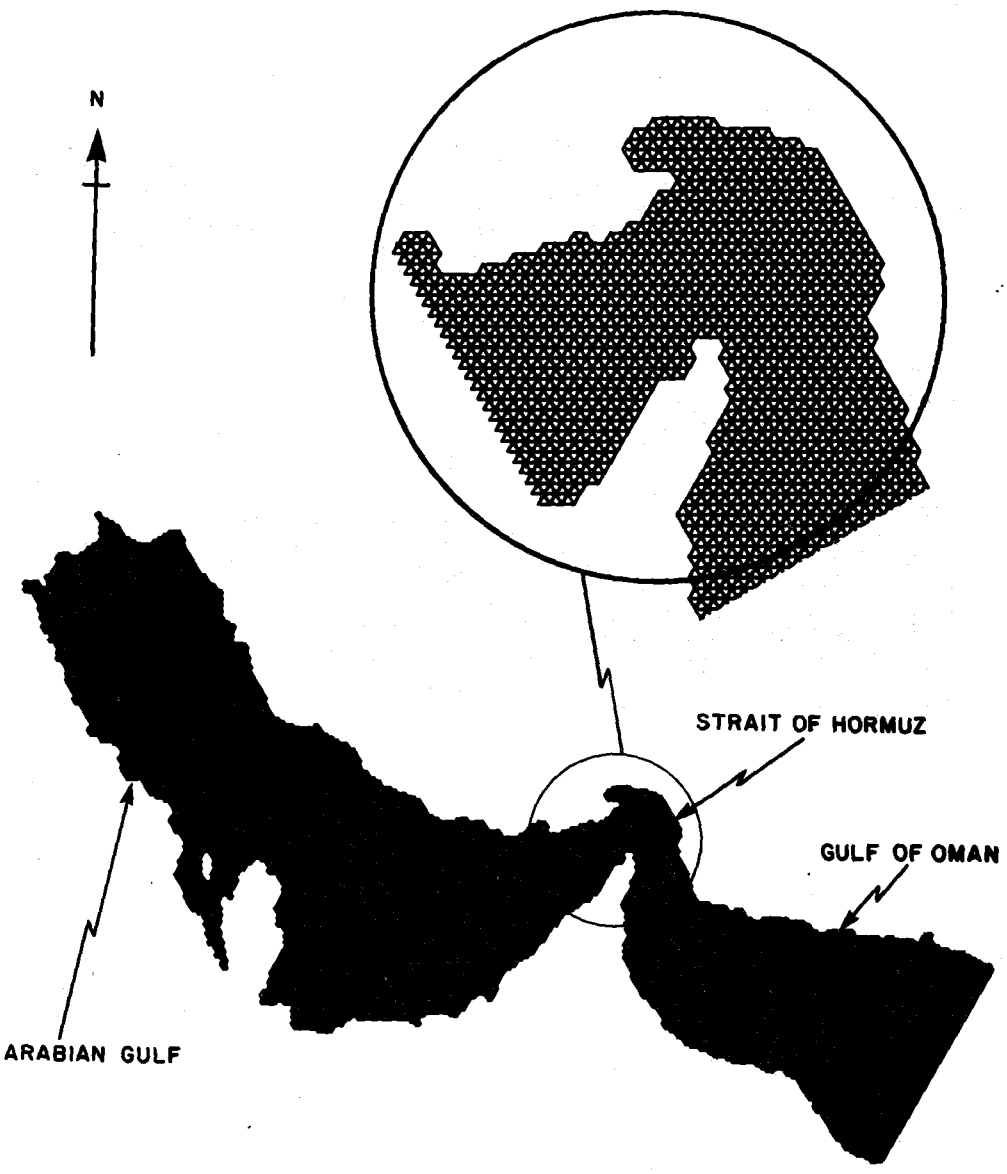

Figure 11: Regular Triangular grid for the Strait of Hormuz.

SIMULATION MODELS FOR POLLUTANT TRANSPORT IN THE MARINE ENVIRONMENT: CAPABILITIES AND LIMITATIONS

by

J. Post

Preussag Marine Technology, Hannover

ABSTRACT

Industrial activities and antropogene near-shore pollution are two important reasons for the development of dispersion models. The physical process of dispersion is given by the well known transport diffusion equation. The quality of a dispersion model depends strongly on the accuracy of the circulation model, since the advection is the most important part of the equation.

The development of circulation models has a long history in the Institute of Oceanography at the University of Hamburg. Over the last 30 years, various one, two and three-dimensional baroclinic and barotropic models based on explicit or implicit finite difference schemes have been designed. The models show reasonable agreement with actual measurements and seem to provide a good basis for transport models. The latest stage is the development of a three-dimensional baroclinic model based on a semi-implicit difference scheme; it is one of the quickest algorithms in the world. Besides the circulation models, various dispersal models have been constructed for the transport and diffusion of heat, salt, radioactive waste, sewage and chemical or biological properties. Some of these models employ a Lagrangian tracer technique for passive tracers as well as active tracers, such as density. The main advantage of this technique is that numerical diffusivity is omitted. These models are in excellent agreement with measurements and have a high accuracy in both hindcasting and forecasting. Examples of circulation and dispersal models are presented.

INTRODUCTION

Antropogene impacts in the marine environment, such as the dumping of waste material and hazerdous accidents, have largely determined the scope of oceanographers' studies in recent years. Besides extensive field studies and the simulation of natural processes through the application of hydraulic models, one of the most effective tools for investigating physical processes in the marine environment is the numerical simulation model. It is quick, flexible and, compared with other methods, requires only low cost.

Spreading predictions and risk assessments of intentional or accidental waste releases have led to the development of numerous circulation, transport and dispersal models.

Some recently developed transport models are presented and their capabilities and limitations discussed below.

FUNDAMENTALS OF THE MODELS

The basis of numerical simulation models is given by the fundamental thermodynamic and hydrodynamic equations of conservation, that is,

- conservation of momentum;
- conservation of mass;
- conservation of energy; and
- equation of state.

From these equations it is possible to determine the relationship between acting forces (tides, winds, etc.) the boundary conditions (e.g. heat exchange or waste discharge) and the resulting physical state of a certain water body. The state of the water body can be described by the

- current pattern;
- pressure distribution;
- temperature, salinity and density distribution;
- distribution of dispersed material;
- distribution of dissolved constituents; and
- distribution of properties.

Because turbulent processes have not yet been completely described mathematically and would, in any case, require a vast computational effort, turbulence factors, such as bottom friction, viscosity and diffusion, are described by empirical parameters which need to be calibrated by measurements.

The equations of conservation mentioned above lead to non-linear partial differential equations, which, especially for complex natural topographies, do not give exact analytical results. A feasible way to solve this problem is by the application of numerical approximation methods. The entity composed of the basic physical equation, the initial and boundary conditions, the discretization and the numerical methods is called a numerical simulation model. One, two or three-dimensional models are developed depending on the geographical context and the statement of the problem. The scope of interest determines whether models are applied which take density gradient-driven processes into account (baroclinic), or

which neglect these forces and calculate a non-stratified homogeneous water body (barotropic).

Finite difference methods and the Monte Carlo Method are generally applied to simulate spreading. The finite difference scheme is based on a rectangular grid and provides the opportunity of nesting or telescoping on areas of particular interest. It is mainly used within general circulation models. The Monte Carlo Method works with a defined number of particles distributed over the entire water body. The particles (or tracers) are marked with certain properties (e.g., temperature and pollutant) and are moved both by advective transport induced by the mean currents, and by turbulent diffusion, simulated by the random procedure known as the Monte Carlo Method. The latter is mainly used for transport and dispersion calculations. Mathematical approximation methods require conditions of convergence and stability. The Courant Stability Condition, i.e., that the numerical propagation of a wave ($\frac{\Delta t}{\Delta x}$) must be higher than the propagation of the gravity wave $\sqrt{g \times h}$, is the most important. For high resolution (i.e., small Δx), this condition leads to a small time step, Δt, and thus to lengthy computation time for the simulation of natural processes. The Courant Stability Condition restricts the so-called explicit methods where the new state (at the new time step) is exclusively calculated from the old state. The application of implicit methods, where already new, calculated values are used to determine the new state, is independent of the Courant Criterion and, consequently, gives a better ratio between computer time and actual simulated natural process time.

MODELS

Initial approaches to simulating physical processes, especially within areas with a complicated topography, were carried out at the Hamburg University in the early 1960s using the so-called Hydrodynamic Numerical Method. The simulation of the semidiurnal M_2-tide the Inner Gulf (von Trepka, 1976) may serve as an example.

Inner Gulf M_2 tide model

The tides in the Inner Gulf are mainly co-oscillating, generated in the very narrow Strait of Hormuz and caused by the Indian Ocean tides. The Gulf's tides are of mixed type with the M_2-tide dominating. Due to the very limited computer capacity available at that time, a horizontal resolution of 14 km was chosen. The tides were generated at the model's open boundary within the Strait of Hormuz. The model was based on the non-linear Navier-Stokes equations (two-dimensional) and the equation of continuity (mass conservation) written in finite difference form. In spite of insufficient resolution for some coastal areas, the results of the model show good agreement with observations and measurements (Figure 1).

The model's generating forces such as tides and wind were subsequently tested in numerous areas and for extreme situations (e.g., storm surges), one of the main objectives being the simulation of long-term processes, such as general circulation and transport in the oceans and adjacent seas. The rapid increase in computer speed and capacity over the last decade has favoured the development of highly efficient models.

General circulation model of the Red Sea

In the course of an extensive environmental impact study within the Red Sea a number of different model investigations were carried out. The aim of this set of models was to simulate the spreading and dispersion of pollutants released during potential mining activities within the central Red Sea and make a prediction of the potential accumulation area. The general circulation model[1/] developed for this purpose (König, 1982) provides the basic input for the transport of material after release and plume development. It is a three-dimensional multi-level baroclinic model which computes the monthly mean currents in the entire Red Sea and the adjacent Gulfs of Suez and Aqaba. Main features of the model are:

- Navier-Stokes, continuity and hydrostatic equations;
- finite difference approximation;
- spherical coordinate system;
- horizontal resolution of one third of a degree;
- vertical resolution of twelve levels;
- input of monthly mean temperature, salinity, wind and evaporation fields;
- tides are neglected; and
- output of monthly mean current pattern for each level and each month (see Figure 2)

A combination of the monthly mean currents resulting from the general circulation model with a meso-scale model which simulates the release of material and plume development is in preparation.

Still more powerful, however, regarding the relationship between computer time and actual simulated natural time are the implicit calculated models, where the Courant criterion restriction is omitted. A three-dimensional baroclinic model based on a semi-implicit difference scheme has recently been developed, and it is one of the quickest algorithms in the world.

A semi-implicit shelf sea model

This model applies a semi-implicit scheme for the numerical solution of the shallow water equation. It is suitable for the simulation of shelf sea dynamics and, due to its optimal computing time economy, designed to serve as a basic long-term transport model for hindcasting and forecasting calculations. In addition, computation time is gained by applying a simple but very effective trick. Backhaus (1982) describes it as follows. The idea is to eliminate the divergence terms defined at the future time-step in the equation of continuity in order to obtain a system of linear equations for the sea surface elevation ζ. This is done by inserting the equation of motion into the divergence terms and so reducing the equation of continuity to a system of linear equations for the scalar function ζ. It is recommended that this system be solved by means of an iteration procedure, to be carried out at each time-step. Trials with different iteration techniques have shown that the most rapid convergence is obtained by using the method of successive overrelaxation.

1/ Work on this model was financed by the Ministry of Research and Technology of the Federal Republic of Germany and the Saudi Sudanese Red Sea Commission.

Applications to different areas (e.g. North Sea, Baltic, Elbe estuary) have shown that the new model used in conjunction with the successive overrelaxation method lowers computer times to as little as 15 times less than those of the earlier explicit schemes.

A mixed Eulerian-Lagrangian Spreading model

This model attempts to reproduce the measured Cs 137 distribution in the North Sea, which has been fed for several years through the English Channel. In the first step, the equations of motion and the continuity equation are calculated. The predominating semi-diurnal M_2-tide and mean wind stress are the generating forces. After a short period of time, the model becomes stationary with the M_2-tide in a periodical step.

In the next step, the water mass transport is calculated by integration of the two horizontal velocity components over one M_2 period. This procedure results in a transport pattern defined for each Υ-gridpoint and the duration of one M_2 period. As is obviously essential for long-term simulations, it is possible to change from the 5 minute time-step, necessarily applied in the first computation step, to a 12 hour time-step for the subsequent spreading model.

Due to the fact that Cs^{137} is a passive tracer which has no influence on the water motions, it is possible to apply the Monte Carlo method. In the calculation for each time-step, one particle is added to the model area at the grid point near Dover. The particles belonging to a certain Υ-gridpoint at a certain time-step are moved by the transport vector at this gridpoint. In addition, the movement of the particles is influenced by a displacement which is randomly taken from a defined statistical distribution F(dx, dy). The trajectories of the particles and the resulting distribution and concentrations are shown in Figures 3 and 4. The qualitative distribution is in good agreement with the measured results obtained by the Hydrographic Institute of the Federal Republic of Germany.

DISCUSSION

This paper has mentioned a number of the capabilities and advantages of numerical simulation models. It would far exceed the scope of the paper to try to specify all the capabilities and different applications of marine simulation models. A good insight can, moreover, be gained into recently acquired modelling capabilities from the Symposium report. In contrast, the limitations of marine modelling are seldom specified in detail. One main limitation of numerical simulation models, limited computer capacity and computation speed, has become increasingly unimportant due to recent developments in computers and software. Nevertheless, in some cases (long-term processes, world ocean processes, etc.), computer capabilities continue to be restrictive. A major problem is still the lack of knowledge of how to treat turbulent processes, which gear into each other from micro-scale to macro-scale. A great deal of physical oceanographers' work is and will be focused in future on this complex of problems. A further limitation on marine modelling became apparent recently in attempts to combine physical, chemical and biological processes to investigate the interaction between these different components of the marine environment. It is difficult to put these process, especially the biological processes, into mathematically treatable form.

It is obvious from a reviewing of oceanographers' efforts to computerize the complexity of the marine environment that there is still a lot to be done. In the end, the task may turn out to be Sisyphean.

REFERENCES

Backhaus, J.O. (1982) A semi-implicit three-dimensional tidal model for shelf seas (submitted for publication).

König, P. (1982) General circulation model of the Red Sea, Saudi Sudanese Red Sea Commission Techn. Rep. No. 38.

Maier-Reimer, E. (1975) On the influence of a mean wind stress on the residual currents of the North Sea. DHZ, 28, No.6, 253-262 (in German).

Maier-Reimer, E. and Sündermann, J. (1981) On tracer methods in computational hydrodynamics. In: Engineering application of computation hydraulics, Abott, M.B. and Cunge, J.A. (ed.) Pitman, London.

Von Trepka, L. (1968) Investigations of the tides in the Arabian Gulf by means of a hydrodynamic-numerical model. Mitt. des Institutes f. Meereskunde, Univ. Hamburg, No. 10.

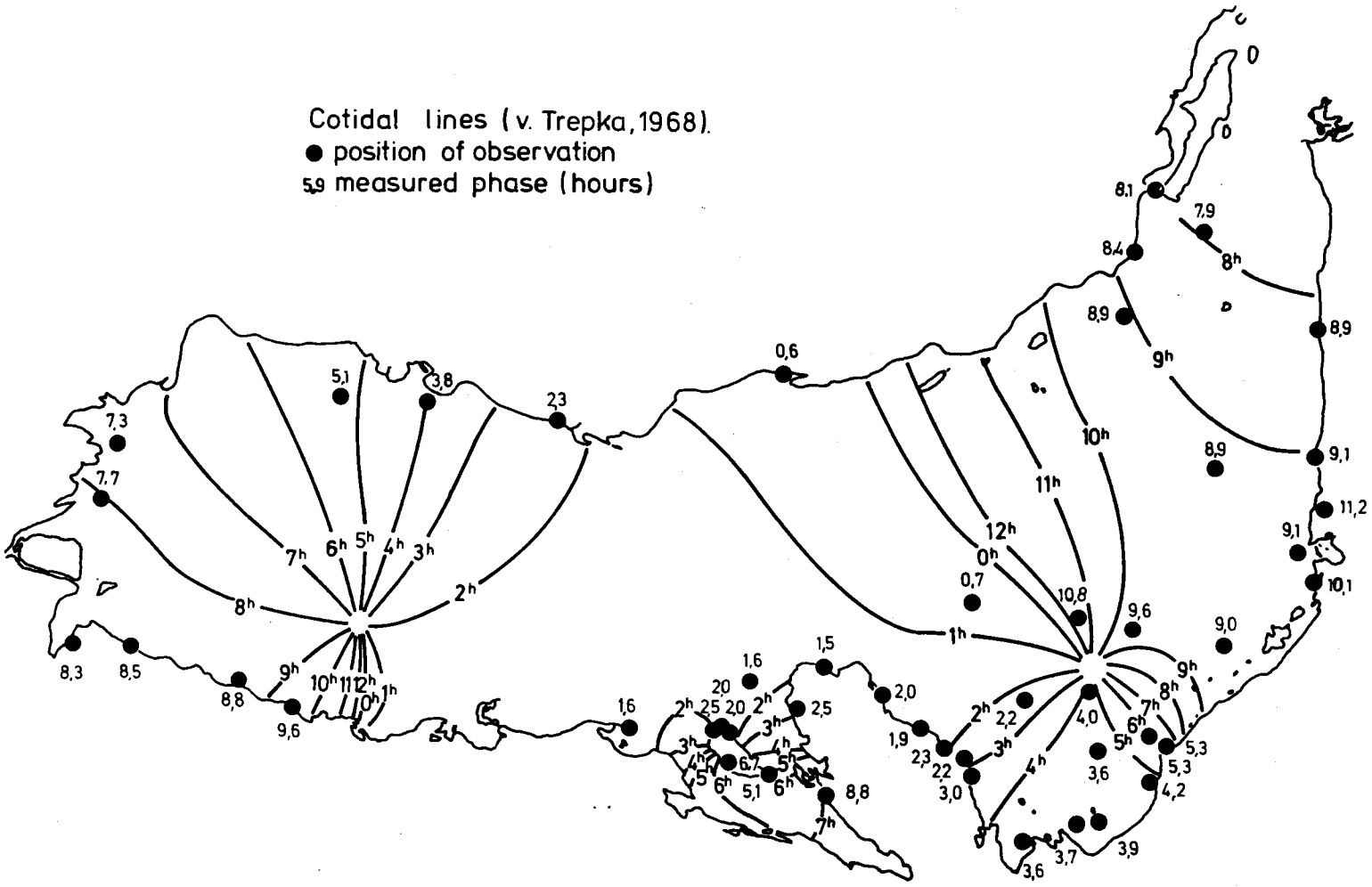

Figure 1: Inner Gulf M_2-tide: comparison of model with observations.

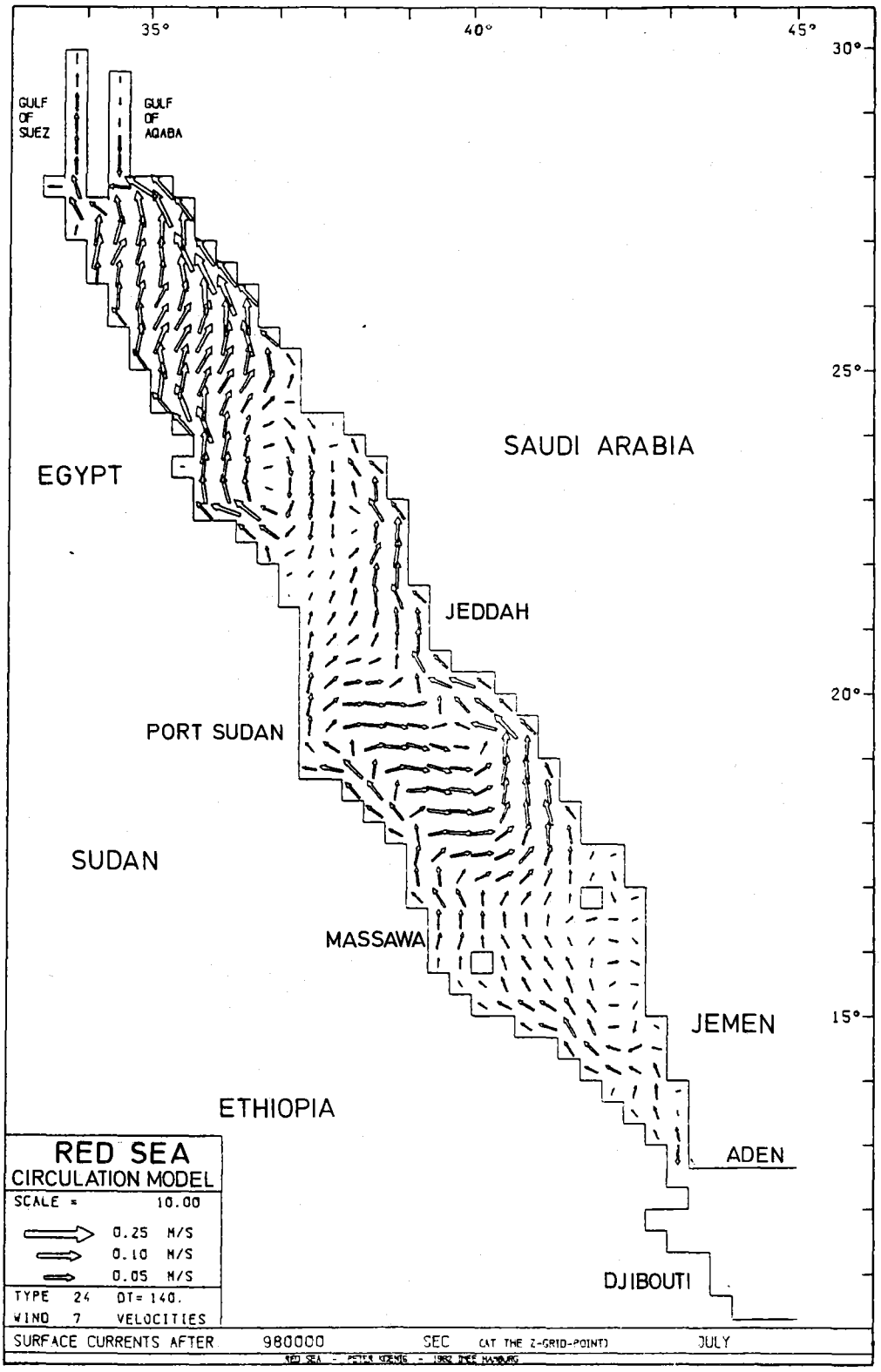

Figure 2: Red Sea surface mean current pattern in July.

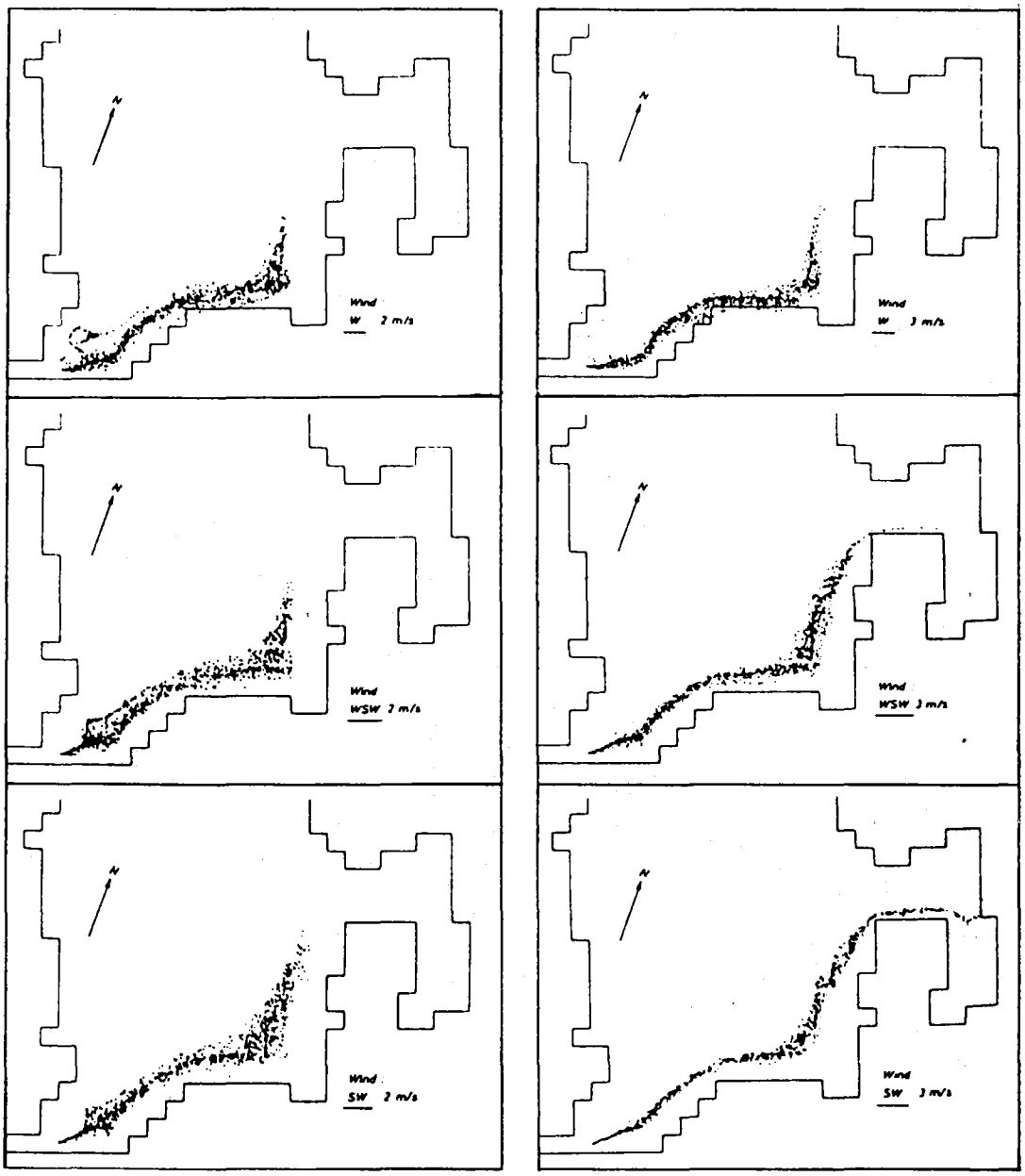

Figure 3: Propagation over 2 years, with continous source in the Channel, calculated for different wind stresses from West to South-West (Maier-Reimer, 1975).

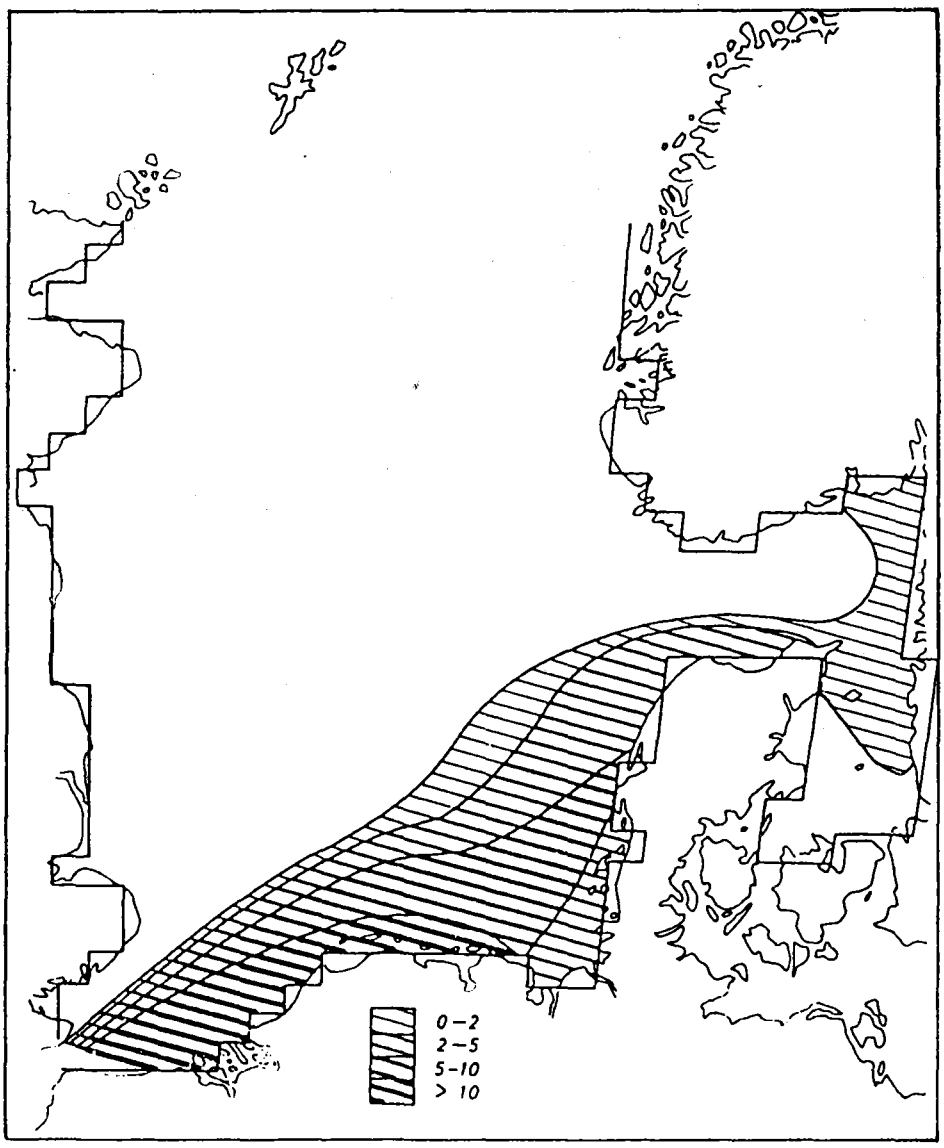

Figure 4: Propagation of a point sssrce near Dover over 2 years, WSW -Wind 3m/s, A=25m^2/s; lines of equal concentration (arbitary units) (Maier-Reimer, 1975).

OCEANOGRAPHIC MODELLING APPLICATIONS FOR INDUSTRY IN THE INNER GULF

by

R.O. Williams
Arabian American Oil Company
Dhahran, Saudi Arabia

ABSTRACT

The modelling of meteorological and oceanographic processes has numerous applications for coastal and offshore industries, providing a basis for both design and operations.

The design of facilities typically requires analyses of extreme event and joint probabilities, based on the modelling of long term continuous meteorological and oceanographic data. Major storm data are used for developing hindcast models of winds, waves, currents and storm surges and, for example, of the inter-relationships that lead to the "100 year storm".

Industrial operations require meteorological and oceanographic modelling for day-to-day activities, such as vessel operation and berthing, and emergencies, such as oil spill tracking and clean-up.

INTRODUCTION

As is the case for other countries of the world with coastlines, the Inner Gulf countries have a concentration of industry and population along the coast because of the many advantages such a location offers. The import and export of goods, for example, is easily forwarded by ships calling on Gulf ports; fisheries operate in the Gulf waters, and the seawater is used not only as a source of cooling water for industries, but also as a community water supply.

The coastal facilities supporting these industries and populations are numerous and include harbours with breakwaters, jetties, piers and intake/discharge structures for power and desalination plants. Extension of the industries offshore is mainly related to oil pipelines and platforms, as well as vessels trafficking in the open Gulf.

Environmental parameters such as winds, waves, currents, tides and seawater quality are of great importance to the design and operation of these commercial activities. Working values of these parameters are generally obtained from physical or numerical models. The unique climate, as well as the basin geometry and topography would, however, be expected to require complex model development. General small scale models of the entire Inner Gulf may act as boundary conditions for the modelling of specific coastal areas.

EXTREME EVENT ANALYSES

Although there are numerous small earthquakes to the East of the Inner Gulf within the Zagros Mountains of Iran, the Inner Gulf is generally thought to be aseismic, indicating no risk of tsunami generation. This is not, however, to say that research into this particular hazard assessment should not be undertaken. Numerous earthquakes have been reported near Bandar Abbas near the Straits of Hormuz and the potential for tsunamis, together with threats of associated coastal inundation, merit investigation.

The main type of extreme event analyses required for facility design, however, concerns storms and astronomical tides. The northwest Shamal is the predominant [illegible]d and it can generate severe conditions. There is, on average, one severe storm [illegible]t winds for a period of 12 hours) per year.

[illegible] needed in[illegible]ht and period of the design wave is usually the most critical value reliance is p[illegible] structure design. Since wave data for the Inner Gulf are sparse, the wave generati[illegible]n the fairly good data base of winds and on various models of [illegible]ential of wind.

A commonly applied [illegible] wave height and period [illegible]d of correlating wind speed/duration and fetch with forecasting chart. In additio[illegible]he use of Bretschneider's (1970) deep water wave also shallow water limitations whe[illegible]etch limitations of the enclosed Gulf, there are of less than half a wavelength. A[illegible]allow water is defined as water with a depth of 5 seconds has a wavelength of about 40[illegible]1 1 m wave in the Inner Gulf with a period in water less than 20 m deep. This acc[illegible]so that shallow water waves are found particularly the low sloping South and Western [illegible]s for much of the entire Gulf basin, [illegible]ves.

Storm waves in fully developed sea conditions have been recorded with associated wavelengths of 100 m in the Southern Gulf. Such waves would therefore be shallow water waves for almost the entire Western Gulf.

More sophisticated techniques are required for modelling shallow water waves and these must consider the effects of refraction and bottom friction. Such models require the input of details of bathymetric observations, direction of wave approach and period, bottom type and wave interactions.

Storm surge associated with wind can be either positive or negative, depending on the direction of the storm approach and fetch. Besides flooding hazard or negative surge impact on industrial cooling intakes, the water level modifies the height of possible waves along a coast.

Sea currents, though usually dominated by tidal dynamics in the Inner Gulf, can be significantly controlled by winds in the shallow shelf areas. Progressive vector plots of winds and currents have shown significant correlations between the net transport of each parameter in water depths of less than 20 m.

A critical factor in undersea pipeline design, particularly for buoyant natural gas pipelines, is the near bottom current velocity. Research has been limited to the 1 to 2 m boundary layer near the seabed. The motion components of the total bottom current would be tidal, wind driven and residual current, orbital wave particle velocities and vortices associated with flow over the pipeline.

Extreme event analyses are required for design purposes. For critical structures such as offshore oil platforms, a "100 year" design value is usually specified. This is something of a misnomer; it should really be considered as a 0.01 probability that a storm value of a specified intensity would occur in any one year.

There are various methods of determining the probability of occurrence of extreme values (Gumbel, 1958). As with any statistical analysis, however,the accuracy of results increases with the increase in the population of values. In climatology, data must be collected for many years to yield representative trends or characterize extreme events. At least 10 years of data are generally required. Tidal levels and currents can be well described with 29 days of data, though seasonal meteorological trends require longer observations. A 369 day tidal analysis will account for most of the secondary astronomical harmonic constituents.

As the cost of coastal and offshore industrial development increases, more work is being done to characterize the joint probability occurrence of extreme events instead of vectorially adding all the values. The assumption that maximum tidal currents occur simultaneously with maximum waves and wind generated currents is a conservative one. More appropriate values may be developed using statistical independence assumptions and defining the phase difference between storm build up, peak and decay in terms of wind waves, currents and storm surge. Little research worldwide has addressed this issue and no published works have been found thus far for the Inner Gulf.

OPERATIONAL MODELLING

Recirculation studies for power plant and refinery cooling and desalination plants are most commonly required in the Inner Gulf to optimize the design configuration of intake and discharge structures. The design requirements are the prevention or reduction of the reentrainment of heated or briny water and a reduction in the impact of heated, saline and/or chemically treated water on marine organisms. To model these situations more accurately requires further research into parameters of the Inner Gulf. For example, the author is not aware of any well defined values for dispersion coefficients. Values reported in the literature vary from 0.08 to 0.30 m2/sec.

Desalination plant discharges are typically a dense plume that follows the bottom topography in shallow coastal areas. Toxic chemicals such as copper sulphate, which are typically injected to control marine biofouling, may act quite differently from the briny discharge and may require special modelling efforts.

Power plants typically have a heated and buoyant discharge. For both desalination and power plants, consideration must be given to tidal current reversal and the artificially induced influence of the intake. Withdrawal volumes of large desalination plants can be near 100 MGD and nearfield current velocities can reach 2 m/sec. Physical modelling may actually be more realistic in complex bathymetric areas such as the Western Inner Gulf coast. Some physical models have been constructed for specific industrial projects in this area.

Finally, sediment transport models are important to littoral zone structures as well as to dredging for channel approaches, under pipeline corridors, etc. Accretion and erosion of coastlines are well known phenomena when longshore sediment transport is interrupted by coastal works. Calculations off Ras Tanura indicate that sediment transport rates may be as high as 100,000 m3/year. Dispersion modelling of dredge spoil to minimize environmental impacts on marine organisms as well as to maintain open channel approaches are but two further applications of such modelling.

BIBLIOGRAPHY

Banerji, B.N. (1932) The Bahrain storm and some studies of cold wedges over the Persian Gulf. Beitr. Phys. Frei Atmos. 19, p. 34.

De Sylva, D.P. (1979) A bibliography of oceanography of the Arabian Gulf 1859-1978, Univ. of Miami, Florida, 444 references.

Dubach, H.W. (1964) A summary of temperature-salinity characteristics of the Persian Gulf. U.S. National Oceanographic Data Center General Ser. Pub. G-4.

Emery, K.O. (1956) Sediments and water of the Persian Gulf. Bull. Am. Assoc. Petrol. Geologists, 40(10), pp. 2354-2383.

Feteris, P.J. (1973) The role of convection and strong winds aloft in triggering gales over the Persian Gulf: comparative case studies. Monthly Weather Review, 101(5), pp. 455-460.

Gumbel, E.J. (1958) Statistics of extremes. Columbia University Press, New York, 347 pp.

Kihara, K. (1974) Bathythermography and the stratification of temperature and salinity in the Arabian Gulf, December 1968. In: Kuronuma, K. (ed.) Trans. Tokyo Univ. Fish., No. 1.

Kuo, W.S. (1965) A study of weather over the Arabian Peninsula. Taipei, Met. Bull. 2, pp. 25-35.

La Violette, P.E. and Frontenac, T.R. (1967) Temperatures, salinity and density of the world's seas: Arabian Sea, Persian Gulf and Red Sea. U.S. Naval Oceanographic Office Report.

Leony, E. (1970) Model tests and studies for Port Rashid, Dubai. American Society of Civil Engineers, Proc. of the 12th Coastal Engineering Conference, p. 1137-1149.

Perry, K., (1965) Results of the Persian Gulf-Arabian Sea oceanographic surveys 1960-1961. U.S. Naval Oceanographic Office Technical Report, No. 176.

Smith, S.D. (1981) Factors for adjustment of wind speed over water to a 10-meter height. Bedford Institute of Oceanography Report BI-R-81-3.

Tetra Tech, Inc. (1979) Oceanographic study in the Straits of Hormuz and over the Indian shelf in the Persian Gulf. Report to Sultanate of Oman.

Tetra Tech, Inc., (?) Study of wind generated currents in the Gulf between Iran and the Arabian Peninsula. Report to Continental Oil Co., U.A.E.

Tetra Tech, Inc., (?) Wind, wave and statistical analyses to assess general circulation and littoral zone dynamics in the Gulf. Report to Continental Oil Co., U.A.E.

Wang, S. and LeMeHaute B. (1983) Duration of measurements and long term wave statistics. Am. Soc. of Civ. Eng. Jour. of Waterway, Port, Coastal and Ocean Division (In Press).

Williams, R.O. (1979) Meteorologic and oceanographic data book for the Eastern Province Region of Saudi Arabia, Arabian American Oil Company, 132 pp.

_____, (1962) Geophysics and oceanology in the ocean and Persian Gulf: Surveys of H.M.S. Owen and H.M.S. Dalrymple Nature, London, Vol. 194(4832):919.

AN EVALUATION OF JUBAIL METEOROLOGICAL DATA TO PROVIDE WIND PARAMETERS FOR OIL SPILL MOVEMENT PREDICTIONS

by

Karl F. Zeller
and Asad T. Amr,
Royal Commission, Jubail, Saudi Arabia

ABSTRACT

The Royal Commission for Jubail and Yanbu has been collecting meteorological and air quality data at eight locations in and around Madinat Al-Jubail Al-Sinaiyah since August 1978. Four of the eight sites are adjacent to the Inner Gulf of the Kuwait Action Plan (KAP) Region, and the other four sites are located several kilometres inland. One of the inland sites has a 90 m tower and continually collects meteorological data at 10, 50 and 90 m above ground. The other seven sites have 10 m meteorological towers and also collect data continuously.

Surface oil spill movement is dependent upon wind turbulence, wind speed and wind direction. Oil spill models require wind parameter m as input. Computing surface wind fields over sea from sparse measurements obtained at coastal and inland stations has to be done with great care because of the differences in surface roughness. This paper evaluates selected 5-minute meteorological data obtained at Jubail during homogeneous wind turbulence periods. Data from one of the coastal sites are compared with data from the inland 90 m tower site. Values of the friction velocity (u_*), roughness length (z_o), coefficient of friction, (C_d); and power law exponent are investigated. Wind speeds from these selected data periods are then correlated for subcategories of bulk Richardson number, vertical temperature lapse rate and wind direction.

INTRODUCTION

Wind blowing over a water surface causes a stress, s, on the water surface in the direction of the wind. Thus, wind at the surface must be taken into account when predicting oil spill movement. The wind (or eddy) stress can be expressed as:

$$s = d_a C_d U^2 \qquad (1)$$

where, d_a is the density of the air, C_d is the drag coefficient and U is the wind velocity (wind speed and direction) (Kullenburg, 1982). In Ekman's (1905) classical analysis, s is related to the water surface current speed, V, by:

$$V = s (A f d_w)^{-0.5} \qquad (2)$$

where A is the wind eddy coefficient, f is the Coriolis parameter and d_w is the water density.

In practice, the "ground level" wind velocity is usually measured at 10 m above ground. This 10 m wind velocity must therefore be adjusted to represent the wind flowing adjacent to the ground or sea. This paper describes the existing meteorological monitoring programme at Madinat Al-Jubail Al-Sinaiyah and then examines some of the wind parameter m used to calculate wind speed change with height as determined from data averaged over a 5-minute period during selected homogeneous turbulence periods that occurred in March and May 1983.

JUBAIL METEOROLOGICAL MONITORING PROGRAMME

The Royal Commission for Madinat Al-Jubail Al-Sinaiyah has been engaged in the collection of meteorological and air quality data at eight fixed sites located in the Jubail vicinity since August 1978. The locations of the sites are shown in Figure 1. The continuous meteorological data collected at the sites are listed in Table 1. Site 1 is located approximately 8 km inland from the Inner Gulf coast and has a 90 m meteorological tower. This is the most important site in the network for the collection of meteorological data. The area surrounding Site 1 is relatively flat except for a 3 m elevated roadway 100 m to the Northeast and a 5 m high building 100 m to the Southeast.

Site 2 is situated 50 m from the coast line and is the closest network site to the Inner Gulf waters. Site 2 is strategically located adjacent to the Industrial Sea Water Cooling Canal intake and to the stand-by desalination plant. Wind data measured at Site 2 would logically to be most representative of wind conditions affecting the sea surface flow near these vital industrial facilities.

At each site, data sensors are automatically queried every 5 seconds (every 2 seconds for wind parameters) and data are temporarily stored as 5-minute averages. The 5-minute averages are then relayed by radio to a central computer where the data are calibrated and edited, and one-hour averages are calculated and stored in a data base for multiple users. Typically, only the one-hour averaged data are available to data users. The 5-minute data are only stored temporarily in the computer. This paper, however, examines selected periods of 5-minute data as stated above. The periods studied vary from one to five hours in length. They were initially selected based on periods of relatively stable one-hour standard deviations of the 10 m wind direction (normally called sigma theta). Sigma theta is referred to as SIG1 in the tables and is reported as an angle in degrees.

A total of 39 periods was studied. A summary of the data results is presented in Table 2. The data in table 2 were further separated into 11 categories. Wind parameter averages within each category were calculated and are discussed below. The eleven categories were:

(1) Site 1:10 to 50 m vertical temperature lapse rate greater than 0 °C/40 m.

(2) Site 1:10 to 50 m vertical temperature lapse rate less than 0 °C/40 m but greater than -0.24 °C/40 m.

(3) Site 1:10 to 50 m vertical temperature lapse rate less than 0.24 °C/40 m but greater than -0.5 °C/40 m.

(4) Site 1:10 to 50 m vertical temperature lapse rate less than -0.5 °C/40 m.

(5) Site 1:10 to 50 m bulk Richardson number greater than .03.

(6) Site 1:10 to 50 m bulk Richardson number less than .03 but greater than -.03.

(7) Site 1:10 to 50 m bulk Richardson number less than -.03.

(8) Site 1 wind direction between 0 and 89°.

(9) Site 1 wind direction between 90 and 179°.

(10) Site 1 wind direction between 180 and 269°.

(11) Site 1 wind direction between 270 and 359°.

The vertical temperature lapse rate categories and the bulk Richardson number categories were chosen to distinguish atmospheric stability cases and also to give an adequate number of cases in each category for this selected data set.

CONSTRUCTING A WIND PROFILE USING MEASURED DATA

There are several methods for computing wind profiles (i.e., wind speed change with height above ground or sea) in the lower layer of the atmosphere (Goodin and McRae 1980, McLellan 1968, Hess 1959). This paper examines the Jubail Site 1 90 m tower data using the power-law, the logarithmic profile and a boundary layer drag coefficient.

Power-law wind profile

$$U_1 = U_2 \, (z_1/z_2)^{1/n} \qquad (3)$$

where, U^1 and U^2 are mean wind speeds at heights z_1 and z_2, respectively; n is non-dimensional and varies with thermal stability, which is related to vertical temperature lapse rate (change in ambient temperature with height). The power-law profile is used for all stabilities and n is found to have a value of 7 for the neutral stability case (i.e., adiabatic lapse rate).

In this study, n was calculated for three layers using the Site 1 5-minute wind data: 50 to 90 m , 10 to 50 m , and 10 to 90 m . These 5-minute results for n were then averaged to produce an overall average for the homogeneous sample period.

The data listed in Table 2 show the averages for n calculated between 10 and 90 m only. These varied from 2.1 to 23.7. If the data in Table 2 are segregated by the 10-50 m lapse rate categories, the averages for n within each category vary from 3.7 for stable cases to 16.5 for unstable cases (see Table 3). Segregating the same data by the bulk Richardson number category (see Appendix) calculated between 10 and 50 m and averaging within each category produces values for n that vary from 4.0 for stable cases to 15.2 for unstable cases. Wind direction data segregation by quadrant shows the northeast quadrant (category 8) having the highest value for n (13.8). This would be expected since northeast winds are onshore winds and are typically stable. In this category, however, the average bulk Richardson number and lapse rate indicate that most of the cases were unstable.

Logarithmic wind profile

$$U = (u_*/k)\ \ln(z/z_o) \qquad (4)$$

where U is the desired mean wind speed (m/sec) at height z (m), u_* is the the friction velocity in m/sec which is related to the surface wind stress (see Appendix, equation (7)), k is the von Karman constant or universal turbulence constant (taken to be 0.4 in this study) and z_o (reported in centimeters) is the roughness length giving an indication of the theoretical elevation above ground where the wind speed goes to zero.

Equation (4) was used to extract u_* and z_o values between the elevations 10 and 50 m , 50 and 90 m , and 10 and 90 m . The wind speeds at 10, 50 and 90 m for each study period were also averaged, and u_* and z_o were calculated from a correlated straight line fit of ln(z) plotted against U. The correlated u_* and z_o are tabulated in Table 2. The u_* and z_o values were also averaged for the eleven lapse rate, bulk Richardson number and wind direction categories discussed above. These results are listed in Table 3. The value of u_* varies from 0.60 to 0.20 m/sec for stable to unstable conditions based on the lapse rate categories and from 0.57 to 0.15 m/sec for stable to unstable conditions based on the bulk Richardson number categories. The average u_* for northeast quadrant wind directions was 0.24, much lower than that for the other quadrants.

Drag coefficient

$$U_z = (u_*^2/C_d)\,\emptyset.5 \qquad (5)$$

Once u_* is known, C_d can be calculated as discussed in the Appendix (equations (7) to (9)). C_d is a non-dimensional number which relates the stress in the boundary layer to the wind speed at a chosen level, customarily 10 or 15 m (McLellan, 1968). This number is probably the most useful for predicting surface water movement. C_d was calculated using the Site 1:10 m wind speed and the correlated u_* value discussed above. C_d values for each study period are listed in Table 2. C_d values were also segregated according to lapse rate, bulk Richardson number and wind direction categories (Table 3). C_d averages varied from 0.0440 to 0.0008 for stable to unstable conditions using the lapse rate categories and from 0.0548 to 0.0015 for stable to unstable conditions based on the bulk Richardson number categories. The average C_d value for the northeast wind quadrant was 0.0030, much lower than the other quadrants. This is because the average u_* value was lower for this category.

DISCUSSION

The extrapolation of meteorological measurements obtained on land at coastal stations to estimate offshore winds must be done with care since the wind profile can experience large changes due to differences in surface roughness and surface heating. The values of u_*, z_o, C_d and n reported above as calculated from the limited sampling of data are representative of Site 1, 8 km inland from the Inner Gulf. The averages of these parameters m as reported in Table 3 are within reasonable expected limits, although some individual values were extreme. The use of the logarithmic profile was extended beyond its applicable limit of neutral stability cases. This extension is in agreement with the u_* and z_o results for non neutral cases.

The question regarding the usefulness of this analysis for oil spill applications is whether the Jubail Site 1 meteorological tower data can be used to provide adjusted wind parameter m for oil spill model prediction. An attempt to answer this question was made by comparing the wind speed data studied above with simultaneous Site 2:10 m wind speed data (see Table 4). The comparisons were made for the same lapse rate, bulk Richardson number and wind direction categories used above. For this comparison, wind speed categories were: 10 m Site 1 to 90 m Site 1; 10 m Site 2 to 90 m Site 1; and 10 m Site 1 to 10 m Site 2. In all categories except the most unstable, the average coastal (Site 2) 10 m wind speeds were greater than the inland (Site 1) 10 m wind speeds. The fact that the coastal site would generally have greater wind speeds is expected and indicates that the extrapolation of Site 1 tower data to estimate sea surface winds would probably best be achieved by lowering the values of n and C_d. Adjusting u_* and z_o would be a different matter since lapse rate considerations would have to be taken into account. As discussed above, equation (4) only applies for the neutral stability case and must be altered to incorporate the stable or unstable case (see Hess 1959 or Goodin and McRae 1980).

The correlation values shown in Table 4 were only reasonable for the 10 to 90 m wind comparison at Site 1 during unstable cases. If the number of available cases were larger, it would be reasonable to further sort the wind parameter m according to finer categories of wind direction and to add time of day as another independent variable. The low correlation between the 90 m Site 1 winds and the 10 m Site 2 winds is an indication that the 90 m winds might provide good data for distant offshore oilspill modelling, since Site 2 10 m winds are influenced by local surface conditions.

RECOMMENDATIONS

The data analysis and results described above show promise for using Site 1 tower data to calculate sea surface wind parameter m for oil spill modelling. The data set evaluated is, however,too small a sample to provide any specific guidelines as to how to adjust the Site 1 tower data for model input. The analysis presented in this paper should be expanded to include sufficient data for each season to obtain a significant sample number for predominant wind directions, stability cases and times of day. The logarithmic wind profile must also be adjusted for stable and unstable cases. To further the study of the use of Jubail meteorological data for Inner Gulf oil spill modelling, the following recommendations are made:

(a) 2 m wind speed sensors should be added to both the inland 90 m tower site and to the coastal 10 m tower site to better describe the surface friction layer at both sites.

(b) An investigation should be made of the use of 90 m wind data to represent offshore winds while using the coast 10 m wind data for near-shore winds. This is particularly important for sea-breeze periods.

(c) The Jubail wind data should be correlated with actual offshore meteorological data by temporarily siting a meteorological ocean buoy offshore. This would provide information for use in adjusting the boundary layer wind parameter m obtained onshore to estimate offshore winds.

ACKNOWLEDGEMENTS

The data collection and analysis presented in this paper was supported by the Royal Commission for Jubail and Yanbu Contract No. 001-T17. The results presented and the recommendations made are the responsibility of the authors alone.

The authors would like to express their appreciation to Mr. Arthur Noguerola for computer programming support and useful suggestions relative to data handling, and to Mr. Barry Neal for his editorial review and suggestions.

APPENDIX

Bulk Richardson number

The bulk Richardson number, Rib, was calculated between two elevations using the following formula (Hanna et al., 1977):

$$Rib = (g/T)\ ((d\Theta)\ (dz)/U^2) \qquad (6)$$

where

g = acceleration due to gravity in m/sec2

T = temperature at the lower level in degrees Kelvin

dΘ = difference in potential temperature between the higher and lower level in degrees Kelvin

dz = elevation difference between levels in m

U = average wind speed between the two levels in m/sec

In this study, the bulk Richardson number was calculated for each 5-minute period between 50 and 90 m, 10 and 50 m, and 10 and 90 m. The 10 to 50 m bulk Richardson number, referred to as R1050 in the tables, was found to be most representative and was used to segregate the data shown in Table 3.

Friction velocity and drag coefficient

The friction velocity, u_*, is site and direction specific and is considered constant within the boundary layer. It is a measure of the transfer of momentum due to turbulent eddies. It is related to the wind stress, s, by the following expression:

$$u_* = (s/d_a)^{0.5} \qquad (7)$$

substituting Equation 1 for s gives:

$$u_* = (C_d\ U^2)^{0.5} \qquad (8)$$

C_d is calculated in this study by rearranging the terms in equation 8 to give:

$$C_d = u_*^2/U^2 \qquad (9)$$

The wind speed, U, used for this calculation is the 5-minute 10 m Site 1 wind speed.

u_* can be calculated using the wind speed data from any two heights and solving equation (4) for each height, then the equation for one height is subtracted from the other giving:

$$u_* = (U_1 - U_2)k\ /\ \ln(z_1/z_2) \qquad (10)$$

REFERENCES

Ekman, V.W. (1905) On the influence of the Earth's rotation on ocean currents. Ark. Mat. Astron. Fys., 2, 1.

Goodin, W.R. and McRae G.J. (1980) A procedure for wind field construction from measured data which utilizes local surface roughness. Second Conference on Coastal Meteorology, Preprint, Am. Meteor. Soc.

Hanna, S.R. et al. (1977) AMS Workshop on Stability Classification and Sigma Curves: Summary of Recommendations. Bull. of Am. Meteor. Soc. Vol. 58, No. 12.

Hess, S.L. (1959) Introduction to theoretical meteorology. Holt, Rinehart and Winston, NY.

Kullenberg, G. (1982) Pollutant transfer and transport on the sea. Vol 2, CRC Press. Florida 1982.

McLellan, H.J. (1968) Elements of physical oceanography. Pergamon Press, Oxford.

Table 1: Continous Meteorological Data collected at Madinat Al-Jubail Al-Sinaiyah

Parameters	Averaging Period (hrs)	Site 1	Site 2
Wind Speed and Direction (vector and scaler)			
90 meters	1	x	
50 meters	1	x	
10 meters	1	x	x
Sigma theta (all levels)	1	x	x
2-second maximum gust	-	x	x
Temperature Difference			
10-50 meters	1	x	
10-90 meters	1	x	
Temperature (10 m)	1	x	x
Dew Point (10 m)	1	x	
Solar Radiation	1	x	
Barometric Pressure	1	x	
Rainfall	1	x	x
Evaporation	24	x	
Mixing Height (Acoustic Sounder)	1	x	
Soil Temperature (5 cm, 1 m and 2 m)	1	x	

Table 2: Summary of Meteorological Parameters from the Selected Homogeneous Turbulence Periods at Jubial

DATE	TIME	WD10 s1	U10 s1	U90 s1	SIG1 s1	T10 s1	USTAR	ZZERO	R1050	R5090	T1050	N	Cd	WD10 s2	U10 s2	SIG10 s2	T10 s2
01/3	11-1500	336	8.6	10.3	8.2	13.9	.30	.011	-.02	-.01	-.78	12.9	.001	348	9.2	5.7	13.3
01/3	19-2000	343	2.9	6.1	4.8	11.5	.58	130.409	.01	-.02	.47	3.0	.039	328	4.7	4.4	12.3
02/3	20-2100	315	1.6	4.1	4.1	12.6	.45	237.874	.19	-.04	1.14	2.4	.076	306	2.3	4.1	13.3
04/3	21-2200	130	6.8	8.2	18.1	18.5	.27	.048	-.01	-.01	-.04	21.4	.002	130	8.1	8.4	17.6
04/3	24-0100	132	6.3	9.2	17.7	17.3	.54	12.048	-.02	-.01	-.15	6.0	.007	132	7.0	7.6	17.1
05/3	01-0300	130	5.7	9.1	18.2	17.1	.63	33.296	-.02	-.01	-.09	5.0	.012	138	7.9	6.3	17.2
05/3	04-0500	131	5.5	10.1	18.5	16.9	.86	98.904	-.01	-.01	-.05	3.7	.024	137	7.7	6.3	17.1
05/3	06-0700	137	6.5	10.4	16.7	17.2	.72	33.454	-.01	-.01	-.15	4.9	.013	141	8.6	6.2	17.4
06/3	15-1600	0	9.3	11.2	7.0	18.4	.36	.035	-.01	-.01	-.53	12.9	.002	0	9.9	4.9	17.1
06/3	18-1900	358	6.6	9.0	7.1	15.9	.42	1.840	-.02	-.01	-.25	7.7	.004	358	9.4	5.0	16.2
08/3	03-0400	306	3.8	8.0	4.6	9.9	.76	135.788	.04	.04	.98	3.0	.040	307	4.3	3.5	11.6
08/3	05-0600	304	4.0	7.4	5.3	9.5	.67	89.471	.04	.04	1.20	3.8	.028	304	4.1	4.4	11.5
08/3	07-0800	291	3.9	5.8	4.9	10.0	.36	12.479	-.04	.08	-.16	5.7	.008	285	2.9	6.5	11.5
08/3	17-1800	7	8.6	10.5	5.1	13.7	.34	.049	-.01	-.01	-.32	11.6	.002	5	10.2	5.5	14.1
08/3	19-2000	353	4.7	7.6	6.9	13.2	.52	30.369	-.03	-.02	-.15	4.7	.012	358	8.3	5.6	13.9
08/3	21-2200	334	3.4	6.5	6.0	13.0	.56	91.980	-.03	-.02	.02	3.4	.027	331	5.7	3.9	13.4
11/3	11-1300	14	5.6	6.4	10.4	17.6	.13	.000	-.04	-.03	-.64	16.4	.001	5	5.4	3.9	15.8
15/3	08-0600	161	15.9	20.8	4.2	22.6	.89	.921	-.00	.00	-.38	8.4	.003	162	13.1	6.7	15.4
18/3	01-0300	253	2.5	3.7	2.5	14.5	.23	11.578	.25	-.02	2.05	6.3	.008	253	3.8	2.3	13.3
23/3	17-2000	326	3.6	6.6	7.6	19.7	.55	84.525	.01	-.01	.24	3.8	.024	341	6.3	4.2	19.7
01/5	06-0700	339	9.2	12.2	6.7	25.1	.55	1.246	-.01	-.00	-.35	8.6	.004	341	10.8	4.0	24.5
01/5	16-1600	254	3.7	4.7	9.2	30.0	.18	.308	-.06	-.04	-.28	9.8	.002	297	3.7	8.2	27.1
03/5	10-1200	337	5.3	6.2	12.9	30.7	.16	.001	-.05	-.02	-.78	16.6	.001	12	4.1	3.9	26.9
03/5	16-1700	64	4.7	5.6	6.1	28.9	.16	.010	-.04	-.02	-.40	18.8	.001	50	4.1	3.6	26.0
04/5	02-0300	220	2.5	7.4	3.6	21.2	1.01	368.774	.12	.07	2.57	2.1	.163	231	3.7	5.4	22.6
04/5	13-1300	75	5.2	5.6	9.5	34.1	.10	.000	-.05	-.02	-.67	19.8	.000	75	4.6	3.4	28.4
07/5	10-1100	96	5.3	5.8	8.8	33.2	.11	.000	-.04	-.02	-.66	19.0	.000	102	5.8	5.4	28.3
08/5	09-1000	34	1.5	1.6	23.2	36.7	.02	.000	-.69	-.54	-.46	5.9	.000	63	4.1	3.4	29.5
08/5	15-1600	78	4.6	5.0	9.1	32.7	.09	.000	-.05	-.03	-.46	23.7	.000	93	3.7	5.9	28.2
08/5	18-1800	88	2.5	3.4	7.1	31.2	.17	2.842	.08	.09	.93	7.9	.005	112	2.8	6.3	28.1
08/5	20-2000	334	2.9	3.9	11.6	30.8	.19	2.912	.73	.55	1.20	4.6	.005	269	2.6	13.7	28.8
09/5	00-0000	312	2.5	5.2	9.1	29.2	.48	130.060	.01	.03	.58	3.0	.036	318	2.4	5.0	28.6
09/5	03-0400	5	5.5	9.9	8.0	29.0	.80	70.474	.01	.00	.57	3.7	.021	350	6.0	5.3	28.2
09/5	11-1300	5	7.6	8.6	8.1	36.4	.20	.000	-.02	-.01	-.82	19.2	001	14	4.2	3.6	29.7
09/5	15-1700	44	6.7	8.7	5.7	33.6	.35	.507	-.02	-.00	-.42	9.6	003	47	4.8	4.0	29.5
21/5	10-1000	329	8.5	9.8	7.8	35.8	.25	.001	-.02	-.01	-.75	15.5	001	330	8.9	3.3	33.3
23/5	02-0300	322	5.3	10.4	6.2	30.1	.93	116.297	-.00	-.00	.35	3.3	.031	326	6.8	4.0	30.3
23/5	21-2300	147	3.1	8.9	9.1	31.5	1.04	329.021	.06	.02	1.52	2.1	.114	143	3.6	5.1	31.2
26/5	14-1600	28	6.1	7.0	7.9	34.1	.17	.001	-.03	-.01	-.40	16.3	.001	8	4.1	3.6	30.3

Table 3: Average and Standard Deviation of Categorized Wind Parameters (Average/Standard Deviation)

Category*	Cases # no.	U10 s1	SIG1 s1	U10 s2	SIG1 s2	U90 s1	T10 s1	T10 s2	n s1	USTAR s1	ZZERO s1	Cd s1	R5090 s1	T1050 s1
(a)	14	3.3	6.4	4.2	5.1	6.6	21.0	20.9	3.7	.60	129	.0440	+.11	+1.0
		1.1	2.5	1.5	2.7	2.3	9.0	8.1	1.6	.29	112	.0449	.19	.7
(b)	7	5.6	14.4	7.2	6.7	8.6	15.8	16.0	7.3	.56	31.5	.0112	-.02	-.1
		1.0	5.9	2.0	1.0	1.6	3.0	2.4	6.2	.20	32.4	.0069	.01	.1
(c)	9	6.8	8.5	7.1	5.2	8.7	26.6	23.4	11.5	.33	.54	.0021	-.09	-.4
		4.2	5.8	3.7	1.6	5.6	7.9	6.3	5.8	.27	.66	.0014	.22	.1
(d)	9	6.8	8.9	6.3	4.2	7.9	28.2	24.8	16.5	.20	.01	.0008	-.03	-.7
		1.6	1.8	2.4	.9	2.1	8.9	7.3	2.5	.09	.01	.0004	.01	.1
(e)	8	2.9	6.0	3.4	5.6	5.9	20.1	20.0	4.0	.57	147	.0548	.19	1.5
		.8	3.1	.7	3.5	2.3	9.8	8.5	2.1	.36	148	.0584	.23	.6
(f)	21	6.7	9.4	7.6	5.2	9.6	21.3	20.3	8.2	.53	39.8	.0127	-.01	-.1
		2.9	5.0	2.5	1.4	3.1	8.0	6.8	5.5	.22	48.9	.0128	.01	.4
(g)	10	4.6	10.2	4.3	4.8	5.4	28.8	25.2	15.2	.15	1.28	.0015	-.11	-.5
		1.3	5.1	.8	1.6	1.5	8.4	6.3	6.1	.09	3.94	.0025	.20	.2
(h)	12	5.7	8.9	5.3	4.5	7.0	28.9	25.4	13.8	.24	6.2	.0030	-.07	-.3
		2.3	4.8	2.3	1.1	2.9	7.9	6.0	6.2	.20	20.3	.0059	.20	.5
(i)	8	6.9	13.9	7.7	6.5	10.3	21.8	20.2	8.8	.63	63.5	.0219	-.01	-.0
		3.8	5.6	2.7	1.1	4.5	6.8	6.0	7.3	.32	112	.0380	.03	.6
(j)	3	2.9	5.1	3.7	5.3	5.3	21.9	21.0	6.0	.47	127	.0578	.10	1.4
		.7	3.6	.0	3.0	1.9	7.8	7.0	3.8	.47	209	.0911	.15	1.5
(k)	16	4.8	7.1	5.8	5.1	7.5	19.4	19.3	6.4	.48	66.5	.0210	.05	.2
		2.3	2.5	2.8	2.5	2.4	9.2	8.0	4.6	.20	71.3	.0208	.19	.7

* See text for explanation of categories

Table 4: Comparison of Wind Speed at Site 1 and Site 2 by Lapse Rate, Bulk Richardson Number and Wind Direction Categories

Category 1	Number of Cases	Slope	Offset	Correlation Coeff.
U10 (Site 1) vs U90 (Site 1)	14	1.7	0.8	.666
U10 (Site 2) vs U90 (Site 1)	14	1.1	2.0	.494
U10 (Site 1) vs U10 (Site 2)	14	1.1	0.5	.647
Category 2				
U10 (Site 1) vs U90 (Site 1)	7	1.1	2.3	.541
U10 (Site 2) vs U90 (Site 1)	7	0.6	4.3	.555
U10 (Site 1) vs U10 (Site 2)	7	1.3	-0.2	.479
Category 3				
U10 (Site 1) vs U90 (Site 1)	9	1.3	-0.5	.994
U10 (Site 2) vs U90 (Site 1)	9	1.3	-0.9	.793
U10 (Site 1) vs U10 (Site 2)	9	0.8	1.7	.772
Category 4				
U10 (Site 1) vs U90 (Site 1)	9	1.3	-1.0	.994
U10 (Site 2) vs U90 (Site 1)	9	0 7	3.2	.697
U10 (Site 1) vs U10 (Site 2)	9	1.2	-2.1	.696
Category 5				
U10 (Site 1) vs U90 (Site 1)	8	1.8	0.7	.382
U10 (Site 2) vs U90 (Site 1)	8	2.1	-1.4	.493
U10 (Site 1) vs U10 (Site 2)	8	0.7	1.3	.577
Category 6				
U10 (Site 1) vs U90 (Site 1)	21	1.0	3.0	.855
U10 (Site 2) vs U90 (Site 1)	21	1.0	2.1	.613
U10 (Site 1) vs U10 (Site 2)	21	0.7	3.1	.633
Category 7				
U10 (Site 1) vs U90 (Site 1)	10	1.1	0.5	.884
U10 (Site 2) vs U90 (Site 1)	10	0.3	4.1	.027
U10 (Site 1) vs U10 (Site 2)	10	0.2	3.1	.158

Table 4: (continued)

Category 8	Number of Cases	Slope	Offset	Correlation Coeff.
U1Ø (Site 1) vs U9Ø (Site 1)	12	1.2	Ø.1	.867
U1Ø (Site 2) vs U9Ø (Site 1)	12	Ø.9	1.9	.572
U1Ø (Site 1) vs U1Ø (Site 2)	12	Ø.8	Ø.9	.561
Category 9				
U1Ø (Site 1) vs U9Ø (Site 1)	8	1.1	2.9	.843
U1Ø (Site 2) vs U9Ø (Site 1)	8	1.4	-Ø.3	.7Ø5
U1Ø (Site 1) vs U1Ø (Site 2)	8	Ø.7	3.1	.866
Category 1Ø				
U1Ø (Site 1) vs U9Ø (Site 1)	3	-Ø.8	7.7	.Ø8Ø
U1Ø (Site 2) vs U9Ø (Site 1)	3	-2Ø1.7	779.1	.792
U1Ø (Site 1) vs U1Ø (Site 2)	3	Ø.Ø	3.8	.Ø77
Category 11				
U1Ø (Site 1) vs U9Ø (Site 1)	16	Ø.9	3.1	.781
U1Ø (Site 2) vs U9Ø (Site 1)	16	Ø.7	3.2	.771
U1Ø (Site 1) vs U1Ø (Site 2)	16	1.1	Ø.7	.76Ø

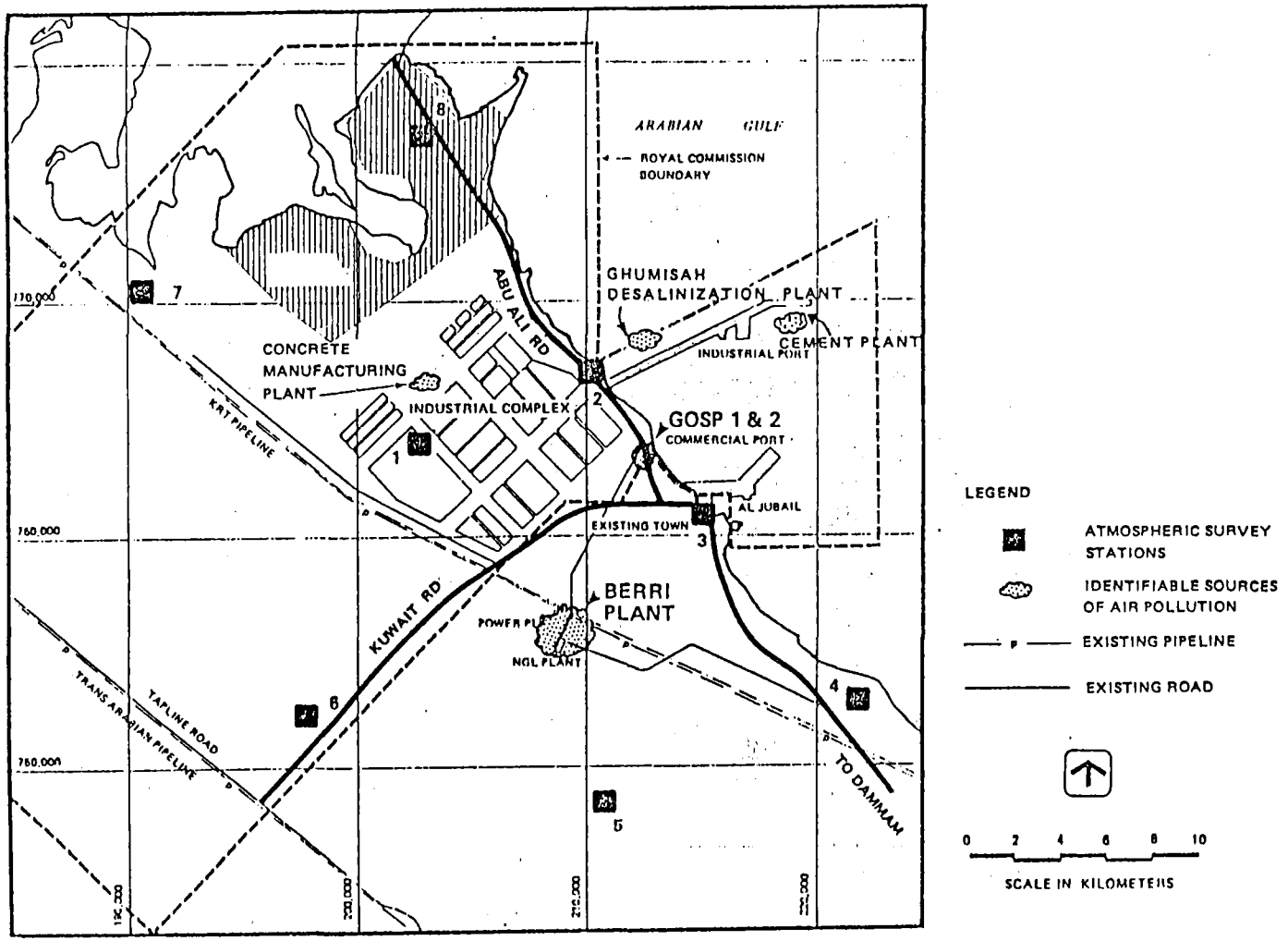

Figure 1: Study Region with station location (numbers 1 to 8)

RECOMMENDATIONS

THE SYMPOSIUM/WORKSHOP

Considering that the numerical modelling of oceanographic phenomena can provide a powerful tool for assisting in the decision-making processes leading to environmental management policy;

Considering the requirement for predictive models dealing with the dispersion of certain pollutants in marine environments;

Considering the importance of propagating the idea of oceanographic modelling among marine scientists in the KAP Region and the necessity to continue with such action;

Considering the enthusiastic response from marine scientists participating in this and former symposia and workshops;

Considering the lack of oceanogrphic data that exists in the KAP Region;

Recognizing that the acquisition of sufficient baseline data is a necessary prerequisite for any successful modelling effort.

Considering the need to update marine scientists in the methodology of modelling;

Recognizing the importance of maintaining continuous interaction between regional research groups;

Being aware of the fact that the available data base for the Gulf of Oman was not adequate for a comprehensive numerical model;

MAKES THE FOLLOWING RECOMMENDATIONS:

1. Form a group from the region to inventory available oceanographic and atmospheric data pertaining to the KAP Region;

2. Reinforce the efforts made toward the establishment of a regional data center in order to archive and disseminate such data;

3. Collect additional data for use in specific modelling projects in the following fields:

   (a) Tides and storm surges
   (b) Residual currents and mixing processes
   (c) Oil Slicks
   (d) Ecosystems

For (a) and (b), data particularly required are:

(i) long-period current measurements taken at key sites and different depths throughout the KAP Region;

(ii) long-period measurements of sea-level variations taken simultaneously around the Gulf, offshore, and in the Gulf of Oman;

(iii) better and more detailed measurements of the wind waves and swell in the KAP Region;

(iv) development of theoretical relationships between wind speed and wave height in shallow water.

In addition, for (b) data include:

(v) large-scale conventional oceanographic observations over the KAP Region and, in particular, during the summer;

(vi) fresh water input to the KAP Region;

(vii) measurements of evaporation throughout the Gulf at different times of the year;

(viii) mixing experiments involving the use of tracers especially to determine vertical mixing time.

For (c), data required are:

(ix) characterization of the oil in particular with regard to properties like weathering, toxicity, dispersibility, which bear directly on the environment.

4. Investigate the use of remote sensing techniques to augment, reinforce, and calibrate conventional observation programs in the KAP Region.

5. Establish a regional center for numerical modelling at a research institution in the region to act as a focus for the free exchange of ideas, develop a regional focus and avoid needless duplication of effort, making use of existing facilities in the region.

6. Hold a follow-up workshop/symposium in two years time to review progress and update recommendations.

7. Encourage training of young scientists in the KAP Region in the field of oceanographic modelling.

PUBLICATIONS IN THE UNEP REGIONAL SEAS REPORTS AND STUDIES SERIES

No. 1 UNEP: Achievements and planned development of UNEP's Regional Seas Programme and comparable programmes sponsored by other bodies. (1982)

No. 2 UNIDO/UNEP: Survey of marine pollutants from industrial sources in the West and Central African region. (1982)

No. 3 UNESCO/UNEP: River inputs to the West and Central African marine environment. (1982)

No. 4 IMCO/UNEP: The status of oil pollution and oil pollution control in the West and Central African region. (1982)

No. 5 IAEA/UNEP: Survey of tar, oil, chlorinated hydrocarbons and trace metal pollution in coastal waters of the Sultanate of Oman. (1982)

No. 6 UN/UNESCO/UNEP: Marine and coastal area development in the East African region. (1982)

No. 7 UNIDO/UNEP: Industrial sources of marine and coastal pollution in the East African region. (1982)

No. 8 FAO/UNEP: Marine pollution in the East African region. (1982)

No. 9 WHO/UNEP: Public health problems in the coastal zone of the East African region. (1982)

No. 10 IMO/UNEP: Oil pollution control in the East African region. (1982)

No. 11 IUCN/UNEP: Conservation of coastal and marine ecosystems and living resources of the East African region. (1982)

No. 12 UNEP: Environmental problems of the East African region. (1982)

No. 13 UNEP: Pollution and the marine environment in the Indian Ocean. (1982)

No. 14 UNEP/CEPAL: Development and environment in the Wider Caribbean region: A Synthesis. (1982)

No. 15 UNEP: Guidelines and principles for the preparation and implementation of comprehensive action plans for the protection and development of marine and coastal areas of regional seas. (1982)

No. 16 GESAMP: The health of the oceans. (1982)

No. 17 UNEP: Regional Seas Programme: Legislative authority. (1985)

No. 18 UNEP: Regional Seas Programme: Workplan. (1982)

No. 19 Rev. 2. UNEP: UNEP Oceans Programme: Compendium of projects. (1985)

No. 20 CPPS/UNEP: Action Plan for the protection of the marine environment and coastal areas of the South-East Pacific. (1983)

No. 21 CPPS/UNEP: Sources, levels and effects of marine pollution in the South-East Pacific. (1983) (In Spanish only)

No. 22 Rev. 2. UNEP: Regional Seas Programme in Latin America and Wider Caribbean. (1985)

No. 23 FAO/UNESCO/IOC/WHO/WMO/IAEA/UNEP: Co-ordinated Mediterranean Pollution Monitoring and Research Programme (MED POL) - Phase I: Programme Description. (1983)

No. 24 UNEP: Action Plan for the protection and development of the marine and coastal areas of the East Asian region. (1983)

No. 25 UNEP: Marine pollution. (1983)

No. 26 UNEP: Action Plan for the Caribbean environment programme. (1983)

No. 27 UNEP: Action Plan for the protection and development of the marine environment and coastal areas of the West and Central African region. (1983)

No. 28 UNEP: Long-term programme for pollution monitoring and research in the Mediterranean (MED POL) - Phase II. (1983)

No. 29 SPC/SPEC/ESCAP/UNEP: Action Plan for managing the natural resources and environment of the South Pacific region. (1983)

No. 30 UNDIESA/UNEP: Ocean energy potential of the West and Central African region. (1983)

No. 31 A. L. DAHL and I. L. BAUMGART: The state of the environment in the South Pacific. (1983)

No. 32 UNEP/ECE/UNIDO/FAO/UNESCO/WHO/IAEA: Pollutants from land-based sources in the Mediterranean. (1984)

No. 33 UNDIESA/UNEP: Onshore impact of offshore oil and natural gas development in the West and Central African region. (1984)

No. 34 UNEP: Action Plan for the protection of the Mediterranean. (1984)

No. 35 UNEP: Action Plan for the protection of the marine environment and the coastal areas of Bahrain, Iran, Iraq, Kuwait, Oman, Qatar, Saudi Arabia and the United Arab Emirates. (1983)

No. 36 UNEP/ECLAC: The state of marine pollution in the Wider Caribbean region. (1984)

No. 37 UNDIESA/UNEP: Environmental management problems in resource utilization and survey of resources in the West and Central African region. (1984)

No. 38 FAO/UNEP: Legal aspects of protecting and managing the marine and coastal environment of the East African region. (1983)

No. 39 IUCN/UNEP: Marine and coastal conservation in the East African region. (1984)

No. 40 SPC/SPEC/ESCAP/UNEP: Radioactivity in the South Pacific. (1984)

No. 41 UNEP: Socio-economic activities that may have an impact on the marine and coastal environment of the East African region. (1984)

No. 42 GESAMP: Principles for developing coastal water quality criteria. (1984)

No. 43 CPPS/UNEP: Contingency plan to combat oil pollution in the South-East Pacific in cases of emergency. (1984)

No. 44 IMO/ROPME/UNEP: Combating oil pollution in the Kuwait Action Plan region. (1984)

No. 45 GESAMP: Thermal discharges in the marine environment. (1984)

No. 46 UNEP: The marine and coastal environment of the West and Central African region and its state of pollution. (1984)

No. 47 UNEP: Prospects for global ocean pollution monitoring. (1984)

No. 48 SPC/SPEC/ESCAP/UNEP: Hazardous waste storage and disposal in the South Pacific. (1984)

No. 48/Appendices SPC/SPEC/ESCAP/UNEP: Hazardous waste storage and disposal in the South Pacific. (1984)

No. 49 FAO/UNEP: Legal aspects of protecting and managing the marine and coastal environment of the East African region: National Reports. (1984)

No. 50 IUCN/UNEP: Marine and coastal conservation in the East African region: National Reports. (1984)

No. 51 UNEP: Socio-economic activities that may have an impact on the marine and coastal environment of the East African region: National Reports. (1984)

No. 52 UNEP: Arab co-operation for the protection and development of the marine environment and coastal areas resources of the Mediterranean. (1984)

No. 53 UNEP: UNEP Regional Seas Programme: the Eastern African Experience. (1984)

No. 54 UNIDO/UNEP: Contingency planning for emergencies associated with industrial installations in the West and Central African region. (1985)

No. 55 FAO/UNEP: Marine mammals: global plan of action. (1985)

No. 55/Annex FAO/IUCN/IWC/UNEP: Marine mammals: global plan of action. (1985)

No. 56 GESAMP: Cadmium, lead and tin in the marine environment. (1985)

No. 57 IMO/UNEP: Oil spills and shoreline clean-up on the coasts of the Eastern African region. (1985)

No. 58 UNEP: Co-operative programmes sponsored by UNEP for the protection of the marine and coastal environment in the wider Indian Ocean region. (1985)

No. 59 UNEP: Environmental problems of the marine and coastal area of India: National Report. (1985)

No. 60 IUCN/UNEP: Management and conservation of renewable marine resources in the Indian Ocean region: Overview. (1985)

No. 61 UNEP: Action Plan for the protection, management and development of the marine and coastal environment of the Eastern African region. (1985)

No. 62 IUCN/UNEP: Management and conservation of renewable marine resources in the South Asian Seas region. (1985)

No. 63 IUCN/UNEP: Management and conservation of renewable marine resources in the Kuwait Action Plan region. (1985)

No. 64 IUCN/UNEP: Management and conservation of renewable marine resources in the Red Sea and Gulf of Aden region. (1985)

No. 65 IUCN/UNEP: Management and conservation of renewable marine resources in the East Asian Seas region. (1985)

No. 66 IUCN/UNEP: Management and conservation of renewable marine resources in the Eastern African region. (1985)

No. 67 UN/UNEP: Coastal erosion in West and Central Africa. (1985)

No. 68 GESAMP: Atmospheric transport of contaminants into the Mediterranean region. (1985)

No. 69 UNEP: Environment and resources in the Pacific. (1985)

No. 70 UNESCO/ROPME/UPM: Proceedings of the Symposium/Workshop on oceanographic modelling of the Kuwait Action Plan (KAP) region. (1985)

No. 71 IUCN/ROPME/UNEP: An ecological study of the rocky shores on the southern coast of Oman. (1985)

No. 72 IUCN/ROPME/UNEP: An ecological study of sites on the coast of Bahrain. (1985)

No. 73 SPC/SPEC/ESCAP/UNEP: Ecological interactions between tropical coastal ecosystems. (1985)